

Jeong-Yeol Yoon

Introduction to Biosensors

From Electric Circuits to Immunosensors

Second Edition

Jeong-Yeol Yoon

Introduction to Biosensors

From Electric Circuits to Immunosensors

2nd ed. 2016



Jeong-Yeol Yoon
University of Arizona, Tucson, AZ, USA

ISBN 978-3-319-27411-9 e-ISBN 978-3-319-27413-3
DOI 10.1007/978-3-319-27413-3

Library of Congress Control Number: 2015958324

© Springer International Publishing Switzerland 2013, 2016

This work is subject to copyright. All rights are reserved by the Publisher, whether the whole or part of the material is concerned, specifically the rights of translation, reprinting, reuse of illustrations, recitation, broadcasting, reproduction on microfilms or in any other physical way, and transmission or information storage and retrieval, electronic adaptation, computer software, or by similar or dissimilar methodology now known or hereafter developed.

The use of general descriptive names, registered names, trademarks, service marks, etc. in this publication does not imply, even in the absence of a specific statement, that such names are exempt from the relevant protective laws and regulations and therefore free for general use.

The publisher, the authors and the editors are safe to assume that the advice and information in this book are believed to be true and accurate at the date of publication. Neither the publisher nor the authors or the editors give a warranty, express or implied, with respect to the material contained herein or for any errors or omissions that may have been made.

Printed on acid-free paper

This Springer imprint is published by SpringerNature The registered company is Springer International Publishing AG Switzerland

Preface to the Second Edition

Since I wanted my textbook to serve as an “introduction” to biosensors with hands-on laboratory demonstrations, I deliberately made the first edition of my book as concise as possible. Therefore, many different advanced topics had to be forgone in the first edition. However, some of those advanced topics are too important to be dismissed—for example, pulse oximeter, glucose meter, lateral flow assay, paper-based lab-on-a-chip, nano-biosensors, and microcontroller. These important topics were either very briefly mentioned without laboratory exercises or not mentioned at all in the first edition. Therefore, I decided to add these topics to the second edition with appropriate laboratory exercises, while not compromising the concise nature of this book.

Here is a list of the major additions made to the second edition:

- Most circuit photos were retaken at higher resolution with an easy-to-recognize layout.
- Added a section on op-amp filters.
- The spectrophotometry chapter was fully rewritten to focus on pulse oximeter, not on glucose sensing. Added new laboratory procedures on hemoglobin sensing and meat quality monitoring.
- The fluorescence chapter was fully rewritten to incorporate advanced fluorescent dyes, autofluorescence, and different methods of fluorescence detection. Added a new laboratory procedure on fluorescence detection from urine. The fluorescent lamp measurement laboratory in the first edition was removed.
- Added advanced topics on electrochemical sensors.
- Added a new laboratory procedure on fluoride sensing from tap water and toothpaste to the electrochemical sensor chapter.
- Glucose sensing in the spectrophotometry and electrochemical sensor chapters were consolidated into the new glucose sensor chapter.
- Added additional details on various glucose sensing methods.
- Added a new laboratory procedure on lateral flow assay (pregnancy test) and subsequent smartphone-based quantification to the immunosensors chapter.
- Added advanced topics on lab-on-a-chip.
- Added a section and two new laboratory procedures on paper-based lab-on-

a-chip.

- Added a new chapter on nano-biosensor.
- Added a new appendix on microcontroller (Arduino) and two new laboratory procedures.

I hope the newly added materials would provide the most up-to-date and comprehensive introduction to the modern biosensor research and their commercialization efforts.

Some of these newly created laboratory procedures have been implemented in my Sensors and Controls class in Fall 2013, Fall 2014, and Fall 2015, with assistance from my teaching assistants and postdocs—Dr. David You, Dr. Pei-Shih Liang, Dr. Tu San Park, Dr. Christopher Fronczek, Dr. Scott Angus, Dr. Dustin Harshman, Ms. Katrina DeCook, Mr. Tigran Nahapetian, Ms. Katherine McCracken, and Mr. Kevin Okarski, all at the University of Arizona, who provided very important feedback, corrections, and suggestions. I would also like to thank the other students in my research laboratory—Ms. Cayla Baynes, Ms. Ariana Nicolini, Ms. Soohee Cho, Ms. Robin Sweeney, Ms. Alexandra Downs, Mr. Tyler Toth, and Mr. Collin Gilchrist, who have also provided feedback and corrections to the draft manuscript. I also thank my former and current department heads, Dr. Urs Utzinger and Dr. Arthur Gmitro in the Biomedical Engineering Department, and Dr. Donald Slack and Dr. Kathryn Farrell-Poe in the Agricultural and Biosystems Engineering Department, who have supported my class through providing personnel, equipment, and laboratory space at the University of Arizona. Support and suggestions from the editorial office at Springer, especially Ms. Marta Moldvai, is greatly appreciated. Finally, I would like to mention my wife's name one more time, Dr. Sunhi Choi (Mathematics Department at the University of Arizona), for her continuous inspiration and support during the preparation of this second edition.

Preface to the First Edition

The title of this textbook, *Biosensors: From Electric Circuits to Immunosensors*, implies that we are going to learn both electric circuitry (in relation to conventional sensors such as temperature sensors) and biosensors (such as antibody-based immunosensors). The idea of putting these two topics together into a single book came from my decision to add biosensor topics to the “Sensors and Controls” class taught at the University of Arizona. At that time, I realized there was no available textbook that equally addressed these two topics. In typical sensor textbooks, biosensor topics are relatively sparse. In biosensor textbooks, fundamental electric circuitry is rarely addressed. More importantly, none of those textbooks address the necessary link between these two topics. After all, most biosensors require electric circuit components.

This textbook is designed not only for college undergraduate students but also for the scientists and engineers working in the sensor or biosensor industries as a hands-on guide. Although this book may seem to be a collection of laboratory procedures (and certainly can be used for a college-level laboratory class), its primary aim is to deliver hands-on guidance and visual demonstrations of biosensor applications. Readers can complete virtual experiments by reading the lab procedures and viewing the photographs taken during the lab exercises. They can also carry out their own experiments by purchasing the necessary equipment and supplies. This book takes a step-by-step approach towards the end result of building an antibody-based immunosensor from scratch.

Many people have provided invaluable help in creating this textbook. First of all, I wish to express my deepest appreciation to my wife, Dr. Sunhi Choi, for her support and advice throughout the writing of this textbook. I also wish to thank my former graduate student Dr. Lonnie J. Lucas (at Applied Energetics) for all the time he spent with me in shaping the entire book, in providing numerous ideas and suggestions, and in proof-reading the entire draft. This collaboration with Lonnie was one of the most pleasant collaborations in my entire life. Specifically, Chap. 9 was written jointly with Lonnie. I also thank the students enrolled in my Sensors and Controls class in Fall 2009, Fall 2010, and Fall 2011 at the University of Arizona, who have provided corrections and constructive suggestions on the draft lab procedures. The help of my teaching assistants for this class, Zachary S. Dean, C. Christopher Stemple, and Scott V. Angus, is greatly appreciated as well. Specifically, Zach collected many photographs of lab exercises and proof-read many parts of the manuscript. Dr. David J. You, my former graduate student and current post-doc, provided

important help in creating Chap. 15 lab exercise. Other students and post-docs in my lab have also provided numerous corrections and suggestions. My former and current department heads, Dr. Donald C. Slack and Dr. Mark R. Riley, have also provided support and suggestions for my class. I also thank the late Dr. Kenneth Jordan (University of Arizona), who taught the Sensors and Controls class for many years before me and laid the foundations for the lab procedures from Chaps. 2–6. Finally, support and suggestions from the editorial office at Springer, Alison Waldron and Steven M. Elliot, are greatly appreciated. None of this would have been possible without the contributions of all of my students, co-workers and collaborators.

Contents

1 Introduction

1.1 Sensors

1.2 Transducers

1.3 Biosensors

1.4 Bioreceptors

1.5 Transducers for Biosensors

1.6 Overview of This Textbook

References and Further Readings

2 Resistors

2.1 Electric Circuit

2.2 Current and Voltage

2.3 Resistance and Ohm's Law

2.4 Resistors in Series, or Voltage Divider

2.5 Potentiometer, or Pot

2.6 Resistors in Parallel, or Current Divider

2.7 Reading Resistor Values

2.8 Breadboards

2.9 Laboratory Task 1: Resistors in Series

2.10 Laboratory Task 2: Resistors in Parallel

2.11 Laboratory Task 3: “Droop”

2.12 Laboratory Task 4: Potentiometer (Pot)

2.13 Further Study: Thévenin’s Theorem

References and Further Readings

3 Diodes and Transistors

3.1 Semiconductors

3.2 Diodes

3.3 Zener Diode

3.4 Transistors

3.5 Operational Amplifier to Protect Your Circuit

3.6 Laboratory Task 1: LED

3.7 Laboratory Task 2: Zener Diode

3.8 Laboratory Task 3: Transistor

References and Further Readings

4 Temperature Sensors

4.1 Thermocouple

4.2 Thermistor

4.3 Diode Temperature Sensor

4.4 Transistor Temperature Sensor

4.5 Laboratory Task 1: Thermistor

4.6 Laboratory Task 2: Zener Diode Temperature Sensor

4.7 Laboratory Task 3: Transistor Temperature Sensor

References and Further Readings

5 Wheatstone Bridge

5.1 Wheatstone Bridge

5.2 Strain Gauge

5.3 Cantilever Biosensor

5.4 Laboratory Task 1: Wheatstone Bridge

5.5 Laboratory Task 2: Wheatstone Bridge for a Thermistor

5.6 Laboratory Task 3: Wheatstone Bridge for a Strain Gauge

References and Further Readings

6 Op-Amp

6.1 Op-Amp

6.2 Basics of Op-Amp

6.3 Voltage Follower or Buffer Op-Amp

6.4 Non-Inverting Op-Amp

6.5 Inverting Op-Amp

6.6 Summing Op-Amp

6.7 Differential Op-Amp

6.8 Laboratory Task 1: Non-inverting Op-Amp Operation

6.9 Laboratory Task 2: Signal Conditioning for Temperature Sensor

6.10 Further Study: Op-Amp Filters

References and Further Readings

7 Light Sensors

7.1 Light

7.2 Photoresistor

7.3 Photodiode

7.4 Phototransistor

7.5 Light-Emitting Diode (LED)

7.6 Laser Diode

7.7 Laboratory Task 1: Photoconductive Operation

7.8 Laboratory Task 2: Photovoltaic Operation

References and Further Readings

8 Spectrophotometry

8.1 Spectrophotometry

8.2 Spectrophotometry Biosensor Example: Pulse Oximeter

8.3 Miniature Spectrophotometer

8.4 Optical Fibers

8.5 Laboratory Task 1: Hemoglobin Quantification with a Spectrophotometer

8.6 Laboratory Task 2: Hemoglobin Quantification with LED/PD Circuit

8.7 Laboratory Task 3: Meat Quality Monitoring with Reflection Probe

References and Further Readings

9 Fluorescence

9.1 Fluorescence

9.2 Fluorescent Dyes

9.3 Advanced Fluorescent Dyes: GFP, SYBR, and QD

9.4 Autofluorescence

9.5 Detection of Fluorescence

9.6 Laboratory Task 1: 180° Back Scatter Fluorescence Detection for Fluorescein

9.7 Laboratory Task 2: 90° Side Scatter Fluorescence Detection for Urine

References and Further Readings

10 Electrochemical Sensors

10.1 Electrolytic and Electrochemical Cells

10.2 Ion-Selective Electrodes (ISEs; Potentiometric)

10.3 pH Electrode (Potentiometric)

10.4 Amperometric Biosensors

10.5 Conductometric Biosensors

10.6 Laboratory Task 1: Buffer Preparations and Their pH Measurements

10.7 Laboratory Task 2: pH Meter Circuit

10.8 Laboratory Task 3: Fluoride Ion Selective Electrode with PH Meter

10.9 Laboratory Task 4: Fluoride Ion Selective Electrode with Circuit

References and Further Readings

11 Piezoelectric Sensors

11.1 Piezoelectricity

11.2 Pressure Sensors

11.3 Crystal Oscillators

11.4 Quartz Crystal Microbalance (QCM)

11.5 Viscoelasticity Consideration in QCM

11.6 Flow Cell QCM as Biosensor

11.7 Laboratory Task 1: Quantifying BSA Adsorption on QCM Sensor

References and Further Readings

12 Glucose Sensors

12.1 Optical Glucose Sensor

12.2 Electrochemical Glucose Sensor

12.3 Other Electrochemical Biosensors

12.4 Continuous Glucose Monitoring (CGM)

12.5 Laboratory Task 1: Glucose Assay Kit with a Spectrophotometer

12.6 Laboratory Task 2: Glucose Assay Kit with LED/PD Circuit

12.7 Laboratory Task 3: Commercial Electrochemical Glucose Sensor

References and Further Readings

13 Immunosensors

13.1 Enzyme-Linked Immunosorbent Assay (ELISA)

- 13.2 Antibodies**
 - 13.3 Antibody Fragments and Aptamers**
 - 13.4 Lateral-Flow Assay (LFA)**
 - 13.5 Optical Immunosensors**
 - 13.6 Surface Plasmon Resonance (SPR) Immunosensor**
 - 13.7 Electrochemical Immunosensors**
 - 13.8 Impedance Immunosensors: Interdigitated Microelectrode (IME) Immunosensor**
 - 13.9 Piezoelectric Immunosensors: QCM Immunosensor**
 - 13.10 Immunosensing Kits Versus Handheld Immunosensors**
 - 13.11 Laboratory Task 1: Insulin ELISA Kit**
 - 13.12 Laboratory Task 2: Insulin ELISA Kit with Smartphone Camera**
 - 13.13 Laboratory Task 3: Pregnancy Test (LFA) with Smartphone Camera**
 - 13.14 Further Study: DNA Sensors**
- References and Further Readings**

- 14 Lab-on-a-Chip Biosensors**
 - 14.1 What Is Lab-on-a-Chip (LOC)?**
 - 14.2 How to Make LOCs: Photolithography and Soft Lithography**
 - 14.3 Early LOC: Capillary Electrophoresis (CE)**
 - 14.4 LOCs for Point-of-Care Testing (POCT)**
 - 14.5 Use of Optical Fibers in LOCs**

14.6 Sample/Reagent Introduction

14.7 Mixing in LOC

14.8 Paper-Based LOCs

14.9 LOC Sensing with a Smartphone Camera

14.10 Other Applications of LOCs

14.11 Laboratory Task 1: Fabrication of LOC by Soft Lithography

14.12 Laboratory Task 2: Mixing in LOC

14.13 Laboratory Task 3: Fabrication of a Paper-Based LOC

14.14 Laboratory Task 4: Bradford Assay with Paper-Based LOC

14.15 Further Study: Latex Immunoagglutination Assay (LIA) in LOC

14.16 Further Study: Polymerase Chain Reaction (PCR) in LOC

References and Further Readings

15 Nanobiosensors

15.1 Gold Nanoparticles (AuNPs)

15.2 Quantum Dots (QDs)

15.3 Zinc Oxide (ZnO) Nanostructures

15.4 Carbon Nanotubes (CNTs) and Graphene

15.5 Nanoporous Gold

15.6 Concluding Remarks

References and Further Readings

Appendix: Microcontroller

Index

About the Author

Jeong-Yeol Yoon

received his B.S., M.S., and Ph.D. degrees in Chemical Engineering from Yonsei University, Seoul (South Korea) in 1992, 1994, and 1999 respectively, under the guidance of Dr. Woo-Sik Kim, in collaboration with Dr. Jung-Hyun Kim, where he worked primarily on polymer colloids. He received his second Ph.D. in Biomedical Engineering from the University of California, Los Angeles (UCLA) in 2004, working on lab-on-a-chip and biomaterials, under the guidance of Dr. Robin L. Garrell. He joined the Agricultural and Biosystems Engineering faculty in August 2004 and holds joint appointment in the Department of Biomedical Engineering and BIO5 Institute at the University of Arizona. Dr. Yoon is currently Professor and is directing the Biosensors Lab (<http://biosensors.abe.arizona.edu>). He is a member of the Institute of Biological Engineering (IBE), American Society of Agricultural and Biological Engineers (ASABE), and SPIE —The International Society for Optics and Photonics. He was an elected president of IBE (<http://www.ibe.org>) for the 2015 calendar year. Dr. Yoon currently serves as one of two Editor-in-Chief's for Journal of Biological Engineering (<http://jbioleng.biomedcentral.com>), the official journal of IBE, published by BioMed Central. He also serves (or had served) as Associate Editor and Editorial Board Members for numerous journals, including Scientific Reports, Journal of Biological Engineering, Biological Engineering Transactions, and Transactions of the ASABE.

1. Introduction

Jeong-Yeol Yoon¹✉

(1) University of Arizona, Tucson, AZ, USA

✉ Jeong-Yeol Yoon
Email: jyyoon@email.arizona.edu

1.1 Sensors

As implied in the title of this textbook, *Biosensors: From Electric Circuits to Immunosensors*, we are going to learn both electric circuitry (in relation to conventional sensors such as temperature sensors) and biosensors (such as antibody-based immunosensors), with equal emphasis on both. The overarching aim is to build an antibody-based immunosensor from scratch. Before we begin this textbook, let us define two important terms: sensors and biosensors. Let us start with sensors.

Literally, a *sensor* is a device used to sense a physical variable, which includes, but is not limited to: temperature, strain, humidity, pressure, mass, light, and voltage . To sense these variables, we need to convert them into a universal and easily accessible *signal*—usually a *voltage*. This voltage signal changes continuously with time, and is directly proportional to a corresponding physical variable. A component responsible for this conversion is a *transducer* . The resulting voltage signal is usually an *analog* signal.

The analog voltage signal is usually transferred to a computer or a microprocessor, which recognizes *digital* signals only. An analog signal is converted into a series of high and low voltages (i.e., binary numbers), such that a small fluctuation in the analog signal (i.e., noise) does not affect the overall digital signal. An analog-to-digital converter (A/D converter) performs this conversion. Today, all-in-one type sensors have become very popular. They incorporate a transducer, an A/D converter, a microprocessor, and a small liquid

crystal display (LCD) panel. The signal can also be sent to a computer's universal serial bus (USB) from an A/D converter.

1.2 Transducers

The most common transducers for physical sensors are those used to measure temperature, strain , pressure and light; however, the other variables listed in Fig. 1.1 can also be measured from these four basic transducers: for example, humidity from a set of temperature transducers or mass from a strain transducer (electronic balance). Voltage measurements require no transducers.

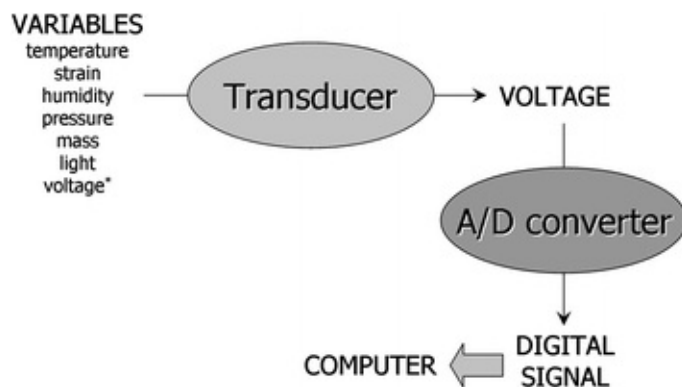


Fig. 1.1 A typical sensor

Let us begin with *temperature transducers*. The oldest and the simplest temperature transducer is a *thermocouple* . Details will be discussed later in Chap. 4. Thermocouples can be made by simply connecting two different types of metal wires and then attaching them to a *voltmeter* (a device that measures voltage) (Fig. 1.2). We normally use a *digital multimeter (DMM)* that can measure not only voltage, but current and resistance as well.

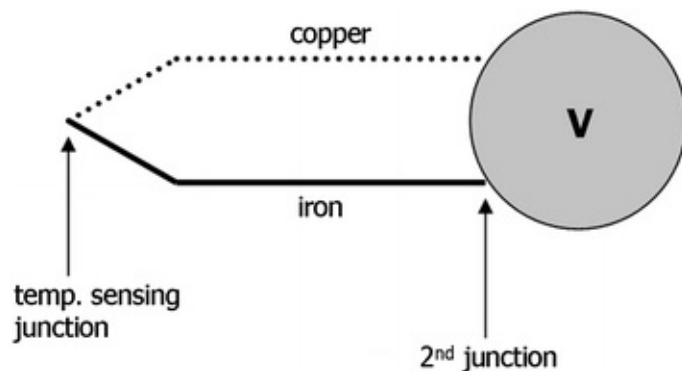


Fig. 1.2 A thermocouple

Semiconductors, including a *resistor*, a *diode* or a *transistor* can also be used to measure temperature, as the semiconductors' current-voltage responses are affected by ambient temperature. A resistor-type temperature transducer is specifically called a *thermistor*. Semiconductor transducers generally provide more accurate temperature information and are smaller in size than a thermocouple. This book includes a lab procedure (Chap. 4) for all three types of semiconductor temperature transducers: a thermistor, a diode temperature transducer, and a transistor temperature transducer.

The *strain transducer* obviously measures *strain*, the deformation of a body. Figure 1.3 shows a typical setup of a *strain gauge*, which is attached to a body. As the body elongates horizontally, the physical width of a metal coil decreases and the length of a metal coil increases, leading to the change in resistance. This resistance change is very small and generally requires a circuit layout known as a *Wheatstone bridge*. A lab procedure is available in this book for a strain gauge (Chap. 5), used as part of a Wheatstone bridge experiment. The strain gauge is widely used in civil and mechanical engineering applications. It is also used widely in an electronic balance.

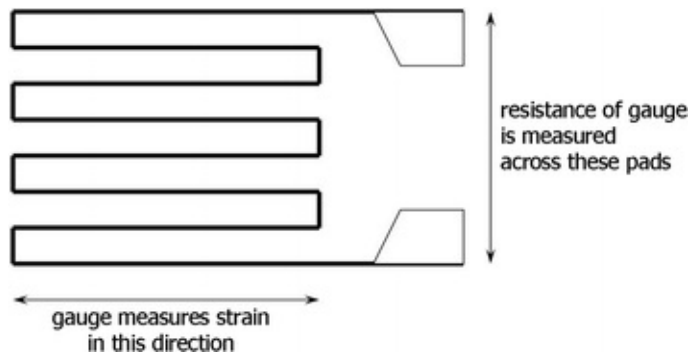


Fig. 1.3 A strain gauge

Pressure transducers measure pressure, a force applied to a unit area of surface. In the field applications, pressure is generally measured with a *capacitor*. A capacitor is comprised of two metal plates (conductors), separated by a dielectric (electrical insulator). Air or vacuum is commonly used as a dielectric. Once voltage is applied to a capacitor, electrons accumulate on the plates. The amount of electrons is determined by (1) the distance between the two plates, (2) the dielectric constant, and (3) the voltage applied to it. A pressure transducer is basically a special type of capacitor, where one plate is replaced with a *diaphragm*. As shown in Fig. 1.4, this diaphragm can be deformed depending on the outside pressure, causing a change in the distance between the two plates

and a subsequent change in the capacitance of the pressure transducer. We do not have a lab procedure for pressure sensors, since they are rarely used in biosensor applications.

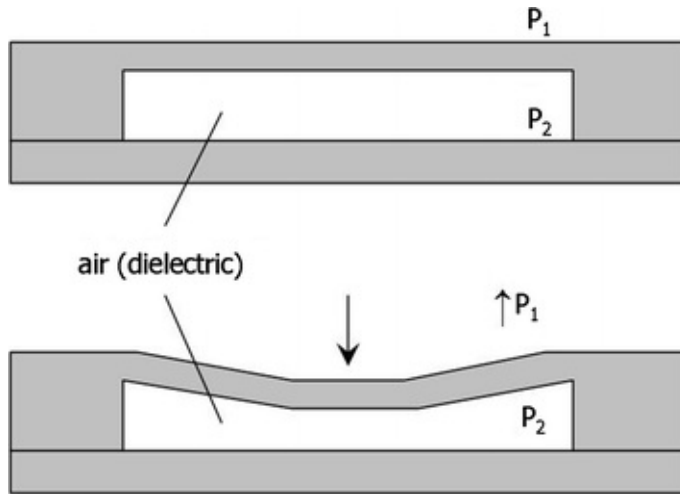


Fig. 1.4 A pressure transducer

Light transducers sense light, which is a wave of photons. Like temperature transducers, three major types of semiconductors can be used as light transducers, namely the *photoresistor*, the *photodiode*, and the *phototransistor*. The photodiode (PD) is probably the most popular. Similar to a diode-type temperature transducer, the current–voltage response from a PD is affected by photons. A PD is usually combined with a *light-emitting diode (LED)* or a *laser diode*, as the light transducer requires a light source. There are lab procedures for the LED and PD in this book (Chaps. 7 and 8) (Fig. 1.5).

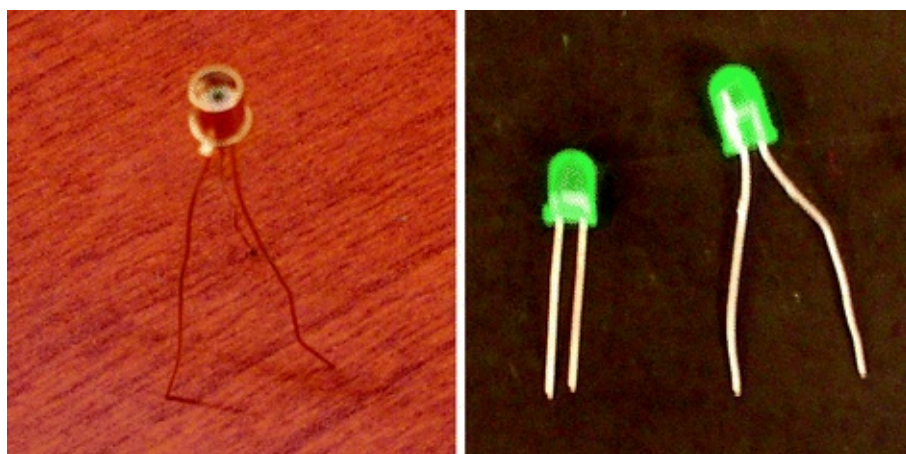


Fig. 1.5 Photodiode (PD) and light-emitting diodes (LEDs)

Modern biosensors employ advanced optics components, such as *optical fibers*, *charge-coupled device array* (*CCD array*), and *complementary metal oxide semiconductor array* (*CMOS array*). Details can be found in Chap. 9. An optical fiber is used to deliver light similar to the way an electric wire delivers electricity. CCDs can be arranged in a one-dimensional (1-D) array to be used as a detector for a *spectrophotometer*, or in a 2-D array for acquiring an optical image. Similarly, CMOS can be arranged in a 2-D array for imaging. CCD array or CMOS array are commonly found in modern digital cameras and *smart phones*. We have lab procedures for the optical fiber and 1-D CCD array used as a spectrophotometer as shown below (Chaps. 8 and 9). We also have lab procedures using a digital camera or a smart phone (with CCD or CMOS array in it) as an optical detector (Chaps. 13 and 14) (Fig. 1.6).

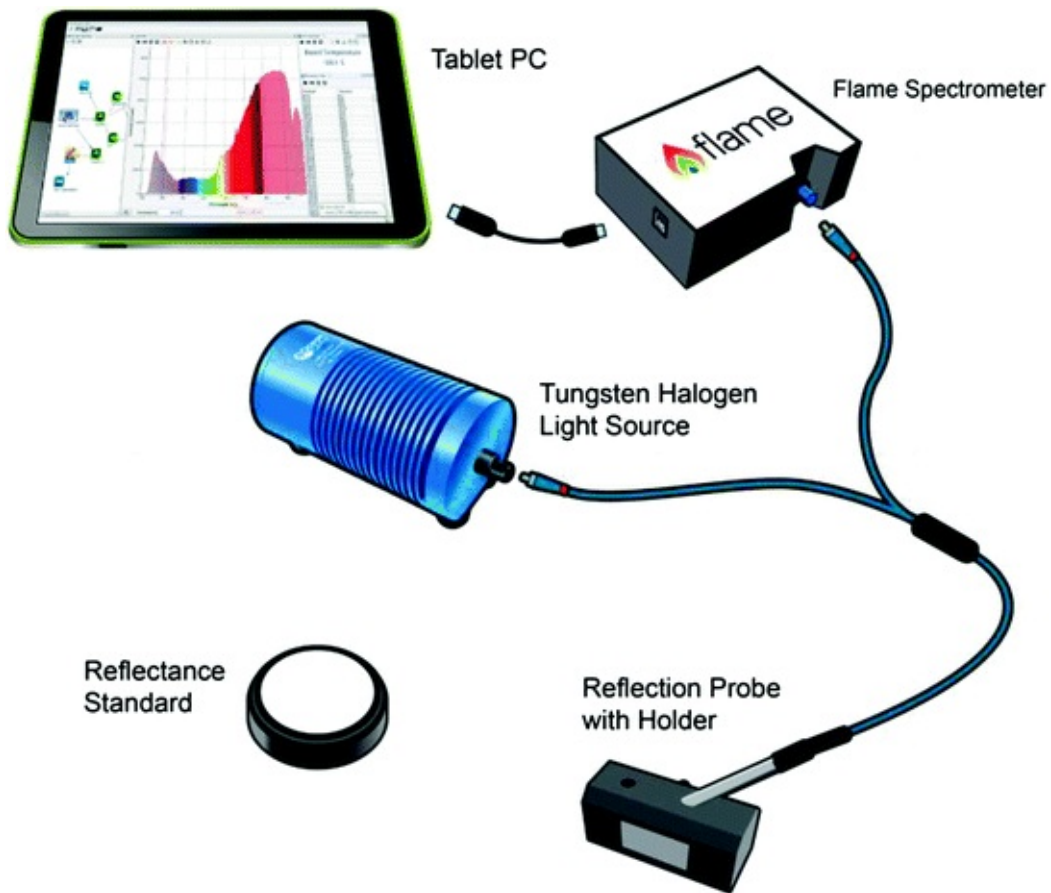


Fig. 1.6 A reflection probe is measuring optical signal, connected to a light source and a miniature spectrometer. Accessed in October 2015 from <http://oceanoptics.com/wp-content/uploads/FlameIO.pdf>. Reprinted with Ocean Optics permission. © Ocean Optics 2015

1.3 Biosensors

As shown in Fig. 1.7, the variables of interest in *biosensors* are typically the type and the concentration of a specific analyte, which can be a simple biochemical compound (e.g., glucose), a sequence of nucleic acid (DNA or RNA), a specific protein, a virus particle, a bacterium, and so forth. These variables cannot be determined with the conventional sensors discussed earlier (temperature, strain, pressure, or light transducers). Therefore, we need another component known as a *bioreceptor*. This bioreceptor is a biological material or a biomimetic, which includes antibodies, enzymes, nucleic acids, viruses, bacteria, tissues, etc. A bioreceptor will specifically bind to a target analyte and cause a transducer to generate a voltage signal.

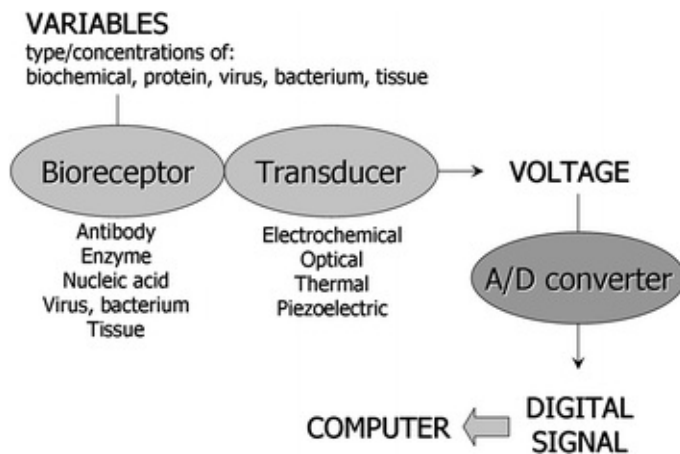


Fig. 1.7 A typical biosensor

The binding process between bioreceptors and target biomolecules is highly specific. For example, the use of an antibody to *Escherichia coli* (anti-*E. coli*) as a bioreceptor will generate a voltage signal only when *E. coli* exists in the sample, but other bacteria or viruses present in the sample will not affect the voltage. Among the bioreceptors, antibodies and nucleic acids (DNA and RNA) are the most popular; the antibody bioreceptor will be demonstrated in the lab procedure described in this book.

The transducers mentioned in Sect. 1.2 may be used for biosensors, with some modifications. The most commonly used transducers for biosensors include: electrochemical (by measuring voltage or current), optical (by measuring light intensity), thermal (by measuring temperature), and piezoelectric (this will be discussed later).

The most successful commercial biosensor application that has been

developed thus far is the glucose sensor used to monitor the blood glucose content for diabetes patients. The glucose sensor has driven the recent growth of the biosensor market and now accounts for over 85 % of the commercial biosensor market. Other new biosensors are currently being investigated and developed for medical diagnostics, environmental monitoring, and water/food safety.

1.4 Bioreceptors

One of the first attempts in biosensor development was based on the *enzyme*, which also serves as a fundamental basis for the glucose sensor. An enzyme is a protein molecule that acts as a biological catalyst, and it always binds to a specific substrate molecule, which is usually a chemical compound smaller than a protein molecule. Upon binding, the enzyme chemically converts the substrate into a different molecule. This enzyme–substrate binding is highly specific to shape, similar to a lock-and-key mechanism (Fig. 1.8).

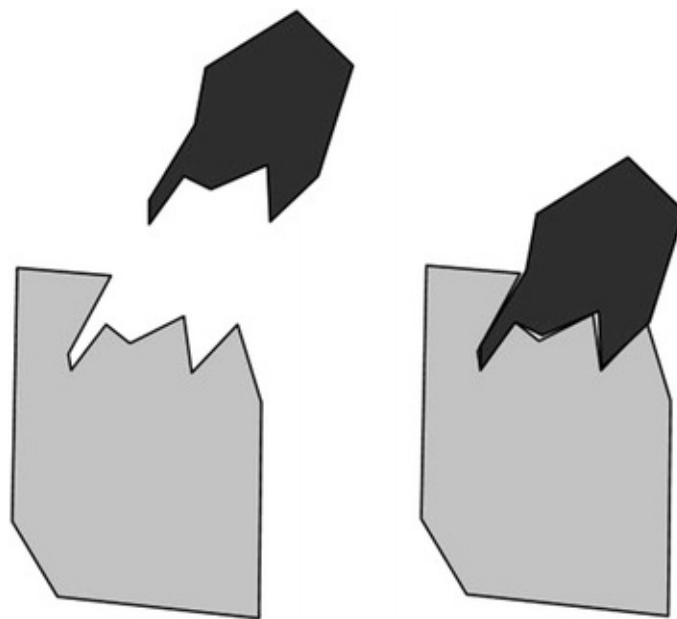


Fig. 1.8 Enzyme (bottom)–substrate (top) binding

In a glucose sensor, an enzyme called *glucose oxidase (GOx)* is used to capture and detect the glucose molecule (Note that the names of enzymes usually end with -ase.). GOx binds only to glucose, and oxidizes it into another chemical called gluconolactone, and eventually to gluconic acid. A series of further reactions creates an oxidation/reduction cycle that generates/consumes electrons,

and can be represented as an electric current. This current is directly proportional to the concentration of glucose. The current can be converted easily into voltage using a resistor. This transducer is specifically called an *electrochemical transducer* (Fig. 1.9).



Fig. 1.9 A commercial glucose meter is reading the glucose level from blood, using an electrochemical transducer

Enzyme–substrate binding can also be quantified with an *optical transducer*. For example, the above-mentioned oxidation/reduction cycle for glucose sensing generates a by-product, hydrogen peroxide (H_2O_2), which converts a benzidine derivative [specifically, tetramethylbenzidine (TMB)] into a blue-colored polymer. This color development can be detected by a light transducer. In fact, the first generation of glucose sensors was based on this color development on a test strip, where the detection was made by the human eye. These days, commercial glucose sensors are based on the electrochemical transducer;

however, recent advancements in light transducers make the use of optical transducers in glucose sensing very popular in research and development (R&D) applications. In this book, I have included a laboratory procedure on glucose sensors with both optical and electrochemical transducers (Chap. 12).

An *antibody* is also a very popular bioreceptor—perhaps more popular than enzymes in R&D. An antibody, which is a protein molecule, is the basis of the immune system. When a foreign molecule invades the body, the immune system recognizes and memorizes the molecule's shape by creating an antibody molecule that is a perfect fit to the molecule (similar to the lock-and-key mechanism of enzyme–substrate binding). Note that the antibody is drawn as a Y-shape, which represents the most common form of antibody, immunoglobulin G (IgG) (Fig. 1.10).

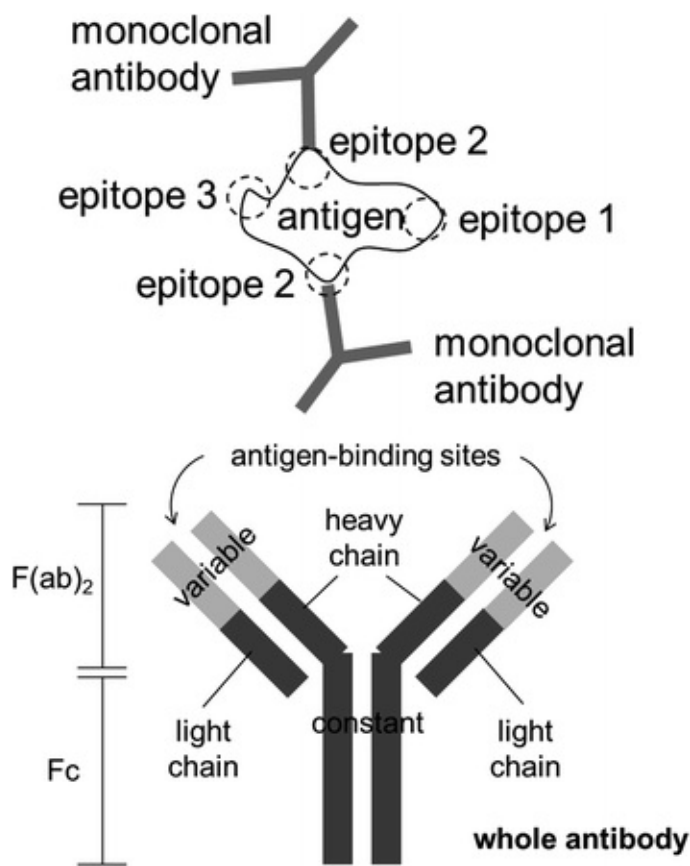


Fig. 1.10 Monoclonal antibodies bind to a single type of epitopes of an antigen (top). A whole antibody molecule, showing heavy and light chains, variable and constant regions, $F(ab)_2$, and Fc portions

The molecule that is recognized by an antibody is called the *antigen*, which is generally a protein molecule. An antibody can also recognize a virus particle or a bacterium by recognizing the proteins on the surface. Therefore, antibodies

can be used as excellent bioreceptors for a wide variety of protein molecules, as well as viruses and bacteria. Antibody-based biosensing is often referred to as an *immunoassay*; an assay mimicking the immune system. A huge inventory of antibodies is available commercially throughout the world, although they can be quite expensive (a few hundred US dollars per milligram).

Antibody–antigen binding can also be quantified with both electrochemical and optical transducers as shown in Fig. 1.11. First, the antibody is immobilized on a solid surface. Empty spaces on a surface are filled with a *passivating protein*, typically bovine serum albumin (BSA), to prevent *nonspecific reaction* (we will cover this topic later). A specimen containing the target molecule (protein, virus, bacterium, etc.) is added. Upon rinsing, only a target molecule specific to an antibody remains on the surface. The same antibody is added again (secondary antibody), followed by the addition of “antibody-to-antibody” (or anti-IgG) that is tagged with an enzyme or a fluorescent dye. Because two identical antibodies sandwich the target molecule, this scheme is often called a *sandwich immunoassay*.

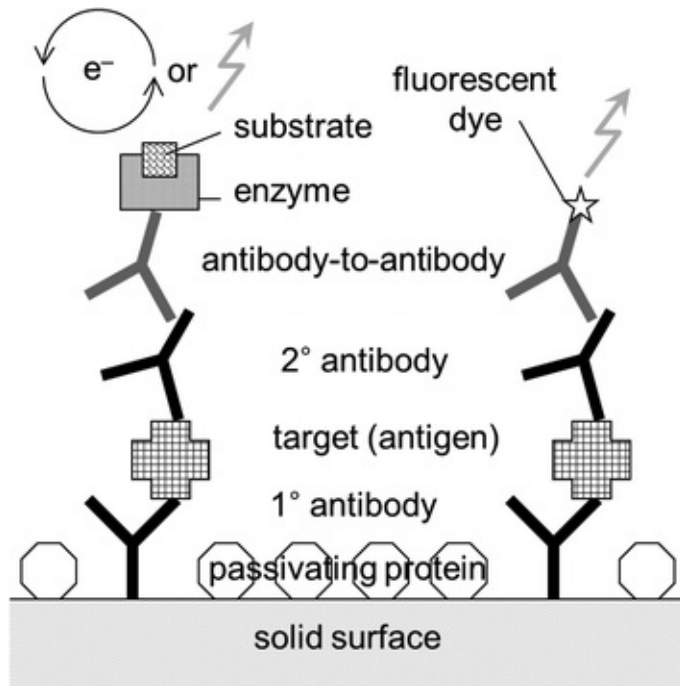


Fig. 1.11 An example of an antibody bioreceptor: sandwich immunoassay with an enzyme (left) or a fluorescent dye (right)

If the antibody-to-antibody is tagged with an enzyme, a substrate can be added, which can be detected electrochemically or optically as mentioned above. If it is tagged with a fluorescent dye, a light source and a light transducer pair are

used to detect its optical signal. This sandwich immunoassay is typically performed on a multi-well platform called *microwell plate* or simply *microplate*, which is shown in Fig. 1.12. This book includes a laboratory procedure for a sandwich immunoassay (Chap. 13).

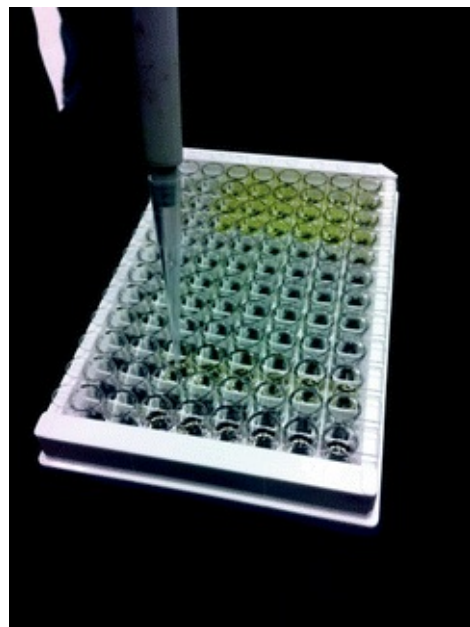


Fig. 1.12 Adding and rinsing a solution inside each microwell using a pipette, on a 96-well microplate

For analyzing a single type of target with a single sample, there is a simpler format available in the market, called *lateral flow immunochromatographic assay* or simply lateral flow assay (LFA). The most well-known example is the pregnancy test. Figure 1.13 shows two different formats of LFAs, cassette and strip types. This topic will be covered in Chap. 13.

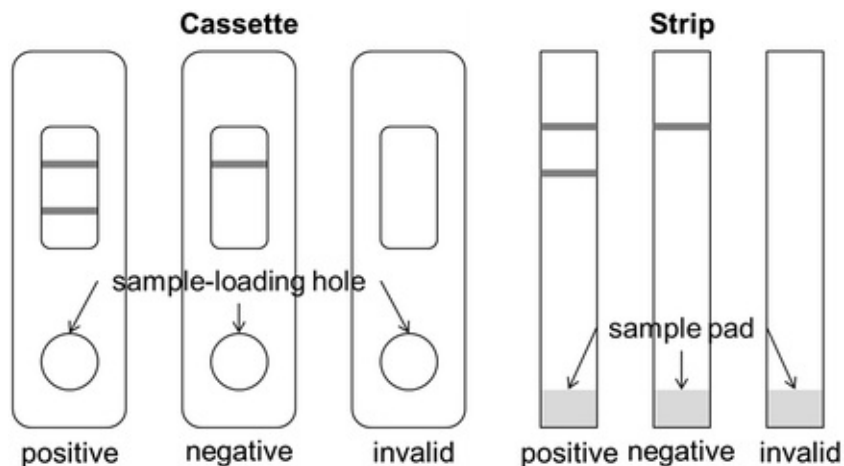


Fig. 1.13 Cassette-type and strip-type lateral flow immunochromatographic assays (LFAs)

Nucleic acids can also serve as good bioreceptors. These include specific sequences of deoxyribonucleic acid (DNA) or ribonucleic acid (RNA). We all know that genetic information is stored within a huge inventory of DNA or RNA. In a way, it is very similar to the hard disk drive on your personal computer: lots of programs are stored in many different places, with a great deal of garbage information here and there. The major difference is that genetic information is stored in a quaternary (base-4) system consisting of four different bases: *adenine* (A), *thymine* (T), *guanine* (G) and *cytosine* (C) for DNA; and adenine (A), *uracil* (U), guanine (G), and cytosine (C) for RNA. A always binds to T (U for RNA) and G always binds to C. Therefore, a specific RNA sequence of these bases, for example, AGA GGA GAU, can be used to detect the existence of their complementary sequence, UCU CCU CUA. The specificity of the nucleic acid bioreceptor is enhanced simply by increasing the length of the DNA/RNA sequence. In fact, lengths of several hundred such codes can be used for practical applications.

The nucleic acid bioreceptor is especially powerful in identifying different species of viruses or bacteria. For example, it is possible to make a distinction between the influenza A virus subtype H1N1 (initially known as swine flu) and the subtype H5N1 (highly pathogenic bird flu), with a well-designed nucleic acid sequence. The longer the sequence is, the better the specificity is, although the binding of complementary sequences becomes harder and harder.

Figure 1.14 illustrates one example of a nucleic acid bioreceptor. The schematic is largely identical to that of Fig. 1.11, where two antibodies to target (1° and 2° antibodies) are replaced with *capture probe* and *detector probe*. *Probes* are short nucleic acid sequences that recognize and specifically bind to the target nucleic acid. Note that the capture probe is immobilized on a solid surface through the binding of *neutravidin* (a variant of *avidin*) to *biotin*. *Avidin* is a protein that has a very strong affinity for the chemical *biotin*. This neutravidin–biotin (alternatively, streptavidin–biotin) pair is currently the most frequently used in many nucleic acid-based biosensor applications.

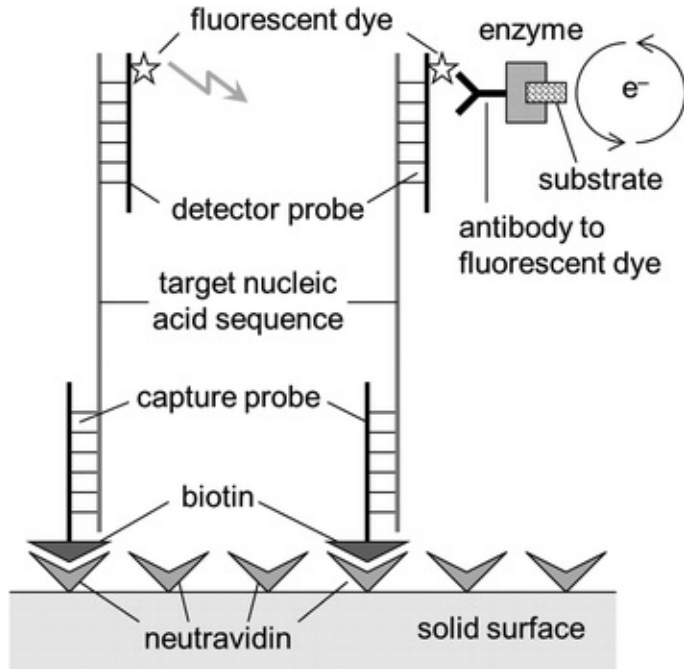


Fig. 1.14 An example of a nucleic acid bioreceptor with a fluorescent dye (left) or an enzyme (right)

Certain *cells* that possess a strong affinity for a specific target can also be used as a bioreceptor. The *T cell* is a good example. Recall that the antibody is one of the major players in the immune system. There are three other important cells in charge of the body's immune response: the *B cell*, the *T cell*, and the natural killer cell (*NK cell*). The *B cell* produces antibodies to fight against foreign molecules, whereas the *T cell* recognizes and fights against the foreign molecules by itself. This indicates that the *T cell* can also be used as an excellent bioreceptor.

In fact, any group of cells that forms a *tissue* can also be used as a bioreceptor provided that they can recognize and bind to a target molecule. Certain virus particles or bacteria that bind to a specific cells and/or tissues can also be used as good bioreceptors.

1.5 Transducers for Biosensors

In the previous section, two types of transducers have been discussed for antibody and nucleic acid bioreceptors: electrochemical and optical. Electrochemical transducing can be used by tagging an enzyme to the antibody-to-antibody (Fig. 1.11) or the detector probe (Fig. 1.14), while optical transducing by tagging a fluorescent dye to it.

Electrochemical transducer typically measures tiny small changes in voltage

(*potentiometry*), current (*amperometry*), or resistance/conductance (*conductometry*). Potentiometry usually involves the use of an electrode that is sensitive to a certain chemical species, and they are often used as a stand-alone chemical sensor without using bioreceptors. Examples include the pH electrode and ion-selective electrodes. I have included a laboratory exercise for a pH sensor (Fig. 1.15) as well as for a fluoride ion selective electrode (Chap. 10). Amperometry and conductometry usually involves the use of two electrode plates under the voltage applied, where the bioreceptors (antibody or nucleic acid) are immobilized onto it.



Fig. 1.15 A fluoride ion selective electrode is measuring fluoride concentration from tap water

Optical transducer measures the voltage signals coming from light transducers, most notably PD. It almost always requires the use of light source, typically LED or laser diode. Advanced light transducers are often utilized in optical transduction biosensors, including optical fibers, CCD/CMOS arrays, and recently smart phones.

The *piezoelectric transducer* is also used in the field of biosensors, although it is not yet as popular as electrochemical and optical transducers. Originally a nano-mass detector, piezoelectric transducers can be used to detect antigens, substrates, nucleic acids, and other target molecules by immobilizing antibodies, enzymes, nucleic acids, and cells on the transducer surface. I have included a basic laboratory exercise for a protein immobilization study using a piezoelectric transducer (Chap. 11) (Fig. 1.16).



Fig. 1.16 A piezoelectric biosensor measures protein immobilization

1.6 Overview of This Textbook

Recall that the goal of this book is to build knowledge step-by-step, enabling the reader to eventually build an antibody-based immunosensor from scratch. We will start by learning some basic electric circuitry, which is focused on measuring electric voltage, current, and resistance. This will serve as a fundamental basis for understanding electrochemical transducers with enzyme, antibody, nucleic acid, or cell bioreceptors . Then we will investigate further into the other types of physical transducers based on temperature, strain, and light.

We will then move forward into a group of biosensor topics. Laboratory procedures include spectrometric sensors (including pulse oximeter), fluorescence-based sensors, electrochemical sensors (including pH sensor and ion-selective electrodes), piezoelectric sensor, various glucose sensors (with both optical and electrochemical transducers), and a sandwich immunoassay sensor (including ELISA and LFA). Additional topics include: *lab-on-a-chip* (system integration) (Fig. 1.17), nano-biosensors, and *microcontroller* .

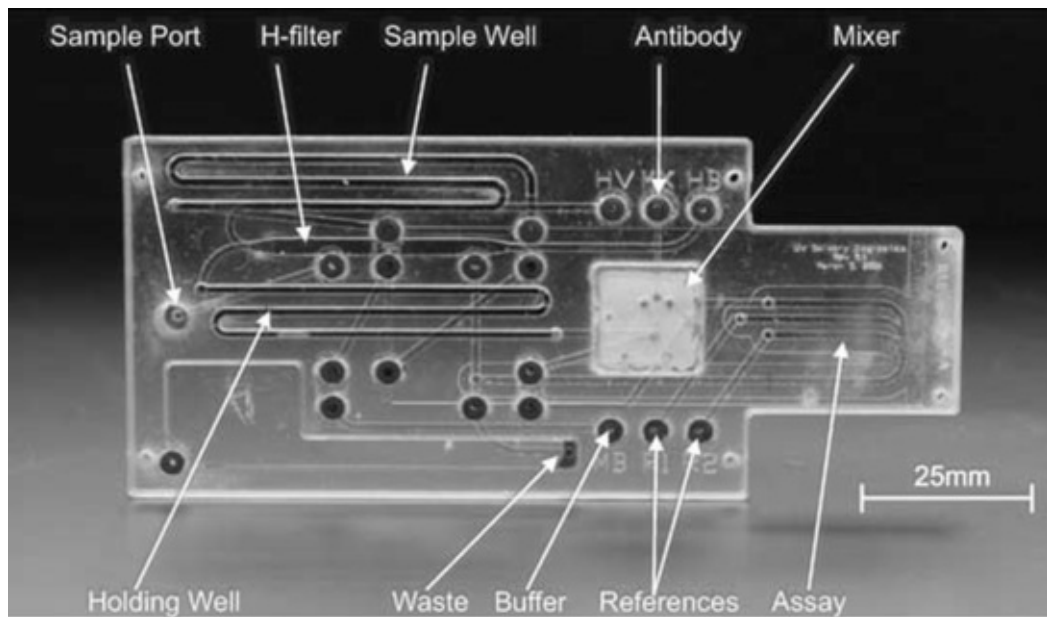


Fig. 1.17 “Integrated” biosensing system utilizing lab-on-a-chip (LOC) technology. Fu et al. (2007), © John Wiley and Sons 2007, reprinted with permission

There are laboratory sections in all chapters (except for Chaps. 1 and 15), which will deliver hands-on guidance and visual demonstrations of biosensor applications (Fig. 1.18).

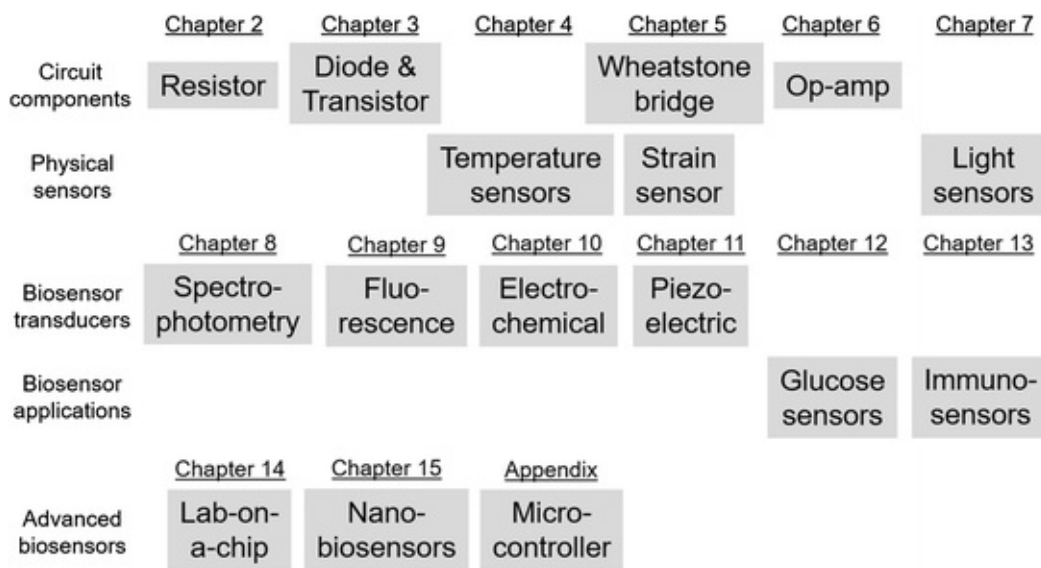


Fig. 1.18 The overview of this textbook

References and Further Readings

- Christian GD (2004) Analytical chemistry, 6th edn. Wiley, Hoboken
- Cooper J, Cass T (eds) (2004) Biosensors, 2nd edn. Oxford University Press, Oxford
- Egging BR (2002) Chemical sensors and biosensors. Wiley, West Sussex
- Fu E, Chinowsky T, Nelson K, Johnston K, Edwards T, Helton K, Grow M, Miller JW, Yager P (2007) SPR imaging-based salivary diagnostics system for the detection of small molecule analytes. *Ann NY Acad Sci* 1098:335–344 (Figure 1.19)
- Gu MB, Kim H-S (eds) (2014) Biosensors based on aptamers and enzymes. Springer, Heidelberg
- Holme DJ, Peck H (1998) Analytical biochemistry, 3rd edn. Pearson Education, Essex
- Ristic L (ed) (1994) Sensor technology and devices. Artech House, Norwood
- Skoog DA, Holler FJ, Nieman TA (2006) Principles of instrumental analysis, 6th edn. Saunders College Publishing, Philadelphia
- Tiwari A, Turner APF (eds) (2014) Biosensors nanotechnology. Scrivener Publishing, Beverly
- Webster JG (ed) (2000) Mechanical variables measurement: solid, fluid, and thermal. CRC Press, Boca Raton

2. Resistors

Jeong-Yeol Yoon¹✉

(1) University of Arizona, Tucson, AZ, USA

✉ Jeong-Yeol Yoon
Email: jyyoon@email.arizona.edu

In the previous chapter, we learned that all transducers for sensors and biosensors generate voltage. In this regard, it is important that we begin our study with a basic understanding of electronics and circuitry.

2.1 Electric Circuit

Figure 2.1 shows an *electric circuit* that includes a battery (power source), a lamp (load), wires (conductors), and a switch to turn the circuit on or off.

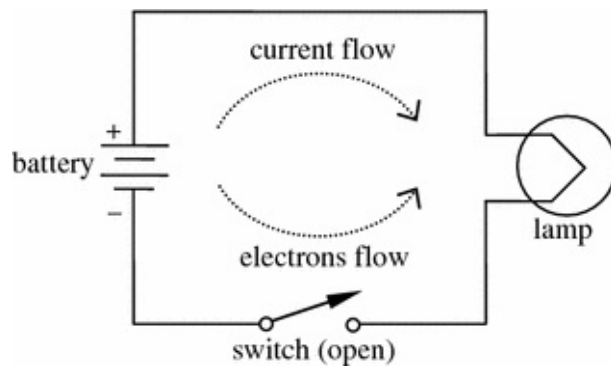


Fig. 2.1 A simple electric circuit

Benjamin Franklin (the father of electronics) thought that positive charges move from the positive to the negative terminal of a battery, which he defined as

electric current. Figure 2.2 is a redrawing of Fig. 2.1 that illustrates this concept. We will use this type of circuit diagram throughout this textbook.

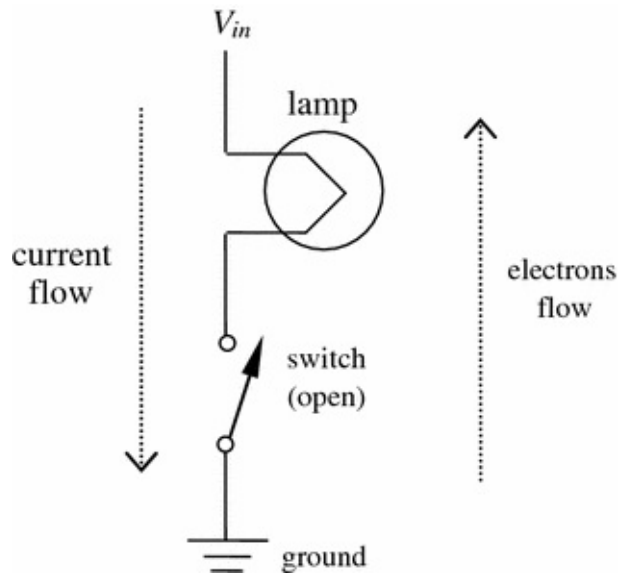


Fig. 2.2 Redrawing of Fig. 2.1. The battery power source is divided into high voltage (V_{in}) and ground

Franklin's definition was apparently an error, as Joseph Thompson later found that the moving charges in an electric circuit were not positive charges but free electrons, which move in the opposite direction. As of today, however, we are still pretending that there are positive charges that move from the positive to the negative side of a power source, or from the *high voltage* to the *ground*, which works perfectly okay as long as we stick to this convention.

2.2 Current and Voltage

As defined previously, *electric current*, or simply *current*, is the flow of hypothetical positive charges from a region of positive net charge to a region of relative negative charge, which is the opposite of the flow of electrons from a negative to a positive charge. To measure current, we need to define a unit for electrical charge. A coulomb (C) is used for such a unit, which is equal to the charge of 6.25×10^{18} electrons or comparable positive charges. Current is the rate at which positive charges or electrons flow through a given point in a circuit. Current is given in unit amperes (A):

$$\text{amperes (A)} = \text{coulombs (C)}/\text{seconds (s)} \quad (2.1)$$

Another important term in basic circuitry is *electrical voltage*, or simply *voltage*. Voltage is an electromotive force (EMF) that moves positive charges or

electrons from one point to another. Voltage at a given point in a circuit is always measured against the ground, which is usually the negative terminal of a power supply. The voltage of a battery, therefore, is the voltage at its positive terminal (high voltage) measured against its negative terminal (ground). A battery has an excess of electrons at negative terminal and a deficiency of electrons at the other.

When the movement of one coulomb of positive charges or electrons between two points (or the given point of a circuit and the ground) generates one joule of work, the voltage between these two points is defined as one volt (V), which is the unit of voltage:

$$\text{volts (V)} = \text{joules (J)} / \text{coulombs (C)} \quad (2.2)$$

The voltages of typical AA or AAA batteries are 1.5 V and that of your car is 12 V.

Figure 2.3 shows a circuit with two identical lamps connected in series with 3 V battery. The voltage of the battery is measured at its positive terminal (V_{in}) with reference to its negative terminal (ground). This particular voltage is referred to as a *voltage rise*, as it generates necessary voltage to the circuit. This voltage is dropped upon traveling the two lamps. As the two lamps are identical, equal amount of *voltage drop* should occur for these lamps, which is 1.5 V each. Therefore, the voltage at the point in between the two lamps (with reference to the ground) should be 1.5 V. In this way, the sum of voltage drops in a given circuit becomes the same as the sum of voltage rise.

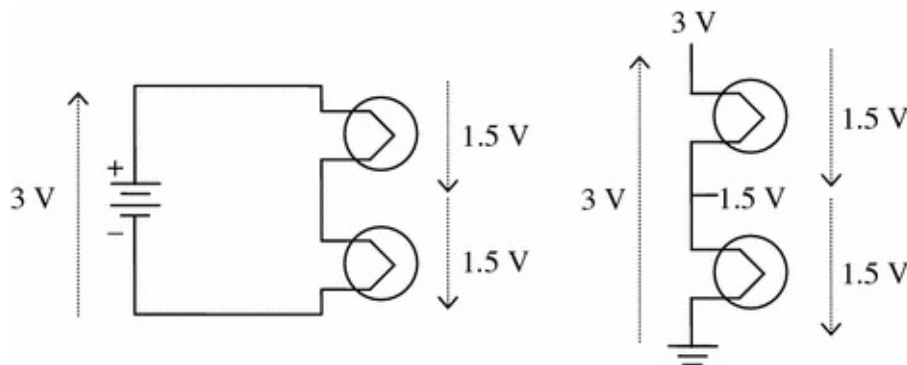


Fig. 2.3 Voltage rise and voltage drop

2.3 Resistance and Ohm's Law

If a copper wire is connected across the 3 V battery, huge current will flow. If a piece of rubber is connected, however, almost no current will flow. The ratio of voltage over current should tell you how resistive your wire is in delivering

electric charges with a given voltage. This ratio is called *resistance* (R). The unit of resistance is the *ohm* (Ω):

$$\text{ohms } (\Omega) = \text{volts } (V) / \text{amperes } (A) \quad (2.3)$$

More generally,

$$R = \frac{V}{I} \text{ or } V = IR \quad (2.4)$$

which is known as *Ohm's law*. Obviously the resistance of conductors is very low, while that of insulators is very high. *Conductors* are the substances that have many free electrons, like metals ($R \rightarrow 0$). The best metallic conductors are gold, silver, and copper among common materials. As gold and silver are very expensive, copper is usually the one most frequently used in wiring electric circuits. *Insulators* are the substances that have fewer free electrons ($R \rightarrow \infty$). The best insulators are glass and rubber among common materials.

Resistors are the passive devices that resist current flow, and are typically made out of materials that fall somewhere in between the properties of conductors and insulators. Resistors are often connected in series or in parallel, which will be discussed in the next sections.

2.4 Resistors in Series , or Voltage Divider

Figure 2.4 shows a circuit with two different resistors connected in series. There is only one path for current to pass through the circuit, meaning that the current flowing through two different resistors should be the same. The input voltage, V_{in} , is the voltage rise. V_1 is the voltage drop across R_1 , and V_2 is across R_2 . As the sum of the voltage rise should be the same as the sum of the voltage drop,

$$V_{in} = V_1 + V_2 \quad (2.5)$$

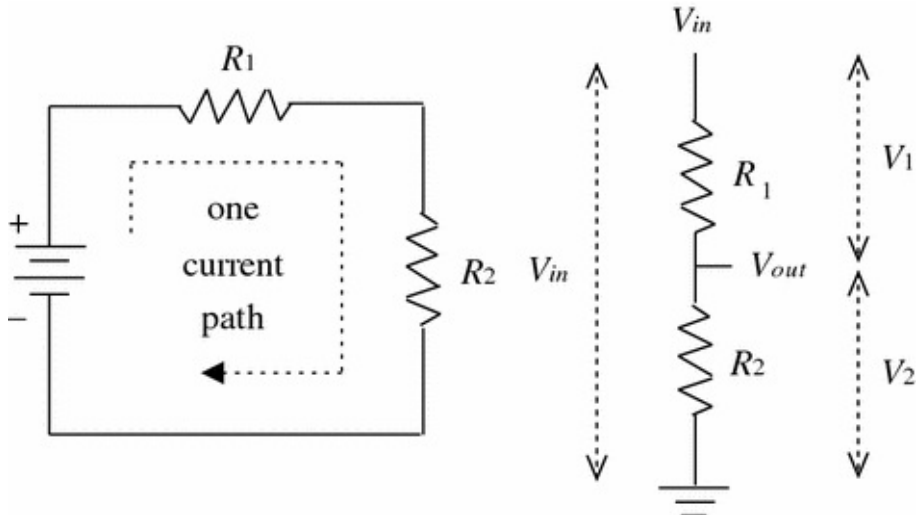


Fig. 2.4 Resistors in series, or voltage divider

As explained earlier, there is only one path for the current flow to pass through. The currents flowing through R_1 and R_2 are identical. Let us designate that current as I . Using Ohm's law:

$$I = \frac{V_1}{R_1} \text{ (current through } R_1) = \frac{V_2}{R_2} \text{ (current through } R_2) \quad (2.6)$$

Equation 2.6 can be expressed for V_1 and V_2 :

$$V_1 = I \cdot R_1 \text{ and } V_2 = I \cdot R_2 \quad (2.7)$$

Plugging Eq. 2.7 into Eq. 2.5 gives:

$$V_{in} = I \cdot R_1 + I \cdot R_2 = I(R_1 + R_2) \quad (2.8)$$

For the entire circuit, using the equivalent total resistance R_T and Ohm's law:

$$V_{in} = I \cdot R_T \quad (2.9)$$

Comparing Eqs. 2.8 and 2.9 gives:

$$R_T = R_1 + R_2 \quad (2.10)$$

Equation 2.10 indicates that the total resistance R_T is equal to the sum of the two resistors. In general, the total resistance of the resistors in series can be expressed as:

$$R_T = R_1 + R_2 + \dots + R_n \quad (2.11)$$

This particular circuit is also known as a *voltage divider*, as the voltage at the point in between the two resistors (with reference to the ground), V_{out} , is a fraction of the input voltage V_{in} , depending on the ratio of the two resistors R_1 and R_2 . In other words, the voltage divider "divides" the input voltage using two (or more) resistors connected in series.

The output voltage V_{out} is essentially the same as V_2 . From Eq. 2.7:

$$V_{\text{out}} = V_2 = I \cdot R_2 \quad (2.12)$$

To express V_{out} in terms of V_{in} , R_1 , and R_2 , let us use Eqs. 2.9 and 2.10:

$$I = \frac{V_{\text{in}}}{R_T} = \frac{V_{\text{in}}}{R_1 + R_2} \quad (2.13)$$

Plugging Eqs. 2.13 to 2.12:

$$V_{\text{out}} = V_{\text{in}} \frac{R_2}{R_1 + R_2} \quad (2.14)$$

This is the voltage divider relationship, without the need for measuring the current I in evaluating its voltage output V_{out} .

Question 2.1

Calculate V_{out} of a voltage divider for:

(a) $R_1 = 10 \Omega$ and $R_2 = 5 \Omega$

(b) $R_1 = 1 \text{ k}\Omega$ and $R_2 = 1 \Omega$

2.5 Potentiometer , or Pot

The voltage divider divides the input voltage at the fixed ratio set by the two resistors. A *potentiometer*, or simply a *pot*, is a variable voltage divider made as a single piece. It is essentially a single resistor with an additional, third terminal. This third terminal is made to mechanically slide through the resistor so that the length of the top and bottom resistors can be altered. Figure 2.5 shows a graphical representation of a pot. Note that the arrow indicates the third terminal, or slider, and its direction does not indicate the flow of current. Pots are commonly used in many different applications, including the volume control of a radio or stereo system, and as position transducers such as a joystick (Fig. 2.6).

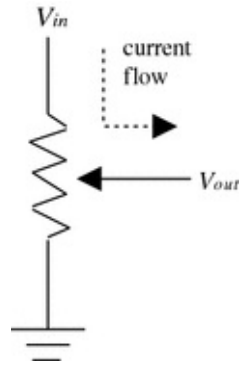


Fig. 2.5 A potentiometer or a pot

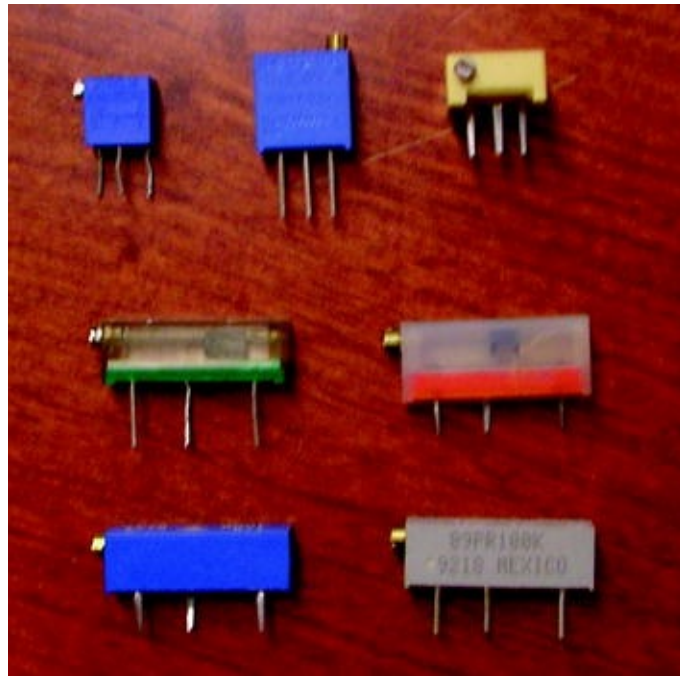


Fig. 2.6 Various single-turn and multi-turn potentiometers for infrequent adjustments, typically mounted directly on PCBs

2.6 Resistors in Parallel , or Current Divider

Figure 2.7 shows a circuit with two different resistors connected in parallel. There are two paths for current to pass through the circuit, meaning that the current is divided into two different resistors. Therefore:

$$I_{in} = I_1 + I_2 \quad (2.15)$$

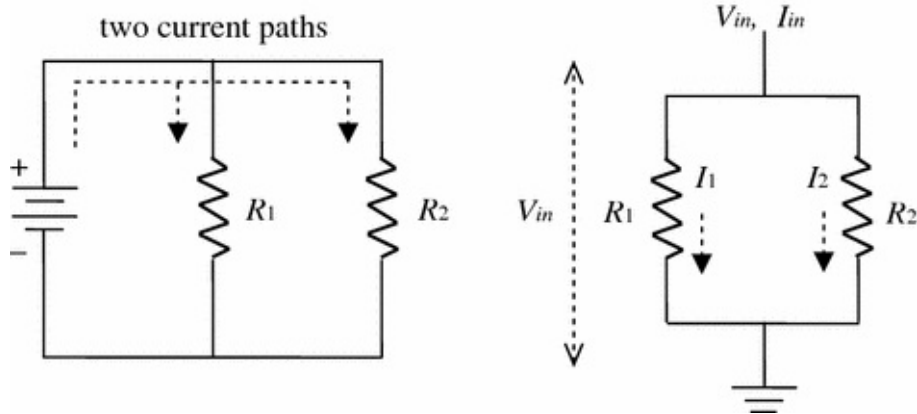


Fig. 2.7 Resistors in parallel or current divider

The voltage drops across the two different resistors should, however, be the same (V_{in}).

$$I_1 = \frac{V_{in}}{R_1} \text{ and } I_2 = \frac{V_{in}}{R_2} \quad (2.16)$$

Plugging Eq. 2.16 into Eq. 2.15:

$$I_{in} = \frac{V_{in}}{R_1} + \frac{V_{in}}{R_2} = V_{in} \left(\frac{1}{R_1} + \frac{1}{R_2} \right) \quad (2.17)$$

For the entire circuit, using the equivalent total resistance R_T and Ohm's law:

$$I_{in} = \frac{V_{in}}{R_T} \quad (2.18)$$

Comparing Eqs. 2.17 and 2.18 gives:

$$\frac{1}{R_T} = \frac{1}{R_1} + \frac{1}{R_2} \text{ or } R_T = \frac{R_1 \cdot R_2}{R_1 + R_2} \quad (2.19)$$

In general, the total resistance of the resistors in parallel can be expressed as:

$$\frac{1}{R_T} = \frac{1}{R_1} + \frac{1}{R_2} + \dots + \frac{1}{R_n} \text{ or } R_T = \frac{1}{\frac{1}{R_1} + \frac{1}{R_2} + \dots + \frac{1}{R_n}} \quad (2.20)$$

This particular circuit is also known as a *current divider*, as the current is divided into two paths, I_1 and I_2 . Let us express I_1 in terms of I_{in} , R_1 , and R_2 (i.e. without using V_{in}). Plugging Eq. 2.19 into Eq. 2.18 gives:

$$V_{in} = I_{in} R_T = I_{in} \frac{R_1 \cdot R_2}{R_1 + R_2} \quad (2.21)$$

Plugging Eq. 2.21 into the first equation of Eq. 2.16:

$$I_1 = \frac{V_{in}}{R_1} = I_{in} \frac{R_1 \cdot R_2}{R_1 + R_2} \frac{1}{R_1} = I_{in} \frac{R_2}{R_1 + R_2} \quad (2.22)$$

Similarly,

$$I_2 = I_{in} \frac{R_1}{R_1 + R_2} \quad (2.23)$$

Equations 2.22 and 2.23 are the current divider relationships. The current flowing through branch 1 is affected by the second resistor, and that through branch 2 by the first resistor. This indicates that more current flows through a smaller resistor, while less current flows through a larger resistor.

Question 2.2

Calculate I_1 and I_2 of a current divider for:

(a) $R_1 = 10 \Omega$ and $R_2 = 5 \Omega$

(b) $R_1 = 1 \text{ k}\Omega$ and $R_2 = 1 \Omega$.

Does less current flow through the resistor with higher resistance?

2.7 Reading Resistor Values

We have just learned some basic fundamentals of electric circuitry, primarily Ohm's law. The resistor is a cornerstone in understanding Ohm's law, and also one of the most frequently used components in building circuits. A resistor is used to convert electric current into voltage signals. The resistor is also the main component in a voltage divider circuit. Before we begin our lab exercises, we need to learn some fundamental basics, including how to read resistor values.

Figure 2.8 shows a photograph of a resistor with four different colored bands around it. You will notice that the left-end color band is very close to the lead while the right band is further away from the other lead. If not, you have to flip it around. In some cases, there may exist some distance between the third and fourth bands. (Note that this direction does not matter in actual circuit building, as resistors have no polarity.) Assume that the sequence of the colored bands is: Brown—Black—Red—Silver.



Fig. 2.8 Resistors

Table 2.1 shows a resistor color code, for identifying the color code. The first two bands correspond to two significant digits: in this case, brown for 1 and black for 0. The third band represents a multiplier; in this case, red for 10^2 . Therefore, we can come up with the formula, $10 \times 10^2 = 1,000 \Omega$ or $1 \text{ k}\Omega$. The fourth band represents *tolerance*, i.e., a maximum error; in this case, silver for 10 %. As 10 % of $1,000 \Omega$ is 100Ω , the actual resistor value would be somewhere between 900Ω and $1,100 \Omega$. As the tolerance band is typically either silver (10 %) or gold (5 %), only two significant digits are necessary to show the resistor size.

Table 2.1 Resistor color code

	1st band	2nd band	3rd band	4th band
	1st digit	2nd digit	Multiplier	Tolerance (%)
Silver	–	–	10^{-2}	± 10
Gold	–	–	10^{-1}	± 5
Black	0	0	10^0	–
Brown	1	1	10^1	± 1
Red	2	2	10^2	± 2
Orange	3	3	10^3	–
Yellow	4	4	10^4	–
Green	5	5	10^5	± 0.5
Blue	6	6	10^6	± 0.25
Violet	7	7	10^7	± 0.1

Gray	8	8	10^8	-
White	9	9	10^9	-

If the tolerance is less than or equal to 1 %, three significant digits are necessary. In this case, a 5-band color code becomes necessary with the first three corresponding to significant digits, the fourth the multiplier, and the fifth the tolerance. In some cases, a 6-band color code is possible, where the sixth represents the *temperature coefficient*. Four colors are used for the temperature coefficient band; brown (100 ppm), red (50 ppm), orange (15 ppm), and yellow (25 ppm). This coefficient represents the fractional decrease of resistor value per 1 °C rise from room temperature (25 °C). If the temperature coefficient of the above 1,000 Ω resistor is 100 ppm (brown), $1,000 \Omega \times 100 \times 10^{-6} = 0.1 \Omega$. If the temperature rises from 25 to 55 °C, then it follows that $1,000 - (0.1 \times (55 - 25)) = 997 \Omega$.

Question 2.3

- (a) Identify the resistor values and tolerances of the following resistors.

Green—Brown—Red—Gold

Orange—Black—Black—Orange—Brown—Brown

- (b) For a resistor of exactly 30.0 kΩ at 25 °C with a 100 ppm temperature coefficient, calculate its resistance at 37 °C.

2.8 Breadboards

Circuits are typically soldered into a printed circuit board (PCB) (Fig. 2.9), the wiring layout of which is chemically written on a board. This is a common practice in many commercial electrical devices, but not at all appropriate in testing and/or developing a new circuit (prototyping).



Fig. 2.9 A computer “mother board” is a good example of a PCB

Breadboards make this prototyping really easy (Fig. 2.10); all you have to do is insert the leads into the tiny holes to construct a circuit and power it up by connecting the breadboard to the power supply. You can change the circuit layout anytime by simply removing, adding, and relocating components. You can also measure the voltage difference between any two points using a voltage meter (commonly known as a *voltmeter*), or more practically, with a digital multimeter (DMM) .

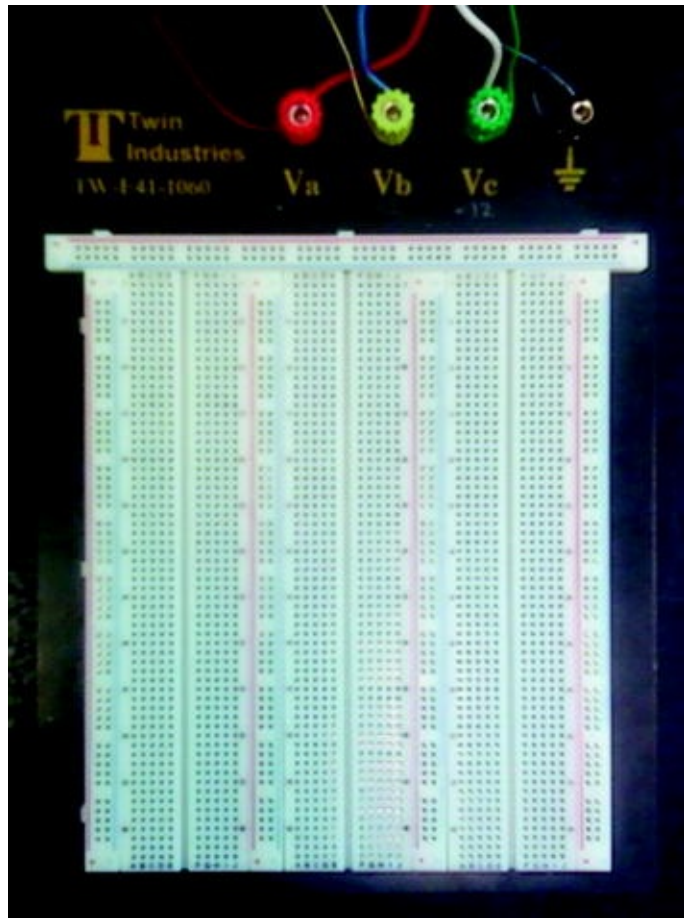


Fig. 2.10 A breadboard

The early prototyping was made on a plain wooden plate that looked like a breadboard, on which bread is cooled and/or sliced after baking. The current prototyping breadboard, however, no longer look like a real breadboard.

2.9 Laboratory Task 1: Resistors in Series

In this task, you will need the following:

- Breadboard
- Three-output low-capacity AC-to-DC power supply (+5, +12 and -12 V)
- Standard wire (wire gauge 22)
- Wire cutter/stripper
- Resistors (1 k Ω)

Let us learn about breadboards with a practical example: resistors in series

(i.e., a *voltage divider*). Figure 2.11 shows the circuit diagram.

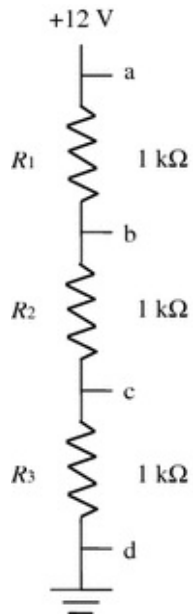


Fig. 2.11 Circuit diagram for Task 1

You need a power supply that generates +12 V, three 1 kΩ resistors, a couple of wires, and a breadboard. These items can generally be purchased from an online vendor; use any search engine, and look for the term “breadboard” or “resistor” and you will find appropriate vendors in your area.

First, hook up a power supply to a breadboard (Fig. 2.12). The previous Fig. 2.10 shows a typical breadboard with power connectors. At the top are *binding posts* which allow you to hook up power to the breadboard tie points. You may use batteries as a power source, but we recommend you use an AC-to-DC power supply that generates +5, +12 and -12 V (three outputs). Again, this kind of power supply can be purchased from online vendors as mentioned above. Note that a high-capacity power supply is not necessary; choose one whose current capacity is less than 2 A (it usually costs less than \$10 in the U.S.) (Fig. 2.12).

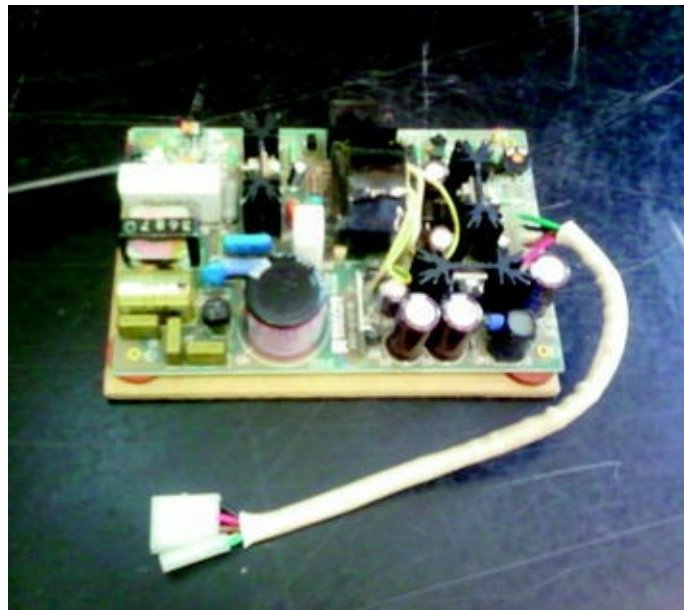


Fig. 2.12 Three-output low-capacity power supply

Your power supply may come with a connector for plugging into the breadboard. If not, you can simply connect it using standard wire. Most breadboards accept wire gauge sizes from 19 to 29, but 22 is probably the most common. Strip off about a quarter inch or half a centimeter of the insulation at each end of the wire. Figure 2.13 shows how to strip off a wire using a wire cutter/stripper. Note that the same job can be done with a nipper, but we recommend using a wire cutter/stripper).

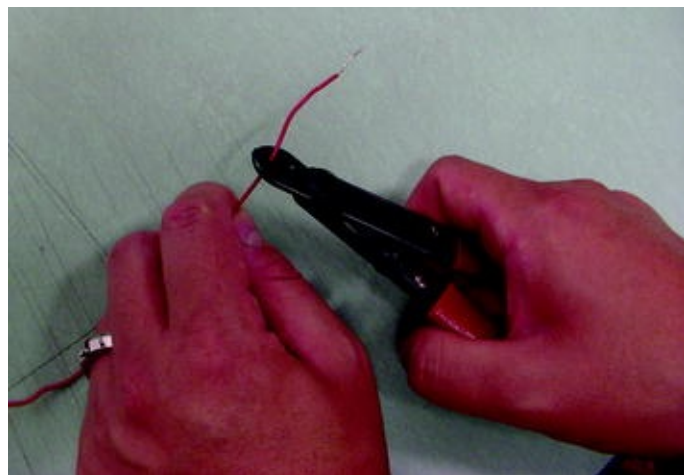


Fig. 2.13 Wire stripping

Figure 2.14 also demonstrates how the wire can be fixed to a binding post on

a breadboard. Note that other connecting means are also available, such as alligator clips, mount clips, and banana plugs (Fig. 2.15).

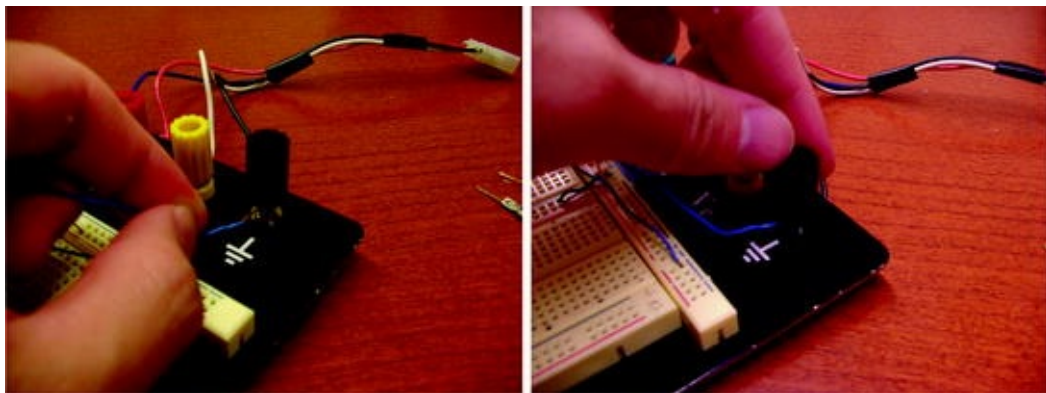


Fig. 2.14 Wire mounting to a binding post (of a breadboard)

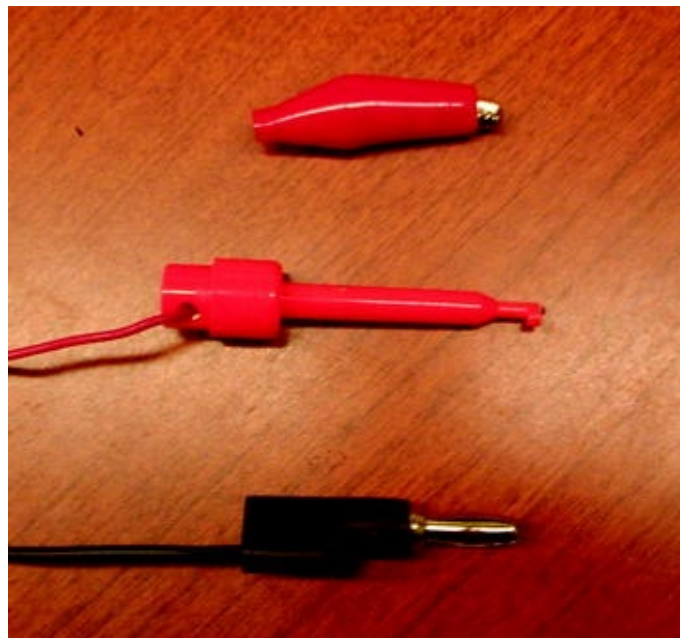


Fig. 2.15 Top Alligator clip. Middle Mount clip. Bottom Banana plug

Let us connect wires from the power supply to the breadboard. You will need to connect three different DC voltages (+5, +12 and -12 V) and a ground (GND; 0 V; a reference point) that is shared by the above three voltages. Do not connect the power supply to the AC power outlet yet.

Now, return back to the breadboard. Notice that the tie points come in groups of five, horizontally. These five points are electrically connected to each other, allowing you to connect one wire to four others. There are also *distribution*

strips which are usually used for distributing power (+5, +12 or -12 V) and ground (0 V) around the breadboard, since the circuit will likely connect to these in several places. On the breadboard shown in Fig. 2.14, these distribution strips are conveniently marked with red or blue lines, indicating they are also electrically connected throughout the entire line. For example, the distribution strips on top are horizontally connected, while the others are vertically connected.

You should have three $1\text{ k}\Omega$ resistors. Insert the first lead to one horizontal tie point and the second lead to the other tie point. Then insert one lead of your *digital multimeter (DMM)* to each of the tie points. As the resistor does not have any polarity, you can connect it any way you want.

The DMM can measure electric current, resistance, and voltage. Each measurement comes with a different measurement range. Set up the DMM to measure resistance, with a maximum range of $2\text{ k}\Omega$. It is okay to use the 20 or $200\text{ k}\Omega$ range to measure $1\text{ k}\Omega$ resistors, but we would not get sufficient significant digits. Record the exact resistance values of all three resistors (Fig. 2.16).

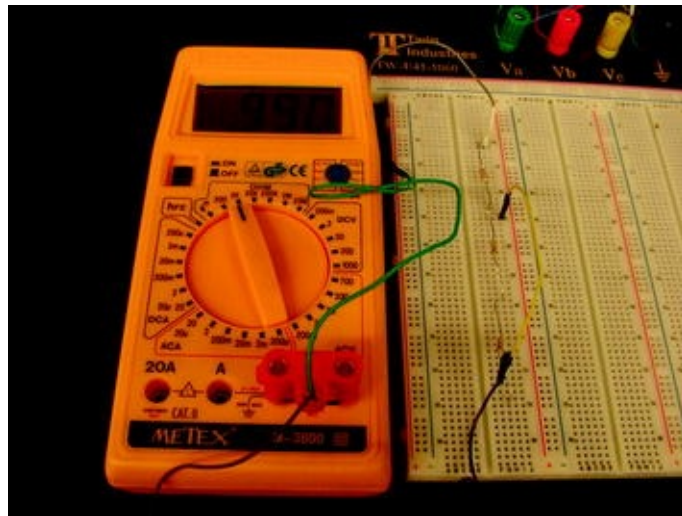


Fig. 2.16 Resistance measurements with a DMM

You should not measure the resistance values while the circuit is connected to a power supply. Even if the power supply is not connected to the AC outlet, the power supply itself contains many components, especially resistors, which will affect your resistance readings.

For the next question and subsequent experimental procedures, assume your measurements showed resistance values of $990\text{ }\Omega$ for the first resistor (R_1), $1020\text{ }\Omega$

Ω for the second (R_2), and 980Ω for the third (R_3).

Question 2.4

If the tolerance band is gold, are the above resistors within their acceptable tolerance?

Power one pair of distribution strips with +12 V and GND by connecting wires from the binding posts onto the breadboard. Then connect three $1 \text{ k}\Omega$ resistors in series as shown below. Use additional wires to connect these series resistors to the DC power source (+12 V and GND).

The setup in Fig. 2.17 is not very ideal. Generally, the wires should be cut as short and as close to the board as possible to prevent possible signal interference and so forth. If you have the luxury of owning a collection of pre-cut and pre-stripped wires, you may choose to use those; however, the above practice is generally acceptable.

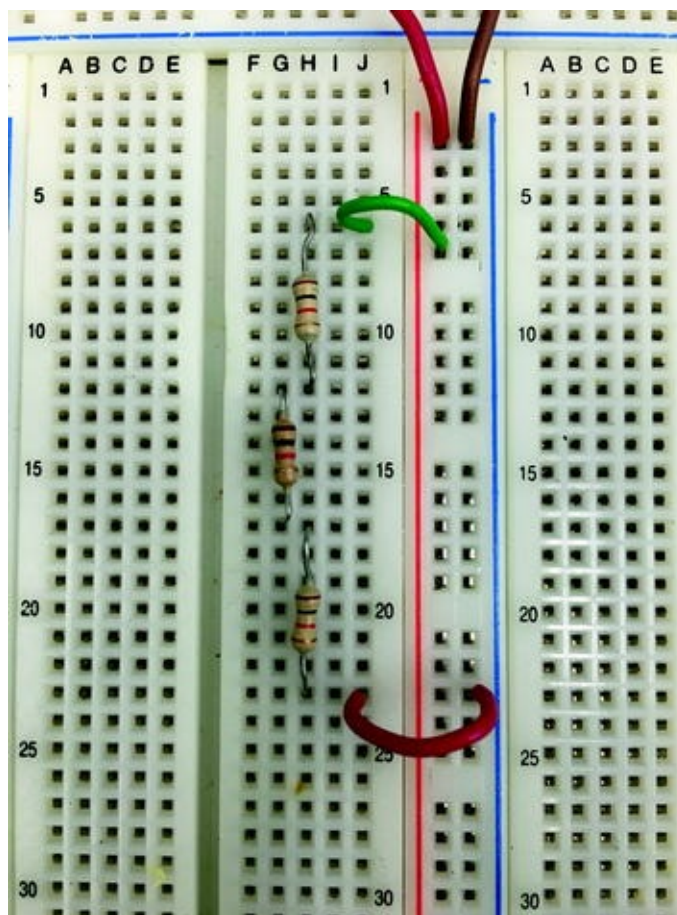


Fig. 2.17 Circuit photo of Task 1

The theoretical voltages at four different points (*a*, *b*, *c*, and *d*) in Fig. 2.11 can be calculated. V_a should be measured by inserting the positive lead of your DMM to point *a* and the ground lead to point *d*. Make sure your DMM is set to measure DC voltages, not AC. You can also connect the ground lead to any location within the distribution strip that is connected to GND. Remember that electric voltage is always measured with reference to ground (GND). Set your DMM to voltage measurement with a 20 V range. V_d is 0 V and there is no need to measure it. The experimental measurement should show $V_a = 12.5$ V. (Note that the power supply is supposed to generate 12.0 V, but the actual output will vary depending on the output from your AC outlet). This is your input voltage, V_{in} .

Now calculate the voltage at point *b*. Given the three resistor values previously measured ($R_1 = 990 \Omega$, $R_2 = 1020 \Omega$ and $R_3 = 980 \Omega$), the top resistor is equal to R_1 (990Ω) and the bottom to $R_2 + R_3$ ($1020 \Omega + 980 \Omega$). From the voltage divider relationship,

$$V_b = V_{in} \frac{R_{bottom}}{R_{top} + R_{bottom}} = (12.5) \frac{1020 + 980}{990 + 1020 + 980} = 8.36 \text{ V} \quad (2.24)$$

We can repeat the same for point *c*. The top resistor is $R_1 + R_2$ ($990 \Omega + 1020 \Omega$) and the bottom is R_3 (980Ω).

$$V_c = V_{in} \frac{R_{bottom}}{R_{top} + R_{bottom}} = (12.5) \frac{980}{990 + 1020 + 980} = 4.10 \text{ V} \quad (2.25)$$

Experimental measurements of voltages at point *b* (with reference to GND) and point *c* (with reference to GND) should not differ very much from these calculations.

Alternative Task 1: Resistors in Series

Change the three resistors on the breadboard to $R_1 = 3 \text{ k}\Omega$, $R_2 = 8 \text{ k}\Omega$ and $R_3 = 1 \text{ k}\Omega$ (the actual resistance values will vary), and repeat Task 1.

- Identify color bands for all three resistors.
- Measure the actual resistor values using a DMM.
- Measure V_{in} ($= V_a$).
- Calculate V_b and V_c using the voltage divider relationship.
- Experimentally measure V_b and V_c and compare with the calculations.

Repeat the whole experiment with $R_1 = R_2 = R_3 = 100 \text{ k}\Omega$ (the actual resistances will vary).

2.10 Laboratory Task 2: Resistors in Parallel

Use the same materials and equipment used for Task 1. Let us construct a circuit that contains resistors in parallel (i.e., *current divider*) (Figs. 2.18 and 2.19).

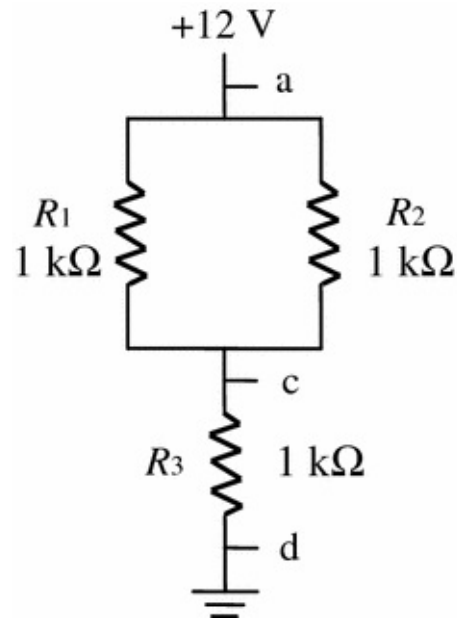


Fig. 2.18 Circuit diagram for Task 2

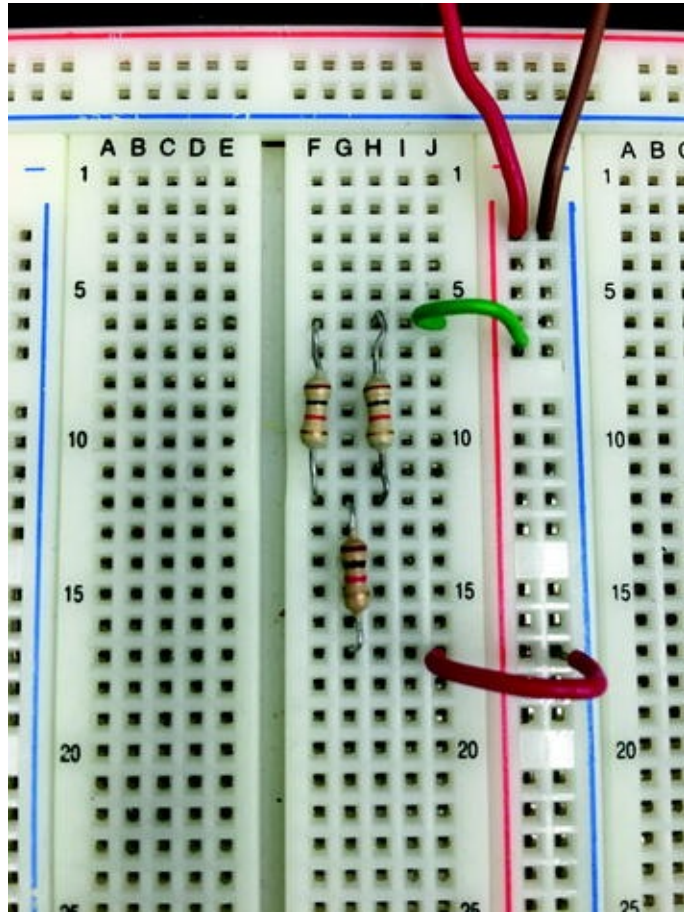


Fig. 2.19 Circuit photo of Task 2

Note that R_1 and R_2 are connected to the same row of tie points. If we are using identical resistors from Task 1 ($R_1 = 990 \Omega$, $R_2 = 1020 \Omega$ and $R_3 = 980 \Omega$), the total resistance of the two resistors in parallel, i.e., between the points a and c , is:

$$R_{\text{total}} = \frac{R_1 R_2}{R_1 + R_2} = \frac{990 \cdot 1020}{990 + 1020} = 502 \Omega. \quad (2.26)$$

Compare this value with the actual resistance reading of your DMM between points a and c . Remember that the power from the resistor circuit should be disconnected before making any resistance measurements, as the power supply circuit can function as a resistor even if it is not connected to the AC outlet.

Using this “total” resistance, we can calculate the voltage output at point c using the voltage divider relationship:

$$V_c = V_{\text{in}} \frac{R_{\text{bottom}}}{R_{\text{top}} + R_{\text{bottom}}} = (12.5) \frac{980}{502 + 980} = 8.27 \text{ V}. \quad (2.27)$$

Compare this value with the actual voltage measurement at point c (again,

with reference to GND) using a DMM.

Alternative Task 2: Resistors in Parallel

Repeat Task 2 with $R_1 = 3 \text{ k}\Omega$, $R_2 = 8 \text{ k}\Omega$ and $R_3 = 1 \text{ k}\Omega$, and $R_1 = R_2 = R_3 = 100 \text{ k}\Omega$.

2.11 Laboratory Task 3: “Droop”

Repeat Tasks 1 and 2 with $R_1 = R_2 = R_3 = 10 \text{ M}\Omega$ (Fig. 2.20). The actual resistance measurements show $R_1 = 9.9 \text{ M}\Omega$, $R_2 = 10.1 \text{ M}\Omega$ and $R_3 = 10.2 \text{ M}\Omega$. $V_{\text{in}} = V_a = 12.5 \text{ V}$. For Task 1:

$$V_b = V_{\text{in}} \frac{R_{\text{bottom}}}{R_{\text{top}} + R_{\text{bottom}}} = (12.5) \frac{10.1 + 10.2}{9.9 + 10.1 + 10.2} = 8.40 \text{ V} \text{ and} \\ V_c = V_{\text{in}} \frac{R_{\text{bottom}}}{R_{\text{top}} + R_{\text{bottom}}} = (12.5) \frac{10.2}{9.9 + 10.1 + 10.2} = 4.22 \text{ V}, \quad (2.28)$$

and for Task 2:

$$V_c = V_{\text{in}} \frac{R_{\text{bottom}}}{R_{\text{top}} + R_{\text{bottom}}} = (12.5) \frac{10.2}{\frac{9.9+10.1}{9.9+10.1} + 10.2} = 8.39 \text{ V}. \quad (2.29)$$

However, the experimental measurements for Task 1 show:

$$V_b = 5.05 \text{ V}, V_c = 2.52 \text{ V}$$

and for Task 2:

$$V_c = 6.28 \text{ V}$$

These measurements are significantly lower than our calculations. This phenomenon is known as *voltage droop*, or simply *droop*.

Even though a DMM has its own power supply (typically a 9 V battery), a small portion of electric current flowing through our circuit is bypassed through the DMM to make the actual measurement. A large resistor, typically around 10 MΩ, is installed in a DMM. The resistor sizes of our main circuit are substantially lower than 10 MΩ, so that almost all of the electric current flows through our main circuit, while only a very small portion of current flows through the DMM. However, if the main circuit consists mostly of large resistors (i.e., high loads), relatively large currents will flow through the DMM, resulting in a voltage loss within the main circuit.

Calculate the actual voltage at point c with resistors in series. Figure 2.20 below shows that a DMM is trying to measure the voltage at point c. The “top” part resistance is:

$$R_1 + R_2 = 9.9 + 10.1 = 20.0 \text{ M}\Omega \quad (2.30)$$

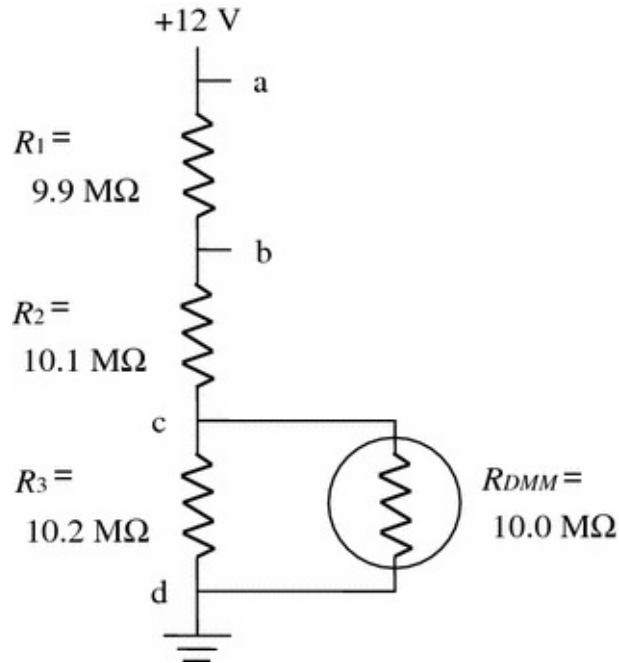


Fig. 2.20 Circuit diagram for Task 3

The “bottom” part can be treated as resistors in parallel,

$$\frac{R_3 \cdot R_{\text{DMM}}}{R_3 + R_{\text{DMM}}} = \frac{10.2 \cdot 10.0}{10.2 + 10.0} = 5.05 \text{ M}\Omega \quad (2.31)$$

The voltage divider relationship yields:

$$V_c = V_{\text{in}} \frac{R_{\text{bottom}}}{R_{\text{top}} + R_{\text{bottom}}} = (12.5) \frac{5.05}{20.0 + 5.05} = 2.52 \text{ V.} \quad (2.32)$$

Obviously it is possible to back-calculate the resistor value inside of a DMM with experimental data for V_c .

Question 2.5

Repeat the above calculation (with a 10 MΩ DMM connected) for V_b of Task 1 with 10 MΩ resistors and V_c of Task 2 with 10 MΩ resistors.

Question 2.6

Back-calculate the value of the resistor inside of the DMM in Fig. 2.21, given the following experimental measurements.

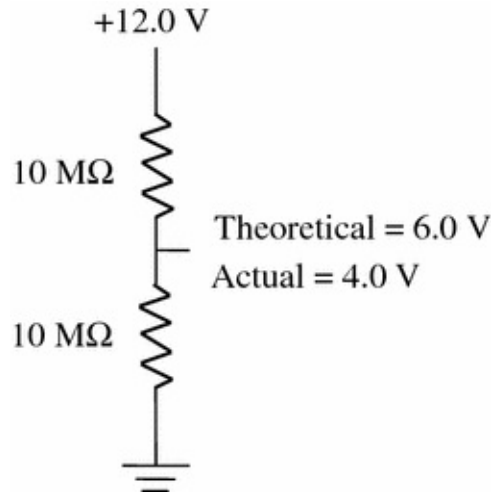


Fig. 2.21 Calculating DMM resistance

2.12 Laboratory Task 4: Potentiometer (Pot)

A pot is basically a variable voltage divider. The circuit layout shown in Figs. 2.22 and 2.23 includes a 20 k Ω pot, where a small adjustment shaft can be found on its top or side, and three terminals (usually labeled 1, 2 and 3) can be found at the bottom. Typically terminal 1 is connected to GND and terminal 3 to the high potential. In reality, terminals 1 and 3 can be swapped as there is no polarity in pots. Within a pot, terminal 2 is connected to a slider whose position can be adjusted with an adjustment shaft on the top. Based on the actual location of a slider, the top and bottom resistances are varied such that the output voltage from terminal 2 can be varied as well; thus it is a variable voltage divider. If only terminals 1 and 3 are used, it will simply work as a 20 k Ω resistor. If only terminals 1 and 2 (or 2 and 3) are used, it will become a variable resistor.

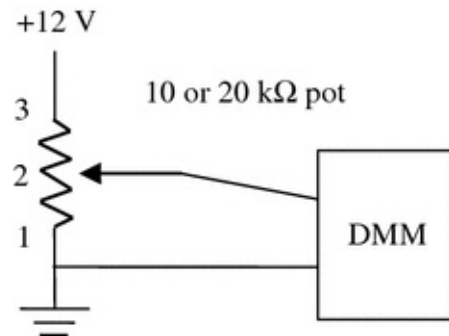


Fig. 2.22 Circuit diagram for Task 4

As the output voltage of a voltage divider simply depends on the ratio of top

and bottom resistances, the “size” of a pot (i.e., whether it is 1 or 20 k Ω pot) does not really affect the output voltage. However, it does affect the current applied to the given circuit. Pots are very useful in adjusting input voltages for a given circuit, and will be used throughout this textbook.

In a single-turn pot, a single 360° turn of a shaft would make the slider move from one end to the other. With +12 V input voltage, the output from terminal 2 would vary from 0 to 12 V with a single 360° turn. In a multi-turn pot, 10–20 × 360° turns may be required to make the slider move from one end to the other. We will use a multi-turn pot for more subtle control of output voltage.

In this task, you will need the following:

- A breadboard, wires, wire cutter/stripper, a power supply and a DMM.
- 10 or 20 k Ω pot.
- A small, flathead screw driver.

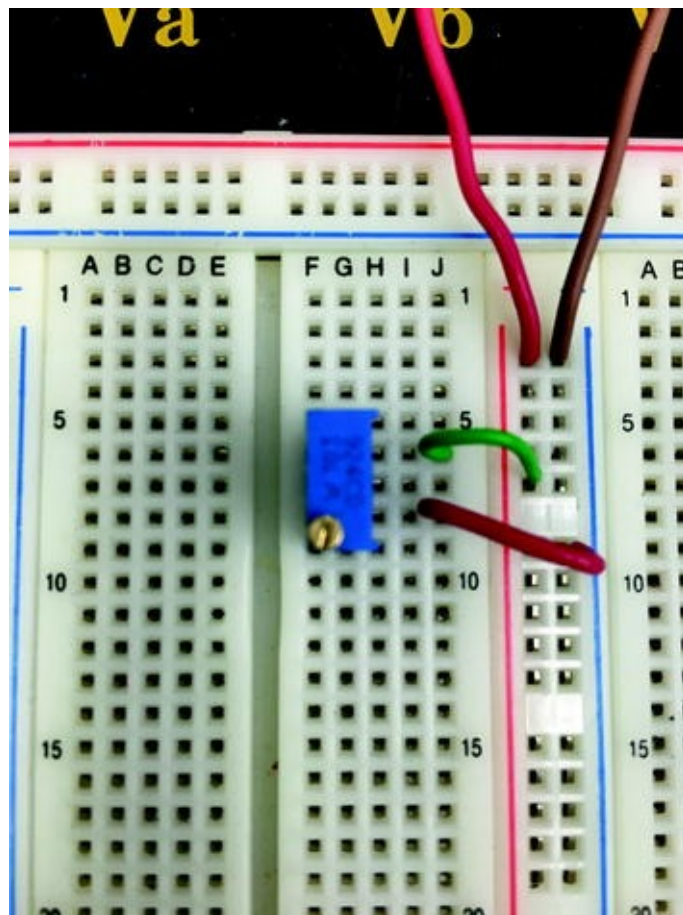


Fig. 2.23 Photo of a pot circuit to be used in Task 4

Here is the circuit diagram:

- As the pot itself does not have any polarity, switching pins 1 and 3 from top to bottom position does not make any difference. You should measure voltage output from pin 2 of your pot (with reference to ground).
 - Read the output voltage from your pot. A voltage close to 12 V indicates the slider (terminal 2) is located very close to terminal 3. A voltage close to 0 V indicates the slider is located very close to terminal 1. Turn the adjustment shaft using an appropriate screw driver to make the output voltage 0 V. This is usually achieved by turning the shaft clockwise. Once you reach the end point, you will hear a clicking sound, indicating you have gone too far. Record the output voltage.
 - Make a full (360°) counterclockwise turn of the adjustment shaft. This action should decrease the output voltage a little bit. Record the output voltage.
 - Continue this until you reach the maximum voltage ($V_{in} \approx 12$ V).
 - Record your data.
 - Plot the output voltage against the number of turns. Perform linear regression and obtain the equation and R^2 value. You will notice that the output voltage is linearly proportional to the number of turns (Fig. 2.24).
-

2.13 Further Study: Thévenin’s Theorem

You may have found it a bit difficult to solve Question 2.6 earlier, back-calculating the inner resistance of a DMM. For this kind of complicated circuit calculation, you may find *Thévenin’s theorem* useful. Thévenin’s theorem states that a portion of an electric circuit can be simplified as a single voltage source (V_{Th} —Thévenin equivalent voltage or simply *Thévenin voltage*) and a single resistor (R_{Th} —Thévenin equivalent resistance or simply *Thévenin resistance*).

# turns	0	1	2	3	4	5	6	7	8	9	10	11
V	0.09	0.71	1.26	1.9	2.49	3.11	3.65	4.21	4.71	5.29	5.82	6.33
# turns	12	13	14	15	16	17	18	19	20	21	22	23
V	6.88	7.41	8.01	8.56	9.08	9.58	10.1	10.5	11	11.4	11.8	12.3

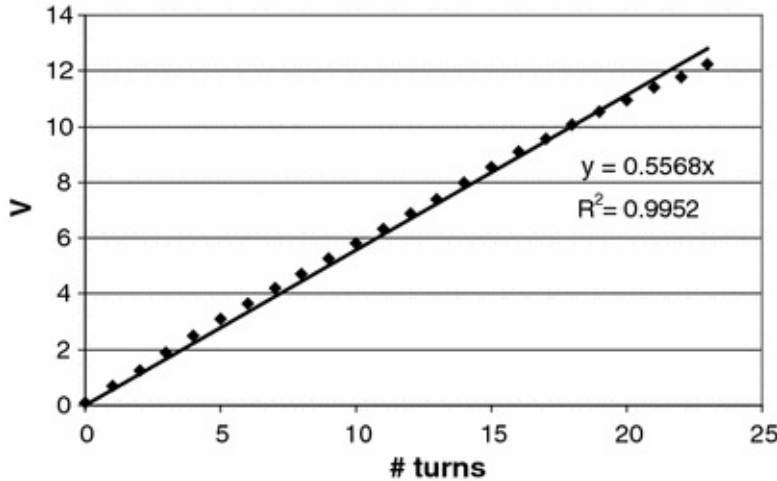


Fig. 2.24 Experimental data for Task 4

Your voltage output to the DMM comes from point *c*. You are trying to simplify the circuit that is circled with a dotted line in Fig. 2.25. Let's first assume that this is your only circuit; i.e. your DMM is disconnected. With the DMM disconnected, we know that the voltage output at point *c* should be 4.0 V from the voltage divider principle. This (4.0 V) is your V_{Th} .

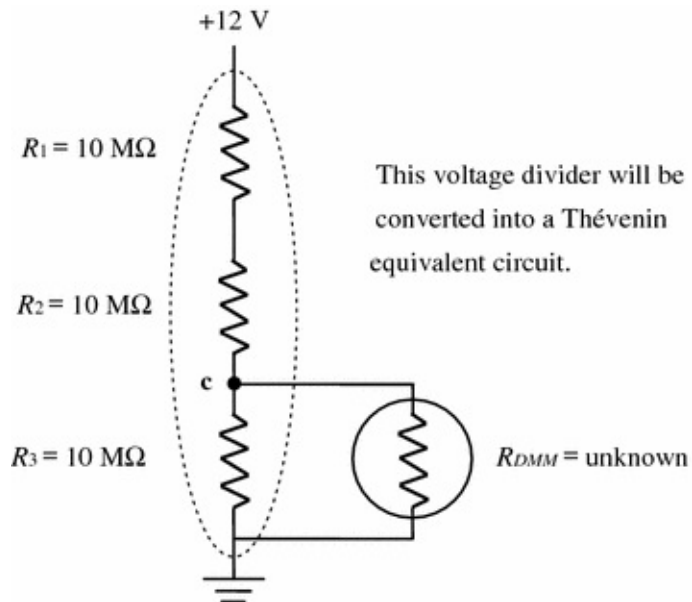


Fig. 2.25 Circuit used for Question 2.6

Figure 2.26 shows we now have a new voltage source at point *c*, you want to relocate the voltage source to this hypothetical point. This relocation implies that the original voltage source of +12 V should be eliminated, while the high voltage and ground should be connected to each other. From this new voltage source, you can look back at the circuit and find there are two branches, one with two $10 \text{ M}\Omega$ resistors and the other with one $10 \text{ M}\Omega$ resistor. This is equivalent to parallel resistors with 20 and $10 \text{ M}\Omega$ resistors. The total resistance can be calculated as: $(20 \times 10)/(20 + 10) = 6.67 \text{ M}\Omega$. This is your R_{Th} .

Hence the components circled with a dotted line in Fig. 2.25 are now converted into an open circuit consisting of a single voltage source ($V_{Th} = 4.0 \text{ V}$) and a single resistor ($R_{Th} = 6.67 \text{ M}\Omega$). If you connect your DMM (with unknown inner resistance x) to this open circuit, you can use the voltage divider principle to evaluate x . If your actual voltage reading at point *c* is 2.4 V ,

$$V_{out} = V_{in} \frac{R_{bottom}}{R_{top} + R_{bottom}}$$

$$2.4 = (4.0) \frac{x}{6.67 + x}$$

$$x = 10$$
(2.29)

You can also calculate the actual voltage reading at point *c* with the known inner resistance of the DMM ($10 \text{ M}\Omega$): $(4.0) \times [10/(6.67 + 10)] = 2.4 \text{ V}$ (Fig. 2.26).

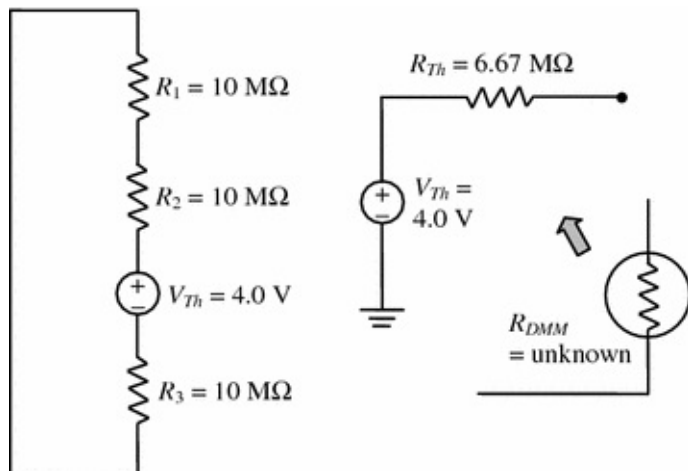


Fig. 2.26 Thévenin circuit for Question 2.6

Question 2.7

Determine V_{ab} in Fig. 2.27 using Thévenin's theorem. Hint: Make the first Thévenin equivalent circuit (short dotted line) at point c. Then the circuit becomes a voltage divider problem with three resistors (R_{Th} , 3 and 4 k Ω) with the input voltage V_{Th} .

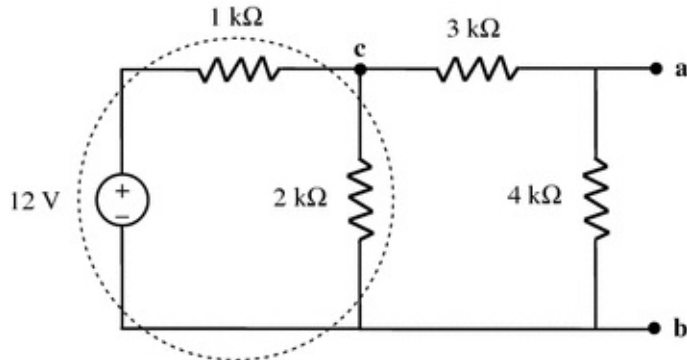


Fig. 2.27 Circuit used for Question 2.7

References and Further Readings

Gibilisco S (2006) Teach yourself electricity and electronics, 4th edn. McGraw-Hill, New York

Kybett H, Boysen E (2008) All new electronics self-teaching guide, 3rd edn. Wiley, Hoboken

Mims III F (2003) Getting started in electronics, 3rd edn. Master Publishing, Lincolnwood

Scherz P (2006) Practical electronics for inventors, 2nd edn. McGraw-Hill, New York

3. Diodes and Transistors

Jeong-Yeol Yoon¹✉

(1) University of Arizona, Tucson, AZ, USA

✉ Jeong-Yeol Yoon
Email: jyyoon@email.arizona.edu

In the previous chapter, we learned the fundamental basics of electronic circuitry using resistors. Many resistors are neither conductors nor insulators. Rather, they are somewhere in between the two. This class of materials is called *semiconductors*. Semiconductors are the building blocks of many other electronic components, such as diodes and transistors—the subjects of this chapter.

3.1 Semiconductors

The most popular semiconductor material is silicon (Si). It belongs to the group IV elements in the periodic table (Fig. 3.1). Group IV elements have four electrons in their outermost (valence) shell. As the valence shell wants to hold a total of eight electrons, a single silicon atom can be covalently attached to four nearby silicon atoms, thus creating a crystal structure. Through this sharing, all silicon atoms have four electrons in their valence shells, leaving no free electrons. Therefore, a pure silicon crystal is nearly an insulator.

For electronic applications, however, this silicon crystal undergoes a process called *doping*, so that it turns into a semiconductor. Doping is essentially the addition of small impurities to a silicon crystal. In *N-type* doping, phosphorous (P) is typically added to a silicon crystal. This small impurity is called *dopant*. Phosphorous belongs to group V elements, meaning there are five electrons in its valence shell (Fig. 3.1). The fifth electron has nothing to bond to, so it becomes

a free electron. Overall, N-type silicon (or *N-doped* silicon) carries negative charges because of these free electrons, but not as many as electric conductors.

If the dopant is boron (B), which belongs to group III elements (i.e., three electrons in its valence shell), there should be a lack of an electron wherever there is boron (Fig. 3.1). This lack of an electron is called a *hole*, which is equivalent to the hypothetical positive charge. *P-type* silicon (or *P-doped* silicon) carries positive charges because of these holes, but again, not as many as electric conductors.

Other atoms can be used for semiconductor materials. For example, germanium (Ge) can be used instead of silicon (Si), both of which belong to the group IV elements. For positive dopant, arsenic (As) can be used in place of phosphorous (P), both of which belong to the group V elements. For negative dopant, gallium (Ga) can be used instead of boron (B), both of which belong to the group III elements.

5 B Boron	6 C Carbon	7 N Nitrogen
13 Al Aluminum	14 Si Silicon	15 P Phosphorous
31 Ga Gallium	32 Ge Germanium	33 As Arsenic

Fig. 3.1 Semiconductor materials (*middle column*) and their positive dopants (*left column*) and negative dopants (*right column*) from the periodic table of elements

3.2 Diodes

When you sandwich together P-type and N-type silicon, it becomes a *diode*. This particular type of diode is sometimes called a P–N junction diode. The primary function of a diode is to allow current to flow only in one direction, i.e., a one-way street for electric current.

When the P-side is connected to the high voltage side of a battery and the N-side to the ground, as shown on the left in Fig. 3.2, it is called *forward biasing*. Electrons are generated from the ground of a battery and flow toward the N-type silicon. The excess electrons in the N-type silicon are forced to jump into the holes of the P-type silicon, and continue to travel to the high voltage side of a

battery. Therefore, the diode allows the electrons to flow from the ground to the high voltage of a battery.

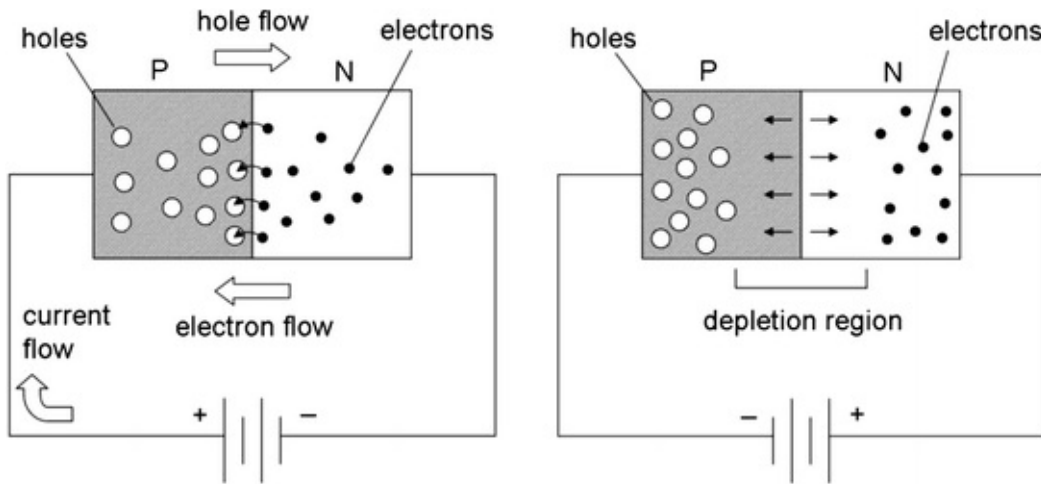


Fig. 3.2 A P–N junction diode in forward (left) and reverse (right) bias

When the battery is reversed, as shown in Fig. 3.2 in the right, it is called *reverse biasing*. Electrons from the ground of a battery attract the holes in the P-type silicon, forcing the holes to move to the left. Holes from the high voltage of a battery attract the electrons in the N-type silicon, again forcing the electrons to move to the right. This results in an empty zone that is nearly free of holes and electrons, called a *depletion region*. As there are almost no holes or electrons in this region, it acts as an insulator, meaning that the diode does not allow the electrons or current to flow through it.

Figure 3.3 shows a typical package of a diode and its schematic symbol. The P-type side is called the *anode* and the N-type side is called the *cathode*. Typically, there is a colored band in the diode package to indicate its cathode (N-type side). Current flows from anode to cathode (or P-type to N-type side), and the triangle symbol of a diode indicates this direction of current flow.

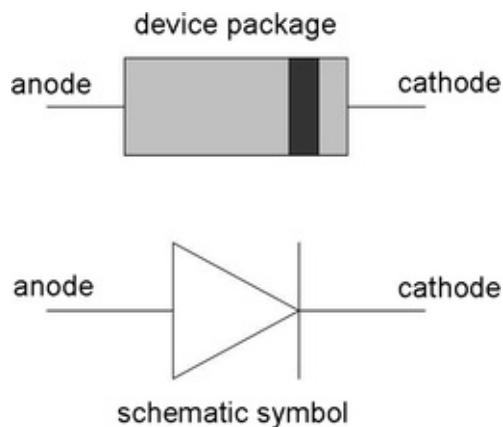


Fig. 3.3 Diode

Diodes are primarily used to allow forward current but to block reverse current. This is a fundamental basis for converting alternating current (AC) to direct current (DC), which is called *rectification* (Fig. 3.4). Many power adaptors for laptop computers, smartphones, and other electronic gadgets use this type of circuit to convert AC outlet power (100–240 V) to useable DC power (3–9 V).

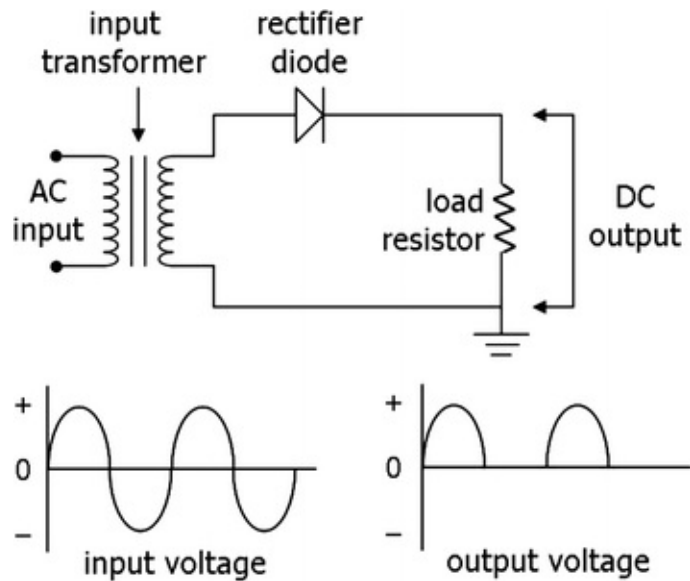


Fig. 3.4 Converting AC into DC with a rectifier diode

Diodes do not allow the forward-biased current to flow if the applied voltage is too low. The minimum voltage required to drive a diode is called the *barrier voltage*. Additionally, diodes may allow the reverse-biased current to flow if the applied voltage is substantially high. The voltage that enables this reverse-biased current flow is called *breakdown voltage*. This behavior is graphically illustrated

in Fig. 3.5 with the voltage versus current (V - I) curve of a typical silicon diode.

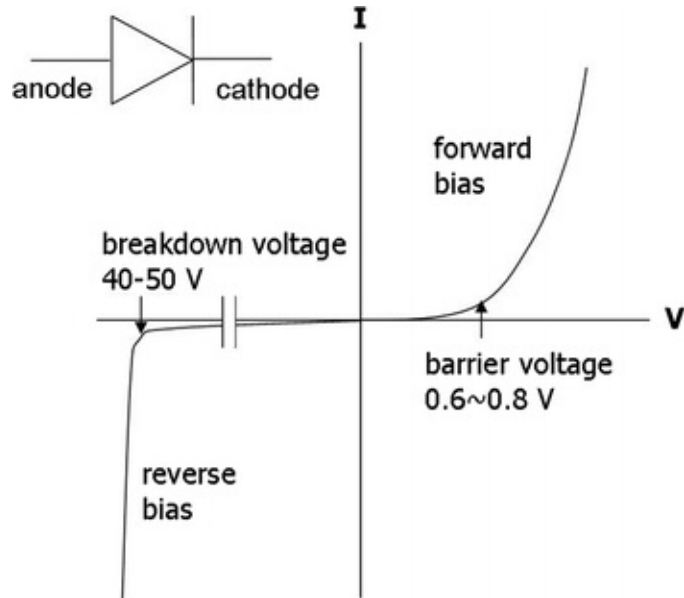


Fig. 3.5 V - I curve for a typical diode with barrier and breakdown voltages

The forward-biased current that flows through a typical silicon diode (I_D) is related to the applied voltage (V_D) with the following equation:

$$I_D = I_S(e^{qV_D/kT} - 1) \quad (3.1)$$

where

I_S saturation current, characteristic to each diode, $10^{-8}\sim10^{-14}$ A

q charge of an electron

k Boltzmann's constant

T temperature in Kelvin

At room temperature (298 K), $kT/q = 0.026$ V. Therefore, the curve is really an exponential curve. Practically speaking, however, it is safe to assume that the current is zero until the barrier voltage and linearly increases thereafter.

For most diodes, the V - I curve is very steep and the voltage drop across the diode is roughly the same regardless of the current flowing through it. We can use this feature to drop the voltage by a constant value. Figure 3.6 shows such a circuit, called a *voltage dropper*.

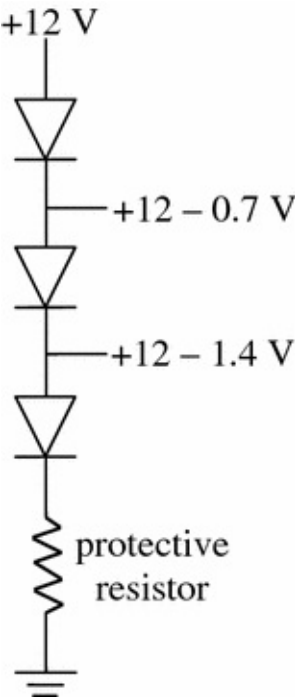


Fig. 3.6 Voltage dropper

Because the $V-I$ curve of a diode is exponential, the voltage drop by a diode is not really constant and varies slightly by the input current. Note that there is a protective resistor in the voltage dropper circuit. A diode is not a resistor, and the current increases exponentially upon increasing the voltage, according to Eq. 3.1. This often leads the diodes to burn. The protective resistor prevents that from happening.

The reverse-bias behavior of a typical diode is somewhat similar to that of forward bias, except for the fact that the magnitude of a breakdown voltage is much higher than that of a barrier voltage. Figure 3.5 shows a breakdown voltage of ~ 45 V, which varies by the types of diodes. After the breakdown point, the slope of the $V-I$ curve becomes infinity, i.e., the voltage across a diode remains constant regardless of the amount of current flowing through it. As this breakdown voltage and accompanying current are typically very high, it usually leads to permanent damage of diodes.

3.3 Zener Diode

The reverse bias of a typical diode shows very interesting behavior. There is almost no current flowing when the applied voltage is below its breakdown point. After that point, the voltage drop across the diode remains constant,

regardless of the current flowing through it. A *Zener diode* is a special type of diode that is able to utilize this reverse-bias behavior at a lower applied voltage.

Figure 3.7 shows the V–I curve of a typical Zener diode, which is identical to Fig. 3.5, except that the breakdown voltage is much smaller. This lower breakdown voltage is called *Zener voltage*. Obviously the forward bias behavior of a Zener diode is exactly identical to that of a typical diode. Therefore, a Zener diode is almost exclusively used with reverse biasing. As the Zener voltage is much lower than the breakdown voltage of a typical diode, no permanent damage is made to the Zener diode and the process is entirely reversible.

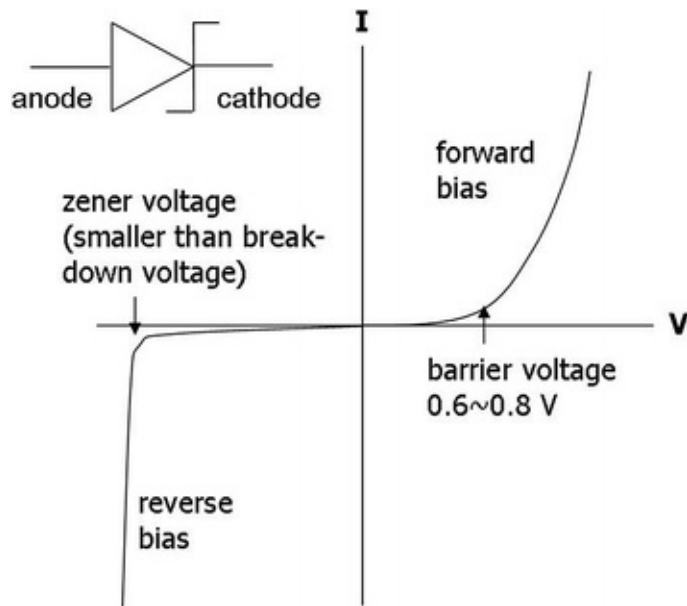


Fig. 3.7 V–I curve of a Zener diode, with its schematic symbol shown in the top left corner (the line in the cathode is replaced with Z-shape, representing “Zener”)

Zener diodes have been primarily used for stabilizing and regulating voltages. Figure 3.8 shows a circuit called a *voltage regulator*. When $V_{\text{out}} < V_{\text{Zener}}$, no current flows through the Zener diode, and the entire circuit behaves simply as the circuit with a single resistor (R_{load}). When $V_{\text{out}} > V_{\text{Zener}}$, however, a huge current will flow through the Zener diode, and no current will flow through the R_{load} . If the Zener voltage is 3 V, only voltages below 3 V will be allowed to pass through the load, while any voltages above 3 V will be blocked from the load.

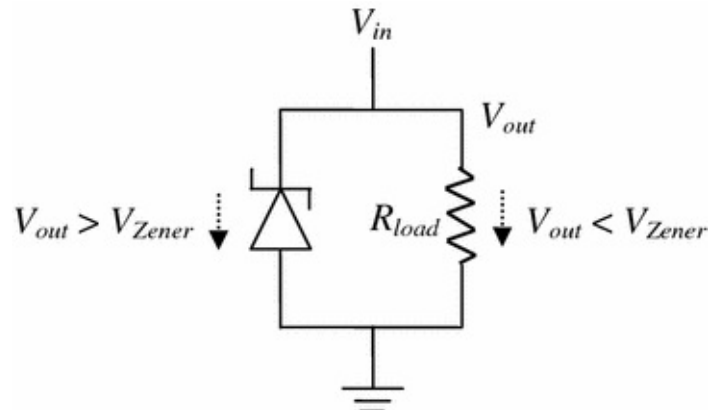


Fig. 3.8 Voltage regulator

The Zener voltage does not change with the input voltage or current, but it is a function of temperature, which means that we can utilize it as a temperature sensor. This Zener diode temperature sensor will be discussed further in the next chapter.

3.4 Transistors

Transistors are very similar to diodes, except for the fact that they are three-element devices. If you sandwich together N-type, P-type, and N-type silicon, it becomes an *NPN transistor*. If you sandwich together P-type, N-type, and P-type silicon, it becomes a *PNP transistor*. (These specific types of transistors are referred to as bipolar junction transistors —see below). Let us start our discussion with an NPN transistor, which is graphically illustrated in Fig. 3.9 with a correct bias.

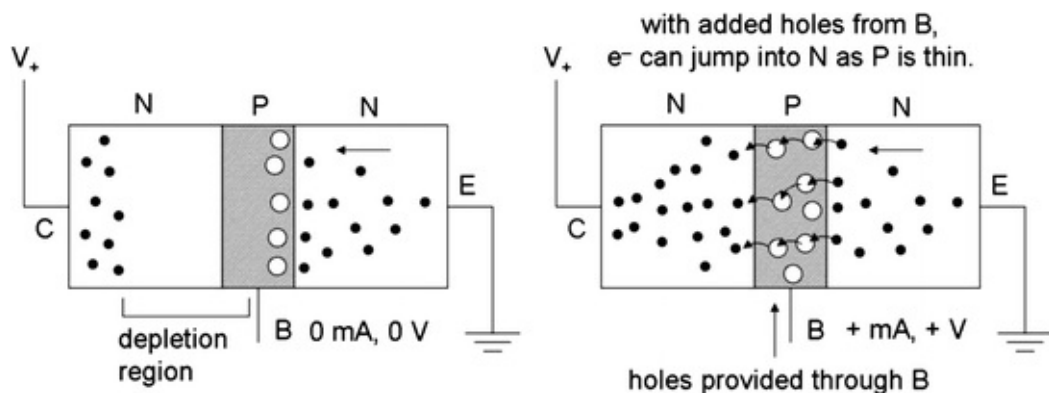


Fig. 3.9 Correct bias for an NPN transistor

Note that the left N-type silicon is connected to a high voltage (V_+), which is called the *collector* (C), and the right N-type silicon to a ground, which is called the *emitter* (E). The lead that is connected to the central P-type is called the *base* (B). A flow of electrons is provided from the ground to the emitter N-type silicon. Just like the diode in the forward bias, the excess electrons want to jump into the P-type silicon, attracting its holes. In the meantime, high voltage is applied to the collector N-type silicon, attracting their electrons to the left side. Because the holes in the P-type silicon are already attracted to the right emitter N-type silicon, a depletion region forms. Therefore, the left N–P junction is essentially a diode in reverse bias, while the right P–N junction is a diode in forward bias. Because of the depletion region formed in the left N–P junction, no current flows through this NPN transistor.

When you apply a small, positive current to the central P-type silicon (base), things change. The small depletion region in the P-type silicon is now filled with holes, converting the P-type silicon back to a conductor. As the P-type silicon is made very thin in transistors, the electrons attracted to the right P–N junction can “jump” to the left N–P junction as the thin P-type silicon is now fully conductive. If you increase the current flowing into the base, more electrons flow from the emitter to the collector, i.e., more current flows from the collector to the base.

To summarize, a very small current to the base (called base current, I_B) determines the amount of current flowing from the collector to the emitter (called collector current, I_C , and emitter current, I_E). A water flow analogy has been used to describe how transistors work, shown in Fig. 3.10. A reservoir of water is stored in C (collector) and wants to flow toward E (emitter). There is a plunger in between C and E, which is connected to the smaller reservoir of water in B (base). If we pour a small amount of water into B, it will push the plunger upwards, allowing the water to flow from C to E. Some of the water from B joins the flow, but its amount is negligible compared to those of C and E. If more water is poured into B, the plunger moves further upward and an even greater amount of water flows from C to E.

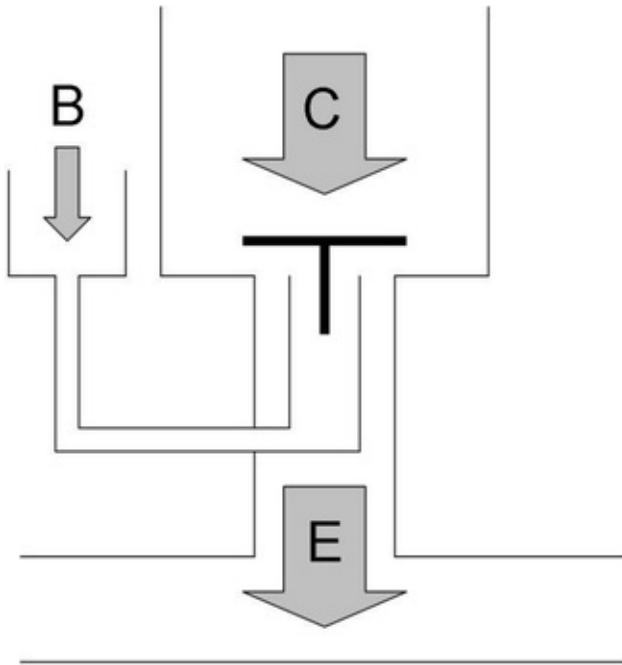


Fig. 3.10 Water flow analogy for a transistor

Figure 3.11 shows the package of a typical transistor, with the three leads for the emitter (E), the base (B), and the collector (C). Figure 3.12 shows the schematic diagrams for NPN and PNP transistors, along with their circuit symbols. PNP transistors work exactly opposite to NPN transistors. Negative current is applied to the base (or current output rather than input), which controls the current flowing from the emitter to the base. With either transistor, the main direction of current flow is always designated with an arrow within the transistor symbol.

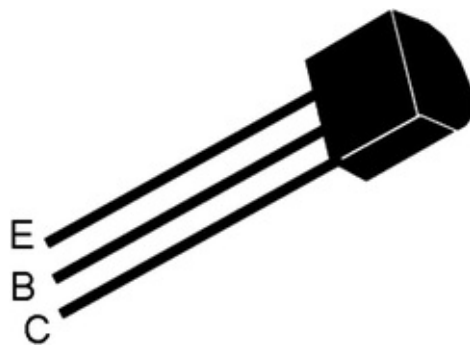


Fig. 3.11 A transistor

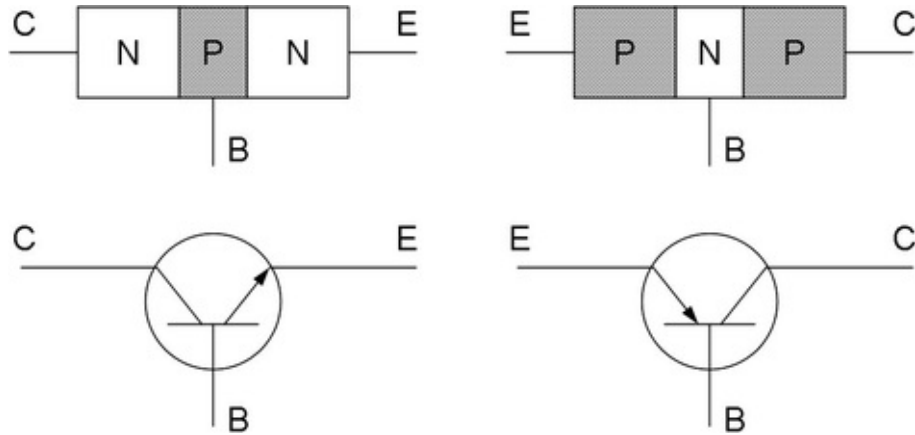


Fig. 3.12 An NPN (left) and PNP (right) transistor

The primary function of a transistor is *amplification*, as the small base current (I_B) enables much larger collector and emitter currents (I_C and I_E). For all transistors:

$$I_C = I_B \times \beta \quad (3.2)$$

where β = *current gain*, a value that varies by transistor model.

The current gain of the transistor used in Task 3 of this chapter is around 150. As the collector and base currents join together toward the emitter (for an NPN transistor):

$$I_E = I_C + I_B \quad (3.3)$$

Plugging Eq. 3.2 into Eq. 3.3:

$$I_E = I_B \times \beta + I_B = (1 + \beta) I_B \quad (3.4)$$

As I_B is very small compared to I_C :

$$I_C \approx I_E \quad (3.5)$$

Question 3.1

Calculate V_C , V_E , I_C , I_E , and I_B for the following transistor circuit (Fig. 3.13). The current gain β is 100. V_{BE} is 0.67 V, and is nearly constant for this transistor for a range of input voltage and current.

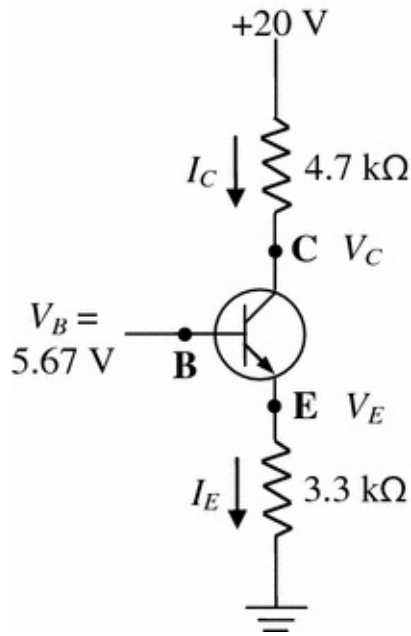


Fig. 3.13 A transistor circuit for Question 3.1

Solution

$$\begin{aligned}
 V_{BE} &= V_B - V_E \\
 V_E &= V_B - V_{BE} = 5.67 \text{ V} - 0.67 \text{ V} = 5 \text{ V} \\
 I_E &= (V_E - 0 \text{ V}) / 3.3 \text{ k}\Omega = 5 \text{ V} / 3.3 \text{ k}\Omega = 1.5 \text{ mA}
 \end{aligned} \tag{3.6}$$

Using Eq. 3.4:

$$\begin{aligned}
 I_E &= 1.5 \text{ mA} = (1 + \beta) I_B = 101 I_B \\
 I_B &= 1.5 \text{ mA} / 101 = 0.015 \text{ mA} \text{ or } 15 \mu\text{A}
 \end{aligned} \tag{3.7}$$

Using Eq. 3.5:

$$\begin{aligned}
 I_C &\approx I_E = 1.5 \text{ mA} \\
 I_C &= 1.5 \text{ mA} = (20 \text{ V} - V_C) / 4.7 \text{ k}\Omega \\
 V_C &= 13 \text{ V}
 \end{aligned} \tag{3.8}$$

Figure 3.14 shows characteristic curves for a typical NPN transistor. Once a sufficient voltage is applied across the transistor (V_{CE}), an almost constant amount of current flows (I_C , which is almost the same as I_E) through it. This current is not really affected by the applied voltage (V_{CE}), as shown in the figure. What really affects I_C is the base current, I_B .

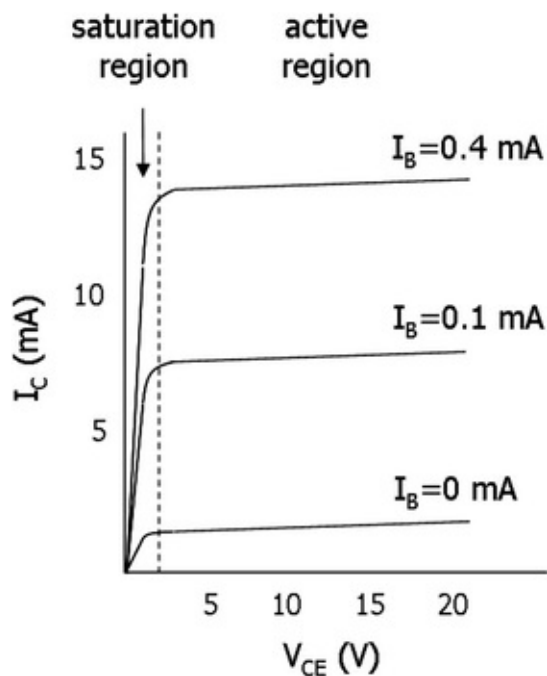


Fig. 3.14 Characteristic curves for an NPN transistor

As mentioned briefly in Question 3.1, V_{BE} is also almost constant regardless of the input voltage and current. However, V_{BE} is a function of temperature (just like in the Zener diode), which means that we can utilize it as a temperature sensor. Again, this feature will be discussed further in the next chapter.

In addition to the apparent use of a transistor for current amplification, a transistor can also be used for a *current biasing circuit* (Fig. 3.15). The left-hand side is essentially a voltage divider, and its output flows toward the base. By adjusting V_B (and thus I_B), the current flowing through R_{load} (collector current I_C) can be regulated. Integrated circuits that provide constant current source are built upon the current biasing circuit.

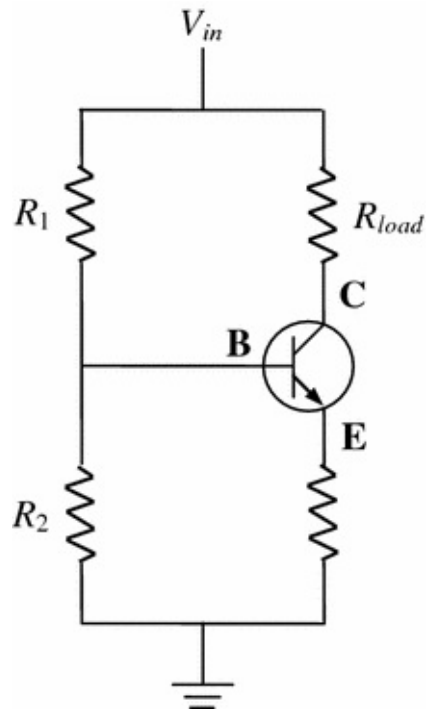


Fig. 3.15 Current biasing circuit

The transistors described previously are in fact an old type of transistor, called the *bipolar junction transistor (BJT)*. They are still being used today, especially for analog circuits, which are essential components for physical sensors and biosensors. In modern digital applications, however, a new type of transistor is commonly used, called the *junction field-effect transistor (JFET)*. Rather than sandwiching P-type and N-type silicon, channels are fabricated on semiconductor substrates to create NPN or PNP junctions. Unlike BJT, which is current-controlled, JFET is voltage-controlled, and it draws little or no input current. This is a very useful feature in chemical or biosensor applications. For example, the output from a typical pH electrode comes with very small current (Chap. 10).

3.5 Operational Amplifier to Protect Your Circuit

We have just learned the basic fundamentals of diodes and transistors. In the following laboratory section, we will have a hands-on experience with two different types of diodes: the light emitting diode (LED) and the *Zener diode*. A section of the lab also focuses on transistors. The LED will be revisited in the optoelectronics chapter, and the Zener diode will be revisited in the temperature sensor chapter.

Although all diodes require voltage, care should be taken to not apply excess current. In fact, only a small amount of current should be applied in order to protect any type of diode. In this regard, we will use a pot and an *operational amplifier* (or “*op-amp*”). Although op-amps will be investigated in a later chapter, remember for now that they are used to amplify voltage while using almost no current. The op-amp used in the following lab is configured as a *buffer stage*, a configuration that results in no gain. Therefore, the primary purpose of using an op-amp in the following lab is to create a voltage signal with almost zero current, primarily to protect our LED and Zener diode.

Throughout this textbook, we will use either the *LM741* (a single op-amp) or the *LM324* (consisting of four op-amps). As their patents are expired, there are many manufacturers worldwide that make these op-amps. Use an appropriate online search engine using *LM741* and *LM324* as keywords for further information on the devices.

Both the *LM741* and the *LM324* have two input terminals, negative (−) and positive (+), and one output terminal. The signal from the negative terminal is amplified using +12 V power, and that from the positive terminal is amplified using −12 V power, as seen in Fig. 3.16. Some other op-amps use ±10 or ±9 V. Note that GND (0 V) does not need to be connected to power up the op-amps.

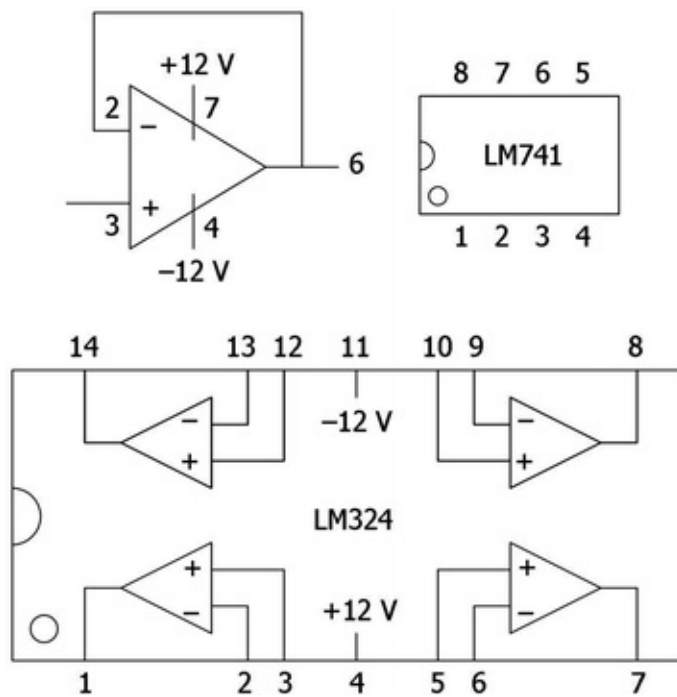


Fig. 3.16 Op-amps *LM741* and *LM324*. Note that terminals 1, 5, and 8 in the *LM741* are generally not used

Since we will build a relatively simple circuit, a single op-amp LM741 is appropriate. The layout shown in Fig. 3.16 is a top view. The eight terminals of the LM741 can be inserted directly into a breadboard, but you do not want to tie the terminals 1 and 8, 2 and 7, 3 and 6, and 4 and 5 together. Figure 3.17 shows how to connect the op-amp onto a breadboard while isolating the pins correctly.

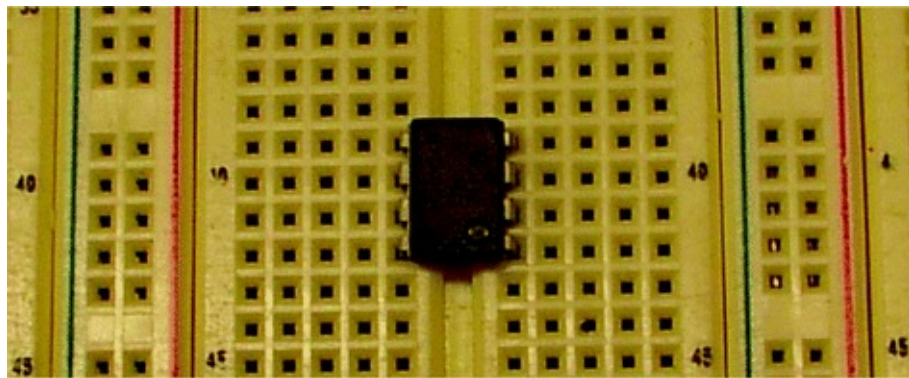


Fig. 3.17 A correct op-amp (LM741) installation on a breadboard

Improper connection of an op-amp with the terminals tied together will lead to the smell of burning plastic, or smoke. Obviously, this causes permanent damage to the op-amp, and could also damage the breadboard.

3.6 Laboratory Task 1: LED

For this task, you will need the following:

- A breadboard, wires, wire cutter/stripper, a power supply, and a DMM.
- 10 or 20 $\text{k}\Omega$ pot, and a screw driver
- Op-amp LM741
- Green or red LED
- 0.1 $\text{k}\Omega$ resistor

Figures 3.18 and 3.19 show the circuit layout. The op-amp simply acts as a buffer stage, providing necessary voltage to the LED but with a very small current, to protect the LED. The maximum output current of LM741 is 25 mV, according to its specification sheet.

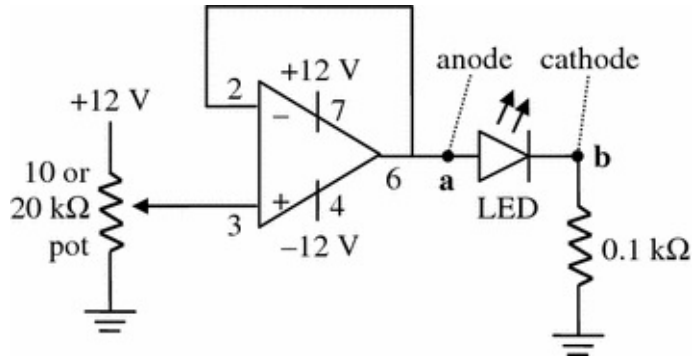


Fig. 3.18 Circuit diagram for Task 1. A single +12 V voltage source can be used to power both the pot and the op-amp

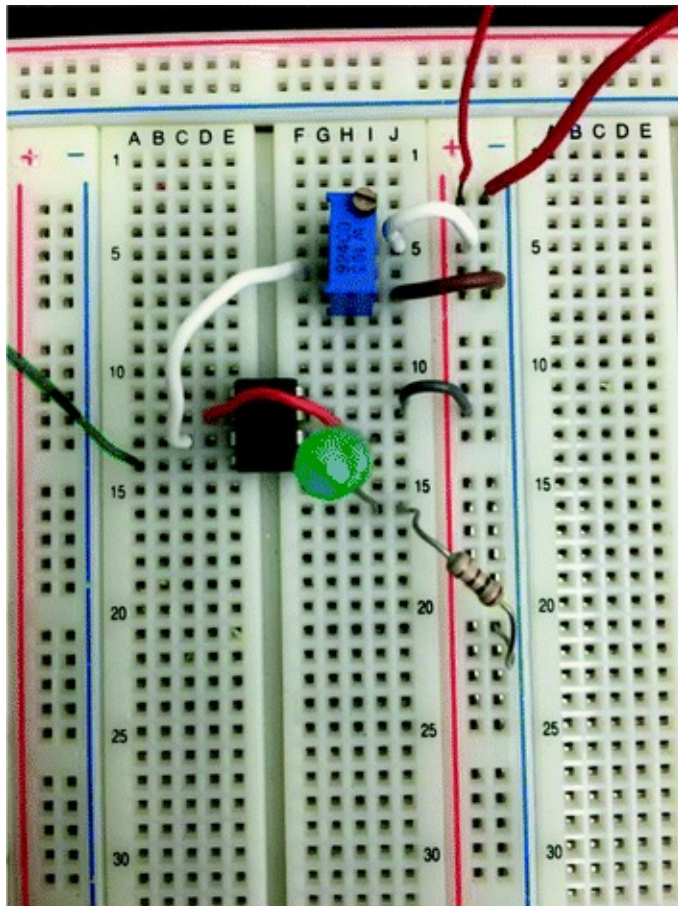


Fig. 3.19 Circuit photo of Task 1

As a positive voltage is applied to the anode of the LED, we say that the LED is configured in a *forward bias*. For diodes, the anode is referred to as (−) and the cathode as (+). Typically, the anode terminal is longer than the cathode terminal. Light emission from an LED also indicates that the LED is positioned

in a forward bias . The voltage nomenclature is as follows:

- V_a = voltage applied to an LED. Can be measured in 20 V scale.
- $V_{ab} = V_a - V_b$ = voltage drop across the LED. You may want to measure V_a and V_b separately and subtract them, or connect the positive lead of DMM to point a and the GND lead of DMM to point b .
- V_b = voltage drop across the 0.1 k Ω resistor. Using Ohm's law, you can calculate the current flowing through the 0.1 k Ω resistor. This current will be identical to the current flowing through the LED, as the LED and the resistor are connected in series (conservation of current).

Change the voltage output of the pot from 0 to +12 V. The voltage output from terminal 2 of the pot should be identical to terminal 6 of the LM741 (V_a). As you turn the pot, record V_a , V_{ab} , and V_b at the end of each turn. Unlike the potentiometer lab (Task 4 of the previous chapter), V_{ab} and V_b will not change linearly against the number of pot turns. You may want to start with quarter turns of the pot, especially at low V_a .

Now you can calculate the voltage drop across the LED (V_{LED}) from V_{ab} , and the current flowing through the LED (I_{LED}) from V_b . Let us plot an I - V curve for an LED from our sample experimental data (Fig. 3.20).

V_{ab}	0	0.04	0.77	1.18	1.57	1.72	1.81	1.88	1.95	2.01	2.06	2.11
V_b	0	0	0	0.02	0.13	0.42	0.81	1.18	1.62	2.02	2.43	2.82

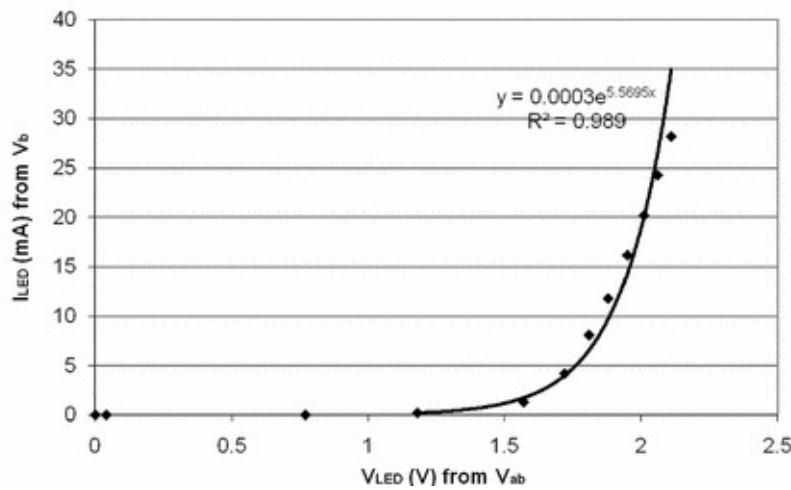


Fig. 3.20 Experimental data from Task 1

You can clearly notice the barrier voltage of 1.6 V, where you are able to see

the light emission from your LED. You can also notice I_{LED} starts to level off at 25 mA, which is the maximum output current of LM741.

Question 3.2

Draw the I - V curve for an LED if it is connected in a reverse bias.

3.7 Laboratory Task 2: Zener Diode

In this task, you will need the following:

- A breadboard, wires, wire cutter/stripper, a power supply, and a DMM.
- 10 or 20 k Ω pot, and a screw driver
- Op-amp LM741
- 5.1 V Zener diode
- 1 k Ω resistor

Figures 3.21 and 3.22 show the circuit layout. The main power supply is set to -12 V, indicating that we are doing this experiment in a *reverse bias*. There is a colored band on the Zener diode, indicating the cathode.

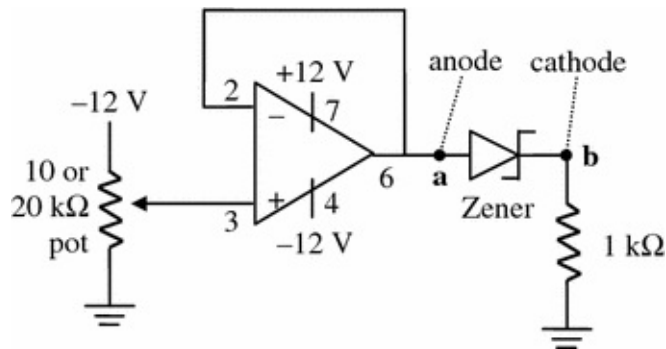


Fig. 3.21 Circuit diagram for Task 2. A single -12 V voltage source can be used to power both the pot and the op-amp

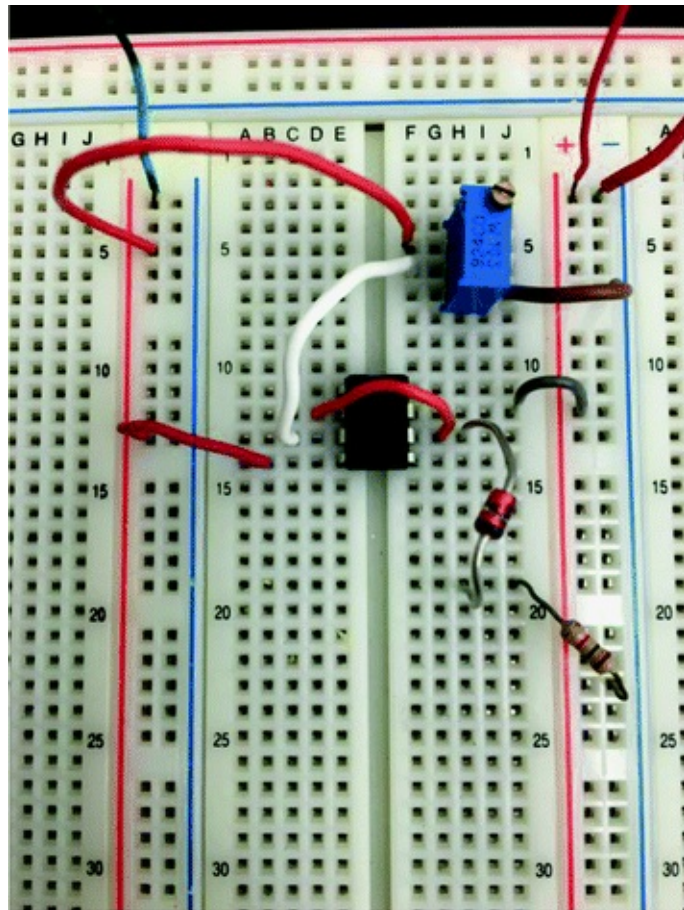


Fig. 3.22 Circuit photo for Task 2

As explained earlier, a Zener diode behaves similar to other diodes in a forward bias, which is not very useful. After all, Zener diodes are more expensive than regular diodes or light emitting diodes. Zener diodes are almost always used in reverse bias , which exhibits a Zener voltage. After this point, the current increases almost vertically against the voltage drop across the Zener. Note that we are using a larger resistor ($1\text{ k}\Omega$) than that used in Task 1, indicating that a higher current is flowing though the Zener diode than our LED.

Repeat the experiments the same as Task 1. Calculate V_{zener} from V_{ab} , and I_{zener} from V_b (both should be negative). Then plot an I - V curve for a Zener diode, which should be shown in the third quadrant (Fig. 3.23). You can clearly identify the Zener voltage of around -5.1 V .

V_{ab}	0	-0.33	-0.73	-1.17	-1.62	-2.07	-2.51	-2.96	-3.42	-3.83	-4.17	-4.4
V_b	0	0	0	0	0	0	0	0	-0.02	-0.07	-0.19	-0.38
V_{ab}	-4.57	-4.69	-4.78	-4.85	-4.89	-4.96	-4.97	-4.98	-5	-5.01	-5.02	-5.02
V_b	-0.68	-1.02	-1.42	-1.88	-2.32	-2.75	-3.17	-3.59	-3.99	-4.42	-4.57	-4.57

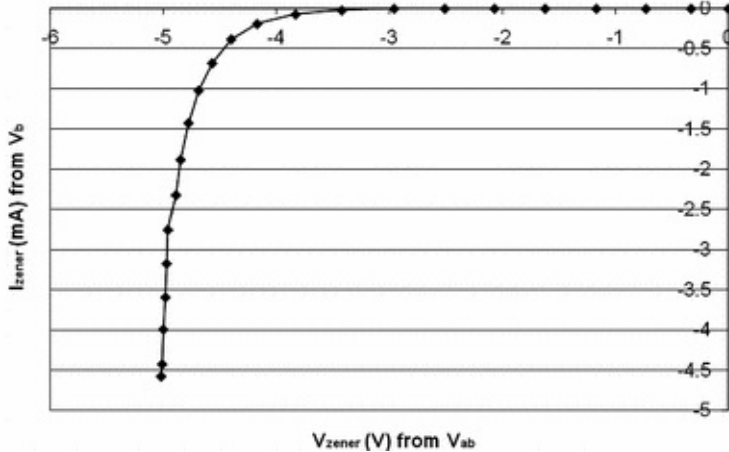


Fig. 3.23 Experimental data from Task 2

Question 3.3

Plot $-V_{\text{zener}}$ (y-axis) against $-I_{\text{zener}}$ (x-axis) for the above data in the first quadrant. Did you notice the voltage is almost constant for a certain window of current?

3.8 Laboratory Task 3: Transistor

In this task, you will need the following:

- A breadboard, wires, wire cutter/stripper, a power supply, and a DMM
- 1 and 10 k Ω pots, and a screw driver
- Bipolar transistor 2N4401 (NPN-type)
- 100 and 1 k Ω resistors

Figures 3.24, 3.25 and 3.26 show the circuit layout, 2N4401 pin configuration, and circuit photo. Transistors come in several different packages, but the TO-92 plastic package is the most common (Fig. 3.25).

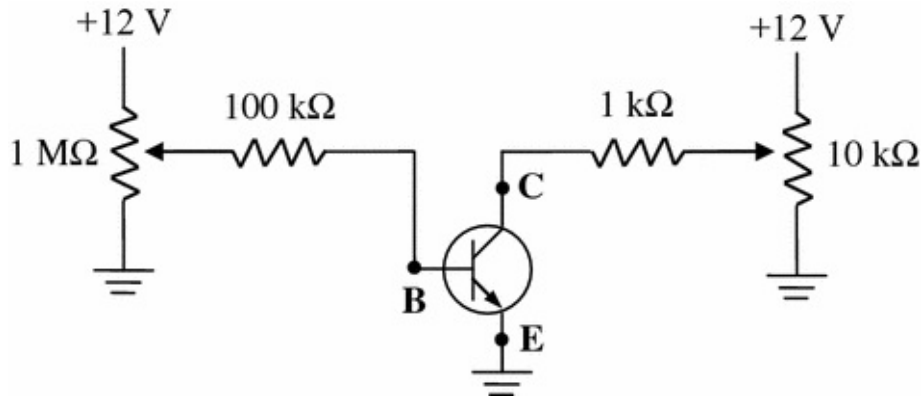


Fig. 3.24 Circuit diagram for Task 3

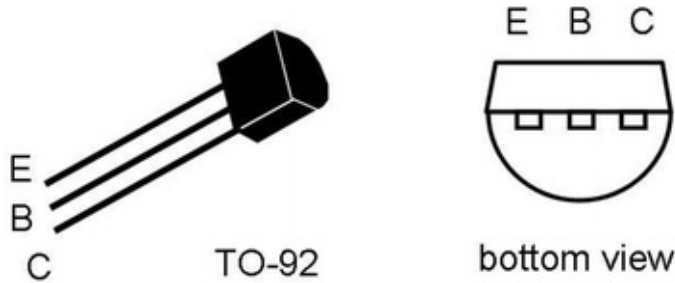


Fig. 3.25 TO-92 plastic package for 2N4401 transistor. *E*—Emitter; *B*—Base; *C*—Collector. *Left* view with the flat face toward you. *Right* view with the leads pointing toward you

The circuit layout indicates a larger pot and resistor are used on the base side of a transistor, while smaller ones are used on the collector side. Why? A transistor is basically a current amplifier; a small current to the base produces a much larger current flow from the collector to the emitter. Like a water faucet, the amount of current applied to the base controls the collector–emitter current.

Figure 3.26 shows the base current, I_B , can be measured from the voltage drop across the $100\text{ k}\Omega$ resistor, just like we did in Tasks 1 and 2. The collector current, I_C , can be measured from the voltage drop across the $1\text{ k}\Omega$ resistor. Let us initially set $I_B = 0\text{ mA}$ by adjusting the $1\text{ M}\Omega$ pot, and set $V_{CE} = +5\text{ V}$ by adjusting the $10\text{ k}\Omega$ pot.

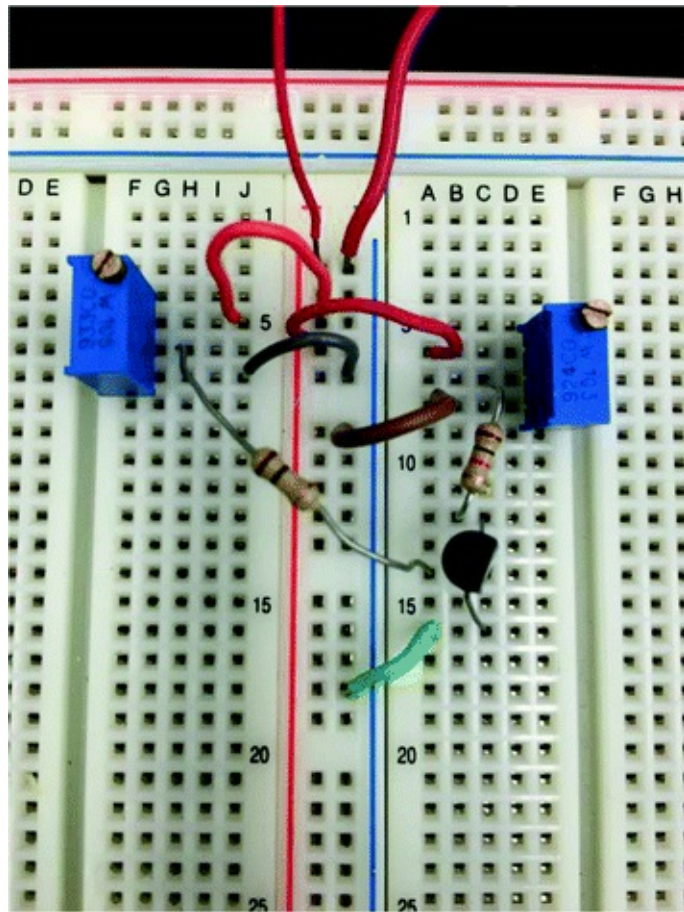


Fig. 3.26 Circuit photo for Task 3

Change I_B by adjusting the $10\text{ M}\Omega$ pot. Each time you make turns of the pot, try to bring V_{CE} back to $+5\text{ V}$. Then record I_B , I_C and V_{BE} . Note that you already know $V_{CE} = +5\text{ V}$. Stop when you either can not make V_{CE} equal to $+5\text{ V}$ or when $I_C \geq 60\text{ mA}$.

Once you are finished, you can plot I_C against I_B , showing how I_B can amplify and control I_C ($\approx I_E$). The transistor gain β can be easily calculated from the slope of the $I_C - I_B$ curve (Fig. 3.27).

V_{100k}	0	0.01	0.45	1.01	1.51	1.96	2.43	2.87	3.34		
V_{1k}	0	0.01	0.75	1.36	2.37	3.27	3.86	4.34	4.74		

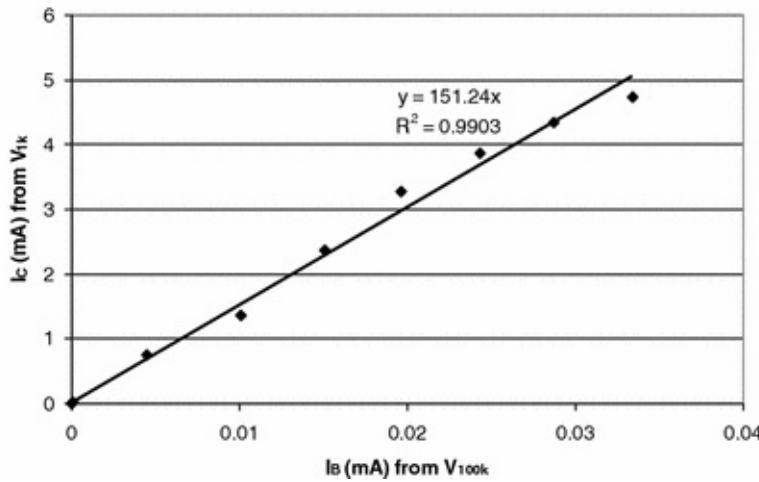


Fig. 3.27 Experimental data of Task 3: I_C against I_B

You can also plot I_C against V_{BE} , and will notice a certain amount of voltage is needed to make the current flow (Fig. 3.28). This curve looks very similar to that of Task 2. This is because the base-emitter part (P–N) of a bipolar transistor is a diode (P–N).

V_{1k}	0	0.01	0.75	1.36	2.37	3.27	3.86	4.34	4.74	4.79	4.85
V_{BE}	0	0.5	0.62	0.63	0.63	0.65	0.66	0.66	0.66	0.67	0.67

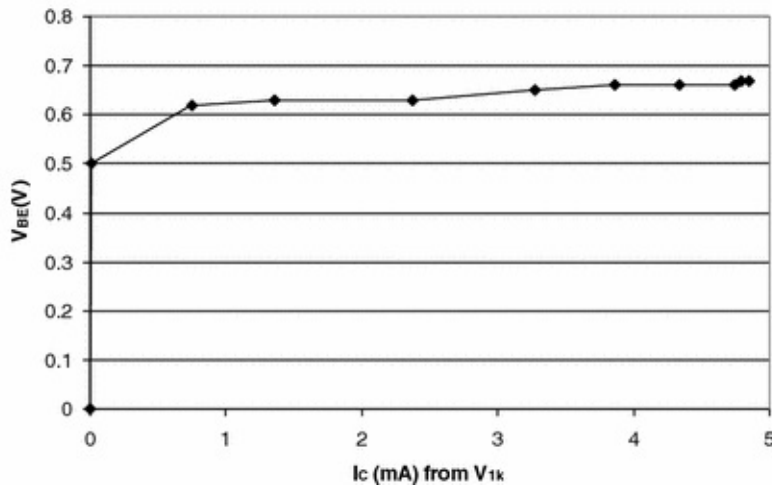


Fig. 3.28 Experimental data from Task 3: V_{BE} against I_C

Alternative Task 3: Transistor

Repeat Task 3 while maintaining V_{CE} at +10 V. This curve should look very

similar to that of Task 3. Estimate the transistor gain β .

Question 3.4

Determine the transistor gain β from the specification sheet of the 2N4401, which can be easily found on the web. For the given I_C and V_{CE} , is the measured transistor gain β in the acceptable range?

References and Further Readings

- Gibilisco S (2006) Teach yourself electricity and electronics, 4th edn. McGraw-Hill, New York
- Kybett H, Boysen E (2008) All new electronics self-teaching guide, 3rd edn. Hoboken, Wiley
- Mims F III (2003) Getting started in electronics, 3rd edn. Master Publishing, Lincolnwood
- Neamen D (2005) An introduction to semiconductor devices. McGraw-Hill, New York
- Pierret R (1996) Semiconductor device fundamentals, 2nd edn. Addison Wesley, Upper Saddle River
- Scherz P (2006) Practical electronics for inventors, 2nd edn. McGraw-Hill, New York
- Sze S (2008) Semiconductor devices: physics and technology, 2nd edn. Wiley, Hoboken
- Turley J (2002) The essential guide to semiconductors. Prentice-Hall, Upper Saddle River

4. Temperature Sensors

Jeong-Yeol Yoon¹✉

(1) University of Arizona, Tucson, AZ, USA

✉ Jeong-Yeol Yoon
Email: jyyoon@email.arizona.edu

In the previous chapters, we have learned about the very basic building blocks for constructing an electronic circuit—resistors, diodes, and transistors. In this chapter, we will learn how these basic components can be used as transducers to sense physical variables (or *physical sensors*).

Temperature sensors are probably the most studied and the most widely used type of physical sensors . Temperature sensors are commonly used together with biosensors, as temperature is a very important parameter for many biological systems. Especially for this type of application, temperature sensors must exhibit high sensitivity and fast response. The semiconductor temperature sensors, i.e., resistor-, diode-, and transistor-based, show much higher sensitivity compared to the others. These are typically operated in direct contact with media (usually water), and their response is very fast. Therefore, we will focus on the semiconductor temperature sensors in this chapter; namely, thermocouple, thermistor, diode, and transistor temperature sensors.

4.1 Thermocouple

A *thermocouple* is perhaps the oldest type of temperature sensor . It consists of two dissimilar metals joined together as shown in Figs. 4.1 and 4.2. The temperature where two metals joined together is referred to as the *hot junction temperature* , or T_{hot} ; the temperature at the open junction is the *cold junction temperature* , or T_{cold} . If there is temperature difference between T_{hot} and T_{cold} ,

heat flows through these metals. In turn, this heat flow creates a flow of electrons (thus electric current) which is known as the *Seebeck effect*.

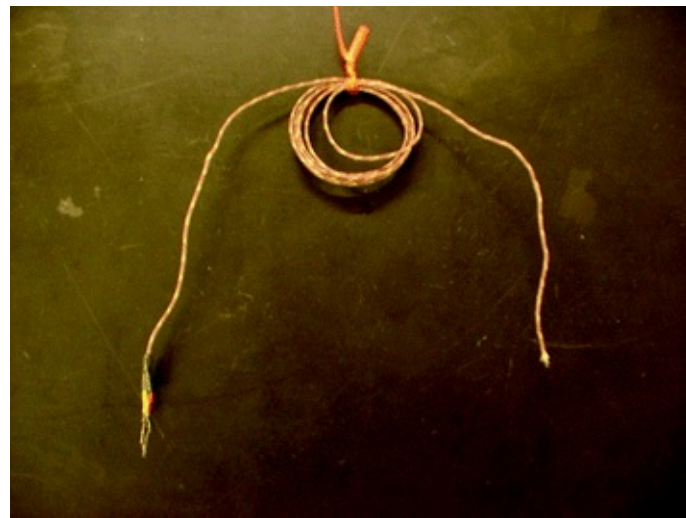


Fig. 4.1 A thermocouple (type K)

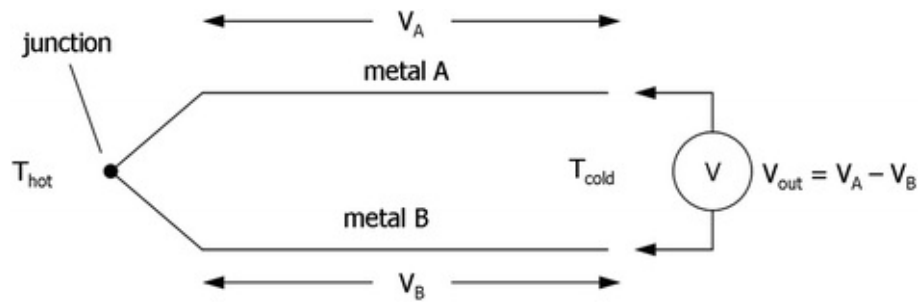


Fig. 4.2 Working principle of a thermocouple

Although metals are considered conductors, they do have a small degree of resistance, which should create voltage drops for each metal. As two different types of metals are used which have different resistances, the voltage drops should be also different from each other. $V_{out} = V_A - V_B$ is measured at the cold junction, which is a function of the metal pair used and the temperature difference ($T_{hot} - T_{cold}$). V_{out} is linearly proportional to the temperature difference, and the slope is determined by the metal pair used. Essentially, the thermocouple is a resistor-type temperature sensor, where the pair of metals acts as resistors with extremely low resistance values.

The typical voltage output of thermocouples is usually between 15 and 40 μV per $^{\circ}\text{C}$. The actual slope of the V_{out} —temperature curve varies with the choice of metal pair. Several metal combinations are referred to as Type E, J, K,

R, S and T, as shown in Fig. 4.3.

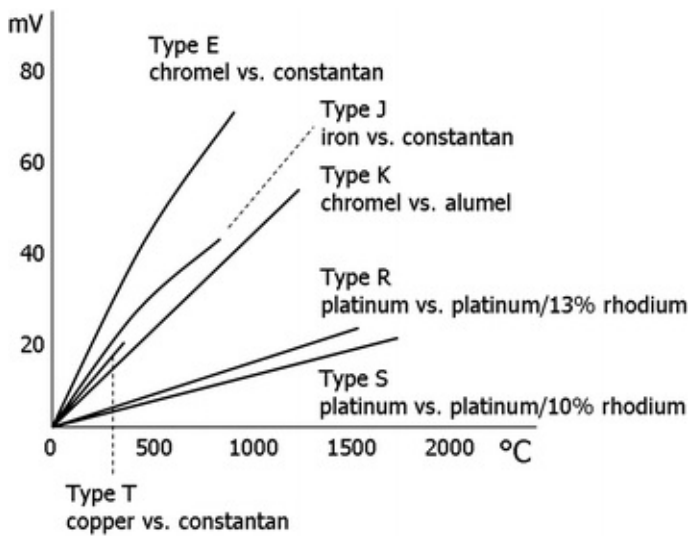


Fig. 4.3 The choice of metal combination affects the voltage output of a thermocouple



Fig. 4.4 A thermistor

As shown in Fig. 4.3, a thermocouple can be used for a wide range of temperatures up to 1500 °C, and its temperature response is quite linear. Its sensitivity, however, is inferior to the other temperature sensors described in this chapter—thermistor, diode and transistor temperature sensors.

4.2 Thermistor

If conductor metals can be used to sense temperature, perhaps conventional

resistors may be used as temperature sensors as well. In fact, there is a special type of resistor that is very sensitive to temperature changes, which is called a *thermistor* (thermal resistor) (Fig. 4.4).

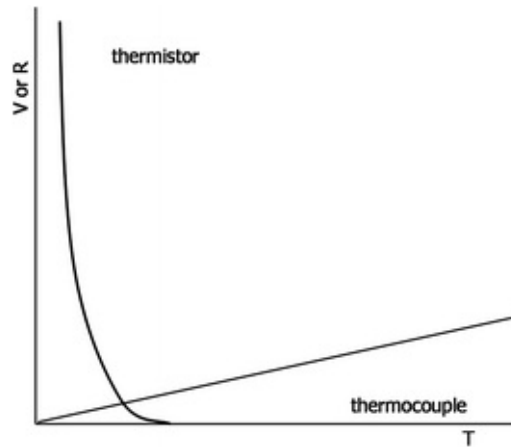


Fig. 4.5 Temperature response curves for thermistor and thermocouple

Unlike a thermocouple, however, the voltage drop across a thermistor (resulting from the resistance of thermistor) is inversely related to the temperature. This means that the voltage drop, or resistance, decreases as temperature increases. More specifically, this relationship is approximated through the use of following curve-fitting equation

$$1/T = A + B \ln R + C(\ln R)^3 \quad (4.1)$$

where

T degrees Kelvin (K)

R resistance of thermistor (Ω)

A, B and C curve-fitting constants

This equation is called the *Steinhart-Hart equation*. This temperature response of thermistor is shown in Fig. 4.5 in comparison with that of the thermocouple. In the low temperature region, the voltage drop or resistance of thermistor changes a lot more than that of the thermocouple. A thermistor is essentially a superior temperature sensor compared to a thermocouple, if it is used within a limited temperature range of usually -90°C to 130°C . For most temperature sensing purposes, especially for use in conjunction with biosensors, this range is more than enough. Any temperatures outside this range can cause permanent damage to thermistors. An additional benefit of a thermistor is its

compact size; it is essentially a single piece of resistor, which can be incorporated in any part of a circuit.

Despite being inferior to the thermistor, thermocouples are still being used today for applications that require (1) a linear signal and/or (2) the ability to sense very high temperature (over 130 °C and up to 1500 °C; like ovens and furnaces).

4.3 Diode Temperature Sensor

Both diodes and transistors can be used to sense temperature, just like resistor-based temperature sensors (thermocouples and thermistors). The specific type of diode that can be used for temperature sensing is the *Zener diode*. The I - V curve of a typical Zener diode is illustrated in Fig. 4.6.

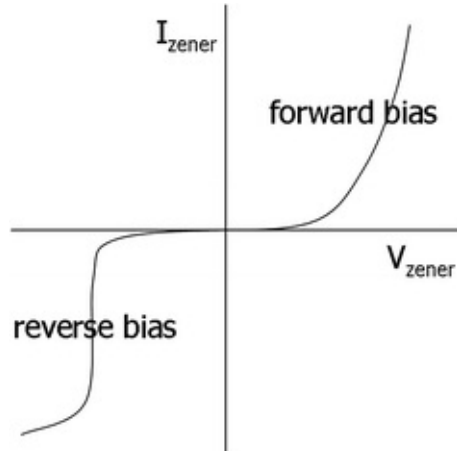


Fig. 4.6 Typical I - V curve of the Zener diode

The Zener diode is especially important in a reverse bias configuration, which makes the Zener a unique type of diode. The reverse bias operation of a Zener diode can be redrawn using negative quadrants in Fig. 4.7.

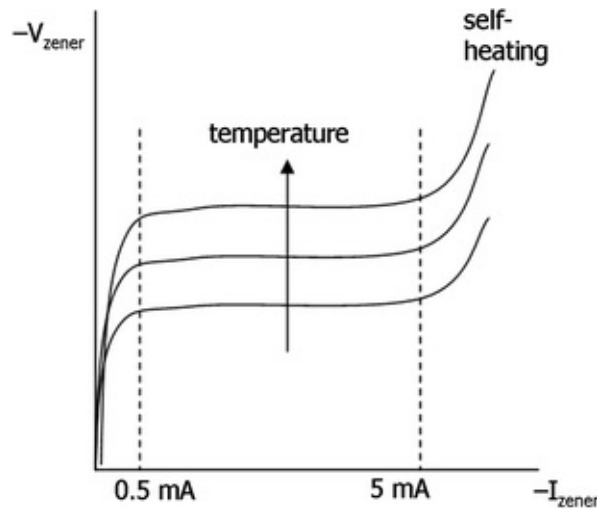


Fig. 4.7 V–I curve of a Zener diode in reverse bias

For a certain range of Zener currents, 0.5–5 mA in the above case, the Zener voltage stays constant. This plateau voltage changes with the environmental temperature. Additionally, this plateau voltage is linearly proportional to the temperature value (degrees in Kelvin). This indicates that we can use a Zener diode to sense temperature within a certain current range. Figure 4.7 shows that if the Zener current is too low, you will get a voltage output which is also low; if the Zener current is too high, it will heat itself (self-heating). However, depending on the diode model, this self-heating effect may not be significant.

Most Zener diode temperature sensors are designed to generate a voltage signal that conveniently matches the temperature value. For the *LM335* that we will use in this chapter's laboratory exercise, it generates 2.73 V for 273 K, 3.00 V for 300 K, and so forth. The accompanying circuit to achieve this goal is integrated together with a Zener diode in the form of an *integrated circuit (IC)*. The typical temperature range of Zener diode sensors is -40 to $+120$ °C, which is not very different from that of a thermistor. Its sensitivity is also comparable to that of a thermistor. The real benefit of a Zener diode temperature sensor is its linear signal. This linearity comes at a price, however; a Zener diode temperature sensor is an IC and quite expensive while thermistors are essentially a single-piece resistor and thus are relatively cheap.

4.4 Transistor Temperature Sensor

From Task 3 of Chap. 3, we learned that the I_C – V_{BE} curve of a transistor was very similar to that of a Zener diode, because the base-emitter part (P–N) of a

bipolar transistor is actually a diode (P–N). If we connect the base and collector leads together, the bipolar transistor behaves very similar to a diode (Fig. 4.8). The temperature range of transistor is about the same as that of a Zener diode, and its signal is linear over a range of temperatures.

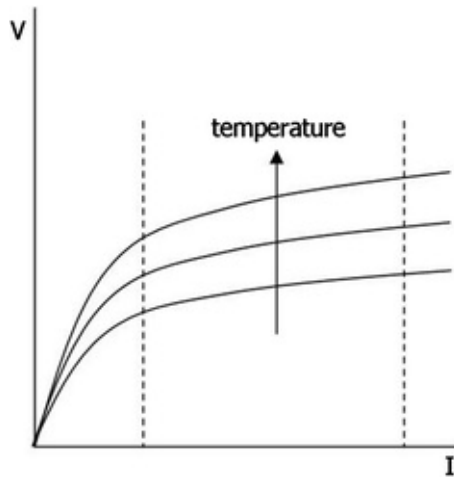


Fig. 4.8 V–I curve of a bipolar transistor

Unfortunately, the output voltage varies slightly against the input current. Therefore, we need to provide a fixed amount of current to get a constant voltage reading. This can be achieved easily by using a constant current source, such as the LM334 . Note that the LM334 is very similar to the LM335, which is a Zener diode temperature sensor. The major difference between these two integrated circuits is that the LM335 generates a constant voltage output for a wide range of input current, while the LM334 generates constant current output for a wide range of input voltage. In this regard, the LM334 can also be used as a temperature sensor.

Despite this small dependency on input current, a transistor temperature sensor is an economical choice over a Zener diode temperature sensor, as transistors are much cheaper in general because they are mass produced. The demand for transistors is much greater than that of Zener diodes or their IC version such as the LM335. This is especially true when a single current source (LM334) can be used to power up multiple transistor temperature sensors. Let us take an example of installing 20 temperature sensors. If 20 LM335's (Zener diode ICs) are used, the total cost is $\$1.35 \times 20 = \27 . If a single LM334 (a constant current source) is used to power up 20 2N4401's (transistors), the total cost is $\$1.20$ (LM334) + $\$0.03$ (2N4401) $\times 20 = \$1.80$. If the accuracy is not a major concern and the circuit provides relatively constant current, a transistor

can be used stand-alone, which only costs pennies.

4.5 Laboratory Task 1: Thermistor

In this task, you will need the following:

- Breadboard, wires, wire cutter/stripper, a power supply, and a DMM.
- A thermistor ($30\text{ k}\Omega$ at 25°C)
- $1\text{ k}\Omega$ resistor

Figures 4.9 and 4.10 show the circuit layout. This circuit is essentially a voltage divider, with the top resistor replaced with a thermistor. Let us measure V_{in} , V_{out} , and the resistor values of R_1 (thermistor) and R_2 ($1\text{ k}\Omega$) at room temperature. You can calculate the theoretical voltage output V_{out} using the input voltage V_{in} and the measured resistances of R_1 and R_2 . Compare this theoretical V_{out} with the experimentally obtained V_{out} . Then, repeat the whole experiment while holding the thermistor firmly with your finger, to increase its temperature.

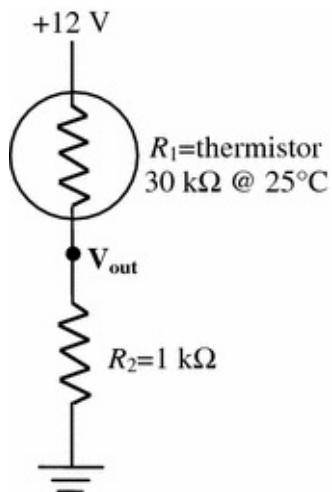


Fig. 4.9 Circuit diagram for Task 1

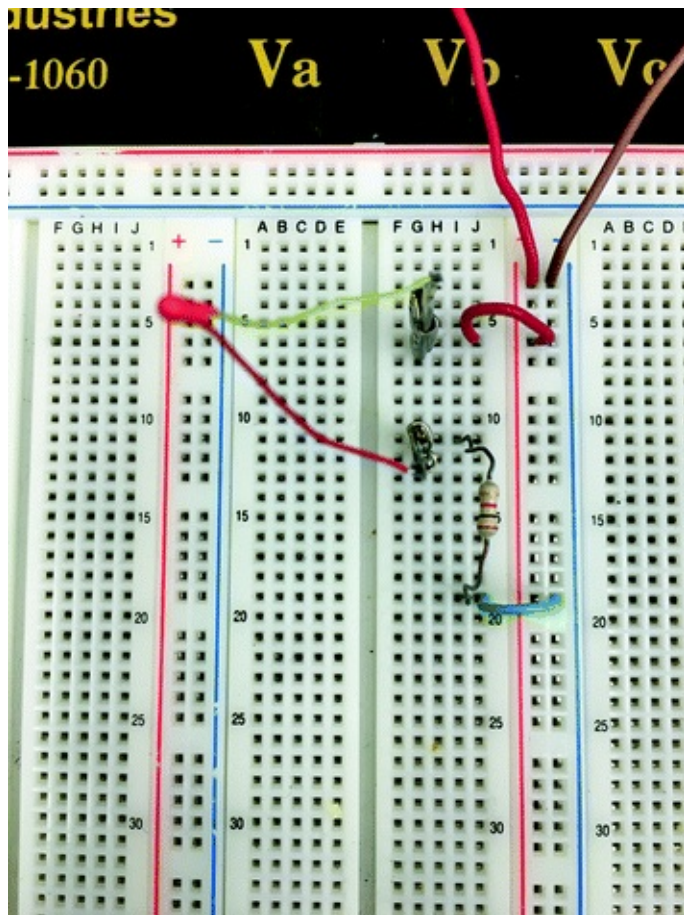


Fig. 4.10 Circuit photo of Task 1

Table 4.1 clearly indicates the nonlinear, inversely proportional response of a thermistor.

Table 4.1 Experimental data from Task 1

	V _{in} (V)	R ₁ (kΩ)	R ₂ (kΩ)	V _{out} , theoretical (V)	V _{out} , experimental (V)
RT	12.00	31.4	0.986	0.365	0.395
w/finger	12.00	23.2	0.986	0.489	0.500

Alternative Task 1a: V-T or R-T Curve of a Thermistor

Expose the thermistor to various temperatures; preferably take more than four data points. Measure the actual temperatures using a thermometer. Using the same circuit of Task 1, measure V_{in} , V_{out} , R_1 (thermistor), and R_2 (1 kΩ) for each temperature. The voltage drop across the thermistor should be $V_{in} - V_{out}$. Then plot both the voltage drop and R_1 against temperature and see whether it behaves the same as Fig. 4.5. In addition, plot the inverse of temperature ($1/T$)

against the log resistance ($\log R$) of a thermistor. Perform linear regression to Eq. 4.1 and evaluate the curve-fitting constants A , B , and C of Steinhart–Hart equation.

Alternative Task 1b: Regular Resistor as Temperature Sensor

Regular resistors can be used as temperature sensors, which should behave the same as thermistors. The only difference is its inferior sensitivity. Repeat the whole Task 1 using 1 k Ω resistor and see if you can get any change in resistance or voltage drop across it.

4.6 Laboratory Task 2: Zener Diode Temperature Sensor

In this task, you will need the following:

- Breadboard, wires, wire cutter/stripper, a power supply, and a DMM.
- 10 or 20 k Ω pot and a screw driver
- Diode temperature sensor LM335
- 1 Ω resistor
- Thermometer (optional)

Figures 4.11, 4.12 and 4.13 show the circuit layout, LM335 pin configuration, and circuit photo. As explained earlier, the *LM335* is an integrated circuit which contains more than a Zener diode. However, for this exercise, treating it as a single Zener diode is sufficient. The cathode (+) of the LM335 is connected to the positive voltage and the anode (−) is connected to GND, indicating that the Zener diode is configured in a reverse bias. The third lead, labeled “adj,” is not used in most cases. Leave this lead open; do not insert this lead into the breadboard.

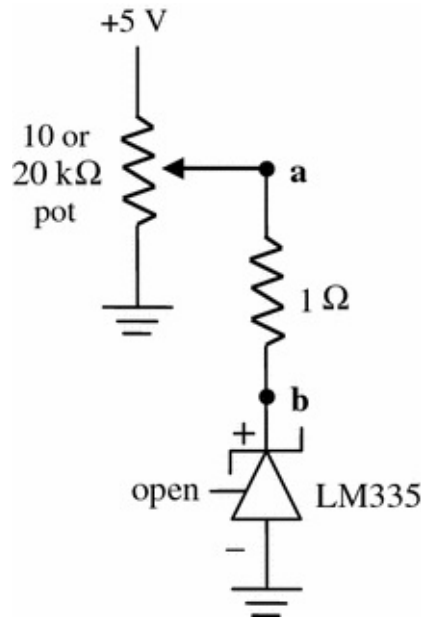


Fig. 4.11 Circuit diagram for Task 2

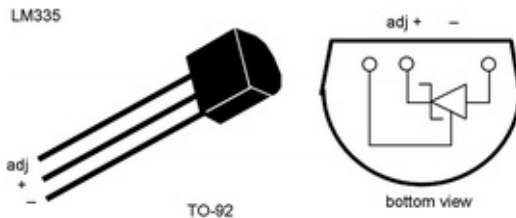


Fig. 4.12 TO-92 plastic package for LM335 diode temperature sensor. *Left* view with the flat face toward you. *Right* view with the leads pointing toward you

The $1\ \Omega$ resistor is used to evaluate the current flowing in this circuit. Compare this setup with Tasks 1 and 2 of Chap. 3. Since the LM335 is set to reverse bias, both $V_{ab} (=V_a - V_b)$ and I_{LM335} should have negative values. You may think that you can measure V_a and V_b separately and make a subtraction, but that is not really possible. Both V_a and V_b are on a scale of several volts, while their difference is only in millivolts (mV scale). You want to insert the two leads of your DMM to directly measure V_{ab} . V_{LM335} is the voltage drop across the LM335, which should be the same as V_b .

Adjust your pot to produce a stepwise change in I_{LM335} (from V_{ab}) and record V_{LM335} (from V_b). Plot V_{LM335} against I_{LM335} . Note that your readings of V_{ab} and V_b are all positive, even though the LM335 is configured in reverse bias. That is because you used a positive voltage source. From the LM335's viewpoint, these readings are all (actually) negative.

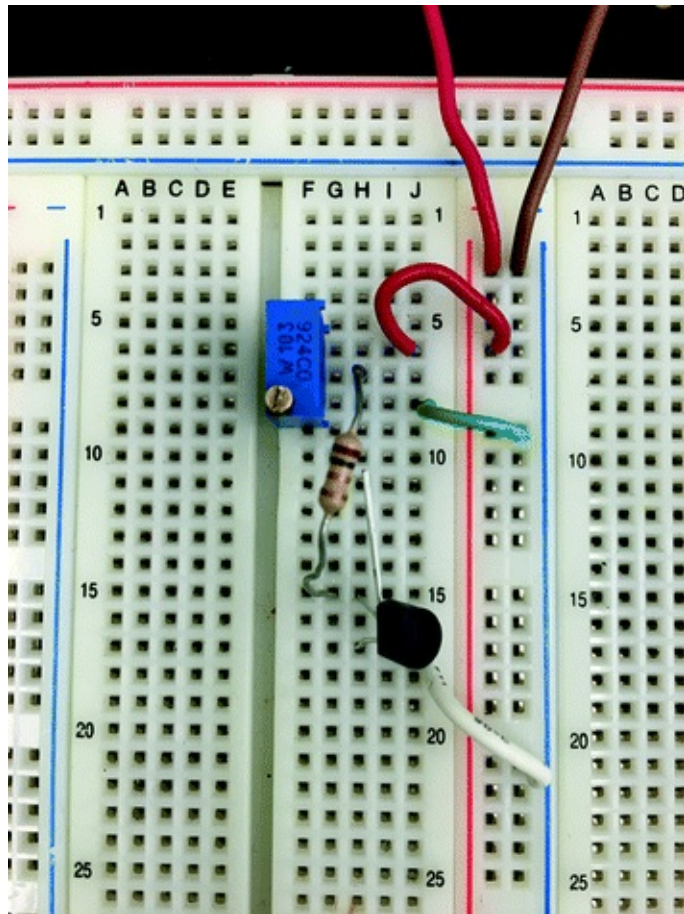


Fig. 4.13 Circuit photo of Task 2

Figure 4.14 shows the experimental result obtained with an ambient temperature of 298 K. For a current range of 0.5–5 mA, the output voltage remained constant at 2.98 V, corresponding to the 298 K temperature.

V_{ab}	0	0	0	0	0.1	0.1	0.1	0.3	0.4	0.5	1	1.5
V_b	0	0.18	0.3	1.25	1.31	1.51	1.61	2.72	2.97	2.97	2.97	2.98
V_{ab}	2	2.5	3.7	4.4	5.8	6.8	8.6	72.1	121.3	132	135	
V_b	2.98	2.98	2.98	2.99	2.99	3	3.08	3.28	3.41	4.36	5.05	

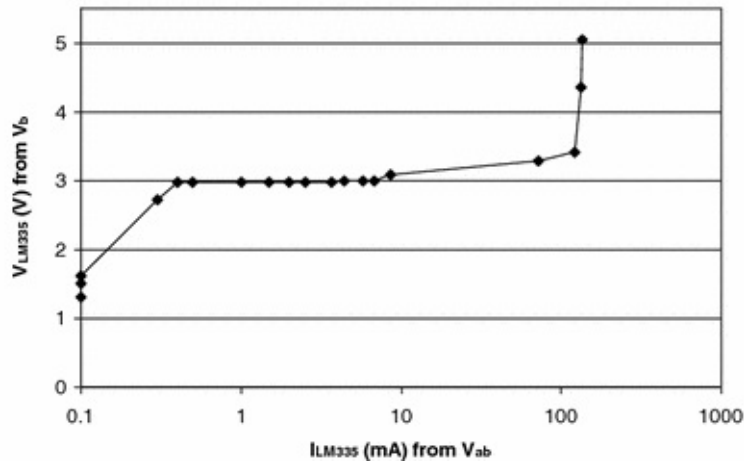


Fig. 4.14 Experimental data from Task 2

You can repeat this experiment while holding the LM335 with your finger to increase the temperature. The open symbols in Fig. 4.15 show a higher voltage output, 3.03 V, indicating the experimenter's finger temperature is 303 K. Note that this is somewhat lower than the normal internal body temperature of a human, 310 K (37 °C).

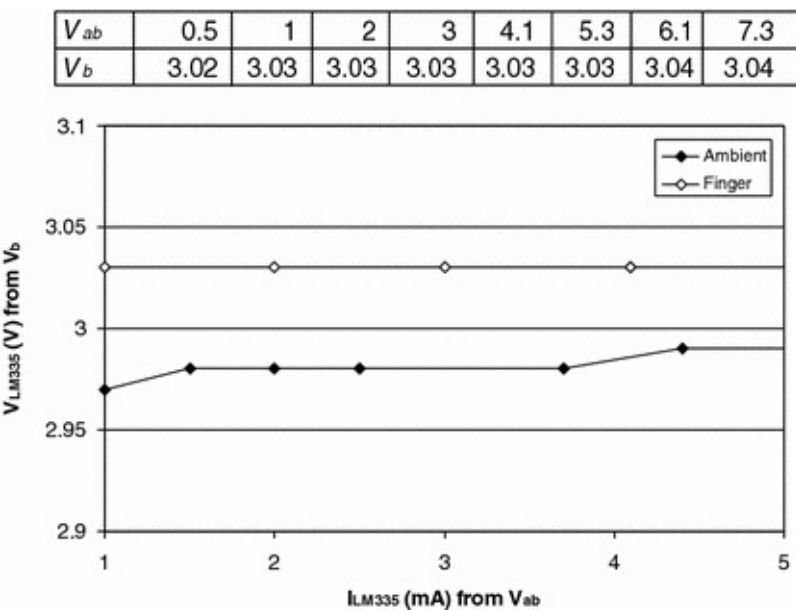


Fig. 4.15 Experimental data from Task 2, LM335 held in fingers (open symbols)

Question 4.1

Apply a current higher than 5 mA to the circuit, so that the LM335 self-heats. Assume that the voltage output is 3.10 V. What will happen to the output voltage if you hold this self-heated LM335 with your finger? Assume your finger temperature is 300 K.

4.7 Laboratory Task 3: Transistor Temperature Sensor

In this task, you will need the following:

- Breadboard, wires, wire cutter/stripper, a power supply, and a DMM.
- 10 or 20 k Ω pot and a screw driver
- Constant current source LM334
- Four 68 Ω resistors
- Transistor 2N4401
- 1 Ω resistor
- Thermometer

Figures 4.16, 4.17 and 4.18 show the circuit layout, LM334/2N4401 pin configurations, and circuit photo. There is a bypass resistor circuit, consisting of one 68 Ω resistor or four 68 Ω resistors in parallel. The input set current will be divided into two branches:

$$I_{\text{set}} = I_R + I_{\text{bias}} = \frac{V_R}{R_{\text{set}}} + I_{\text{bias}} \quad (4.2)$$

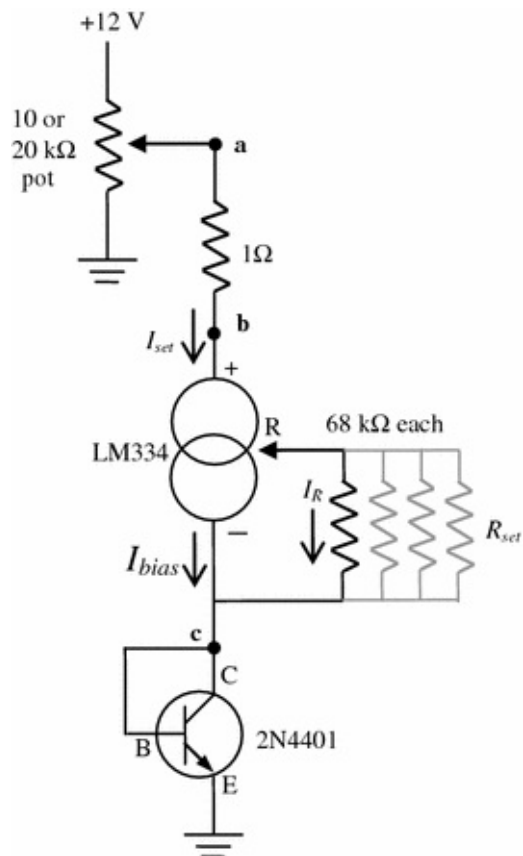


Fig. 4.16 Circuit diagram for Task 2

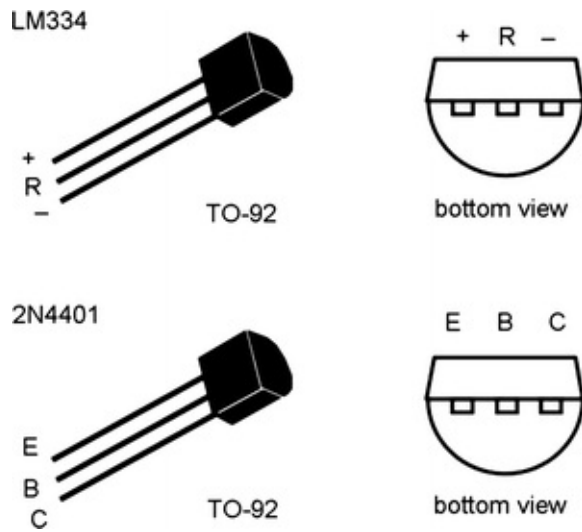


Fig. 4.17 TO-92 plastic package for LM334 constant current source (*top*) and 2N4401 transistor (*bottom*). *Left* view with the flat face toward you. *Right* view with the leads pointing toward you

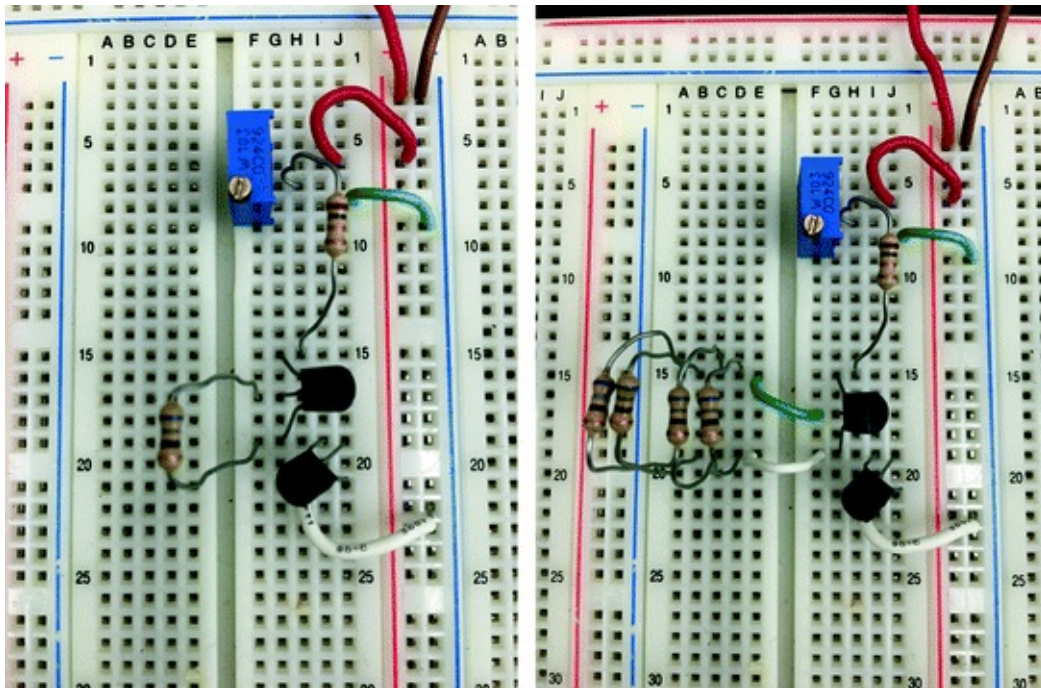


Fig. 4.18 Circuit photos of Task 3, with one $68\ \Omega$ resistor (left) or four $68\ \Omega$ resistors (right)

The ratio of I_{set} to I_{bias} is constant for a given range of input set current. For the LM334, $n = I_{\text{set}}/I_{\text{bias}} = 18$. Therefore, $I_{\text{bias}} = I_{\text{set}}/18$. Plugging this I_{bias} into Eq. 4.2 gives

$$I_{\text{set}} = \frac{V_R}{R_{\text{set}}} + \frac{I_{\text{set}}}{18}$$

$$I_{\text{set}} = \frac{V_R}{R_{\text{set}}} (1.059) \quad (4.3)$$

V_R is a function only of temperature, $V_R = 0.227\ \text{mV/K}$. At room temperature of $25\ ^\circ\text{C} = 298\ \text{K}$, $V_R = 67.6\ \text{mV}$. With $R_{\text{set}} = 68\ \Omega$, you should get a current output of $1.05\ \text{mA}$ for a range of voltage supply. Although LM334 can also be affected by the ambient temperature, its sensitivity ($0.227\ \text{mV/K}$) is much inferior to $10\ \text{mV/K}$ of LM335 ($2.98\ \text{V}$ for $298\ \text{K}$), thus functioning as a reliable constant current source under small temperature variations.

Adjust the pot to generate a voltage supply (V_a) from 0 to 12 V, and using one $68\ \Omega$ resistor with the LM334, evaluate the current output by measuring V_{ab} . Remember that the current flowing through the $1\ \Omega$ resistor should be identical to the current flowing through the LM334 and 2N4401 by conservation of current.

V_a	0	0.18	0.4	0.72	0.97	1.24	1.29	1.32	1.36	1.39	1.4	1.42
V_{ab}	0	0	0	0	0.1	0.2	0.4	0.4	0.5	0.6	0.7	0.8
V_c	0	0.03	0.13	0.32	0.44	0.57	0.58	0.59	0.6	0.6	0.61	0.61
V_a	1.48	1.52	3.21	4.69	7.88							
V_{ab}	0.9	1	1	1	1							
V_c	0.62	0.62	0.62	0.62	0.62							

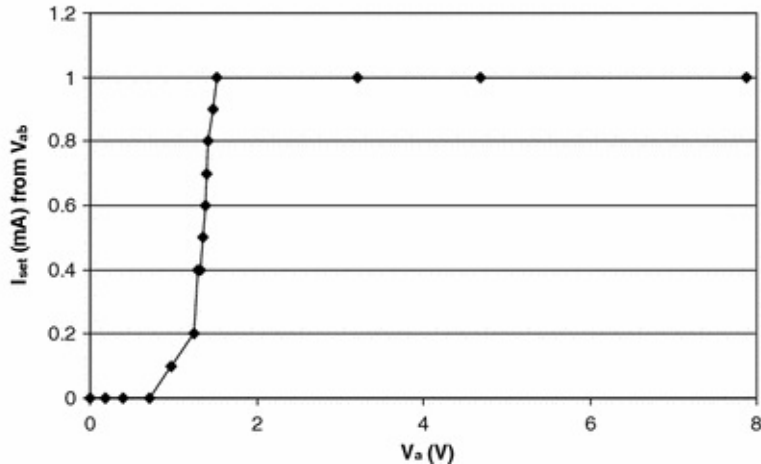


Fig. 4.19 Experimental data from Task 3: LM334 constant current source

I_{set} initially increases rapidly in the low voltage region, but it levels off after a certain point and remains constant (~ 1 mA) beyond this point (Fig. 4.19).

During these measurements, also simultaneously measure V_c , the voltage drop across the 2N4401 transistor, which acts like a diode in this setup. Notice that V_c becomes constant once you achieve the constant current output from the LM334. Note that this V_c is equal to V_{BE} as well as V_{CE} , since the base and collector are connected together (Fig. 4.20).

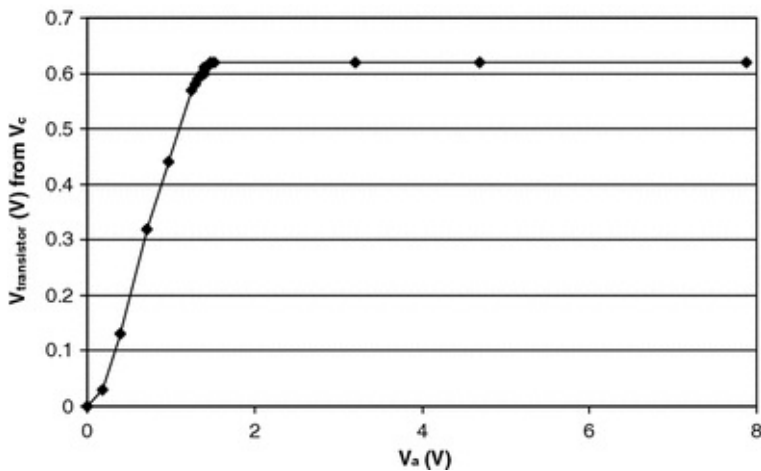


Fig. 4.20 Experimental data from Task 3: transistor temperature sensor

V _a	0	0.21	0.71	1.17	1.24	1.3	1.34	1.36	1.39	1.4	1.42	1.45
V _{ab}	0	0	0	0	0.1	0.2	0.4	0.4	0.6	0.6	0.7	0.8
V _c	0	0.05	0.31	0.54	0.57	0.59	0.61	0.61	0.62	0.62	0.62	0.62
	1.6	2.5	4	7.2	11.46							
	1	1	1	1	1							
	0.62	0.63	0.63	0.63	0.63							

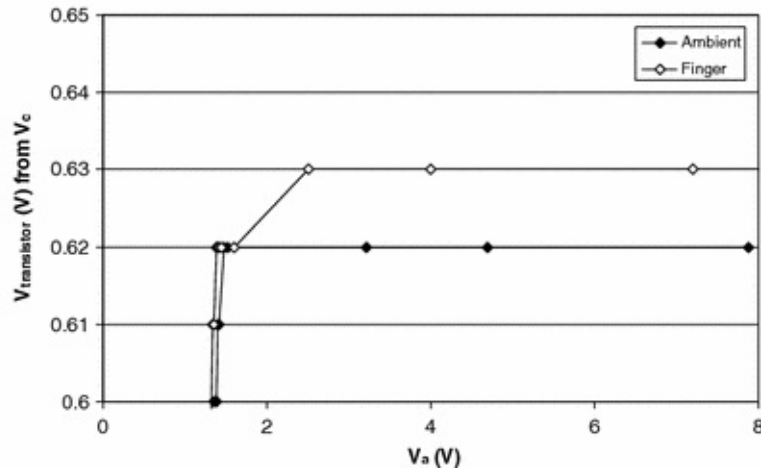


Fig. 4.21 Experimental data from Task 3, with 2N4401 held in fingers (open symbols)

The open symbols show the same curve while holding the 2N4401 between your fingers, showing slightly higher voltage output (Fig. 4.21).

Alternative Task 3: Transistor Temperature Sensor

Install four $68\ \Omega$ resistors in parallel to the LM334. R_{set} is now a quarter of $68\ \Omega$, i.e., $17\ \Omega$, and I_{set} should be quadrupled, i.e., $\sim 4\ \text{mA}$. Repeat Task 3. You should get somewhat higher voltage readings for both ambient and finger-holding conditions.

Question 4.2

Calculate I_{set} of the LM334 if $R_{\text{set}} = 1\ \text{k}\Omega$. Can you estimate $V_{\text{transistor}}$ with this I_{set} ?

References and Further Readings

Michalski L, Eckersdorf K, Kucharski J, McGhee J (2001) Temperature measurement, 2nd edn. Wiley, Hoboken

Pertijs M, Huijsing J (2006) Precision temperature sensors in CMOS technology, 1st edn. Springer, New York

Pollock D (1991) Thermocouples: theory and properties, 1st edn. CRC Press, Boca Raton

Ristic L (ed) (1994) Sensor Technology and Devices. Artech House: Norwood, MA

Webster J (1998) The measurement, instrumentation and sensors handbook, 1st edn. CRC Press, Boca Raton

5. Wheatstone Bridge

Jeong-Yeol Yoon¹✉

(1) University of Arizona, Tucson, AZ, USA

✉ Jeong-Yeol Yoon
Email: jyyoon@email.arizona.edu

In Tasks 2 and 3 of previous chapter's laboratory (diode and transistor temperature sensors), we measured V_{ab} across the $1\ \Omega$ resistor to evaluate the current. We did not measure V_a and V_b separately and make a subtraction, as both are on a scale of several volts (measured in 0–20 V scale), while their difference is only in millivolts (measured in 0–200 mV scale). If you have a DMM, you can connect one of its leads to the position a and the other to b to measure this tiny voltage drop. This is not really possible if you plan to develop a stand-alone sensing device.

In fact, this type of voltage measurement is known as a differential measurement, a common metric particularly in biosensor applications. Many biosensors measure a tiny difference in voltage, current or resistance in comparison with that of a blank or a negative control. If you try to make measurements for the target and the blank separately and evaluate their tiny difference by subtraction, you will need a sensor that has extremely high accuracy and sensitivity, perhaps with six or more significant digits.

There is a simple solution for it: a *Wheatstone bridge*. In the past, it has been used primarily for strain gauge applications, but more recently for a bio-application in the form of a cantilever biosensor. In reality, a Wheatstone bridge can be used for any differential measurement for both physical and biosensors.

5.1 Wheatstone Bridge

A Wheatstone bridge is an electrical circuit used to measure a very small change in resistance, such as a $10\ \Omega$ decrease for a $10\ k\Omega$ resistive load. This small change is not readily detectable by a typical DMM in the $0\text{--}20\ k\Omega$ range. The Wheatstone bridge consists of four resistors arranged in a diamond configuration. An input DC voltage, or excitation voltage, is applied between the top and bottom of the diamond, and the output voltage is measured across the middle. When the output voltage is zero, the bridge is said to be balanced. One (or more) of the legs of the bridge may consist of a resistive transducer, such as a thermistor or a strain gauge (often as R_4 in Fig. 5.1). The other legs of the bridge are simply completion resistors with resistance equal to that of a selected resistive transducer. As the resistance of one of the legs changes, the previously balanced bridge becomes unbalanced; this can occur when a temperature or strain from a resistive transducer changes, for example. The unbalance in the bridge causes a voltage to appear across the middle of the bridge. This induced voltage may be measured with a voltmeter, or the resistor in the opposite leg to the changed resistor may be adjusted to rebalance the bridge. In either case, the change in resistance that caused the induced voltage may be measured and converted to obtain the engineering units of temperature or strain.

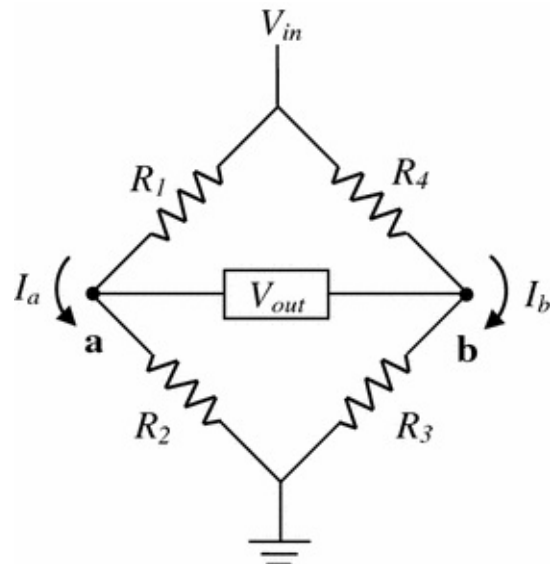


Fig. 5.1 A wheatstone bridge

The Wheatstone bridge circuit in Fig. 5.1 contains four resistors arranged in a diamond configuration. A voltage, V_{in} , is supplied across the vertical diagonal of the diamond. The voltage, V_{out} , appears across the pair of terminals connected along the horizontal diagonal.

$$V_{\text{out}} = V_a - V_b = I_a R_2 - I_b R_3 \quad (5.1)$$

and,

$$I_a = \frac{V_{\text{in}}}{R_1 + R_2} \quad \text{and} \quad I_b = \frac{V_{\text{in}}}{R_3 + R_4} \quad (5.2)$$

therefore,

$$\frac{V_{\text{out}}}{V_{\text{in}}} = \frac{R_2}{R_1 + R_2} - \frac{R_3}{R_3 + R_4} \quad (5.3)$$

When the voltages V_a and V_b are equal, V_{out} will be zero; at this point, the bridge is said to be balanced. In addition, the value of R_4 can be found from:

$$R_1 R_3 = R_2 R_4 \quad \text{or} \quad R_4 = \frac{R_1 R_3}{R_2} \quad (5.4)$$

Assume that the bridge is initially balanced. R_4 is your resistive transducer. The resistance of R_4 is slightly changed. This change can be measured in two different ways:

- Measure V_{out} to calculate the new value of R_4 , using Eq. 5.3.
- Use a variable R_1 and adjust it until $V_{\text{out}} = 0$. Use Eq. 5.4 with the adjusted R_1 value to calculate the new value of R_4 .

Curiously enough, the Wheatstone bridge was not invented by Charles Wheatstone (1802–1875), but by Hunter Christie. However, Wheatstone was responsible for popularizing the arrangement of four resistors, a battery and a galvanometer. He gave Hunter Christie full credit for the Wheatstone bridge in his 1843 Bakerian Lecture. Wheatstone called the circuit a “*differential resistance measurer*.” In regards to Wheatstone’s diamond-pattern, it has been suggested that a set of blue willow pattern China, decorated with cross-hatching on an arched bridge, suggested the shape to him.

5.2 Strain Gauge

The oldest yet still popular application of a Wheatstone bridge would be a *strain transducer*, also known as a *strain gauge*. Obviously *strain* is measured with a strain gauge. Strain (ϵ) is a measure of a body’s deformation, and its definition for either compression or tension is:

$$\epsilon = \frac{\Delta l}{l_0} \quad (5.5)$$

where

Δl change in length

l_0 original length

Figure 5.2 shows a typical setup of a *strain gauge*, which is attached to a body (Fig. 5.3). As the body elongates horizontally, the physical width of a metal coil decreases and the resistance changes accordingly. This resistance change is very small and generally requires a circuit layout known as a *Wheatstone bridge*. The strain gauge is widely used in civil and mechanical engineering applications, but it is also used for an electronic balance.

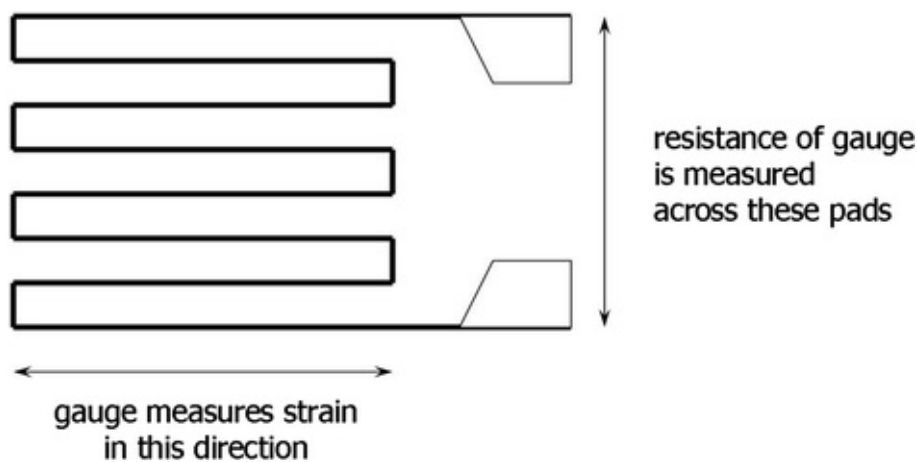


Fig. 5.2 A strain gauge

Strain gauge can also be used to indirectly measure stress (σ), because stress is linearly proportional to strain for a limited range of strain.

$$\sigma = E\varepsilon \quad (5.6)$$

where E = elastic modulus (for compressive or tensile strain)

The elastic modulus E is generally known in literature for many types of materials.

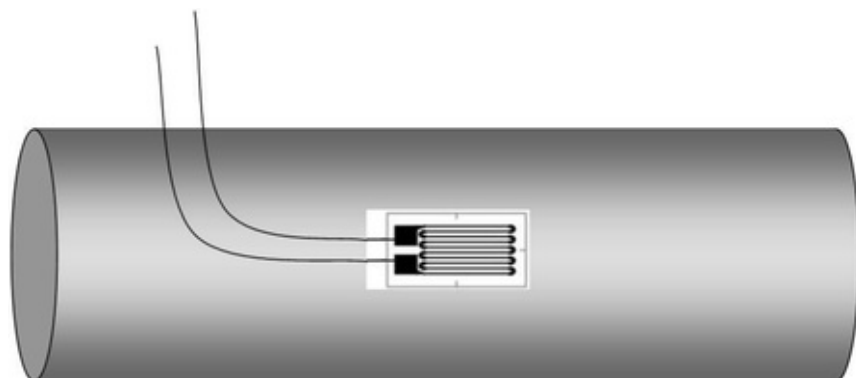


Fig. 5.3 A strain gauge attached to a metal specimen

5.3 Cantilever Biosensor

Recently, strain gauges have been applied to monitor biological reactions, which are often referred to as cantilever bending biosensors, or just *cantilever biosensors*. The working principle of a cantilever biosensor is shown in Fig. 5.4. Upon downward bending of the cantilever, the resistor on top of the cantilever is elongated, which results in an increase in its resistivity. This change in resistivity is read out as an electrical signal via a Wheatstone bridge configuration.

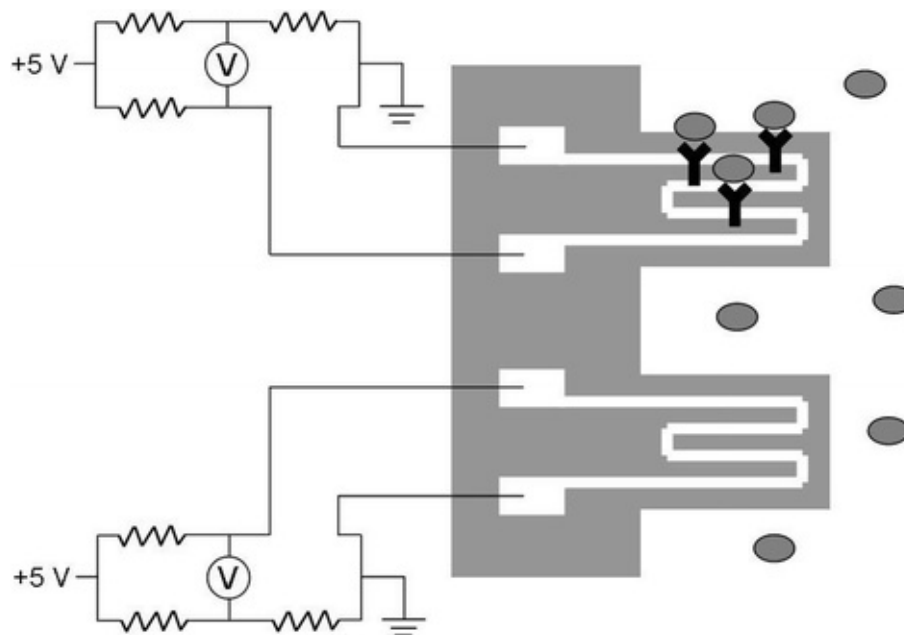


Fig. 5.4 A cantilever biosensor. The antibodies (*Y-shaped*) immobilized on the *top* cantilever capture target molecules, causing it to bend

Many bioreceptors can be used with cantilever biosensors, including antibodies, enzymes, and nucleic acids (Fig. 5.5). For diagnostics, each measuring cantilever is paired with an inert reference cantilever. The reference cantilever is used to filter out thermal and chemical interactions between the surrounding media and the measuring cantilevers, since the reference cantilever is not affected by the molecular reaction on the measuring cantilevers.

The first applications of cantilever sensors for biological systems were reported in 1996 with a single cantilever. The first biosensing experiments with cantilever arrays were demonstrated in 2000, showing the proof-of-principle for DNA detection and the ability to identify single-base mismatches between

sensing and target DNA oligonucleotides.

These cantilever biosensors can be integrated into a lab-on-a-chip device, which also requires a Wheatstone bridge to read out small changes in resistance.

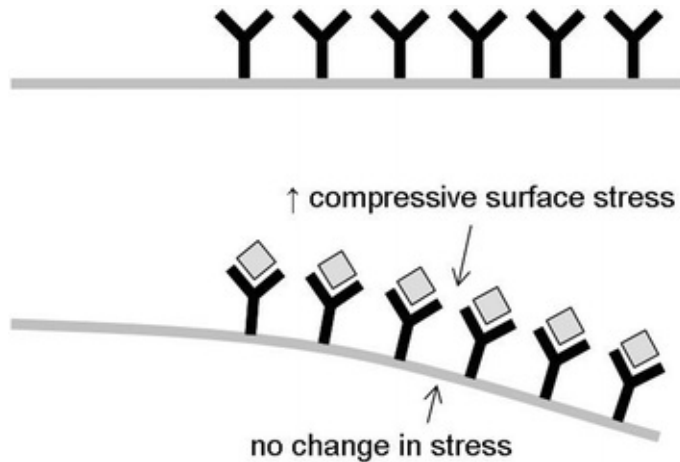


Fig. 5.5 Cantilever bending upon antibody-antigen binding. Antigen binding to the antibodies increases compressive surface stress (i.e., surface tension) on the *top* of the cantilever, while there is no such change on the other side, leading to cantilever bending downwards. If a tensile surface stress is generated, cantilever will bend upwards

5.4 Laboratory Task 1: Wheatstone Bridge

In this task, you will need the following:

- A breadboard, wires, wire cutter/stripper, a power supply, and a DMM.
- Four $1\text{ k}\Omega$ resistors.

Figures 5.6 and 5.7 show the circuit layout. Before beginning this task, the exact resistance values for the four resistors should be measured with a DMM. Label the resistors R_1 , R_2 , R_3 , and R_4 , respectively. Table 5.1 show the DMM readings.

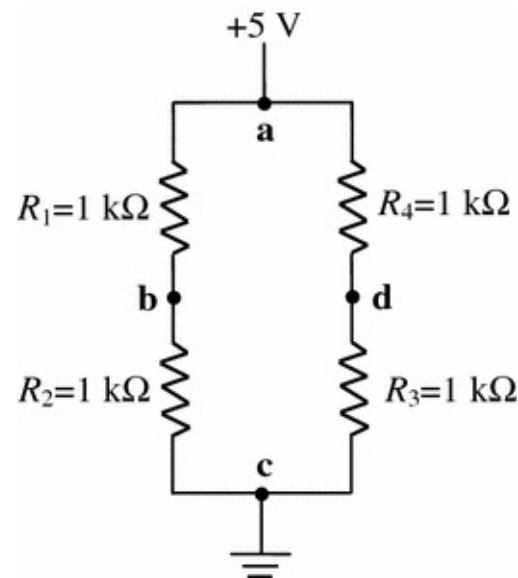


Fig. 5.6 Circuit diagram for Task 1

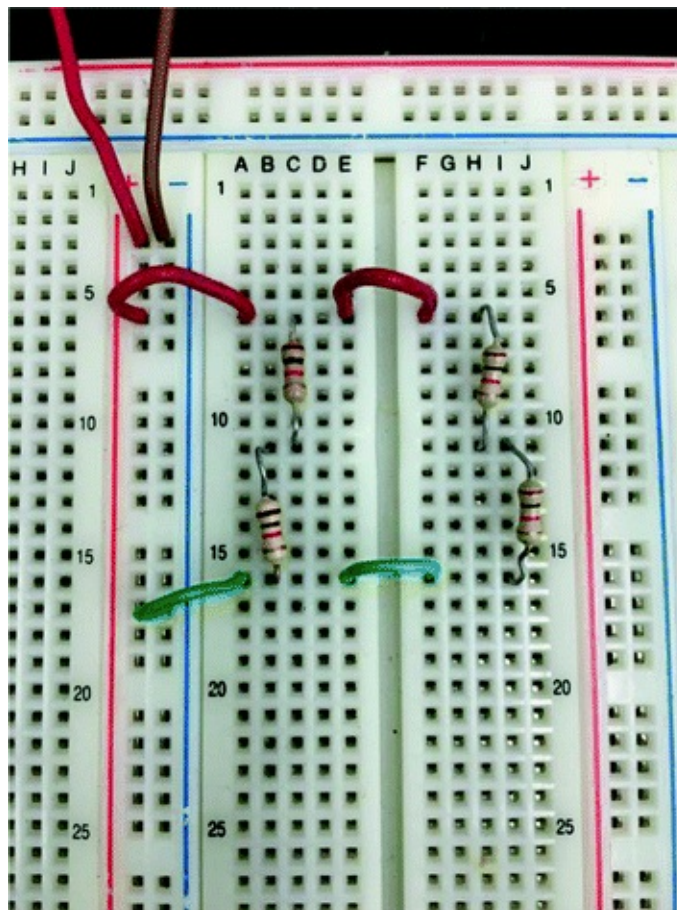


Fig. 5.7 Circuit photo for Task 1

Table 5.1 Experimental data from Task 1

V_{in} = V_a	R₁	R₂	R₃	R₄	V_{bd} (experimental)
5.04 V	0.988 kΩ	0.989 kΩ	0.988 kΩ	0.986 kΩ	0.0 mV

Theoretical V_{bd} can be calculated from Eq. 5.3, using the experimentally measured V_{in} , R_1 , R_2 , R_3 , and R_4 values

$$V_{bd} = V_{in} \left(\frac{R_2}{R_1 + R_2} - \frac{R_3}{R_3 + R_4} \right) = (5.04) \left(\frac{989}{988 + 989} - \frac{988}{988 + 986} \right) \\ = -0.0013 \text{ V} = -1.3 \text{ mV.}$$
 (5.7)

The experimental reading is off by +1.3 mV from its theoretical reading, but they are very close to each other.

Question 5.1

You constructed the Wheatstone bridge circuit first and tried to measure the R_1 value by connecting the DMM leads to the points ‘a’ and ‘b’. Your DMM reading was 0.75 kΩ rather than 1 kΩ. Why is this happening? Hint: Between points ‘a’ and ‘b’, there are two branches of resistors, one with R_1 and the other with $R_2 + R_3 + R_4$.

Alternative Task 1: Wheatstone Bridge

Switch the locations of the four resistors and calculate V_{bd} . Compare this with the actual DMM measurement. Try several different combinations until the V_{bd} value (both calculated and measured) becomes close to 0 mV.

5.5 Laboratory Task 2: Wheatstone Bridge for a Thermistor

In this task, you will need the following:

- A breadboard, wires, wire cutter/stripper, a power supply and a DMM.
- 20 kΩ pot and a screw driver.
- 100 kΩ resistor.
- 30 kΩ thermistor.
- 30 kΩ resistor.
- Two 1 kΩ resistors.

Figures 5.8 and 5.9 show the circuit layout. The resistance value of typical resistors varies as the environmental temperature changes. A thermistor is a resistor that is much more sensitive to temperature than typical resistors. We will use a thermistor whose resistance is $30\text{ k}\Omega$ at 25°C (room temperature or RT). Before you begin, measure the resistance value of your thermistor with your DMM. If the DMM reading is $32\text{ k}\Omega$, you should change R_1 to $32\text{ k}\Omega$.

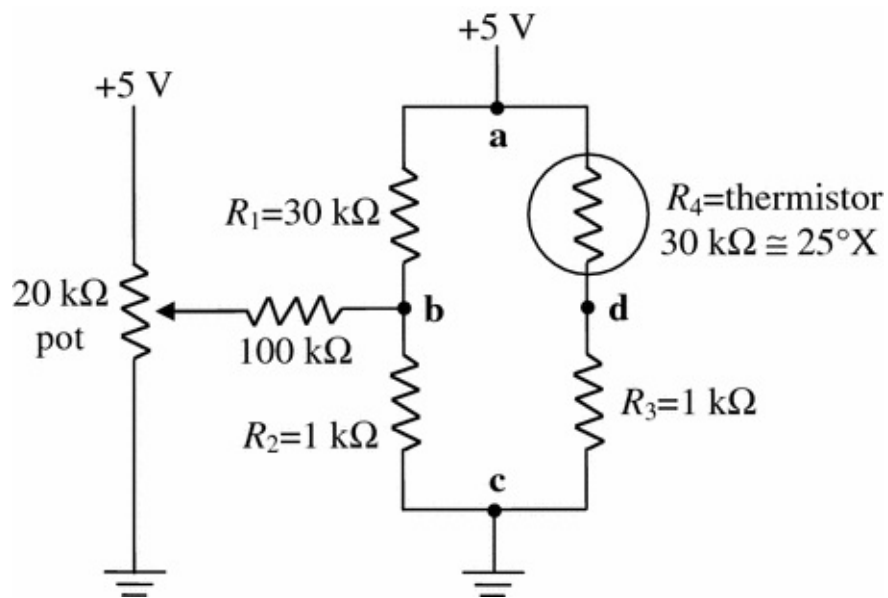


Fig. 5.8 Circuit diagram for Task 2

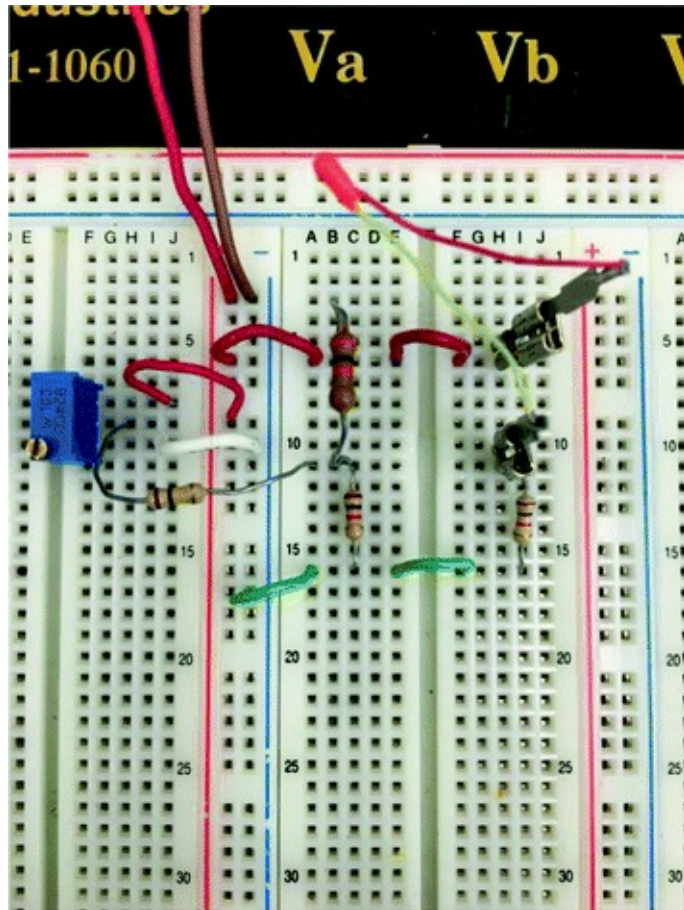


Fig. 5.9 Circuit photo for Task 2

The $20\text{ k}\Omega$ pot and the $100\text{ k}\Omega$ resistor attached in parallel with R_1 act as a “fine-tuner” for R_1 . As they are parallel to R_1 , the actual resistance between the points a and b should be slightly smaller than R_1 . Adjust the $20\text{ k}\Omega$ pot from one end to the other and measure V_{bd} for those two extremes. (The easy way to do this is to set your pot to generate 0 V and measure V_{bd} , then simply flip its direction to generate maximum voltage.) The voltage at one extreme should be positive while that at the other extreme negative. This indicates you are able to balance the bridge. If not, try to swap R_2 and R_3 , or use a different resistor for R_1 .

Once the bridge is balanced, the overall equivalent resistance on the top left part of the bridge (i.e., the whole part including R_1 , the pot, and the $100\text{ k}\Omega$) can be easily calculated from Eq. 5.4 ($R_1 R_3 = R_2 R_4$), shown in Table 5.2.

Table 5.2 Experimental data from Task 2

$V_{in} = V_a$	$R_{1,eq}$	R_2	R_3	$R_4 @ RT$	$R_{1,eq} = R_2 R_4 / R_3 @ balanced$
5.04 V	unknown	0.989 kΩ	0.988 kΩ	30.8 kΩ	
V_{bd}					
@ $V_{pot} = 0$ V	@ $V_{pot} = V_{in}$ (5.04 V)		@ balanced		= $0.989 \times 30.8 / 0.988$
-6.5 mV	+36.9 mV		0.0 mV		= 30.83 kΩ
V_{bd} w/finger	R_4 w/finger				
-62.0 mV	21.8 kΩ				

Now, hold the thermistor with your fingers to increase the temperature that it is exposed to. Do not touch the pot. The resistance value should decrease, changing the balance of the bridge (in other words, V_{bd} is no longer 0 mV).

Given the $R_{1,eq}$ obtained above and experimentally measured V_{bd} , V_{in} , R_2 and R_3 , we can calculate the new R_4 with finger heating, also shown in Table 5.2.

R_4 with finger was calculated as follows:

$$V_{bd} = V_{in} \left(\frac{R_2}{R_1 + R_2} - \frac{R_3}{R_3 + R_4} \right) = (5.04) \left(\frac{989}{30830 + 989} - \frac{988}{988 + R_{4,finger}} \right) = -0.0620 \quad (5.8)$$

Solving for $R_{4,finger}$ gave 21.8 kΩ. Apparently, the temperature rise caused the resistance of our thermistor to drop by 9.0 kΩ.

Question 5.2

Calculate the current flowing through the two branches when the bridge is balanced ($V_{bd} = 0$ mV). Hint: Use R_2/V_b and R_3/V_d to calculate the current. V_d ($= V_b$; why?) can be measured from V_{in} , R_3 and R_4 . Are they identical?

Question 5.3

Calculate the current flowing through R_1 and the 100 kΩ resistor, using the values shown in Table 5.2. (Note that the arrow symbol on the pot does not represent the direction of current, but simply a schematic symbol for a pot.) Hint: The sum of these two currents should be the same as the current flowing through R_2 .

Question 5.4

Calculate R_4 using the above calculation and measurement when $V_{bd} = +50$ mV.

Alternative Task 2: Wheatstone Bridge for a Resistor

Task 2 can be repeated with regular $1\text{ k}\Omega$ resistors for both R_1 and R_4 . In this case, a $1\text{ k}\Omega$ resistor (R_4) acts as a very insensitive thermistor. Repeat the entire Task 2.

5.6 Laboratory Task 3: Wheatstone Bridge for a Strain Gauge

In this task, you will need the following:

- A breadboard, wires, wire cutter/stripper, a power supply and a DMM.
- $20\text{ k}\Omega$ pot and a screw driver.
- $10\text{ k}\Omega$ resistor.
- A strain gauge, $120\ \Omega$, with ribbon leads.
- Three $120\ \Omega$ resistors.

Figures 5.10 and 5.11 show the circuit layout. Similar to Task 2, you will need to balance the bridge; in other words, you need to make $V_{bd} = 0\text{ mV}$. Once you achieve the zero balance, try to bend the strain gauge (by touching it with your finger) and record V_{bd} . You can back-calculate the new resistance value for the strain gauge ($R_{4,\text{strain}}$) (Table 5.3).

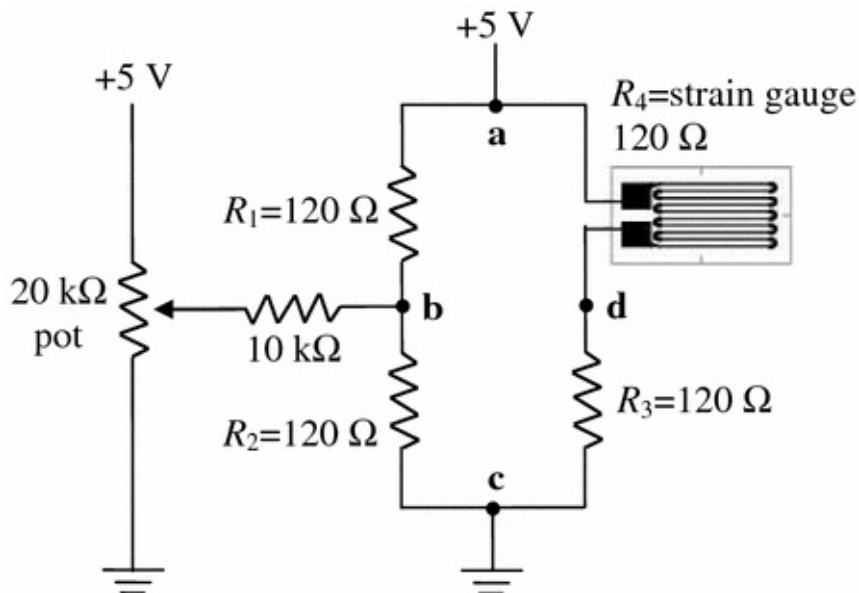


Fig. 5.10 Circuit diagram for Task 3

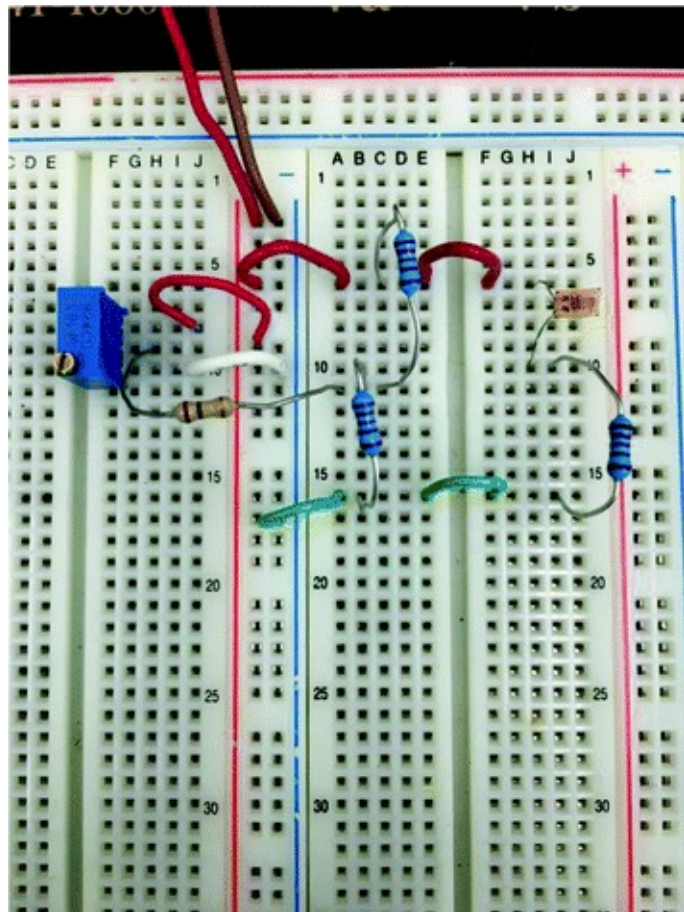


Fig. 5.11 Circuit photo for Task 3

Table 5.3 Experimental data from Task 3

$V_{in} = V_a$	$R_{1,eq}$	R_2	R_3	R_4 w/no strain	$R_{1,eq} = R_2 R_4 / R_3$ @ balanced
5.04 V	unknown	119 Ω	120 Ω	118 Ω	= $119 \times 118 / 120 = 117 \Omega$
V_{bd} w/strain	R_4 w/strain				
-40.4 mV	114 Ω				

R_4 with strain was calculated from the following:

$$V_{bd} = V_{in} \left(\frac{R_2}{R_1 + R_2} - \frac{R_3}{R_3 + R_4} \right) \quad (5.9)$$

$$= (5.04) \left(\frac{119}{117 + 119} - \frac{120}{120 + R_{4,\text{strain}}} \right) = -0.0404$$

Resistance decreased by 4 Ω ($118 \Omega \rightarrow 114 \Omega$) with strain, indicating the strain gauge was compressed (shorter length of wires). If the resistance increased, the strain gauge would be stretched (longer length of wires).

Question 5.5

Calculate R_4 using the above calculation and measurement when $V_{bd} = +5$ mV.

References and Further Readings

Baselt DR, Lee GU, Natesan M, Metzger SW, Sheehan PE, Colton RJ (1998) A biosensor based on magnetoresistance technology. *Biosens Bioelectron* 13:731–739

[[CrossRef](#)]

Edelstein R, Tamanaha C, Sheehan PE, Miller MM, Baselt DR, Whitman LJ, Colton RJ (2000) The BARC biosensor applied to the detection of biological warfare agents. *Biosens Bioelectron* 14:805–813

[[CrossRef](#)]

Fritz J (2008) Cantilever biosensors. *Analyst* 133:855–863

[[CrossRef](#)]

Harborn U, Xie B, Venkatesh R, Danielsson B (1997) Evaluation of a miniaturized thermal biosensor for the determination of glucose in whole blood. *Clin Chim Acta* 267:225–237

[[CrossRef](#)]

Hierlemann A, Lange D, Hagleitner C, Kerness N, Koll A, Brand O, Baltes H (2000) Application-specific sensor systems based on CMOS chemical microsensors. *Sens Actuators B* 70:2–11

[[CrossRef](#)]

Hosaka S, Chiyoma T, Ikeuchi A, Okano H, Sone H, Izumi T (2006) Possibility of a femtogram mass biosensor using a self-sensing cantilever. *Curr Appl Phys* 6:384–388

[[CrossRef](#)]

Khan AS, Wang X (2000) Strain measurements and stress analysis, 1st edn. Prentice Hall, Upper Saddle River

Morgenshtein A, Sudakov-Boreysha L, Dinnar U, Jakobson CG, Nemirovsky Y (2004) Wheatstone-bridge readout interface for ISFET/REFET applications. *Sens Actuators B* 98:18–27

[[CrossRef](#)]

Murray W (1992) The bonded electrical resistance strain gage: an introduction, 1st edn. Oxford University Press, New York

Ramanathan K, Danielsson B (2001) Principles and applications of thermal biosensors. *Biosens Bioelectron* 16:417–423

[[CrossRef](#)]

Tamanaha C, Mulvaney S, Rife JC, Whitman LJ (2008) Magnetic labeling, detection, and system integration. *Biosens Bioelectron* 24:1–13

[[CrossRef](#)]

Window AL (1992) Strain gauge technology, 2nd edn. New York, Springer

Xie B, Danielsson B, Norberg P, Winquist F, Lundström I (1992) Development of a thermal micro-biosensor fabricated on a silicon chip. *Sens Actuators B* 6:127–130

[CrossRef]

Xie B, Danielsson B, Winquist F (1993) Miniaturized thermal biosensors. *Sens Actuators B* 15–16:443–447
[CrossRef]

Yang SM, Chang C, Yin TI (2008) On the temperature compensation of parallel piezoresistive microcantilevers in CMOS biosensor. *Sens Actuators B* 129:678–684
[CrossRef]

6. Op-Amp

Jeong-Yeol Yoon¹✉

(1) University of Arizona, Tucson, AZ, USA

✉ Jeong-Yeol Yoon
Email: jyyoon@email.arizona.edu

So far, we have learned about a couple of physical sensors, including a thermistor, diode temperature sensor, transistor temperature sensor, thermistor, strain gauge, and more. For practical applications, the voltage signals generated from these sensors must be conditioned and appropriately amplified. This task is usually achieved by an *operational amplifier*, more commonly referred to as an *op-amp*, which we briefly used in Chap. 3 laboratory.

6.1 Op-Amp

The op-amp is an integrated circuit (IC); more specifically, an *analog IC* or *linear IC*. Most ICs deal with digital signals, called *digital IC* or *logic IC*, and are used primarily in microprocessors and memory applications. Op-amps, however, deal mostly with analog signals (voltage signals). Other examples of analog or linear IC include timers and oscillators.

A typical op-amp, shown in Fig. 6.1, is an integrated device with a non-inverting input, an inverting input, two DC power supply leads (positive and negative), an output terminal, and a few other specialized leads used for fine-tuning (Figs. 6.2 and 6.3).

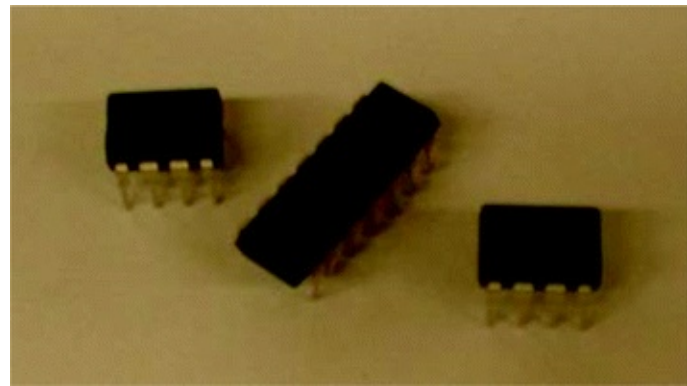


Fig. 6.1 Op-amps (LM741 , LM324 and TL082)

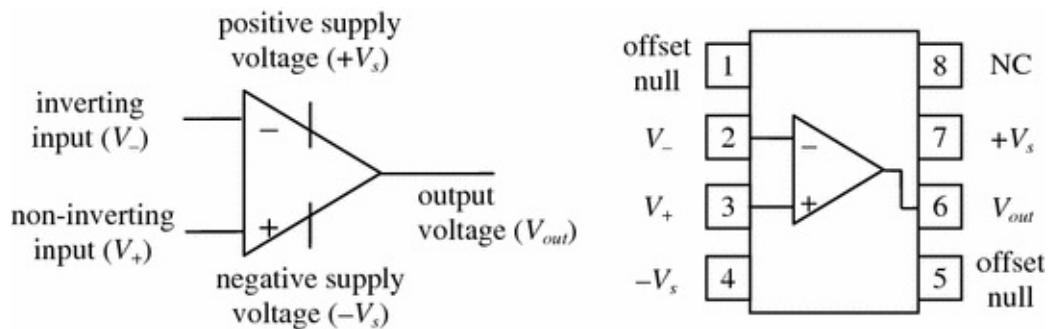


Fig. 6.2 A schematic symbol of an op-amp (left) and its pin configuration (right; for LM741)

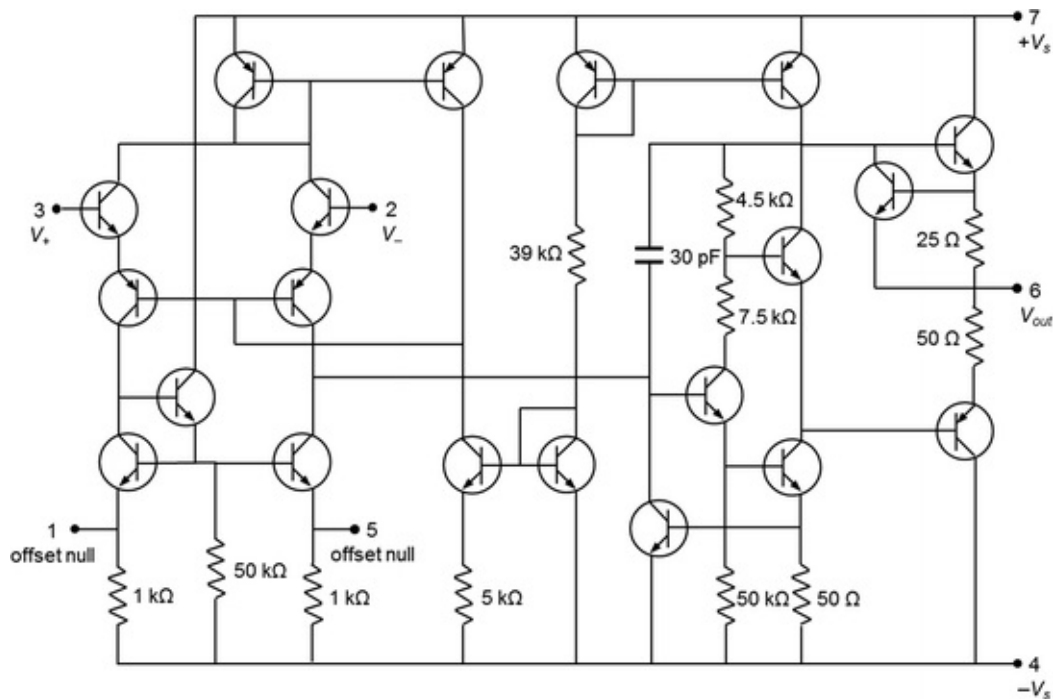


Fig. 6.3 A component level diagram of LM741, consisting of transistors and resistors

6.2 Basics of Op-Amp

The following is an expression for an op-amp's output voltage as a function of its input voltages V_+ (non-inverting) and V_- (inverting) and of its *open-loop voltage gain* A_o :

$$V_{\text{out}} = A_o(V_+ - V_-) \quad (6.1)$$

Figure 6.4 compares an ideal op-amp (left) with a real op-amp (right). We must take into account the real features of an op-amp, such as its input resistance R_{in} and output resistance R_{out} . To understand and compare the ideal and real equivalent circuits, know that the values of A_o , R_{in} , and R_{out} are defined by the following rules (*rules of op-amp*):

- Rule 1: For an ideal op-amp, the open-loop voltage gain is infinite ($A_o = \infty$). For a real op-amp, the gain is between 10^4 and 10^6 .
- Rule 2: For an ideal op-amp, the input resistance is infinite ($R_{\text{in}} = \infty$). For a real op-amp, the input resistance is finite, typically between 10^6 and 10^{12} . The output resistance for an ideal op-amp is zero ($R_{\text{out}} = 0$). For a real op-amp, R_{out} is typically between 10 and 1000 Ω .
- Rule 3: The input terminals of an ideal op-amp draw no current. Practically speaking, this is also true for real op-amps since input current is usually in the pA or nA range.

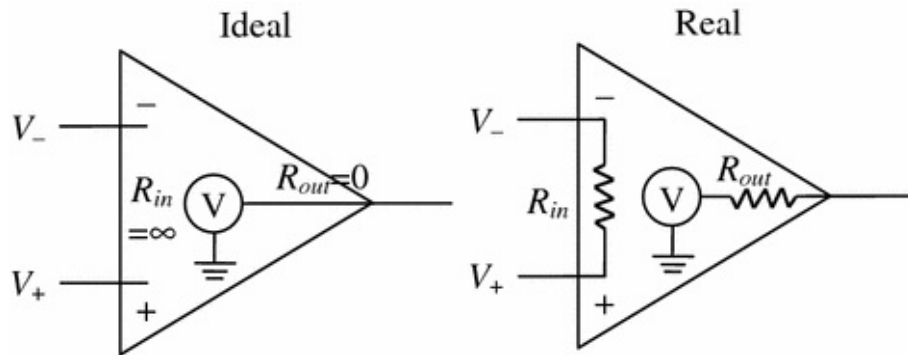


Fig. 6.4 Ideal versus real op-amp

As an example, we can solve for the gain of the circuit shown in Fig. 6.5. Since V_- is grounded (0 V) and V_+ is simply V_{in} the open-loop voltage gain expression becomes

$$V_{\text{out}} = A_o(V_+ - V_-) = A_o(V_{\text{in}} - 0) = A_o V_{\text{in}} \quad (6.2)$$

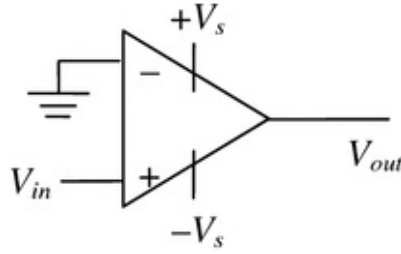


Fig. 6.5 Non-inverting setup

Rearranging this equation gives this expression for the *gain*

$$\text{Gain} = \frac{V_{\text{out}}}{V_{\text{in}}} = A_o \quad (6.3)$$

If we treat the op-amp as ideal, A_o would be infinite. However, if we treat the op-amp as real, A_o is finite (around 10^4 – 10^6). This circuit acts as a simple *non-inverting comparator* with ground as a reference. If $V_{\text{in}} > 0$, the output ideally goes to $+\infty$; if $V_{\text{in}} < 0$, the output ideally goes to $-\infty$. With a real op-amp, the output is limited by the supply voltages $+V_s$ and $-V_s$. These maximum output voltages are called the positive and negative *saturation voltages*.

Next, we will solve for the gain of the inverting setup in Fig. 6.6. Since V_+ is grounded (0 V) and V_- is simply V_{in} , the open-loop voltage gain expression becomes

$$V_{\text{out}} = A_o(V_+ - V_-) = A_o(0 - V_{\text{in}}) = -A_o V_{\text{in}} \quad (6.4)$$

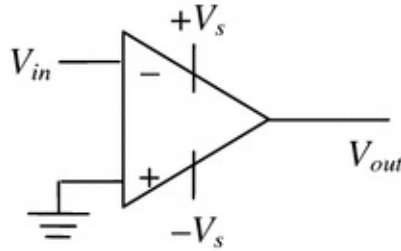


Fig. 6.6 Inverting setup

Rearranging this equation gives this expression for the gain

$$\text{Gain} = \frac{V_{\text{out}}}{V_{\text{in}}} = -A_o \quad (6.5)$$

If we treat this op-amp as ideal, then $-A_o$ is negatively infinite. However, if

we treat the op-amp as real, then $-A_o$ is finite (around 10^4 – 10^6). This circuit acts as a simple *inverting comparator* with ground as reference. If $V_{in} > 0$, then the output ideally goes to $-\infty$; if $V_{in} < 0$, the output ideally goes to $+\infty$. With a real op-amp, the outputs are limited to the saturation voltages; i.e., the output V_{out} cannot exceed V_s .

6.3 Voltage Follower or Buffer Op-Amp

Figure 6.7 shows a negative feedback loop for an op-amp.

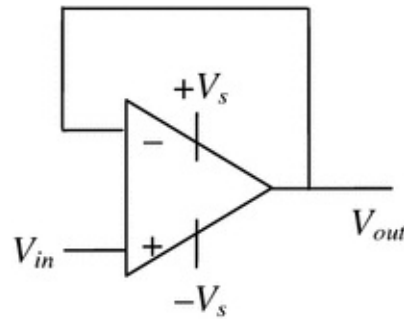


Fig. 6.7 Negative feedback loop: voltage follower or buffer

Here is the fourth *rule of an op-amp* to describe this feedback loop,

- Rule 4: With feedback, the op-amp will strive to reduce $V_+ - V_-$. In other words, it wants $V_+ = V_-$.

For the setup shown in Fig. 6.7,

$$\begin{aligned} V_+ &= V_{in}, \\ V_- &= V_{out} \text{ (connected with a feedback loop), and} \\ V_+ &= V_- \text{ (rule 4).} \end{aligned} \tag{6.6}$$

This gives

$$V_{in} = V_{out} \text{ and Gain} = 1. \tag{6.7}$$

The output follows the input (no sign inversion) and is therefore called a *voltage follower*. The input impedance is high since the current is very low (it is assumed to be zero). Thus, no loading occurs and the input is buffered, giving it the name: *buffer op-amp*. This voltage follower or buffer configuration is a good way to test your chips. We have already used this configuration to protect our LED and zener diode in Chap. 3 laboratory, as it draws almost no current.

6.4 Non-Inverting Op-Amp

The non-inverting setup shown in Fig. 6.5 is not entirely practical since the gain is either infinite (ideal) or very high (real). We can place a resistor at the input terminal (R_i) and another within the feedback loop (R_f) of the voltage follower to fix the gain at a desired number (*non-inverting op-amp*) (Fig. 6.8).

We can calculate the gain of the above circuit by using *Kirchhoff's current law* (also known as *Kirchhoff's first law*) for the black dot (*summing junction*) that is connected to the inverting input (V_-).

- Kirchhoff's current law: At any point in an electrical circuit that does not represent a capacitor plate, the sum of current flowing toward that point is equal to the sum of the currents flowing away from that point.

$$\sum_{k=1}^n I_k = 0. \quad (6.8)$$

For the summing junction shown in Fig. 6.8,

$$I_i + I_f + I_- = 0 \quad (6.9)$$

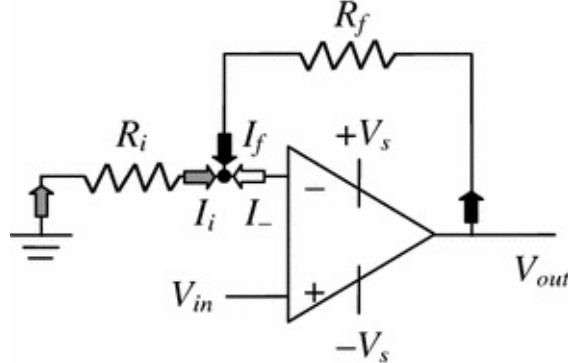


Fig. 6.8 Non-inverting op-amp

As the voltage at this summing junction (V_-) should be the same as $V_+ = V_{in}$ (rule 4),

$$\begin{aligned} I_i &= \frac{0 - V_-}{R_i} = \frac{0 - V_{in}}{R_i} \\ I_f &= \frac{V_{out} - V_-}{R_f} = \frac{V_{out} - V_{in}}{R_f} \end{aligned} \quad (6.10)$$

$I_- = 0$ (rule 3, input terminal draws no current)

If V_{in} is positive, I_i becomes negative, indicating that the I_i current is flowing away from the junction. If the above circuit is really amplifying (i.e., V_{out}

$V_{\text{out}} > V_{\text{in}}$, I_f becomes positive, indicating that the I_f current is flowing toward the junction.

Plugging Eq. 6.10 into Eq. 6.9 gives

$$\frac{V_{\text{out}} - V_{\text{in}}}{R_f} = \frac{V_{\text{in}}}{R_i}$$

$$\text{Gain} = \frac{V_{\text{out}}}{V_{\text{in}}} = \frac{R_f}{R_i} + 1 \quad (6.11)$$

Therefore, the *gain* of non-inverting op-amp configuration can be set by the ratio of two resistors, R_f and R_i . Note that the gain is always positive, indicating a non-inverting configuration.

6.5 Inverting Op-Amp

In the non-inverting op-amp, V_{in} is supplied to the non-inverting input (V_+). We can supply V_{in} to the inverting input (V_-) to create an inverting amplification setup (*inverting op-amp*) (Fig. 6.9).

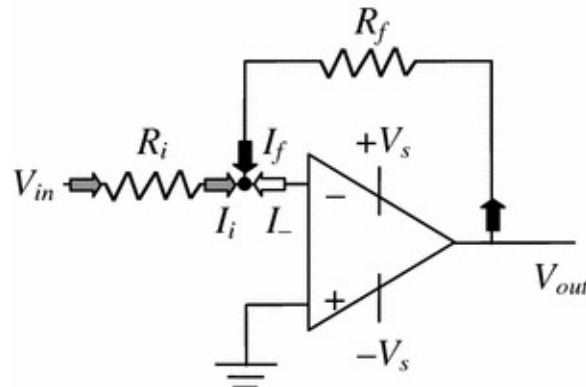


Fig. 6.9 Inverting op-amp

This time, the non-inverting input is connected to ground ($V_+ = 0$). From rule 4 ($V_+ = V_-$), V_- should also be 0.

$$I_i = \frac{V_{\text{in}} - V_-}{R_i} = \frac{V_{\text{in}} - 0}{R_i}$$

$$I_f = \frac{V_{\text{out}} - V_-}{R_f} = \frac{V_{\text{out}} - 0}{R_f} \quad (6.12)$$

$$I_- = 0 \text{ (rule 3)}$$

Both I_i and I_f are positive if V_{in} is positive, indicating they are flowing toward the junction. Plugging Eq. 6.12 into Eq. 6.9 gives

$$\frac{V_{\text{out}}}{R_f} = -\frac{V_{\text{in}}}{R_i}$$

$$\text{Gain} = \frac{V_{\text{out}}}{V_{\text{in}}} = -\frac{R_f}{R_i}$$
(6.13)

Note that the *gain* is always negative, indicating an inverting configuration.

6.6 Summing Op-Amp

We can also add two voltages together and amplify them using an op-amp (*summing op-amp*) (Fig. 6.10).

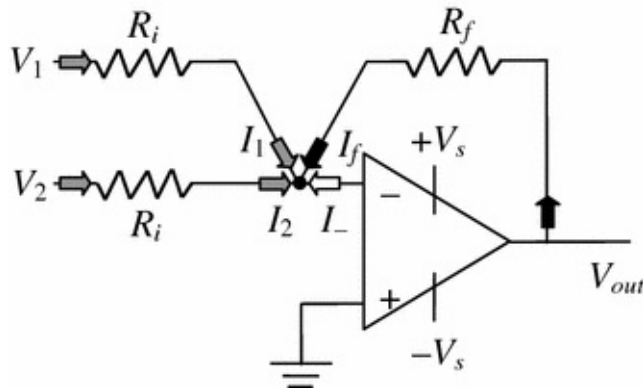


Fig. 6.10 Summing op-amp (inverting)

Again, $V_+ = V_- = 0$. Note that identical resistors (R_i) are used for the two input voltages (V_1 and V_2).

$$I_1 = \frac{V_1 - 0}{R_i}, I_2 = \frac{V_2 - 0}{R_i}$$

$$I_f = \frac{V_{\text{out}} - 0}{R_f}$$
(6.14)

$I_- = 0$ (rule 3)

Thus,

$$\frac{V_{\text{out}}}{R_f} = -\left(\frac{V_1}{R_i} + \frac{V_2}{R_i}\right)$$

$$V_{\text{out}} = -\frac{R_f}{R_i}(V_1 + V_2)$$
(6.15)

The result indicates that the sum of two voltages (V_1 and V_2) is amplified by a *gain* of $-R_f/R_i$ (inverting).

6.7 Differential Op-Amp

We can also subtract two voltages and amplify them using an op-amp (*differential op-amp*) (Fig. 6.11).

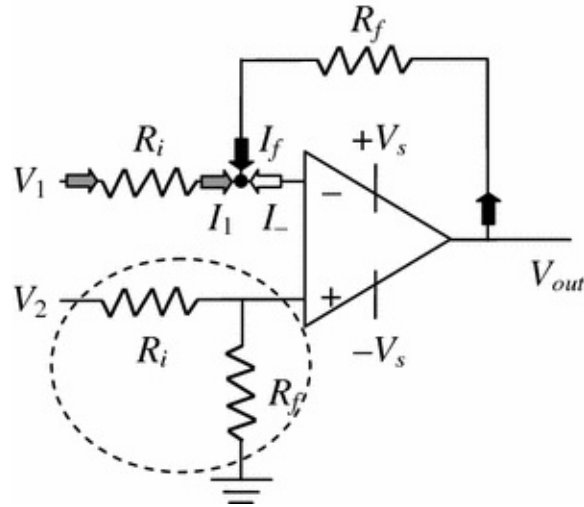


Fig. 6.11 Differential op-amp

The bottom part (dashed circle) is a simple voltage divider. The voltage output from this voltage divider should be the same as the non-inverting input voltage of the op-amp. This voltage should also be the same as V_- (rule 4).

$$V_+ = V_- = V_2 \frac{R_f}{R_i + R_f} \quad (6.16)$$

Solving for three currents,

$$\begin{aligned} I_1 &= \frac{V_1 - V_-}{R_i} = \frac{1}{R_i} V_1 - \frac{R_f}{R_i(R_i + R_f)} V_2 \\ I_f &= \frac{V_{\text{out}} - V_-}{R_f} = \frac{1}{R_f} V_{\text{out}} - \frac{R_f}{R_f(R_i + R_f)} V_2 \end{aligned} \quad (6.17)$$

$$I_- = 0 \quad (\text{rule 3})$$

Therefore,

$$\begin{aligned} \frac{1}{R_f} V_{\text{out}} &= \frac{R_f}{R_i + R_f} \left(\frac{1}{R_i} + \frac{1}{R_f} \right) V_2 - \frac{1}{R_i} V_1 \\ V_{\text{out}} &= \frac{R_f^2}{R_i + R_f} \frac{R_i + R_f}{R_i R_f} V_2 - \frac{R_f}{R_i} V_1 = \frac{R_f}{R_i} (V_2 - V_1) \end{aligned} \quad (6.18)$$

The result indicates that the difference of two voltages V_2 and V_1 is amplified by a *gain* of R_f/R_i (non-inverting).

6.8 Laboratory Task 1: Non-inverting Op-Amp Operation

In this task, you will need the following:

- A breadboard, wires, wire cutter/stripper, a power supply, and a DMM
- 10 kΩ or 20 kΩ pot and a screw driver
- Op-amp LM741 or LM324
- Five 1 kΩ resistors

Figures 6.12, 6.13 and 6.14 show the circuit layout, op-amp pin layouts, and circuit photo. The input voltage (V_{in}) is connected to the positive input (pin 3) of the op-amp, indicating this is non-inverting operation. Note that the output (pin 6) of the op-amp is left open. You can connect the positive DMM lead to this output and connect the other to GND in order to measure the op-amp output. You can also use one quarter of a quadruple op-amp LM324 instead of a single LM741 op-amp. Be careful with the different pin configurations, though. The pin layouts of LM741 and LM324 are shown again in Fig. 6.13.

Set $V_{in} = 2.5$ V by adjusting the pot. The gain will change depending on the number of 1 kΩ resistors that are connected to the negative input. As two 1 kΩ resistors in parallel are equivalent to 1/2 kΩ, three to 1/3 kΩ, and four to 1/4 kΩ, the gains for this non-inverting setup are

$$\begin{aligned}\text{Gain} &= \frac{R_f}{R_i} + 1 = \frac{1}{1} + 1 = 2 \text{ (one } 1 \text{ k}\Omega \text{ resistor)} \\ &= \frac{1}{1/2} + 1 = 3 \text{ (two } 1 \text{ k}\Omega\text{'s)} \\ &= \frac{1}{1/3} + 1 = 4 \text{ (three } 1 \text{ k}\Omega\text{'s)} \\ &= \frac{1}{1/4} + 1 = 5 \text{ (four } 1 \text{ k}\Omega\text{'s)}\end{aligned}$$

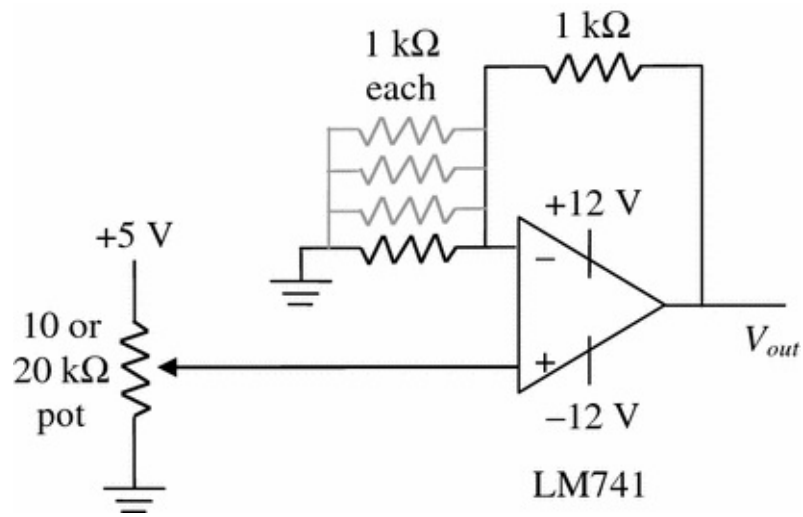


Fig. 6.12 Circuit diagram for Task 1

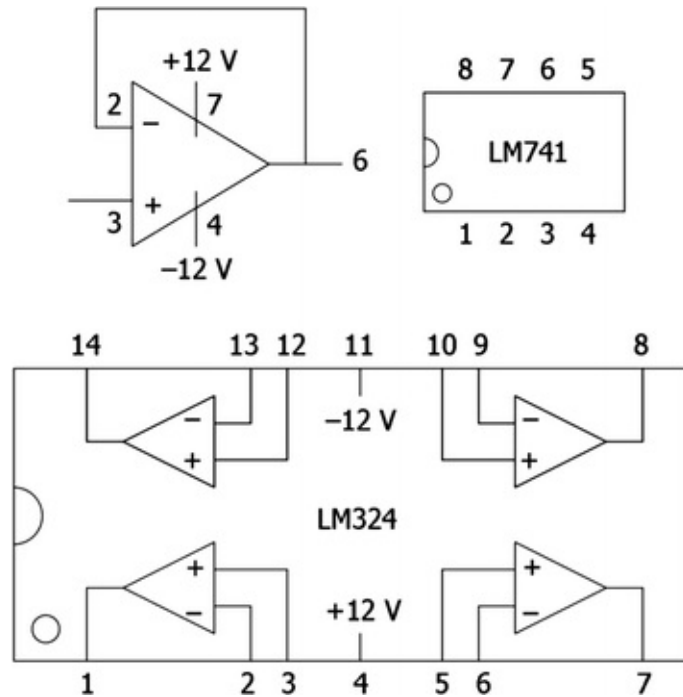


Fig. 6.13 Op-amps LM741 and LM324

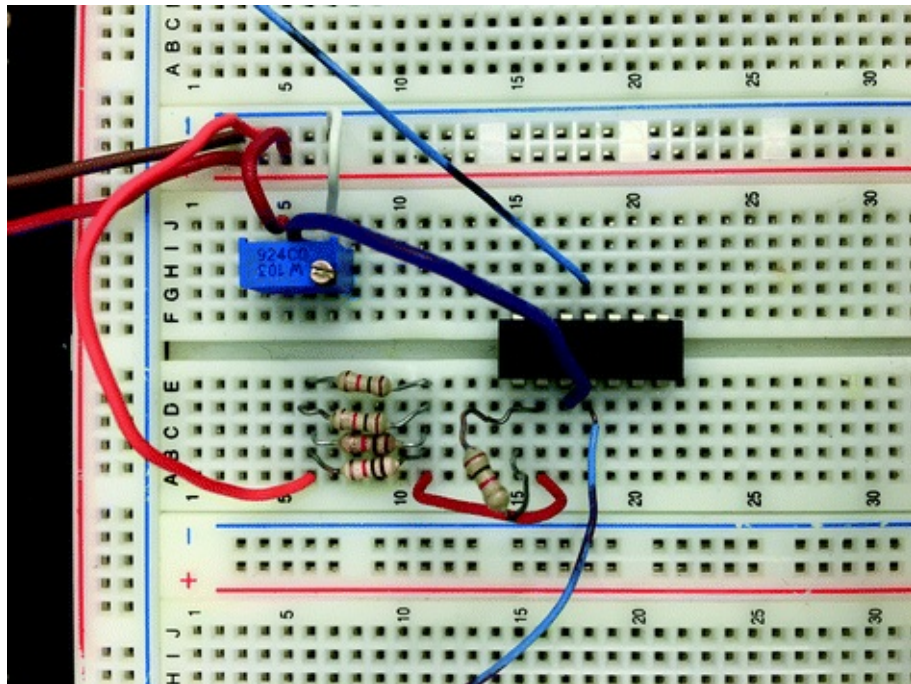


Fig. 6.14 Circuit photo of Task 1 with four $1\text{ k}\Omega$ input resistors (R_i). The top left part of LM324 is used

Table 6.1 shows some experimental data that closely corresponds to the above calculations.

Table 6.1 Experimental data from Task 1

V _{in}		2.5 (V)	Gain
V _{out}	One $1\text{ k}\Omega$	5.0	2.0
	Two $1\text{ k}\Omega$'s	7.5	3.0
	Three $1\text{ k}\Omega$'s	10.0	4.0
	Four $1\text{ k}\Omega$'s	11.0	4.4

As the theoretical gain with four $1\text{ k}\Omega$ resistors is 5, the expected V_{out} should be 12.5 V for this case; however, the actual reading for this case is 11.0 V. As discussed earlier, the output of an op-amp is limited by its voltage supply. Both the LM741 and LM324 are powered by +12 V at the negative input terminal and -12 V at the positive input terminal, so the output voltage will not exceed +12 V or -12 V. Actually, it saturates slightly lower than these limits, around +11 V or -11 V.

Alternative Task 1: Inverting Op-Amp Operation

Apply V_{in} to the negative input and ground the positive input of the op-amp.

This is an inverting setup. Repeat all of Task 1 and measure V_{out} for four different gains. Are you able to observe saturation?

Question 6.1

Estimate V_{out} with $V_{\text{in}} = 3.0 \text{ V}$ for (a) non-inverting setup with one, two, three, or four $1 \text{ k}\Omega$ resistors in parallel to the negative input (i.e., Task 1), and (b) inverting setup with one, two, three or four $1 \text{ k}\Omega$ resistors in parallel to the negative input (i.e., Alternative Task 1). For which case are you able to observe saturation?

6.9 Laboratory Task 2: Signal Conditioning for Temperature Sensor

In this task, you will need the following:

- A breadboard, wires, wire cutter/stripper, a power supply, and a DMM.
- Two pots ($10 \text{ k}\Omega$ or $20 \text{ k}\Omega$) and a screw driver
- Diode temperature sensor LM335
- Op-amp LM324
- Resistors: 1Ω , three $1 \text{ k}\Omega$'s, 100Ω , and $5.1 \text{ k}\Omega$

Figures 6.15, 6.16 and 6.17 show the circuit layout, LM335 pin layout, and circuit photo. Table 6.2 shows experimental data.

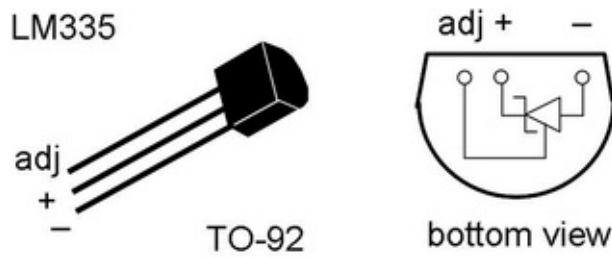
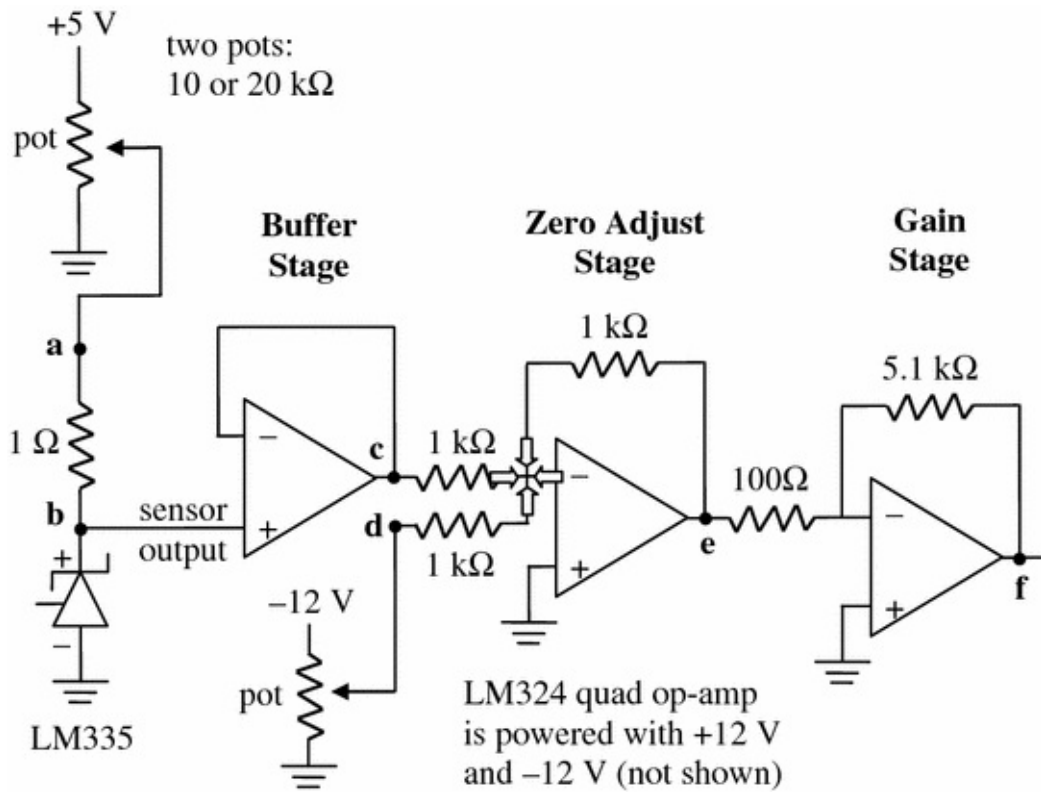


Fig. 6.16 TO-92 plastic package for LM335 diode temperature sensor. Left view with the flat face toward you. Right view with the leads pointing toward you

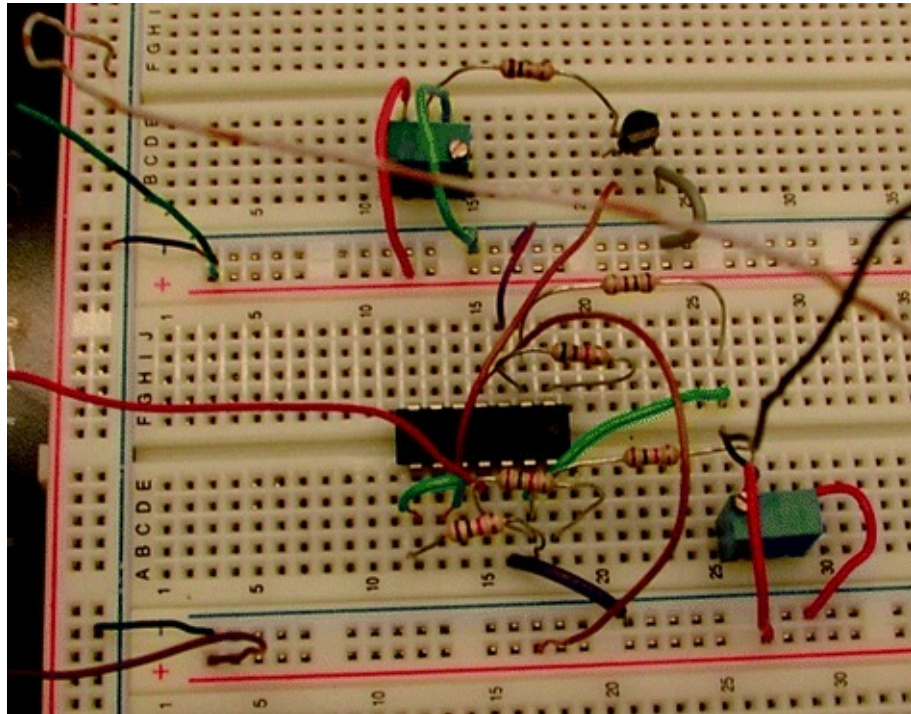


Fig. 6.17 Circuit photo for Task 2. LM324 quad op-amp is used for buffer stage (bottom left), zero adjust stage (bottom right) and gain stage (top right)

Table 6.2 Experimental data from Task 2

V_b (V)	V_c (V)	V_d (V)	V_e	V_f (V)
+2.98	+2.98	-2.98	+2.1 mV	-0.10
+3.00 V	+3.00	-2.98	-0.02 V	+1.02

Note that there was a small $V_e = +2.1$ mV even with the zero adjustment, which was amplified to -0.10 V

LM335 temperature sensor: Set your first pot (top left corner of the circuit layout) to generate the proper current, 0.5–5 mA, to your LM335 temperature sensor. This current can be measured by checking the voltage drop across the $1\ \Omega$ resistor (V_{ab} from 0.5 to 5 mV). Now, make sure that the LM335 generates a proper voltage output; it should correspond to the ambient temperature, $V_b = +2.98$ V for 298 K (25°C).

Buffer stage: The first op-amp is a buffer stage , generating the same voltage output as the input (voltage follower). Since the current generated from the op-amp output is very small (actually, it can be assumed to be zero), the LM335 circuit is isolated from the op-amp circuit. This causes the buffer action of the op-amp. Note that the sensor output is connected to the positive input of the op-

amp, so V_c should be identical to V_b , +2.98 V.

Zero adjust stage: As the indoor temperature normally changes from 10 to 30 °C, or 283 to 303 K, V_b and V_c also vary from 2.83 to 3.03 V. If you want to amplify these signals with a gain of 50, the output signals will surely saturate. Therefore, you want to set a new zero point to prevent this saturation. Let's set the room temperature, 25 °C or 298 K, as our new zero point. To make this happen, you want to use the “summing” op-amp setup. As $V_c = +2.98$ V, you want to provide an additional branch of $V_d = -2.98$ V to the negative input of the op-amp. This additional branch is powered by a pot that is connected to -12 V power (if available; -5 V should also do the job). As the summing junction is connected to the negative input of an op-amp, the output signal will be inverted, and the gain will be $1 \text{ k}\Omega / 1 \text{ k}\Omega = 1$. Adjust your second pot (bottom of the circuit layout) to make $V_d = -2.98$ V, causing the output of this stage to become zero ($V_e = 0$ V).

Gain stage: Again , this is an inverting setup, and the gain is $5.1 \text{ k}\Omega / 100 \Omega = 51$. As $V_e = 0$ V, the final output should also be 0 V, although you will observe a small voltage due to noise amplification.

Finger temperature: Now, hold the LM335 with your fingers, and measure the voltage at various points. V_b should read: +3.00 V. V_c should be the same as V_b . As V_d is still -2.98 V, the sum of these two voltages should be +0.02 V. The output, V_f , should be inverted -0.02 V. At the final gain stage , the signal is again inverted with a gain of 51, $V_f = (-51) \times (-0.02 \text{ V}) = + 1.02 \text{ V}$.

Question 6.2

Determine V_c , V_e , and V_f if $V_b = +3.08$ V. V_d is still set to -2.98 V. If this op-amp saturates at 11.0 V, what is the highest temperature this system can measure?

Question 6.3

Four arrows are located in the circuit layout at the summing junction of the zero adjust stage (Fig. 6.18). Identify those four currents (with sign) flowing toward the *summing junction* for the above two cases ($V_b = + 2.98$ V and +3.00 V with $V_d = -2.98$ V). Hint: the voltage at the summing junction is zero, since the input terminals of an op-amp drives no current.

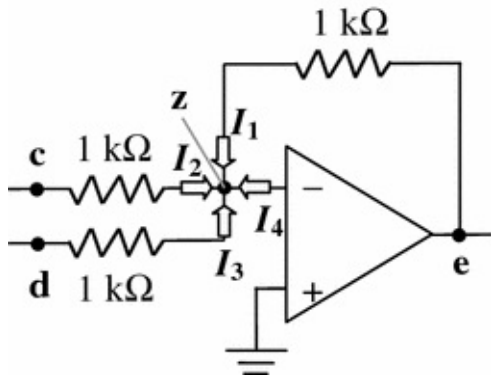


Fig. 6.18 Question 6.3

Solution

From the hint, $V_z = 0 \text{ V}$ and $I_4 = 0 \text{ mA}$.

For $V_b = +2.98 \text{ V}$:

$$I_1 = (V_e - V_z)/1 \text{ k}\Omega = (0 - 0)/1000 = 0 \text{ mA}$$

$$I_2 = (V_c - V_z)/1 \text{ k}\Omega = (+2.98 - 0)/1000 = +2.98 \text{ mA}$$

$$I_3 = (V_d - V_z)/1 \text{ k}\Omega = (-2.98 - 0)/1000 = -2.98 \text{ mA}$$

$$\Sigma I = I_1 + I_2 + I_3 + I_4 = 0 + 2.98 - 2.98 + 0 = 0 \text{ mA}.$$

For $V_b = +3.00 \text{ V}$:

$$I_1 = (V_e - V_z)/1 \text{ k}\Omega = (-0.02 - 0)/1000 = -0.02 \text{ mA}$$

$$I_2 = (V_c - V_z)/1 \text{ k}\Omega = (+3.00 - 0)/1000 = +3.00 \text{ mA}$$

$$I_3 = (V_d - V_z)/1 \text{ k}\Omega = (-2.98 - 0)/1000 = -2.98 \text{ mA}$$

$$\Sigma I = I_1 + I_2 + I_3 + I_4 = -0.02 + 3.00 - 2.98 + 0 = 0 \text{ mA}.$$

Alternative Task 2: Signal Conditioning for Strain Gauge

Repeat Task 2 for the strain gauge with a Wheatstone bridge, the same experiment as Task 3 of the previous lecture. The outputs from the Wheatstone bridge, V_b and V_d , should be connected to both positive and negative input terminals of an op-amp, a differential op-amp setup. A zero adjust stage is not necessary (why?).

6.10 Further Study: Op-Amp Filters

In some cases, the op-amp output could be quite noisy (i.e., changing over time). There is a way to reduce this “noise” in op-amp signal amplification, referred to as *-op-amp filters*. In fact, most commercial sensors and biosensors (including light sensors, spectrometric sensors, pH/ion selective electrodes, glucose sensors, piezoelectric sensors, immunosensors, etc., which will be discussed in the later chapters) utilize op-amp filters.

There are two types of op-amp filters: (1) *low-pass filter* and (2) *high-pass filter*. The circuit diagrams of both filters are shown in Fig. 6.19.

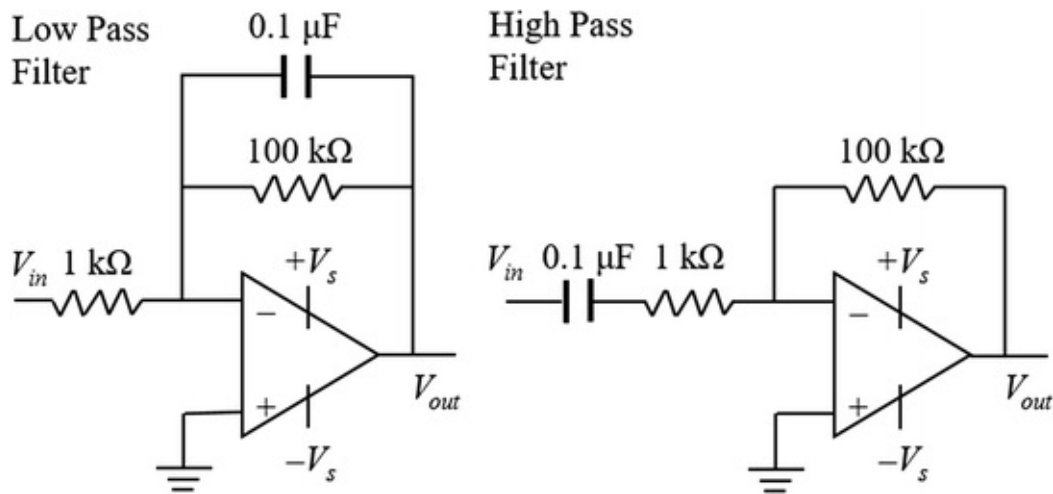


Fig. 6.19 Low-pass (left) and high-pass op-amp filters

Note that both op-amps are inverting op-amps with a gain of -100 ($= -100 \text{ k}\Omega / 1 \text{ k}\Omega$). (Of course, low-pass and high-pass filters can also be used for non-inverting op-amps.) In the low-pass op-amp filter, a $0.1 \mu\text{F}$ capacitor is added in parallel to the feedback loop resistor ($100 \text{ k}\Omega$). In the high-pass op-amp filter, the same capacitor is added in series to the input resistor ($1 \text{ k}\Omega$).

Capacitor is a device that stores electrical energy (i.e., holes and electrons) for a short amount of time. Capacitor is essentially two electrode plates separated by nonconductive materials, which include glass, paper, air, or even vacuum. The unit of a capacitor is farad (F), named after Michael Faraday, which is defined by the electrical charge per given voltage

$$F \text{ (farad)} = C \text{ (coulomb)} / V \text{ (volt)} \quad (6.19)$$

Using the current and resistance definitions,

$$A \text{ (ampere)} = C \text{ (coulomb)} / s \text{ (second)} \quad (6.20)$$

$$\Omega \text{ (ohm)} = V \text{ (volt)} / A \text{ (ampere)} \quad (6.21)$$

leads to the following:

$$F = A \cdot s/V = s/\Omega \quad (6.22)$$

Many noisy voltage signals change at a very fast rate, i.e., in high frequency. To eliminate such high-frequency noises, you may wish to cut off or attenuate such high-frequency signals, while retaining the signals that change in low frequency. This is what low-pass filter does. If the signal changes in high frequency, the capacitor is never fully charged, and the current mostly flows through the capacitor rather than the feedback resistor. This effectively reduces the overall resistance in the feedback loop, substantially lowering the gain, thus attenuating or virtually eliminating such high-frequency signal. If the signal changes in low frequency, the capacitor can be fully charged, and the current flows mostly through the feedback resistor, allowing the op-amp to function normally.

The *corner frequency* f_c (or *cut-off frequency*) for RC (resistor-capacitor) filter is defined as:

$$f_c = 1/(2\pi RC) \quad (6.23)$$

where R is the resistance (in Ω) and C is the capacitance (in F). For the above low-pass filter

$$f_c = 1/(2\pi \times 10^5 \Omega \times 10^{-7} F) = 16 \Omega^{-1} F^{-1} \quad (6.24)$$

Since $F = s/\Omega$, f_c becomes $16 s^{-1} = 16 \text{ Hz}$. This indicates that any signals changing faster than 16 Hz (16 times per second) will be attenuated (Fig. 6.20).

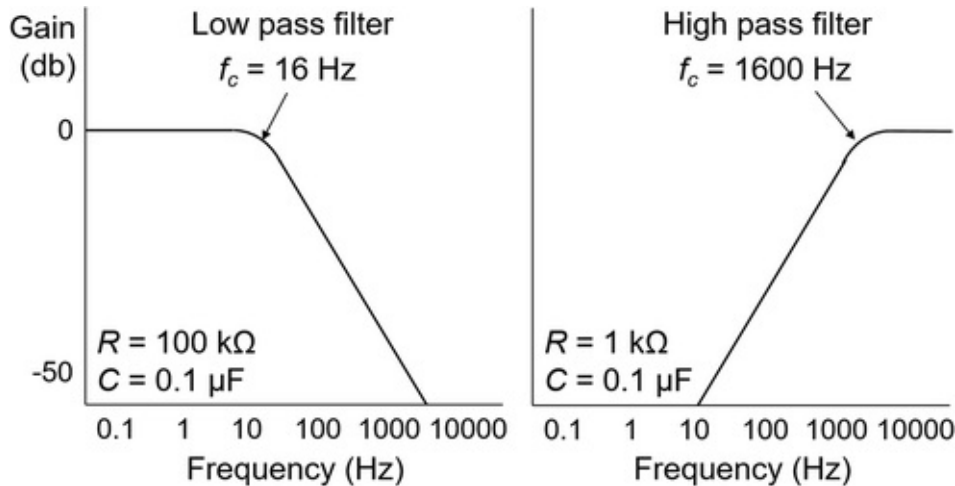


Fig. 6.20 Frequency responses of low-pass (left) and high-pass (right) op-amp filters. In the low-pass filter, any signals that change faster than the corner (cut-off) frequency ($f_c = 16 \text{ Hz}$) are attenuated (negative gain), allowing only the low-frequency signals to be delivered. In the high-pass filter, any signals that change slower than $f_c = 1600 \text{ Hz}$ are attenuated (negative gain), allowing only the high-frequency signals to be delivered

For the high-pass filter, the high-frequency signal makes the capacitor never fully charged, enabling the current to flow through the capacitor, and subsequently to the input resistor ($1\text{ k}\Omega$), allowing the op-amp to function normally. The low-frequency signal, however, makes the capacitor fully charged, and the current does not really flow through the capacitor, and subsequently to the input resistor. This will effectively attenuate or virtually eliminate such low-frequency signal ($1\text{ k}\Omega$). The corner frequency in this case is

$$f_c = 1/(2\pi \times 10^3 \Omega \times 10^{-7} \text{ F}) = 1600 \Omega^{-1} \text{ F}^{-1} = 1600 \text{ Hz} \quad (6.25)$$

indicating that any signals changing slower than 1600 Hz will be attenuated (Fig. 6.20).

If both low-pass and high-pass filters are used for a single op-amp, only a certain range of frequency signals can be chosen, while attenuating or virtually eliminating out-of-range frequency signals. This particular setup is known as *band-pass filter*, which is quite useful for audio applications.

References and Further Readings

- Carter B, Mancini R (2009) Op amps for everyone, 3rd edn. Newnes, Burlington
- Grey P (2009) Analysis and design of analog integrated circuits, 5th edn. Wiley, Hoboken
- Johns D, Martin K (1996) Analog integrated circuit design, 1st edn. Wiley, Hoboken
- Jung W (2004) Op amp applications handbook, 1st edn. Newnes, Burlington
- Rabaey JM, Chandrakasan A (2003) Digital integrated circuits, 2nd edn. Prentice Hall, Upper Saddle River
- Scherz P (2006) Practical electronics for inventors, 2nd edn. McGraw-Hill, New York

7. Light Sensors

Jeong-Yeol Yoon¹✉

(1) University of Arizona, Tucson, AZ, USA

✉ Jeong-Yeol Yoon
Email: jyyoon@email.arizona.edu

Light sensors have become very popular in many practical applications, perhaps more so than other physical sensors such as temperature, strain, and pressure sensors. They are also becoming very important in many biosensor applications, commonly used in conjunction with fluorescent dyes. In this chapter we will examine a group of light sensors that are made out of semiconductors, namely photoresistor, photodiode (PD), and phototransistor. Light sensors are typically used together with light sources; hence we will cover them (light emitting diode (LED) and laser diode) as well.

7.1 Light

Before we begin our discussion, we need to understand what light is. *Light* is a part of *electromagnetic radiation* that is visible to human eye. However, people also use the word light for some electromagnetic radiations that are not visible to human eye, for example, ultraviolet (UV) light or infrared (IR) light. Because of this, the light that can be seen by human eye is specifically called *visible (Vis)* light .

Light exists in tiny “packets of energy” called *photons* , and it exhibits properties of both waves and particles (called *wave–particle duality*). As light (and all other electromagnetic radiations) is a wave, we can draw its wave form as shown in Fig. 7.1. The wave is sinusoidal and its peak-to-peak distance is called *wavelength (λ)* .

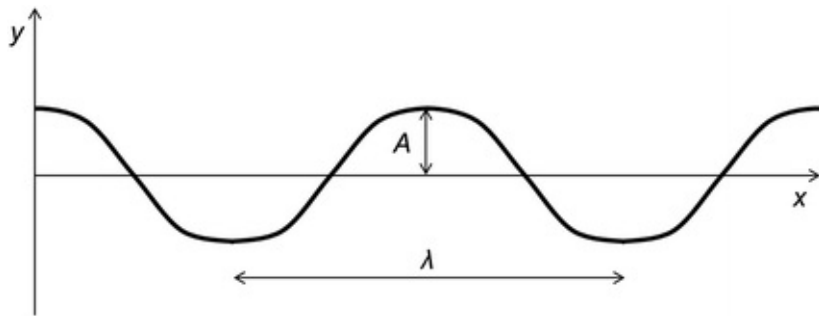


Fig. 7.1 Wavelength (λ) and amplitude (A) of light (electromagnetic wave)

In visible light, the wavelength determines its color. There may be a single wavelength (*monochromatic*), or a mixture of multiple wavelengths (*polychromatic*) that is more common.

The speed of light (and all other electromagnetic radiations) under vacuum is a universal constant and does not vary with the wavelength. The speed of light in air is almost the same as that under vacuum. This value is 3.0×10^8 m/s. If we divide the speed of light (m/s unit) with the wavelength (m unit), we will get a unit of s^{-1} , indicating the number of wave oscillations per second. The SI unit of s^{-1} is Hz (hertz), and this is specifically called *frequency*, in this case, frequency of light (or electromagnetic radiation).

$$\nu = c/\lambda \quad (7.1)$$

where

- ν frequency of light (or electromagnetic radiation)
- c speed of light under vacuum = 3.0×10^8 m/s
- λ wavelength of light (or electromagnetic radiation).

Electromagnetic radiations can be categorized into several different groups, as summarized in Table 7.1, depending on its wavelength or frequency. While *micro* and *radio waves* are commonly used in wireless (TV, radio, and cell phone) telecommunications and *IR* in wired telecommunications (fiber optic telephone and internet), and *X ray* in medical imaging, UV and Vis are more important in many biosensor applications.

Table 7.1 Electromagnetic radiations

Type	Wavelength (λ)	Frequency (ν)
γ (gamma) ray	<10 pm	
X ray	0.01–10 nm	

Ultraviolet (UV) light	10–400 nm	
Visible (Vis) light	400–750 nm	
Infrared (IR) light	0.8–300 μm	1–400 THz
Micro wave	1 mm–1 m	0.3–300 GHz
Radio wave	>1 m	<300 kHz

Note frequency is not commonly used for γ and X-rays , UV, and Vis lights

7.2 Photoresistor

In Chap. 4, we learned that all three basic semiconductors—resistor, diode, and transistor—can be used as temperature sensors. We can do the same for light sensors; hence we have photoresistor, PD, and phototransistor.

A *photoresistor* (also known as *photoconductive cell* , but we will not use this term to avoid confusion with the photoconductive mode of a PD) is a resistor that changes its resistance when it is exposed to light (i.e., photons). Any resistors can be used to sense light, but there are special types of semiconductor materials that change resistance upon light irradiation more significantly than the others. These include cadmium sulfide (CdS), lead sulfide (PbS), and cadmium selenide (CdSe). Figure 7.2 shows a working principle of a photoresistor. The resistor is S-shaped, to increase the area of light exposure and its length. This is initially a big resistor, with typical resistance in the $M\Omega$ scale, which behaves almost like an insulator. The electrons and holes are firmly bound together. When light (i.e., photons) hits this material, however, things change. Remember the photons are packets of energy, thus they provide extra energy that can strip valence electrons off a molecule. This process creates extra electrons and leaves the atom positively charged (extra holes), i.e., electron–hole pairs. This separation makes the material more conductive, thus lowering its resistance. The overall mechanism is very similar to that of a thermistor.

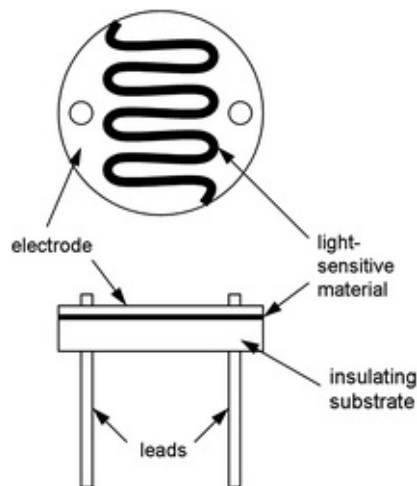


Fig. 7.2 A photoresistor

Just like a thermistor, a photoresistor is extremely sensitive to light irradiation, and generally more sensitive than PDs and phototransistors. Similar to a thermistor, a photoresistor does not show linear response against light irradiation, which may be a concern in constructing a control circuit.

7.3 Photodiode

A PD is a special type of diode that is sensitive to photons. A typical PD is shown in Fig. 7.3.

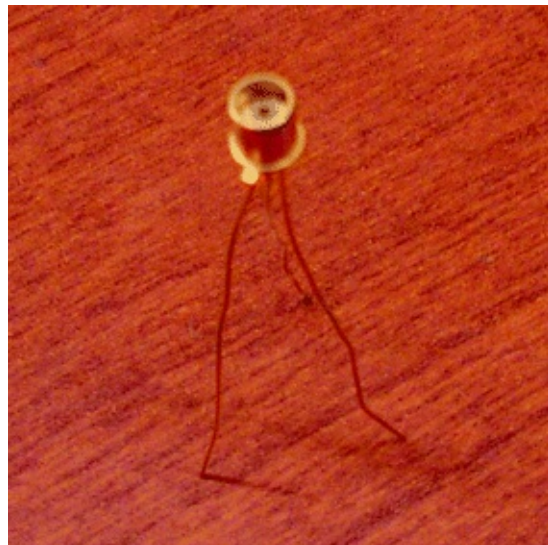


Fig. 7.3 A photodiode

PDs can be used with or without applied voltage to sense light. Unlike the regular diodes, PDs are made with very thin P-type semiconductor that is diffused into the N-type semiconductor. P-side is exposed to external light during PD operation. Figure 7.4 shows the schematic illustration of a PD, without applied voltage. This specific mode of operation is called *photovoltaic mode*.

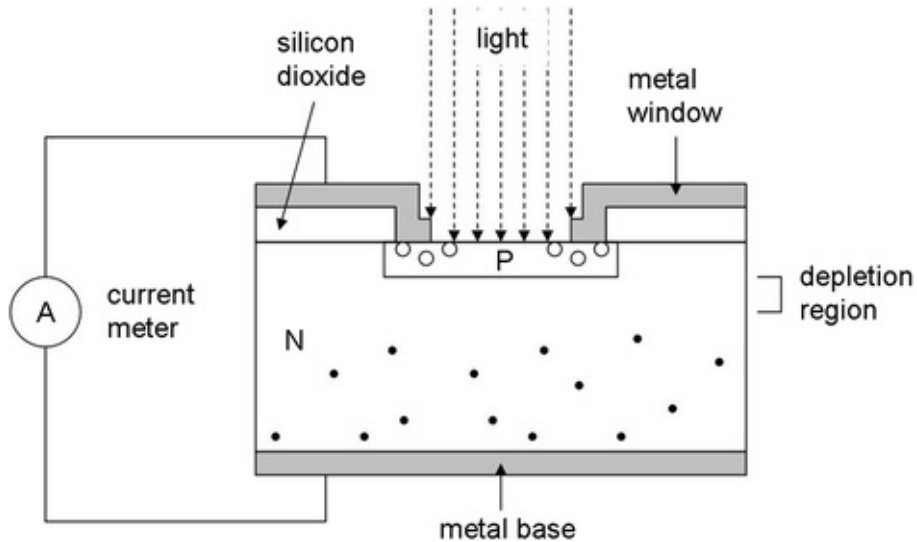


Fig. 7.4 Photodiode in photovoltaic mode . Depletion region is formed because of the repulsion between P- and N-type semiconductors. Photons (light) provide extra electrons and holes to the depletion region, making it more conductive

P-type semiconductor contains holes and N-type semiconductor contains free electrons. Because holes and electrons repel from each other, a small depletion region (void of holes and free electrons) will form at the PN junction. This depletion region is sometimes not recognized as “true” depletion but rather a “less conductive” region. When light (waves of photons) hits the P-type semiconductor, it will strip the valence electrons off from the molecules, creating extra free electrons and holes (electron–hole pairs), just like the photoresistors. As P-type semiconductor is made very thin, some light will be able to penetrate into the N-type semiconductor as well, also creating electron–hole pairs. The extra electrons in the P-type substrate move to the N-type substrate, and the extra holes in the N-type substrate move to the P-type substrate. Therefore, with sufficient supply of photons, the depletion region is filled with extra holes (in the P-type side) and extra electrons (in the N-type side). Hence the depletion region becomes more conductive. If you connect the P-type semiconductor to the N-type semiconductor using a wire, the extra holes in the P-type side move to the N-type side and the extra electrons in the N-type side to the P-type side. This

should create a noticeable electric current, which can be measured with a current meter. More light (more photons) should generate higher current.

This current signal can be amplified if a voltage is applied to a PD. This mode of PD operation is called *photoconductive mode*, shown in Fig. 7.5.

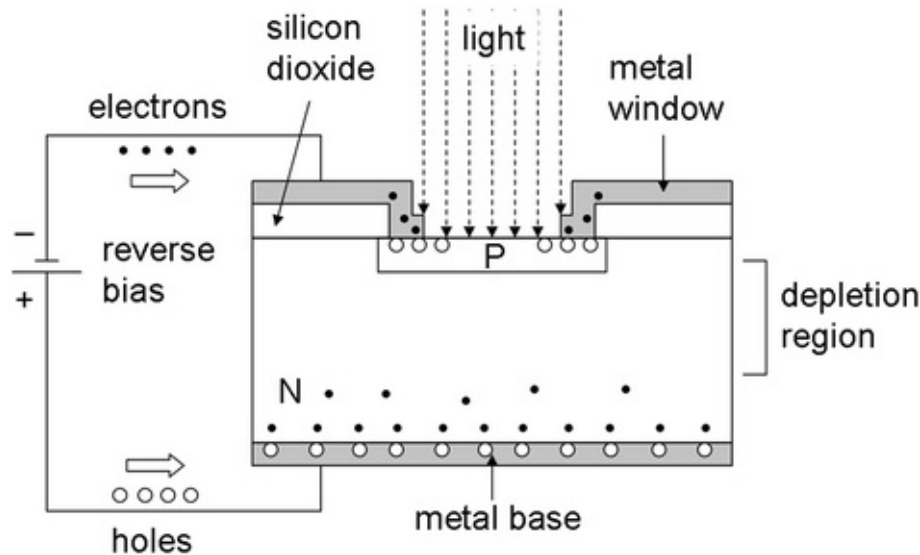


Fig. 7.5 Photodiode in photoconductive mode . Depletion region forms because of the reverse-biased applied voltage

In the photoconductive mode, a reverse bias is applied to the PN PD, i.e., high voltage to the N-type semiconductor and ground to the P-type semiconductor. In this mode, a near-insulator-like depletion region will be formed because of the reverse-biased voltage. Obviously, the depletion region in the photoconductive mode is much more apparent than that in the photovoltaic mode . Higher reverse-biased voltage makes this depletion region even thicker. When light hits the P-type semiconductor, electron–hole pairs are generated in the depletion region. As the depletion region is thicker, it can generate much higher number of electron–hole pairs with proper light exposure, capable of generating much higher current than the photovoltaic mode. The dynamic range of the photoconductive mode is much broader than the photovoltaic mode. In addition, the reverse-biased voltage also consumes the extra holes (in the P-type side) and the extra electrons (in the N-type side) quickly, making this mode a lot more sensitive than the photovoltaic mode .

It may seem that photovoltaic mode is never used and the photoconductive mode is the only choice in practical applications. However, there is another way to take advantages of the simplicity of photovoltaic mode and sensitivity of photoconductive mode: *PIN PD* . As shown in Fig. 7.6, a PIN PD has an

additional layer in between the P-type and N-type semiconductors, called *intrinsic (I) layer*, which is almost an insulator. This intrinsic layer should act as a naturally occurring depletion region, without necessarily applying a reverse-biased voltage. Therefore, a PIN PD in photovoltaic mode can generate about the same dynamic range and sensitivity of a PN-junction PD in the photoconductive mode. If a PIN PD is used in the photoconductive mode, there is not much advantages in dynamic range and sensitivity, but it does show better linear response than a PN-junction PD in photoconductive mode.

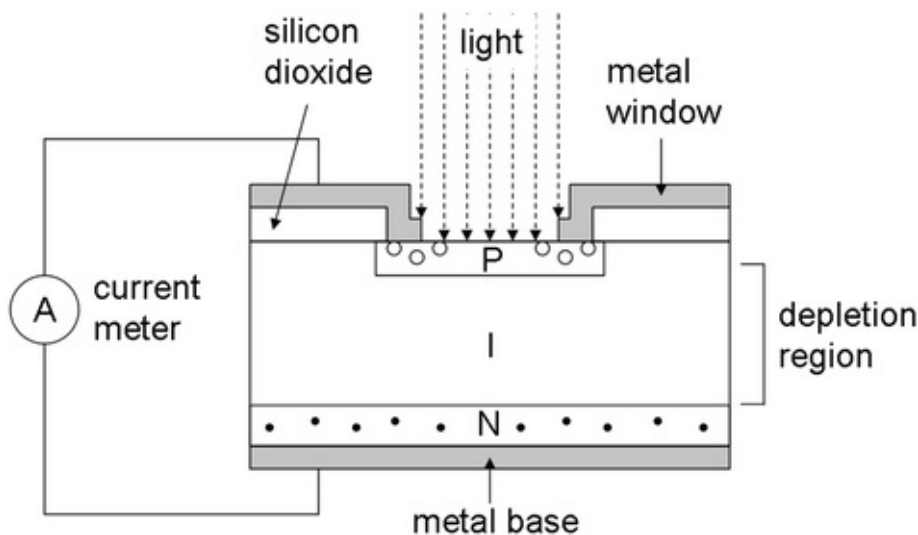


Fig. 7.6 PIN photodiode in photovoltaic mode. Thicker depletion region is formed because of intrinsic (*I*) layer, without reverse-biased voltage

PDs in photovoltaic mode generate electric current without applied voltage, i.e., they convert light energy into electrical energy. This is the working principle of a *solar cell*. Basically, a solar cell is a PD in photovoltaic mode, with much larger surface area. Solar cell is sometimes referred to as a *photovoltaic cell* to address this relationship.

Multiple PD-like components can be integrated together to form a one-dimensional (linear) or two-dimensional arrays. This integrated-array-type light detector is called charge-coupled device array (CCD array). 1-D CCD is used for a miniature spectrometer (see Chap. 8) or a scanner, while 2-D CCD is primary used for digital camera (see Chap. 13 Lab).

CCD is essentially a metal oxide semiconductor (MOS). Complementary metal oxide semiconductor array (CMOS array) is also widely used for digital camera and smartphone.

7.4 Phototransistor

In a conventional NPN bipolar transistor, the small current flowing into the base (P-type semiconductor) controls the bulk current flow from the collector to the emitter. In an NPN *phototransistor*, that base current is replaced with light (photons). Photons create electron–hole pairs, and it enables the electrons to jump from the emitter toward the collector (and the holes to jump from the collector toward the emitter), just like the normal operation of an NPN bipolar transistor (Fig. 7.7).

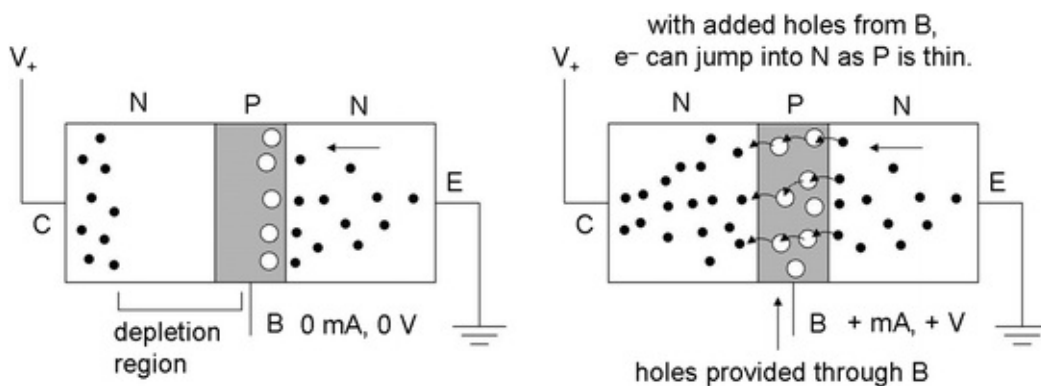


Fig. 7.7 A conventional NPN transistor (identical to Fig. 3.9)

A NPN phototransistor is fabricated first by diffusing P-type silicon (base) into the N-type (collector), followed by diffusing the N-type (emitter) into the P-type. A PNP phototransistor can be fabricated in a similar manner.

Phototransistors do not have a base prong; they only have two prongs, collector and emitter, as the light irradiation replaces the base current. In addition, the phototransistor is mounted under a clear window so that light can strike its upper surface (Fig. 7.8).

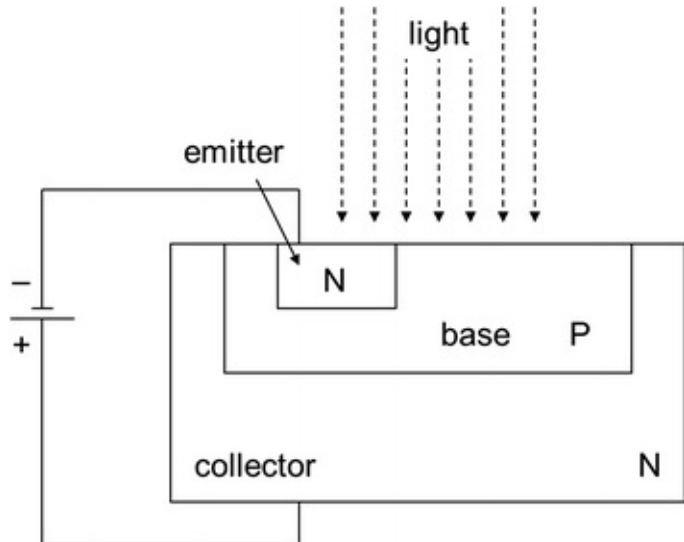


Fig. 7.8 An NPN phototransistor

A phototransistor can produce much higher output currents than a PD because the phototransistor is also a transistor, i.e., has a built-in amplifying ability. Despite this superiority over a PD, it has a disadvantage: it is more vulnerable to device failure (can be damaged easily) because it handles much higher current than a PD.

7.5 Light-Emitting Diode (LED)

We have already used the LED as an example of a diode in Chap. 2. In theory, every single diode should emit light with forward bias. An LED is simply a special version of a diode that comes with transparent plastic packing (so that it can emit light) and is optimized for generating light at a certain wavelength (or color). Figure 7.9 shows green LEDs.

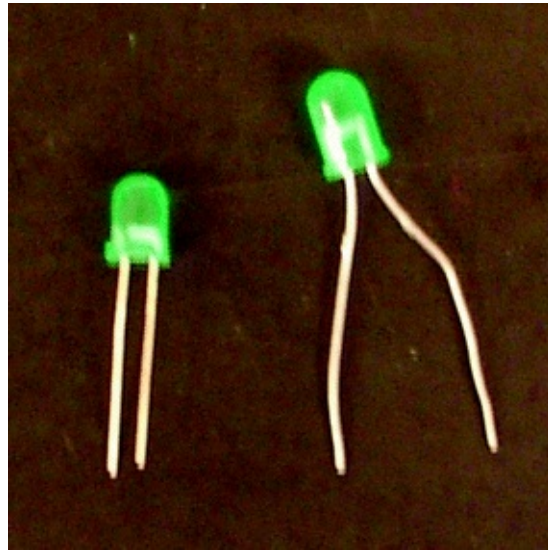


Fig. 7.9 Light-emitting diodes (LEDs)

Figure 7.10 shows a PN-junction diode. With forward bias, electrons bind to holes at the PN junction. In all three light sensors we learned in this chapter (photoresistor, PD, and phototransistor), light (photons) is able to strip the electrons off the molecules, creating electron–hole pairs. When electrons and holes combine together, the reverse happens: light emission.

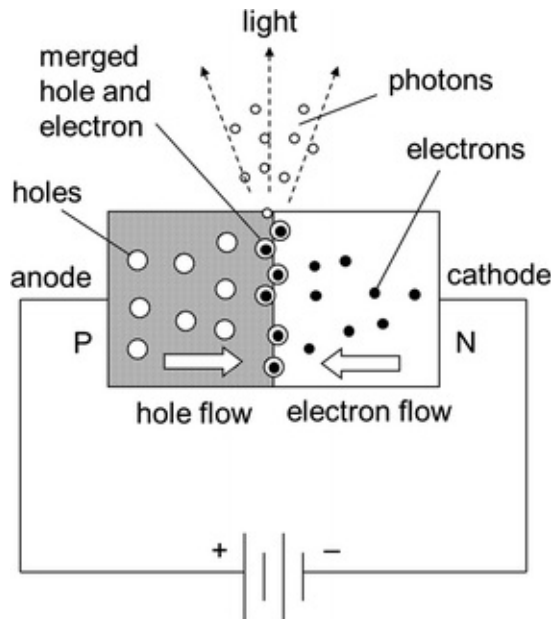


Fig. 7.10 Working principle of an LED

The wavelength of light emission is determined by the type of semiconductor

material used in constructing LEDs. The ability of light emission for ordinary diodes is very poor, as they are mostly made with silicon, which is opaque material. A red LED, meanwhile, uses gallium arsenide phosphide (GaAsP), which is semitransparent and primarily generates red light emission.

The relationship between forward current and voltage in a typical GaAsP LED is shown in Fig. 7.11. Once the forward bias is increased to ~ 1.2 V, the current increases rapidly. The forward voltage does not increase beyond ~ 1.6 V and is essentially constant. Only the current continues to increase, so we should be very careful not to apply too much current into an LED to prevent damaging it. This was already observed in Chap. 3 laboratory.

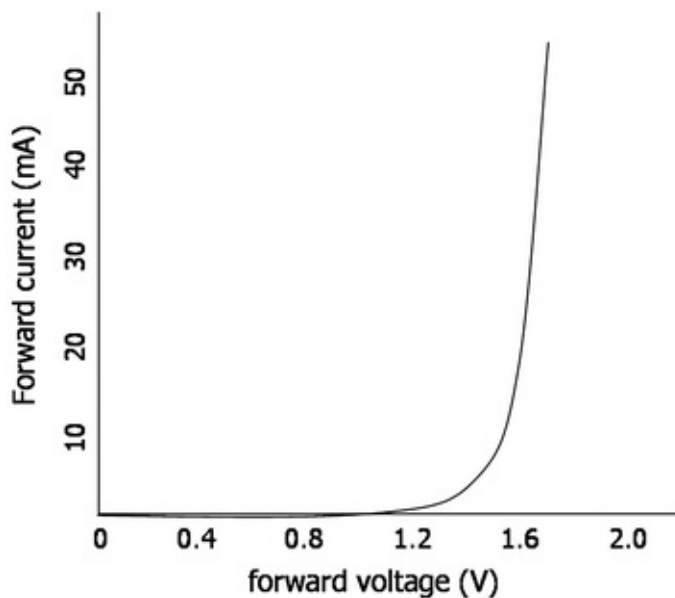


Fig. 7.11 I–V curve for GaAsP LED

The popularity of LED in light sensor application is its low power consumption. As observed in Chap. 3, LED consumes much less power compared to the other types of light sources, such as incandescent, halogen, gas-discharge, xenon flash, or even fluorescent light bulbs. In addition, LEDs generate nearly monochromatic light, i.e., light at a single color, while incandescent light bulbs generate white light, i.e., mixture of light with wide range of wavelengths (colors). This is a very important feature in many biosensor applications using fluorescent dyes, where each fluorescent dye must be excited with different color.

There is another type of LED that generates “white” light, mimicking the natural sunlight, referred to as *white LED*. White LED is essentially a hybrid of two different LEDs, one in blue and the other in yellow (i.e., at the boundary of

green and red), thus covering the all three basic colors (RGB) of visible spectrum. White LED is popularly used as a flash for digital cameras and smartphones.

7.6 Laser Diode

A *laser diode* is a special type of LED that generates *laser*, which is a coherent beam of light that is extremely monochromatic. Figure 7.12 in the previous page shows the extremely monochromatic character of laser in comparison with LED.

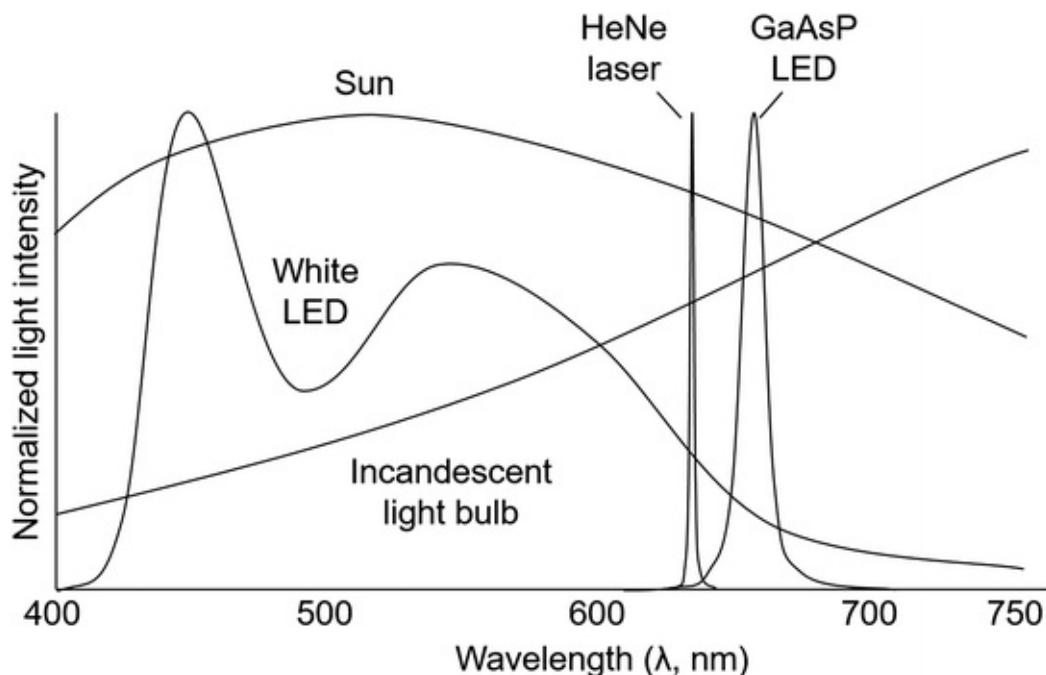


Fig. 7.12 Light intensity— λ curves (spectra) of various light sources

Let us begin our study with laser first. Laser is an acronym for Light Amplification by Stimulated Emission of Radiation. Figure 7.13 shows a basic apparatus for generating laser. Two mirrors are sandwiching a small column, called *gain medium*. In a HeNe laser, the earliest yet still very popular type of lasers, the gain medium is helium–neon gas. When a DC voltage is applied into this gain medium, photons are generated at a very specific wavelength. For HeNe laser, $\lambda = 633$ nm (red color). These photons will bounce back and forth between two mirrors, thus amplifying the light intensity. The right mirror is made partially transparent, and some of this amplified, monochromatic light can escape from the system. Note that only the light that bounces perpendicular to two mirrors will be bounced and amplified. Because of this, the light beam

generated from the right mirror is made extremely coherent.

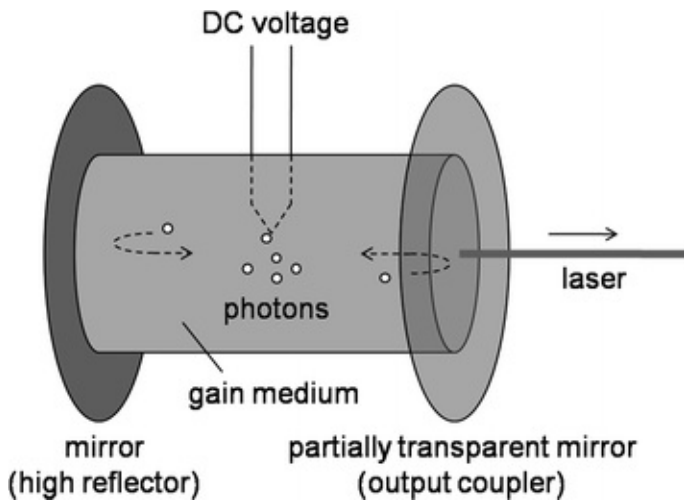


Fig. 7.13 Working principle of laser

In a laser diode, the gain medium is replaced with an LED, with two surrounding mirrors attached to it. Application of DC voltage to the PN junction of LED obviously creates the photons. With sufficient amount of current, these photons can travel to the mirrors and bounce back and forth, so that the light intensity is amplified and a coherent beam of light is created. Unlike the other type of lasers, especially the gas lasers such as HeNe laser, the laser diodes require much less voltage power, is much smaller (about the same size of typical LEDs), and a lot cheaper. Despite this simplicity and low cost, it is still laser; the spectrum width is around 1 nm (see Fig. 7.12), and can focus radiation to a spot as small as 1 μm in diameter. One disadvantage of laser diodes (compared to gas or other types of lasers) is that its beam is divergent, typically elliptical or wedge-shaped, and astigmatic, requiring refocusing.

Laser diodes are most commonly used in CD, DVD and blu-ray players, laser printers, and barcode/UPC scanners. They are also becoming very important in many biosensor applications, especially when the light needs to be irradiated to the small area of interest, such as microcapillary channels, and when the light source needs extremely narrow spectrum width.

7.7 Laboratory Task 1: Photoconductive Operation

In this task, you will need the following:

- A breadboard, wires, wire cutter/stripper, a power supply and a DMM.

- 20 k Ω pot, and a screw driver.
- 1 Ω resistor.
- Planar diffused silicon PD (metal package; *PIN-040A* from UDT Sensors, Inc.).
- Incandescent light bulbs: 15, 40 and 60 W.
- Sockets for light bulbs.
- Ruler.

Figures 7.14, 7.15 and 7.16 show the circuit layout, photodiode pin layout, and circuit photo. The PD is aligned in reverse bias, indicating this is a photoconductive operation. Without light, a depletion region forms between the P- and N-type semiconductors (because it is set to reverse bias), and no current flows. With light, this depletion region gradually disappears and the current starts to flow.

The 1 Ω resistor is used for measuring the current flowing through the PD. Before applying the voltage to the circuit, make sure that the voltage output from the 20 k Ω pot is less than 10 V, so that a huge current is not applied to the PD.

Expose the PD to the 60 W light bulb (630 lm) by bringing the light bulb as close as possible, as shown in the following figure.

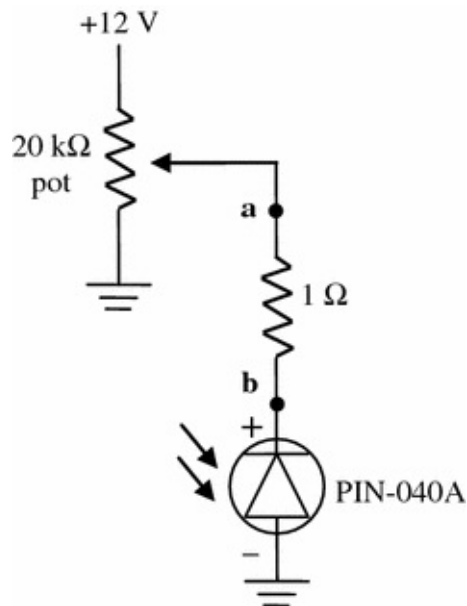


Fig. 7.14 Circuit diagram of Task 1

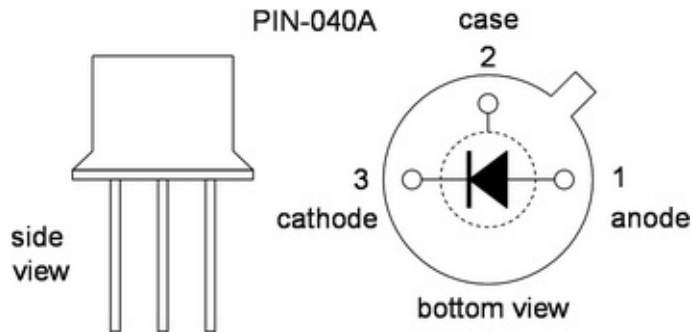


Fig. 7.15 TO-18 metal packaging for PIN-040A photodiode

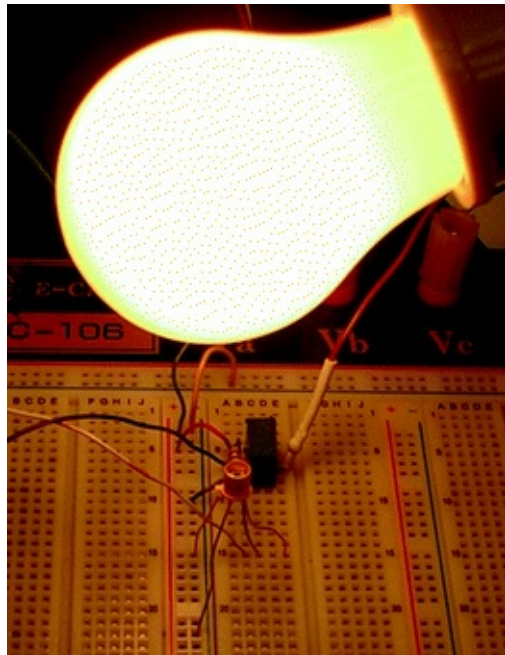


Fig. 7.16 Circuit photo of Task 1

While changing our pot from 0 to 10 V, measure the voltage applied to the system ($V_a = V$), and the voltage drop across the $1\ \Omega$ resistor (V_{ab}) to evaluate current (I). Figure 7.17 summarizes the experimental results (current against voltage), indicating almost constant current readings over the voltage range. Take the average of the currents that are “plateaued.” This is your sensor reading.

Voltage (V , from V_a)	Current (mA, from V_{ab})			
	ambient	15 W	40 W	60 W
0	0	0	0	0
1	0	0.1	0.5	0.7
3	0	0.1	0.5	0.7
5	0	0.1	0.5	0.7
9	0	0.1	0.5	0.7

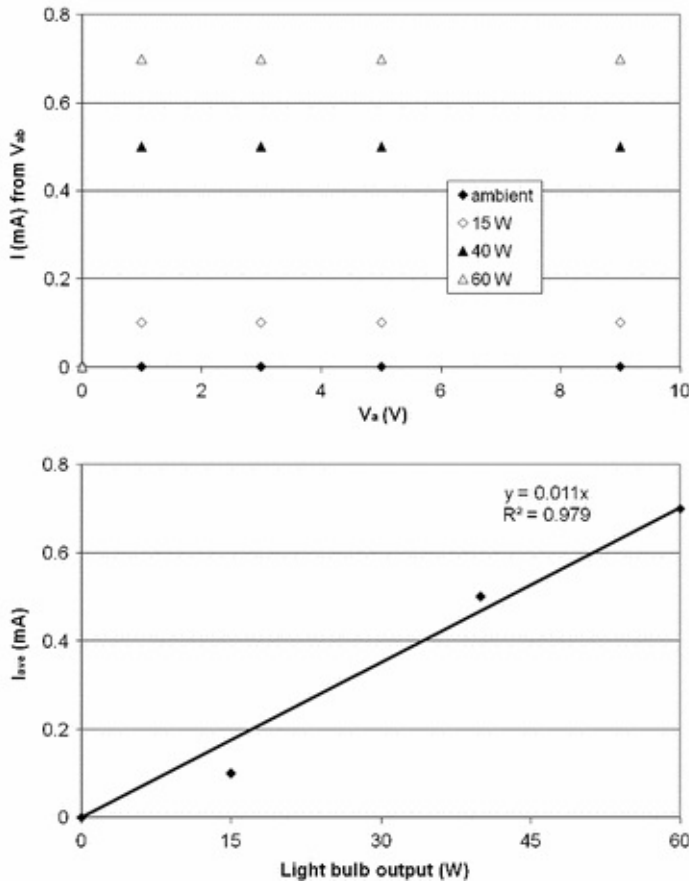


Fig. 7.17 Experimental data from Task 1: I – V and I_{ave} —light bulb output. We notice that the I —light bulb output graph is quite linear

Repeat the experiments with a 40 W light bulb (480 lm), with a 15 W light bulb (110 lm), and with ambient light. Plot the average current readings against the light bulb output (W), provided by the bulb manufacturer.

Question 7.1

The experimental data shown above indicates almost no current for the ambient light, and the I —light bulb output curve passes thru the origin. If the current for ambient light is 0.1 mA, can you estimate the light intensity of ambient light using the above data (in W)?

Continue this experiment by adjusting the distance between the light bulb and the PD. Pick the 60 W light bulb, and fix your pot to certain voltage that generates acceptable current readings. Vary the distance between the light bulb and the PD, and measure the current from V_{ab} . The distance should be measured with a ruler. Plot the current against this distance. Determine the distance where the current becomes the same as the ambient light current. This is the maximum distance that the PD is usable under ambient light conditions (Fig. 7.18).

Distance (cm)	0	0.5	0.8	1.3	3.0	4.1	5.6	7.4
I (mA, from V_{ab})	0.7	0.6	0.5	0.4	0.3	0.2	0.1	0

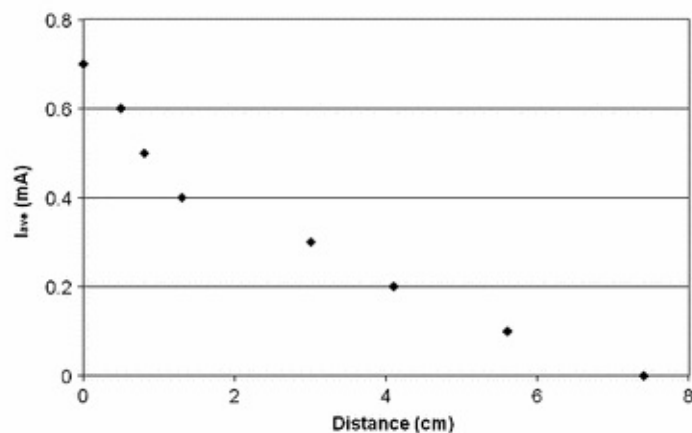


Fig. 7.18 Experimental data from Task 1: I —distance (60 W)

Alternative Task 1: Photoconductive operation—maximum distance

Repeat the I —distance experiment for the other two light bulbs (the 15 and 40 W). Evaluate the maximum detectable distance for those light bulbs as well. Plot the maximum detectable distance against the outputs (W) of the light bulbs, and perform an appropriate linear regression on the data.

7.8 Laboratory Task 2: Photovoltaic Operation

For regular PN PDs, the photovoltaic mode should be less sensitive to light than the photoconductive mode. This is not the case for PIN PDs, since they already have a thick enough depletion region (I-type material). In reality, applying a reverse bias voltage (photoconductive mode) is not necessary because the PIN PD has its own depletion region. As a result, the photovoltaic mode is also sensitive enough for a PIN PD.

In this task, you will need the following:

- A breadboard, wires, wire cutter/stripper, a power supply, and a DMM.
- Two $1\text{ k}\Omega$ and two $10\text{ k}\Omega$ resistors.
- PIN-040A PD.
- Op-amp LM741 (or LM324).
- Incandescent light bulbs (with sockets): 15, 40 and 60 W.
- Ruler.

Figures 7.19 and 7.20 show the circuit layout. No voltage is applied to the PD, and the current flows from the positive to the negative terminals of an op-amp, so this circuit is set up for photovoltaic operation. Upon light exposure, a small current flows from the anode ($-$) to the cathode ($+$). The op-amp is configured as a “differential” setup; in other words, the voltage drop across the PD is measured. The gain is 10.

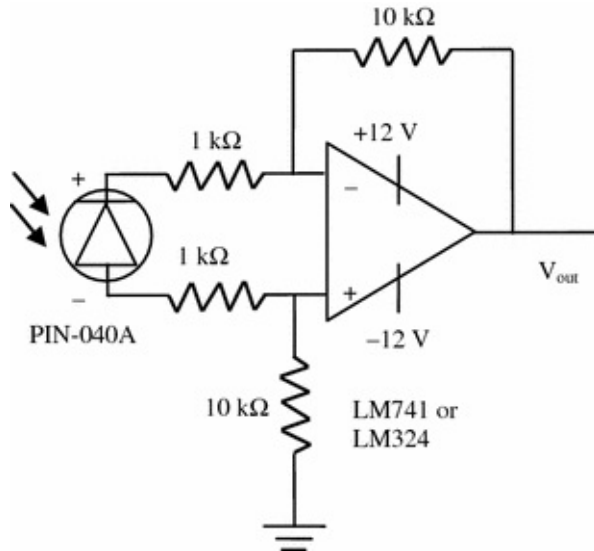


Fig. 7.19 Circuit diagram for Task 2

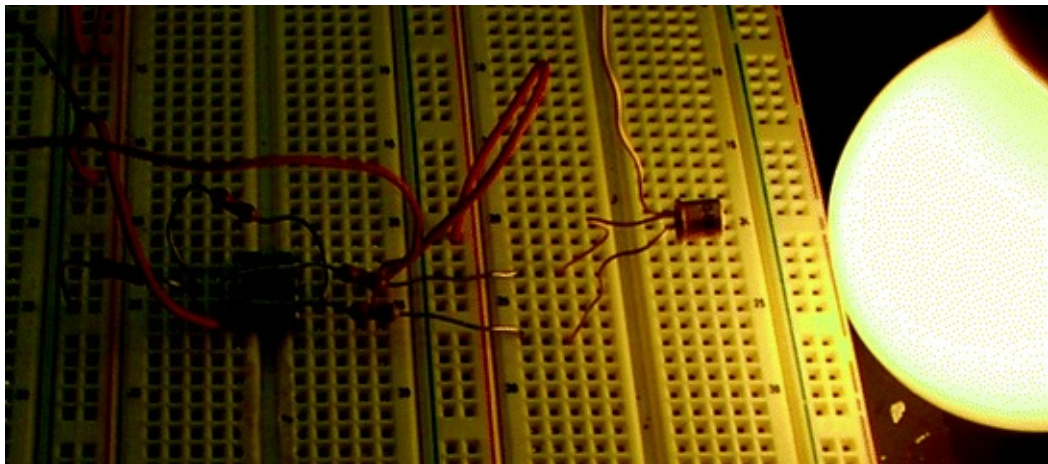


Fig. 7.20 Circuit photo of Task 2

Record V_{out} under ambient light, and for the 15, 40, and 60 W light bulbs (with bulbs as close as possible). Plot V_{out} against the light intensities specified by the light bulb manufacturer. Also, repeat the second half of Task 1, the I —distance experiments (Figs. 7.21 and 7.22). The op-amp layouts are shown in Fig. 7.23 to assist circuit construction.

Light bulb output (W)	0	15	40	60
V_{out} (V)	0	4.03	4.56	5.13

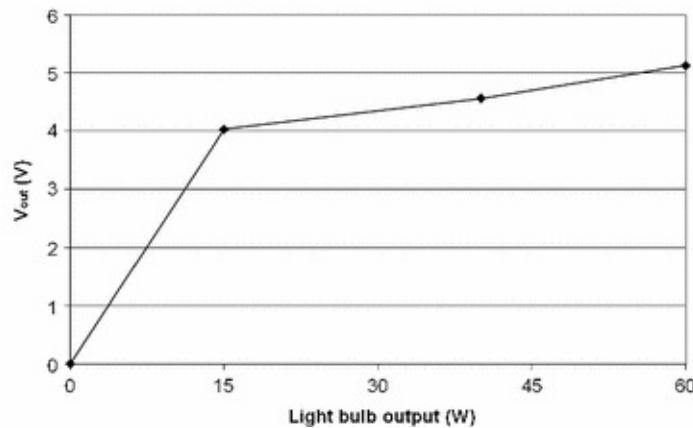


Fig. 7.21 Experimental data from Task 2: V_{out} —light bulb output

Distance (cm)	0	2	8	18	34	50	72	98
$V_{out}(V)$	5.13	3.26	0.96	0.31	0.12	0.06	0.02	0.01

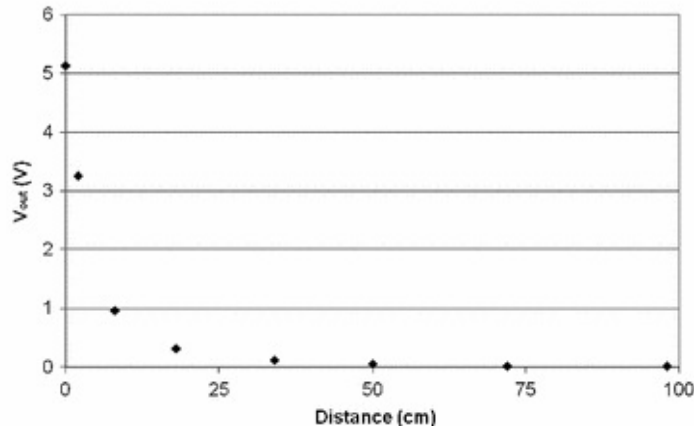


Fig. 7.22 Experimental data from Task 2: V_{out} —distance (60 W)

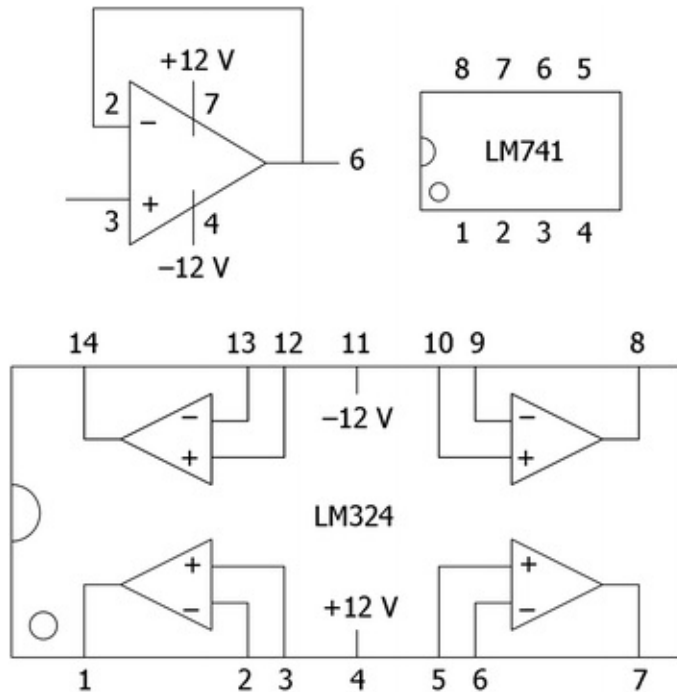


Fig. 7.23 Op-amps LM741 and LM324

Alternative Task 2: Photovoltaic operation—maximum distance

Repeat the V_{out} —distance experiment with a different gain. Change both $10\text{ k}\Omega$ resistors to $5\text{ k}\Omega$ such that gain becomes 5. Is there any difference in the maximum detectable distance? Note that when you amplify your signal, you are amplifying both the signal and the noise from the environment, so the signal-to-noise ratio (S/N) will stay the same. If needed, however, an op-amp filters can

also be used to filter the noise within an electric circuit.

References and Further Readings

- Bhattacharya P (1996) Semiconductor optoelectronic devices, 2nd edn. Prentice Hall, Upper Saddle River
- Cardinale G (2003) Optoelectronics: introductory theory and experiments, 1st edn. Delmar Cengage Learning, Clifton Park
- Kasap S (2000) Optoelectronics and photonics: principles and practices, 1st edn. Prentice Hall, Upper Saddle River
- Litwiller D (2001) CCD versus CMOS: facts and fiction. Photonics Spectra. Available at: http://www.teledynedalsa.com/public/corp/Photonics_Spectra_CCDvsCMOS_Litwiller.pdf. Accessed Jan 2001
- Litwiller D (2005) CMOS versus CCD: maturing technologies, maturing markets. Photonics Spectra. Available at: http://www.teledynedalsa.com/public/corp/CCD_vs_CMOS_Litwiller_2005.pdf. Accessed Aug 2005
- Parker M (2005) Physics of optoelectronics, 1st edn. CRC Press, Boca Raton
- Ristic L (ed) (1994) Sensor technology and devices. Artech House, Norwood
- Rosencher E, Vinter B (2002) Optoelectronics, 1st edn. Cambridge University Press, Cambridge
- Scherz P (2006) Practical electronics for inventors, 2nd edn. McGraw-Hill, New York
- Webster J (1998) The measurement, instrumentation and sensors handbook, 1st edn. CRC Press, Boca Raton

8. Spectrophotometry

Jeong-Yeol Yoon¹✉

(1) University of Arizona, Tucson, AZ, USA

✉ Jeong-Yeol Yoon
Email: jyyoon@email.arizona.edu

In the previous chapter we learned about optoelectronic light sensors, especially photodiode. Although many photodiodes are made to be specifically sensitive to a certain range of colors, e.g., UV-blue, red-IR, etc., they cannot tell the exact color or color combination of a light signal. Photodiodes (and most other optoelectronic light sensors) simply inform us of the intensity of light signals. Detailed information on color combination can be obtained using a technique known as *spectrophotometry*, which involves an instrument known as a *spectrophotometer*. Spectrophotometers are quite bulky, relatively expensive, and have not been considered as a topic for sensors or biosensors. In recent years, however, very small spectrophotometers (of size comparable to a smartphone) have become commercially available. Because of this, spectrophotometers are becoming an integral part of many sensor and biosensor devices.

8.1 Spectrophotometry

A spectrophotometer measures the light intensity that is absorbed or transmitted through (sometimes scattered or reflected from) a sample material, which is typically liquid solution in a container, but sometimes gas in a container. This intensity measurement can be made at a specific wavelength, or scanned through a range of wavelengths. If the measurement is made at a specific wavelength, it is called *photometry*. If the measurement is made for a range of wavelengths, it

is called *spectrometry*, and the resulting light intensity—wavelength curve is called a *spectrum* (plural: *spectra*). Therefore, you can see that spectrophotometry is a collective term for both spectrometry and photometry. Most commercial instruments are capable of conducting both spectrometry and photometry, hence they are called spectrophotometers. Most spectrophotometers measure absorbance, thus they are specifically called *absorption spectrophotometers*, and the resulting spectrum is called the *absorption spectrum*.

Many different types of light can be used for spectrophotometry, including, but not limited to: X-ray, ultraviolet (UV), visible (Vis), infrared (IR), etc. The most common types of spectrophotometers are the ones that use both UV and Vis (called *UV/Vis spectrophotometer*) and IR (typically with Fourier transform feature, hence *FT-IR spectrophotometer*) (Fig. 8.1).

Figure 8.2 is a schematic illustration for the simplest possible spectrophotometer. The light source is a lamp, which is typically a xenon (Xe) arc lamp, deuterium (D_2) arc lamp, and/or a tungsten (W) incandescent lamp for UV/Vis spectrophotometer. These types of lamps generate light at all wavelengths (in their appropriate ranges), in almost equal proportions, and are considered to be “white” light sources. This white light passes through a *monochromator*, consisting of a prism, a couple of mirrors (not shown above), and a slit, which chooses a particular wavelength. This selected beam of light finally passes through a rectangular container that holds a liquid solution. This container is called a *cuvette*. Depending on the type and concentration of solute in the solution, as well as the type of liquid medium (typically water), the intensity of light is attenuated. Finally a light detector (photodiode in Fig. 8.2) measures the intensity of this attenuated light. By comparing this light intensity (I) with that from the light source (I_0), we can measure the light absorbance A :

$$A = -\log \frac{I}{I_0} = \log \frac{I_0}{I} \quad (8.1)$$

where

I light intensity after passing through the material (typically liquid)

I_0 light intensity from the light source



Fig. 8.1 Left a UV/Vis spectrophotometer. Right a FT-IR spectrophotometer . Pictures taken by Tim Vickers in July 2008 (left) and S. Levchenkov in June 2008 (right) and placed in public domain. Accessed October 2015 from http://commons.wikimedia.org/wiki/File:DU640_spectrophotometer.jpg (left) and http://commons.wikimedia.org/wiki/File:IR_spectrometer.jpg (right)

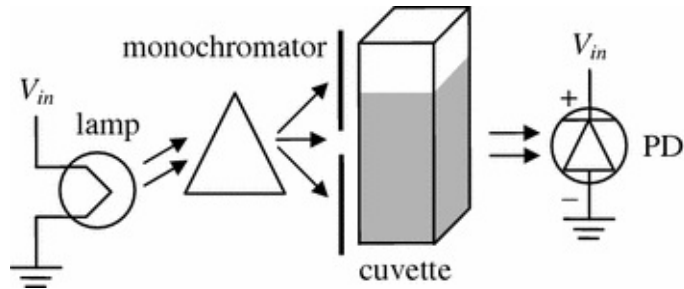


Fig. 8.2 A simple spectrophotometer

I_0 can easily be measured by eliminating the cuvette in the above configuration. In some cases, transmittance T is used instead of absorbance:

$$T = \frac{I}{I_0}, \quad \text{where } A = -\log T \quad (8.2)$$

Absorbance is more common than transmittance, as it is related to the concentration of a specific component in a solution:

$$A = \epsilon lc \quad (8.3)$$

where

ϵ molar absorptivity

l path length (the distance the light travels through the material)

c molar concentration of a specific component

Equation 8.3 is called *Beer-Lambert law* . Note that the path length of a

typical cuvette is 1 cm ($=l$). The *molar absorptivity* may be obtained from literature, but it is usually better to obtain it each time conducting experiments, through constructing a standard curve .

A *standard curve* is made by preparing a series of solutions (typically five to six) containing the target; each solution only varies by a difference in concentration. Absorbance is measured and plotted against the given concentration. A linear regression is performed to obtain $A = (\text{slope}) \times c$. The concentration of a target in the unknown sample can be evaluated by first measuring A , then back-calculating c using the above experimental equation (Fig. 8.3).

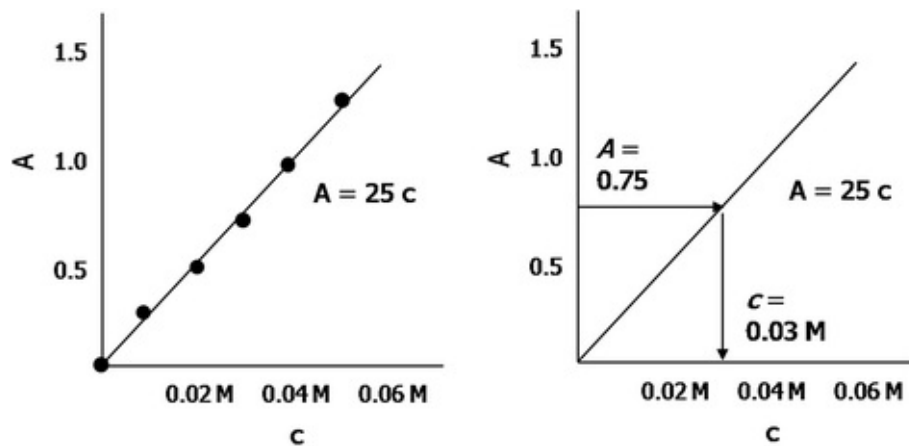


Fig. 8.3 Construction of a standard curve and determination of target concentration with it, using a UV/Vis spectrophotometer

Absorbance (or transmittance) can also be measured for a gas sample if a proper container is available. However, if the sample is a solid plate, it is not possible to measure absorbance (or transmittance). In that case, we need to measure the intensity of reflected light (*reflection spectrophotometry*), where the light detector (photodiode in Fig. 8.2) should be placed at the same side of a light source. This type of instrument is specifically called *reflectometer* .

What we discussed above is just about photometry, i.e., light intensity measurement at a fixed color (or wavelength λ). Recall that most instruments are capable of conducting both photometry and spectrometry (hence spectrophotometers). Spectrometry is achieved by mechanically rotating and/or moving a prism and a mirror such that the wavelength λ of the light passing through a cuvette can be gradually changed against time. Absorbance A is recorded continuously while varying λ , and the instrument provides a plot of $A-\lambda$, which is called a *spectrum* (more specifically, *absorption spectrum*).

For a UV/Vis spectrophotometer, the measured wavelength range is typically from 200 to 900 nm. For an FT-IR spectrophotometer , the measured wavelength range is typically from 2.5 to 20 μm (in wavenumber v unit, which is the inverse of wavelength and more commonly used in FT-IR spectrophotometry, from 4000 to 500 cm^{-1}). Figure 8.4 show the example spectra of UV/Vis and FT-IR spectrometry. While $A-\lambda$ plot is the most common in UV/Vis spectrometry, $T-v$ plot is more common in FT-IR spectrometry.

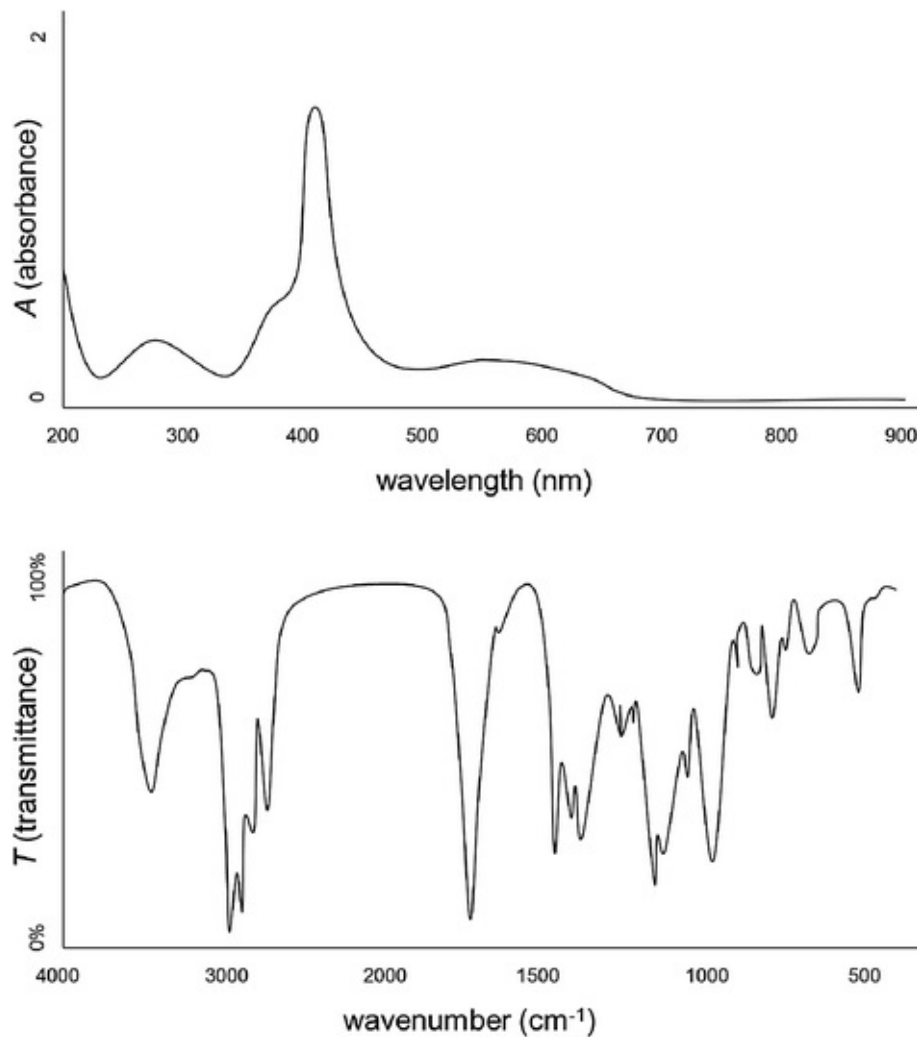


Fig. 8.4 Top a UV/Vis spectrum. Bottom an FT-IR spectrum

Peaks at certain wavelength or wavenumber are characteristic to a certain chemical structure. For example, the peak at 280 nm corresponds to a benzene ring, while the one at 405 nm corresponds to a heme group. The UV/Vis spectrum shown in Fig. 8.4 is actually for the solution of protein called hemoglobin that contains heme group and responsible for oxygen transport

within red blood cells (RBCs). In the case of FT-IR spectrum shown in Fig. 8.4, the big peak around 3000 cm^{-1} corresponds to the C-H stretching and the one around 1700 cm^{-1} corresponds to C=O (carbonyl group). These peak wavelengths can provide useful information on estimating possible chemical structures of an unknown solute, or at least confirming the presence of an expected solute in a solution.

In chemical and biosensor applications, however, photometry at a fixed wavelength is the most frequently used method, as spectrometry is a matter of analytical chemistry rather than sensor application.

8.2 Spectrophotometry Biosensor Example: Pulse Oximeter

The most well-known and commercially successful example of spectrophotometry-based biosensors is the *pulse oximeter*, which measures two important clinical parameters—*oxygen saturation in blood ($\text{SpO}_2\%$)* and *heart rate (pulse)*—in a noninvasive and continuous manner. The first pulse oximeter was developed by Takuo Aoyagi in 1973, and it became very commercially successful since 1980s. Pulse oximeters are being used in almost every hospital throughout the world. It is essentially a spectrophotometer, whose design is very similar to that of Fig. 8.2.

A pulse oximeter measures the absorbance spectra of *hemoglobin* through a human tissue, usually a finger. Hemoglobin is a protein found in RBCs within blood that is responsible for delivering oxygen throughout the body. In fact, the UV/visible spectrum, shown in Fig. 8.4, is the one for hemoglobin, showing a strong peak at 405 nm (at the boundary of UV and blue color), and another one at 280 nm (short wavelength UV). The concentration of hemoglobin can be evaluated by measuring the absorbance at either 280 or 405 nm, using a standard curve and Beer-Lambert law as depicted in Fig. 8.3. In pulse oximeter, however, we are more interested the “status” of hemoglobin, i.e., whether it contains oxygen (*oxyhemoglobin*), or not (*deoxyhemoglobin*), or denatured (*methemoglobin*). Such information can be found in much longer wavelength, in green and red color regions. In Fig. 8.4, a smaller peak can be identified in the green color region, although it is quite smaller than the ones at 405 or 280 nm. Figure 8.5 is the magnified version of Fig. 8.4 for green, red, and near-infrared (NIR) wavelengths, for three different types of hemoglobin: oxyhemoglobin (solid), deoxyhemoglobin (long dash), and methemoglobin (short dash). Oxyhemoglobin, the desired form of hemoglobin in blood, shows two distinct

peaks in the green color region, while the red and NIR absorbance are close to zero (i.e., transparent). Deoxyhemoglobin, where the oxygen is removed, shows only one peak in the green color, while the red absorbance is somewhat increased (i.e., less transparent) and the NIR is still close to zero. Therefore, by measuring absorbance at two different wavelengths, typically 660 nm (red) and 940 nm (NIR), we can estimate the ratio of oxyhemoglobin against the total hemoglobin amount. The 660 nm measurement is the actual signal while the 940 nm signal serves as a reference. Acceptable SpO_2 values are 95–100 % for healthy adults, although 90–95 % or even below 90 % is sometimes possible.

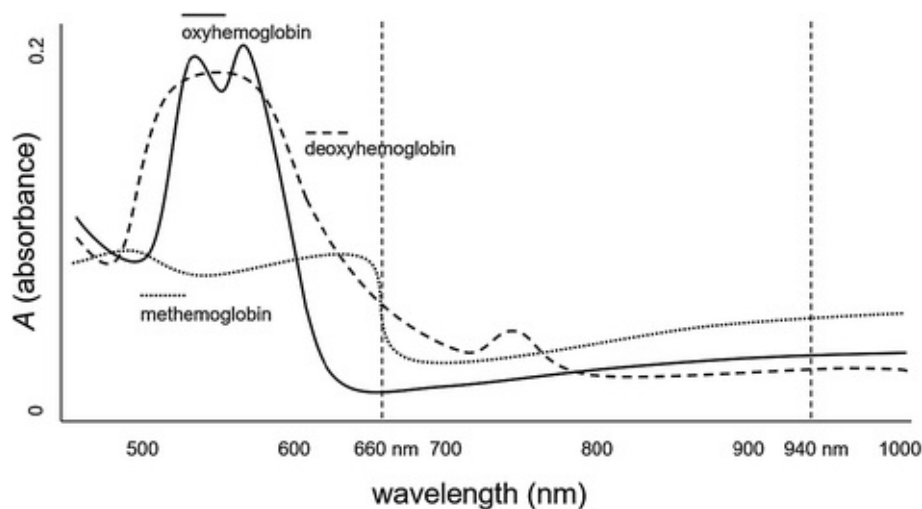


Fig. 8.5 Working principle of pulse oximeter: absorbance spectra of oxy-, deoxy-, and methemoglobin

Methemoglobin can be considered to be a denatured form, showing reduced peak in green color, about the same red absorbance as that of deoxyhemoglobin , and negligible absorbance in NIR. When you purchase a lyophilized powder of hemoglobin from commercial vendors, they are most likely in the form of methemoglobin.

Figure 8.6 shows a simplified schematic of a pulse oximeter. This is essentially a double-beam spectrophotometer, i.e., with two light sources (NIR and red LEDs) and two photodiode detectors, where the cuvette is replaced with a human finger. The actual signals from a human finger are pulsating because of the heartbeat. We can actually use this pulsation to measure the *heart rate* (or *pulse*) of a patient. All pulse oximeters, therefore, measures two parameters, oxygen saturation (SpO_2) and heart rate (pulse) simultaneously. This pulsation does not cause any problem in obtaining SpO_2 as the signal is always normalized by measuring at two different wavelengths.

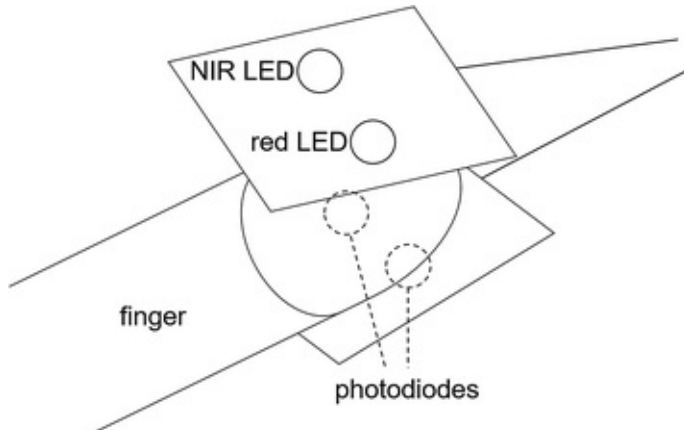


Fig. 8.6 Simplified schematic of a pulse oximeter, which is essentially double-beam spectrophotometer with NIR and red LEDs and two photodiodes

8.3 Miniature Spectrophotometer

As shown in Fig. 8.1, spectrophotometers are often bulky and quite expensive, and difficult to be used in field applications. In recent years, however, several attempts have been made to reduce the size of these spectrophotometers to that of a smartphone. This specific version of spectrophotometer is called *miniature spectrophotometer*, and one example is shown Figs. 8.7 and 8.8.

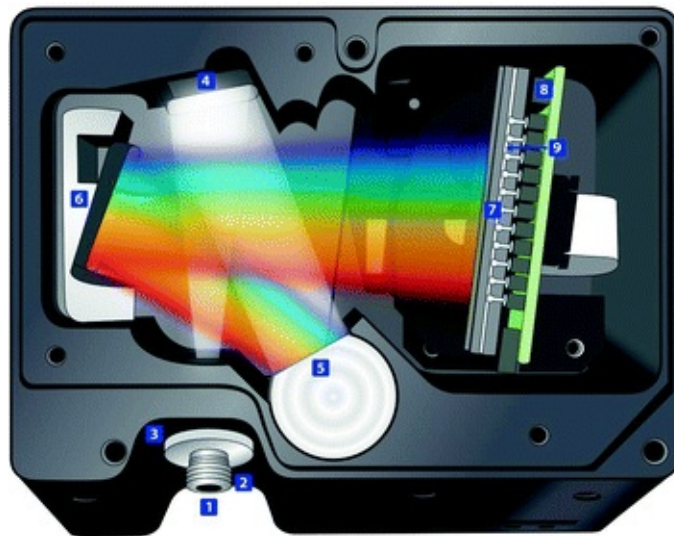


Fig. 8.7 Cut-away view showing internal components of Ocean Optics USB4000 miniature spectrometer. 1 fiber connector, 2 slit, 3 filter, 4 collimating mirror, 5 grating, 6 focusing mirror, 7 detector collection lens, 8 detector (1-D CCD array), 9 filter, 10 quartz window (optional). Accessed in October 2015 from <http://oceanoptics.com/wp-content/uploads/FlameIO.pdf>. Reprinted with Ocean Optics permission. © Ocean Optics 2015



Fig. 8.8 A miniature spectrophotometer (flame) from Ocean Optics. Accessed in October 2015 from <http://oceanoptics.com/wp-content/uploads/FlameIO.pdf>. Reprinted with Ocean Optics permission. © Ocean Optics 2015

In a miniature spectrophotometer, a monochromator is no longer used; instead, a “white” light passes through a cuvette. This light then hits the prism, which spreads light to a rainbow-like spectrum. Instead of using a single PD (or other light detector), a one-dimensional array of charge-coupled devices (CCDs) catches this spectrum, delivering the whole spectrum instantaneously to a computer. This linear or 1-D CCD is essentially the same thing as the one used in digital cameras except for the fact that the CCDs for digital cameras are 2-D. (Note: Some digital cameras use *CMOS array*; refer to the end of Sect. 7.3). This elimination of monochromator makes the device a lot smaller. In addition, a whole spectrum can be obtained almost instantaneously, without “scanning” through a range of wavelengths.

Miniature spectrophotometers are designed to be used with optical fibers, which will be discussed in the next section, and provide versatility in many physical, chemical, and biosensor applications. They can be used as is as an integral part of a biosensor, or a similar concept can be utilized in constructing a modern biosensor.

Unlike the benchtop version of a spectrophotometer, the miniature spectrometer requires a separate computer, typically a laptop or a tablet, connected via a USB port. Separate software is necessary, and it is the *OceanView™* (previously *SpectraSuite™*) for the Ocean Optics miniature spectrophotometer (*USB4000* or *Flame*) (Fig. 8.9). *OceanView™* can measure optical signals in absorbance, reflection, transmittance, reflectance, and irradiance. If your spectrometer is not directly attached to the light source/cuvette holder as shown in Fig. 8.8, the software can only measure the

raw light intensity. To measure absorbance, you will need to acquire a reference spectrum (i.e., I_0 plot over a range of λ). This reference spectrum can be measured with nothing placed on the cuvette holder. In this case, the resulting standard curve should have a y-intercept, which represents the collective background absorbance for a cuvette and water. If you place a cuvette with deionized water while acquiring a reference spectrum, the y-intercept of a standard curve should be zero, since the cuvette and water absorbance has already been accounted for.

The maximum light intensity is 65535 (16-bit). You can zoom in or out as necessary using the toolbox at the left of a main toolbar. You can also set the x- and y-axis ranges manually by clicking the magnifier icon on it. On the top left, you can adjust the integration time. A longer integration time makes the signal (as well as the noise) stronger. Note that a longer integration time does not really improve your sensitivity, since it strengthens both the signal and the noise. Leave the “scans to average” to 1, and the “boxcar width” to 0 for now.

These explanations will not be applicable to the equipment and software from any company other than Ocean Optics; however, the concepts explained here should be useful in understanding miniature spectrometers in general.

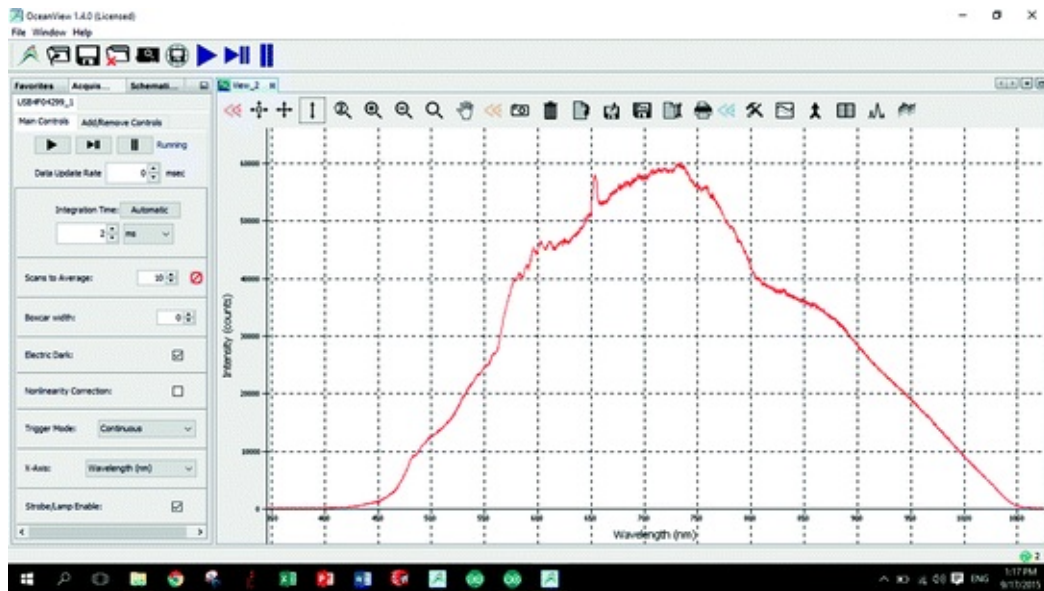


Fig. 8.9 OceanView™ software (from Ocean Optics). Reprinted with Ocean Optics permission. © Ocean Optics 2015

8.4 Optical Fibers

In most equipment-based spectrophotometry, experiments are performed in a

completely dark environment. This dark environment typically makes the equipment quite bulky and expensive. Toward portable spectrophotometry, one needs to concentrate the light on a specific area and capture its transmitted and/or reflected light that can be delivered to a transducer with its full extent. Therefore, a need for guiding light has emerged for portable spectrophotometry measurement, which can be achieved using optical fibers . In portable spectrophotometry, optical fibers are almost always used in conjunction with a miniature spectrophotometer.

An *optical fiber* is a very thin piece of glass or plastic, which acts as a pipe through light can pass. It operates on a principle known as total internal reflection (TIR) (Fig. 8.10). TIR was first observed in 1840s, when scientists found that light could be guided along jets of water for fountain displays. By definition, TIR confines light in a material (*core*) that is surrounded by other material (*cladding*) with a lower *refractive index* n . In the above fountain case, a jet of water acts as the core ($n = 1.33$) and the surrounding air acts as the cladding ($n = 1.0$). The most common materials used in optical fibers are glass (silica) and plastics.

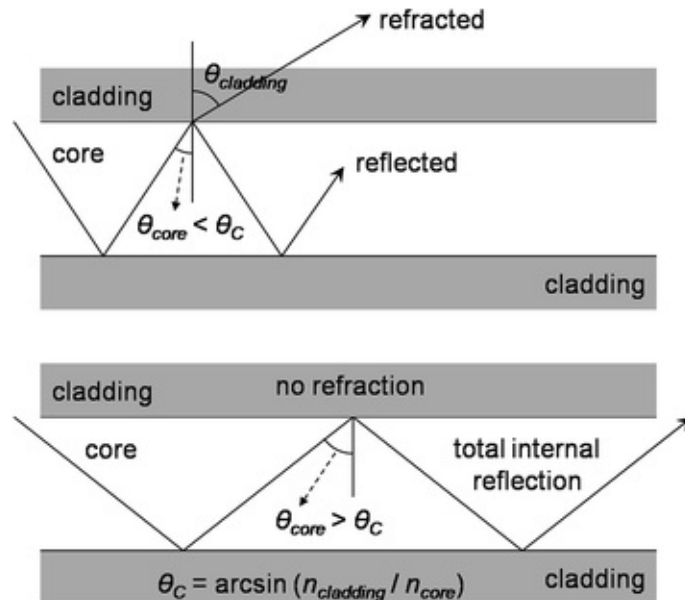


Fig. 8.10 Total internal reflection (TIR)

Refractive index is actually a ratio of light velocities in a vacuum and in medium. When the light hits at the interface of two different materials (in the above case, water and air), the light passes through at a different angle (refraction) according to the *Snell's law* :

$$\frac{\sin \theta_{\text{water}}}{\sin \theta_{\text{air}}} = \frac{n_{\text{water}}}{n_{\text{air}}} = \frac{n_{\text{air}}}{n_{\text{water}}} = \frac{1.0}{1.33} = 0.75 \quad (8.4)$$

If $\theta_{\text{air}} = 90^\circ$, the light cannot pass through the interface, i.e., the light is confined within the core (jet of water). As $\sin 90^\circ = 1$, Eq. (8.4) becomes:

$$\theta_{\text{water}} = \arcsin \frac{n_{\text{air}}}{n_{\text{water}}} = \arcsin \frac{1.0}{1.33} = 49^\circ \quad (8.5)$$

Any θ_{water} that is larger than 49° is reflected back to the core. Due to the nature of the beam that is transferring through the core, the chance for $\theta_{\text{water}} < 49^\circ$ is very small; hence the light travels mostly through the core. In general, this critical angle is defined as

$$\theta_C = \arcsin \frac{n_{\text{cladding}}}{n_{\text{air}}} \quad (8.6)$$

The greater difference in refractive indices of core and cladding makes the critical angle θ_C very small thus ensuring TIR at almost any angles of θ_{cladding} .

Initially, optical fibers have been used for telecommunications (telephone and internet), which is still the majority of optical fiber applications. Light is turned on (1) and off (0) to transmit digital signals. The frequency is extremely high to allow large amount of data transmission. Longer wavelengths are typically preferred for telecommunications, usually IR, as they involve less energy ($E = hc/\lambda$; will be discussed in the next chapter) thus less vulnerable to noise. In addition, signal attenuation is not a significant issue as the signal is digital and carries less energy; in fact, it can travel as much as hundreds of kilometers.

In sensor and biosensor applications, however, the light signal must be transferred in analog form for both light excitation and emission detection. Both UV/Vis and IR can be used for sensor/biosensor applications, although UV/Vis is more common. Due to the high energy of UV/Vis light and its analog nature, optical fibers are more vulnerable to noise and cannot travel for long distance. However, these do not pose any problems in actual applications, as the optical fibers used in sensor/biosensor applications are quite short in length (less than a few meters).

Typical optical fibers can handle wavelengths from 300 nm (longer wavelength UV) to 2 μm (NIR). Core materials should be made transparent to the desired range of wavelengths. Most silica glasses are transparent from 700 nm to 1.6 μm (NIR), while many plastics are transparent for visible light. Both silica glass and plastics will not transmit very efficiently below 400 nm (longer wavelength UV), the core materials for longer wavelength UV should be either quartz or doped silica glass. This doping involves with a high hydroxyl (–

OH) content. The choice of cladding material is also important in sensor/biosensor applications, to ensure proper TIR as well as preventing nonspecific fluorescence.

Typical construction of an optical fiber is shown in Fig. 8.11. The diameters of core ($50 \mu\text{m}$) and cladding ($125 \mu\text{m}$), shown in Fig. 8.11, are typical of the fibers used in some biosensor devices, although these diameters should vary depending on its applications. Note that the diameter of the core ($50 \mu\text{m}$) shown in Fig. 8.11 is substantially larger than the wavelengths of light used in optical fiber applications ($300 \text{ nm} - 2 \mu\text{m}$). In this schematic, thousands of rays of light (light modes) can travel through a core at the same time, which is called *multimode fiber*. This is the most common type of optical fiber, and the equipment needed for connections is relatively cheap. As multiple light modes travel at the same time; however, the signal may be spread over time, which is called *model dispersion*. This problem can be resolved by making the core smaller, $8 - 10 \mu\text{m}$, such that only a single ray of light (a single light mode) can travel. This type of fiber is called *singlemode fiber*, although it requires very expensive connectors and specifically designed op-amps, as the signal is very weak.

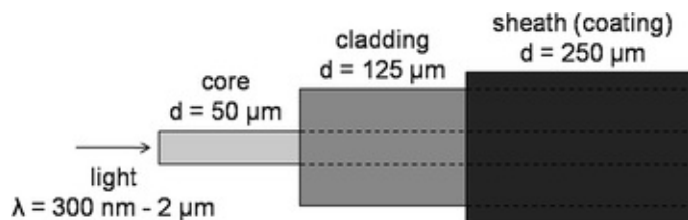


Fig. 8.11 Construction of an optical fiber

Another important feature of optical fibers is numerical aperture (NA). For the light to properly travel through an optical fiber, it must enter and reflect at the cladding at an angle (θ_{core}) greater than the critical angle (θ_C); otherwise, a portion of light may pass through the cladding and TIR would not be achieved. Collecting the rays of light that reflect at the critical angle would draw a cone at the entrance of an optical fiber, which is called *acceptance cone*. The sine of the half angle of this cone is called NA, and for the case shown in Fig. 8.12, it is $\text{NA} = \sin 20^\circ = 0.34$. NA depends on the diameter of a core and the critical angle θ_C . Obviously, the optical fibers with high NAs will accept more light than fibers with low NAs (hence high NAs for multimode fibers and low NAs for singlemode fibers). When the light source and/or the emission signal are weak, one must consider the optical fibers with high NAs.

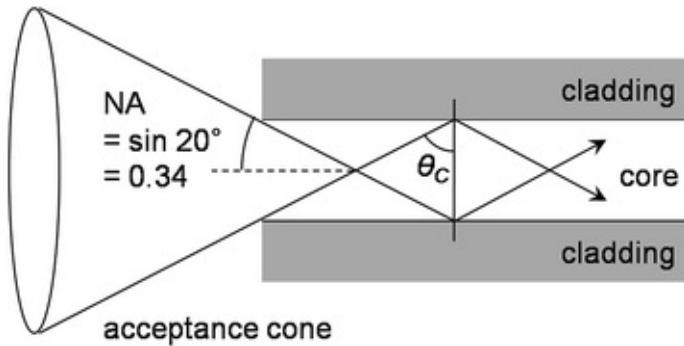


Fig. 8.12 Numerical aperture (NA) of an optical fiber

A typical optical sensor setup with optical fibers is not very different from that of a spectrophotometer (refer to Fig. 8.2): a light source, an optical fiber, material or system under test, another optical fiber, and a miniature spectrometer. Some suppliers offer a simpler alternative to this system, known as a *reflection probe* (Fig. 8.13).

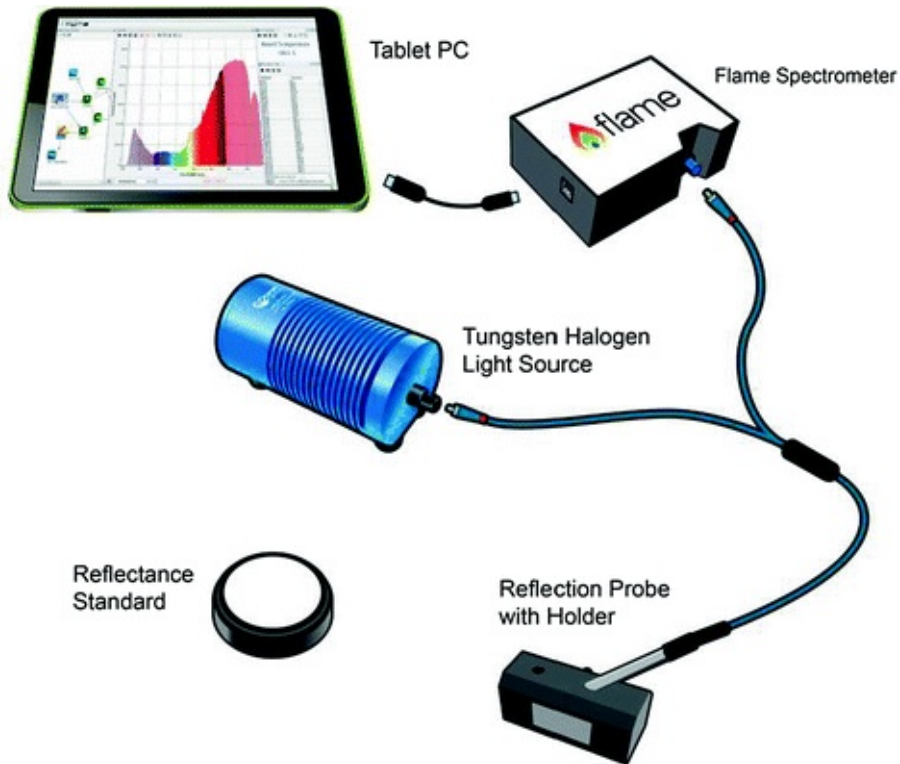


Fig. 8.13 A reflection probe is measuring optical signal, connected to a light source and a miniature spectrometer. Accessed in October 2015 from <http://oceanoptics.com/wp-content/uploads/FlameIO.pdf>. Reprinted with Ocean Optics permission. © Ocean Optics 2015

A reflection probe is a core-shell bundle of optical fibers. The light from a

source is delivered through a core, and the material or system reflects or backscatters this light. (It can also emit fluorescence upon light excitation). The light is then transferred into the shell-side bundle of fibers (as shown in Fig. 8.14), which are eventually delivered to a miniature spectrometer. The probe is connected to Y-shaped optical fiber, with one leg to the light source and the other leg to the miniature spectrometer. This probe can be used to measure optical signals from the ambient air, from the solid surface, in the liquid, in a dark chamber, and more.



Fig. 8.14 Cut-away view of a reflection probe. The core fiber delivers the incident light, and the shell-side bundle of fibers detects the reflected or backscattered light. Accessed in October 2015 from <http://oceanoptics.com/product/premium-grade-reflection-probes>. Reprinted with Ocean Optics permission. © Ocean Optics 2015

8.5 Laboratory Task 1: Hemoglobin Quantification with a Spectrophotometer

In the following tasks, you will use a miniature spectrophotometer and a simplified LED-PD circuit to evaluate the concentration of hemoglobin. As shown in Fig. 8.4, the concentration of hemoglobin can be best evaluated by measuring absorbance at 405 nm (very short wavelength blue color), or by measuring at 280 nm (UV). The primary aim of this laboratory exercise is, however, to identify the different status of hemoglobin (oxy-, deoxy-, and met-), we will focus on measuring green absorbance.

In this task, you will need the following:

- Hemoglobin (in lyophilized powder, mostly methemoglobin)
- Electronic balance, weighing paper, laboratory spatula

- Distilled and/or deionized water
- Centrifuge tubes (1.5 mL)
- Pipettes and pipet tips (1000 μ L)
- A vortex mixer
- A spectrophotometer with white light source and a cuvette holder (CHEMUSB4 or FLAME-CHEM from Ocean Optics) and appropriate software (OceanView™ from Ocean Optics)
- Disposable plastic cuvettes
- Latex gloves, delicate task wipers (KimWipes®)

Preparation of Solutions

- Using an electronic balance (Fig. 8.15), dissolve 3 mg of hemoglobin in 1 mL of deionized or distilled water in a 1.5 mL centrifuge tube. Use a vortex mixer to dissolve (Fig. 8.16). This will make a 3 mg/mL hemoglobin stock solution.
- Using a pipette (Fig. 8.17), dilute the standard in water using 1.5 mL centrifuge tubes as follows (Fig. 8.18).



Fig. 8.15 Weighing lyophilized powder of hemoglobin using an electronic balance



Fig. 8.16 A vortex mixer dissolving hemoglobin in a centrifuge tube



Fig. 8.17 How to use a pipette

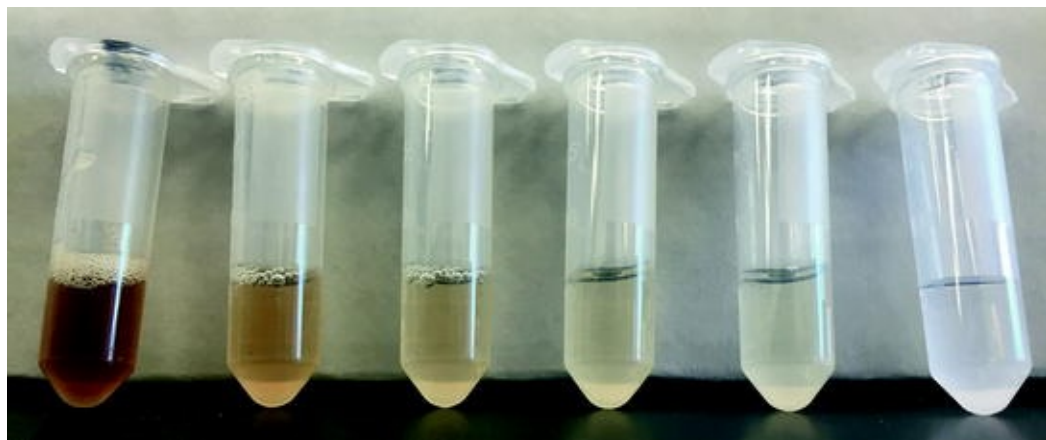


Fig. 8.18 Hemoglobin solutions

No.	Stock + water	Volume (μL)	Hemoglobin (mg/mL)
1	200 μL + 400 μL	600	1.00
2	100 μL + 500 μL	600	0.50
3	50 μL + 550 μL	600	0.25
4	25 μL + 575 μL	600	0.125
5	0 μL + 600 μL	600	0

How to Use a Miniature Spectrophotometer

- The miniature spectrophotometer, CHEMUSB4 or FLAME-CHEM from Ocean Optics, is a combination of a miniature spectrometer USB4000 or Flame, and a light source with a cuvette holder (Fig. 8.19).



Fig. 8.19 A miniature spectrophotometer (*left*), coupled with a light source and a cuvette holder (*right*), from Ocean Optics (FLAME-CHEM spectrometer system). Accessed in October 2015 from <http://oceanoptics.com/product/flame-chem-spectrometer-systems>. Reprinted with Ocean Optics permission. © Ocean Optics 2015

- USB4000 or Flame miniature spectrometer draws its power from a computer via USB port, while the light source and the cuvette holder require a separate power supply using its power adaptor. Although the light source/cuvette holder is powered separately, it still communicates with the computer via USB4000 or Flame miniature spectrometer.
- Make all necessary USB and power connections.
- Launch OceanView™ software. Initially, the software can collect only the raw light intensities. To make the software to measure absorbance, you will need to go through the following calibration procedure.
- At the Welcome Screen, choose “Run a Wizard.”
- Choose “Spectroscopy,” and “Absorbance.”
- Place a cuvette filled with deionized water into the cuvette holder. A raw spectrum of the light source will show up on the screen. Note that the light intensities vary substantially over the wavelengths (λ). If the raw intensity of the light source is high at a certain wavelength, the absorbance measurement at that wavelength will be quite sensitive. If it is low at other wavelength, the absorbance measurement at that wavelength will become less reliable.
- If your spectrum is saturated (i.e., many data points are at their maximum, 65535), decrease the integration time so that no part of your spectrum is saturated. If your light intensities are too low, increase the integration time until the signals start to saturate.

- Click the yellow bulb icon to store the reference spectrum. Click “Next.”
- The yellow bulb icon becomes dark gray bulb, and the light source is now turned off. The resulting spectrum is a dark spectrum (i.e., background noise). Click the dark gray bulb icon to store the dark spectrum.
- Now the software has information for both maximum and minimum signals at all wavelengths, and can convert the raw intensities to the absorbance data.
- Click the magnifier icon to reset the x- and y-axis ranges. For example, the x-axis from 400 to 800 nm (visible light), and the y-axis from 0 to 2.0 (absorbance larger than 1.5 is typically discouraged). Note that your plastic cuvettes are not transparent for wavelengths below 300 nm.
- Transfer each solution into a disposable, plastic cuvette using a pipette. Do not touch the bottom surface, as fingerprints may dramatically affect the absorbance readings.
- Do not recycle the plastic cuvettes. They are for single use.
- The dimension of the bottom portion of a plastic cuvette is $0.5\text{ cm} \times 1\text{ cm}$. A longer path length (1 cm) gives a higher absorbance according to Beer-Lambert law (Eq. 8.3), which is desirable for most cases. However, if your absorbance readings are too high, you may want to try a shorter path length (0.5 cm).
- Once you obtain a spectrum, click around the peak of interest (i.e., 530 nm). Numerical absorbance data at a given wavelength will appear at the bottom. You can also fine-tune the wavelength by clicking it.
- The easiest way to save your result is to press the PrtScn key you’re your keyboard and paste it (Ctrl-V) into your word processing software (Fig. 8.20).

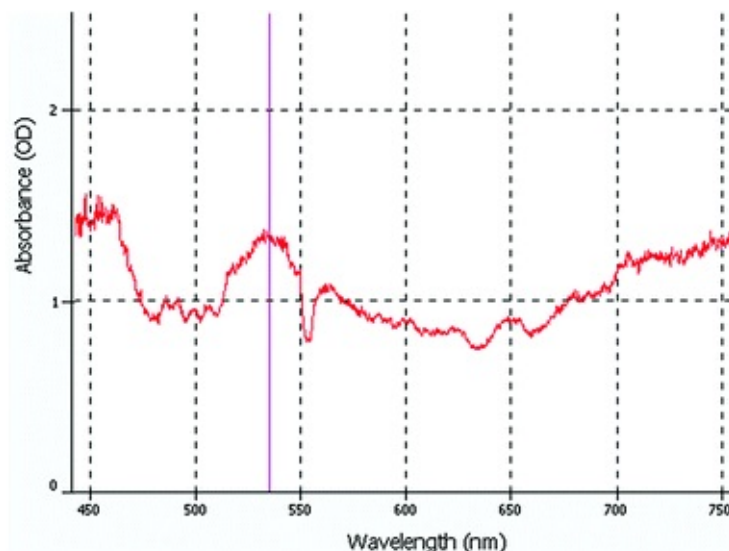


Fig. 8.20 Absorbance spectrum of hemoglobin

Question 8.1

Compare your spectrum to the ones shown in Fig. 8.5. Is your hemoglobin oxy-, deoxy-, or methemoglobin? Explain why your hemoglobin is in that state.

Hemoglobin Quantification Using Beer-Lambert Law

- Read the absorbance A at 520–560 nm (peak absorbance around 530 nm) against the blank. Repeat these measurements for all five samples.
- Theoretically, A at 0 mg/mL concentration should be zero, making the standard curve to pass through origin. In reality, however, the cuvette and water absorb light, leading to positive y-intercept in the standard curve. Although it is okay to use this standard curve as is, one may find it more useful to zero-adjust the entire curve by subtracting with A at 0 mg/mL concentration.
- Subtract blank absorbance (water, #5) from the standard absorbance values (#1–#4), and plot the absorbance against standard concentrations. Determine the slope using linear regression fitting. The y-intercept should be set to zero. This is your “standard curve.”
- Obtain one hemoglobin sample from the other team, without knowing its concentration. This is your “unknown” sample.
- Using this standard curve, determine the hemoglobin concentration of the unknown sample (Fig. 8.21).

Hemoglobin (mg/mL)	0	0.125	0.25	0.50	1.00	unknown
Absorbance	0.01	0.12	0.14	0.89	2.33	1.20

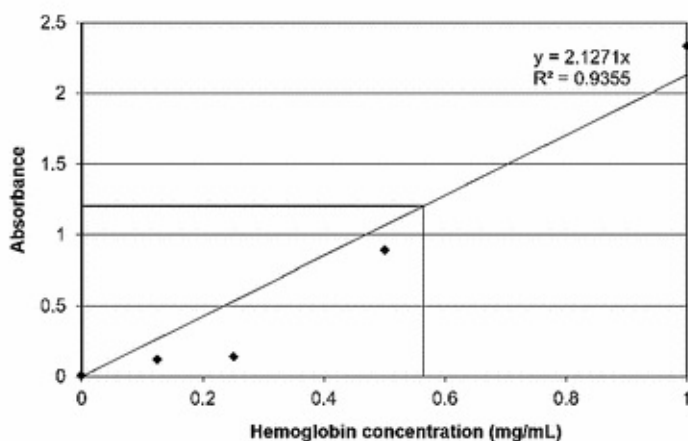


Fig. 8.21 Experimental data from Task 1: absorbance—hemoglobin concentration plot. The hemoglobin concentration of an unknown sample can be calculated from the regression equation: $1.20 = 2.1271x$, $x = 0.564$ mg/mL

8.6 Laboratory Task 2: Hemoglobin Quantification with LED/PD Circuit

We will replace the UV/Vis spectrophotometer with a green LED and a photodiode, using the same five samples from Task 1 in cuvettes. The *LED* circuit is identical to the one we studied in Chap. 3 Task 1, using a green LED (green laser diode can also be used) that generates a maximum light intensity around 530 nm. The photodiode circuit is identical to the one we studied in Chap. 7 Task 2, PIN photodiode in photovoltaic mode with differential op-amp.

In this task, you will need the following:

- A breadboard, wires, wire cutter/stripper, a power supply, and a DMM.
- 10 or 20 $k\Omega$ pot, and a screw driver
- Three $100\ \Omega$ and two $1\ M\Omega$ resistors
- Green LED
- PIN-040A photodiode
- Op-amp LM741 (or LM324)
- Five samples in cuvettes from Task 1

Figures 8.22, 8.23, 8.24 and 8.25 show the circuit layout, photodiode pin layout, op-amp pin layout, and circuit photo. The left-hand side is identical to Chap. 3 Task 1 and the right-hand side is identical to Chap. 7 Task 2 with a much larger gain of 10,000 (Figs. 8.22 and 8.25).

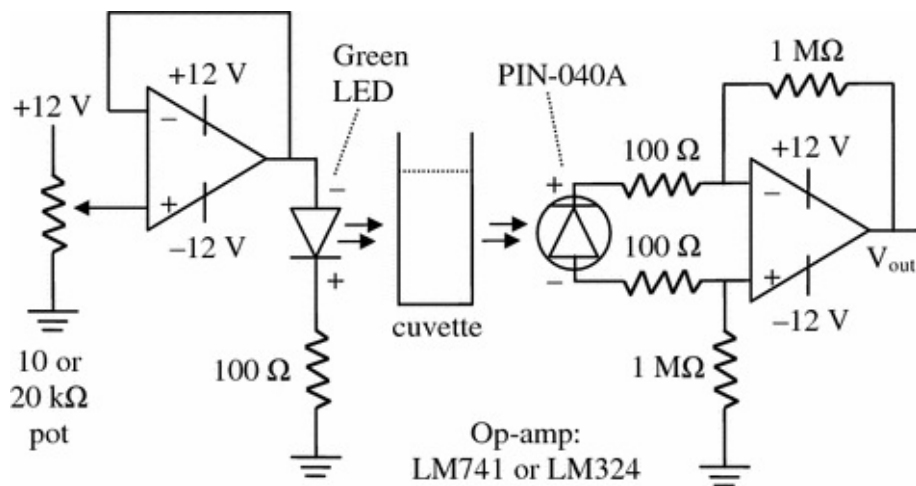


Fig. 8.22 Circuit diagram of Task 2

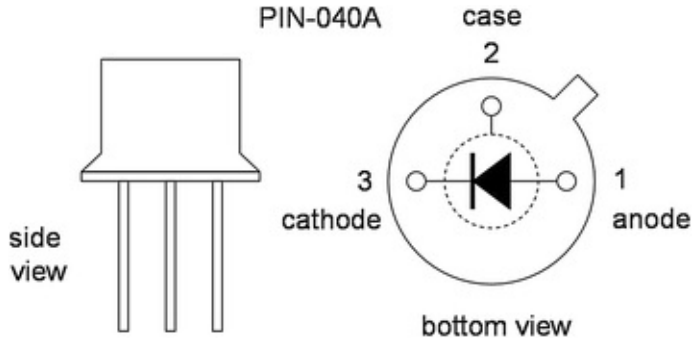


Fig. 8.23 TO-18 metal packaging for PIN-040A photodiode

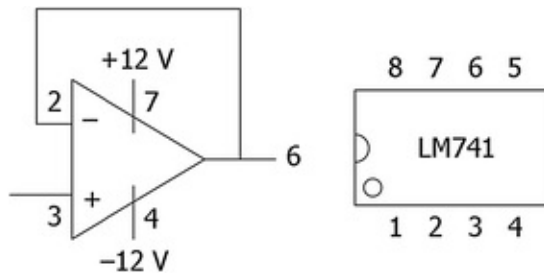


Fig. 8.24 Op-amp LM741

Absorbance is evaluated by measuring light intensities before entering the material (I_0) and after passing through the material (I). Absorbance (A) is defined by $A = \log_{10} (I_0/I)$ (Eq. 8.1). The absorbance is related to the concentration of substance in the medium, with the Beer-Lambert law, $A = \varepsilon lc$ (Eq. 8.3), where ε is the molar absorptivity , l is the path length, and c is the concentration of substance.

As V_{out} from a PD circuit will be divided by that of 0 mg/mL hemoglobin solution, not I_0 , the A at 0 mg/mL automatically becomes 0. This will make the standard curve pass through origin, or zero-adjusted (Fig. 8.26).

As shown in Fig. 8.25, the cuvettes are aligned to have 0.5 cm path length, compared to 1 cm path length in Task 1, the absorbance should be roughly a half of those in Task 1 (consider the Beer-Lambert law, $A = \varepsilon lc$, where l is the path length).

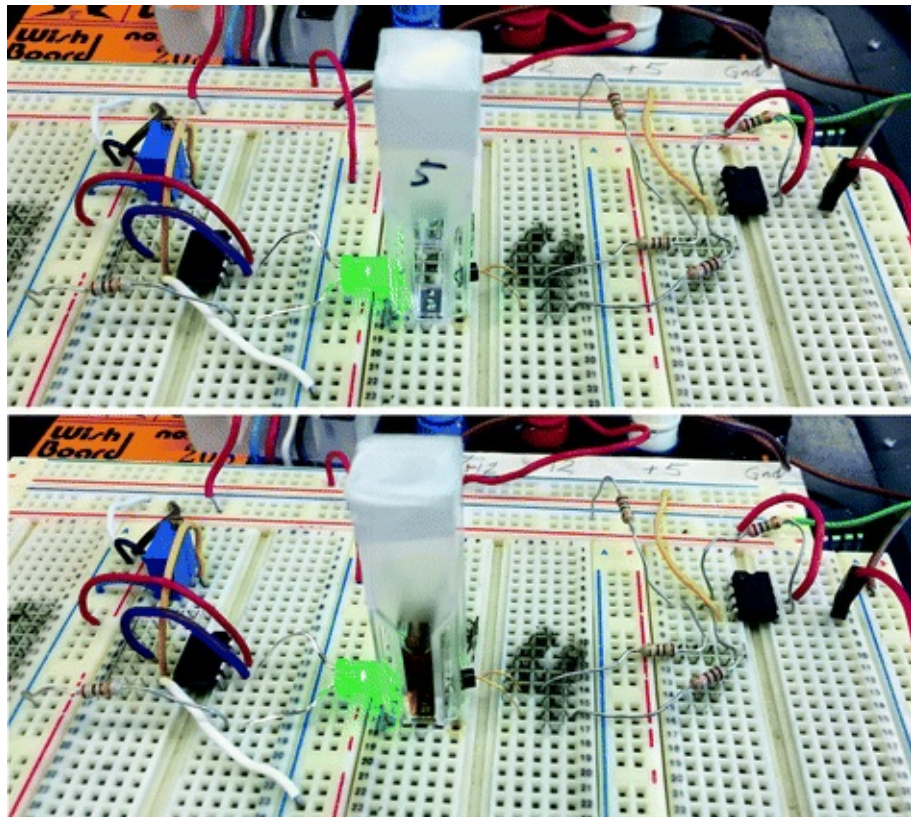


Fig. 8.25 LED-PD circuit is measuring the hemoglobin concentration in a cuvette. Top 0 mg/mL. Bottom 1.00 mg/mL

Hemoglobin (mg/mL)	0	0.125	0.25	0.50	1.00
V_{out}	3.30	2.83	2.69	2.30	1.34
$A = \log(I_0/I) = \log(V_{out,0}/V_{out})$	0	0.0667	0.0888	0.157	0.391

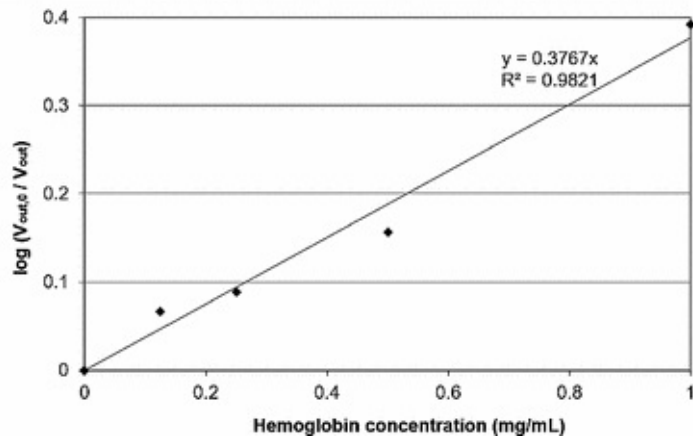


Fig. 8.26 Experimental data of Task 2: $\log(V_{out,0}/V_{out})$ —hemoglobin concentration plot. $V_{out,0}$ is the voltage output with 0 mg/mL hemoglobin solution

Question 8.2

Compare the absorbance readings (zero-adjusted) of Task 1 and Task 2. The absorbance readings of Task 2 are likely smaller than a half of those of Task 1. What factors are responsible for this deviation?

Question 8.3

Does the absorbance (1) increase, (2) decrease, or (3) stay the same if the gain is decreased to 1000?

8.7 Laboratory Task 3: Meat Quality Monitoring with Reflection Probe

Tasks 1 and 2 are designed to quantify the amount and the status of hemoglobin using a miniature spectrophotometer and an LED-PD circuit. It will be best to use a pair of LED-PD circuits to perform pulse oximetry on a human finger. However, typical SpO₂ level of human adult is over 95 %, and the signals fluctuate relatively fast (60–100 beats per minute or bpm), such measurement would be quite challenging. Differences among oxy-, deoxy-, and methemoglobin would not be quite obvious if the human fingers are used for experiments.

There is a good alternative. We can take spectra of beef. Beef consists primarily of muscle tissue, with varying amounts of fats. In the muscle tissue, there is a protein called *myoglobin*, which is very similar to hemoglobin. While there are four subunits (two alpha and two beta) in hemoglobin, myoglobin has only one subunit and may be approximated to the one quarter of hemoglobin. Similar to hemoglobin, myoglobin carries heme group and its spectrum is very similar to that of hemoglobin.

One would consider the beef with bright cherry red color to be very fresh. Indeed, myoglobin found in such color is primarily oxymyoglobin, i.e., myoglobin bound mostly to oxygen. Once the beef undergoes aging and/or denaturation, oxymyoglobin becomes metmyoglobin, changing its coloration to brown. Figure 8.5 clearly indicates a decrease in green absorbance and an increase in red (shorter wavelength) absorbance, resulting in increased green and decrease red coloration, thus brown coloration.

Sometimes, you may notice darker coloration (not brown; rather purple red) deeper inside the meat, even though it was packaged very recently. The reason for this darker coloration is not due to the metmyoglobin, but rather deoxymyoglobin. As shown in Fig. 8.5, deoxymyoglobin shows an increase in red absorbance but not much change in green absorbance, resulting in somewhat

reduced red coloration. In fact, most vacuum-packaged frozen beef carries this coloration (darker purple red), which does not necessarily indicate its freshness. Upon thawing and contacting with ambient oxygen, its color changes back to bright cherry red color.

In this task, you will need the following:

- Ground beef
- A miniature spectrometer (USB4000 or Flame from Ocean Optics) with appropriate software (OceanView™ from Ocean Optics)
- A desktop or laptop computer
- A reflection probe with optical fibers (R400-7-UV-VIS)
- A white light source (fluorescent lamp, white LED flash of a smartphone, or incandescent light bulb, etc.)
- Latex gloves, delicate task wipers (KimWipes®)



Fig. 8.27 A reflection probe is measuring a spectrum of ground beef

The reflection probe needs to be connected to a light source and a miniature spectrophotometer (USB4000 or Flame). You may want to use the white LED light source that can be connected to an optical fiber. A white LED generates blue and yellow color, and covers the entire spectrum of visible light, thus generating white light. To make the experiment simple, let us use the fluorescence lamp or incandescent light bulb in the laboratory ceiling as your light source. You may also want to use the white LED flash of your smartphone as your white light source.

- Prepare two different ground beef sample, one fresh, and the other aged at

room temperature for 2–4 h.

- Place a white paper on your bench. Make sure the paper is well exposed to the fluorescent lamp or incandescent light bulb in your laboratory.
Alternatively, you may want to place a smartphone with its white LED flash on.
- Place a reflection probe on top of your white paper, at a fixed distance, e.g., 1 cm.
- Adjust the integration time accordingly.
- Store a reference spectrum.
- Turn off the light source, and store a dark spectrum.
- Switch to “A” (absorbance) mode.
- Place the ground beef sample on top of a white paper (Fig. 8.27).
- Collect spectrum.
- Repeat the experiments for aged ground beef.
- Identify whether the “aged” ground beef contains mostly met- or deoxyhemoglobin (Fig. 8.28).

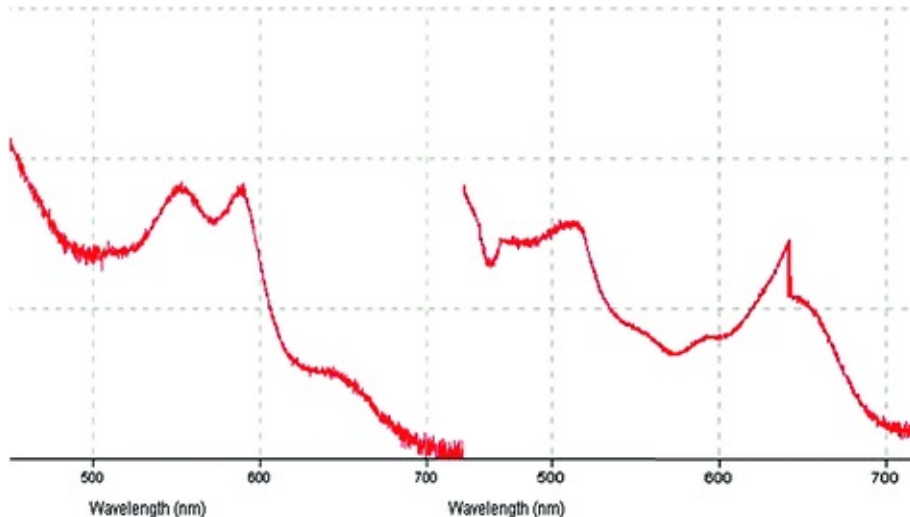


Fig. 8.28 Experimental data of Task 3: absorbance spectra of fresh (*left*) and aged (*right*) ground beef samples

Question 8.4

Compare the above spectra with the actual coloration of ground beef (fresh vs. aged). Do they match?

Question 8.5

Why are the spectra noisy beyond 700 nm?

Alternative Task 3: Simple Pulse Oximeter with Reflection Probe

Use the smartphone's white LED flash as your light source, and the reflection probe as your detector, to obtain a spectrum from your finger. How can you evaluate the pulse and SpO₂?

References and Further Readings

General

- Christian GD (2004) Analytical chemistry, 6th edn. Wiley, Hoboken
- Cooper J, Cass T (eds) (2004) Biosensors, 2nd edn. Oxford University Press, Oxford
- Eggins BR (2002) Chemical sensors and biosensors. Wiley, West Sussex
- Hollas J (2004) Modern spectroscopy, 4th edn. Wiley, Hoboken
- Holme DJ, Peck H (1998) Analytical biochemistry, 3rd edn. Pearson Education, Essex
- Kissinger P (2005) Biosensors—a perspective. Biosens Bioelectron 20:2512–2516
[CrossRef]
- Koschwanez H, Reichert W (2007) In vitro, in vivo and post explantation testing of glucose-detecting biosensors: current methods and recommendations. Biomaterials 28:3687–3703
[CrossRef]
- Pavia D, Lampman G (2008) Introduction to spectroscopy, 4th edn. Brooks Cole, Florence
- Skoog DA, Holler FJ, Nieman TA (2006) Principles of instrumental analysis, 6th edn. Saunders College Publishing, Philadelphia

Pulse Oximeter (Sect. 8.2)

- Bowes WA III, Corke BC (1989) Pulse oximetry: a review of the theory, accuracy, and clinical applications. Obstet Gynecol 74:541–546
- Mendelson Y (1992) Pulse oximetry: theory and applications for noninvasive monitoring. Clin Chem 38:1601–1607
- Tremper KK, Barker SJ (1989) Pulse oximetry. Anesthesiology 70:98–108
[CrossRef]

Optical Fibers (Sect. 8.4)

- Lucas LJ, Yoon J-Y (2008) On-chip detection using optical fibers. In: Li D (ed) Encyclopedia of microfluidics and nanofluidics. Springer, Heidelberg, pp 1515–1530

Ristic L (ed) (1994) Sensor technology and devices. Artech House, Norwood

9. Fluorescence

Jeong-Yeol Yoon¹✉

(1) University of Arizona, Tucson, AZ, USA

✉ Jeong-Yeol Yoon
Email: jyyoon@email.arizona.edu

In the previous chapter, we learned about spectrophotometric detection for biosensor applications, namely, detection of light absorbance at a certain wavelength. This method works well for a variety of applications. Despite its popularity, it has some limitations. The target molecule must exhibit specific coloration(s), i.e., absorption peaks at certain specific wavelength(s). It is possible to use a combination of an enzyme and a substrate that will exhibit a specific coloration. An example of this would be glucose oxidase and benzidine in detecting glucose (will be discussed later in Chap. 12). However, such enzyme–substrate colorimetric assay is not always possible. Sometimes, when the target is a complicated biomolecule, such as a protein, virus, or even bacterium, this is not an easy task because such an enzymatic reaction is generally not possible.

A more generalized approach is to “label” the target molecule with a specific dye, and quantify the concentration of the dye. This dye can be conjugated directly to the target, but a more generalized approach is the use of a secondary bioreceptor that is conjugated with a dye. Figure 9.1 graphically illustrates this concept:

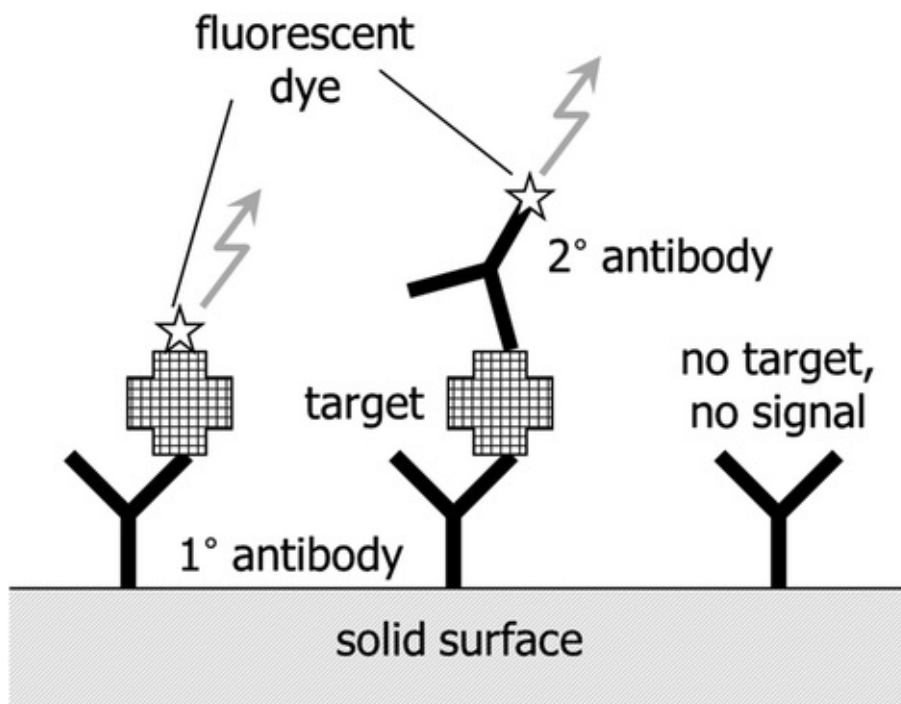


Fig. 9.1 Use of fluorescent dye in biosensing

Bioreceptors (primary antibodies in Fig. 9.1) are pre-immobilized on a solid surface prior to the assay. A solution that may contain target molecules (antigen to the primary antibody in Fig. 9.1) is added. Upon washing, all unbound molecules are washed away. If dye (fluorescent dye in Fig. 9.1) is conjugated to the target prior to the assay, we simply need to monitor fluorescent emission coming from the solid surface. This monitoring confirms the existence of target molecules and possibly quantifies its concentration through light intensity measurement. However, this direct dye conjugation is impractical, as the other molecules in a test solution may also be conjugated with fluorescent dyes. Therefore, secondary antibodies, identical to the primary antibodies but pre-conjugated with fluorescent dyes, are added to the surface followed by washing. These secondary antibodies will bind to captured target on the surface if it is present. Again, measurement of fluorescent emission from the surface can confirm the existence of a target and/or quantifying its concentration. Other types of bioreceptors can also be used, including DNA/RNA and enzymes.

Two different types of dyes have been used—*radioisotope* and *fluorescent dyes*. Radioisotopes are extremely powerful, as a tiny amount of them can exhibit significant magnitude of radioactive decay, leading to extreme sensitivity. Due to the strict regulation on the use of radioisotopes and the difficulty of their use, however, radioisotopes are losing their popularity. Fluorescent dyes have

mostly replaced the applications of radioisotope labeling. Due to the recent advancements in optoelectronic components and devices, fluorescent dyes have become at least comparable to radioisotope dyes in terms of their sensitivity. Fluorescent dyes are not toxic, safe to use, and relatively easy to conjugate to bioreceptors for labeling.

9.1 Fluorescence

Before we begin learning about fluorescent dyes , we should first learn the definition of *fluorescence*, especially in comparison with absorption spectrophotometry. In absorption spectrophotometry, the wavelengths of incident light do not change when the light passes through a cuvette—only its intensity is attenuated at certain wavelengths. If the solute in a solution is *fluorescent* (i.e., fluorescent dyes), the color of emitted light from the cuvette is altered to the longer wavelength. This difference is schematically illustrated in Fig. 9.2.

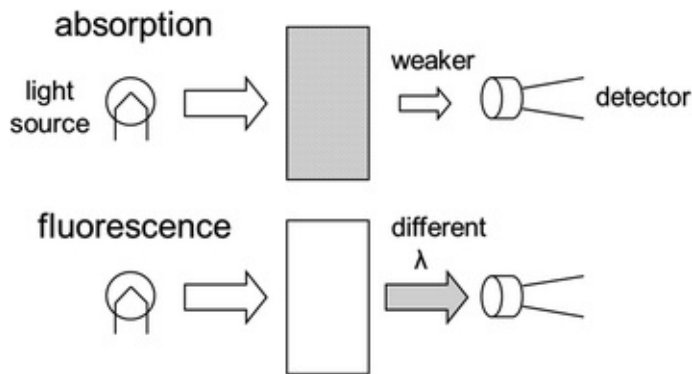


Fig. 9.2 Absorption versus fluorescence

An easy example of fluorescence is a *fluorescent lamp* , which has mostly replaced incandescent light bulbs in lighting industry (although fluorescent lamps are recently being challenged by LED lamps). In a fluorescent lamp, the tube is charged with mercury vapor, which produces UV light upon applying electrical voltage. The inner surface of the tube is coated with fluorescent coatings, which absorb UV light and emit visible lights (excitation = UV, shorter wavelength; emission = visible, longer wavelength). The term fluorescence was derived from the mineral *fluorite* , which is largely calcium fluoride.

When molecules are exposed to light irradiation (exposure to photons), the energy carried by the photons is transferred to the electrons in the molecules, which moves them from the stable ground state to the unstable excited states. As these excited states are not preferable to the molecules, they want to lose this

excess energy and return back to the ground state. This can happen by emitting the photons at the identical wavelength as that of initial light irradiation. When it occurs, it will look like nothing has ever happened. Molecules may also use this excess energy for molecular rotations and/or vibrations (internal energy U), or production of heat (Q). For most molecules, both happen at the same time, resulting in a light emission from the molecules that is attenuated, hence absorption. As certain molecules do convert more photons to U and Q at a specific wavelength than the other wavelengths, we should get different absorption intensities over a range of wavelengths, which is an absorption spectrum.

For the molecules that exhibit fluorescence , they do absorb more photons at a specific wavelength (e.g., for the mineral fluorite , the maximum absorption occurs at UV color). The excited electrons return back to the ground state mostly by emitting photons (but not U and Q), but the energy loss happens in two stages. A small amount of energy is lost in the first stage, which shifts the excited electrons to the less excited state (known as *Stokes shift*). Later, a large amount of energy is lost, returning the excited electrons back to the ground state. Therefore, the emitted light from the fluorescent molecule should carry less energy than the incident light. The energy of light, or more generally electromagnetic wave, is related to the wavelength by the following equation:

$$E = \frac{hc}{\lambda} \quad (9.1)$$

where

E = energy, h = Planck's constant = 6.6×10^{-34} J s,

c = speed of light = 3×10^8 m s⁻¹, λ = wavelength.

Therefore, the emitted light should have a longer wavelength than the incident (excited) light. The optimum wavelengths of excitation and emission vary by the type of fluorescent dyes . For the fluorescent lamp , excitation is UV and emission is visible light. For the example shown in Fig. 9.3, excitation is blue and emission is green.

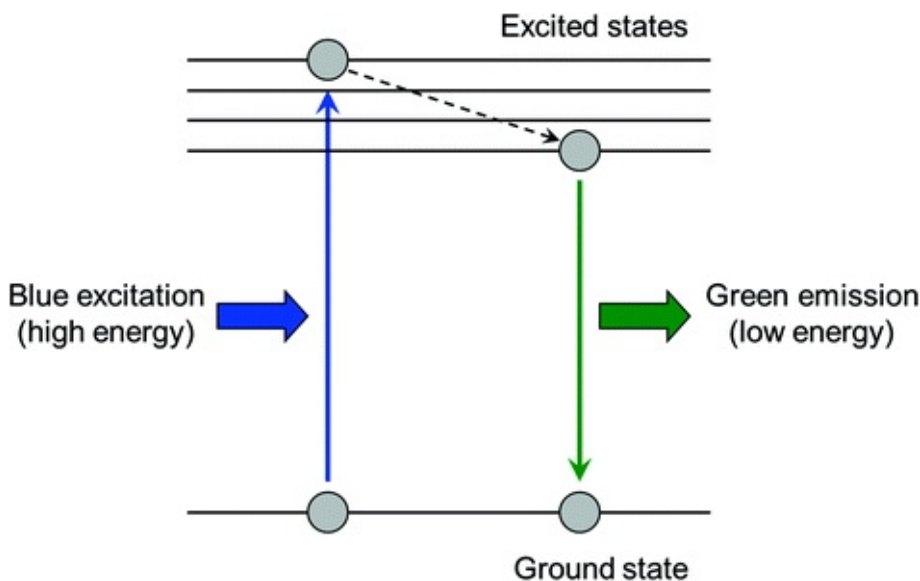


Fig. 9.3 Fluorescence

9.2 Fluorescent Dyes

At this point you may wonder why fluorescent dyes are better than regular absorption dyes. This is due to the superior sensitivity of fluorescence photometry over absorption photometry. Pico- (10^{-12}) or even femtograms (10^{-15}) of fluorescent dyes per 1 mL solution can be detected, which is not possible with conventional absorption dyes. This superiority is due to the fact that many solvents (especially water) are “transparent” to the fluorescence measurement, as those solvents are not fluorescent. In absorption measurement, however, almost all solvents do attenuate some light (absorption by solvents), which creates unnecessary background noise and affects its sensitivity. Many different fluorescent dyes have been identified and used in numerous chemical and biological applications. The following list is just a small fraction of available fluorescent dyes (Fig. 9.4). All fluorescent dyes possess a couple of aromatic ring structure, which is primarily responsible for the loss of small energy shift (Stokes shift). You can also notice that the molecular size of a fluorescent dye is correlated with the wavelengths of excitation and emission maxima.

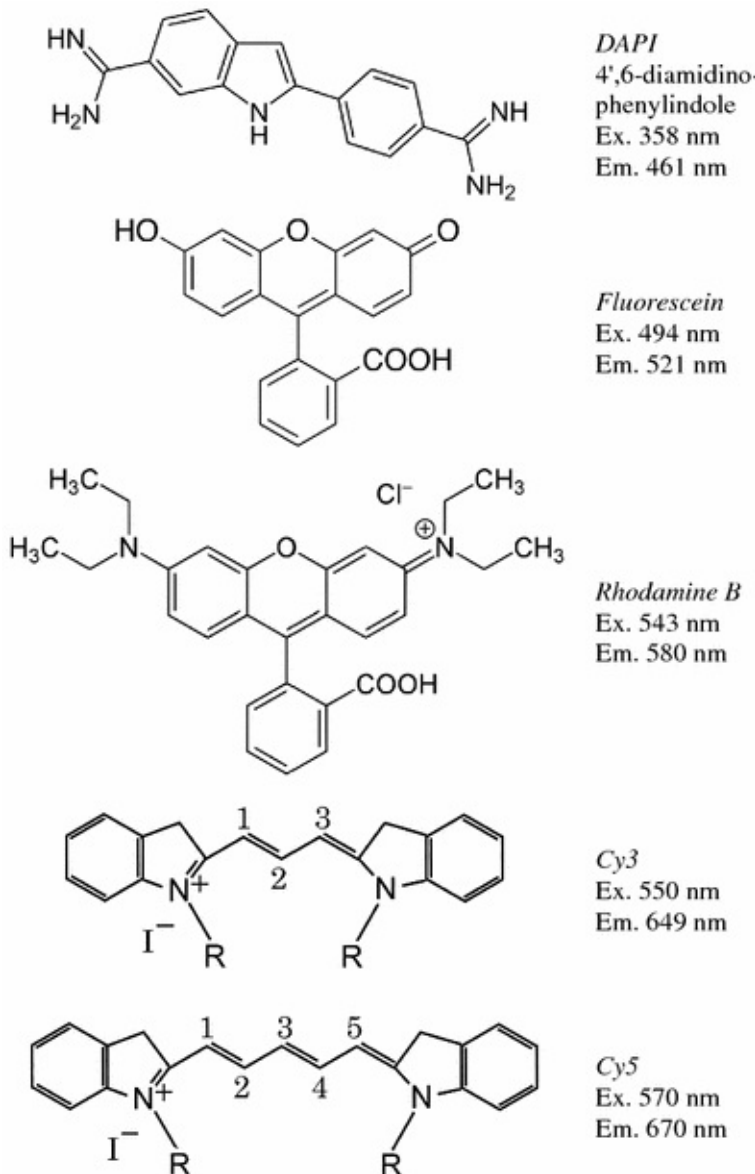


Fig. 9.4 Fluorescent dyes

Note that both fluorescein and rhodamine dyes are typically conjugated with isothiocyanate ($-\text{N}=\text{C}=\text{S}$) at the bottom aromatic ring to facilitate chemical conjugation to proteins, called fluorescein isothiocyanate (FITC) and tetramethyl rhodamine isothiocyanate (TRITC).

Fluorescent dyes have frequently been used in many life science applications. The most common example would be fluorescence microscopy. In *fluorescence microscopy*, we typically label two or three different portions of a target (typically cells) with two or three different fluorescent dyes. For the example shown in Fig. 9.5, three different fluorescent dyes are used—DAPI,

FITC, and TRITC—each conjugated to different portions of a cell. The microscopic slide is first excited with UV for DAPI to emit blue light. This image is captured in black and white to maximize its resolution, as we already know its color. Next, the slide is excited with blue for FITC to emit green color. The image is again captured. Finally, the slide is excited with green for TRITC to emit yellow-red color. Again, the black and white image is captured. Computer software then assigns an appropriate pseudo-color to each black and white image, and superimposes all three images to obtain a nice image shown at the bottom right corner in Fig. 9.5.

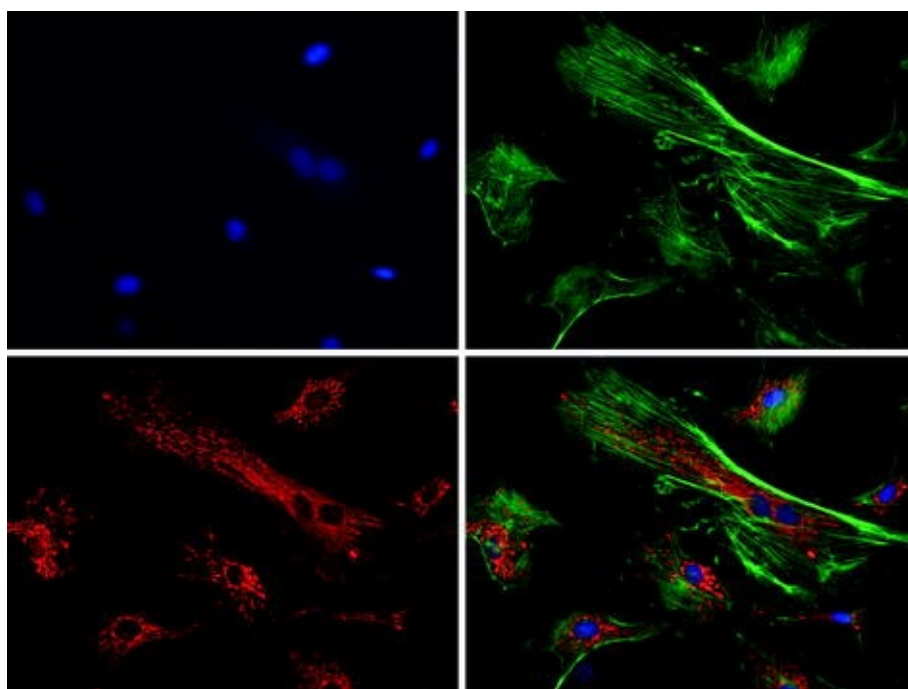


Fig. 9.5 The fluorescence microscopic images of a cell. Different portions of a cell are conjugated with different fluorescent dyes. Excitation/emission colors: UV-blue (top left), blue-green (top right), green/red (bottom left), and combined (bottom right)

To obtain fluorescence microscopic images, we need a fluorescence microscope (Fig. 9.6), which is essentially a regular light microscope equipped with a fluorescent light source, filter cube, and an appropriate computer software. A *filter cube* is an essential component in a fluorescence microscope, which delivers excitation light only to the specimen but not to the eyepiece or camera and emission light only to the eyepiece or camera.

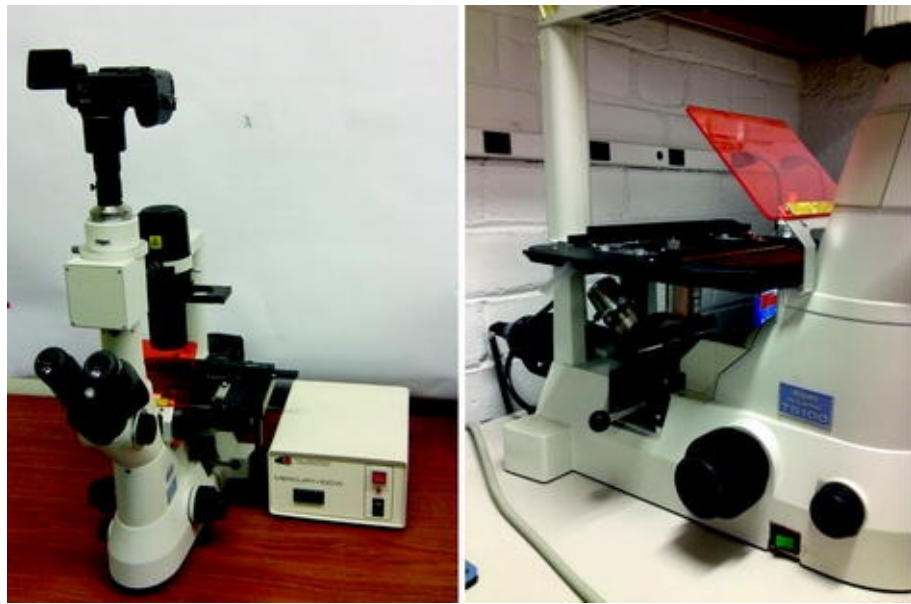


Fig. 9.6 Inverted fluorescence microscope showing the overall shape (*left*) and objective lenses/filter cubes (*right*)

Figure 9.7 shows two different versions of a fiber cube, one for an upright microscope and the other for an inverted microscope. In both cases, a dichroic mirror (also known as a beam-splitting mirror) reflects the short excitation light but lets the long emission light to pass through. For imaging with three different fluorescent dyes, we need three different filter cubes that can mechanically slide through a microscope horizontally. A fluorescent light source is also important to deliver just the color that is needed for excitation.

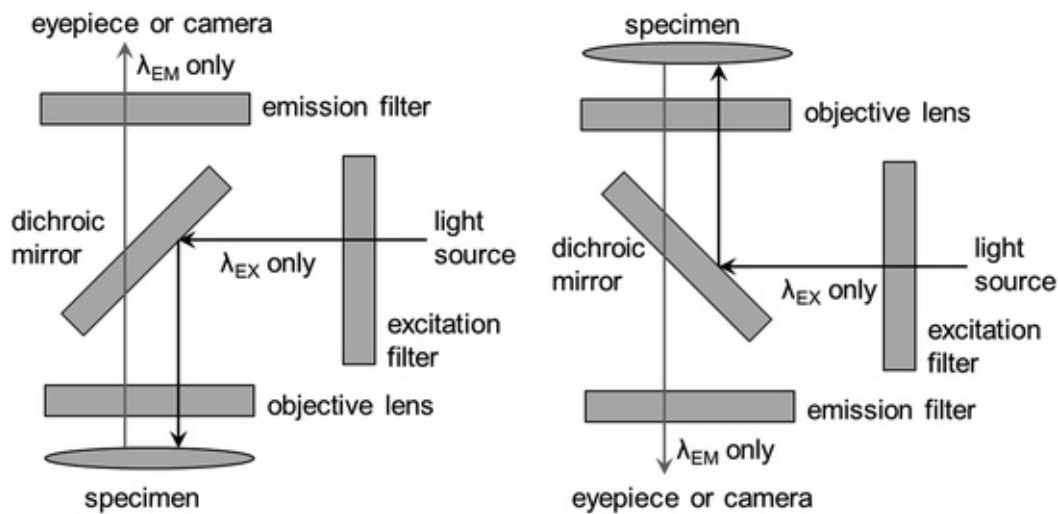


Fig. 9.7 Filter cubes for upright (*left*) and inverted (*right*) fluorescence microscopes

9.3 Advanced Fluorescent Dyes: GFP , SYBR , and QD

Fluorescent dyes typically need to be conjugated to either a target molecule or a bioreceptor (e.g., antibody) prior to the assay. There are several examples of “advanced” fluorescent dyes that do not require such pre-assay conjugation.

The first example is green fluorescent protein (GFP) , which is actually a protein rather than a chemical. This protein exhibits green fluorescence, with excitations at 395 or 475 nm and emission at 509 nm. First isolated from the jellyfish, *Aequorea victoria*, GFP has frequently been used as a marker for gene expression. When a target gene is inserted into an organism, the gene for GFP is also inserted. If the gene insertion is successful, GFP will be synthesized, and green fluorescence can be observed.

The second example is SYBR family of dyes from molecular probes (the most well-known example is SYBR Green I). *SYBR Green I* itself is a cyanine dye (Fig. 9.8), whose structure is similar to Cy3 and Cy5 shown in Fig. 9.4. SYBR Green I has a strong, specific affinity to double-stranded DNA (dsDNA), and when it binds to dsDNA, it exhibits strong green fluorescence (excitation at 497 nm and emission 520 nm). SYBR Green I is frequently used to identify and quantify dsDNA in the sample, where it functions as both fluorescent dye and bioreceptor. SYBR Green I is particularly useful in monitoring the progress of polymerase chain reaction (PCR) . PCR is the process of amplifying the amount of target DNA sequence from the sample, and the production of target dsDNA can easily be monitored by adding SYBR Green I dye to the PCR mixture. PCR assay with this fluorescence monitoring feature is known as real-time PCR or quantitative PCR (qPCR). PCR will be further discussed later in this textbook (Chap. 14).

There are other examples of DNA intercalating dye that can be used for DNA sensing and PCR. The most well-known example is *ethidium bromide* (Fig. 9.8), which has been known long before the introduction of SYBR family dyes. Ethidium bromide also intercalates the dsDNA and exhibits strong orange/yellow fluorescence (emission at 590 nm) with UV excitation (excitation at either 300 or 360 nm). Ethidium bromide has been used to identify and quantify dsDNA in *gel electrophoresis* , which has also been popularly used as an endpoint identification tool for conventional PCR assays.

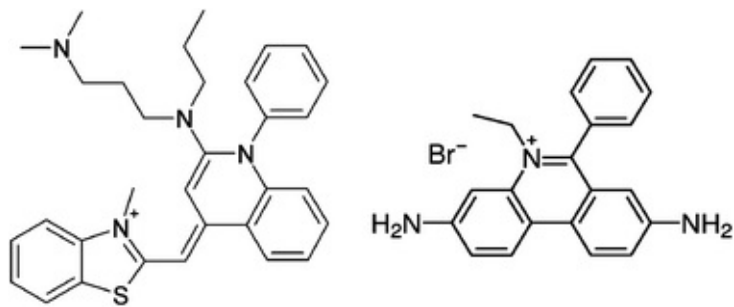


Fig. 9.8 DNA intercalating dyes: SYBR Green I (left, Ex. 497 nm, Em. 520 nm) and ethidium bromide (right, Ex. 300 or 360 nm, Em. 590 nm)

The last example of advanced fluorescent dyes is not about pre-assay conjugation, but rather about overcoming the disadvantage of fluorescent dyes: *photobleaching*. Continuous light exposure to fluorescent dyes leads to their destruction, thus fluorescent emission decays over time. To overcome this problem, a new type of fluorescent-like dye has been developed: *quantum dots*. Quantum dots are not fluorescent dyes, as they are essentially colloidal semiconductor nanocrystals. Despite this difference, they do absorb UV light (UV excitation) and emit visible light (visible emission), which is very similar to fluorescent dyes (hence, it is called *artificial fluorescence*). The emission wavelength becomes longer as the size of quantum dots gets bigger, although they are all excited by UV regardless of their size. Quantum dots are much brighter, yet exhibit much less photobleaching than fluorescent dyes, at a cost of possible toxicity to cells. Quantum dots will be further discussed in Chap. 15.

9.4 Autofluorescence

Autofluorescence is a naturally occurring fluorescence emission, mostly from biological samples such as cells and tissues. Since there exist so many different types of chemicals and biomolecules in cells and tissues, it is natural that some of them exhibit fluorescent characteristics. In fluorescence microscopy and fluorescence biosensing, this autofluorescence comes largely from sample matrices, such as blood, urine, saliva, cell culture, water, food, etc. Such autofluorescence from sample matrices can be quite problematic, since it obscures the true fluorescence signal from the target molecules. Examples of autofluorescence include nicotinamide adenine dinucleotide (NAD^+/NADH), Flavin adenine dinucleotide ($\text{FADH}_2/\text{FADH}_2$), urobilin, polymers, paper, chlorophyll, etc.

Nicotinamide adenine dinucleotide (NAD^+/NADH) from cell and tissue

samples (Fig. 9.9): NAD⁺/NADH is a common co-enzyme found in many types of cells, involved in several different redox reactions. Both NAD⁺ (oxidized form) and NADH (reduced form) strongly absorb deep UV (peak at 260 nm), while only NADH shows blue fluorescence (emission peak at 460 nm). This unique distinction between NAD⁺ and NADH has been utilized in many different biological assays (and subsequently in biosensing), although the presence of NADH in biological sample can cause some trouble in detecting other types of fluorescent molecules.

Flavin adenine dinucleotide (FAD⁺/FADH/FADH₂) from cell and tissue samples (Fig. 9.9): FAD⁺/FADH/FADH₂ is another common co-enzyme found in many types of cells, again involved in several different redox reactions. FAD⁺ is the fully oxidized form, FADH is the partially reduced form, and FADH₂ is the fully reduced form. All three forms strongly adsorb blue light (peak at 450 nm), and the oxidized FAD⁺ emits green fluorescence (emission peak at 520 nm). Both NAD⁺ and FAD⁺ have been utilized in glucose sensing, which will be discussed later in Chap. 12.

Urobilin from urine samples (Fig. 9.9): This is the molecule responsible for yellow coloration and green fluorescence of urine. In the body, the aged red blood cells, which are essentially a sack containing hemoglobin (refer to the previous chapter), are cleared in spleen. The heme portion of hemoglobin is turned into bilirubin, and excreted as bile into the small intestine. The microbes in the large intestine further break the bilirubin into urobilinogen (colorless). Some of the urobilinogen is converted into sterobilin (brown color), responsible for the coloration of feces. Some of urobilinogen is reabsorbed back into the bloodstream, oxidized to urobilin (yellow color), and excreted as urine, responsible for the coloration of urine. Urobilin strongly absorbs blue color (peak at 450 nm), resulting in yellow (=green + red) coloration. This blue absorption also leads to a small amount of green fluorescence (emission peak at 530 nm), again causing some troubles in biosensing from urine samples.

Polymers used for sensor platforms/substrates: Many polymeric materials are known to exhibit fluorescence upon UV irradiation. The emission wavelengths are quite broad, typically ranging from blue to green color. Since the polymers exist in varying chain lengths and different molecular conformations, several different modes of fluorescence can be found from a single polymeric sample, resulting in multiple peaks of fluorescent emissions.

Paper (cellulose fibers) from sensor platforms/substrates (Fig. 9.9): Like polymers, most papers (cellulose fibers) also exhibit blue to green fluorescence

upon UV irradiation. Autofluorescence of polymers and papers is quite important in biosensing applications, since many biosensors are being developed using polymers or papers as a substrate material. For example, many glucose test strips (Chap. 12), lateral flow assays (Chap. 13), and lab-on-a-chip biosensors (Chap. 14) are being fabricated using either polymers or papers.

Chlorophyll from plant samples: Chlorophyll is the chemical responsible for the green coloration of many plants. Most chlorophylls (note that there exist several different forms of chlorophyll, while *chlorophyll a* being the most common and well-known) absorb blue and red colors, thus generating green coloration. In addition, chlorophyll exhibits red fluorescence, with a very strong peak at 670–680 nm (red) and the second one around 720–730 nm (far red). This red fluorescence must be considered in testing any plant samples, including algae, which has been a quite popular theme for bioenergy research.

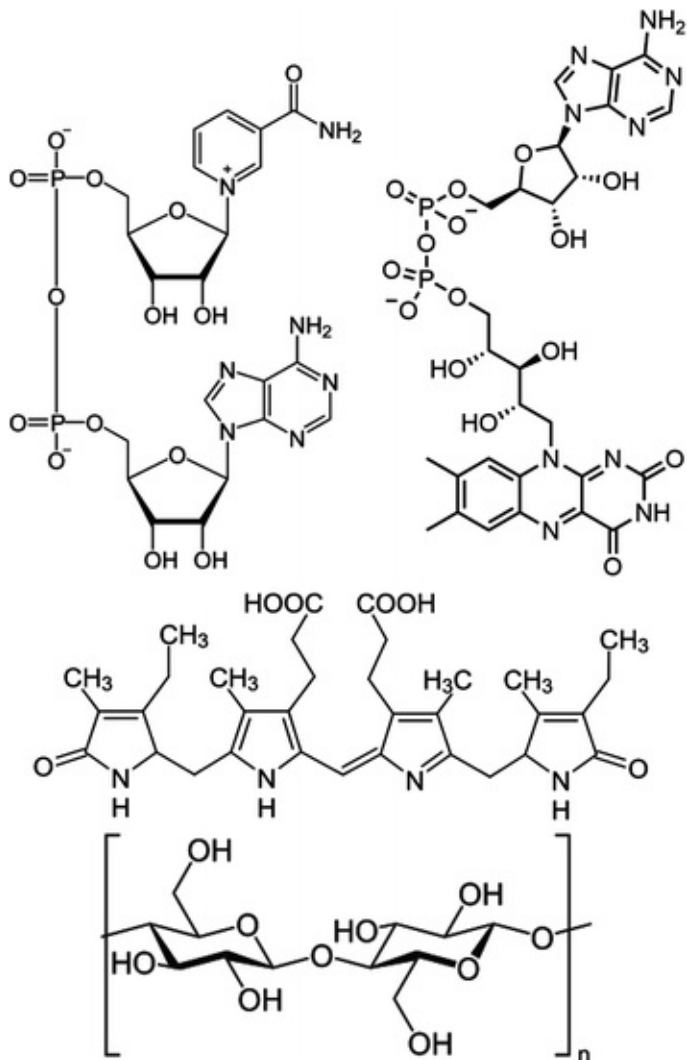


Fig. 9.9 Chemicals responsible for autofluorescence: NADH (top left) and FAD⁺ (top right), urobilin (second row), and cellulose (third row)

9.5 Detection of Fluorescence

The main difference between spectrophotometry and fluorescence sensing is illustrated in Fig. 9.2: difference in wavelength (λ). Therefore, isolation of emission light from excitation light becomes critical in fluorescence sensing. In fluorescence microscopy, this isolation is achieved using a dichroic mirror, which reflects the excitation light and pass the emission light (Fig. 9.7). To prevent the excitation light leaking into the emission wavelength and the emission light leaking into the excitation wavelength, excitation filter and emission filter are also required. These *optical filters* are either *low-pass filters*, *high-pass filters*, or *band-pass filters*. Similar to op-amp filters, a low-pass filter passes the light whose wavelength is shorter than a certain wavelength, a high-pass filter longer than a certain wavelength, and a band-pass filter a small range of wavelengths. Same optical filters can be utilized in developing fluorescence-based sensors, in a layout similar to that of a fluorescence microscope.

In practical fluorescence sensing, simpler fluorescence sensing is possible using optical fibers, LEDs, and/or laser diodes. Excitation with an LED or a laser diode makes the excitation light monochromatic, eliminating the need for an excitation filter. Delivering this excitation using an optical fiber or a collimating lens make the excitation light delivered coherently to the sample. The excitation light that passes through the sample (i.e., transmitted light) can be detected at 0° (relative to the light source). The fluorescent emission light can be detected at any angle other than 0°, since the excitation beam is coherent (or concentrated to one direction). The most commonly used angle of fluorescent detection is either 180° (*back scatter*) or 90° (*side scatter*). As the excitation light is coherent, no excitation light can be detected at these angles (180° or 90°), eliminating the need for an emission filter as well as a dichroic mirror (or a dichroic filter).

Figures 9.10 and 9.11 show the schematic diagrams of these angled detection of fluorescence, for the case of a green fluorescent dye (excitation at 475 nm and emission at 530 nm). Figure 9.10 shows the schematic of 180° back scattering fluorescence detection, using a *reflection probe*, which we briefly discussed in the previous chapter (Chap. 8). The blue LED light (475 nm) is delivered through the core of the reflection probe, while the back scattered green fluorescence (530 nm) is picked up through the shell-side bundle of fibers, eventually delivered to the *miniature spectrometer*. If there is no reflection, this

particular setup is quite easy-to-use and usable for various field applications. Unfortunately, reflections from the sample container as well as the liquid–air interface are quite common, as shown in the left side of Fig. 9.10, and the miniature spectrometer may pick up both excitation and emission lights. Therefore, the reflection probe must be dipped into the liquid sample, but not too close to the side walls or the bottom surface of the sample container (e.g., beaker), as shown in the right side of Fig. 9.11. This may not be practical in using small sample containers such as centrifuge tubes or cuvettes.

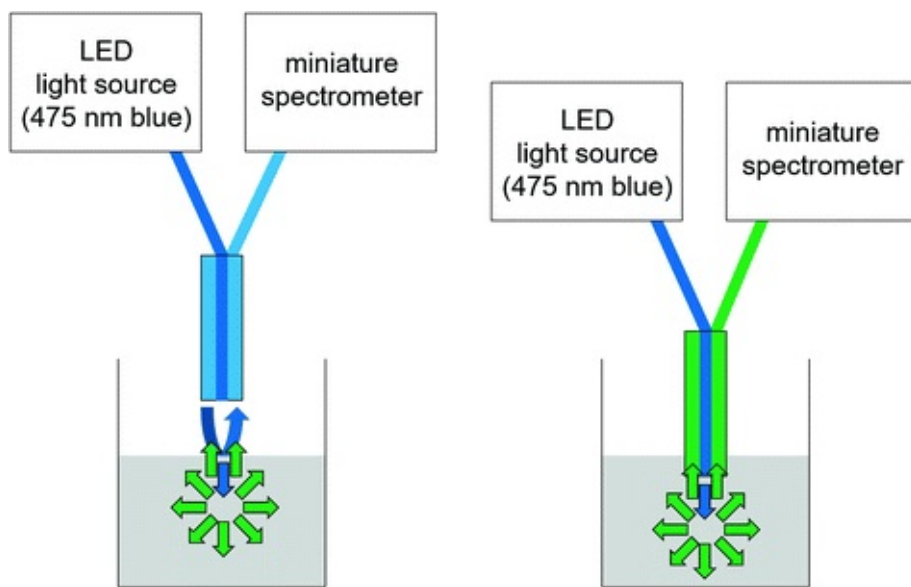


Fig. 9.10 A reflection probe captures green fluorescence from a liquid sample. Both excitation and emission lights are picked up in the *left* setup, due to the reflection at the air–liquid interface, while only emission light is picked up in the *right* setup with the probe dipped into the liquid sample

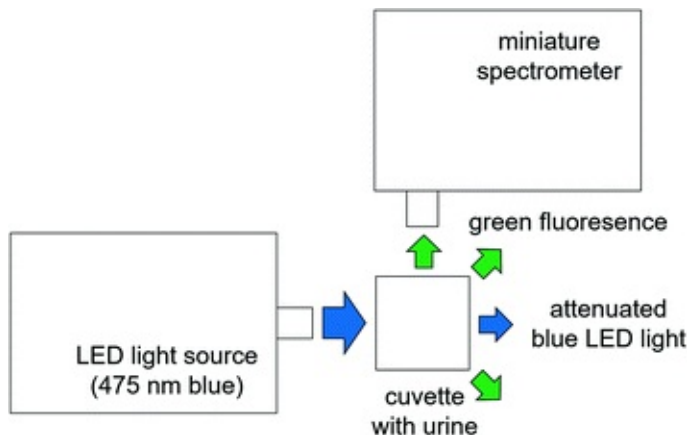


Fig. 9.11 An LED light source and a miniature spectrometer are aligned at 90° for side scatter fluorescence detection

Figure 9.11 shows the schematic of 90° side scattering fluorescence detection, which is more appropriate in dealing with small-sized sample containers (a cuvette in this case).

In the following two laboratory tasks, we will learn these two types of filter-free detection of fluorescence: 180° back scatter detection using a reflection probe for a fluorescein solution (Task 1) and 90° side scatter detection for human urine (Task 2). Other types of filtered or filter-free fluorescence detection are possible, e.g., utilizing laser diodes, quantum dots, smartphones, 30° forward scatter, 45° forward scatter, etc.

9.6 Laboratory Task 1: 180° Back Scatter Fluorescence Detection for Fluorescein

In this task, you will need the following:

- A miniature spectrometer (USB4000 or Flame from Ocean Optics) with appropriate software (OceanView™ from Ocean Optics)
- A desktop or laptop computer
- A reflection probe with optical fibers (R400-7-UV–VIS)
- A light source with blue LED (LS-450 from Ocean Optics)
- Electronic balance, weighing paper, laboratory spatula
- Distilled and/or deionized water
- Beakers
- A vortex mixer; A sonicator (optional)
- Fluorescein
- Latex gloves, delicate task wipers (Kimwipes®)
 - Locate the LS-450 blue LED light source that produces either pulsed or continuous output at 475 nm (the blue region) for fluorescence measurements.
 - The 475 nm blue LED is slightly off from the optimum excitation peak (494 nm), but it should still provide sufficient fluorescence signals. If possible, try to use a different LED that is closer to 494 nm.
 - Insert the input leg of the optical fibers from the reflection probe into the light output port on the LS-450, hand-tighten only.
 - Make sure to place the switch in the “off” position. Plug the 12 V DC/1.5 mA power supply into the LS-450 before plugging it into a 115

AC power outlet. Note: Do not plug in the serial port connector.

- Switch to continuous mode. The blue LED should light up.
- Dispense 40 mL of deionized or distilled water into a 50-mL glass beaker.
- Point the probe down at the water with the probe tip height set equal to the top of the beaker.
- Take the spectrum. Adjust the integration time to make the peak bigger or to prevent signal saturation. If the spectrum is noisy, you may wish to increase the scans to average to reduce the noise over time, or increase the boxcar width to smoothen the spectrum over the wavelengths. The blue illumination should be reflected at the air–water interface, and you should get a peak at 475 nm.
- You should also get multiple peaks from the fluorescent lights at the ceiling of your lab. Turn off the lab lights and check whether those peaks have disappeared.

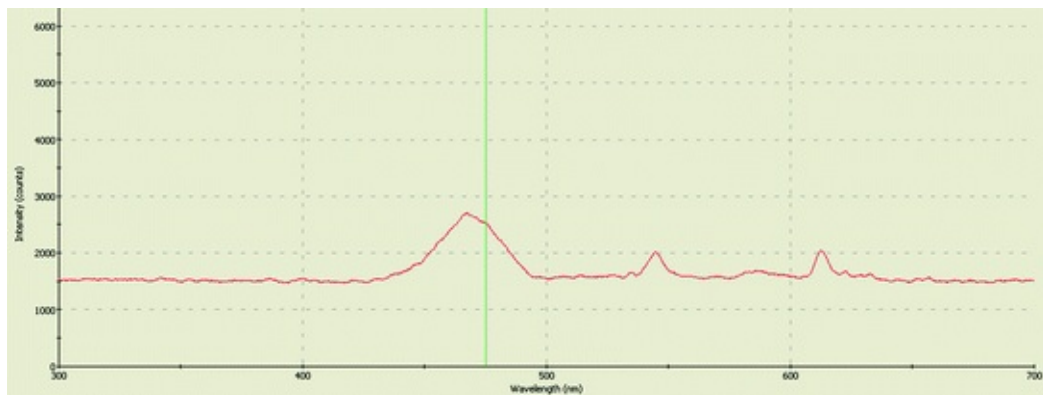


Fig. 9.12 Experimental data of Task 1—blue illumination (475 nm) with ambient light interference

- Dispense 40 mL of deionized or distilled water into a 50-mL glass beaker. Add fluorescein to a final concentration of 0.25 mg/mL.
- Cover the beaker with a sealing film (e.g., Parafilm), and vortex it for 1 min. Sonicate the solution as desired (optional), since the fluorescein has limited solubility in water.
- Point the probe down at the water with the probe tip height set equal to about 1 cm above the solution. Make sure that the probe tip is dry. Take the spectrum (Probe Dry). Most of your blue illuminations will be reflected at the air–water interface, with limited fluorescent emission coming from your solution. Therefore, you should have a bigger peak of blue (475 nm—reflection) and a smaller peak of green (525 nm—fluorescent emission) (Fig. 9.12).
- Now, immerse the probe 1 cm down from the air–water interface (Fig.

9.13). Take the spectrum (Probe Wet). Since there is no reflection at the air–water interface you should have only green fluorescent emission (525 nm) (Fig. 9.14). If you immerse your probe too deep, the probe starts to catch the reflection at the bottom of the beaker, and the blue peak may re-emerge.

- Repeat the Probe Dry and Probe Wet experiments with the lab lights turned off.

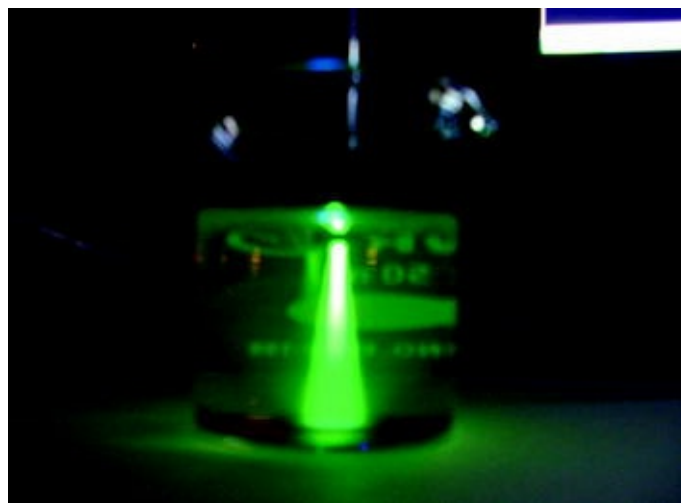


Fig. 9.13 Blue irradiation from the probe excites fluorescein to emit green color

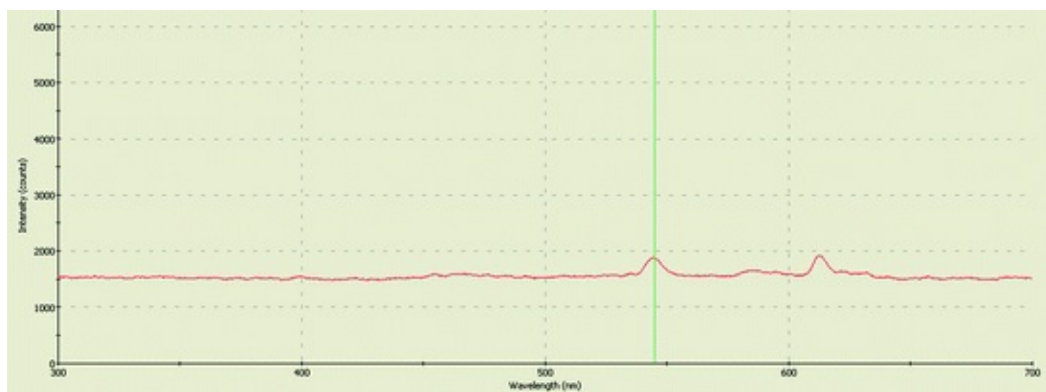


Fig. 9.14 Experimental data of Task 1—fluorescent emission (545 nm) with ambient light interference under “probe wet” condition. Note that fluorescent excitation (475 nm) cannot be seen

Alternative Task 1: Reflection Probe for Other Fluorescent Dyes

Repeat Task 1 with other fluorescent dyes, such as rhodamine. As the excitation wavelength of rhodamine is different from that of fluorescein, you should change the LED of the LS-450 light source.

Question 9.1

For a mixture of fluorescein and rhodamine solutions, roughly sketch the spectra with (a) blue light source (475 nm), (b) green light source (555 nm), and (c) incandescent light bulb. Assume “probe wet” condition (i.e., no reflection of excitation light).

9.7 Laboratory Task 2: 90° Side Scatter Fluorescence Detection for Urine

In addition to the materials and equipment required for Task 1, you will need:

- Human or animal urine samples
- Filter paper (optional)
- Cuvette
 - As explained in Sect. 9.4, urobilin in urine is responsible for the yellow coloration of urine (absorbs blue but not green and red, resulting yellow coloration), as well as green fluorescence (excitation at 450 nm = blue and emission at 530 nm = green).
 - The 475 nm blue LED is slightly off from the optimum excitation peak (450 nm) of urobilin, but it should still provide sufficient fluorescence signals. If possible, try to use a different LED that is closer to 450 nm.
 - Fill the cuvette with various human or animal urine samples. For this laboratory exercise, a sterilized human urine sample from pooled human donors is used.
 - Using a filter paper, filter this urine sample (optional).
 - Align the LED light source and the miniature spectrometer at 90° to the cuvette, as shown in Figs. 9.11 and 9.15.

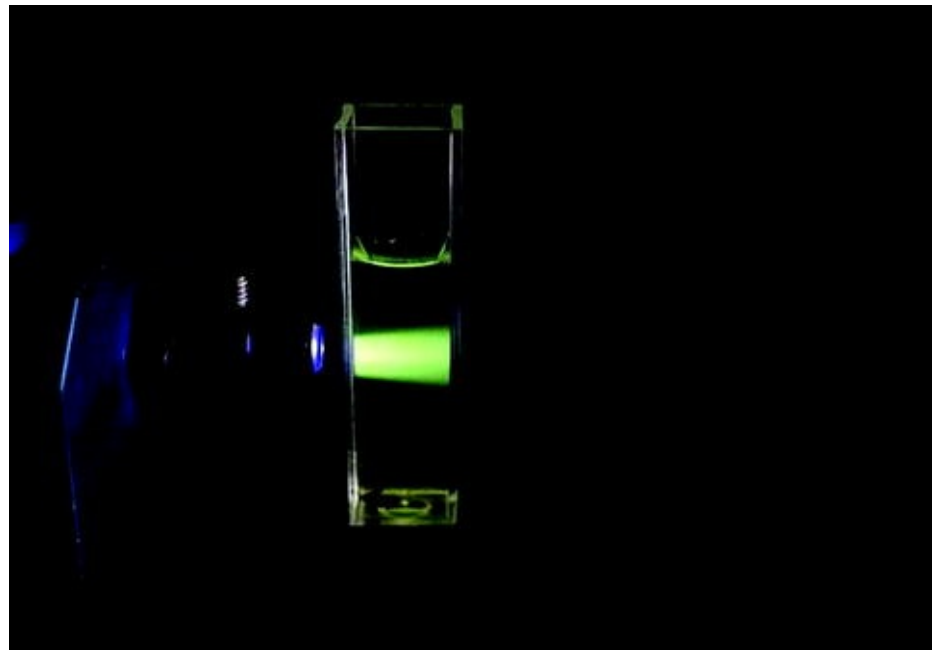


Fig. 9.15 Blue irradiation from the LED light source excites urine sample to emit green color

- Measure fluorescent intensities at its peak (530 nm) (Fig. 9.16).

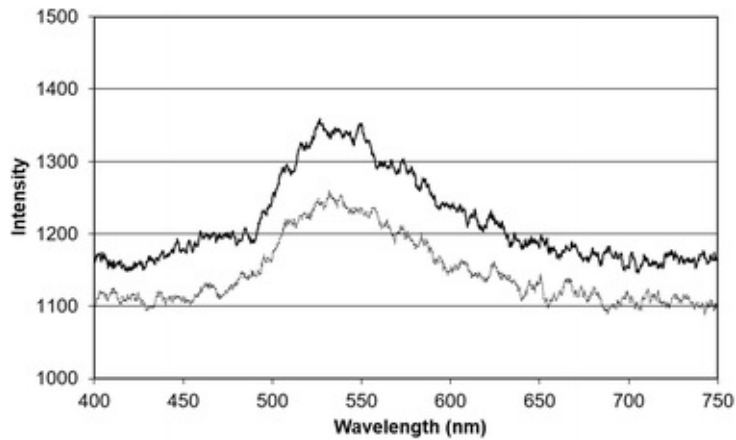


Fig. 9.16 Experimental data of Task 2—fluorescent emission (530 nm) of unfiltered urine (solid line) and filtered urine (dashed line)

- Repeat the same experiment for filtered urine. Can you observe a decrease in fluorescence?

Alternative Task 2: LED–PD Circuit for Urine

Repeat Task 2 with the LED–PD circuit shown in Chap. 8 Task 2. Use blue LED as a light source (Fig. 9.17).

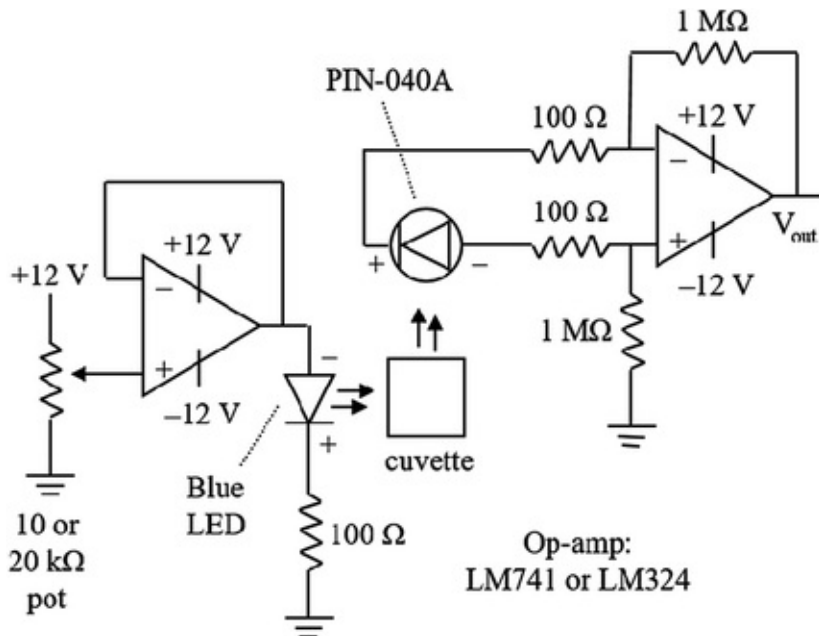


Fig. 9.17 Circuit diagram of Alternative Task 2

References and Further Readings

General

Demchenko A (2008) Introduction to fluorescence sensing, 1st edn. Springer, New York

Goldys E (2009) Fluorescence applications in biotechnology and life sciences, 1st edn. Wiley-Blackwell, Oxford

Lakowicz J (2006) Principles of fluorescence spectroscopy, 3rd edn. Springer, New York
[\[CrossRef\]](#)

Advanced Fluorescent Dyes (Sect. 9.3)

Molecular Probes® (2015) Qdot® Nanocrystal technology overview. <http://www.lifetechnologies.com/us/en/home/brands/molecular-probes/key-molecular-probes-products/qdot/technology-overview.html>

Autofluorescence (Sect. 9.4)

Cho S, Park TS, Nahapetian TG, Yoon J-Y (2015) Smartphone-based, sensitive µPAD detection of urinary tract infection and gonorrhea. Biosens Bioelectron 74:601–611
[\[CrossRef\]](#)

Cornelius CE (1980) Liver Function. In: Kaneko JJ (ed) Clinical biochemistry of domestic animals, 3rd

edn. Academic Press, Burlington

Danielson TL, Rayson GD, Anderson DM, Estell R, Fredrickson EL, Green BS (2003) Impact of filter paper on fluorescence measurements of buffered saline filtrates. *Talanta* 59:601–604
[CrossRef]

Kerkhoff JF, Peters HJ (1968) A reproducible estimation of the urobilin concentration in urine by means of a modified schlesinger test. *Clin Chim Acta* 21:133–137
[CrossRef]

Lakowicz JR, Szmacinski H, Nowaczyk K, Johnson ML (1992) Fluorescence lifetime imaging of free and protein-bound NADH. *Proc Natl Acad Sci USA* 89:1271–1275
[CrossRef]

Nurmukhametov RN, Volkova LV, Kabanov SP (2006) Fluorescence and absorption of polystyrene exposed to UV laser radiation. *J Appl Spectrosc* 73:55–60
[CrossRef]

Plitt KF, Toner SD (1961) A study of the fluorescence of cellulosic polymers. *J Appl Polym Sci* 17:534–538
[CrossRef]

Pedrós R, Moya I, Goulas Y, Jacquemoud S (2008) Chlorophyll fluorescence emission spectrum inside a leaf. *Photochem Photobiol Sci* 7:498–502
[CrossRef]

10. Electrochemical Sensors

Jeong-Yeol Yoon¹✉

(1) University of Arizona, Tucson, AZ, USA

✉ Jeong-Yeol Yoon
Email: jyyoon@email.arizona.edu

As indicated in previous chapters, the top two most popular transducers for biosensors are optical and electrochemical, followed by piezoelectric and thermal. We have already learned a great deal of optical transducers and equipment for biosensor applications in Chaps. 8 and 9. In this chapter, we will learn another very popular transducer for biosensors: electrochemical.

Electrochemical sensors are essentially *electrochemical transducers*, where the concentrations of ions or chemicals are converted into electrical voltage (*potentiometric*), electrical current (*amperometric*), or electrical resistance/conductance (*conductometric*). If electrochemical sensors are used together with bioreceptors (enzymes or antibodies), they become *electrochemical biosensors*.

In this chapter, we will learn the basic electrochemistry (electrochemical cells), which involves:

- (1) Ion-selective electrodes including pH electrode as an example of potentiometric electrochemical sensors;

- (2) Electrochemical glucose sensors as an example of amperometric electrochemical biosensor;

(3) Conductometric electrochemical biosensor.

10.1 Electrolytic and Electrochemical Cells

An *electrolytic cell* decomposes ionic chemical compounds by applying voltage to its solution. Figure 10.1 shows a typical electrolytic cell, where two electrodes (metal rods) are inserted into a solution of metal salts (*electrolytes*). Electrons are taken from metal ions at one electrode (oxidation), and are released to metal ions at the other electrode (reduction). Altogether, the whole reaction is called *redox* (reduction + oxidation) reaction. The current that flows between the electrodes depends not only on the voltage that is applied, but also on the electrical properties of the solution.

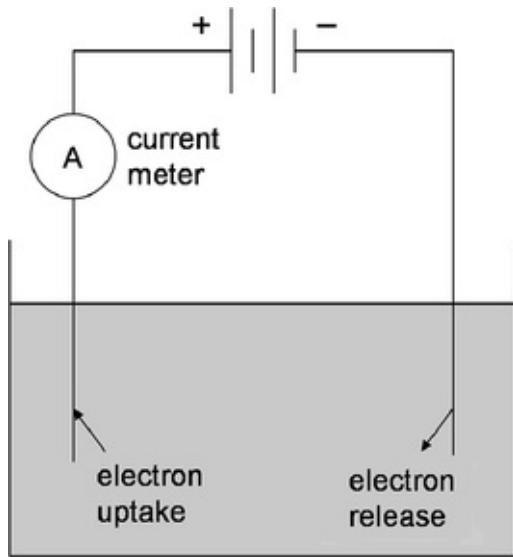


Fig. 10.1 An electrolytic cell

An *electrochemical cell* is a device that generates electrical voltage and current. Two electrodes are inserted into electrolytes that are separated by a salt bridge (example: *Galvanic cell*), or a semi-permeable membrane that replaces the function of a salt bridge (example: *Daniell cell*) (Fig. 10.2).

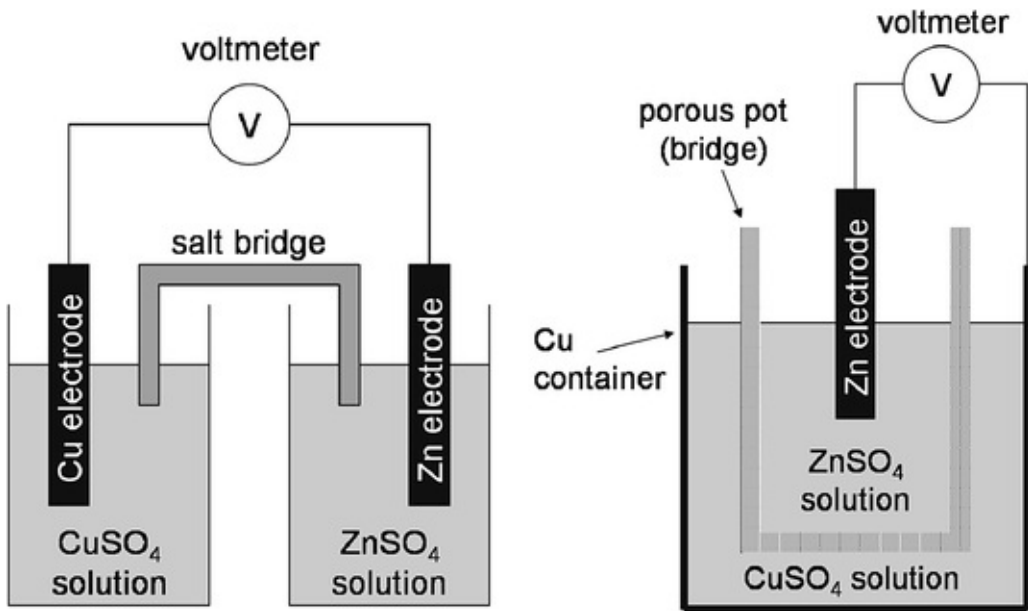


Fig. 10.2 Electrochemical cells: galvanic (left) and Daniell (right) cells

The above cells are essentially identical to each other. Each side of the above cells is referred to as a *half-cell*. To facilitate the notation, the above cell is described as follows:



The following chemical formulas describe the equilibrium of both metal ions:



Combining these two formulas yields:



For this case, a forward reaction is spontaneous, in other words: the change in Gibbs free energy is negative or $\Delta G < 0$. ΔG is defined as

$$\Delta G = -nF\Delta E \tag{10.3}$$

where

n number of electrons

F Faraday constant = 96,487 C mol⁻¹

ΔE electrical potential difference (V)

We also know that

$$\Delta G = RT \ln K \quad (10.4)$$

where

R gas constant = 8.3145 J K⁻¹ mol⁻¹

T temperature (K)

K equilibrium constant

Combining Eqs. 10.3 and 10.4 gives

$$\Delta E = -\frac{RT}{nF} \ln K \quad (10.5)$$

Applying Eq. 10.5 to the left-side half-cell of the above electrochemical cell : $\text{Cu}^{2+} + 2e^- = \text{Cu}$. For this reaction, n is 2, and K is defined by the activity ratio

$$K = \frac{a_{\text{Cu}}}{a_{\text{Cu}^{2+}}} \quad (10.6)$$

The activity of a pure liquid or pure solid is 1 ($a_{\text{Cu}} = 1$), and the activity of metal ions can be approximated by their molar concentration ($a_{\text{Cu}^{2+}} = [\text{Cu}^{2+}]$). ΔE can also be replaced with $E - E^\circ$, where E° refers to the standard electrode potential (reference or ground potential). Plugging all of these into Eq. 10.5 yields

$$E = E^\circ - \frac{RT}{2F} \ln \frac{1}{[\text{Cu}^{2+}]} \quad \text{or} \quad E = E^\circ + \frac{RT}{2F} \ln [\text{Cu}^{2+}] \quad (10.7)$$

Or more generally,

$$E = E^\circ + \frac{RT}{nF} \ln [M^+] \quad (10.8)$$

which is called the *Nernst equation*. Notice that the potential (voltage) is linearly proportional to the *logarithm* of ionic concentration.

We can also convert the natural log into a common log using $\ln X = 2.303 \log X$. In addition, we can plug in universal constants for R , F , and a room temperature of 25 °C (=273.15 K) into Eq. 10.8

$$E = E^\circ + \frac{0.059}{n} \log [M^+] \quad (10.9)$$

For the entire cell,



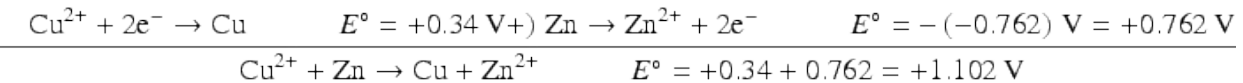
$$K = \frac{a_{\text{Cu}} a_{\text{Zn}^{2+}}}{a_{\text{Cu}^{2+}} a_{\text{Zn}}} = \frac{a_{\text{Zn}^{2+}}}{a_{\text{Cu}^{2+}}} \approx \frac{[\text{Zn}^{2+}]}{[\text{Cu}^{2+}]} \quad (10.10)$$

as the activities of pure solids are 1 ($a_{\text{Cu}} = a_{\text{Zn}} = 1$). Plugging Eq. 10.10 into Eq. 10.5 and repeating the above procedure yields

$$E = E^\circ + \frac{0.059}{2} \log \frac{[\text{Cu}^{2+}]}{[\text{Zn}^{2+}]} \quad (10.11)$$

For either each half-cell or an entire cell, the *standard electrode potential*, E° , should be evaluated before using the Nernst equation. E° for many half-cells can easily be obtained from literature. Table 10.1 show some examples.

For a Galvanic or Daniell cell, the standard electrode potential for the entire reaction can be calculated from those of half-cells. The forward reaction of Eq. 10.2 is spontaneous, which can be split into



(10.12)

If $[\text{Cu}^{2+}] = [\text{Zn}^{2+}] = 0.1 \text{ M}$,

$$E = +1.102 + \frac{0.059}{2} \log \frac{0.1}{0.1} = +1.102 \text{ V} \quad (10.13)$$

If $[\text{Cu}^{2+}] = 1 \text{ M}$ and $[\text{Zn}^{2+}] = 0.1 \text{ M}$,

$$E = +1.102 + \frac{0.059}{2} \log \frac{1}{0.1} = +1.13 \text{ V} \quad (10.14)$$

Typical Galvanic or Daniell cells generate $\sim 1.1 \text{ V}$ unless the ion concentrations of copper and zinc are significantly different by a few orders of magnitude.

Question 10.1

Calculate the cell potential for the following cell:



Use Table 10.1 for the standard electrode potentials. The forward reaction is spontaneous.

Table 10.1 Select standard electrode potentials (E°)

Half-cell reaction	$E^\circ \text{ (V)}$
$\text{Zn}^{2+} + 2e^- \rightleftharpoons \text{Zn}$	-0.762
	-0.44

$\text{Fe}^{2+} + 2\text{e}^- \rightleftharpoons \text{Fe}$	
$2\text{H}^+ + 2\text{e}^- \rightleftharpoons \text{H}_2$	0.0
$\text{Cu}^{2+} + 2\text{e}^- \rightleftharpoons \text{Cu}$	+0.34
$\text{Hg}_2\text{Cl}_2 + 2\text{e}^- \rightleftharpoons 2\text{Hg} + 2\text{Cl}^-$	+0.242

The standard electrode potentials in Table 10.1 are actually obtained with a universal reference electrode since the potential of a half cell is impossible to measure. The above table indicates that the *hydrogen electrode* ($2\text{H}^+ + 2\text{e}^- = \text{H}_2$) is a universal reference, and as such its E° is set to 0 (Fig. 10.3).

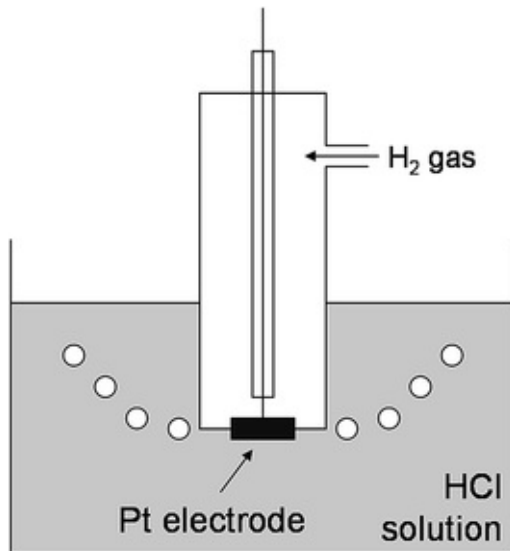


Fig. 10.3 Hydrogen electrode. Hydrochloric acid (HCl) concentration = 1 M. Hydrogen gas (H_2) is bubbled over and absorbed onto the platinum (Pt) electrode at 1 atm

Practically speaking, however, a hydrogen electrode is difficult to use. Therefore, a *saturated calomel electrode* or simply a *calomel electrode*, shown in Fig. 10.4, is often used instead. The half-cell reaction for a saturated calomel electrode is:

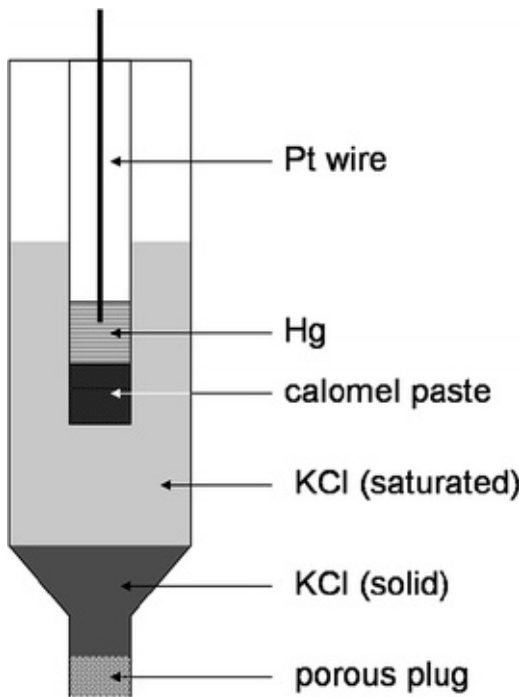


Fig. 10.4 Saturated calomel electrode. Platinum (Pt) wire is connected to metallic mercury (Hg) and a paste that contains calomel (mercury chloride; Hg_2Cl_2) and potassium chloride (KCl). Saturated potassium chloride (KCl) maintains constant ionic concentration and completes the half-cell



The word, “calomel,” refers to the compound: Hg_2Cl_2 . All standard electrode potentials are typically measured against the calomel electrode, followed by subtracting +0.242 V.

10.2 Ion-Selective Electrodes (ISEs; Potentiometric)

The half-cells described above can also be used to measure the concentration of a specific ion. When a half-cell is used in this manner, it is called an ion-selective electrode (ISE) (Fig. 10.5). Typically, the electrolyte solution in the electrode makes contact with the surrounding liquid through a membrane that allows only a specific type of ion to pass through.

ISEs are classified in three types of membranes: solid-state, liquid, and glass membrane.

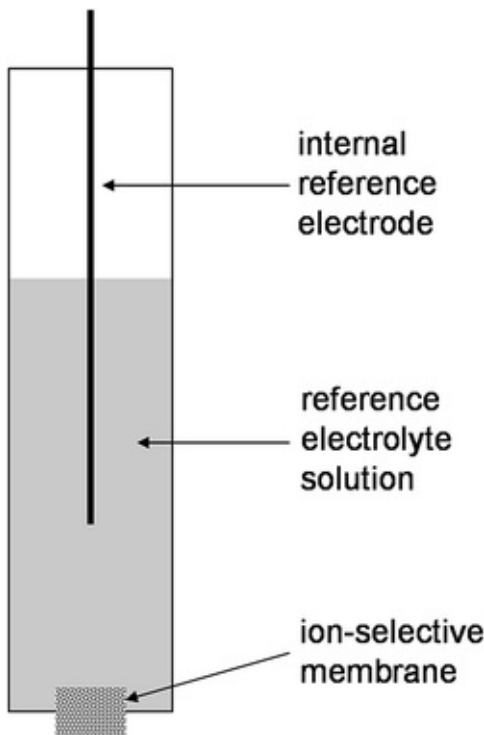


Fig. 10.5 Ion-selective electrode (ISE)

Solid-state ISEs contain a crystalline membrane that is cut from a single crystal. For example, a fluoride ISE uses a solid crystal of LaF_3 , which allows only fluoride ions (F^-) to pass through its membrane. We have a laboratory procedure in this chapter to measure the fluoride concentrations from tap water and toothpaste. Examples of the ions that solid-state ISEs can measure also include: Ag^+ , Cl^- , Br^- , SCN^- , and S^{2-} .

Liquid membrane ISEs contain a plastic membrane, and the liquid ion-exchange material is absorbed into it. Vallinomycin-absorbed polyvinyl chloride (PVC) is a good example of an ISE used to selectively detect potassium ions (K^+). Examples of liquid membrane ISEs include: NO_3^- , Cu^{2+} , Cl^- , BF_4^- , ClO_4^- , and K^+ .

Glass membrane ISEs contain a membrane made from thin glass that is very specific to hydrogen ions (H^+). The usual composition of the glass employed for detecting H^+ is: 22 % Na_2O , 6 % CaO , and 72 % SiO_2 . Glass membrane ISEs, or simply *glass electrodes*, can be used to detect other types of ions, but they are primarily used to measure H^+ , or in other words, pH. An example is shown in Fig. 10.6.

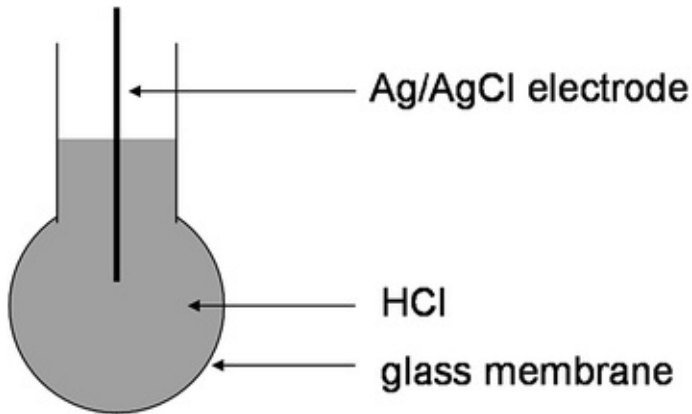


Fig. 10.6 A glass electrode

The detection limit of ISEs is currently very low, ranging between 10^{-8} and 10^{-11} M (10 nM to 10 pM) of target ions. ISEs are suitable for measuring low concentrations in small sample volumes; since they do not chemically influence samples. However, the variety of ions available for low detection limit is quite limited; and they do not include important analytes such as: nickel, manganese, mercury, and arsenate ions.

10.3 pH Electrode (Potentiometric)

pH is a measure of H^+ concentration.

$$\text{pH} = -\log \alpha_{\text{H}^+} \approx -\log [\text{H}^+] \quad (10.17)$$

Plugging Eq. 10.17 into Eq. 10.9 gives

$$E = E^\circ - 0.059 \text{ pH} \quad (10.18)$$

This indicates that the voltage decreases by 0.059 V, or 59 mV, per each pH unit increase.

A glass electrode, such as the one in Fig. 10.6, can be used to measure pH if an appropriate reference electrode is used. A calomel electrode is most frequently used as such reference. These two electrodes can be dipped into a solution, and the voltage difference between them can be measured in order to evaluate the pH of the solution. Today, the two electrodes are typically combined into a single electrode, known as a *combined pH electrode*, shown in Fig. 10.7.

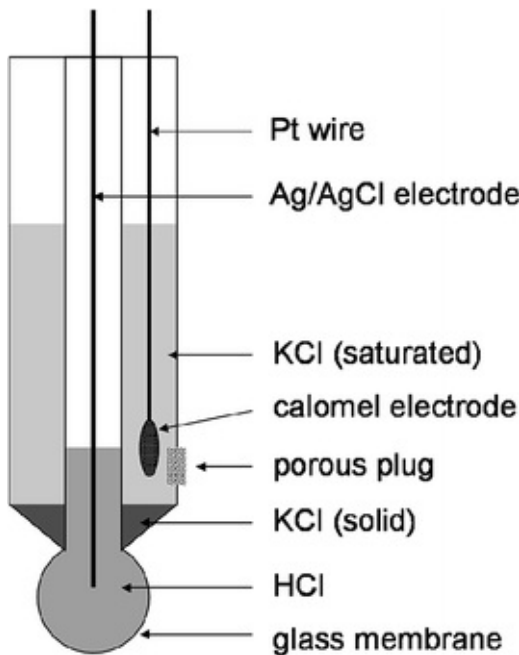


Fig. 10.7 A combined pH electrode

At a neutral pH of 7, the combined pH electrode generates 0 mV. However, if the pH of the target solution increases by a unit, the voltage can drop by 59 mV or vice versa (refer to Eq. 10.18).

As indicated in Eq. 10.18, the pH electrode produces a small voltage, 59 mV/pH unit, which is measured and displayed in pH units by the meter. The meter circuit is fundamentally nothing more than a voltmeter that displays measurements in pH units instead of volts. Since pH electrodes generate a lot of noise, and since 59 mV/pH output is considered relatively low, an op-amp is required in order to construct a pH meter. The input resistance of the meter is very high because of the high resistance (approximately 20–1,000 MΩ) of the glass electrodes used in pH meters. The op-amps used in previous chapters of this book, the *LM741* and the *LM324*, do not meet this requirement. In the following laboratory task, a *TL082* op-amp will be used; it is made with a JFET (junction gate field-effect transistor). A JFET operates with much less base current than the bipolar transistors investigated previously. Therefore, they are appropriate for pH electrodes that have a high resistance, and that generate a very low current.

10.4 Amperometric Biosensors

Enzymes are very popular bioreceptors in identifying and quantifying their

counterpart, substrates. Enzymes are typically proteins, while substrates are generally small chemicals. A good example is the use of glucose oxidase (GOx ; the names of enzymes usually end with -ase; refer to Chap. 1) to quantifying glucose (sugar). GOx converts glucose into gluconic acid while generating hydrogen peroxide as a byproduct. During this reaction, GOx itself is reduced.



An appropriate electron mediator can be added, to regenerate GOx back into its oxidized (i.e., active) form. This *redox* cycle generates electrical current (with no voltage applied; not practical) or change in electrical current (with voltage applied). Since the quantification is made through measuring current, it is referred to as *amperometric electrochemical biosensor* or simply *amperometric biosensor*. This type of biosensor is particularly popular in measuring blood glucose level from diabetic patients. This topic will be separately discussed in Chap. 12.

10.5 Conductometric Biosensors

In *conductometric biosensors*, conductivity (inverse of resistivity) is measured to monitor the redox reactions of enzymatic oxidation. Therefore, there is a lot of similarity between amperometric and conductometric biosensors; the only difference is the current measured in amperometry and conductivity in conductometry.

Conductivity is the inverse of resistivity:

$$\text{resistivity} = \frac{RA}{l} \quad (10.20)$$

where

R resistance (Ω)

A cross-sectional area of a specimen (cm^2)

l length of a specimen (cm)

The typical unit of resistivity is $\Omega \cdot \text{cm}$. Conductivity is defined as:

$$\text{conductivity} = \frac{l}{RA} \quad (10.21)$$

The corresponding unit is $\Omega^{-1} \cdot \text{cm}^{-1}$, or $\text{S} \cdot \text{cm}^{-1}$ (the latter is the standard unit), where the unit, S, is called *Siemens* (identical to Ω^{-1}).

Both resistivity and conductivity are measured typically with a *conductivity cell*, which is shown in Fig. 10.8. It is essentially two metal plates separated by a certain distance. The one shown in Fig. 10.8 has two 1 cm^2 ($=A$) metal plates separated by 1 cm ($=l$). The ratio l/A is referred to as *cell constant*, and it is 1 cm^{-1} ($=1\text{ cm}/1\text{ cm}^2$) for the one shown in Fig. 10.8.

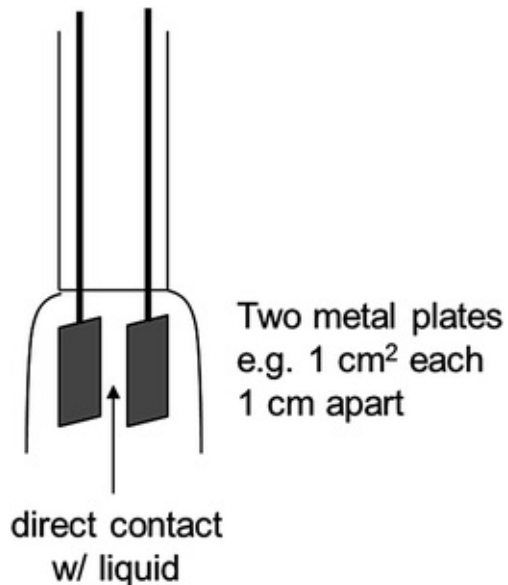


Fig. 10.8 A conductivity cell

This conductivity cell can be used to quantify the extent of the enzymatic redox reactions. Such conductivity changes, however, are generally too small to be detected. Let us recall that conductivity is the inverse of resistivity and that the small resistance change can be measured by a Wheatstone bridge (Chap. 5). If a conductivity cell is used at the place of an unknown resistor (R_4) from a Wheatstone bridge, it is specifically called *conductivity bridge*, which is a basic platform for many conductometric biosensors (Fig. 10.9).

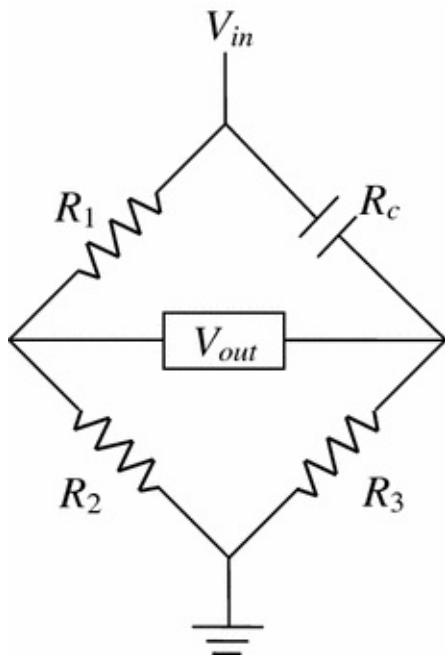


Fig. 10.9 A conductivity bridge

Recently, the conductivity cell portion of conductometric biosensors is further miniaturized to provide better reproducibility and minimize the required sample volume. One good example is interdigitated microelectrode (IME), which will be discussed later in Chap. 13.

As described previously, potentiometric electrochemical sensors are primarily used to monitor the concentrations of specific ions, including hydrogen ion (pH), while amperometric and conductometric electrochemical sensors are almost always used in conjunction with enzymes for redox reaction.

10.6 Laboratory Task 1: Buffer Preparations and Their pH Measurements

The *pH meter* should be calibrated by using two different buffer solutions. A *buffer* is defined as a solution that resists changes in pH when a small amount of an acid or base is added to the solution, or when the solution is diluted. Therefore, a buffer is very useful for maintaining the pH of a reaction at an optimum value. A buffer solution consists of a mixture of a weak acid with its conjugate base, or of a weak base with its conjugate acid at predetermined concentrations, or ratios. In other words, a buffer solution consists of a mixture of a weak acid with its salt, or of a weak base with its salt. For instance, the acetic acid–acetate buffer equilibrium that governs this system is



Since a supply of acetate ions has been added to the system (from sodium acetate, for example), the hydrogen ion concentration is no longer equal to the acetate ion concentration. The hydrogen ion concentration is

$$K_a = \frac{[\text{H}^+][\text{OAc}^-]}{[\text{HOAc}]}, [\text{H}^+] = K_a \frac{[\text{HOAc}]}{[\text{OAc}^-]} \quad (10.23)$$

Taking the negative logarithm of each side of this equation, and using the definitions, $\text{pH} = -\log [\text{H}^+]$ and $\text{p}K_a = -\log K_a$, we have

$$\text{pH} = \text{p}K_a + \log \frac{[\text{OAc}^-]}{[\text{HOAc}]} \quad (10.24)$$

The general form of this equation is called the *Henderson–Hasselbalch equation*.

$$\text{pH} = \text{p}K_a + \log \frac{[\text{A}^-]}{[\text{HA}]} = \text{p}K_a + \log \frac{[\text{conjugate base}]}{[\text{acid}]} \quad (10.25)$$

The equimolar mixture of acetic acid–acetate ($[\text{OAc}^-]/[\text{HOAc}] = 1$) should provide a pH that is equal to the $\text{p}K_a$, which is 4.75.

In this task, you will need the following:

- Electronic balance, weighing paper, laboratory spatula
- Deionized or distilled water
- Beakers, magnetic stir bars, a magnetic stirrer
- Pipettes and pipet tips (1000 μL)
- Monobasic potassium phosphate (KH_2PO_4); dibasic potassium phosphate (K_2HPO_4)
- Acetic acid ($\text{C}_2\text{H}_4\text{O}_2$ or HOAc); sodium acetate ($\text{C}_2\text{H}_3\text{O}_2\text{Na}$ or NaOAc)
- Sodium carbonate (Na_2CO_3); sodium bicarbonate (NaHCO_3)
- Unknown specimen (water sample)
- pH test strips
- pH electrode (PinPoint pH probe from American Marine, Inc.)
- pH meter (PinPoint pH monitor from American Marine, Inc.)
 - Take 10 mmol each of monobasic potassium phosphate (KH_2PO_4) and dibasic potassium phosphate (K_2HPO_4). Dissolve them in 100 mL water using a magnetic stirrer (Fig. 10.10). This procedure

makes 0.1 M pH 7.2 phosphate buffer ($pK_a = 7.20$).

- Take 10 mmol each of acetic acid ($C_2H_4O_2$ or HOAc) and sodium acetate ($C_2H_3O_2Na$ or NaOAc). Dissolve them in 100 mL water. This makes 0.1 M pH 4.75 acetate buffer ($pK_a = 4.75$).
- Take 10 mmol each of sodium carbonate (Na_2CO_3) and sodium bicarbonate ($NaHCO_3$). Dissolve them in 100 mL water. This makes 0.1 M pH 10.3 carbonate buffer ($pK_a = 10.3$).
- Take any water sample of your choice (tap water, toilet, pond, fountain, or something else) as the “unknown” specimen.

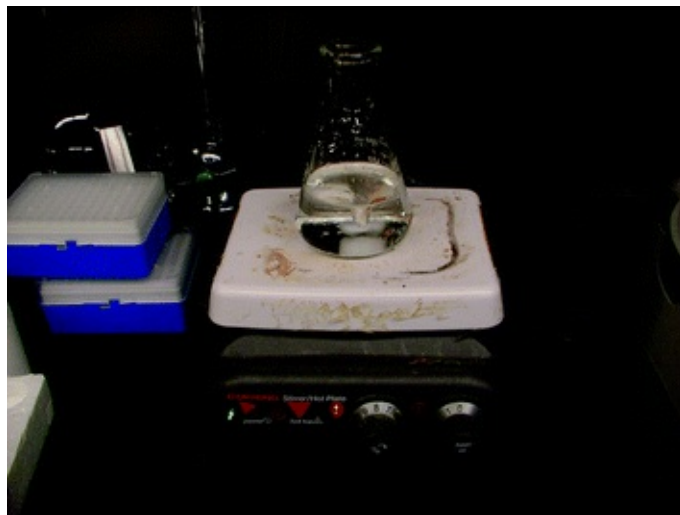


Fig. 10.10 A magnetic stir bar dissolves and mixes chemicals in a beaker, with an external magnetic stirrer. For mixing smaller quantities, a vortex mixer can be used (see Chap. 8)

- Use the test strips to measure the pH of each of the above four solutions. Dip the strip into water for 30 s and move it back and forth. Hold the strip level (flat) for 15 s. Do not shake the excess water from the strip.
- Compare the test pad to the color chart on the side of the container (Fig. 10.11).

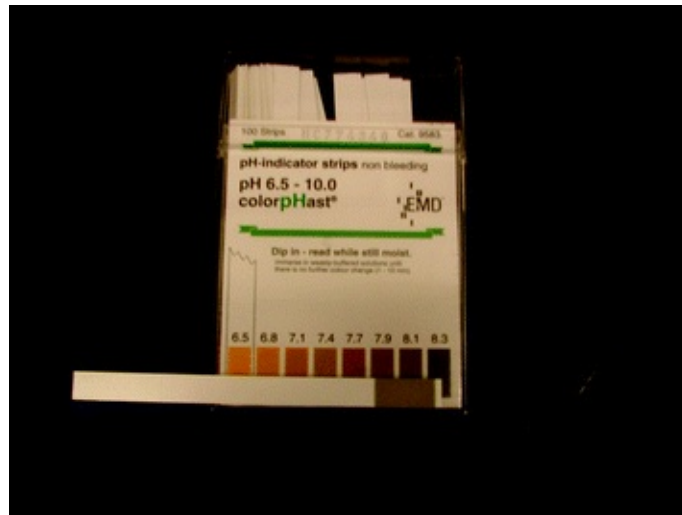


Fig. 10.11 Use of pH test strips

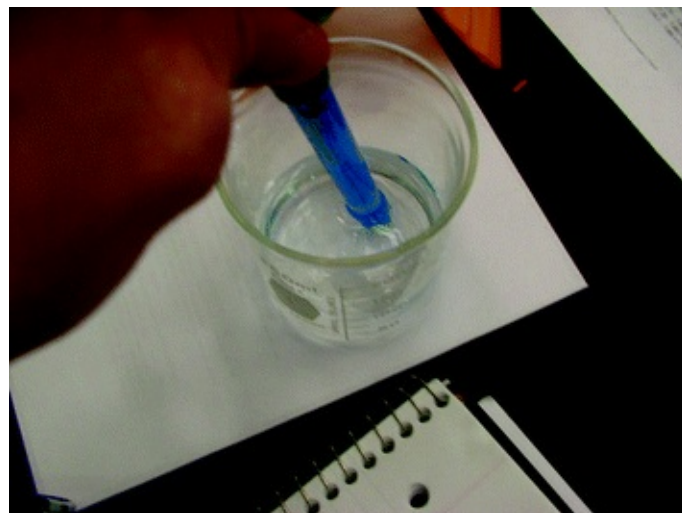


Fig. 10.12 Use of a pH electrode

- Additionally, connect the pH electrode to its meter in order to measure the pH of each of the above four solutions. Gently shake the pH electrode within the solutions (Fig. 10.12). It is desirable to rinse your electrode with distilled and/or deionized water between each measurement. *The pH electrode should always be wet.* Figure 10.13 shows the pH meter connected to its meter, and Table 10.2 shows the experimental results.



Fig. 10.13 A pH meter with a pH electrode

Table 10.2 Experimental data from Task 1. Deionized water was used as the unknown specimen. Note that the results with a pH meter were obtained without calibration (see below for calibration procedure). Normally they are much closer to the theoretical values

	Acetate buffer	Phosphate buffer	Carbonate buffer	Deionized water
pH, theoretical	4.75	7.20	10.30	—
pH test strips	5	7	10.5	6.5
pH meter	6.74	7.28	9.50	7.54

Calibrating pH meter

- The pH meter readings may be different from those of the pH test strips. Once the buffer solutions are made correctly, and the pH test strips are working properly, the pH meter must be calibrated before any measurements.
- The most popular method to calibrate the pH meter is called “two-point” calibration. The pH meter shown above contains two adjustment shafts, which are actually potentiometers (Fig. 10.3).
- The first pot is labeled “7,” indicating that you should calibrate the meter with a pH 7 buffer. Any buffer with a pH close to 7 can be used. Dip the electrode into pH 7.20 buffer, and adjust the pot to make the meter display 7.20. In reality, this pot is the zero-adjustment (refer to Alternative Task 2).
- The second pot is labeled “4 or 10.” Use a pH 4.75, or a pH 10.3 buffer, and adjust the second pot to make the meter display 4.75 or 10.3. In reality, this pot adjusts the gain (refer to Alternative Task 2).

10.7 Laboratory Task 2: pH Meter Circuit

For this task, you will need the following:

- Solutions of buffers and unknown specimen (from Task 1)
- A breadboard, wires, wire cutter/stripper, and a DMM
- TL082 dual op-amp
- A pH electrode (PinPoint pH probe from American Marine, Inc.)
- A BNC connector /adaptor

The following circuit configuration (Fig. 10.14) is simply a voltage follower, or a buffer stage, which allows for stable readings of the voltage outputs. Since the pH electrode has very high resistance, it generates very low current, and an op-amp with very high input resistance is required. The LM741 and the LM324 do not meet this requirement. Instead, TL082 (Fig. 10.15) will be used as described in Sect. 10.3.

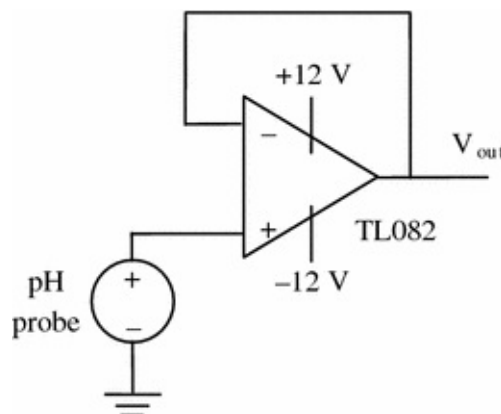


Fig. 10.14 Circuit diagram for Task 2

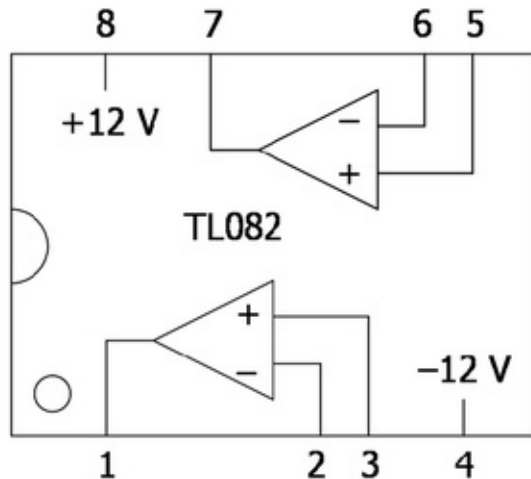


Fig. 10.15 Dual op-amp TL082

According to Eq. 10.18 described above, the voltage output from a pH electrode should be 0 mV at a neutral pH, 7.0. Increasing the pH unit by one unit causes the voltage to decrease by 59 mV. Therefore, the theoretical voltage outputs for three buffer solutions should be

$$\begin{aligned}
 \text{pH 4.75} &: (4.75 - 7.00) \times (-59 \text{ mV}) = +132.8 \text{ mV} \\
 \text{pH 7.20} &: (7.20 - 7.00) \times (-59 \text{ mV}) = -11.8 \text{ mV} \\
 \text{pH 10.3} &: (10.3 - 7.00) \times (-59 \text{ mV}) = -194.7 \text{ mV}
 \end{aligned} \tag{10.26}$$

Initial task: Measure V_{out} for the three different buffer solutions, and for the unknown specimen (Fig. 10.16 and Table 10.3)

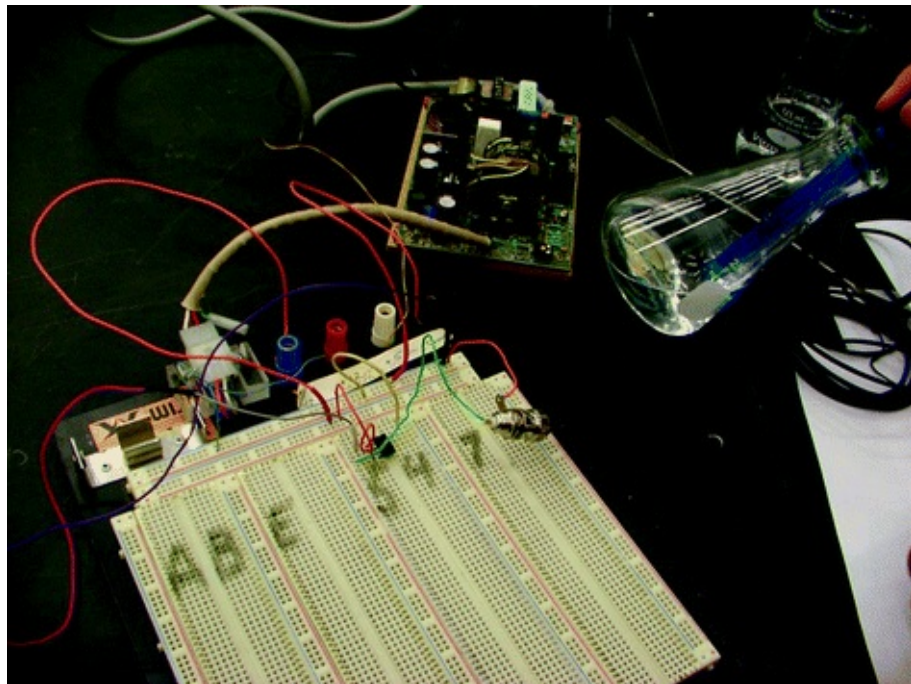


Fig. 10.16 Circuit photo of Task 2

Table 10.3 Experimental data from Task 2. Deionized water was used as the unknown specimen

	Acetate buffer	Phosphate buffer	Carbonate buffer	Deionized water
pH, theoretical	4.75	7.20	10.30	–
V_{out} , theoretical (mV)	+132.8	−11.8	−194.7	–
V_{out} , experimental (mV)	+130.0	−26.5	−177.0	−47.0

A pH electrode is typically connected to its meter through a *BNC (Bayonet Neill-Concelman) connector*. In Fig. 10.16, a female BNC connector is connected to the male connector from a pH electrode, and test clips were used to connect it to the breadboard. The core side is the high voltage (+), and the shell side is the ground (−).

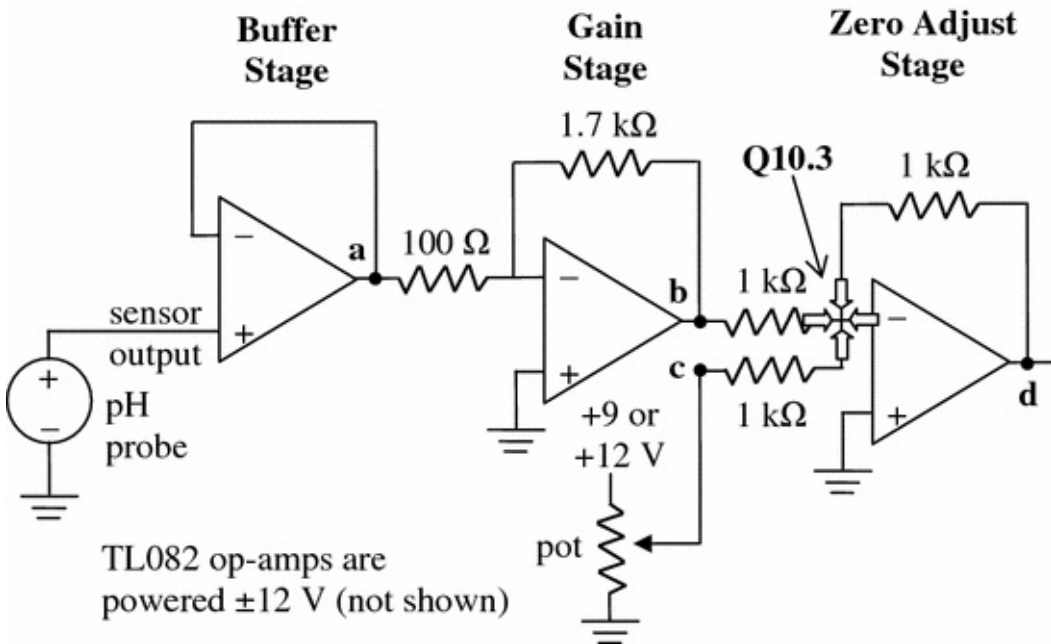


Fig. 10.17 Circuit layout for Task 2a

Alternative Task 2: pH Meter Circuit with Amplification

The actual circuit of a pH meter usually consists of op-amps in an inverting configuration, with a total voltage gain of -17 (Fig. 10.17). The inverting amplifier converts the small voltage produced by the probe (-0.059 V/pH) into pH units, which are then offset by 7 V to give a reading on the pH scale. Similar to the Task 2 circuit of the Chap. 6 Laboratory (op-amp), you will need the following:

- Buffer stage: identical to Task 2 in the above.
- Gain stage: inverting op-amp, gain = -17 .

$$\text{pH 4.75: } (+132.8 \text{ mV}) \times (-17) = -2.25 \text{ V}$$

$$\text{pH 7.20: } (-11.8 \text{ mV}) \times (-17) = +0.20 \text{ V}$$

$$\text{pH 10.3: } (-194.7 \text{ mV}) \times (-17) = +3.30 \text{ V}$$

- Zero-adjust stage: add $+7.00$ V (note that this is also inverting).

$$\text{pH 4.75: } (-2.25 \text{ V} + 7.00 \text{ V}) \times (-1) = -4.75 \text{ V}$$

$$\text{pH 7.20: } (+0.20 \text{ V} + 7.00 \text{ V}) \times (-1) = -7.20 \text{ V}$$

$$\text{pH 10.3: } (+3.30 \text{ V} + 7.00 \text{ V}) \times (-1) = -10.3 \text{ V}$$

Depending on the $+12$ and -12 V power supply, the -10.3 V output may saturate, generating somewhat small magnitude voltage.

Question 10.2

How can you prevent the above saturation with the pH 10.3 buffer?

Question 10.3

Calculate the current of the four branches flowing towards the nodal points shown in Fig. 10.17, for three different buffer solutions (pH 4.75, 7.20, and 10.3).

10.8 Laboratory Task 3: Fluoride Ion Selective Electrode with PH Meter

In this task, you will need the following:

- Fluoride ion selective electrode (Cole-Parmer 27502-19)
- Electronic balance, weighing paper, laboratory spatula
- Deionized or distilled water
- Beakers, magnetic stir bars, a magnetic stirrer
- Pipettes and pipet tips (1000 μ L)
- Sodium fluoride (NaF)
- Unknown specimen 1: tap water
- Unknown specimen 2: solution of toothpaste
- pH meter (PinPoint pH monitor from American Marine, Inc.)
 - Prepare six different fluoride standard solutions (using sodium fluoride = NaF and deionized water), with varying concentrations of 0.01, 0.1, 0.5, 1, 5, and 10 mg/mL.
 - For the first unknown specimen, take tap water. In some countries, including the U.S., fluoride is added to tap water for the benefit of dental health.
 - For the second unknown specimen, dissolve an adequate amount of commercial toothpaste into deionized water. Most toothpastes contain fluoride, again for the benefit of dental health.
 - Connect the fluoride ion selective electrode to the pH meter (used in Task 1) using its BNC connector (Fig. 10.18). Although this particular pH meter does not provide the voltage output (in mV), we can still use its pH reading in lieu of voltage output, since pH and the voltage output are linearly related.

- Take the pH meter readings. Plot these readings against the log concentrations of fluoride solutions (Fig. 10.19).
- Obtain the regression equation. Use this equation to back-calculate the fluoride concentrations in the tap water and the toothpaste solution.



Fig. 10.18 A fluoride ion selective electrode is measuring the fluoride concentration of an unknown specimen

Fluoride conc. ($\mu\text{g/mL}$)	10	100	500	1000	5000	10000
\log_{10} conc.	1	2	2.70	3	3.70	4
pH meter reading	6.20	7.28	7.97	8.27	9.02	9.43
Unknown specimen	Tap water				Toothpaste solution	
pH meter reading	5.50				7.38	
Fluoride conc. ($\mu\text{g/mL}$)	$10^{0.347} = 2.22$				$10^{2.12} = 132$	

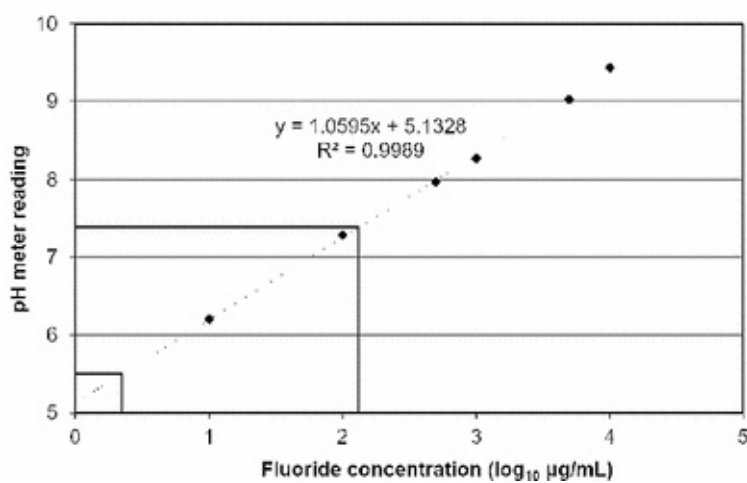


Fig. 10.19 Experimental data of Task 3: pH meter reading from a fluoride ion selective electrode – \log_{10} concentration of sodium fluoride. The fluoride concentrations of the tap water and the toothpaste solution can be calculated from the regression equation: $5.50 = 1.0595x + 5.1328$, $x = 0.347$ ($2.22 \mu\text{g/mL}$) for tap

water; $7.38 = 1.0595x + 5.3128$, $x = 2.12$ ($132 \mu\text{g/mL}$) for toothpaste solution

Question 10.4

Why should the standard curve be plotted against the log concentration of fluoride? (Hint: Use Nernst equation).

Question 10.5

Can you use 0 mg/mL fluoride solution (=deionized water) for the standard curve? Briefly explain why.

10.9 Laboratory Task 4: Fluoride Ion Selective Electrode with Circuit

For this task, you will need the following:

- Fluoride standard solutions and unknown specimen (from Task 3)
- Fluoride ion selective electrode (from Task 3)
- A breadboard, wires, wire cutter/stripper, and a DMM
- TL082 dual op-amp
- A BNC connector/adaptor
 - Construct a circuit identical to that of Task 2.
 - Connect a fluoride ion selective electrode using a BNC connector/adaptor.
 - Make the voltage measurements for the fluoride standard solutions and two unknown specimens.
 - Plot the standard curve and back-calculate the fluoride concentration in the unknown specimens.

Question 10.6

Compare the calculated fluoride concentrations of two unknown specimens using a pH meter (Task 3) and a circuit (Task 4). Is there any discrepancy? (Figs. 10.19 and 10.20).

Question 10.7

Why is the slope of Fig. 10.20 negative, while that of Fig. 10.19 is positive? (Hint: compare with the results of pH meter.)

Fluoride conc. ($\mu\text{g/mL}$)	10	100	500	1000	5000	10000
\log_{10} conc.	1	2	2.70	3	3.70	4
Circuit reading (mV)	+35.0	-25.3	-69.2	-86.3	-125.6	-151.8
Tap water						Toothpaste solution
Circuit reading (mV)	+80					
Fluoride conc. ($\mu\text{g/mL}$)	$10^{0.273} = 1.88$					

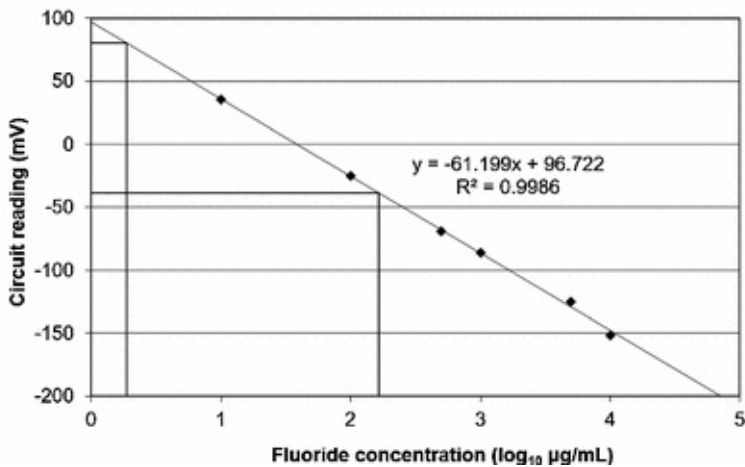


Fig. 10.20 Experimental data of Task 4: circuit reading from a fluoride ion selective electrode— \log_{10} concentration of sodium fluoride. The fluoride concentrations of the tap water and the toothpaste solution can be calculated from the regression equation: $+80 = -61.199x + 96.722$, $x = 0.273$ ($1.88 \mu\text{g/mL}$) for tap water; $-39 = -61.199x + 96.722$, $x = 2.22$ ($165 \mu\text{g/mL}$) for toothpaste solution

References and Further Readings

- Eggins BR (2002) Chemical sensors and biosensors. Wiley, West Sussex
- Grieshaber D, MacKenzie R (2008) Electrochemical biosensors—sensor principles and architectures. Sensors 8:1400–1458
[CrossRef]
- Harborn U, Xie B, Venkatesh R, Danielsson B (1997) Evaluation of a miniaturized thermal biosensor for the determination of glucose in whole blood. Clin Chim Acta 267:225–237
[CrossRef]
- Holme DJ, Peck H (1998) Analytical biochemistry, 3rd edn. Pearson Education, Essex
- Kissinger P (2005) Biosensors—a perspective. Biosens Bioelectron 20:2512–2516
[CrossRef]
- Koschwanez H, Reichert W (2007) In vitro, in vivo and post explantation testing of glucose-detecting biosensors: current methods and recommendations. Biomaterials 28:3687–3703
[CrossRef]
- Lakard B, Herlem G, de Labachelerie M, Daniau W, Martin G, Jeannot J-C, Robert L, Fahys B (2004) Miniaturized pH biosensors based on electrochemically modified electrodes with biocompatible polymers.

Biosens Bioelectron 19:595–606
[CrossRef]

Luong JHT, Male KB, Glennon JD (2008) Biosensor technology: technology push versus market pull. Biotechnol Adv 26:492–500
[CrossRef]

Newman J, Turner A (2005) Home blood glucose biosensors: a commercial perspective. Biosens Bioelectron 20:2435–2453
[CrossRef]

Thevenot D, Toth K (2001) Electrochemical biosensors: recommended definitions and classification. Biosens Bioelectron 16:121–131
[CrossRef]

Wang J (1999) Amperometric biosensors for clinical and therapeutic drug monitoring: a review. J Pharmaceut Biomed Anal 19:47–53

Wang J (2002) Electrochemical nucleic acid biosensors. Anal Chim Acta 469:63–71
[CrossRef]

Wang J (2006) Electrochemical biosensors: towards point-of-care cancer diagnostics. Biosens Bioelectron 21:1887–1892
[CrossRef]

Zhang S, Wright G, Yang Y (2000) Materials and techniques for electrochemical biosensor design and construction. Biosens Bioelectron 15:273–282
[CrossRef]

Zhang X, Ju H, Wang J (eds) (2007) Electrochemical sensors, biosensors and their biomedical applications, 1st edn. Academic Press, London

11. Piezoelectric Sensors

Jeong-Yeol Yoon¹✉

(1) University of Arizona, Tucson, AZ, USA

✉ Jeong-Yeol Yoon
Email: jyyoon@email.arizona.edu

Although optical and electrochemical transducers are the two most popular transducers for biosensors, piezoelectric transducers have also gained some popularity in the past couple of decades. Like optical and electrochemical transducers, piezoelectric transducers can be used as-is as physical sensors (to sense mass), or used with bioreceptors as biosensors (to quantify biomolecules). Collectively they are called *piezoelectric sensors*.

11.1 Piezoelectricity

All piezoelectric sensors work on the principle of piezoelectricity. In the late nineteenth century, the Curie brothers (the younger brother, Pierre, was Marie Curie's husband) found that an electrical voltage was generated when they compressed or stretched *quartz*. This is called *piezoelectric effect*. This effect is reversible, meaning that quartz can be lengthened or shortened when an electrical voltage is applied. *Piezoelectricity* refers to the material's ability to exhibit this piezoelectric effect.

Other materials can also exhibit piezoelectricity, but quartz is still the most popular and the most used material for piezoelectric sensors. Quartz (SiO_2) has a unique, tetrahedron crystal structure as shown in Fig. 11.1. There are four oxygen molecules in a single tetrahedron (SiO_4), where all four oxygen molecules are shared with nearby tetrahedra (thus it becomes SiO_2). These

tetrahedra are stacked up in a highly ordered manner to create a much larger crystal structure.

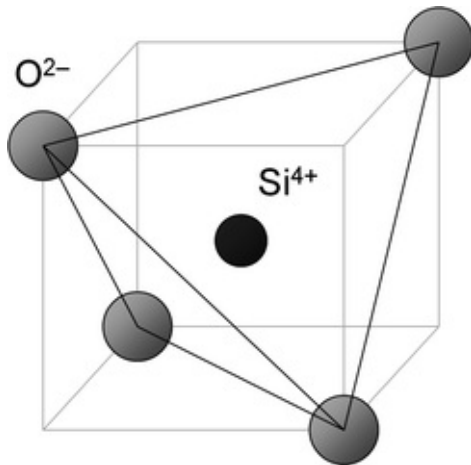


Fig. 11.1 A quartz tetrahedron

Like any other materials, the distribution of polarity is not uniform throughout its crystal structure, creating *dipoles*. As typical quartz is *monocrystal*, indicating all tetrahedra are ordered in one direction, thus the dipoles are also ordered in one direction (Fig. 11.2 top).

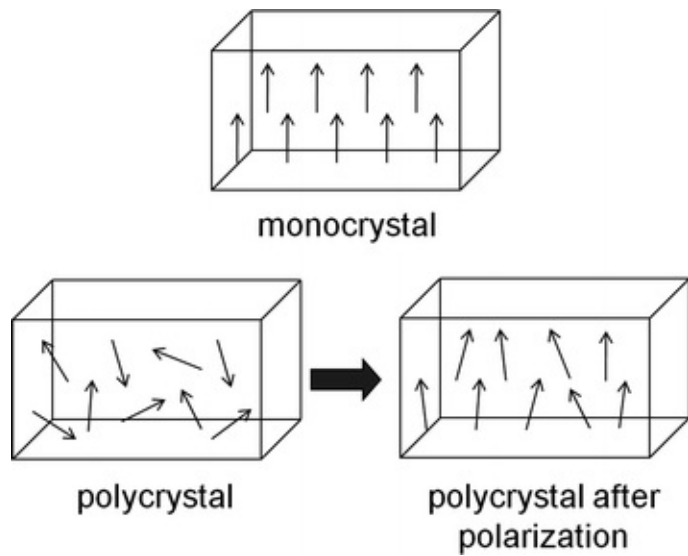


Fig. 11.2 Dipoles are well aligned in monocrystal but random in polycrystal. The dipoles in polycrystal can be aligned through polarization

Some other materials have *polycrystal* structure, meaning that the directions of dipoles are not in one direction. It is possible to use this polycrystal material

as piezoelectric sensor by applying an electrical voltage to the polycrystal to align the dipoles in one direction, called *polarization* (Fig. 11.2 bottom).

To use the monocrystal quartz as a piezoelectric sensor , it is important to cut the crystal in a certain angle so that dipoles are aligned parallel to the electrical voltage. The most widely used angle is $35^\circ 10'$, shown in Fig. 11.3, called *AT-cut*

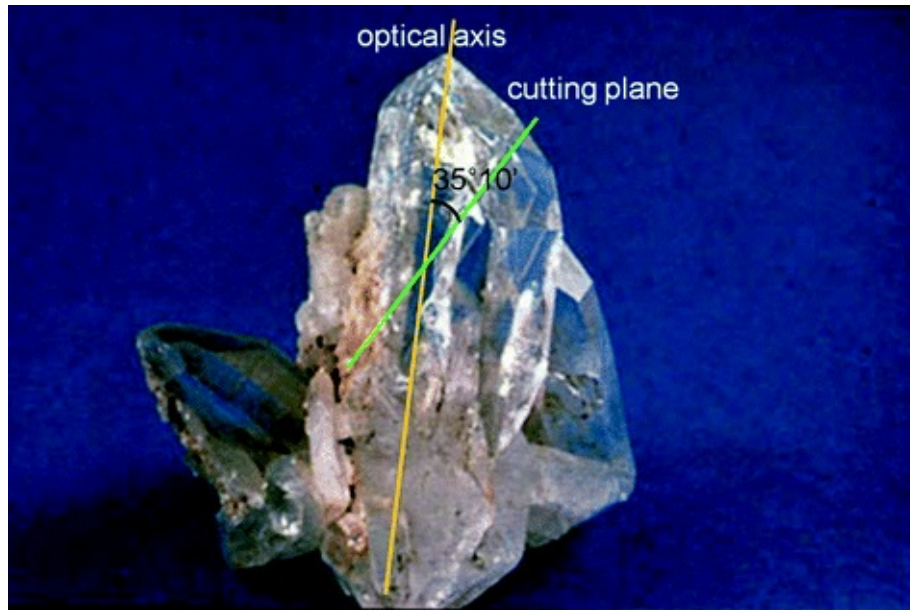


Fig. 11.3 AT-cut quartz crystal. Image adapted from USGS (public domain). Accessed in October 2015 from http://commons.wikimedia.org/wiki/File:Quartz_Crystal.jpg

Once the dipoles are aligned parallel to the electrodes, as shown in Fig. 11.4, piezoelectric effects can be observed. When a quartz crystal is compressed, the dipole itself is also compressed, creating an electrical voltage that has the same direction of the dipole. When the quartz crystal is stretched, the dipole is also stretched, creating a negative electrical voltage.

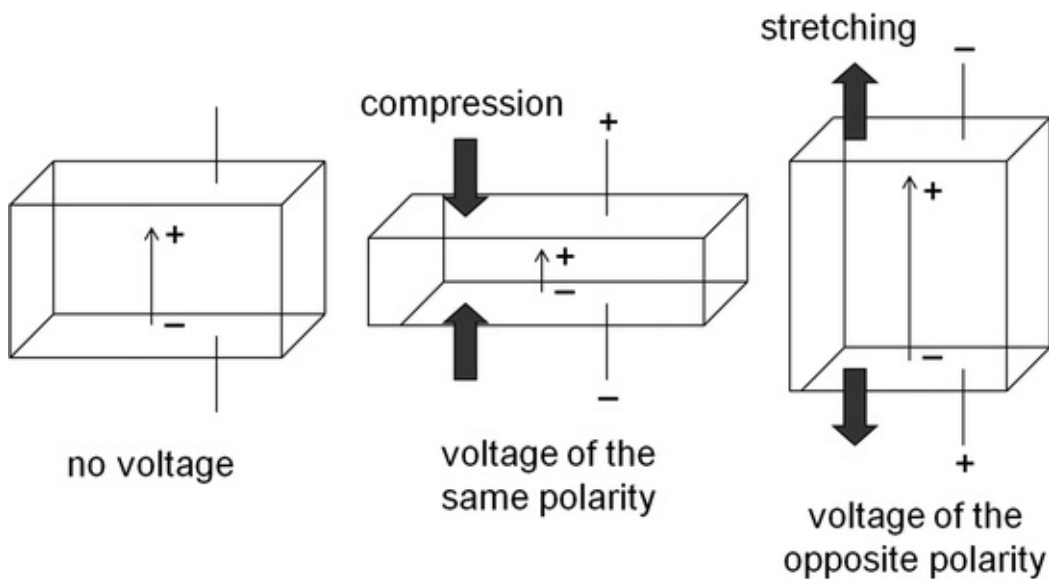


Fig. 11.4 Piezoelectric effect of an AT-cut quartz crystal

Obviously this effect is reversible. When an electrical voltage is applied with the same direction of the dipole, the quartz crystal is compressed. When an electrical voltage is applied with the opposite direction of the dipole, the quartz crystal is stretched. If an alternating current (AC) voltage is applied, the crystal should repeat the compression–stretching cycle.

11.2 Pressure Sensors

The more common pressure sensor would be the capacitor-type pressure sensor that was briefly described in Chap. 1, but the piezoelectric crystal can also be used as a pressure sensor. When one side of the piezoelectric crystal is exposed to a certain pressure, the crystal can be compressed (with positive pressure) or stretched (with negative pressure). This compression or stretching should generate positive or negative voltage, which can be used as a pressure sensor.

The piezoelectric pressure sensor can also be used as an accelerometer, by attaching a mass to the one side of a piezoelectric crystal. When the accelerometer is accelerated or decelerated, the force $F = ma$ is applied to the crystal, which generates a voltage. With the known mass m , acceleration a can be determined.

11.3 Crystal Oscillators

When an electrical voltage is applied to the quartz crystal, the material is

deformed due to the piezoelectric effect. When the voltage is removed, the quartz returns back to its original shape, which also generates electrical voltage (the reverse of the above). Thus the quartz crystal can temporarily store electrical potential and release them later, just like the resistor-inductor-capacitor circuit (RLC circuit). As RLC circuit is capable of generating *harmonic oscillation* at a certain *resonant frequency* (refer to the other electronics textbook for more details), the quartz crystal has the same ability.

The quartz crystal is shock-excited by an applied voltage, and it mechanically vibrates (oscillates) at a resonant frequency to generate AC voltage. To sustain this oscillation, it is necessary to provide another shock-excited voltage before the oscillation is damped. The positive feedback loop of an op-amp can do this function. Unlike the negative feedback loop that we learned previously, positive feedback loop generates the voltage that goes to their extremes, e.g., saturated voltages of +11 or -11 V for LM741 or LM324, which provides the required shock-excited voltages necessary to maintain oscillation. This situation is exactly identical to that of LC or RLC oscillator.

The frequency signal generated from a quartz crystal is generally in the MHz range, which is about the same as an LC or RLC oscillator. Quartz crystals that generate a fixed frequency signal are called *crystal oscillators*. The real advantage of crystal oscillator is its accuracy, with the stability of 0.01–0.001 %; LC oscillators have the stability of 0.01 % at best. The resonant frequency is not affected by environmental parameters, such as external temperature or the magnitude of shock-excited applied voltage. The first application of a crystal oscillator was wristwatch, clock, and radio. The circuit necessary to sustain the crystal oscillation (op-amps or transistors) is available as integrated circuits (ICs), such as 74S124. These days, crystal oscillators are omnipresent in almost all electronic appliances, especially for computers and microprocessors to run at certain clock speed (Fig. 11.5).

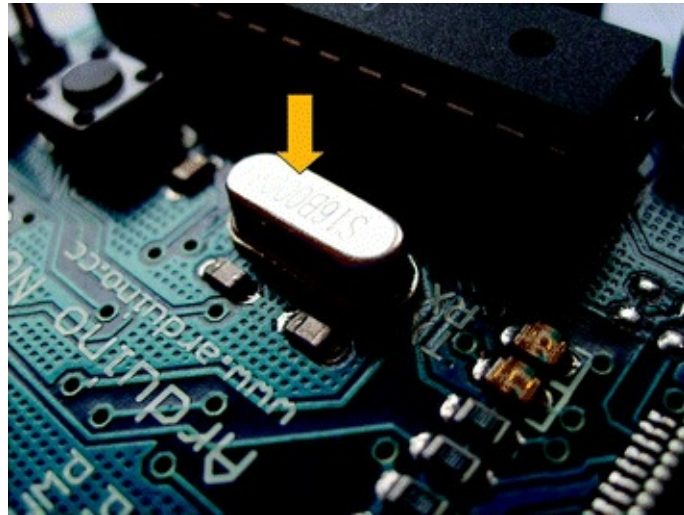


Fig. 11.5 A quartz crystal oscillator in a computer board

11.4 Quartz Crystal Microbalance (QCM)

The most popular biosensor application of piezoelectric sensors would be quartz crystal microbalance (QCM) . QCM is essentially a crystal oscillator that is described in the previous section, utilizing an AT-cut quartz crystal (Fig. 11.6). As described previously, the resonant frequency f is not affected by environmental parameters. However, in 1959, a German physicist Günter Sauerbrey found that this resonant frequency could be decreased when a mass is loaded to one side of a quartz crystal (practically speaking, on the surface of an electrode, as both sides of a quartz crystal must be deposited with metal films to apply voltage). This phenomenon can intuitively be explained in the following manner: suppose an athlete is doing an exercise by moving quickly from the left to the right and coach measures the frequency of such movement per given time. If the coach asks the athlete to do the same exercise but with a heavy backpack, the frequency of such exercise would obviously be decreased.

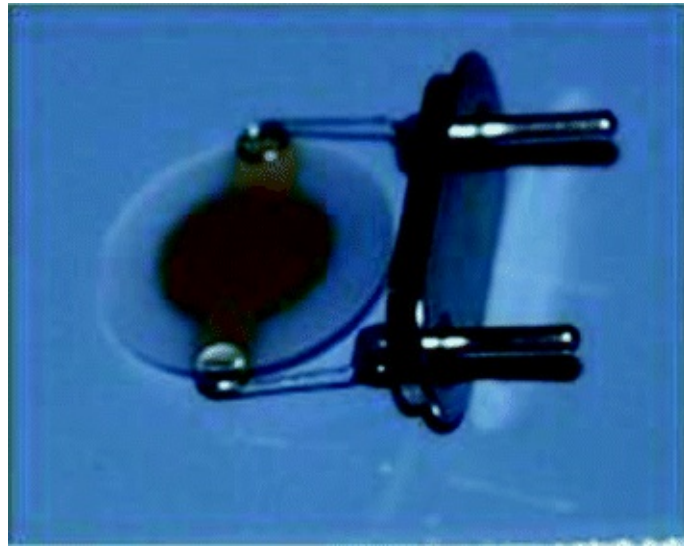


Fig. 11.6 A quartz crystal for QCM. Gold electrodes are deposited on front and back of an AT-cut quartz crystal

Typical resonant frequency of QCM is around 5 MHz. Quartz crystal oscillates at this region of frequency in the *thickness shear mode*, as illustrated in Fig. 11.7. For this reason, QCM is often referred as thickness shear mode resonator (TSM resonator). This thickness shear mode oscillation generates a surface acoustic wave that travels through the film of a loaded mass.

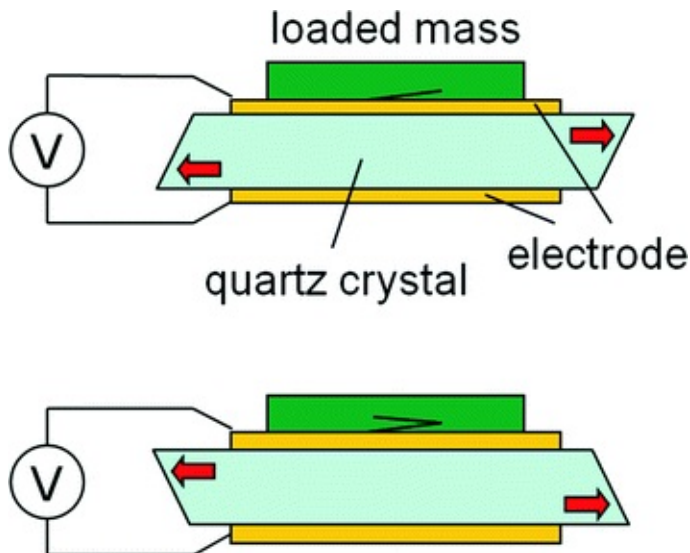


Fig. 11.7 Upon applying voltage, a quartz crystal oscillates to generate a surface acoustic wave into the layer of a loaded mass. With the loaded mass, the quartz crystal oscillates slower than normal, creating a frequency shift

Sauerbrey was able to determine the exact linear relationship between this

frequency change Δf and the loaded mass Δm , called *Sauerbrey equation*:

$$\Delta f = -\frac{2f_0^2}{A \sqrt{\rho_q \mu_q}} \Delta m \quad (11.1)$$

where

f_0 resonant frequency (Hz)

Δf frequency change (Hz)

Δm loaded mass (g)

A piezoelectrically active area (=electrode area) of a crystal (cm^2)

ρ_q density of quartz ($=2.648 \text{ g/cm}^3$)

μ_q shear modulus of AT-cut quartz crystal ($=2.947 \times 10^{11} \text{ g/cm s}^2$)

v_q transverse wave velocity in quartz (m/s)

Note that all parameters in Eq. 11.1 are constant for a given quartz crystal except for the loaded mass Δm ; therefore, the change in frequency is a function of (or proportional to) the change in mass. For the following laboratory, we will use 5 MHz crystals ($f_0 = 5 \times 10^6 \text{ Hz}$) with an active area of 0.4 cm^2 . Then

Eq. 11.1 can be simplified to

$$\begin{aligned} \Delta f (\text{Hz}) &= -0.0565 (\text{Hz/ng}) \times \Delta m (\text{ng}) \quad \text{or} \\ \Delta m (\text{ng}) &= -17.7 (\text{ng/Hz}) \times \Delta f (\text{Hz}) \end{aligned} \quad (11.2)$$

The resonant frequency and its change can accurately be measured with a frequency counter. Since modern QCM sensors have a resolution of 1 Hz or sometimes down to 0.1 Hz, the theoretical resolution of mass detection can be on the nanogram scale. Sub-nanogram mass detection may become possible by increasing the resonant frequency (f_0) to a higher value.

11.5 Viscoelasticity Consideration in QCM

When deriving his equation, Sauerbrey made a very important, yet limiting assumption: the loaded mass is ideally rigid and exhibit no viscoelasticity. In actual situation, however, all materials should exhibit a certain degree of viscoelasticity. The frequency change is no longer a sole function of the loaded mass Δm ; it is also a function of viscoelasticity of the loaded mass. If you use the Sauerbrey equation to estimate the loaded mass that is viscoelastic, you will overestimate the mass. Despite this limitation, Sauerbrey equation is widely used

(and still used today) in estimating the mass loading regardless of its rigidity.

In modern QCM systems, however, an impedance analyzer is typically utilized, where the *impedance* $Z = R + jX$ (R = resistance; X = reactance) is scanned over a range of frequency f , to determine the resonant frequency. Impedance is essentially an extended version of resistance for AC circuits. In a DC circuit, there is no imaginary part of impedance and the impedance simply becomes the same as resistance. Similarly, conductance can be extended to AC circuits by defining the admittance $Y = G + jB$ (G = conductance; B = susceptance). Obviously $Z = 1/Y$.

As the mechanical oscillation of QCM generates AC voltage, either impedance or admittance should be monitored to get an accurate resonant frequency as well as to provide additional information related to its viscoelastic behavior (the latter will be discussed later in this section). For simplification, only the real part of impedance Z or admittance Y can be used, i.e., resistance R or conductance G (Fig. 11.8). It is known that ΔR or ΔG is a stronger function of viscoelasticity of the loaded mass than of Δm ; while Δf is a stronger function of Δm with weaker contribution from viscoelasticity. Obviously, R and G do not change for ideally rigid mass loading, i.e., $\Delta R = \Delta G = 0$. There have been numerous attempts to relate this ΔR or ΔG (with Δf) to a more quantifiable viscoelastic properties, such as the *complex viscosity* (η^*) or the *complex shear modulus* (G^* ; not to be confused with conductance G). However, exact analytical solutions are available only for certain specific situations, such as the films with infinite thickness (i.e., surface acoustic wave decays completely within the film of loaded mass) and homogeneous liquid with no solute adsorption to the electrode surface of a quartz crystal. In most cases, there are more unknown parameters than the number of available equations, leading to an infinite number of possible solutions.

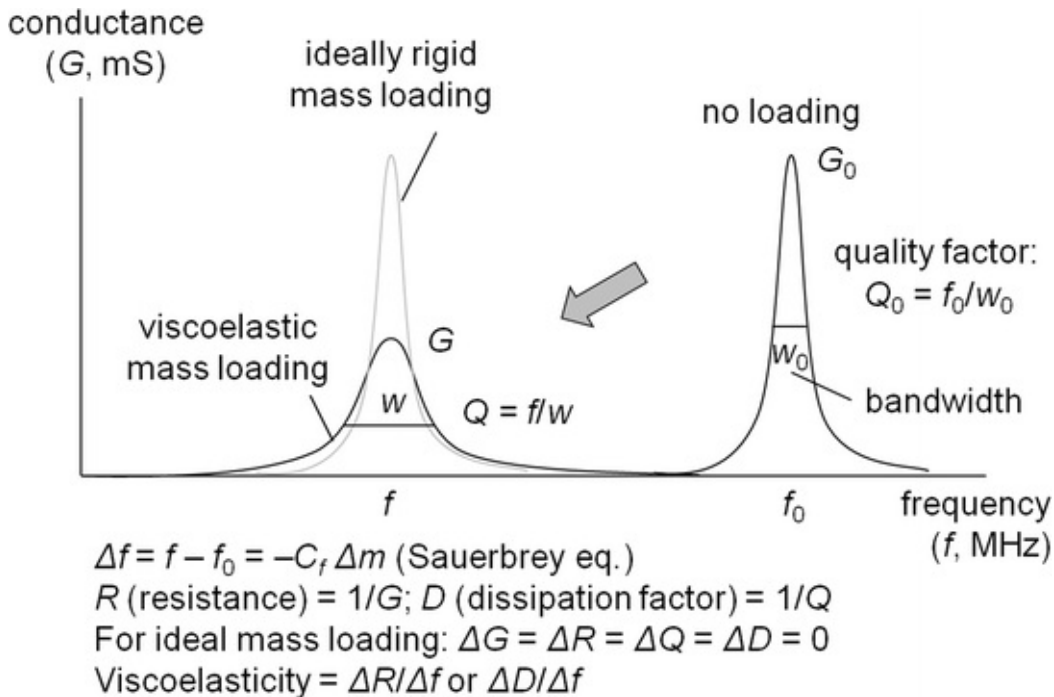


Fig. 11.8 Admittance Y or conductance G is scanned over frequency f to determine frequency change Δf and conductance change ΔG . Similarly, ΔR can be measured. Quality factor Q and dissipation factor D can be used instead of G and R

Despite this difficulty, people have found that the ratio $\Delta R/\Delta f$ is a good qualitative measure of viscoelasticity, though not linearly proportional to it, which people have found useful in many biosensor applications. The QCM equipment shown in this chapter's laboratory is capable of monitoring both ΔR and Δf .

An alternative parameter for viscoelasticity is the *quality factor* Q (Fig. 11.8):

$$Q = f/w \quad (11.3)$$

where

f resonant frequency

w bandwidth (width of a peak at its half height, $G/2$)

Q has a strong correlation with conductance G , because a higher peak gives larger G and smaller w (thus larger Q). Q itself is rarely used in QCM as the bandwidth determination is more difficult than measuring G or R . However, there is an easier way to measure Q through evaluating *dissipation factor* D (Fig. 11.8):

$$D = 1/Q = w/f \quad (11.4)$$

Note that D has a strong correlation with resistance R . Dissipation factor D can be measured by shock-excite the quartz crystal with an applied voltage and measuring its oscillation decay (i.e., no positive feedback loop to sustain its oscillation). By monitoring the exponential decay of oscillation, it is possible to obtain the bandwidth of the original oscillation. The QCM instrument *QCM-D* (trademark of Q-Sense AB, Gothenburg, Sweden) is capable of measuring the dissipation factor. Similar to the conventional QCM, the ratio $\Delta D/\Delta f$ can also be used as a qualitative measure of the viscoelasticity, though still not linearly proportional to it. QCM-D often provides more stable and more reproducible results than conventional QCM, as the energy of crystal oscillation does not accumulate in the loaded mass. In conventional QCM, however, such energy accumulation typically leads to constant drifting of resistance R (and conductance G and quality factor Q) and frequency f .

11.6 Flow Cell QCM as Biosensor

QCM can be used in both air and liquid (mostly water) environment. For the latter, the quartz crystal is typically modified or functionalized with the material of choice, and a solution of biomolecules (typically proteins, DNAs and cells) is introduced onto it. Only one side of a quartz crystal is used for surface modification/functionalization. Occasionally, a bare electrode can also be used without any surface modification/functionalization, where the most typical electrode material for QCM is gold (Au). A *flow cell* is constructed around this side of a quartz crystal oscillator, with an inlet and an outlet, through which a solution of biomolecules is pumped. Figure 11.9 illustrates the schematic of this flow cell for QCM.

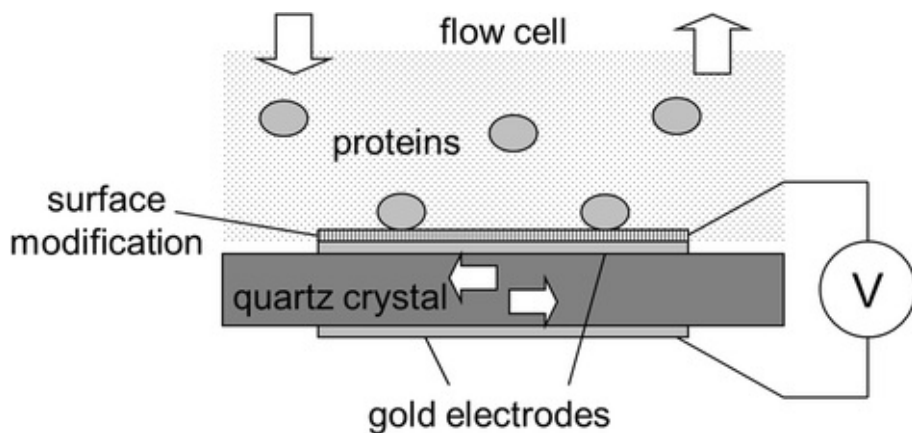


Fig. 11.9 A flow cell for QCM in studying biomolecular adsorption to synthetic surfaces

The QCM has the ability to measure mass deposition/adsorption in nanogram scale, which is three or four orders of magnitude better than any electronic balance. The result can be obtained in real time, such that monitoring the real-time kinetics of biomolecular adsorption to certain surfaces is achievable with extremely high sensitivity. In addition, QCM can also monitor the viscoelasticity change of the adsorbed biomolecules in real time through monitoring $\Delta R/\Delta f$ or $\Delta D/\Delta f$ (though it cannot provide quantitative information). This is an important advantage of using QCM for biological applications. In the following laboratory, we will have a flow cell QCM to study protein adsorption on the bare gold electrode surface.

If the surface modification/functionalization is made with bioreceptors, like enzymes, antibodies, or nucleic acids, the QCM turns into a biosensor. This particular situation will be discussed in detail in Chap. 13 Immunosensors.

11.7 Laboratory Task 1: Quantifying BSA Adsorption on QCM Sensor

The quartz crystal microbalance (QCM) is among the most popular types of piezoelectric sensors. Mass loading onto one side of the electrodes causes the crystal to oscillate at a lower frequency. This decrease in frequency is linearly proportional to the loaded mass, which can be represented by the Sauerbrey equation (Eqs. 11.1 or 11.2). In this laboratory, we will evaluate the adsorption of a model protein molecule, bovine serum albumin (BSA), on a sensor surface.



Fig. 11.10 A complete QCM system with QCM200 digital controller (top), QCM25 crystal oscillator (bottom middle), crystal holder (white plastic piece connected to crystal oscillator), and three 5 MHz quartz crystals. Accessed in October 2015 from <http://www.thinksrs.com/downloads/PDFs/Manuals/QCM200m.pdf>, © Stanford Research Systems 2011, reprinted with permission

In this task, you will need the following:

- QCM (QCM200 from Stanford Research Systems, Fig. 11.10) with a flow cell
- 5 MHz quartz crystals (for QCM200)
- Support stand and clamp for QCM
- A *syringe pump*
- 1 mL syringes and tubings
- Electronic balance, weighing paper, laboratory spatula
- Distilled and/or deionized water
- Beakers, magnetic stir bars, and magnetic stirrer
- Pipettes and pipet tips (1000 μ L)
- Acetic acid ($C_2H_4O_2$ or HOAc) and sodium acetate ($C_2H_3O_2Na$ or NaOAc)
- Monobasic and dibasic potassium phosphate (KH_2PO_4 and K_2HPO_4)
- Bovine serum albumin
- Latex gloves, delicate task wipers (Kimwipes[®]).
 - Acetate buffer: Take 5 mmol each of acetic acid ($C_2H_4O_2$ or HOAc) and sodium acetate ($C_2H_3O_2Na$ or NaOAc). Dissolve them into 100 mL of deionized (DI) water. This makes pH 4.76 100 mM acetate buffer (since $pK = 4.76$).
 - Phosphate buffer: Take 5 mmol each of monobasic potassium phosphate (KH_2PO_4) and dibasic potassium phosphate (K_2HPO_4). Dissolve them into 100 mL of DI water. This makes pH 7.20 100 mM phosphate buffer (since $pK = 7.20$).
 - BSA solution: Add DI water to the vial of protein standard (BSA; bovine serum albumin) to make 400 μ g/mL BSA solution.
 - Prepare 1 mL each of 10 mM acetate and 10 mM phosphate buffer solutions.
 - Also prepare 1 mL each of 40 μ g/mL BSA solutions in (1) 10 mM acetate buffer and (2) 10 mM phosphate buffer.

Why dissolve BSA in two different buffers?

We want to expose our BSA close to its isoelectric point (pH 4.8) and away from it (pH 7.2). The isoelectric point (or pI) of a protein is the pH at which the protein has an equal number of positive and negative charges. Figure 11.11

graphically depicts the surface charge distributions of BSA (left) and lysozyme (right) at pH 7.2. The net surface charge of BSA at pH 4.8 will be close to zero, while that at pH 7.2 will be negative.

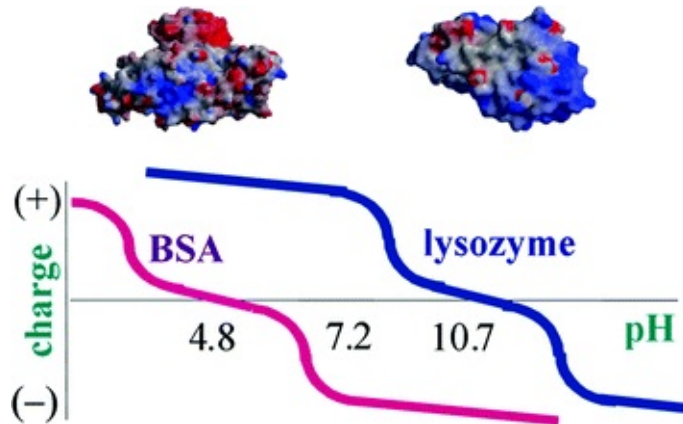


Fig. 11.11 Top surface charge distributions of BSA (left) and lysozyme (right) at pH 7.2. Red negative (-); Blue positive (+). Bottom net charge of BSA and lysozyme plotted against the medium pH

- Get four 1 mL syringes.
- Load two 1 mL solutions (e.g., 10 mM acetate buffer only AND 40 µg/mL BSA in 10 mM acetate buffer) in two different 1 mL syringes (diameter = 5 mm). Be sure to eliminate air bubbles trapped inside.
- Install a syringe onto a syringe pump (Fig. 11.12).

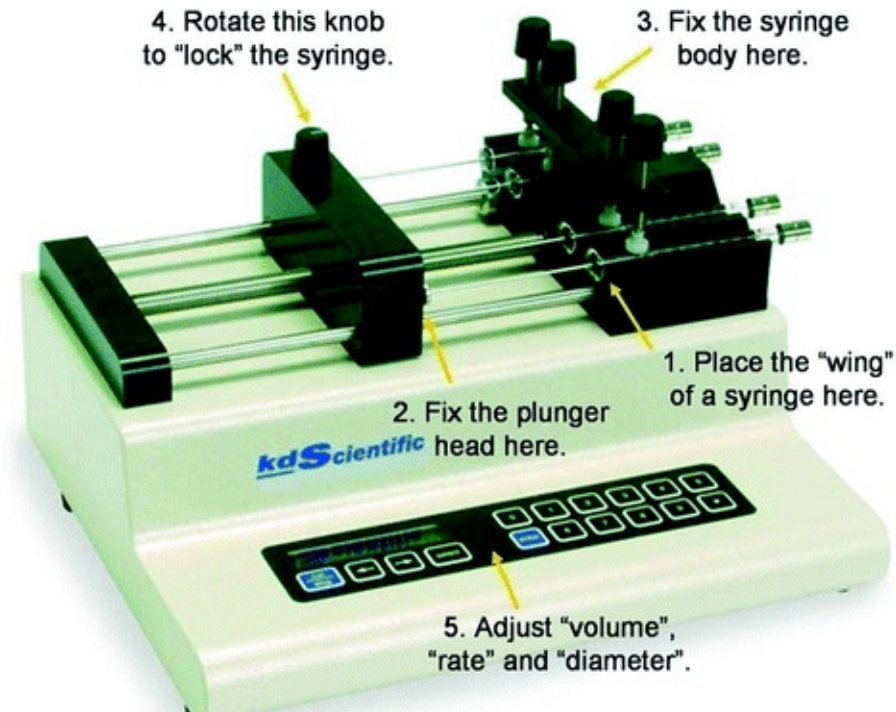


Fig. 11.12 Installing a syringe to a syringe pump

- Install a crystal to the QCM200 system (Fig. 11.13).

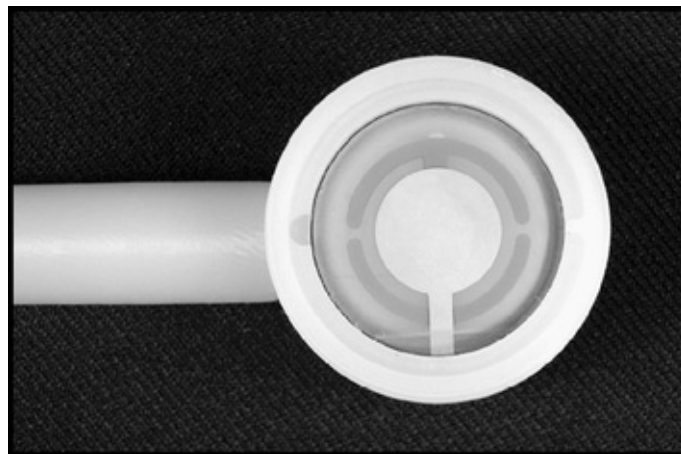


Fig. 11.13 A 5 MHz crystal is placed within the sensor holder of QCM200. In this mode, the QCM can be used as a “balance.” To install a flow cell, the white plastic cap and O-ring should be removed. Accessed in October 2015 from <http://www.thinksrs.com/downloads/PDFs/Manuals/QCM200m.pdf>, © Stanford Research Systems 2011, reprinted with permission

- Cap with a flow cell (Fig. 11.14).

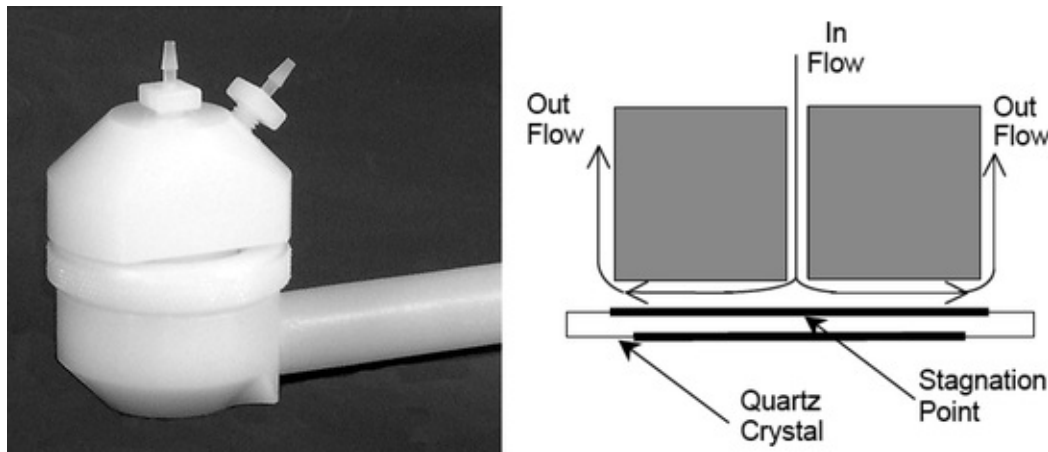


Fig. 11.14 A flow cell for the QCM200. The center connector is for in-flow and the side connector is for out-flow. Accessed in October 2015 from <http://www.thinksrs.com/downloads/PDFs/Manuals/QCM200m.pdf>, © Stanford Research Systems 2011, reprinted with permission

- Experimental setup is shown in Fig. 11.15. Initially, you will need to connect the syringe containing the buffer solution to the QCM flow cell.



Fig. 11.15 Experimental setup of Task 1

- The tubing between the syringe and the inlet of a flow cell should be made as short as possible.
- Turn on the power to the QCM system.
- Turn on the syringe pump and press “select” in order to set-up the diameter of the syringe, the flow rate, and the sample volume. The inner diameter of a 1 mL syringe is 5 mm. If you are using a different syringe and its inner diameter is unknown, you may want to measure the height (h) of a syringe and back-calculate the inner diameter using the following equation (for a 5 mL syringe) (Fig. 11.16):



Fig. 11.16 Determining the inner diameters of disposable syringes

$$5 \text{ mL} = 5 \text{ cm}^3 = 5000 \text{ mm}^3 = \frac{\pi D^2}{4} h \quad (11.5)$$

- Set the flow rate to 0.2 mL/min. This will inject the buffer into the QCM flow cell.
- Wait until both frequency (F) and resistance (R) are stabilized (Table 11.1). Once the crystal makes full contact with water, the resistance (R) should be stabilized around 400–500 Ω . (Note that water is a viscoelastic material, which makes the resistance reading much higher than air.) Less than 400 Ω may indicate the existence of air bubble(s) within a flow cell. Larger than 500 Ω may indicate the existence of viscoelastic mass contamination.

Table 11.1 QCM200 display

Parameter	Value	Symbol	Display
Frequency	Absolute frequency	F	Absolute frequency (Hz) = series resonance frequency of quartz crystal
	Relative frequency	f	Relative frequency (Hz) = absolute frequency – frequency offset
	Mass	m	Mass displacement (ng) = relative frequency/0.0566
Resistance	Absolute resistance	R	Absolute resistance (Ω) = series resonance resistance of quartz crystal
	Relative resistance	r	Relative resistance (Ω) = absolute resistance – resistance offset

- Switch the syringe containing the BSA solution in buffer and inject the solution. Use a clip to hold off the tubing during the syringe exchange. If an air bubble is introduced during the syringe exchange, a sharp peak in frequency curve may be observed and the resistance may drop down significantly.
- Record the frequency and the resistance every 30 s. As the volume is set to 1 mL with a flow rate of 0.2 mL/min, the entire experiment should be finished in 5 min. Typical frequency shift for BSA is a few tens of Hz.
- Repeat the experiment at other pH (10 mM phosphate buffer only AND 40 $\mu\text{g/mL}$ BSA in 10 mM phosphate buffer).
- Remove tubing, flow cell, and crystal holder. Rinse everything (except the

crystal) rigorously with flowing DI water. Place the crystals into the crystal cleaning basket and rinse with DI water. Use wash bottles.

Alternatively, you can use a brand new quartz crystal.

- Plot the frequency and resistance versus time.
- Evaluate “plateaued” Δf and plug into the Sauerbrey equation:

$$\Delta m = -C \cdot \Delta f, \text{ where } C = 17.7 \text{ ng/Hz.}$$

- Divide the mass by the active electrode area of $\sim 0.40 \text{ cm}^2$. Convert this number to units of mg/m^2 or $\mu\text{g/cm}^2$.
- Adsorbed amounts of BSA (trial #1) (Fig. 11.17):

$$\text{pH 7.2: } (17.7 \text{ ng/Hz}) \times (21 \text{ Hz}) / (0.4 \text{ cm}^2) = 929 \text{ ng/cm}^2 = 9.29 \text{ mg/m}^2$$

$$\text{pH 4.8: } (17.7 \text{ ng/Hz}) \times (9 \text{ Hz}) / (0.4 \text{ cm}^2) = 398 \text{ ng/cm}^2 = 3.98 \text{ mg/m}^2.$$

- Adsorbed amounts of BSA (trial #2) (Fig. 11.17):

$$\text{pH 7.2:}$$

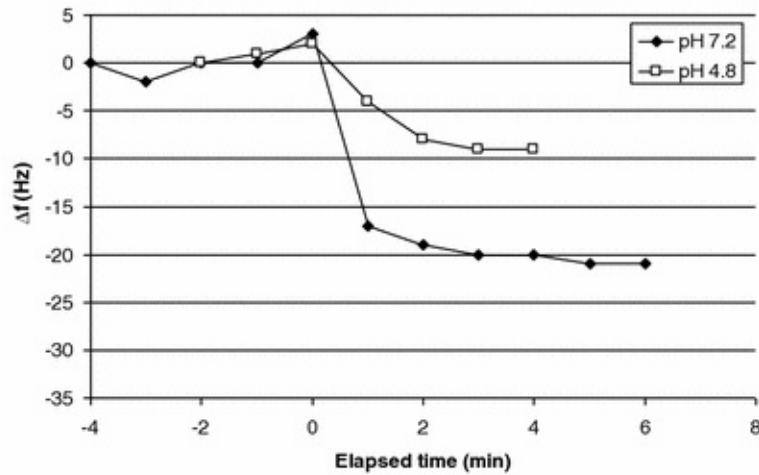
$$(17.7 \text{ ng/Hz}) \times (25 \text{ Hz}) / (0.4 \text{ cm}^2) = 1110 \text{ ng/cm}^2 = 11.1 \text{ mg/m}^2$$

$$\text{pH 4.8:}$$

$$(17.7 \text{ ng/Hz}) \times (19 \text{ Hz}) / (0.4 \text{ cm}^2) = 841 \text{ ng/cm}^2 = 8.41 \text{ mg/m}^2.$$

Trial #1:

	t	-4	-3	-2	-1	0	1	2	3	4	5	6
pH 7.2	Δf	0	-2	0	0	3	-17	-19	-20	-20	-21	-21
pH 4.8	Δf			0	1	2	-4	-8	-9	-9		



Trial #2:

	t	-3	-2	-1	0	1	2	3	4	5	6	7	8
pH 7.2	Δf	0	1	2	3	-30	-25	-25					
pH 4.8	Δf				0	-8	-14	-17	-13	-13	-19	-20	-19

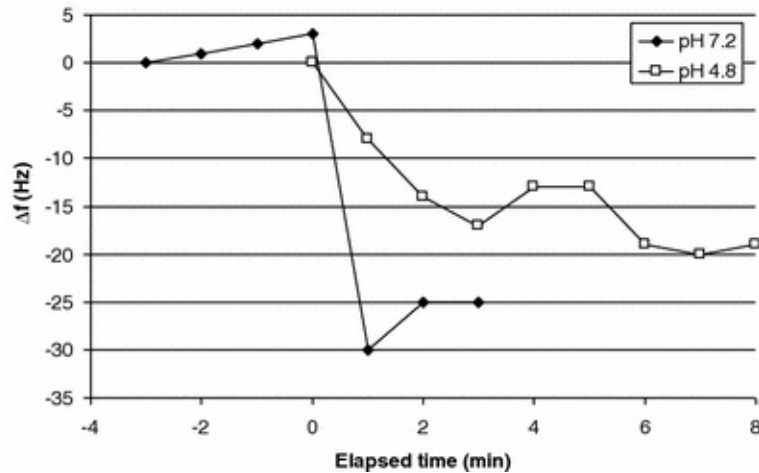


Fig. 11.17 Experimental data of Task 1 (trials #1 and #2): BSA adsorption on QCM sensor surface. More and faster BSA adsorption is observed with pH 7.2, where the net charge of BSA is negative

Question 11.1

More BSA adsorption and faster BSA adsorption was observed for the above experimental results. Explain this in terms of the net charge or the isoelectric point of BSA.

Question 11.2

Figure 11.18 shows BSA has dimensions of $11.6 \times 2.7 \times 2.7 \text{ nm}^3$. Assuming dense hexagonal side-on packing the theoretical adsorbed amount can be calculated by $\Gamma_{\text{theo}} = (\pi/3 \sqrt{3}) \cdot (\delta/v)$, where $\pi/3 \sqrt{3}$ is the packing factor, $\delta = 2.7 \text{ nm}$ (the shortest dimension of BSA because the packing is side-on), and $v = 0.733 \text{ mL/g}$ (the specific volume of BSA, the inverse of its density). Be careful with unit conversions. Compare this with the experimental results obtained in Task 1. Why is there a discrepancy?

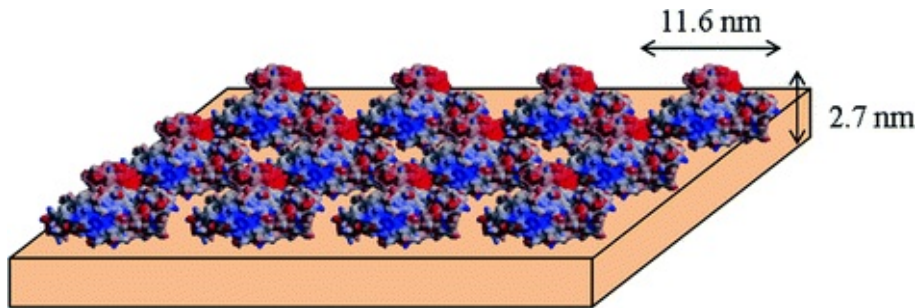


Fig. 11.18 Hexagonal, monolayer packing of BSA on gold surface

Question 11.3

Sketch the frequency shift behavior of lysozyme adsorption on the QCM sensor surface, in pH 7.2 (phosphate) and pH 10.3 (carbonate) buffer. Refer to Fig. 11.11 for the isoelectric point of lysozyme.

References and Further Readings

Crystal Oscillation Theories

- Kao K (2004) Dielectric phenomena in solids, 1st edn. Elsevier, Maryland Heights
- Ristic L (ed) (1994) Sensor technology and devices. Artech House, Norwood
- Scherz P (2006) Practical electronics for inventors, 2nd edn. McGraw-Hill, New York
- Uchino K (2003) Handbook of advanced ceramics, 1st edn. Elsevier, Maryland Heights
- Webster JG (ed) (2000) Mechanical variables measurement: solid, fluid, and thermal. CRC Press, Boca Raton
- Yang J (2004) An introduction to the theory of piezoelectricity, 1st edn. Springer, New York

QCM Mass Sensors

Eggins BR (2002) Chemical sensors and biosensors. Wiley, West Sussex

Smith A (2008) Handbook of thermal analysis and calorimetry, 1st edn. Elsevier, Maryland Heights

Sauerbrey G (1959) Verwendung von schwingquarzen zur wägung dünner schichten und zur mikrowägung (Use of quartz vibrator for weighing thin layers and as a micro-balance). Z Phys 155:206–222
[CrossRef]

Vives A (2008) Piezoelectric transducers and applications, 2nd edn. Springer, New York
[CrossRef]

QCM Viscoelasticity Sensors

Lucklum R, Hauptmann P (2000) The quartz crystal microbalance: mass sensitivity, viscoelasticity and acoustic amplification. Sens Actuators, B 70:30–36
[CrossRef]

Teuscher JH, Yeager LJ, Yoo H, Chadwick JE, Garrell RL (1997) Phase transitions in thin alkane films and alkanethiolate monolayers on gold detected with a thickness shear mode device. Faraday Discuss 107:399–416
[CrossRef]

QCM Immunosensors

Höök F, Rodahl M, Brzezinski P, Kasemo B (1998a) Energy dissipation kinetics for protein and antibody-antigen adsorption under shear oscillation on a quartz crystal microbalance. Langmuir 14:729–734
[CrossRef]

QCM-D

Höök F, Rodhal M, Kasemo B, Brzezinski P (1998b) Structural changes in hemoglobin during adsorption to solid surfaces: Effects of pH, ionic strength, and ligand binding. Proc Natl Acad Sci USA 95:12271–12276
[CrossRef]

Höök F, Kasemo B, Nylander T, Fant C, Sott K, Elwing H (2001) Variations in coupled water, viscoelastic properties, and film thickness of a Mefp-1 protein film during adsorption and cross-linking: a quartz crystal microbalance with dissipation monitoring, ellipsometry, and surface plasmon resonance study. Anal Chem 73:5796–5804
[CrossRef]

QCM-200 from Stanford Research Systems

Stanford Research Systems (2011) Operation and service manual—QCM200 and QCM25. <http://www.thinksrs.com/downloads/PDFs/Manuals/QCM200m.pdf> (Figs. 11.10, 11.13 and 11.14)

12. Glucose Sensors

Jeong-Yeol Yoon¹✉

(1) University of Arizona, Tucson, AZ, USA

✉ Jeong-Yeol Yoon
Email: jyyoon@email.arizona.edu

As we have discussed in Chap. 1 there are four major types of transducers for biosensors: (1) optical, (2) electrochemical, (3) piezoelectric, and (4) thermal. The top two most popular transducers are optical and electrochemical. In reality, these two types are also the ones most commonly used for a glucose sensor, which is one of the most common and the most commercially successful biosensors up to date. In this chapter, we will learn about two different types of glucose sensors, optical and electrochemical, along with other types of enzymatic biosensors.

12.1 Optical Glucose Sensor

A *glucose sensor* (or a *glucose meter*) is a device that monitors the level of blood glucose in humans. Glucose is a simple sugar that exists in the blood stream and comes from the food humans eat. It is essentially a fuel that energizes the cells in a human's body. It is important to maintain a proper level of blood glucose, and in fact, the human body regulates it tightly at a range between 65 and 104 mg/dL (this number can rise up to 140 mg/dL after taking food). The blood glucose level can serve as indicators for variety of medical conditions, but most importantly, this is an indicator for *diabetes*. Blood glucose level higher than 126 mg/dL after 8 h of fasting (typically measured in the morning before breakfast) is diagnosed as diabetes. Most diabetic patients aim to maintain the blood glucose level lower than 120 mg/dL after 8 h of fasting (i.e., in the

morning). Diabetic patients need to monitor the blood glucose level several times a day, so that they can properly control the disease. As it is impractical for the diabetic patients to visit the hospital or laboratory on a daily basis, a need has emerged to develop a handheld, easy-to-use, glucose sensor .

The very first glucose sensor, or rather an assay kit and a reflection photometer (reflectometer), was introduced in the 1970s. The assay utilizes test strips, known as *Dextrostix* , and the accompanying meter was called *Ames Reflectance Meter* (Fig. 12.1). Although this system came with a really high price tag and was primarily used in hospitals only, it basically opened up an entirely new market for glucose sensors and possibly all biosensor markets as well.



Fig. 12.1 Ames reflectance meter that reads from dextrostix . Reprinted from Newman & Turner. *Biosens. Bioelectron.* 20: 2435-2453, © Elsevier 2011, with permission from Elsevier

This glucose sensor is essentially an optical biosensor. In a Dextrostic/Ames Reflectance Meter, glucose in a blood sample is first oxidized into *gluconolactone* , and eventually into *gluconic acid* (Fig. 12.2), under the existence of an enzyme (biological catalyst) called glucose oxidase (GOx). Oxygen (O_2) dissolved in blood is necessary to carry out this oxidation reaction. The byproduct of the reaction is hydrogen peroxide (H_2O_2).

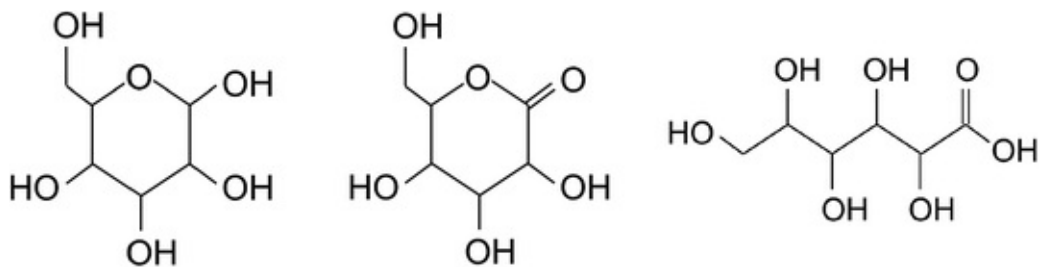
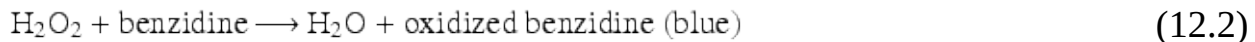


Fig. 12.2 Glucose (left); Gluconolactone (middle); Gluconic acid (right)

In optical glucose sensing, the byproduct, H_2O_2 , is the molecule being detected. For the Ames Reflectance Meter:



This color change (colorless to blue) can be read visually using glucose test strips (Dextrostix), which can be quantified into glucose concentration in mg/dL unit using Ames Reflectance Meter, using the same concept we learned in spectrophotometry.

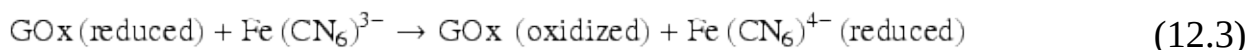
Although modern glucose meters no longer use this optical transduction schematic (they use electrochemical transducers—see the next section), most glucose assay kits still utilize similar optical transduction schematics, as they offer better sensitivity and reproducibility.

Choosing a right transducer is a very important aspect for biosensor development. Electrochemical biosensors can be made very small and inexpensive, typically at the cost of poor sensitivity and poor reproducibility. Optical biosensors are generally considered superior in sensitivity and reproducibility than electrochemical biosensors, at the cost of device complexity and considerable cost for fabrication. Recently, significantly improved sensitivity has been demonstrated for electrochemical biosensors, through utilizing next generation electrode materials, as well as newer types of enzymes and cofactors. Specifically, the introduction of nanotechnology toward electrochemical biosensors has provided their sensitivity and reproducibility comparable to those of optical biosensors (see Chap. 15).

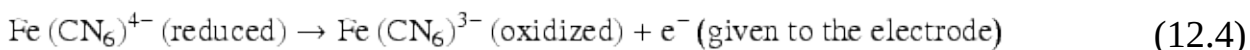
12.2 Electrochemical Glucose Sensor

As discussed in the previous section, glucose sensing involves oxidizing glucose with GOx while generating hydrogen peroxide as a byproduct (Eq. 12.1). During

this process, GOx itself is reduced. If we add a *ferricyanide* ion $\text{Fe}(\text{CN}_6)^{3-}$ (oxidized form) to the reduced GOx, then GOx is oxidized again while ferricyanide is reduced to *ferrocyanide* $\text{Fe}(\text{CN}_6)^{4-}$ (reduced form). Basically, GOx and $\text{Fe}(\text{CN}_6)^{3-}$ are swapping electrons.



The extra electron from ferrocyanide $\text{Fe}(\text{CN}_6)^{4-}$ can be given back to the other electrode.



This cycle generates an electrical current (with no voltage applied; not practical) or change in electrical current (with voltage applied) (Fig. 12.3).

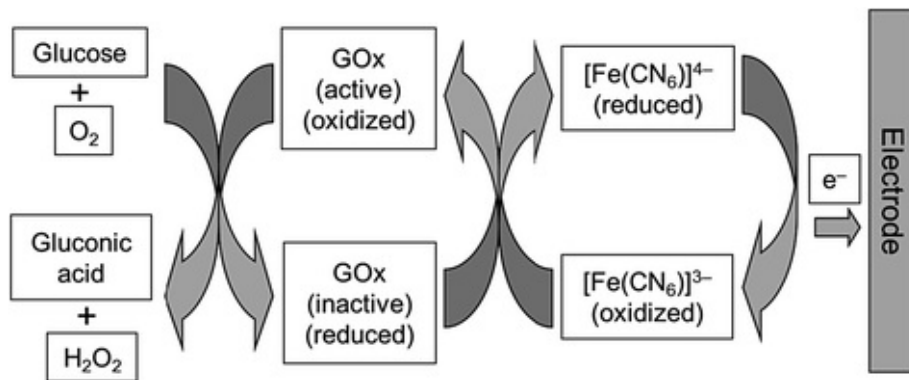


Fig. 12.3 Electrochemical detection of glucose using GOx and ferricyanide ion

In reality, GOx does require a cofactor to truly function as a catalyst. Flavin adenine dinucleotide (FAD^+) is a well-known cofactor for GOx. During the oxidation of glucose to gluconolactone by GOx, FAD^+ works as the electron acceptor and is reduced to FADH_2 .



The cofactor FADH_2 is oxidized back to FAD^+ utilizing O_2 found in blood, while forming H_2O_2 .



H_2O_2 is oxidized back to H_2O at an electrode, generating electrons, and this whole cycle again generates a change in electrical current with a constant voltage applied (Fig. 12.4).

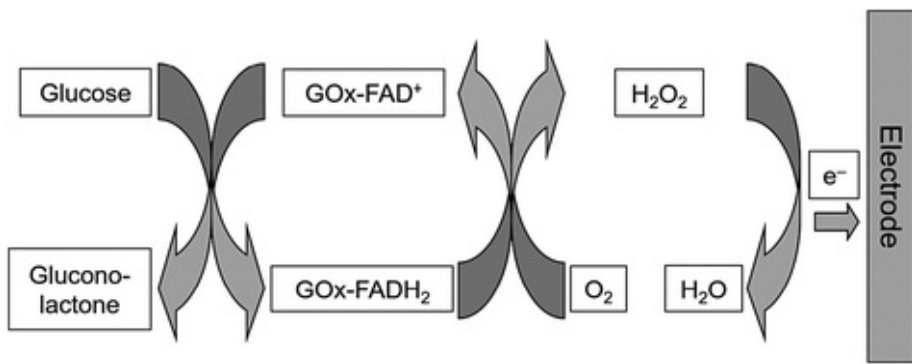


Fig. 12.4 Electrochemical detection of glucose using GOx and FAD^+

Other than GOx, different enzymes can also be used in electrochemically detecting glucose. For example, the enzyme glucose dehydrogenase (GDH) and a cofactor nicotinamide adenine dinucleotide (NAD^+) can function similarly to GOx– FAD^+ combination. In this schematic, oxygen is not required (major benefit over GOx– FAD^+), and GDH converts glucose to gluconolactone while converting NAD^+ into NADH (reduced form):



The reduced NADH will be oxidized back to NAD^+ at the electrode, while generating H^+ and two electrons. This process will again result in a change in electrical current with constant voltage applied.

The use of pyrroloquinoline quinone (PQQ) as a cofactor to GDH has become increasingly popular in electrochemical glucose sensing, due to its rapid electron transfer rate.



Again, the reduced PQQ will be oxidized back to its oxidized form at the electrode, similar to NAD^+ , and a change in electrical current will be observed with constant voltage applied (Fig. 12.5).

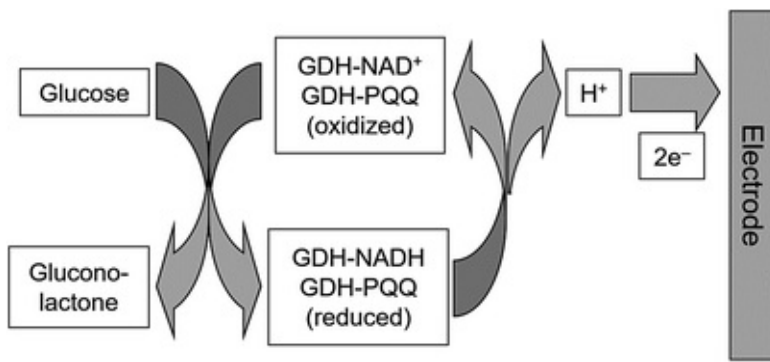


Fig. 12.5 Electrochemical detection of glucose using GDH and NAD⁺/PQQ

This amperometric electrochemical transduction was very popular in the 1980s and quickly became the mainstream in glucose sensing. Electrodes are patterned into a test strip with the necessary enzymes and chemicals immobilized on it. Electrodes are made out of platinum (Pt), gold (Au), or carbon (C), with a reference electrode, so that a small change in current can be measured, usually in μA to nA scale. As it is somewhat difficult to measure this small current change in a reproducible manner, the sensitivity and reproducibility of electrochemical glucose sensors are inferior to those of optical glucose sensors. However, as the system can be made very small and inexpensive, it has quickly dominated the glucose meter market. Many different companies currently manufacture glucose meters and test strips, and use a wide variety of reaction schematics.

Figure 12.6 shows how the commercial glucose meter/strip measures the blood glucose level: (1) sampling a small volume of blood from the patient's finger using a finger-pricking device (referred to as *lancet device*), (2) inserting a glucose strip to its meter, pre-loaded with enzyme (GOx or GDH) and cofactor (FAD⁺, NAD⁺, or PQQ), (3) contacting the inlet of the strip to the blood droplet on a finger, allowing the blood to be absorbed into the strip, and (4) measuring the current change under a constant voltage applied. Diabetic patients need to monitor their blood glucose level several times a day, while the most important reading is the one measured in the morning before taking any food (i.e., after 8 h of fasting). The assay results can be written down in a log book, or can be stored in the small memory of a meter. Some newer versions of glucose meters allow communication with a smartphone for this data logging.



Fig. 12.6 A lancet device pricks the finger to obtain a blood sample (*top left* and *top right*). A glucose meter reads the current change from a glucose strip (pre-loaded with enzyme and cofactor; *bottom left* and *bottom right*)

12.3 Other Electrochemical Biosensors

Since successful demonstration and commercialization of electrochemical glucose sensors, other types of electrochemical enzymatic sensors have been developed. One of the early attempts was cholesterol detection from blood, another important indicator for variety of medical conditions. In cholesterol detection, an enzyme called cholesterol oxidase (ChO_x) oxidizes cholesterol into cholesterol-4-ene-3-one utilizing O₂, while the enzyme itself is reduced, generating H₂O₂. This schematic is identical to Eq. 12.1 (Fig. 12.7).

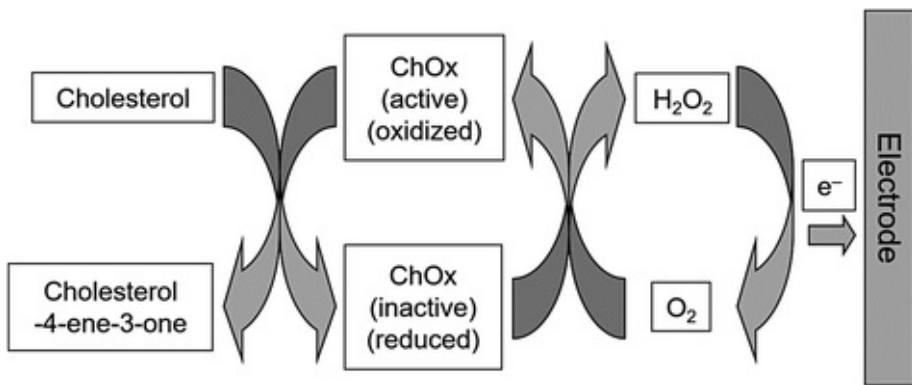


Fig. 12.7 Electrochemical detection of cholesterol using ChOx

Similarly, the level of ethanol in blood (blood alcohol content or BAC) can be detected, for various legal and medical purposes (most notably for identifying drunk driving). An enzyme called alcohol dehydrogenase (ADH) and a cofactor NAD^+ oxidizes ethanol into acetaldehyde without requiring O_2 . This schematic is identical to Eqs. 12.7 and 12.8 (Fig. 12.8).

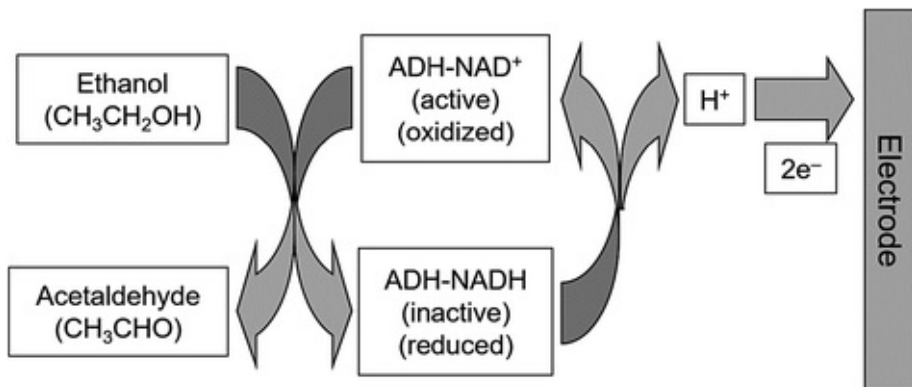


Fig. 12.8 Electrochemical detection of ethanol using ADH- NAD^+

Other detections are also possible: Lactic acid can be detected with lactic oxidase; Uric acid can be detected by uricase; Urea can be detected by urease, etc.

12.4 Continuous Glucose Monitoring (CGM)

While the procedure shown in Fig. 12.6 has been the gold standard in self-monitoring blood glucose level, the patient can obtain only a few data points per day. For some cases, there is a need to monitor the blood glucose level throughout the entire day, e.g., to continuously monitor the blood glucose level,

to figure out the impact of certain type of food or the effect of certain exercise, etc. Therefore, new technology has emerged: continuous glucose monitoring (CGM) . In CGM, an electrode needs to be inserted into the body (to enable in vivo measurements), and the glucose level is measured every 1–5 min (Fig. 12.9).

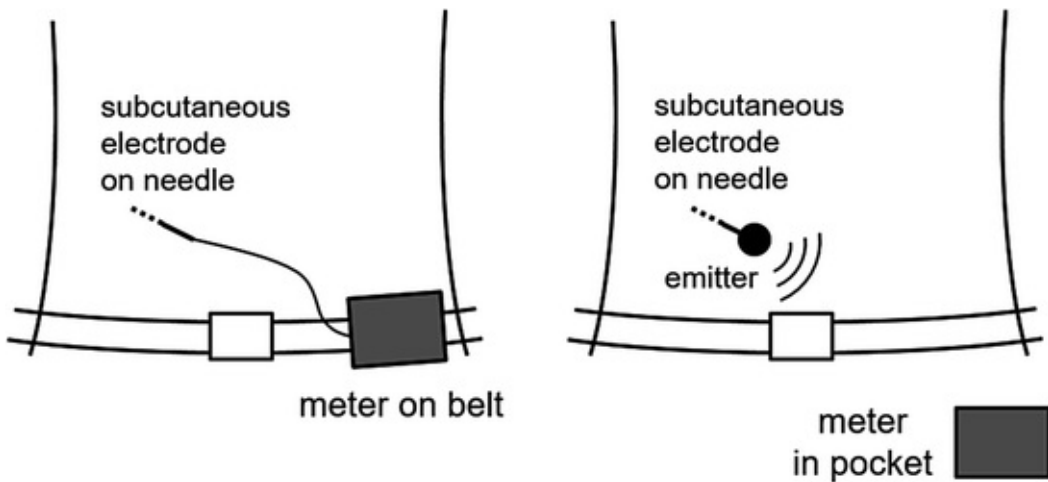


Fig. 12.9 Continuous glucose monitoring (CGM) devices, wired (left) and wireless (right)

Initially, attempts were made to quantify the glucose level directly from blood in a continuous manner. To do this, the electrode is inserted into the capillary blood vessel, and measurements are made every 1–5 min, using the same electrode. Unlike the single-use glucose strips, however, the electrodes are easily contaminated with proteins, especially with blood clots (creating the situation called *thromboembolism* , formation of *thrombus* = stationary blood clot, and *embolus* = circulating blood clot). To avoid this complication, most recent CGM devices measure the glucose level from *interstitial fluid* (=tissue fluid). A needle is inserted through the skin, and the electrode is located at its end, to measure the glucose level of the interstitial fluid (=tissue fluid) right underneath the skin (*subcutaneous measurement*) . The needle-type electrode needs to be replaced before the enzyme and the cofactor become inactive or the electrode becomes contaminated, approximately every 3–7 days.

The earlier models require a physical connection between the needle-based electrode and the meter. The newer models have an emitter fixed to the skin, which transmits the information in a wireless mode to the meter located up a few meters away. In addition, CGM device can be integrated with an *insulin pump* . Based on the measured glucose level, the meter can trigger the insulin pump to inject *insulin* to the patient, to lower the blood glucose level as needed. Note that

diabetes is caused by lack of insulin production (type 1) or insulin resistance (type 2), and injecting insulin to patients is considered as later-stage treatment option.

12.5 Laboratory Task 1: Glucose Assay Kit with a Spectrophotometer

In the first two tasks, you will use a glucose assay kit that utilizes a spectrophotometer. This particular kit does not utilize an enzyme GOx, but directly binds glucose to a chemical o-toluidine under heating and acid conditions. The resulting glucose–toluidine complex has blue-green color. The visible spectrum consists of, from short to long wavelengths, blue-green–yellow-red color. Therefore, coloration of blue-green indicates that absorption occurs yellow-red color from a liquid container (cuvette). The maximum absorption peak occurs at 630 nm.

This reaction is noticeably simpler and easier to use, at a cost of possibility for cross reaction. For example, o-toluidine can also bind to other aldoses such as glyceraldehyde, ribose, or galactose. However, as the concentrations of these chemicals in blood are much lower than that of glucose, this cross reactivity can be often neglected. You can obviously use other glucose assay kits, provided that you follow the manufacturer's protocol line-by-line.

In this task, you will need the following:

- Glucose
- Electronic balance, weighing paper, laboratory spatula
- Deionized or distilled water
- Centrifuge tubes (1.5 mL)
- Pipettes and pipet tips (1000 μ L)
- A vortex mixer
- Glucose assay kit (QuantiChromTM DIGL-100 from BioAssay Systems)
- A heating block (temperature sensor, if needed)
- A spectrophotometer (CHEMUSB4 or FLAME-CHEM from Ocean Optics) and appropriate software (OceanViewTM from Ocean Optics)
- Disposable plastic cuvettes
- Latex gloves, delicate task wipers (KimWipes®)

Preparation of Solutions

- Dissolve 30 mg of glucose in 1 mL of deionized or distilled water in a 1.5-mL centrifuge tube. Use a vortex mixer to dissolve. This will make a 3 g/dL glucose solution.
- Take 100 μ L of 3 g/dL glucose solution and add to 900 μ L distilled and/or deionized water. This will make a 300 mg/dL standard glucose solution (STD).
- Dilute the standard in water using 1.5-mL centrifuge tubes as follows.

No.	STD + water	Vol (μ L)	Glucose (mg/dL)
1	150 μ L + 0 μ L	150	300
2	100 μ L + 50 μ L	150	200
3	50 μ L + 100 μ L	150	100
4	25 μ L + 125 μ L	150	50
5	0 μ L + 150 μ L	150	0

- If you are trained and qualified to use/handle biological specimen and the laboratory is approved for its use, you may obtain blood sample from human subjects, using a lancet device (see Fig. 12.6).
- As this is not a common and easy process, we recommend to take one of the above solutions (#1–#5) from the other team, without knowing its concentration, as your unknown sample.

Colorimetric Detection of Glucose

- Transfer 12 μ L of the above to the other centrifuge tubes. Transfer 1200 μ L QuantiChrom™ Reagent to each tube. Close the tubes tightly and mix with a vortex mixer.
- Place the tubes in a tube holder and heat (100 °C) in a heating block for 8 min (Fig. 12.10). Cool down in cold water for 4 min.

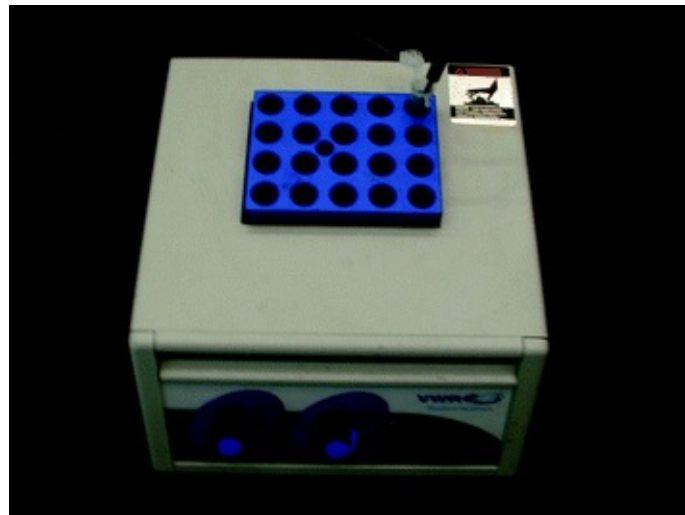


Fig. 12.10 A heating block warms the centrifuge tubes close to 100 °C

- Transfer an appropriate amount of reaction mixture into a cuvette. Read the absorbance at 620–650 nm (peak absorbance at 630 nm) against the blank (Figs. 12.11 and 12.12). The signal will stay stable for 60 min.
- Subtract blank absorbance (water, #5) from the standard absorbance values (#1–#4), and plot the absorbance against standard concentrations. Determine the slope using linear regression fitting. The y-intercept should be set to zero. This is your “standard curve” (Fig. 12.11).
- Using this standard curve, determine the glucose concentration of the “model” urine specimen.
- Refer to Chap. 8 for definitions of absorbance $A = \log_{10} (I_0/I)$, where I_0 is the light intensity before entering the material and I after passing through the material, and *Beer–Lambert law* $A = \varepsilon lc$, where ε is the molar absorptivity, l is the path length, and c is the concentration of substance.
- Theoretically, A at 0 mg/dL concentration should be zero, making the standard curve to pass through origin. In reality, however, the cuvette, water, and the QuantiChrom™ Reagent absorb light, leading to positive y-intercept in the standard curve. Although it is okay to use this standard curve as is, one may find it more useful to zero-adjust the entire curve by subtracting with A at 0 mg/dL concentration (Fig. 12.11).

Glucose concentration (mg/dL)	0	50	100	150	300	unknown
Absorbance	0.23	0.49	0.66	1.05	1.33	0.68

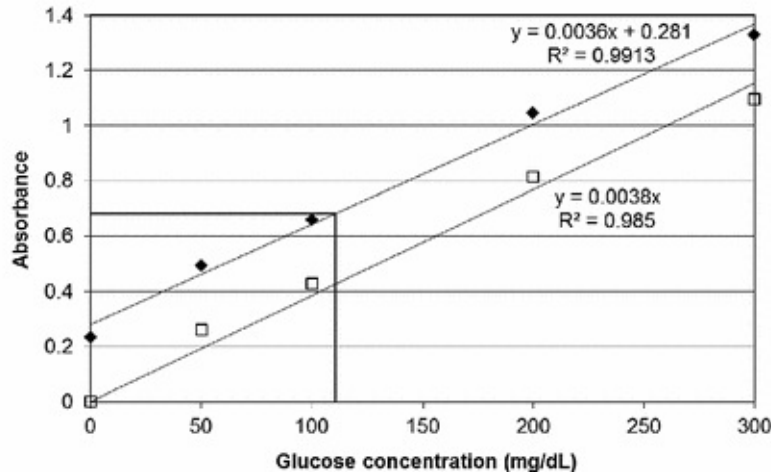


Fig. 12.11 Experimental data from Task 1: absorbance—glucose concentration plot (filled diamond symbols). The glucose concentration of an unknown sample can be calculated from the regression equation: $0.68 = 0.0036x + 0.281$, $x = 110$ mg/dL. The bottom curve (open square symbols) is zero-adjusted by subtracting with the absorbance of 0 mg/dL solution

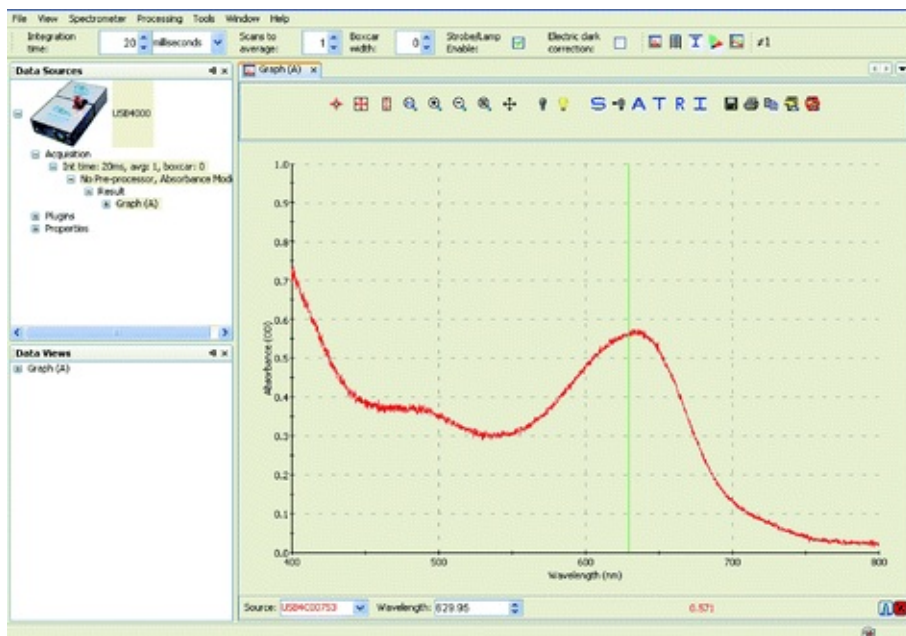


Fig. 12.12 Absorbance spectrum for glucose assay kit

12.6 Laboratory Task 2: Glucose Assay Kit with LED /PD Circuit

In this task, the UV/Vis spectrophotometer will be replaced with a red *LED* and a photodiode, along with accompanying circuit, as described in Chap. 8

(Figs. 12.13 and 12.14). The same glucose solutions from Task 1 will be used.

In this task, you will need the following:

- A breadboard, wires, wire cutter/stripper, a power supply and a DMM
- 10 or 20 k Ω pot, and a screw driver
- Three 100 Ω and two 1 M Ω resistors
- Red LED
- PIN-040A photodiode
- Op-amp LM741 (or LM324)
- Five samples in cuvettes from Task 1 (glucose + QuantiChrom™ reagent + heat-incubated)

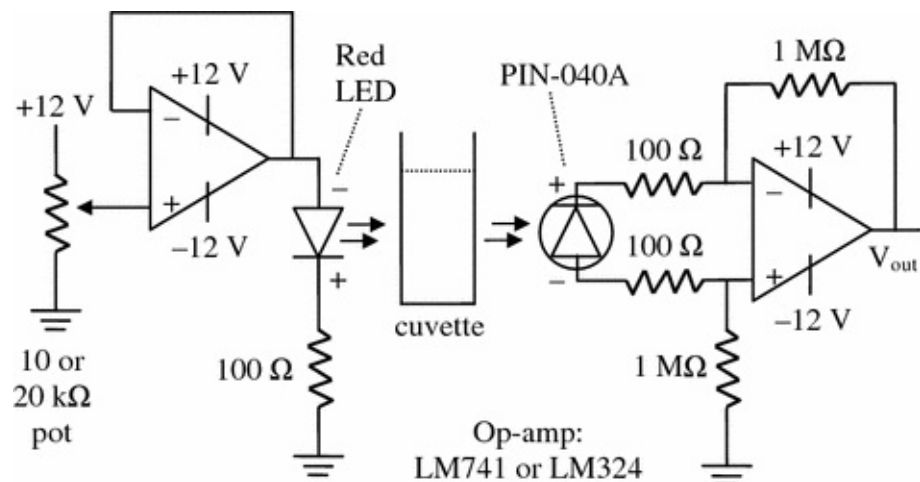


Fig. 12.13 Circuit diagram of Task 2

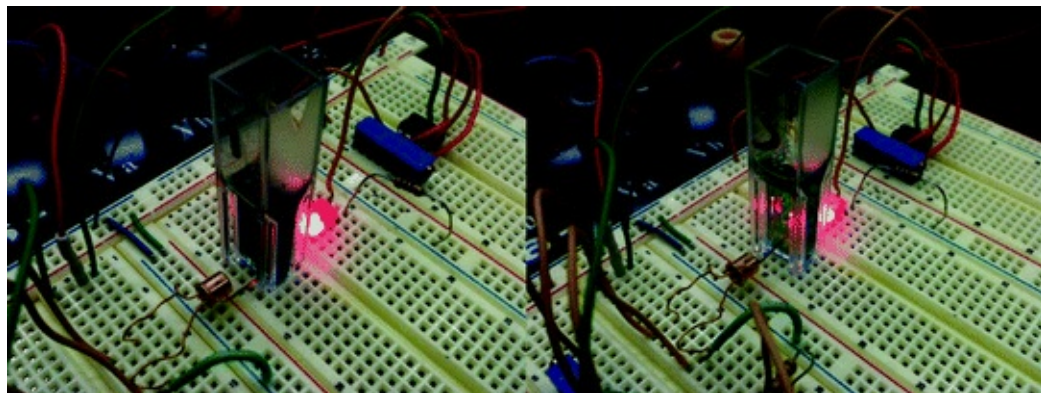


Fig. 12.14 LED–PD circuit is measuring the glucose concentration in a cuvette. Left 300 mg/dL. Right 0 mg/dL

As V_{out} from a PD circuit will be divided by that of 0 mg/dL glucose solution, not I_0 , the A at 0 mg/dL automatically becomes 0. This will make the standard curve pass through origin, or zero-adjusted (Fig. 12.15).

As shown in Fig. 12.14, the cuvettes are aligned to have 0.5 cm path length, and compared to 1 cm path length in Task 1, the absorbance should be roughly a half of those in Task 1 (consider the Beer–Lambert law, $A = \varepsilon lc$, where l is the path length).

Glucose concentration (mg/dL)	0	50	100	150	300
V_{out}	0.195	0.133	0.109	0.076	0.055
$A = \log(I_0 / I) = \log(V_{\text{out},0} / V_{\text{out}})$	0	0.166	0.253	0.409	0.550

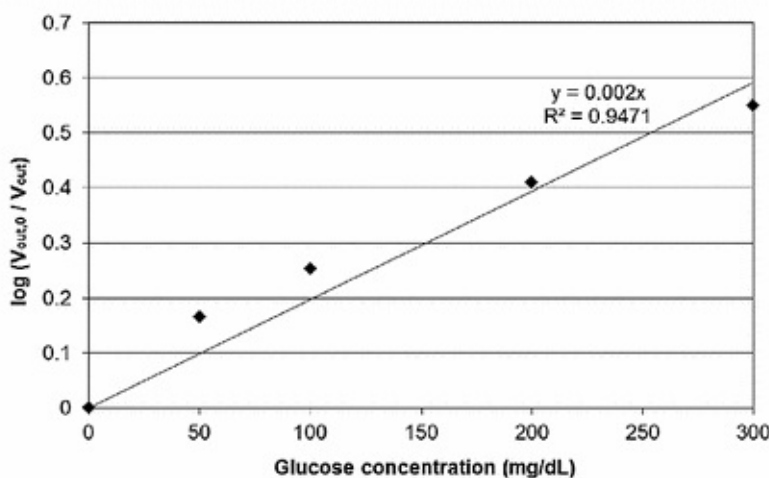


Fig. 12.15 Experimental data of Task 2: $\log(V_{\text{out},0}/V_{\text{out}})$ —glucose concentration plot. $V_{\text{out},0}$ is the voltage output with 0 mg/dL glucose solution

Question 12.1

Compare absorbance readings (zero-adjusted) of Task 1 and Task 2. Probably, the absorbance readings of Task 2 are slightly smaller than a half of those of Task 1. What factors are responsible for this deviation?

12.7 Laboratory Task 3: Commercial Electrochemical Glucose Sensor

In the following task, commercial glucose test strips will be used, which are based on electrochemical detection. Recent glucose test strips are mostly based on GDH–PQQ, although the exact reaction schematics may vary by manufacturer.

In this task, you will need the following:

- Commercial glucose meter and test strips (Accu-Chek from Roche)
- Glucose stock solution (3 g/dL) from Task 1
- Deionized or distilled water
- Centrifuge tubes (1.5 mL)
- Pipettes and pipet tips (10 or 100 μ L)
- A vortex mixer
- Latex gloves, delicate task wipers (KimWipes®)
 - You still have leftover glucose stock solution (3 g/dL). Prepare five different glucose solutions, following the Task 1 protocol. Do not add QuantiChrom™ reagent.
 - Take a test strip from the bottle of new test strips and insert it into a glucose meter to activate.
 - Measure glucose concentrations for the five glucose solutions, by applying a small drop of each to the end of a test strip.
 - Repeat the measurement twice for each solution. Calculate the averages and standard deviations (Figs. 12.16 and 12.17).
 - If possible, try to measure the glucose level of your own blood. Use a lancet device included in the commercial glucose meter.

Glucose concentration (mg/dL)	0	50	100	150	300
Commercial sensor reading (mg/dL)	0	74	230	280.5	421.5

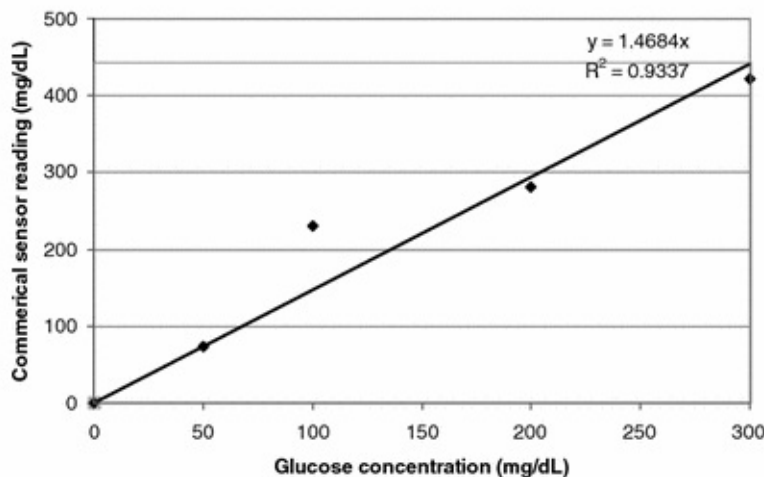


Fig. 12.16 Experimental data of Task 3: commercial sensor reading—glucose concentration plot



Fig. 12.17 A commercial glucose meter is reading the glucose level

Question 12.2

Is there discrepancy between the real concentrations and your meter readings? If so, can you explain why? Hint: many commercial glucose meters show “plasma equivalent” concentrations rather than the actual glucose concentrations.

Question 12.3

When comparing the colorimetric assay kit and the commercial glucose meter, which one shows a larger standard deviation? Can you explain why?

References and Further Readings

Optical Glucose Sensor (Sect. 12.1)

Harborn U, Xie B, Venkatesh R, Danielsson B (1997a) Evaluation of a miniaturized thermal biosensor for the determination of glucose in whole blood. *Clin Chim Acta* 267:225–237
[CrossRef]

Kissinger P (2005) Biosensors—a perspective. *Biosens Bioelectron* 20:2512–2516
[CrossRef]

Koschwanez H, Reichert W (2007) In vitro, in vivo and post explantation testing of glucose-detecting biosensors: current methods and recommendations. *Biomaterials* 28:3687–3703
[CrossRef]

Luong JHT, Male KB, Glennon JD (2008a) Biosensor technology: technology push versus market pull. *Biotechnol Adv* 26:492–500
[CrossRef]

Newman J, Turner A (2005) Home blood glucose biosensors: a commercial perspective. *Biosens Bioelectron* 20:2435–2453 (Figure 12.1)

Electrochemical Glucose Sensor (Sect. 12.2)

Eggins BR (2002) Chemical sensors and biosensors. Wiley, West Sussex

Ferri S, Kojima K, Sode K (2011) Review of glucose oxidases and glucose dehydrogenases: a bird's eye view of glucose sensing enzymes. *J Diabetes Sci Technol* 5:1068–1076
[CrossRef]

Grieshaber D, MacKenzie R (2008) Electrochemical biosensors—sensor principles and architectures. *Sensors* 8:1400–1458
[CrossRef]

Harborn U, Xie B, Venkatesh R, Danielsson B (1997b) Evaluation of a miniaturized thermal biosensor for the determination of glucose in whole blood. *Clin Chim Acta* 267:225–237
[CrossRef]

Luong JHT, Male KB, Glennon JD (2008b) Biosensor technology: technology push versus market pull. *Biotechnol Adv* 26:492–500
[CrossRef]

Newman J, Turner A (2005b) Home blood glucose biosensors: a commercial perspective. *Biosens Bioelectron* 20:2435–2453
[CrossRef]

Thevenot D, Toth K (2001) Electrochemical biosensors: recommended definitions and classification. *Biosens Bioelectron* 16:121–131
[CrossRef]

Yoo E-H, Lee S-Y (2010) Glucose biosensors: an overview of use in clinical practice. *Sensors* 10:4558–4576
[CrossRef]

Wang J (1999) Amperometric biosensors for clinical and therapeutic drug monitoring: a review. *J Pharmaceut Biomed Anal* 19:47–53
[CrossRef]

Wang J (2002) Electrochemical nucleic acid biosensors. *Anal Chim Acta* 469:63–71
[CrossRef]

Wang J (2006) Electrochemical biosensors: towards point-of-care cancer diagnostics. *Biosens Bioelectron* 21:1887–1892
[CrossRef]

Zhang S, Wright G, Yang Y (2000) Materials and techniques for electrochemical biosensor design and construction. *Biosens Bioelectron* 15:273–282
[CrossRef]

Zhang X, Ju H, Wang J (eds) (2007) Electrochemical sensors, biosensors and their biomedical applications, 1st edn. Academic Press, London

Other Electrochemical Biosensors (Sect. 12.3)

Córcoles EP, Boutelle MG (2013) Biosensors and invasive monitoring in clinical applications. Springer, Heidelberg (Chapter 5)

Rahman MM, Ahammad AJS, Jin J-H, Ahn SJ, Lee J-J (2010) A comprehensive review of glucose biosensors based on nanostructured metal-oxides. Sensors 10:4855–4886
[CrossRef]

Tiwari A, Turner APF (eds) (2014) Biosensors nanotechnology. Scrivener Publishing, Beverly (Chapter 1)

13. Immunosensors

Jeong-Yeol Yoon¹✉

(1) University of Arizona, Tucson, AZ, USA

✉ Jeong-Yeol Yoon
Email: jyyoon@email.arizona.edu

As we have learned from Chap. 1, biosensors utilize bioreceptors to capture and analyze specific biomolecules of interest. Antibodies, enzymes, and DNAs have been used commonly as bioreceptors; however, *antibodies* are the most common and widely studied. In addition, *antigens* can also be used as bioreceptors to capture and analyze specific antibodies. Biosensors that utilize antibodies or antigens as bioreceptors are called *immunosensors*.

Immunosensors are being widely investigated and developed for practical applications such as medical and veterinary diagnostics, food safety, and environmental monitoring. Because antibodies are very specific to proteins, viruses, bacteria, cells, etc., the sensitivity and specificity of immunosensors are much more superior to other types of biosensors.

We have learned three major transducers that are commonly used in biosensor applications: optical (Chaps. 8 and 9), electrochemical (Chap. 10), and piezoelectric (Chap. 11). Immunosensors are generally classified depending on the type of transducers: optical immunosensor , electrochemical immunosensor, and piezoelectric immunosensor.

13.1 Enzyme-Linked Immunosorbent Assay (ELISA)

Immunosensors have become very popular recently, although the use of antibodies in biological assays has been and still is a very common practice in laboratory-based analyses. One particular assay protocol that has dominated over

others is the enzyme-linked immunosorbent assay (ELISA) .

We have already learned briefly about the working principle of ELISA in Chap. 1. Figure 13.1 is basically identical to the sandwich immunoassay with enzyme, described previously in Fig. 1.11. In ELISA, a solid support (microwells; described later) is pre-immobilized with antibodies. Any empty spaces are further immobilized with *passivating proteins* , usually bovine serum albumin (BSA) , to prevent any nonspecific bindings. A target solution is added to this surface, and *antibody-antigen binding* occurs if a complementary antigen exists in the target solution. The surface is then rinsed; leaving only the bound target antigens on the surface. Antibody-antigen binding now occurs, but at this moment there is no way to tell whether binding has really occurred or not. Therefore, we need to add additional materials that will bind specifically to the target antigen as well as generate optical or electrochemical signals. To this end, the same antibody is added (called *secondary antibody* or 2° *antibody*) to the surface, which should specifically bind to the target molecule. As a result, the target molecule is sandwiched between two identical antibodies. In this sense, ELISA is often referred to as a *sandwich immunoassay*. The surface is rinsed again to remove excess secondary antibodies. After that, antibody-to-antibody is added that should specifically bind to the secondary antibody, which is typically pre-conjugated (through covalent binding) with an enzyme. To save time, secondary antibody is sometimes pre-conjugated with antibody-to-antibody-enzyme conjugate. Rinsing is then followed to remove any excess antibody-to-antibody-enzyme conjugates. Substrates to the enzyme are finally added, which is usually designed to undergo color change, typically from colorless to yellow or blue colorations. The more targets you have on the surface, the more coloration you should have from the surface.

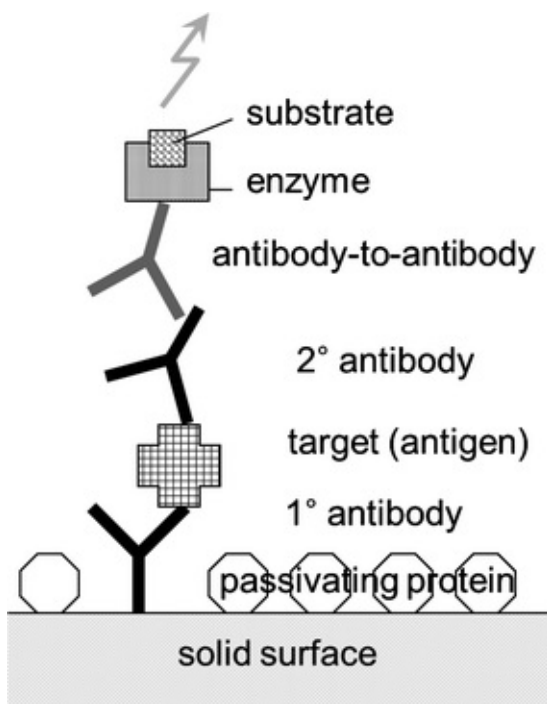


Fig. 13.1 Typical ELISA (identical to the portion of Fig. 1.11)

Note that the above description is about detecting antigens using antibodies. Obviously, the reverse is also possible, i.e., detection of antibodies using antigens. In that case, the ELISA plate should be pre-immobilized with antigens rather than antibodies, and the secondary antigens must be covalently conjugated to an appropriate enzyme. A good example of antibody assay using antigen as bioreceptor is the detection of human immunodeficiency virus (HIV), which causes acquired immune deficiency syndrome (AIDS). The amount of HIVs in the human body is typically very small that is hard to detect. The presence of HIVs in the human body triggers the generation of a substantial amount of antibodies against them (anti-HIV; unfortunately, these antibodies cannot eliminate HIVs), which are a lot easier to detect.

At this point, you may ask: “Why not directly tag the secondary antibody with an enzyme or a fluorescent dye?” The reason is that as there are so many different types of antibodies, it is impractical to tag all the different antibodies with an enzyme or a dye. It is better and more economical to tag the antibody-to-antibody than tagging the entire library of antibodies.

ELISA is typically performed in a plastic container that has multiple wells, typically 8×12 , thus 96 wells. This container is called a *microwell plate* or simply *microplate* (Fig. 13.2). This setup allows the user to perform 96 independent assays at the same time. For example, the glucose assay performed

in the previous chapter would preferably be performed using a microplate. Typical ELISA kits come with all necessary reagents along with a microplate that are pre-immobilized with the antibodies (and of course with passivating proteins). This antibody-immobilized microplate is specifically referred to as *ELISA plate*.

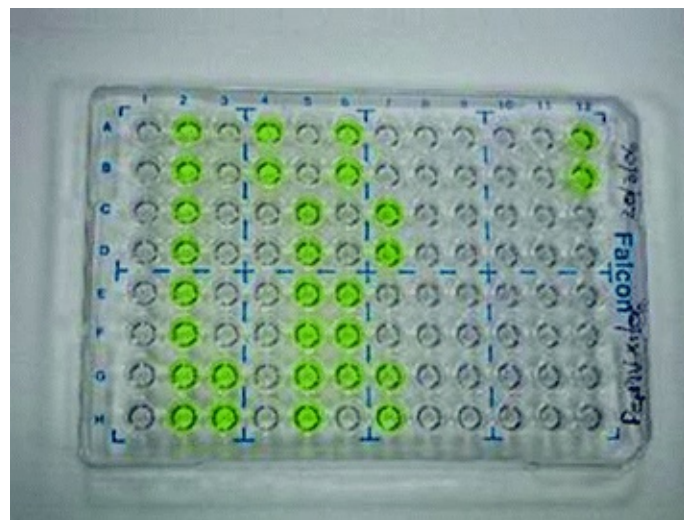


Fig. 13.2 A microplate

Solutions are added to each well of a microplate using a pipette. To speedup the assay, a multi-channel pipette can be used, where 8 pipettes are bundled together to dispense liquid at a single stroke. Since a standard microplate has 8 rows and 12 columns, a multi-channel pipette can feed the entire 96 wells in just 12 strokes. Rinsing is also done using a pipette. One example of rinsing using a pipette is: (1) eliminate the liquid from a well through suction, (2) add a rinsing solution, usually a phosphate-buffered saline (PBS) with a small amount of detergent, (3) wait for a short period of time, and (4) eliminate the rinsing solution. As you can imagine, typical ELISA requires multiple steps of reagent addition and subsequent rinsing, which is highly labor-intensive.

In the earlier days, the light emission from enzyme-substrate binding was visually identified by the naked eye. The light intensity is often classified into several categories such as +++ (strong positive), ++ (very positive), + (positive), w+ (weak positive), and – (negative). Nowadays, of course, we have a sophisticated machine to quantify these light emissions, called the *microplate reader* (Fig. 13.3). The microplate reader is essentially a 2-D version of a spectrophotometer, or a scanner with specific light sources.



Fig. 13.3 A microplate reader. A microplate is placed onto the bottom right tray and inserted into the reader

Many commercial ELISA kits are available on the worldwide market. We perform an ELISA exercise on *insulin* in this chapter, a hormone responsible for the control of glucose metabolism, and thus important in the diagnosis and prognosis of diabetes.

13.2 Antibodies

The choice of antibodies greatly affects the performance of ELISA and other immunosensors. Antibodies can be produced by injecting a specific antigen into animals, typically a mouse, rat, goat, rabbit, pig, or a horse, etc. The animal's immune system will try to recognize the shape of the antigen, and eventually generate a mixture of antibodies that recognizes different portions (called *epitopes*) of the antigen. The resulting "mixture" of antibodies is called polyclonal antibody (pAb) (Fig. 13.4). Despite being a mixture, all of them are still able to recognize the same antigen.

In many cases, certain epitopes may exist over several different antigens. A good example is *Escherichia coli* and *Salmonella*. These two bacteria are somewhat similar to each other and share a certain amount of epitopes. Therefore, pAb to *E. coli* can also bind to *Salmonella*, albeit to a lesser extent, since only a fraction of epitopes are identical to each other. This problem is referred to as *cross-reactivity*. Therefore, there is a need to develop an antibody that recognizes only one type of epitope, called monoclonal antibody (mAb) (Fig. 13.4).

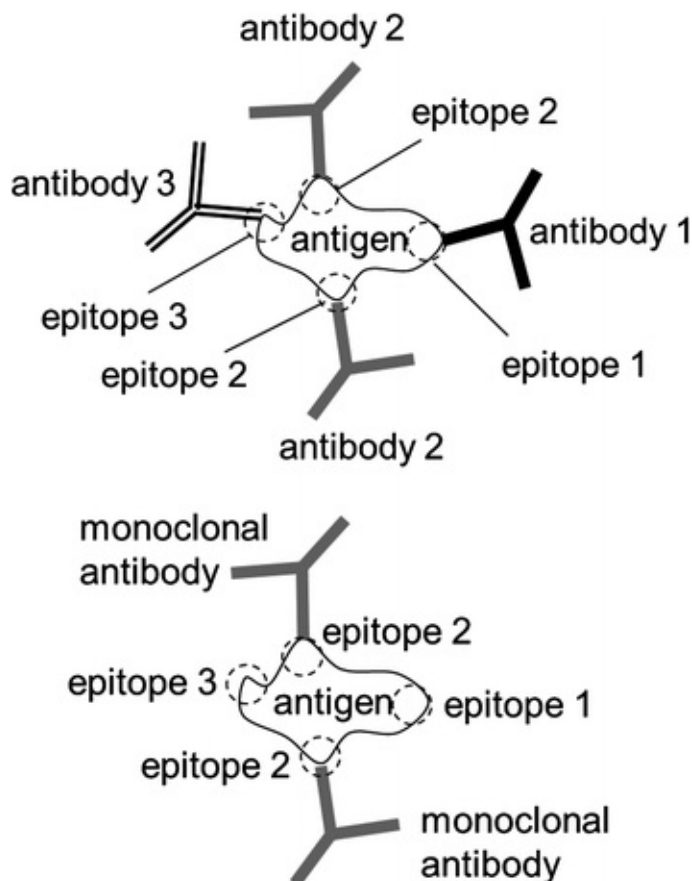


Fig. 13.4 Polyclonal antibodies bind to multiple types of epitopes of a single antigen (top). Monoclonal antibodies bind to a single type of epitope of an antigen (bottom)

Monoclonal antibodies are first produced using spleen cells from mice. The *spleen* is found in all vertebrate animals and one of its functions is to generate antibodies. A specific antigen is injected into a mouse, and the spleen cells (specifically *B cells* that produce antibodies) are harvested. These spleen cells are then fused with *myeloma cells* (*B cell cancer*), resulting in hybrid cells (*hybridoma cell*). These cells do not die but proliferate virtually infinite number of times. A single cell line is chosen and cultured, which will produce only a single type of antibodies (i.e., mAb). Recently, other animal cells have also been used to produce mAb, most notably rabbits. These mAb are widely used in ELISA and other immunosensor applications whenever a higher specificity is required.

13.3 Antibody Fragments and Aptamers

Antibodies are Y-shaped and have two pairs of polypeptide chains: heavy chains

and light chains (Fig. 13.5). The very top portions of both heavy and light chains vary depending on the target antigen that the antibody can recognize (called *hypervariable regions*) and the remainder are identical (called *constant regions*). In general, for ELISA and immunosensing applications, we do not need the constant regions. The top branch portion of antibodies, called *F(ab)₂ fragment*, or even smaller fragments such as single-chain antibody (scAb) fragment and single-chain variable antibody (scFv) fragment, can be used for ELISA and immunosensors (Fig. 13.5). Since these fragments are smaller than whole antibodies, they are potentially more stable, easier to immobilize on solid surfaces, and show better reactivity with the target antigen due to its smaller size. F(ab)₂ fragment can be made by cleaving a whole antibody with *papain enzyme*. The smaller fragments are often synthesized by *recombinant technology*. The recombinant technology has a lot of potential, since they are synthesized within bacteria by inserting a genetic sequence that will synthesize only one type of polypeptide (thus antibody fragment), which may replace the mAb. Currently the binding activity of these recombinant antibody fragments is inferior to that of mAb.

Antibodies have been used as a primary type of bioreceptors in bioanalytical methods and biosensor applications. There are, however, many obstacles in large-scale production of antibodies. They still require animals (polyclonal antibodies) or cell lines (mAb). If the antigens do not trigger the immune response, there is no way to produce antibodies. Some scientists believe aptamers could serve as a good alternative bioreceptor to replace these limitations of antibodies.

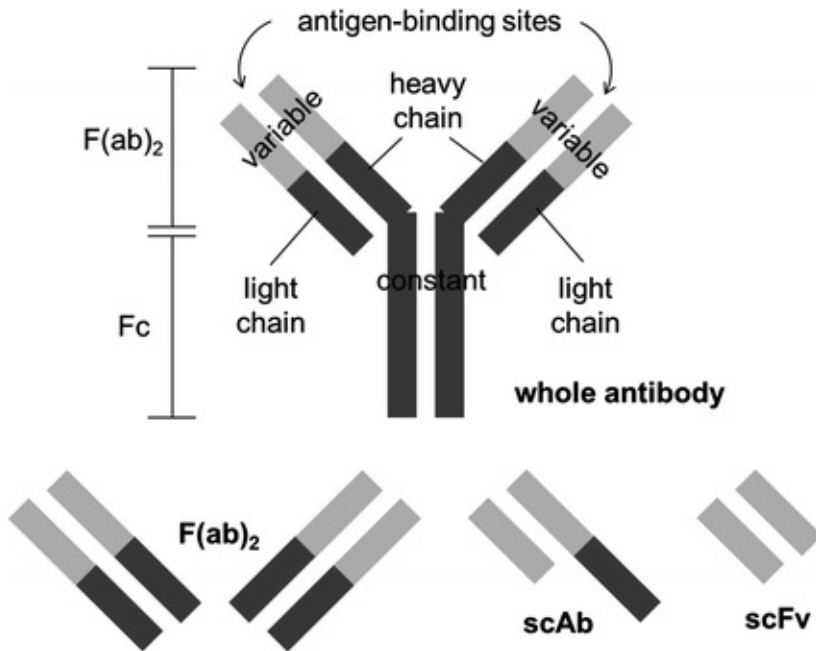


Fig. 13.5 A whole antibody molecule (top), showing heavy and light chains; variable and constant regions; F(ab)₂ and Fc portions. Antibody fragments (bottom), showing F(ab)₂, single-chain antibody (scAb) and single-chain variable fragment (scFv)

Aptamers are essentially artificial nucleic acids (DNA or RNA) that recognize or bind to specific antigens, just like antibodies. Recall that antibodies are proteins, which are made from posttranslational modifications and folding of polypeptide chains. Aptamers are mostly single-chain nucleic acids, either single-stranded DNA (ssDNA) or RNA. (Note that the stable nucleic acids inside the nucleus of a cell are *double-stranded DNA* or *dsDNA*, which has a double-helical structure. RNA is inherently single-stranded.) These single-chain structure can bind partially to itself and/or fold just like proteins, resulting in a 3-D structure. Some single-chain nucleic acids can recognize and bind to a specific molecule, which are called aptamers.

Aptamers are isolated from complex libraries of artificial nucleic acids by an iterative process called systematic evolution of ligands by exponential enrichment (SELEX). A large number of genetic sequences are chosen and synthesized, including a randomized region. The amount of these nucleic acids are amplified through the process called polymerase chain reaction (PCR). The target antigen is added to the resulting mixture, and only a very small portion of candidate nucleic acids are able to bind to the target antigens. The resulting nucleic acid–antigen complex can be filtered, precipitated, or captured with gel, to choose the candidate molecule that possesses the best binding performance. The amount of chosen molecule is again amplified by PCR. The whole cycle is

repeated more than 10 times to select only the best ones.

These aptamers can be used just like antibodies. Figure 13.6 illustrates how aptamers can be used for an ELISA-like process, called enzyme-linked oligonucleotide assay (ELONA), where two aptamers sandwich the target antigen. Aptamer-based biosensors are specifically called *aptasensor*. A hybrid of ELISA and ELONA is also possible. For example, an antibody can be immobilized on a solid surface (as a capture molecule) while an aptamer is used to sandwich the target molecule labeled with an enzyme or a fluorescent dye (as a detector molecule). Conversely, the reverse is also possible: aptamer as a capture molecule and antibody as a detector molecule.

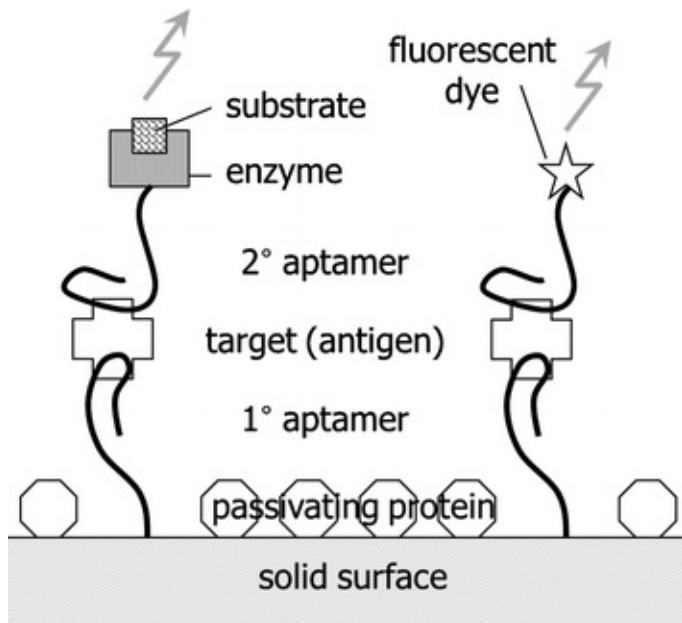


Fig. 13.6 Enzyme-linked oligonucleotide assay (ELONA) or sandwich aptamer assay

Theoretically, we can produce aptamers for any target antigens, as they do not require any immune response of animals or cell lines. Moreover, there are virtually no batch-to-batch variations, which are commonly found in antibodies. The small size of aptamers (antibodies are relatively big, with molecular weight of 150,000) makes it less vulnerable to the denaturation caused by heat and/or long-term storage.

Unfortunately, the number of available aptamers that can readily be used for ELONA and aptasensors is very small at this moment, mainly due to the labor-intensive and time-consuming nature of the SELEX process. For this reason, the commercial market is still dominated with antibodies. However, it may be a matter of time for the aptamers to dominate this market, yet we do not know how

long it will take.

13.4 Lateral-Flow Assay (LFA)

There is a simpler format of immunosensors that gained great popularity in the diagnostics market, called *lateral-flow immunochromatographic assay* or simply lateral-flow assay (LFA). The most well-known example of LFA is the pregnancy test. The user applies a drop of urine sample to a cassette-type device or dips the strip into a urine sample. If two pink lines show up, you are pregnant; and if one pink line shows up, you are not pregnant. No line indicates the test failed (Fig. 13.7).

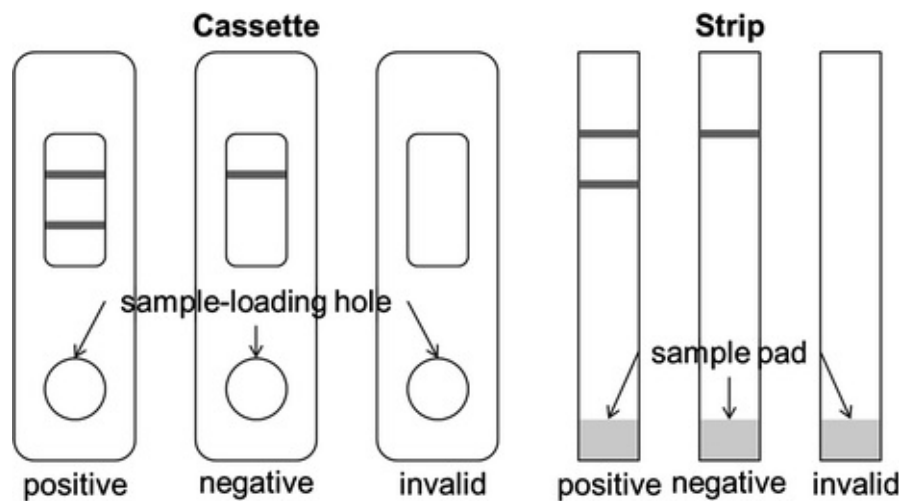


Fig. 13.7 Cassette-type and strip-type LFA

LFA is essentially a membrane that is pre-loaded with a couple of different antibodies. Liquid (urine or blood sample) flows through the membrane by osmotic action. There are two bands in the strip, as shown in Fig. 13.8, one with antibodies to the target (for pregnancy, the target is human chorionic gonadotropin or hCG), the other with antibodies to antibody (anti-IgG). Once the urine/blood sample (which may contain hCG) is applied to the inlet, the anti-hCG-gold nanoparticles (anti-hCG-AuNP ; pre-loaded within the strip) may or may not bind to the target hCG. The liquid travels through the membrane by capillary action. When the liquid hits the test line, the hCG + anti-hCG-AuNP complex is captured there. The unbound, excess anti-hCG-AuNP continues to travel to the control line, which is eventually captured there.

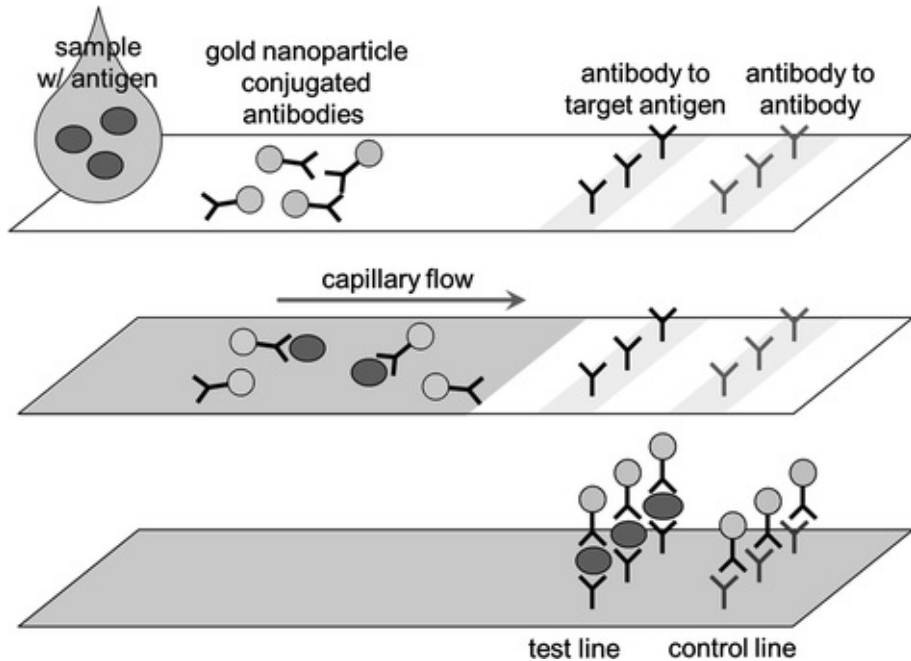


Fig. 13.8 Schematic of LFA

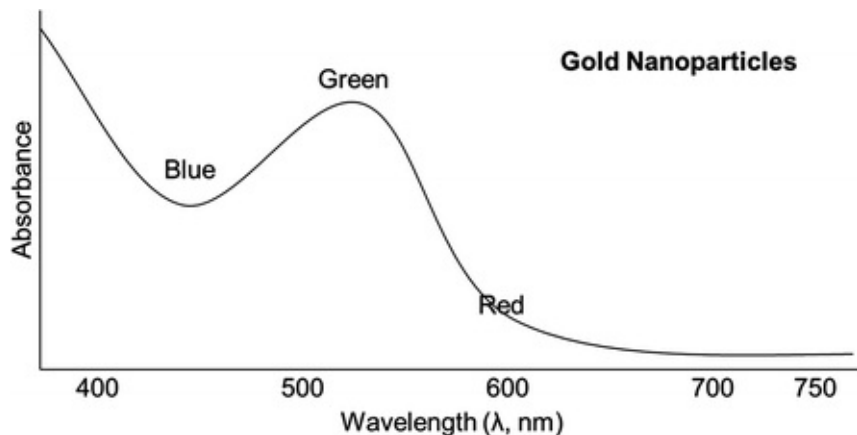


Fig. 13.9 Absorption spectrum of gold nanoparticles (AuNPs), indicating strong absorption in green, moderate absorption in blue, and almost no absorption in red. With white light, it will reflect most of red and some of blue, resulting in a pink coloration

Gold nanoparticles (AuNPs; will be further discussed in Chap. 15) absorb green light and some blue light, so it looks pink (Fig. 13.9). Therefore, two pink bands indicate the presence of target, one band the non-presence of target, and no band the failure of assay (mostly because of not enough sample volume to achieve capillary action).

LFA is an easy-to-use and inexpensive immunosensor, although there is an issue of reproducibility, as well as inferior sensitivity over ELISA (high

detection limit ; *detection limit* is the lowest concentration that can be detected with statistical significance). LFA itself does not provide quantitative readouts, but can be complemented using an optical reader similar to the microplate reader. Recently, the use of a smartphone camera is suggested to obtain quantitative readouts from LFAs.

13.5 Optical Immunosensors

The use of a microplate reader for ELISA is, in a way, a form of *optical immunosensor*. There have been numerous efforts in minimizing the labor required for ELISA, converting the ELISA kit into a user-friendly optical immunosensor. If only a single assay is required, the microplate can be replaced with a single test tube and the microplate reader with a pair of LED and PD (refer to Chap. 8 Laboratory Task 2).

The test tube may be further replaced with an optical fiber probe, where the antibodies are immobilized onto the surface of the exposed optical fiber core, again with some passivating proteins. The probe is then dipped into the target solution, followed by dipping and stirring in the rinsing solution (typically a buffer solution with some detergent). The probe is then dipped into a solution of secondary antibody/antibody-to-antibody conjugate, the latter of which is labeled with a fluorescent dye (Fig. 13.10).

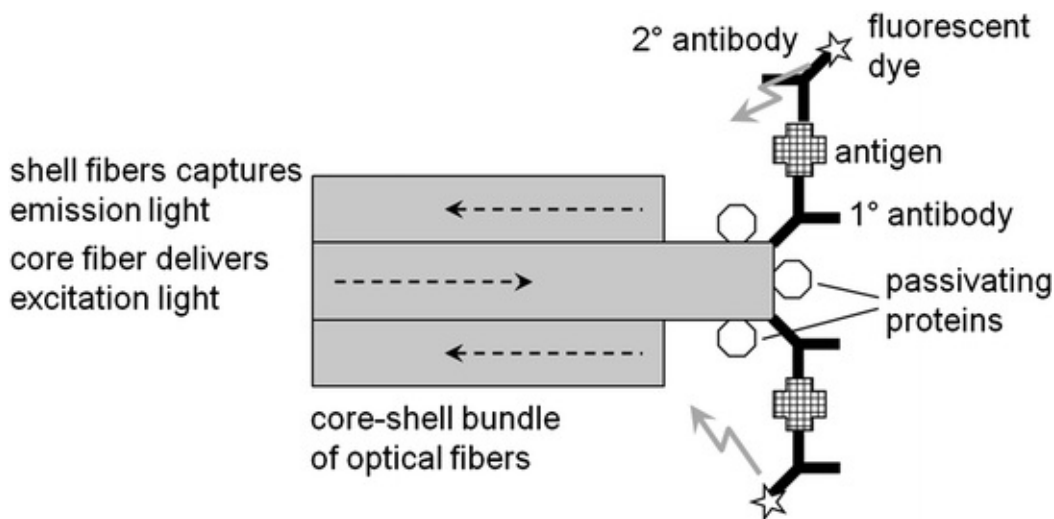


Fig. 13.10 Optical immunosensor using an optical fiber probe. Note that the antibody-to-antibody is omitted here for clarification purpose

The test tube can also be replaced with a microchannel, where the target solution continuously flows through the microchannel (flow injection analysis).

The antibodies are immobilized onto the inner surface, at a specific location, of a microchannel. The continuous flow characteristics make the rinsing very effective. In fact, neither suction-dispensing cycle nor stirring is required, as the flow should remove any excess molecules from the inner surface of a microchannel. Light is irradiated to the location where the antibodies are immobilized; while the light sensor reads the signal from the other side of a microchannel (Fig. 13.11). This schematic is popular in lab-on-a-chip applications, which will be discussed in Chap. 14.

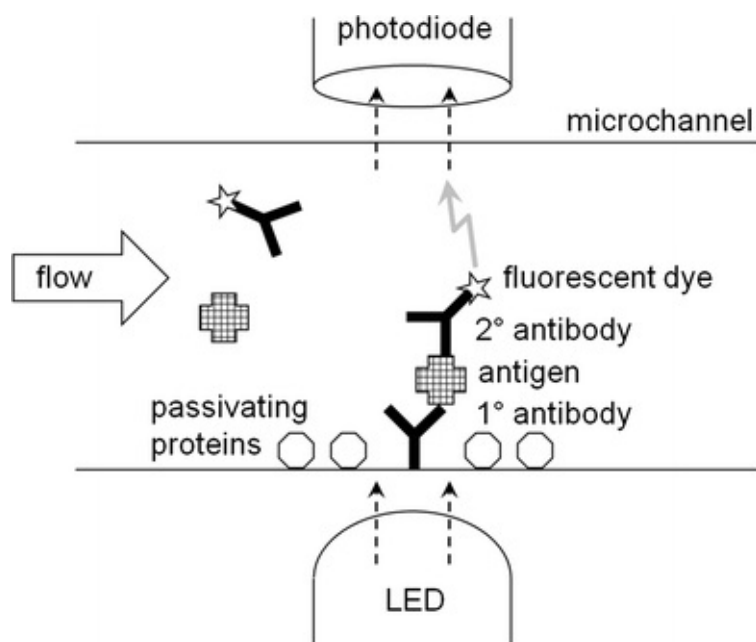


Fig. 13.11 Optical immunosensor using a microchannel

13.6 Surface Plasmon Resonance (SPR) Immunosensor

The above approach is still cumbersome as it requires secondary antibody and subsequently multiple rinsing steps. There is an alternative biosensor that requires neither secondary antibody nor fluorescent dye, called surface plasmon resonance (SPR) immunosensor .

SPR immunosensor is largely based on total internal reflection (TIR) that we have learned in Chap. 8. As shown in Figs. 13.12 and 13.13, light hits the metal–liquid interface, and it exhibits TIR due to the difference in refractive indices of metal and liquid. Light beams are irradiated at a range of incident angles and so are the reflected light beams. In SPR, there are two important modifications: (1) the incident light is polarized and (2) the surface is a thin metal film coating, usually gold. Polarization means that the light is oscillating only at a certain

orientation, where normal light oscillates at various orientations. When light hits the gold surface, electrons and holes are created (just like photoresistor, photodiode, or phototransistor). Because the incoming photons are oscillating only at one orientation, the generation of electrons/holes (electric charges) will also be oscillated in one direction. This charge oscillation can propagate parallel to the gold film, called *evanescent wave*. Also this propagation is short-lived, thus it does affect the reflected light. For a certain angle of incident light, the incident light can be matched to this evanescent wave (resonated). If this resonance happens, the light intensity of reflected light at that angle will be greatly reduced (Fig. 13.12).

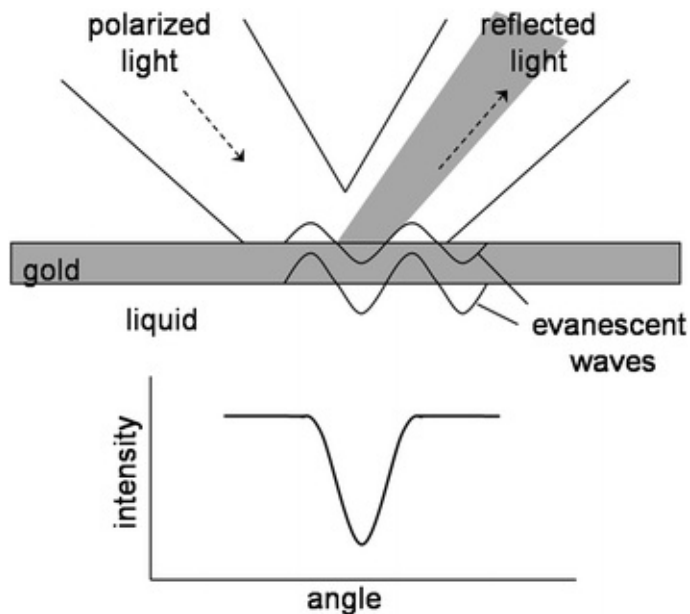


Fig. 13.12 Surface plasmon resonance (SPR)

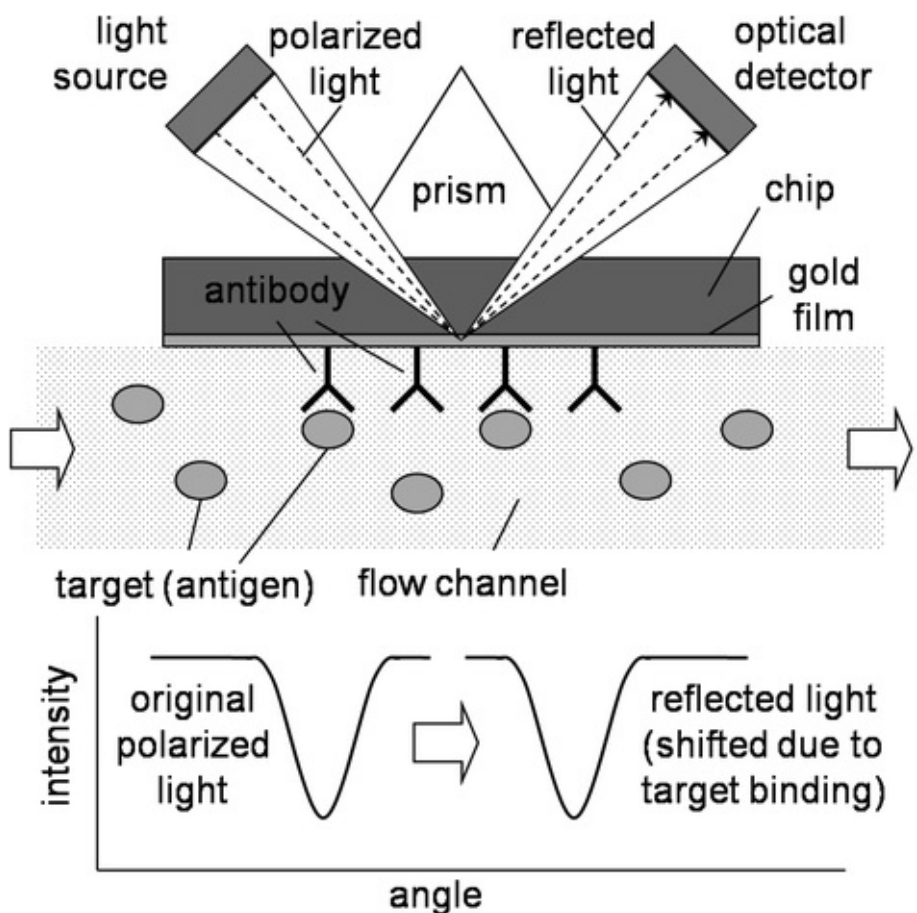


Fig. 13.13 SPR immunosensor

The surface evanescent wave is a function of refractive indices of gold and liquid. If some molecules adsorb to the surface of gold film, the overall refractive index of liquid near the gold film changes, as well as the resonance angle (Fig. 13.13). In a typical SPR apparatus, this change of resonance angle (with reference to a bare surface) is shown as its sensor signal. This sensor signal is roughly equivalent to the mass of the adsorbed molecules. However, exact determination of the adsorbed mass is difficult in SPR sensors, as the refractive indices and other optical properties are quite different from molecule to molecule.

In an SPR immunosensor, the gold surface is pre-immobilized with antibodies, and the SPR signal with these antibodies will serve as a baseline. The sensor chip is exposed to a flow channel to facilitate the introduction of target/reagent solutions and subsequent rinsing. The first commercial SPR-based biosensor was marketed by Biocore AB Corporation based in Sweden; and commonly used in many applications. Recently there have been many attempts to further miniaturize the entire system, especially miniaturizing the flow

channel into a microchannel, thus lab-on-a-chip platform (refer to Chap. 14).

13.7 Electrochemical Immunosensors

As shown in Fig. 13.1, the enzyme-substrate binding typically involves oxidation reaction. This opens up an opportunity to detect ELISA in an electrochemical way (*electrochemical immunosensor*), as shown in Fig. 13.14. This oxidation itself, however, generates too small amount of electrical charges (electrons and holes). Therefore, we need a *mediator*, which can be repeatedly oxidized and reduced under an applied voltage. With the help of a mediator and an applied voltage, the oxidation and reduction reactions can make cycles, which will generate measurable change in electric current (thus *amperometric* detection). This concept is identical to the electrochemical glucose sensing that we have learned in Chap. 12.

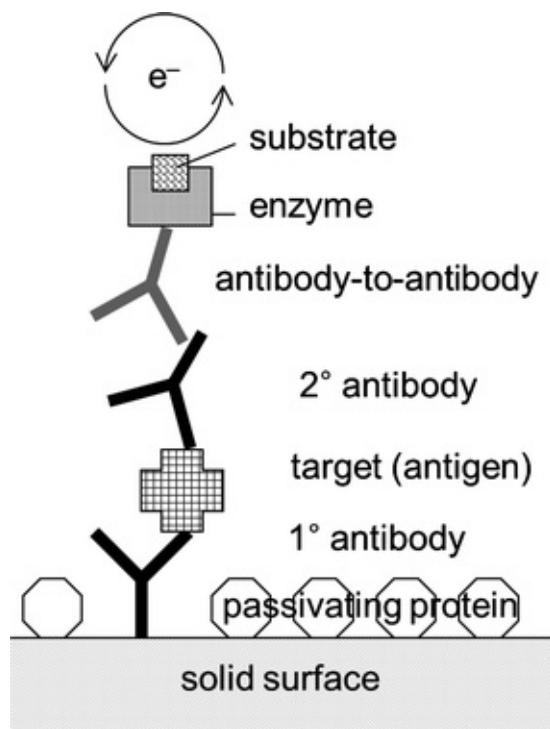


Fig. 13.14 Electrochemical ELISA (identical to the portion of Fig. 1.11)

The most common substrate/mediator pair used for ELISA and other types of electrochemical immunosensors is horseradish peroxidase (HRP) and tetramethylbenzidine (TMB). The substrate for HRP is hydrogen peroxide (H_2O_2) (Fig. 13.15).

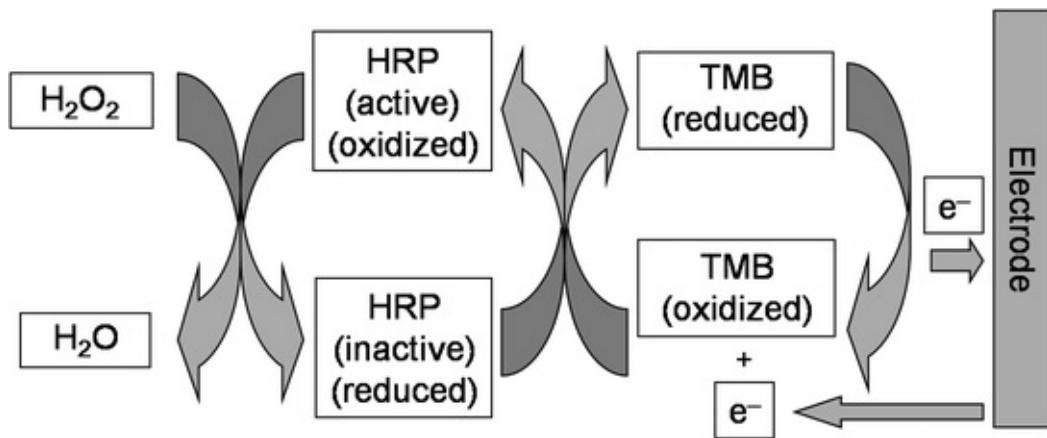


Fig. 13.15 Typical electrochemical detection in ELISA. HRP = horseradish peroxidase; TMB = tetramethylbenzidine

Like electrochemical glucose sensors, typical electrochemical immunosensors involve the use of test strips, shown in Fig. 13.16. The sensor surface is pre-coated with appropriate antibodies (with passivating proteins), and a series of solutions (target, secondary antibody, antibody-to-antibody-enzyme conjugate, and mediator/substrate) are added drop-by-drop onto the sensor surface with appropriate rinsing steps.

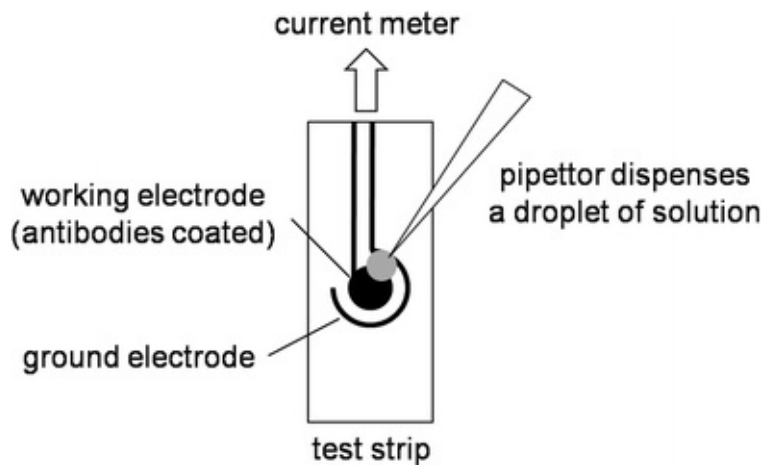


Fig. 13.16 A test strip for a typical electrochemical immunosensor

There have been attempts to embed an array of electrodes to a 96-well ELISA plate. This electrochemical ELISA plate is placed onto an electrochemical microplate reader, which is essentially a current meter that measures current changes from 96 wells simultaneously.

Question 13.1

Electrochemical immunosensors can also be implemented into a microchannel, just like the optical immunosensor. Design the electrode layout around the microchannel, using Figs. 13.1 and 13.11 as the starting point.

13.8 Impedance Immunosensors: Interdigitated Microelectrode (IME) Immunosensor

The SPR immunosensor is a label-free simpler version of optical immunosensors. It does not require secondary antibody, enzyme-substrate pair, or fluorescent dye. There is a similar version for electrochemical immunosensors, called *impedance immunosensors*.

Figure 13.17 shows a schematic of a typical impedance immunosensor. Antibodies are immobilized on a surface where two electrodes are patterned in a configuration called *interdigitated array*. When a big target like bacterium binds to the surface-bound antibodies, some of the target may be able to bridge the two electrodes, thus lowering the resistance. If electrode patterns are made very small (micro or even nanoelectrode), smaller targets such as viruses and proteins may be detectable.

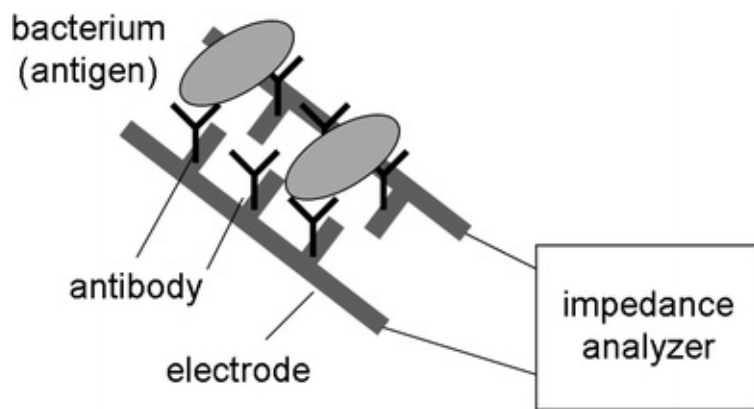


Fig. 13.17 An impedance-based immunosensor

To maintain the antibody-antigen binding and to prevent any possible oxidation/reduction, it is beneficial to apply alternating current (AC) rather than direct current (DC). We need to use an expanded version of resistance with AC power, called *impedance*. Impedance is described as a complex number (refer to Chap. 11):

$$Z(\text{impedance}) = R(\text{resistance}) + jX(\text{reactance}) \quad (13.1)$$

The magnitude of voltage oscillates at a certain frequency with AC power,

and so is the current. The current-to-voltage ratio gives the impedance, where the real part R (resistance) is related to the magnitude of oscillation while the imaginary part X (reactance) is related to the phase shift of oscillation. With DC power, there is no such oscillation and thus no phase shift, resulting in $X = 0$ and $Z = R$.

The interdigitated microelectrode (IME) can be also made as a test strip, similar to what is shown in Fig. 13.16. Significant steps of reagent additions and subsequent rinsing can be eliminated, thus making this assay a lot simpler and easier to use than any other electrochemical immunosensors. The only disadvantage of IME immunosensor is its complexity in microelectrode fabrication and subsequent cost associated with it. *IME immunosensors* have been successfully demonstrated for detecting pathogens in many different sample matrices, including *E. coli*, *Salmonella*, and avian influenza viruses.

Question 13.2

Again, the IME immunosensor can be implemented into a microchannel, as the optical immunosensor. Design the electrode layout around the microchannel, using Figs. 13.11 and 13.14 as the starting point. What is the benefit for incorporating the IME immunosensor in a microchannel rather than in a test strip?

13.9 Piezoelectric Immunosensors: QCM Immunosensor

Piezoelectric transducers can also be used for immunosensor applications, thus *piezoelectric immunosensors*. The quartz crystal microbalance (QCM) shown in Fig. 13.18 is the most popular type of piezoelectric transducer commonly used for immunosensing. (Refer to Chap. 11 for details).

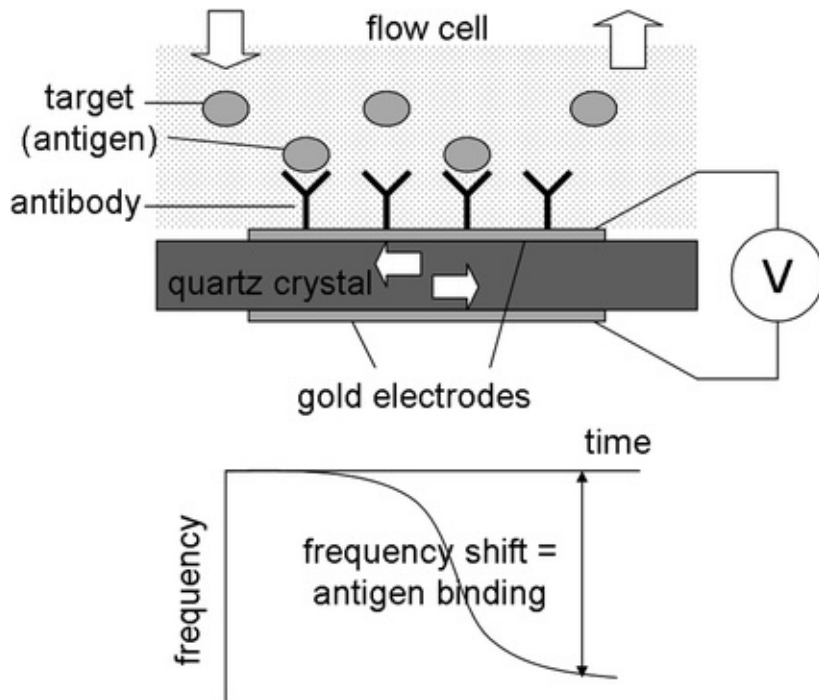


Fig. 13.18 A QCM immunosensor

Like SPR and IME immunosensors, *QCM immunosensor* is a label-free biosensor, i.e., it does not require secondary antibody, enzyme-substrate pair, or fluorescent dye. In addition, QCM immunosensor has the following advantages over SPR and IME immunosensors: (1) smaller and cheaper instrument than SPR immunosensor, potentially comparable to IME immunosensor; (2) simpler fabrication of sensor strips (QCM crystals) than the SPR and IME immunosensors.

Disadvantages of QCM immunosensor include: (1) the need for long incubation times with samples, typically in tens of minutes or more; (2) constant drifting of frequency (f) signal due to the energy accumulation of crystal oscillations (may be avoided by using QCM-D; refer to Sect. 11.5).

13.10 Immunosensing Kits Versus Handheld Immunosensors

All immunosensors described in this chapter require manual liquid handling, including reagent dispensing and subsequent rinsing using a pipettor. Several label-free immunosensors, SPR, IME, and QCM immunosensors, do reduce the amount of such labor, but they still require at least one step for each of reagent dispensing and subsequent rinsing. Many commercial immunosensors, therefore,

are offered as kits, which include several bottles of reagents (some of them need to be refrigerated), disposable sensor strips or a microplate, and a transducer (a microplate reader, an SPR instrument, an impedance analyzer, or a QCM instrument). A pipette is not included in these kits but it is required. Due to the size and AC power requirement of these transducers, and the requirement of sample refrigeration, these assays must be conducted in a wet laboratory.

Nowadays, there have been attempts to convert this immunosensor kit into a handheld immunosensor device. The transducer is made as small as possible, preferably with battery power. It is also equipped with its own microprocessor (for signal processing) and a small liquid crystal display (LCD) panel, with a small user interface (cursor keys and a couple of menu buttons). Reagents that require refrigeration, especially antibodies, are freeze-dried (or vacuum-dried) as powder, so that they can be stored at room temperature at least for a short term. The handheld device usually involves a microchannel to facilitate rinsing without necessarily using a pipette to rinse the surface.

There are other attempts to further automate the assays by incorporating more complicated shapes of microchannels, which enables facilitated mixing, separation, prolonged incubation, heating, etc. This area is called lab-on-a-chip, which will be discussed in Chap. 14.

13.11 Laboratory Task 1: Insulin ELISA Kit

In this task, you will need the following:

- Insulin ELISA kit (IS130D from Calbiotech Inc.)
- Deionized or distilled water
- Pipettes and pipet tips
- A microplate reader (or ELISA reader)
- A vortex mixer or a microplate shaker (optional)
- Absorbent paper towel

The insulin ELISA kit includes the following:

- A microplate, whose wells are coated with mAb to insulin
- Insulin standards
- Insulin enzyme conjugate
- Assay diluent
- TMB substrate

- Stop solution
- Wash solution concentrate

Specimen Collection

- The kit is originally intended for human serum, but we will test the kit using one of the insulin standard solutions. Obtain one of the insulin standard solutions created by the other team, without being informed of its concentration. This is your specimen.

Reagent Preparation

- Insulin enzyme conjugates come as a 20X concentrate. Use the assay diluent to dilute it to 1X, or in other words, 0.1 mL of the stock conjugate in 1.9 mL of assay diluent, which is sufficient for 20 wells.
- The wash solution also comes as 20X concentrate. Add 25 mL of wash stock to 475 mL of distilled and/or deionized water to make it 1X.
- There are six insulin standards in the kit, 0, 6.25, 12.5, 25, 50, and 100 μ IU/mL. IU stands for international unit, an amount of substance based on biological activity of effect. The actual mass varies with substances. For insulin, 1 IU is equivalent to 45.5 μ g. Therefore, the above concentrations correspond to 0, 0.28, 0.57, 1.1, 2.3, and 4.6 ng/mL.

Assay Procedure

- Pipette 25 μ L of six insulin standards into appropriate wells.
- Pipette 25 μ L of three identical urine samples into appropriate wells.
- Add 100 μ L of 1X (i.e., diluted) insulin enzyme conjugate to all wells that contain standards and samples.
- Mix the solutions. You can place a sticker or a lid on top of the microplate to prevent leakage during mixing. You can then mix it manually with your pipette tip, or place the entire microplate onto a vortex mixer (for vigorous mixing) or microplate shaker (for gentle mixing).
- Incubate for 60 min at room temperature (18–26 °C).
- Remove liquids from all wells. Wash wells thrice with 300 μ L of 1X (diluted) wash solution (Fig. 13.19). After the final wash, use an absorbent paper towel to remove all liquids from the wells.
- Add 100 μ L of TMB substrate to all wells that contain standards and specimens.
- Incubate for 15 min at room temperature.
- Add 50 μ L of stop solution to all wells that contain standards and specimens.

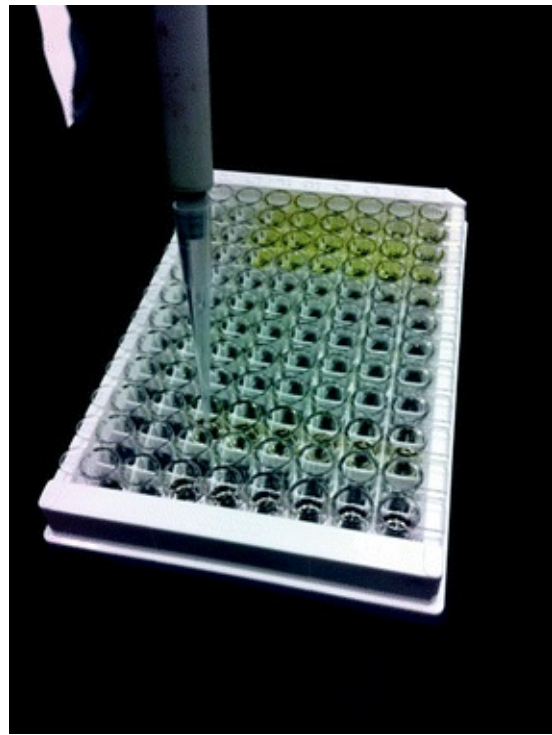


Fig. 13.19 Washing a well with a pipette

Visual Identification

- Visually identify the color intensity. Determine the standard that most closely matches the color intensity of your specimen. For example, if your specimen color is somewhere between 25 and 50 $\mu\text{IU}/\text{mL}$, your specimen's insulin concentration is estimated to be 37.5 $\mu\text{IU}/\text{mL}$.
- Repeat this for all three specimens. Calculate the average and standard deviation.

Microplate Reader

- Read absorbance on a microplate reader at 450 nm within 15 min after adding the stop solution.
- Construct a standard curve from six insulin standards and perform a linear regression (Fig. 13.20).
- Using this equation, determine the insulin concentrations of your three specimens. Calculate the average and standard deviation.

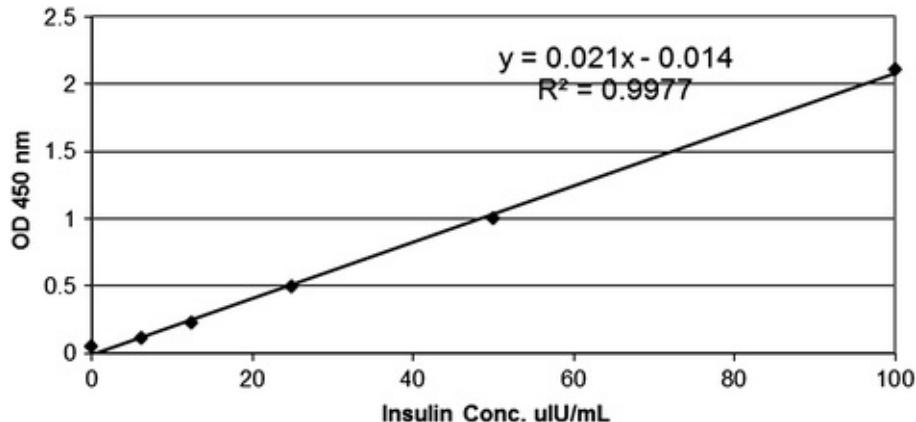


Fig. 13.20 An example of a standard curve from a microplate reader

Question 13.3

Why do you have to construct a standard curve each time you make measurements?

13.12 Laboratory Task 2: Insulin ELISA Kit with Smartphone Camera

Today's *smartphones*, are mostly equipped with a high-resolution digital camera, a very bright white LED flash, and an operating system (either iOS or Android). Recently, there have been various attempts at using this smartphone as all-in-one optical sensing platform, utilizing the flash as a light source, the camera as an optical detector, with the appropriate software (*application* or *app*, loaded in a smartphone) for data storage and processing.

How Digital Camera Stores Images

The resolution of a digital camera is typically represented by megapixels (MP), such as 5, 8, 10 MP, etc. For an 8 MP camera, the resulting size of a digital image is 3266×2450 pixels, which are roughly 8 million pixels. Each pixel is typically stored in 24-bit resolution. This 24-bit is further divided into three 8-bit groups, each corresponding to red (R), green (G), and blue (B) colors. Ideally, it would be great to store an entire visible spectrum (from 400 to 750 nm) per each pixel. However, the human eyes have only three types of *cone cells* that recognize only three different colors: red, green, and blue (*RGB* ; called *trichromatic vision*), hence dividing into three basic colors is sufficient rather than storing an entire spectrum.

From Fig. 13.21, you can probably notice that the green and red spectra are very close to each other. In fact, some humans cannot see the difference between

red and green colors: they see both red and green as a single color. This particular situation is called *color weakness* or *dichromatism*. Bear in mind that most vertebrate animals (e.g., dogs) have *dichromatic vision*. Scientists believe that humans have evolved from dichromatic vision to trichromatic vision, where red-green color differentiation is not substantial compared to green-blue color differentiation.

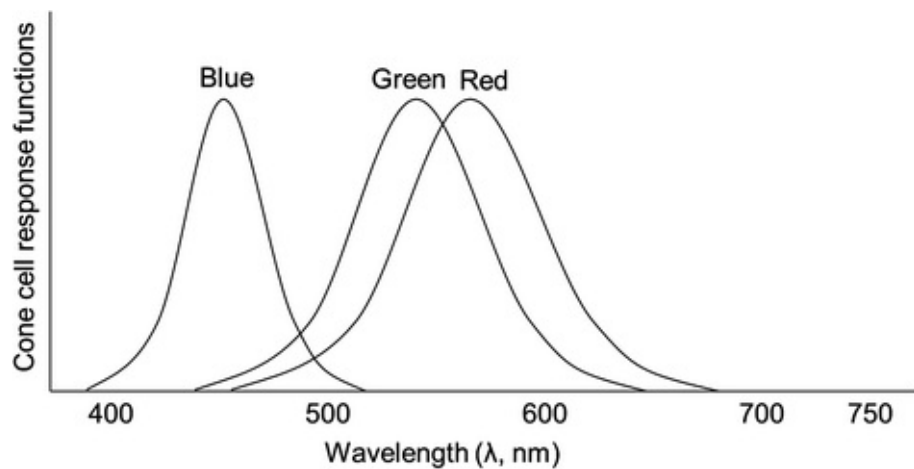


Fig. 13.21 Response functions curves for human cone cells

Simply take a photograph of the microplate using your smartphone, preferably with white background. Figure 13.22 shows the actual image. Using an appropriate software, preferably with ImageJ (free software available from U.S. National Institutes of Health, <http://rsbweb.nih.gov/ij/>) or Adobe Photoshop (commercial software), take 10 pixels from each well and record the RGB color codes. Note that 8-bit resolution enables the color code to change from 0 to 255 ($2^8 = 256$). The average color codes are shown in Fig. 13.23. You can notice that both red and green color intensities are relatively constant (around 126) and do not change over insulin concentration. However, blue color intensities do decrease as increasing insulin concentration. When red, green and blue intensities are about the same and sufficiently bright, the human eye would perceive it as white color (e.g., column A in Fig. 13.22). If blue intensity is significantly lower than red and green intensities, the human eye would perceive it as in-between color of red and green, which is yellow (e.g. columns E and F in Fig. 13.22). Therefore, we need to evaluate blue color intensities to quantify the yellowness of each microplate well. This corresponds very well with Task 1, where we measured the absorbance at 450 nm, which is blue color. Using only the blue intensities, we can calculate the absorbance.

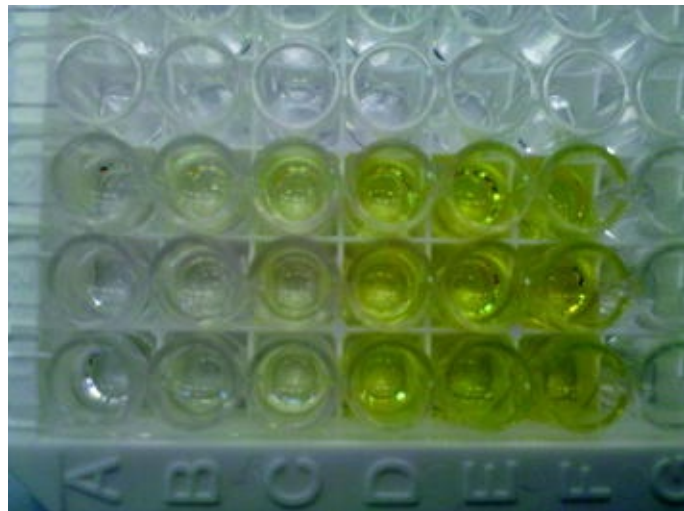


Fig. 13.22 A digital photograph of a microplate from Task 1

Insulin conc. $\mu\text{IU/mL}$	0	6.25	12.5	25	50	100
Red intensity	123	126	128	127	125	116
Green intensity	123	129	132	132	128	120
Blue intensity (I)	127	111	107	75	39	7
$A = \log(I_0 / I)$ [blue]	0	0.0585	0.0744	0.2287	0.5123	1.2587

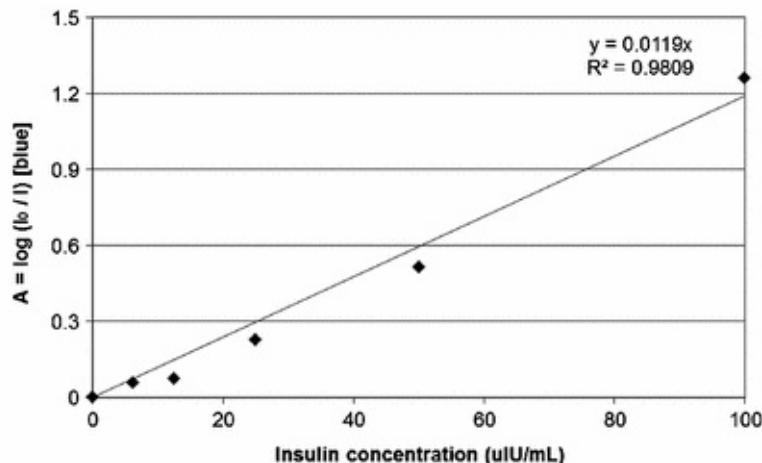


Fig. 13.23 Experimental data of Task 2: standard curve using a smartphone camera. The blue intensity with $0 \mu\text{IU/mL}$ insulin solution was used as I_0

The slopes of two different standard curves are: 0.021 (microplate reader) > 0.012 (cell phone camera).

Question 13.4

If the smartphone camera processes each pixel at 36-bit (12-bit each for three basic colors), can the slope of standard curve with a cell phone camera be

increased (i.e., becomes more sensitive)? Repeat this question if the cell phone camera processes each pixel at 24-bit grayscale.

13.13 Laboratory Task 3: Pregnancy Test (LFA) with Smartphone Camera

By far the most commercially successful LFA is the pregnancy test. These tests detect hCG, a glycoprotein hormone produced in high concentration almost exclusively during pregnancy. Thus, while a female who is not pregnant will have an hCG concentration of <5 mIU/mL in her urine, a female who is pregnant may have early concentrations as high as 500–8000 mIU/mL, and later-term concentrations above 50,000–100,000 mIU/mL. Much of this appears in the urine, which allows for simple and noninvasive pregnancy testing. The extremely high hCG concentration from the pregnant female's urine enabled the popularity and commercial success of pregnancy test. Other LFA's have followed, although most of them have not yet been successful compared to the pregnancy test.

While pregnancy tests are typically analyzed in a positive-or-negative ("yes-or-no") manner, it is actually possible to quantify the concentration of hCG in a sample based on the relative darkness of the positive "test band." In this task, we will be using pregnancy tests to examine three known concentrations of hCG suspended in water. Using a smartphone camera, we will take pictures of the bands and then quantify the concentrations based on the relative pixel intensities in these images. Similarly, we will complete one additional test with an unknown sample and determine its approximate hCG concentration based on the standard curve we develop from the three known samples.

In this task, you will need the following:

- Five pregnancy tests (LFA)
- hCG
- Five centrifuge tubes
- Pipettes and pipet tips
- A vortex mixer
- Smartphone

1. Prepare a stock solution of hCG in 2000 mIU/mL. Using this stock solution, prepare three 500 μ L dilutions of hCG in concentrations of 0, 500, and

1000 mIU/mL. These will be used in forming your standard curve. Also prepare an hCG solution of unknown concentration (e.g., other than 500 and 1000 mIU/mL).

2. With one pregnancy test strip for each of the hCG suspensions, dip the end of the pregnancy test strip into each tube for approximately 3 s. Remove from the tube and set test down horizontally. Streaking may occasionally occur, particularly during the initial flow of the LFA, but your test results should still be valid.
3. Wait for 5–15 min for the band coloring to fully develop. Place the strips directly next to each other on the benchtop.
4. Using a smartphone, take a picture of the band colors from about 4–6 inches above the benchtop.
5. Ensure that your images adequately show the test and control bands for each strip. Flash is not necessary, but you may use it if you choose to (Fig. 13.24).

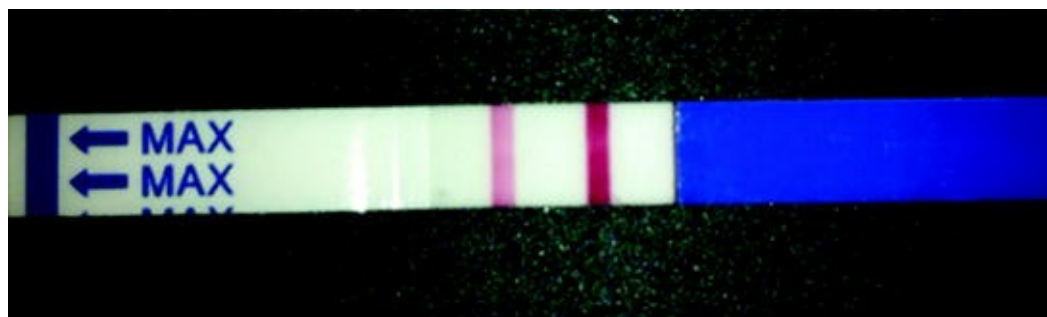


Fig. 13.24 Sample pregnancy test image

6. Load your image into an appropriate software (e.g., ImageJ). Move your mouse over the test line of one of the pregnancy test strips. For 5 separate

points within the test line, record the blue pixel value. Pixel values are listed directly beneath the toolbar as R, G, B. Average these 5 values for each line. This will serve as your blue pixel intensity for each strip (Fig. 13.25).

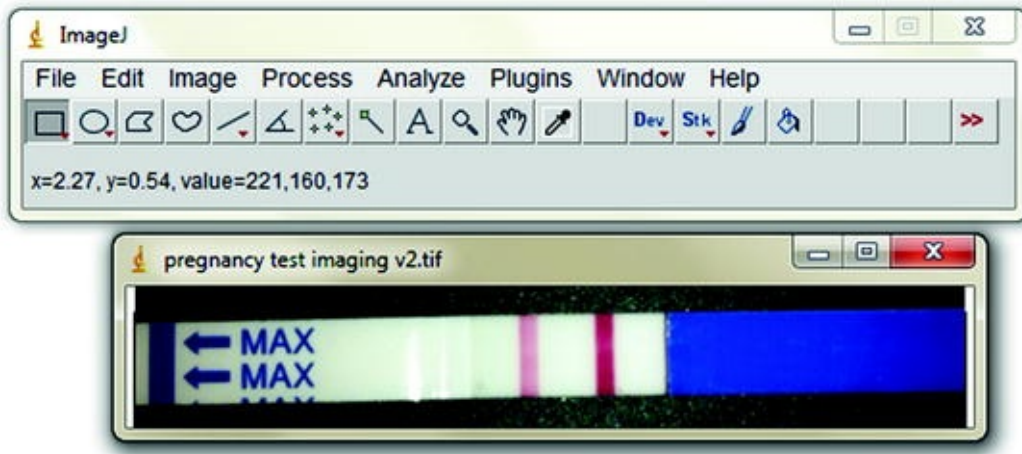


Fig. 13.25 Analyzing the test band pixel intensity within ImageJ

7. With these blue intensity values, determine the red, green, and blue absorbance for each of the hCG concentrations.
8. Plot the red, green, and blue absorbance versus hCG concentration for the three known standard solutions, as well as for the unknown hCG solution. Determine the approximate hCG concentration of this unknown solution (Fig. 13.26).

hCG conc. mIU/mL	0	500	1000
Red intensity	183.4	181.5	172.9
$A = \log(I_0 / I)$ [red]	0	0.00452	0.0256
Green intensity	186.7	174.1	154.5
$A = \log(I_0 / I)$ [green]	0	0.0303	0.0822
Blue intensity (I)	181.3	175.6	163.4
$A = \log(I_0 / I)$ [blue]	0	0.0139	0.0451

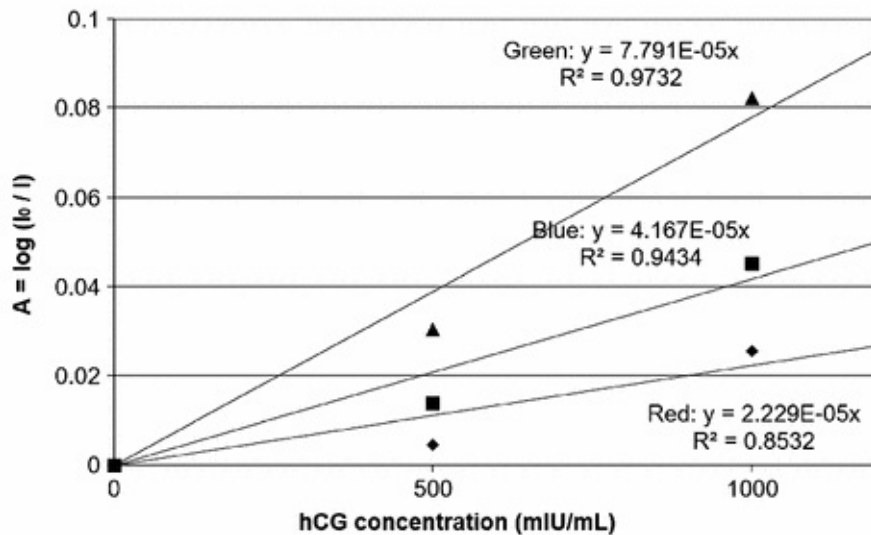


Fig. 13.26 Experimental data of Task 3: standard curve using a smartphone camera. The red, green, and blue intensities with 0 mIU/mL hCG solution was used as I_0

Question 13.5

Compare the standard curves with red, green, and blue pixel intensities. Which color shows the best result, and why? (Hint: use the absorption spectrum of gold nanoparticles—Fig. 13.9).

13.14 Further Study: DNA Sensors

Although antibodies are the most popular bioreceptors in biosensor applications, other types of bioreceptors can be used as well. Nucleic acids, such as DNAs and RNAs are also very popular in biosensor applications. These types of biosensors are typically called *DNA sensors*.

As shown in Fig. 13.27, a relatively short chain of single-stranded DNA (ssDNA) is used in place of a primary antibody. This ssDNA is called *capture probe*, which is complementary to the specific sequence of a desired (target)

DNA. The capture probe is typically conjugated with biotin. The sensor surface is pre-immobilized with either *streptavidin* or its one-quarter version, *neutravidin*. Due to the strong binding of biotin-avidin, the capture probe makes the target DNA firmly bound on the surface.

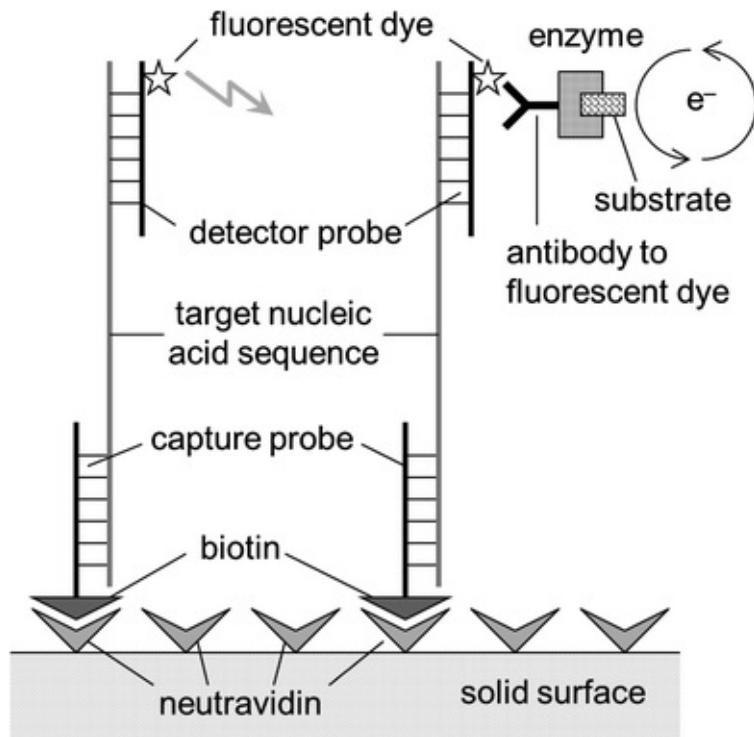


Fig. 13.27 DNA sensors. Identical to Fig. 1.14

To confirm this binding, a secondary ssDNA is needed, which is complementary to the specific sequence of the target DNA (but a different region). This ssDNA is called *detector probe*, and is analogous to the secondary antibody in immunosensors. The detector probe can be conjugated with a fluorescent dye, where any optical detection can confirm the presence of target DNA in a sample. Additionally, antibody to a fluorescent dye that is conjugated to an enzyme (for example, HRP) can be additionally added, where its presence can be detected in an electrochemical way.

Note that it is quite difficult to conjugate proteins such as antibodies and enzymes directly to detector probes. Short ssDNA probes are quite small and significantly smaller than those proteins, and their mobility and binding ability to the target DNA would be greatly affected if they are conjugated with such proteins. These ssDNA probes are almost always conjugated with small chemical compounds, mostly with *biotin* (it is essentially vitamin B₇) and/or

fluorescein.

Question 13.6

Will it be possible to make label-free DNA sensors, using (a) SPR, (b) IME, and (c) QCM transducers? Will the transducer instrumentation and sensor strips remain the same as those of SPR, IME, or QCM immunosensors?

References and Further Readings

- Blake DA, Blake II RC, Abboud ER, Li X, Yu H, Kriegel AM, Khosraviani M, Darwish IA (2007) Antibodies to heavy metals: isolation, characterization, and incorporation into microplate-based assays. In: Van Emon JM (ed) Immunoassay and other bioanalytical techniques (chapter 4). CRC Press, Boca Raton
- Cooper J, Cass T (2004) Biosensors, 2nd edn. Oxford University Press, New York
- Henaresa T, Mizutania F (2008) Current development in microfluidic immunosensing chip. *Anal Chim Acta* 611:17–30
[CrossRef]
- Lucas LJ, Chesler JN, Yoon J-Y (2007a) Lab-on-a-chip immunoassay for multiple antibodies using microsphere light scattering and quantum dot emission. *Biosens Bioelectron* 23:675–681
[CrossRef]
- Lucas LJ, Han J-H, Chesler J, Yoon J-Y (2007b) Latex immunoagglutination for a vasculitis marker in a microfluidic device using static light scattering detection. *Biosens Bioelectron* 22:2216–2222
[CrossRef]
- Morgan C, Newman D (1996) Immunosensors: technology and opportunities in laboratory medicine. *Clin Chem* 42:193–209
- Pemberton R, Hart J (2009) Preparation of screen-printed electrochemical immunosensors for estradiol, and their application in biological fluids. In: Rasooly A, Herold KE (eds) *Biosensors and Biodetection*, 1st edn. Humana Press, Clifton
- Prodromidis M (2010) Impedimetric immunosensors—a review. *Electrochim Acta* 55:4227–4233
[CrossRef]
- Tokarskyya O, Marshall D (2008) Immunosensors for rapid detection of *Escherichia coli* O157:H7—perspectives for use in the meat processing industry. *Food Microbiol* 25:1–12
[CrossRef]
- Tombelli S, Minunni M, Mascini M (2007) Aptamer-based bioanalytical methods. In: Van Emon JM (ed) *Immunoassay and other bioanalytical techniques* (chapter 6). CRC Press, Boca Raton
- Varki A, Cummings RD, Esko JD, Freeze HH, Stanley P, Bertozzi CR, Hart GW, Etzler ME (eds) (2008) *Essentials of glycobiology*, 2nd edn. Cold Spring Harbor Laboratory Press, Plainview
- Wang R, Wang Y, Lassiter K, Li Y, Hargis B, Tung S, Berghman L, Bottje W (2009) Interdigitated array microelectrode based impedance immunosensor for detection of avian influenza virus H5N1. *Talanta*

79:159–164

[CrossRef]

Yang L, Li Y, Griffis CL, Johnson MG (2004) Interdigitated microelectrode (IME) impedance sensor for the detection of viable *Salmonella typhimurium*. Biosens Bioelectron 19:1139–1147

[CrossRef]

14. Lab-on-a-Chip Biosensors

Jeong-Yeol Yoon¹✉

(1) University of Arizona, Tucson, AZ, USA

✉ Jeong-Yeol Yoon
Email: jyyoon@email.arizona.edu

In the previous chapter, we learned that both optical and electrochemical immunosensors can be implemented in a microchannel to facilitate rinsing steps that are labor-intensive and require a skilled operator. In fact, there have been attempts to provide a higher level of automation and to increase ease of use for immunosensors (and certainly other biosensors as well), through fabricating more complicated microchannels. These attempts have usually been achieved by utilizing a concept known as lab-on-a-chip.

14.1 What Is Lab-on-a-Chip (LOC)?

A lab-on-a-chip (LOC) is a device that integrates several laboratory functions onto a small platform, typically only millimeters or centimeters in size. It is essentially a network of channels and wells that are etched onto silicon or polymer substrates to build miniature laboratories (Fig. 14.1). LOCs normally involve the handling of very small fluid volumes, usually on the μL or nL scale and of very small depth and width of channels, $<1 \text{ mm}$, i.e., in μm scale. Pressure or electrokinetic forces move small volumes of liquid in a finely controlled manner through the channels. This introduces the area of *microfluidics* that deals with the control/manipulation of fluids in μm scale. In this sense, LOCs are sometimes referred to as *microfluidic devices* or *microfluidic chips*.

The LOC enables sample handling, mixing, dilution, electrophoresis and

chromatographic separation, staining, and detection on a single, integrated system. The main advantages of the LOC are ease of use, speed of analysis, low sample and reagent consumption, and high reproducibility due to standardization and automation.

The origins of lab-on-a-chip can be found on the miniaturization efforts of analytical and bioanalytical methods, including liquid chromatography (LC) and capillary electrophoresis (CE). The columns for LC and CE should be made as small as possible to achieve better sensitivity and enhance separation performance. Sometime later, scientists and engineers have tested the use of *microchannels* (fabricated on a silicon wafer) for LC and CE, which could be as small as a few micrometers and thus a lot smaller than the small-diameter capillary columns. These microchannel-based LC and CE systems provided even better sensitivity and separation performance. In addition, multiple samples could be analyzed simultaneously on a single device through copying the microchannel pattern multiple times. The CE-based LOC is further explained in Sect. 14.3.

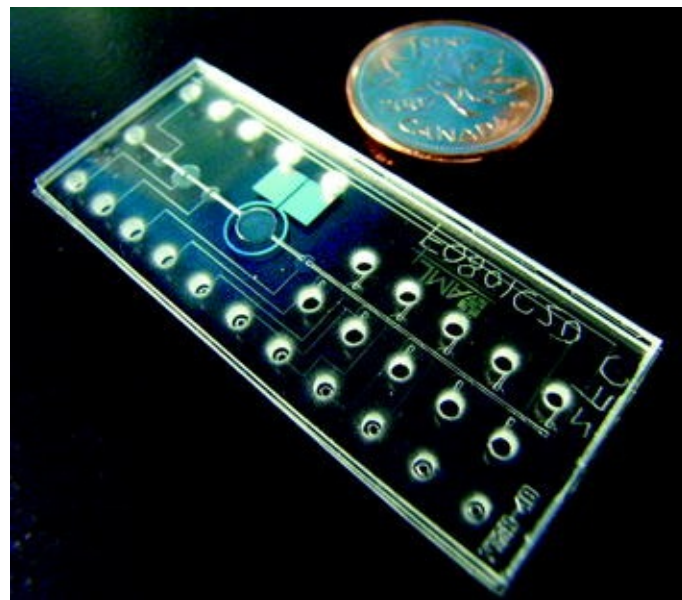


Fig. 14.1 An LOC contains a network of channels and wells. Picture taken by Vjsiebens in March 2009 and placed in public domain. Accessed October 2015 from <http://commons.wikimedia.org/wiki/File:AutoFISH.jpg>

At this time, scientists and engineers have speculated that the microchannels could be used for other types of analytical and bioanalytical methods. “How can we miniaturize all laboratory analytical methods into small microchannel devices?” The microchannels at that time were typically fabricated on a silicon

wafer using *photolithography* technique, which was the same technique used to manufacture semiconductors (i.e., chips). This particular process is also referred to as *microfabrication*. Basically, the laboratory analyses could be miniaturized on a silicon chip, thus the name lab-on-a-chip (LOC).

These microfabrication technologies to fabricate LOCs are a subset of MEMS (micro-electromechanical systems) technologies. Because LOCs are mostly used for biological applications, the microfabrication technologies for LOC fabrication are often referred to as *bioMEMS*. Microfabrication methods are further explained in Sect. 14.2.

In late 1990s and early 2000s, Defense Advanced Research Projects Agency (DARPA) of the United States Department of Defense has started to support a huge research program in this area (called BioFlips). Similar programs have been launched about the same time in the other countries as well. These research funding have made the LOC research extremely popular throughout the world.

Around that time, a new fabrication technology was introduced, called *soft lithography*, where the microchannels were fabricated on a transparent, flexible polymer material, but not on a silicon chip. These days the majority of LOCs are fabricated with polymer materials using soft lithography technique, which are not “chip” any more. However, it should be noted that the soft lithography still requires fabrication of a mold typically made by silicon wafer photolithography. Soft lithography is further explained in Sect. 14.2.

New types of LOCs are currently being designed and fabricated. For example, more complicated and massively parallel LOC systems are currently being developed, that are often capable of handling thousands of different samples or assays. These LOCs are referred to as *high-throughput LOCs*. There are efforts to integrate several different laboratory procedures that are inherently different to each other into a single platform. “Smarter” LOCs are also being developed to perform more complicated analytical procedures, especially integrating the “moving” components in microchannels, such as pumps and valves.

Recently, LOCs are also being tested and used in the areas other than analytical/bioanalytical methods. For example, chemical and biochemical syntheses are currently being attempted in an LOC platform. Mammalian cells are also being cultured in LOCs to provide a tissue-like *in vitro* environment for drug testing/screening.

14.2 How to Make LOCs: Photolithography and Soft

Lithography

The network of channels and wells in an LOC is typically made by either photolithography or soft lithography. Although soft lithography is becoming much more popular than photolithography, it still requires photolithography as a pre-requisite step.

For many years, *photolithography* has been the preferred method of transferring a circuit onto a substrate to make an integrated circuit (IC). The same method can be used to create channels and wells for making an LOC. Photolithography starts with the design of a channel/well network, normally using computer software such as CAD (computer aided design). If the channel/well network is very basic, one may even use simple drawing software, such as PowerPoint™ or Paint™. In either case, the design is printed on a glass or quartz plate. If high resolution is not required, one can simply print on transparency film with a 1200–2400 dpi inkjet or laser printer. (As dpi stands for dots per inch, 2400 dpi corresponds to $1 \text{ in}/2400 = 25.4 \text{ mm}/2400 = 0.01 \text{ mm} = 10 \mu\text{m}$, which is acceptable resolution for the microchannels larger than $100 \mu\text{m}$.) This printout is called a *mask* (Fig. 14.2).

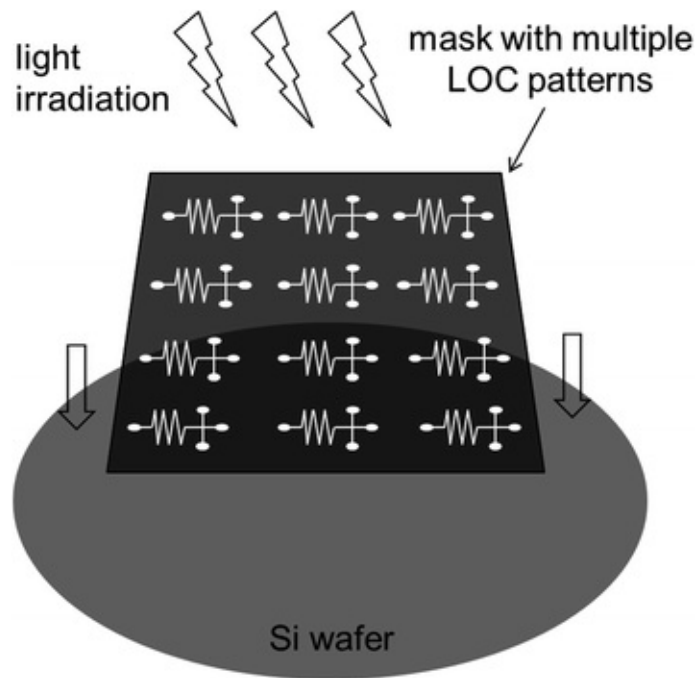


Fig. 14.2 A mask printed on a glass/polymer plate is superimposed on a Si wafer. Multiple LOC patterns are printed on a single mask to fabricate multiple LOCs in a single batch

The mask is then placed on a substrate; typically a *silicon wafer*. The silicon

wafer is pre-coated with an appropriate thin film and photoresist (PR). The mask is placed on this substrate and irradiated with light. Depending on the photoresist material, it can become chemically unstable (*positive resist*) or become hardened (*negative resist*). Figure 14.3 shows the process with a positive resist. In this case, chemical is applied to strip off the portion of PR that became chemically unstable due to light exposure. In the negative resist case, a different chemical is applied to strip off the portion of PR that became not hardened due to light exposure. This procedure (both with positive and negative resists) is called *development*. The portion of thin film that is not protected with the PR is then removed (*etching*). Both *dry etching* (use of plasma or ions) and *wet etching* (use of chemicals) are possible. Removal of the PR results in the final transfer of the mask pattern onto the thin film. The transferred pattern is typically an open trench. Bonding of a cover slide (e.g., glass) makes this open trench into a closed microchannel. Finally, several holes are drilled through the cover slide to create the inlets and outlets to the microchannels.

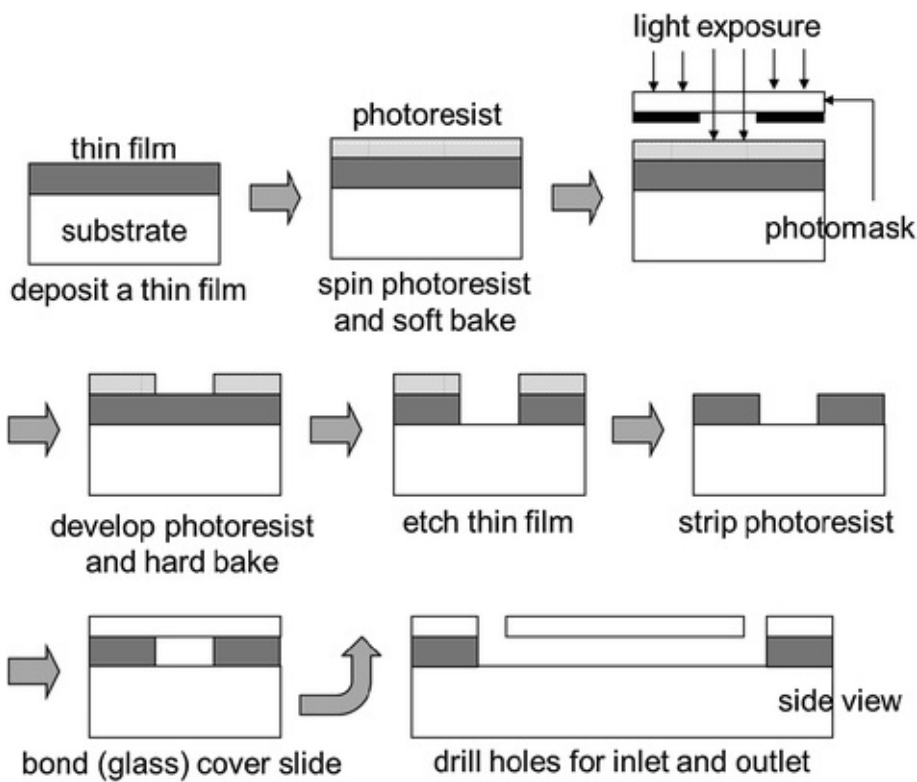


Fig. 14.3 LOC fabrication with photolithography

Earlier days, LOCs were typically fabricated with this photolithographic method. This method normally required a cleanroom environment with expensive equipment, which is the same environment used for semiconductor

manufacturing. To address this issue, a new method was introduced and became very popular in late 1990s and early 2000s, called *soft lithography*. In soft lithography, a *mold* is made with the same photolithography technique. Once a mold is made, polymer gel is poured on and cured via cross-linking. Removal of the mold results in a pattern successfully transferred onto a cross-linked polymer, shown in Fig. 14.4. If the replica is the final product, this method is specifically known as *replica molding* (Fig. 14.5). This process can be repeated multiple times to fabricate multiple LOCs, while it requires neither a cleanroom environment nor expensive equipment. You need to get into the cleanroom only once to make a mold. Low cost and mass production capability are clear advantages of soft lithography over photolithography.

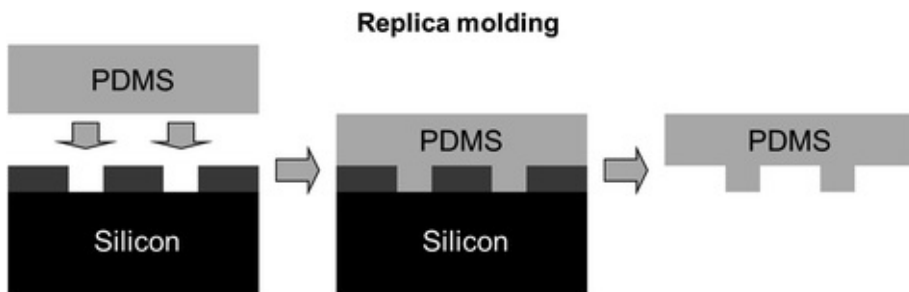


Fig. 14.4 Soft lithography: replica molding



Fig. 14.5 An LOC made out of PDMS replica molding

The most popular material used for soft lithography is polydimethylsiloxane (PDMS). There are added advantages of using PDMS for LOCs. While silicon is optically opaque, PDMS is optically transparent, which facilitates the use of

optical detection in LOCs. While silicon is a rigid material, PDMS is an elastomer, which enables the fabrication of pumps and valves within microchannels.

There are other types of soft lithography techniques based on how the patterns are transferred and whether other chemicals or biomolecules are involved, including microtransfer molding (μ TM) , microinjection molding (μ IM) , and *hot embossing* . Figures 14.6 and 14.7 graphically illustrate how a microstructure can be fabricated by μ TM, μ IM, and hot embossing techniques. Molds are typically fabricated by photolithography. The PDMS replica (Fig. 14.4) can also be used as a mold, if the material property of PDMS is preferred over a silicon wafer or other thin films. Figure 14.6 shows the use of PDMS replica as a mold for μ TM. If the structure does not require high resolution, machine-milled steel or aluminum molds can be used as well.

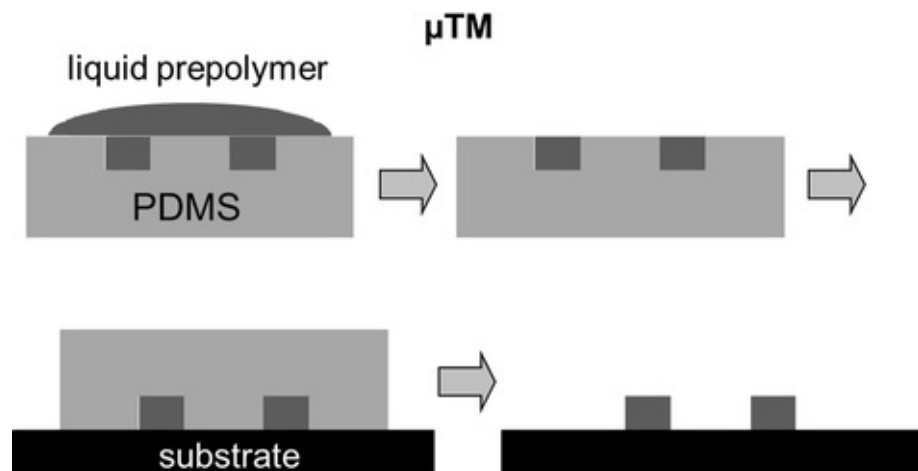


Fig. 14.6 Microtransfer molding (μ TM)

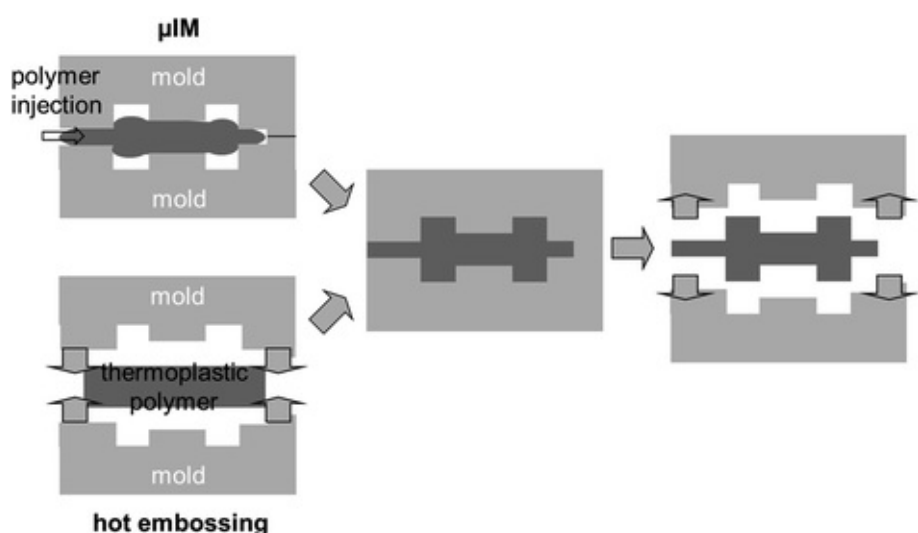


Fig. 14.7 Microinjection molding (μ IM) and hot embossing

Today, much of the exploratory research in LOC is carried out on PDMS chips, the properties of which (soft, optically transparent elastomer) are entirely distinct from those of silicon. It is likely that most LOC devices will ultimately use PDMS or one of the engineered polymers (such as polycarbonate or polyolefin). The ease with which new concepts can be tested in PDMS as well as its ability to support certain components (such as pneumatic valves) have made it the key material for exploratory research and research engineering in the early stages of LOC development.

14.3 Early LOC: Capillary Electrophoresis (CE)

As explained earlier, the origin of LOC lies in miniaturization efforts in liquid chromatography (LC) and capillary electrophoresis (CE), to achieve better sensitivity and enhanced separation performance. Some people believe that the LOC era has begun when the smaller-diameter capillary for LC and CE had been replaced with microchannels. The most studied and successful demonstration at that time was the realization of CE in microchannel format.

Figures 14.8 and 14.9 show the schematics of CE. High voltage (+) is applied to the beginning of a long capillary column and ground (−) to the end of it. The column itself is negatively charged, and an electric double layer (EDL) is formed near at the inner wall of a column. The cations in the first layer are firmly bound to the wall, while those in the second layer are free to move. Because a high voltage is applied along the capillary column, the free cations are pulled towards the anode, and this movement generates the bulk flow of liquid, called electroosmotic flow (EOF). If positively or negatively charged biomolecules (for example, proteins with varying isoelectric points) are introduced into this stream of EOF, they are separated by the differences in their electrophoretic mobility. Positively charged biomolecules are pulled towards the anode faster than those pulled by bulk flow, while negatively charged biomolecules are pulled towards the anode more slowly than those pulled by bulk flow. Thus, a separation of biomolecules is achieved. Detection is typically achieved by using UV/Vis spectrophotometry because many proteins show absorbance in UV and/or visible wavelengths (i.e., without using fluorescent dyes or radioisotopes).

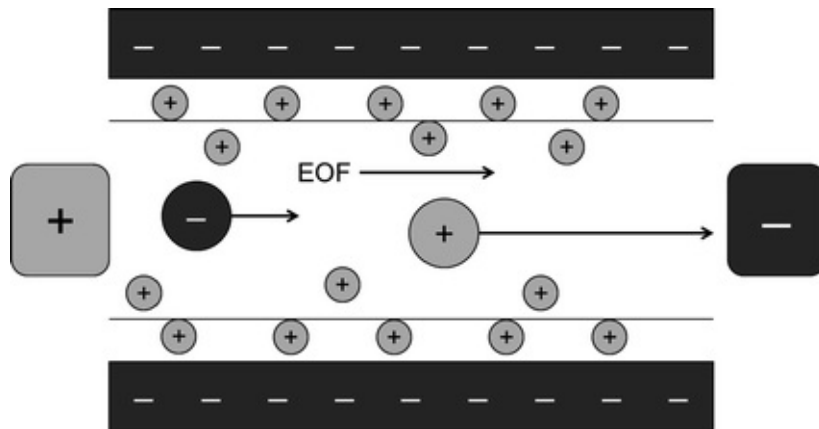


Fig. 14.8 Principle of capillary electrophoresis. Biomolecules flow through a capillary channel under an applied voltage. Depending on their polarity and charge, each biomolecule flows at a different speed

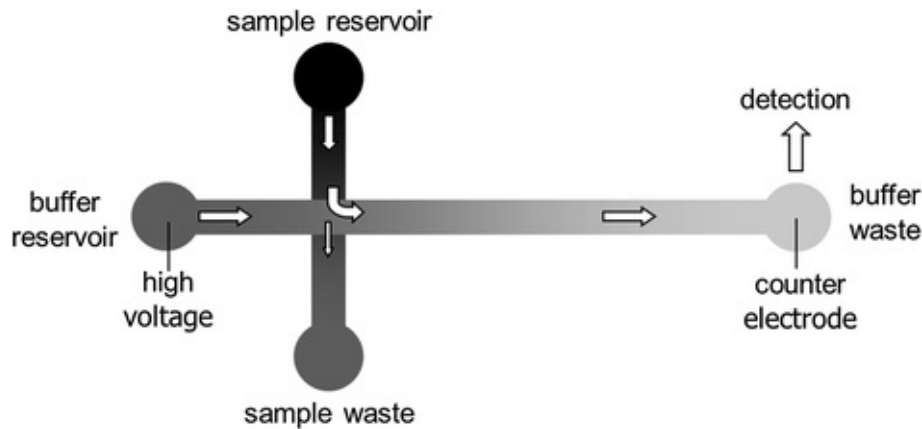


Fig. 14.9 LOC layout for CE

The capillary column can be transformed into microchannels with a couple of wells for applying voltage, introducing sample and making spectrophotometric detection, i.e., in an LOC platform. The typical layout for conducting CE in LOC is shown in Fig. 14.9. This single CE layout can be duplicated, for example, 96 times (12×8), for high-throughput analysis (Fig. 14.10). The entire LOC can be aligned to the microplate reader (refer to Chap. 13), to read the absorbance signals from 96 detection wells.

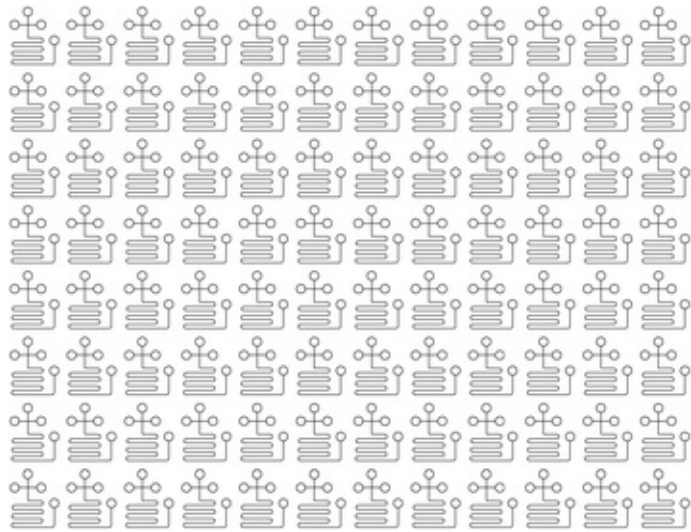


Fig. 14.10 Multiplexed ($12 \times 8 = 96$) CE LOC

14.4 LOCs for Point-of-Care Testing (POCT)

A significant amount of time is often required for clinical diagnostic methods, including immunoassays, from a few hours up to a week. The primary cause of this time lag is not just the assay time, but it is also the distance between the point of subject care and a laboratory facility, as well as the subsequent delivery time. This time lag is often a serious problem, especially when early detection of the disease is important. Thus, the concept of conducting diagnostic experiments at the point of care has emerged. Point-of-care testing (POCT) generates results quickly so that treatment during acute care can be implemented, leading to improved clinical and economic outcomes. POCT can decrease the turnaround time of analysis down to a few minutes. Tests that were sent to an outside lab are now migrating to point-of-care.

The lateral-flow immunochromatographic assay (LFA ; discussed in Chap. 13) has achieved considerable success in the POCT marketplace because the method is rapid and sometimes fairly sensitive. However, the use of LFA is still limited to certain analytes, does not work well with complicated blood or tissue samples, and cannot provide quantitative results. These quantitative immunoassays must still be carried out on microplates (refer to Chap. 13) in laboratories and require skilled personnel. The most appropriate alternative for POCT of quantitative immunoassay with blood or tissue is LOC.

POCT in LOC is generally achieved by incorporating immunosensors into microchannels, as previously described in Chap. 13. Figure 14.11 demonstrates the sandwich immunoassay in a microchannel format, with light source (LED)

and light sensor (photodiode) attached to it.

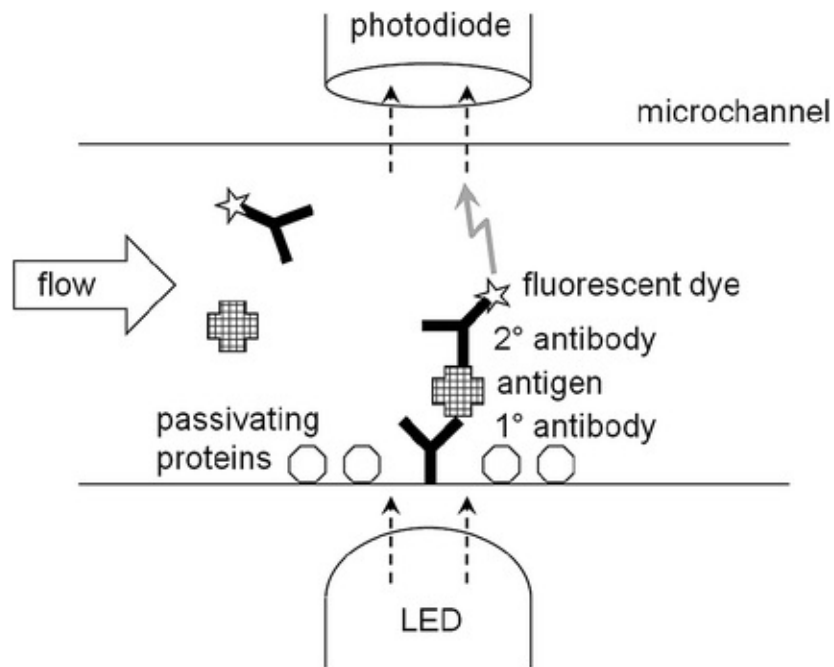


Fig. 14.11 Optical immunosensor LOC (identical to Fig. 13.5)

Figure 14.12 demonstrates the interdigitated microelectrode (IME) immunosensor, a very popular form of impedance-based immunosensor, also in a microchannel format. More advanced immunosensors can also be implemented in LOC platforms; for example, SPR, QCM, electrochemical ELISA, etc. (refer to Chap. 13).

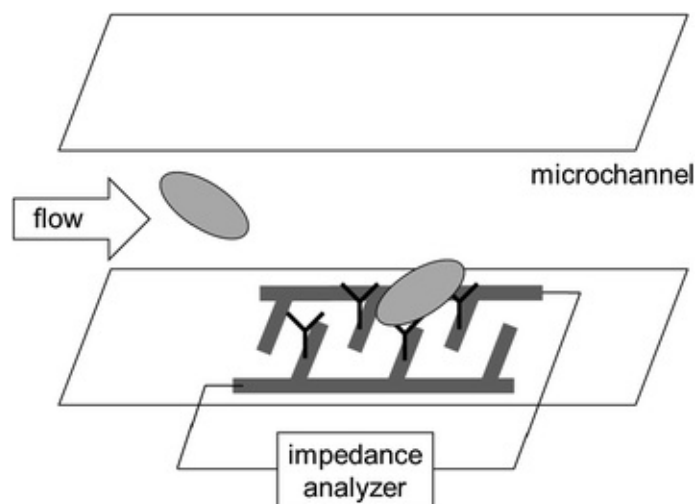


Fig. 14.12 IME (interdigitated microelectrode) immunosensor LOC

Unlike the LFAs, the LOC POCT can incorporate pretreatment procedures for samples, such as filtration and mixing. It is also capable of on-chip electrochemical or optical detection (which will be discussed in the next section). Performing multiple different assays for the same sample is also possible. Figures 14.13 and 14.14 show such examples.

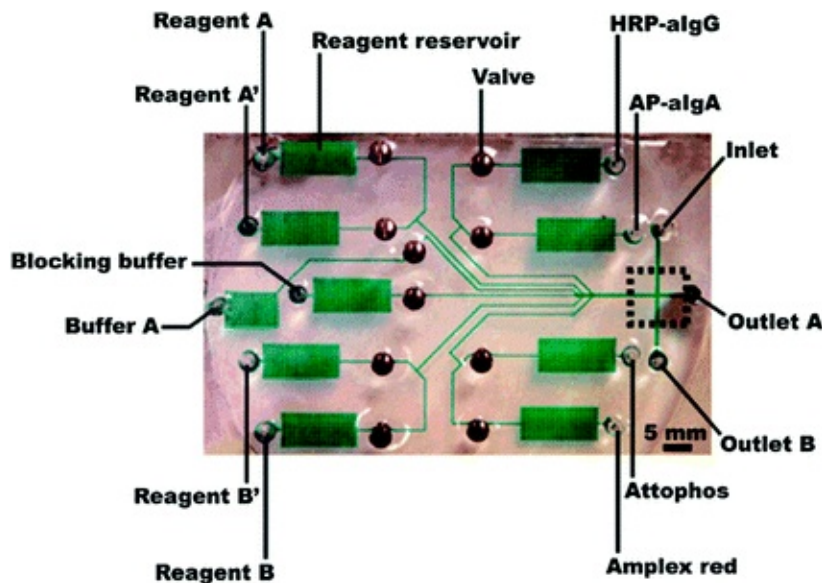


Fig. 14.13 LOC diagnostic device utilizing sandwich immunoassay. Reprinted with permission from Weibel et al. (2005), © 2005 American Chemical Society

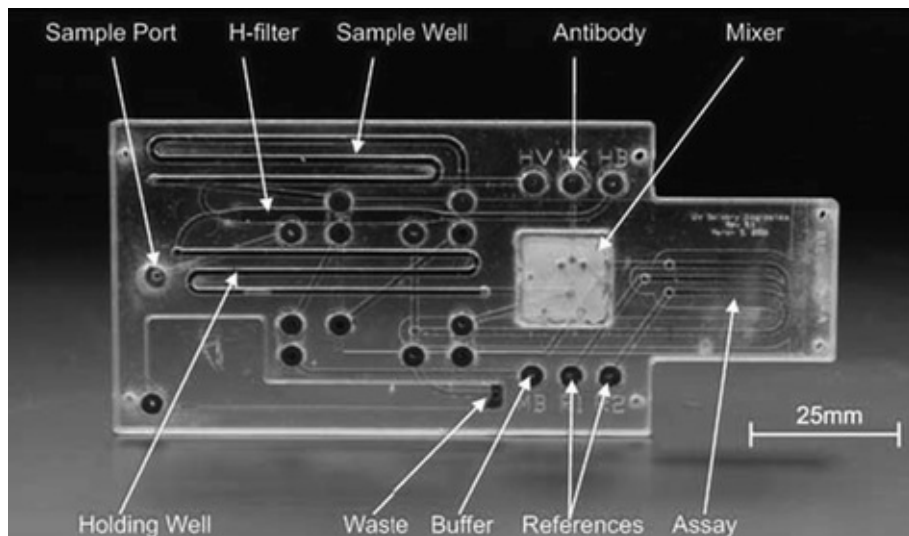


Fig. 14.14 LOC diagnostic device utilizing SPR immunosensing. Reprinted with permission from Fu et al. (2007), © 2007 John Wiley and Sons

In Fig. 14.13, the LOC is designed to perform sandwich immunoassay

(ELISA), where appropriate antibodies are already embedded just like LFAs. A user can manually rotate the screws to open or close each microchannel, thus complicated microchannel actuation is not necessary. The LOC can be used as is, without using any circuitry or microcontrollers.

Figure 14.14 shows a more complicated example of LOC POCT. The loaded sample is filtered, mixed, incubated, and the SPR immunosensor (see Chap. 13) is incorporated within a microchannel.

Although LOCs are still seldom used in commercial immunoassays, this concept is now one of the most studied applications for such devices. Compared to the microplate format, LOCs reduce sample consumption by a factor of 1000 or more. A typical hospital laboratory could save \$1 million per year by decreasing the use of these reagents. Assay time is reduced from hours to minutes by shortening the distance that molecules must travel for diffusion. Precise control and the ability to scale down to small volumes of blood are among the more attractive capabilities of LOC approaches. Compact devices also allow samples to be analyzed at the point-of-care rather than at a centralized laboratory, which could revolutionize medicine.

14.5 Use of Optical Fibers in LOCs

One traditional drawback of LOC devices had been their high *detection limit* (the lowest concentration that can be detected with statistical significance), thus poor sensitivity, which arose because the small volume diminished detectable signals. Today however, much lower detection limits (at the single-molecule level) are being obtained by using optical detection. In the last decade, biosensor researchers have begun to integrate *optical fibers* into LOC devices to enhance sensitivity. Typically, an optical fiber is used to deliver the light source, and another fiber is used to detect bio-reactions. Optical fiber allows pointing the light source and the detector at a precise location, thus providing and collecting light at its maximum. In addition, the disturbance of ambient can also be minimized, greatly enhancing the *signal-to-noise ratio (S/N ratio)*.

However, we must bear in mind that very low detection limits using optical methods are possible only in relatively clean systems. In addition, sample volumes must be sufficiently high to maintain such low detection limits. For instance, one requires at least 100 μL aliquot of a sample to detect 10 CFU (colony forming units) mL^{-1} cells, since this volume contains only one viable cell.

In general, the use of optical fibers in LOCs falls into two categories of fiber

orientation, as shown in Fig. 14.15: (1) *embedded fibers* and (2) *proximity fibers*. Embedded fibers are actually incorporated within an LOC device with physical contact to microchannel structures. This strategy offers the best performance with insignificant signal loss. However, it does require more complicated fabrication processes. Proximity fibers, on the other hand, are located in close proximity to, but not touching the chip. Thus, they are easy to develop, although they may introduce additional noise to the signals.

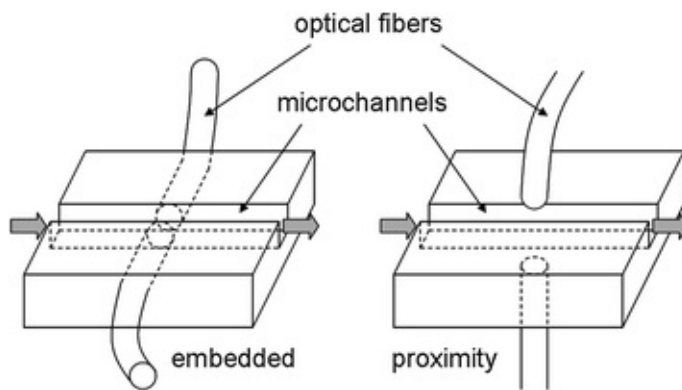


Fig. 14.15 Embedded and proximity optical fibers for LOC. Reprinted from: “latex immunoagglutination assay in lab-on-a-chip” by Yoon (2008). Copyright 2008 American Society of Agricultural and Biological Engineers

14.6 Sample/Reagent Introduction

Solutions of sample and reagent can be introduced to microfluidic channels of the LOC device using microelectronic methods. For example, they can be introduced by utilizing a pump that is micromachined within an LOC device or by applying a very high voltage to the channel to create electroosmotic flow (EOF). The latter (EOF) involves indispensable pumping mechanism for capillary electrophoresis (CE)-based LOC.

Recently, however, the microelectronic methods are being replaced with simpler external pumping methods: *syringe pump* or *peristaltic pump*. These external pumps can be placed at its inlets (injection) or its outlet (suction), as shown in Fig. 14.16.

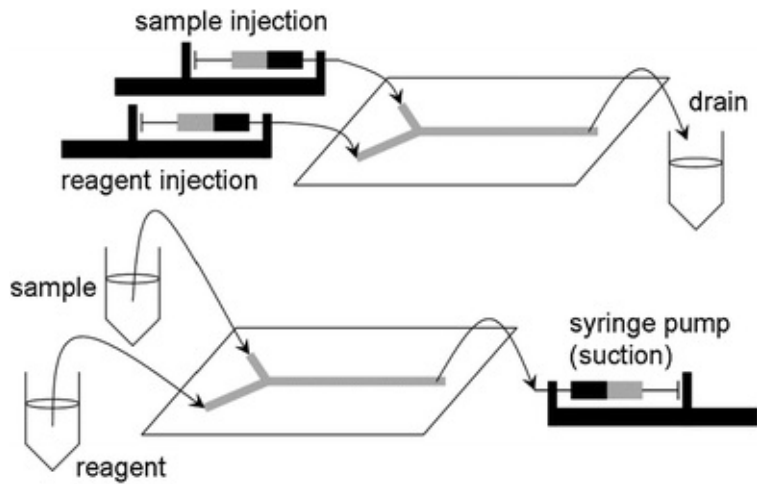


Fig. 14.16 Sample/reagent injection versus suction in POCT LOC

There are attempts to further eliminate the need for pumping. One way to make the liquid flow spontaneously is to make the inner surface of a microchannel *hydrophilic* (meaning water-loving). Once the droplets of sample and reagent are added to the inlets of microchannels, the liquids wet into the microchannel automatically as its inner surface is hydrophilic. The underlying mechanism for this fluid motion is *capillary action*. The lateral-flow assay (LFA) shown in Chap. 13 also works on the principle of capillary action.

Another popular way is the use of CD (compact disc), called *lab-on-a-CD*. Microchannels are fabricated directly on the surface of a CD, from its center to the outside, and the sample/reagent liquid is loaded to the inlet wells. This CD is then loaded into the CD player and rotated, creating a centrifugal force that makes the liquid to flow through the microchannel (Fig. 14.17).

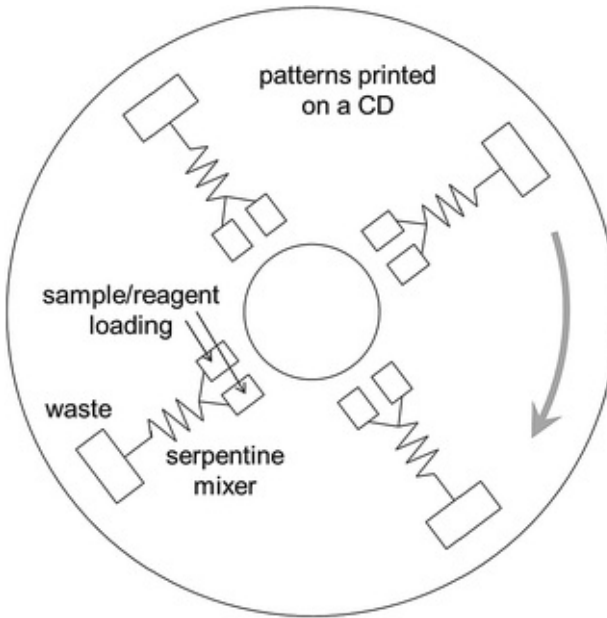


Fig. 14.17 Lab-on-a-CD. Rotation of lab-on-a-CD creates a centrifugal force that pumps the liquid from the center to the outer side

14.7 Mixing in LOC

When working with LOCs, the *Reynolds number*, Re , is a particularly useful dimensionless parameter.

$$Re = \frac{dv\rho}{\eta} = \frac{v\rho}{\eta/d} \quad (14.1)$$

The Reynolds number represents the ratio of inertial forces ($v \cdot \rho$, where v is the flow velocity and ρ the fluid density) to viscous forces (η/d , where η is the dynamic viscosity and d the characteristic length, such as the diameter of the capillary). It is used to characterize the fluid flow as being laminar or turbulent. Once an experiment indicates that a transition will occur (at $Re = 2000$, for example), the outcome of any other experiment and the behavior of the flow can be predicted. Because the Reynolds number is proportional to the characteristic length, d , for miniaturized systems, a small value of Re will indicate strictly laminar flow. In fact, the Re for most LOC systems are extremely low, making it almost impossible to achieve turbulent mixing of reagents as illustrated in Fig. 14.18.

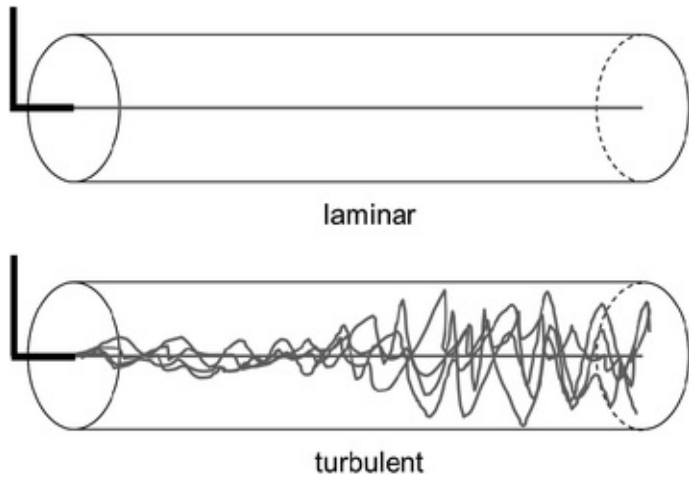


Fig. 14.18 Reynold's experiment: **a** laminar flow and **b** turbulent flow. As the flows are strictly laminar, turbulent mixing would not occur in most LOCs

In LOCs, the molecules flow along the straight stream lines of a strict laminar flow. To achieve effective mixing (without the help of turbulence), the molecules must also move perpendicular to the flow (shown in Fig. 14.19 as *passive mixer*). This is typically achieved by molecular diffusion. While it may be possible to achieve diffusional mixing by using a very long microchannel, this method works only for molecules with very low molecular weight and not for typically high-molecular-weight biomolecules.

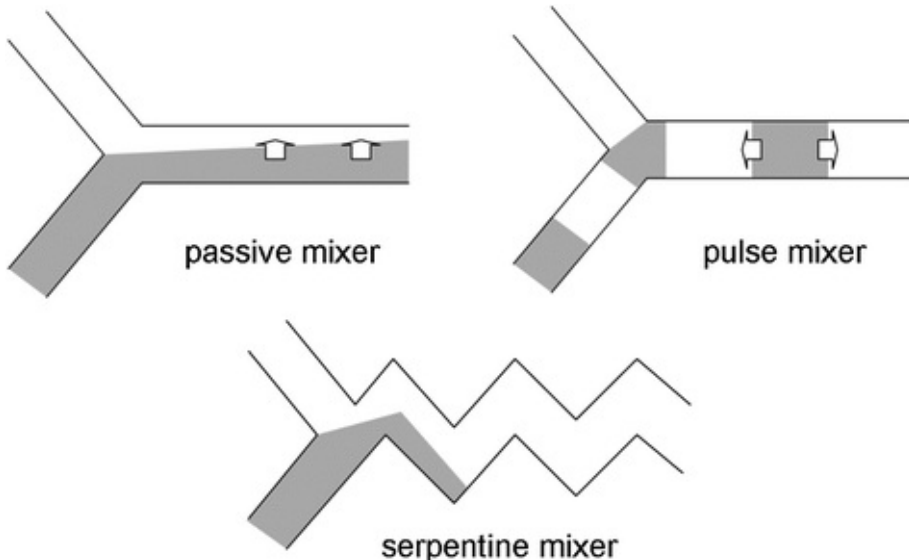


Fig. 14.19 Microfluidic mixers. Pure passive mixer: molecules diffuse to the other side purely by perpendicular diffusion. Pulse mixer: the fluid is supplied with pulse flow, allowing axial (i.e., parallel to the flow) diffusion. Serpentine mixer: allows both perpendicular and axial diffusions

A couple of methods have been suggested to improve this pure passive mixer. For example, the solution can also be introduced as discrete plugs of liquid, called *pulse mixer* (Fig. 14.19). Unlike the passive mixer, the molecular diffusion occurs parallel to the flow, i.e., axial diffusion. More effective and faster mixing can be achieved through making the discrete plugs shorter. The microchannel can also be made as a serpentine shape, so that both perpendicular and axial diffusions occur at the same time (called *serpentine mixer*, Fig. 14.19). More advanced and complicated microfluidic mixers are currently being investigated.

14.8 Paper-Based LOCs

Recently, paper (more specifically chromatography paper) has increased in popularity as an alternative to silicon-based materials for fabricating LOCs. The *paper-based LOCs* are lower in cost, much thinner, easier to fabricate, and easier to use than conventional LOCs. The fabrication and use of such devices are collectively referred to as *paper microfluidics*. Since most paper-based LOCs are used for sensing and biosensing applications, they are typically referred to as microfluidic paper analytic devices, or μ PADs.

Fabrication of paper-based LOCs is not very different from the standard photolithography methods used for typical LOCs. In fact, the only difference is the use of paper in lieu of a silicon substrate. A mask is designed and printed on a glass plate, a quartz plate, or a transparency film (transparency film is preferred for most paper-based LOCs due to simplicity). The paper is pre-coated with an appropriate thin film of photoresist (PR) through spin-coating or by dipping the paper into the PR solution (dipping is preferred for simplicity). Since paper fibers are permeable to most solutions, PR typically penetrates into the paper. While the paper itself is generally hydrophilic due to its cellulosic fiber composition, most PRs are *hydrophobic* (meaning water-hating) and thus cause both the surface and inner paper fibers to become quite hydrophobic. After a drying process, the mask is then placed on the PR-coated paper substrate and both are irradiated with ultraviolet (UV) light. UV radiation causes positive PR to become chemically unstable and able to be removed by a chemical developer. With negative PR, it becomes hardened under UV radiation and the non-hardened PR is removed by a developer. Either way, an area that is free of PR will be generated. Sample liquid can flow through the area that is free of hydrophobic PR, while it cannot flow through the area that is covered and filled with hydrophobic PR. As shown in Fig. 14.20, the fabrication of paper-based LOCs is substantially simpler than that of conventional LOCs. Specifically,

paper-based LOCs do not require a cover slide, thus requiring no bonding procedure. For further simplicity, wax may also be printed directly on the paper, eliminating the need for spin-coating/dipping or a mask.

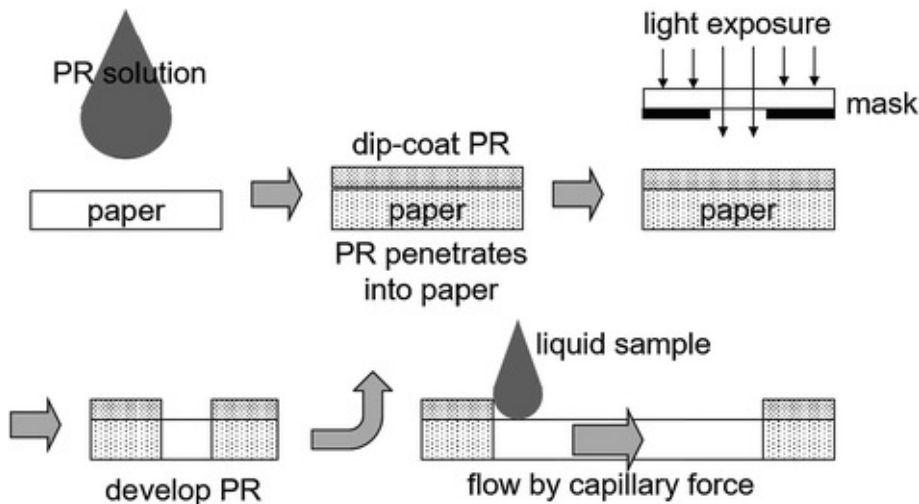


Fig. 14.20 Fabrication of a paper-based LOC

Despite its similarity to conventional LOCs, there is a fundamental difference in paper-based LOCs: its microfluidic channel is not hollow, but is filled with paper fibers. Once a liquid sample is loaded to its inlet, the liquid spontaneously flows through these fibers via *capillary action* (also referred to as *wicking*), thus requiring neither electroosmotic flow nor external pumping. This situation is identical to that of lateral-flow assays, previously described in Chap. 13. This capillary action (or wicking) is perhaps the major advantage of paper-based LOCs over other conventional LOCs.

The presence of paper fibers also causes the flow to slow, and for more viscous liquid samples, the liquid may not be able to flow at all (e.g., whole blood). Depending on the applications, however, this can be beneficial, since we may be able to utilize this flow obstruction as a mechanism for actively filtering certain components from the liquid sample (for example, filtering blood cells from whole blood). More sophisticated filtration can be achieved by utilizing a chromatographic filter paper, with known pore size (narrowly distributed) and known functional groups (nitro- or sulfone-) that are added to the cellulose fibers.

Many different chemical and biological assays have been performed using paper-based LOCs: glucose, cholesterol, lactate, alcohol, heavy metals, enzymes, proteins, etc., utilizing both optical and electrochemical detection.

14.9 LOC Sensing with a Smartphone Camera

Smartphone cameras can be used as powerful optical detectors, as we learned from Laboratory Tasks 2 and 3 of Chap. 13. The same can apply to LOCs. Recent smartphones are equipped with a powerful white flash and a high resolution digital camera, which can function as an effective optical detection system for LOC applications. Although the number of research publications using these for detection is still small, this area is currently growing very rapidly.

One such example is the use of a smartphone camera to count the number of cells that flow through a microchannel. This particular system is known as a *flow cytometer* or *cell counter*, which is normally a very expensive piece of laboratory equipment. The smartphone simply acts as a handheld microscope, which counts the number of cells that flow past.

Another obvious example is the use of a smartphone to read the reflected intensity of light from a test band in a lateral-flow assay (LFA) by utilizing the white flash, digital camera, and software within the phone, as shown in Fig. 14.21. Obviously, any point-of-care testing LOC device (POCT LOC) can be connected to a smartphone, thereby eliminating the need for complicated stand-alone circuitry and microcontrollers that are designed exclusively for optical sensing of this POCT LOC.

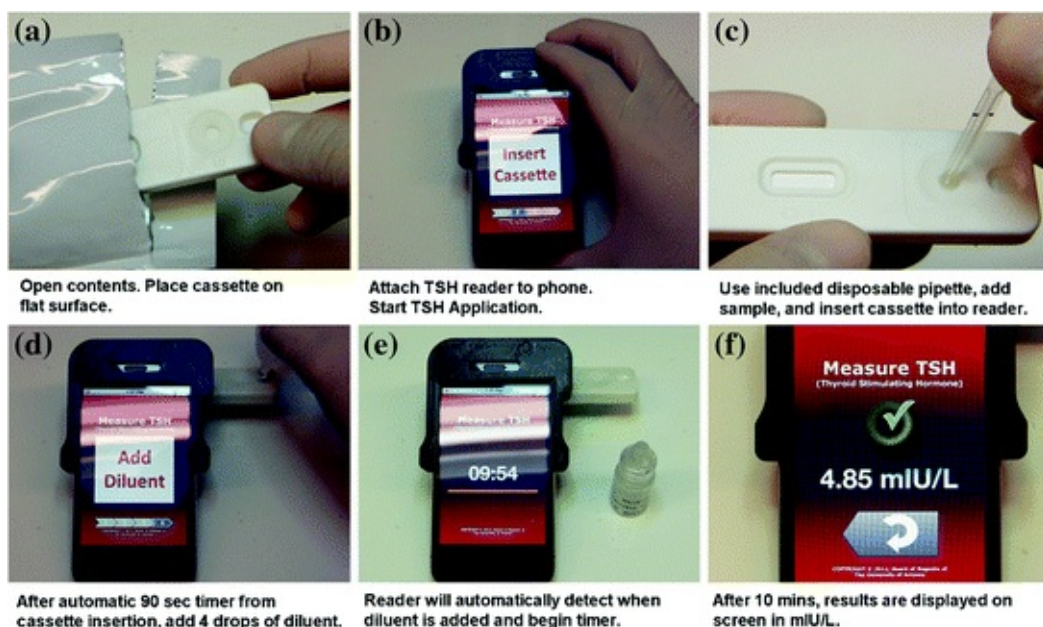


Fig. 14.21 Smartphone-based reader device/software for LFA. You et al. (2013), © Elsevier 2013, reprinted with permission

14.10 Other Applications of LOCs

So far, we have learned about the use of LOCs as advanced, miniaturized, and automated biosensing devices/systems, which can be referred to as POCT LOCs. Obviously, this is just one example of LOC applications, although this is perhaps the most studied and most widely investigated application.

LOCs can certainly be used for chemical analysis, such as mass spectrometry, especially matrix-assisted laser desorption/ionization time-of-flight mass spectrometry (MALDI TOF MS) to analyze the structure of proteins and polymers. Conventional MALDI TOF MS involves a substantial amount of human labor (mostly pipetting) that can be automated through the use of microchannels in LOCs.

Further miniaturization of microchannels and wells can also enable us to isolate and study samples at the single-molecular level, which can be very difficult through conventional laboratory analysis.

Another important application is *cell-on-a-chip*, in which cells or tissues are cultured in microchannels and wells. Through the use of LOC devices, cell proliferation can be guided in a certain direction along a surface pattern, cells can be sorted depending on their type and/or characteristics, and growth factors and/or other chemical/physical stimulation can be applied to specific regions of the cell cultures or tissues.

Recently, *cell-on-a-chip* has been developing into a more sophisticated system known as *organ-on-a-chip* (OOC). OOC is essentially a mimic for human organ or organ component. For example, straight microfluidic channels can be filled with kidney epithelial cells, then proliferated to create a simulated nephron (the basic functional unit of kidney). The resulting OOC can be referred to as *kidney-on-a-chip*. The same channels can be filled with hepatocytes to create a mimic for a liver sinusoid (the basic functional unit of liver). Blood vessel mimic can be created in the same manner using vascular endothelial cells and smooth muscle cells. These OOCs can be utilized to study which chemical and physical factors trigger the formation of cancer and its spread to the other organs (metastasis) by connecting multiple OOCs in a series or in parallel, which is not possible with conventional *in vitro* experiments. Likewise, differentiation of stem cells can better be studied with networked OOC systems. OOCs are also being utilized for evaluating the efficacy and toxicity of new drugs for specific organ or organ networks. OOCs mimic the physicochemical conditions in much more sophisticated ways than static *in vitro* experiments permit, and may potentially replace the need for animal studies in the future.

14.11 Laboratory Task 1: Fabrication of LOC by Soft Lithography

In this laboratory, you will fabricate an LOC device using the PDMS replica molding technique. As it is likely that some readers will not have access to a cleanroom, we will assume that you have purchased a mold produced by standard photolithography, fabricated on a silicon wafer or glass substrate. Many vendors are available to make molds from your CAD or PowerPoint™ drawings. The mold in this laboratory has a simple Y-channel layout, where the specimen and the reagent (typically containing enzymes or antibodies) are introduced separately and merge at its junction.

In this task, you will need the following:

- A LOC mold
- Microscope glass slides
- Clear tape (3 M or Scotch)
- KimWipes (laboratory-level cleaning tissue)
- Isopropanol (IPA)
- Sylgard 184 silicone elastomer curing agent
- Sylgard 184 silicone elastomer base
- Plastic cups, disposable syringes (3 mL)
- A desiccator, connected to a vacuum pump
- An oven
- Latex gloves and paper towels.



Fig. 14.22 An LOC mold in a box structure

1. Using the tape, attach four glass slides to each side of the LOC mold tightly to ensure that there is no space in-between.
2. Fold up the slides to form a box-like structure, and tape it together. Make sure that there are no places where a leak could occur (Fig. 14.22).
3. Clean the mold with IPA using the KimWipes.
4. Wear latex gloves.
5. In a plastic cup, mix 6 mL silicone base with 0.6 mL curing agent.
6. Stir vigorously for 10 min using the syringe plunger (Fig. 14.23).



Fig. 14.23 Mixing of silicone base and curing agent

7.

Place the LOC mold/slides-assembly on the paper towels and pour the mixture from the plastic cup into the mold/slides-assembly. Then, place everything into a desiccator that is connected to a vacuum pump. Apply vacuum for 20 min. as shown in Fig. 14.24.



Fig. 14.24 Vacuuming the chip

8. Place the LOC mold/slides-assembly into the oven at 65 °C, and bake for 1 hour.
9. Remove from the oven, and carefully peel your plastic LOC off of the mold (Fig. 14.25).

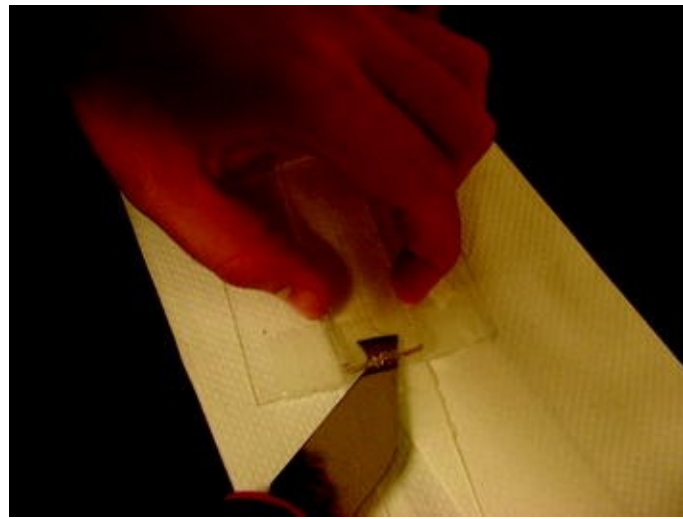


Fig. 14.25 Removal of a mold

14.12 Laboratory Task 2: Mixing in LOC

In this task, you will need the following:

- Your LOC
- Clear tape (3 M or Scotch)
- Two 250 μL syringes with needles
- Microtubing
- Food coloring or edible dye (two different colors)
- Two beakers
- Ruler and stopwatch

1. Tape over the channels in your LOC (make sure there is only one layer of tape over the channels).
2. Poke holes in the tape at the ends of the LOC channels using your syringe needles.

3. Carefully insert your two syringe needles into the micro-tubing (Fig. 14.26).

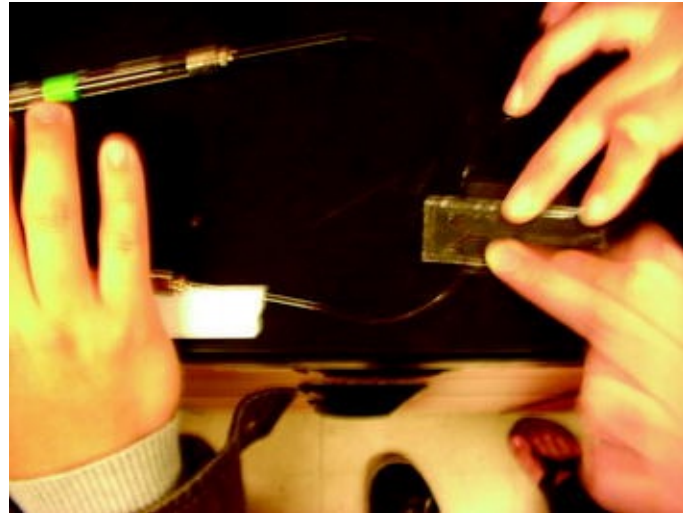


Fig. 14.26 LOC with cover tape and inlet needles

4. In two beakers, drop enough food dye (of two different types) to fill up the syringes (a few drops should work).
5. Fill up the syringes with the dyes.
6. Put the syringes into the holes that you poked at the “y-end” of the LOC.
7. Have one partner SLOWLY inject the fluid into the channels, while the other partner begins the stopwatch when the fluids hit the intersection at the “y-end” of the LOC. The partner with the stopwatch will record the time needed for the fluids to reach the end of the channel.
8. Calculate the flow velocity.

9. Make sure that you note the point along the channel where the fluids start to mix, and measure this distance with the ruler. (This is the diffusional length.) (Fig. 14.27).

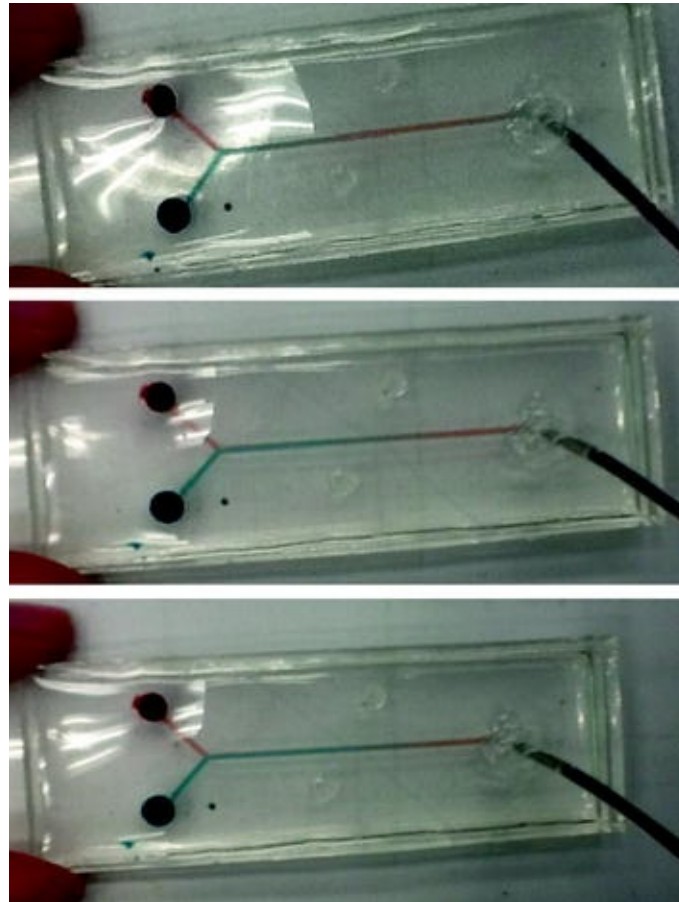


Fig. 14.27 Mixing of two dye solutions within an LOC

10. Try two other flow velocities (by injecting the plunger more slowly) and repeat steps 5–8. Plot the diffusional length (y-axis) against the flow velocity (x-axis) (Fig. 14.28).

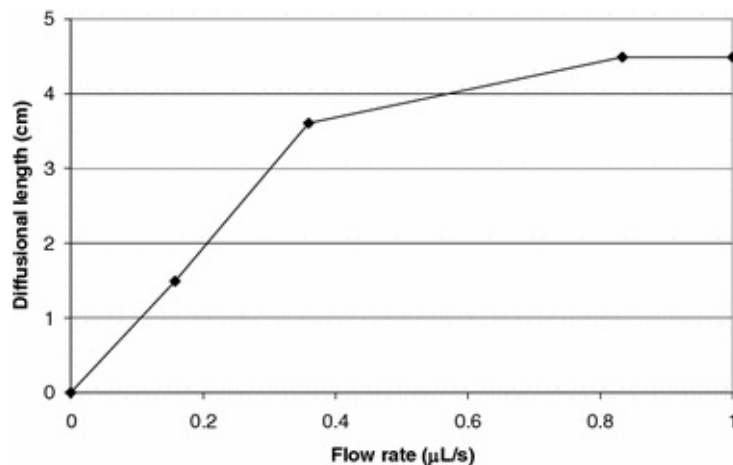


Fig. 14.28 Experimental results from task 2: diffusional length—flow velocity

Question 14.1

Design a glucose assay LOC (Task 2 of the Chap. 12 Laboratory), using optical transducers and the same Y-channel configuration shown earlier. Place an LED and a PD on both sides of the channel as illustrated in Fig. 14.11. Include an overall schematic layout, sample/reagent injections, and circuit diagrams for both the LED and PD.

Question 14.2

Repeat Question 14.1 for an insulin ELISA LOC (Task 1 of the Chap. 13 laboratory).

Question 14.3

Repeat Questions 14.1 and 14.2 using a smartphone as light source and detector.

14.13 Laboratory Task 3: Fabrication of a Paper-Based LOC

In the following two tasks (Task 3 and Task 4), we will fabricate paper-based LOC and use it to assay the total protein concentration. SU-8 will be used as a photoresist (PR). It is a negative PR, indicating that it will be hardened upon UV irradiation. PR coatings exposed to UV irradiation will not be removed upon acetone rinsing, while those not exposed to UV will be removed.

Bradford assay reagent will be used to colorimetrically stain proteins. It is essentially a Coomassie Brilliant Blue G-250 dye that binds to most proteins and emits blue coloration (maximum absorbance at 595 nm = yellow-red; thus blue coloration).

In this task, you will need the following:

- A mask (channel layout printed on a transparency film)
- Filter paper
- SU-8 2010 photoresist (100 %)
- Acetone (100 %)
- Isopropyl alcohol (IPA) (70 %)
- Gel documentation system (for UV irradiation) or a UV lamp
- Hot plate
- Wash bottle
- Tweezers, laboratory spatula, and scissors
- Latex gloves, paper towels, and KimWipes

All steps must be performed in a chemical hood, with the exceptions of mask printing (steps 1–2) and UV irradiation (steps 7–9). Latex gloves should be worn throughout the experiments.

1. Design the layout of a microfluidic channel using an appropriate software system (PowerPointTM or SolidWorksTM). For the sake of simplicity, a layout of three straight channels with a keyhole-shaped design is recommended.

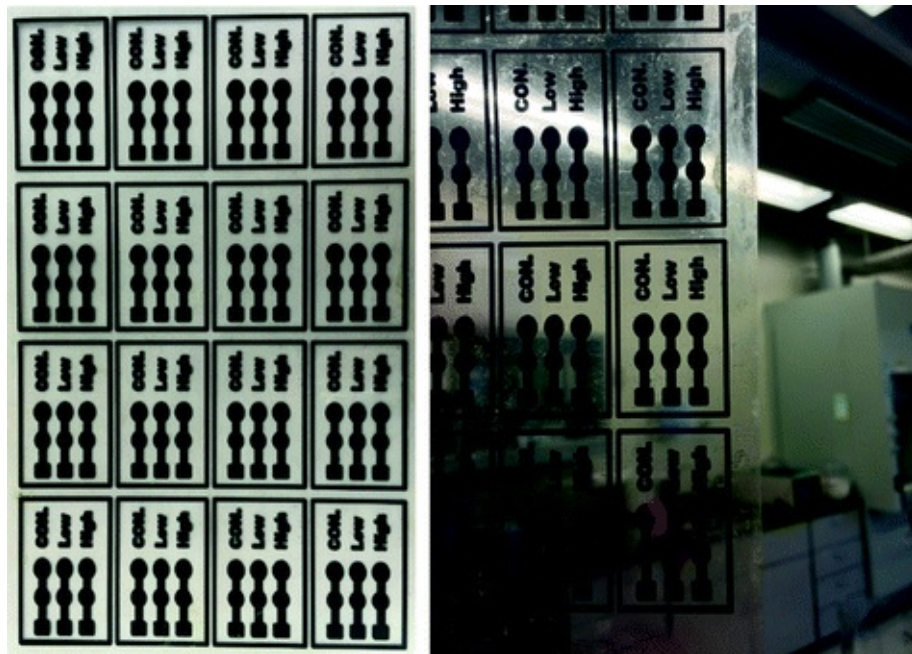


Fig. 14.29 A mask printed on a transparency film. Each LOC pattern consists of three keyhole-shaped straight channels, for a negative control (“CON”), and low- and high-concentration targets (“low” and “high”)

2. Print this pattern, as well as its mirrored inverse, onto a transparency film using a laser printer. Cut these two sides of the transparency pattern out, align them across from one another to form a pattern “sandwich” (with the toner-coated sides facing outward), and tape two adjacent edges together such that a two-sided pocket is formed (Fig. 14.29).
3. Cut a piece of filter paper in an appropriate size that will accommodate the entire microfluidic channel layout, and then immerse the paper into the SU-8 photoresist solution using tweezers. Make sure the entire paper is fully and evenly covered with SU-8. Take the paper out of the SU-8 solution and scrape the excess SU-8 off of the paper using a spatula (Fig. 14.30).

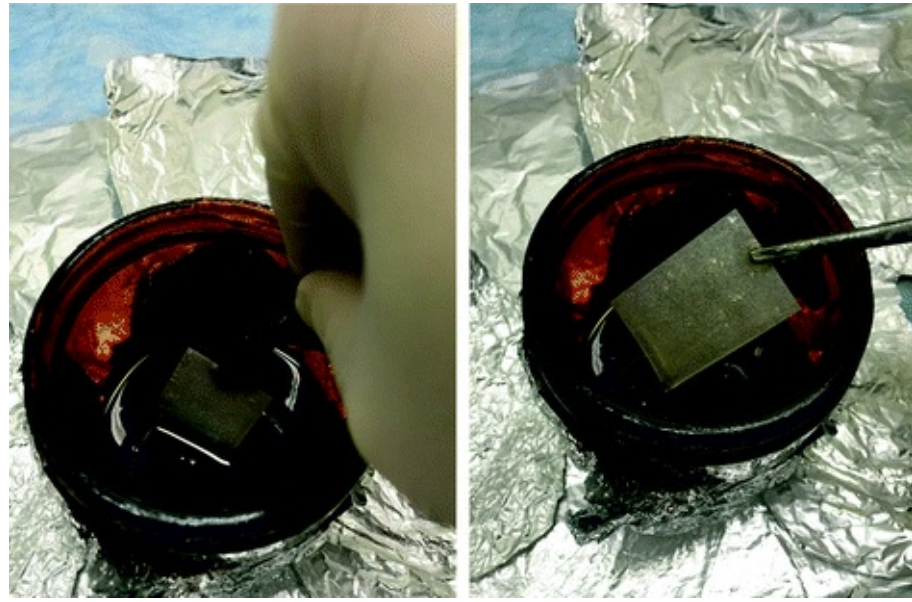


Fig. 14.30 Cut-out paper is immersed into the SU-8 photoresist solution

4. Place the paper between paper towels (preferably KimWipes) and pat until no visible shiny spots are observed. The paper should have a matte appearance.
5. Wrap the paper in a fresh KimWipes and sandwich this between new paper towels on a hot plate ($90\text{ }^{\circ}\text{C}$) until they are fully dried. For better contact between the paper and the hot plate surface, a flat weight (such as a laboratory balance or some other heavy object) can be placed on top of the wrapped paper. Drying typically takes 5–10 min (Fig. 14.31).
6. Remove the paper towels. Place a dried paper coated in SU-8 in the pocket of the mask (the transparency film with the channel layout) to create an SU-8 paper + mask sandwich. Ensure that the channel pattern fits entirely within the bounds of the SU-8 paper. Place a piece of black paper on top of the SU-8 paper + mask sandwich, and then place the black paper + SU-8 paper + mask into the gel documentation system with the black paper positioned on the side opposite of the UV light source (we will use it simply for UV irradiation purposes). Since the UV lamp is located at the base of a typical gel

documentation system, you will need to place the SU-8 paper + mask sandwich underneath the black paper. To hold the paper and the mask together, a weight should be placed on top of the black paper (Fig. 14.32).



Fig. 14.31 Paper is dried on a hot plate. A weight is placed on the paper

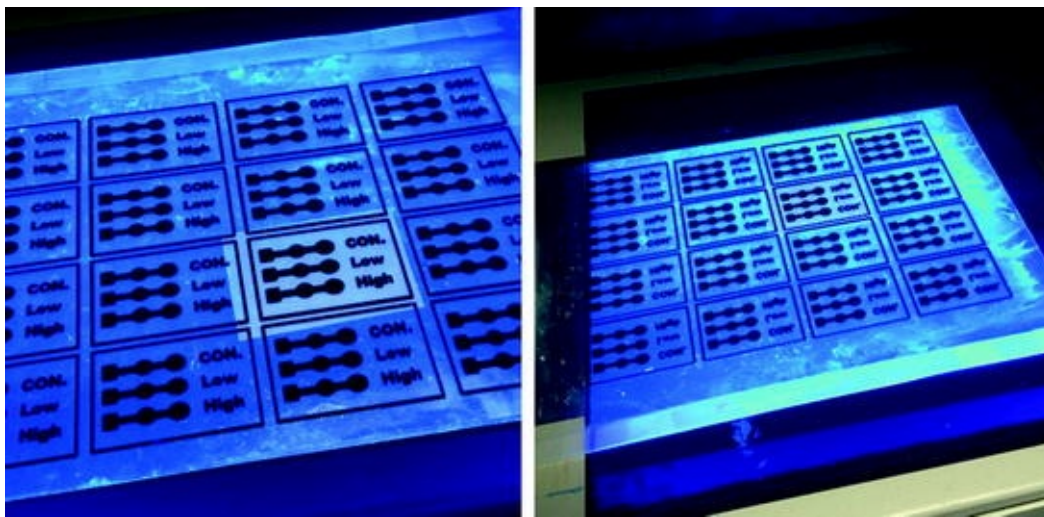


Fig. 14.32 Black paper + SU-8 paper + mask is placed into the gel documentation system

7. If a gel documentation system cannot be used, use an appropriately powerful UV lamp (85 W). When using a UV lamp that irradiates from above, the SU-

SU-8 paper and mask sandwich will be exposed from the top, so a black paper on the top of the mask is not necessary as this would block the mask from UV exposure. The UV lamp must be used in a protective enclosure, or an appropriate pair of UV protective glasses should be worn.

8. After 3 min of UV exposure on the first side of the SU-8 paper, carefully remove the weight and the black paper (if a gel documentation system has been used). Make sure the SU-8 paper and the mask do not shift during this process. Gently flip the SU-8 paper + mask sandwich such that the opposite side may be exposed to the UV light source. Position the black paper and weight as before, and irradiate the second side of SU-8 paper with UV light for 3 min.
9. Remove the SU-8 paper from the mask and immerse the paper in acetone for 2–3 min using a pair of tweezers. This begins to develop the channels. Observe the paper to make sure that the SU-8 is stripping only from the channel and not from the entire paper. The goal is to completely remove SU-8 from the central channel, while retaining SU-8 in all other areas.
10. Remove the developed paper from the acetone bath using tweezers and rinse both sides of the developed paper again with acetone using a wash bottle (Fig. 14.33).

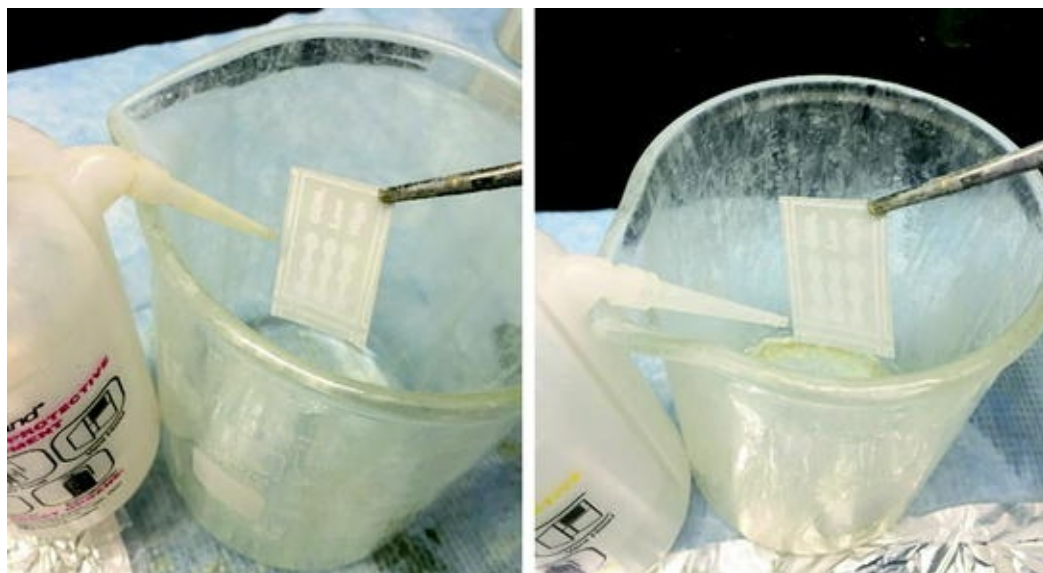


Fig. 14.33 Developed paper is rinsed with acetone using a wash bottle

11. Next, rinse both sides of the developed paper with 70 % isopropyl alcohol (IPA) using a wash bottle.
12. For a final rinse, wash both sides of the developed paper with deionized water using another wash bottle.
13. Finally, place the developed paper between paper towels or KimWipes and dry on a hot plate (90 °C). Again, a weight can be placed on top of the paper to ensure better contact with the heated surface and to allow the paper to flatten. Drying typically takes 5 min. If the paper becomes curled after drying, the developed paper can be immersed back into 70 % IPA, rinsed with deionized water, and dried again on a hot plate.

14.14 Laboratory Task 4: Bradford Assay with Paper-

Based LOC

In this task, you will need the following:

- The paper-based LOC from Task 3
- Bradford assay reagent
- Bovine serum albumin
- Pipettes and pipette tips
- Latex gloves and paper towels (KimWipes)

1. Prepare 1 mL solutions of bovine serum albumin (BSA), with varying concentrations of 2, 1, and 0 mg/ mL (i.e., no BSA).
2. Add 2 μ L of each BSA solution (2, 1, and 0 mg/mL) to the center of separate microfluidic channels. Allow the BSA solutions to dry.
3. Add 8 μ L of the Bradford assay reagent to the inlet of each microfluidic channel. Allow the channels to dry. In the presence of a protein, the Bradford assay reagent will transform from an initial brown coloration toward a blue coloration in a change that is proportional to the solution concentration of protein.
4. Using a smartphone camera, take an image of the paper-based LOC. The smartphone should be placed perpendicular to the paper-based LOC, about 6 inches away from it. Capture one image without flash, and one image with flash (Fig. 14.34).
5. Upload the images onto your computer and open them using an appropriate software package (e.g., ImageJ; refer to Chap. 13 Task 2).
6. Collect red, green, and blue pixel intensities from the appropriate areas of all

three channels in both images (flash, and no flash) separately. Collect the intensities at least from 10 different pixels, and average them. The maximum absorption of the Bradford assay reagent occurs at 595 nm (yellow-red) in the presence of protein, which corresponds to the deepening blue coloration. Absorbance should be calculated using red pixel intensities. For comparison purpose, calculate the absorbance using green pixel intensities (Fig. 14.35).

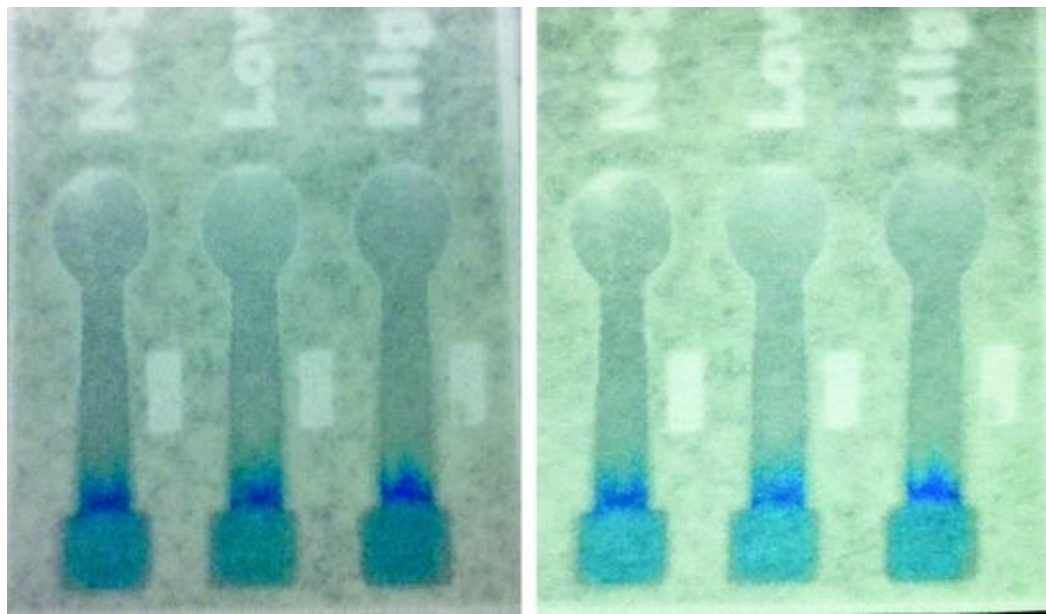


Fig. 14.34 Digital photographs of a paper-based LOC for task 4. *Left* without flash. *Right* with flash

	Without flash			With flash		
	BSA conc. mg/mL	0	1.0	2.0	0	1.0
Red intensity (I)	45.2	36.9	31.4	63.8	47	42.9
Green intensity (I)	112.4	110.9	104.0	140.9	139.8	132.4
Blue intensity	144.3	144	143	177.4	187.9	186.3
A = log (I_0 / I) [red]	0.0	0.088	0.158	0.0	0.133	0.172
A = log (I_0 / I) [green]	0.0	0.006	0.034	0.0	0.003	0.027

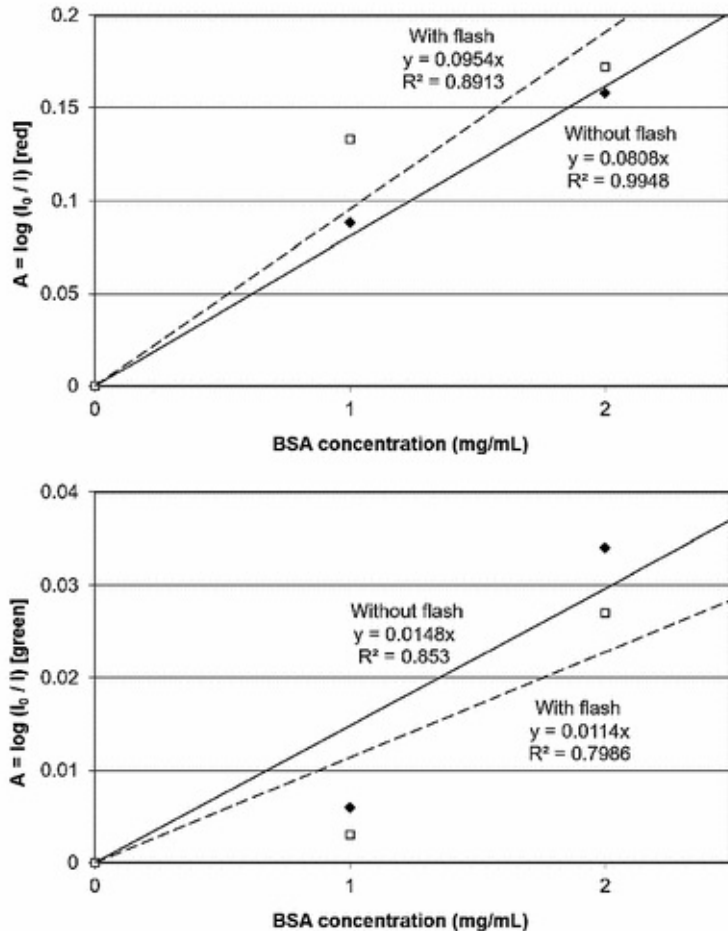


Fig. 14.35 Experimental data of Task 4: standard curves using a smartphone camera. The red and green pixel intensities with 0 mg/mL BSA solution was used as I_0

Question 14.4

Describe the linearity (R^2) of your standard curves with versus without using flash. If nonlinear, briefly explain why.

Question 14.5

Describe the sensitivity (slope) of your standard curves with red versus green pixel intensities.

Question 14.6

If your BSA solutions are not flowing through the channels, how can you fix such problem?

Question 14.7

In Task 4, all three assays were conducted on a single paper-based LOC, thus the variations in paper, light irradiation, focusing, reflection, etc. are minimized. To compare the assays from several different paper-based LOCs, a further “normalization” step would become necessary, typically by taking a photograph of a dry paper-based LOC before and after loading the Bradford assay reagent and BSA solutions. Describe the step-by-step procedures of such background normalization.

14.15 Further Study: Latex Immunoagglutination Assay (LIA) in LOC

Implementing multiple ELISA steps of reagent addition and rinsing into LOC platform is not always easy, as discussed in this chapter. There is an alternative type of immunoassay that is essentially one-step, called latex immunoagglutination assay (LIA) . In LIA, antibodies are immobilized onto the micro- and submicroparticles that are free to move within liquid. (In ELISA, however, antibodies are immobilized on a fixed, non-movable surface.) This antibody-conjugated latex bead suspension is then mixed with a sample solution that may contain antigens. Antibodies can also be detected as target molecule if corresponding antigens are immobilized on the beads. Antigen-antibody binding makes the particle to be glued together (thus the name *agglutination*) leading to the increase in effective bead diameter. This increase typically makes the bead suspension more turbid, which is visually identifiable by naked eye, if the antigen concentration is sufficiently high, or by a microscope, if the antigen concentration is relatively low. No further rinsing and separation is necessary, as unbound antigens do not participate in the immunoagglutination process.

This one-step LIA can easily be implemented in a Y-channel LOC that we learned in this chapter’s laboratory. Antibody-conjugated latex bead suspension is applied to one inlet and a sample solution with target antigen is applied to the other inlet, and mixing occurs at the Y-junction. A pair of optical fibers can be

aligned to the main microchannel (Fig. 14.15 in Sect. 14.5) to illuminate the bead suspension and detect turbidity readings from it.

One method to improve the sensitivity of LIA is the measurement of light scattering rather than turbidity. As shown in Fig. 14.36c, the detector fiber is aligned 45° to the incident fiber, indicating that it detects only the scattered light from the beads and eliminates any light that comes directly from the incident fiber, thus increasing signal-to-noise ratio and subsequently sensitivity. Additionally, the intensity of scattered light is substantially stronger than that of fluorescent emission, which also contributes to the stronger signal and thus better sensitivity. Increases of about three orders of magnitude in lowest detectable concentrations have been reported (see the references under LIA in LOC).

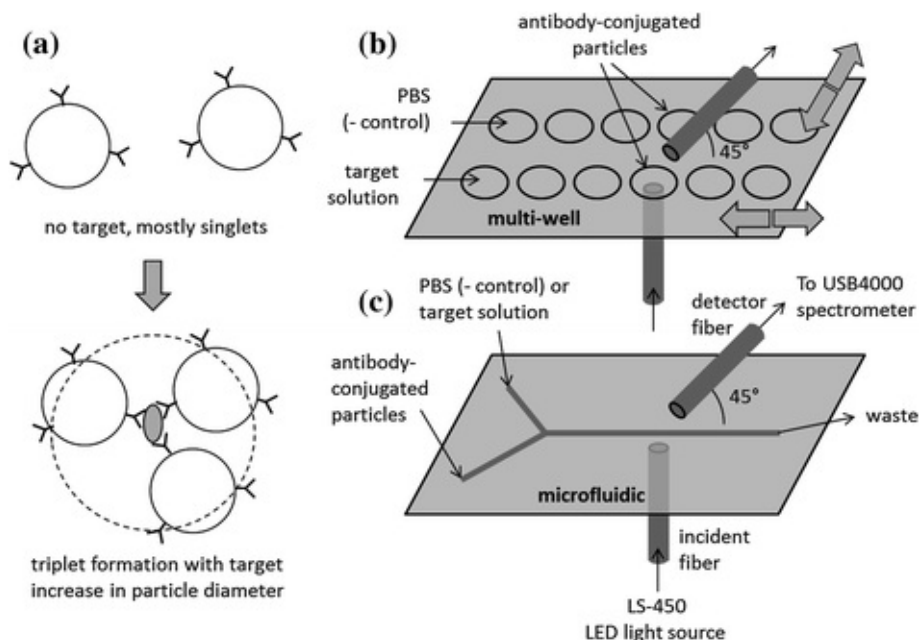


Fig. 14.36 Antibody-conjugated microbeads immunoagglutinates upon binding to a target antigen, increasing their effective diameter (A). “Proximity” fiber optic setup for light scattering detections from a multi-well slide (B) or a microfluidic chip with a Y-microchannel (C). Reprinted with permission Song et al. (2011), © 2011 Elsevier

Fluorescent emission is a special case of light scattering that is inelastic (there is an energy loss), while the emitted light is easily distinguished by its different color. Light scattering from latex beads, however, is elastic and the energy loss is minimal, with the disadvantage of identical wavelengths between incident and scattered lights. The 45° alignment is shown in Fig. 14.36c can solve this problem. The optimum angle of detector fiber is a function of the bead diameter, the refractive indices of bead and sample matrix, the wavelength of

incident light, etc., and is not necessarily 45°. This optimum angle can be determined by a series of experiments, or by *Mie scattering simulation*. The computer code for Mie scattering simulation is publicly available online, for example, the one by Philip Laven <http://philiplaven.com/mieplot.htm>.

Alternative Laboratory Task 2: LIA in LOC

Repeat Task 2 but replace two dyes with (1) anti-mouse IgG-conjugated polystyrene latex beads (anti-IgG is antibody-to-antibody) and (2) any mouse antibody (mouse IgG). Desired bead size is 0.1–1 µm. Set the bead concentration to 0.02 % (w/v). Make serial dilutions of mouse IgG, starting from 1 ng/mL to 1 µg/mL. Use the reflection/backscattering probe (Chap. 9 laboratory) to illuminate the microchannel at UV (380 nm) or blue (475 nm). If possible, use two different optical fibers for illumination and detection as shown in Fig. 14.36c.

14.16 Further Study: Polymerase Chain Reaction (PCR) in LOC

Antibody-based biosensors (immunosensors, discussed in Chap. 13) have also been studied and investigated for POCT LOC devices. Although the specificity of immunosensors is always superior to the other types of biosensors, they are not 100 % accurate. They often fail to recognize different strains of bacteria/viruses, or even show cross reactivity between similar species (e.g., *E. coli* and *Salmonella* spp.). When detecting bacteria and viruses, there is a better way to ensure 100 % specificity: the identification of the genetic sequence of target bacteria or viruses. This genetic identification is typically performed using a procedure called polymerase chain reaction (PCR).

PCR starts with lysing the bacteria or viruses and extracting the genetic material from them (DNA for bacteria and RNA for both bacteria and viruses). DNA is double-stranded (double chains of nucleic acids) and RNA is single-stranded (single chain of nucleic acids). Double-stranded DNA (dsDNA) is used as is, while RNA needs to be converted into dsDNA (the dsDNA made from RNA is referred to as *complementary DNA* or *cDNA*). PCR reagents are added to the target solution, which typically consists of primers, Taq polymerase, dNTPs, and others.

The dsDNAs are heated to 94–96 °C to be *denatured* into two single-stranded DNAs (ssDNAs). They are cooled down to 50–65 °C, and the primers bind to the target sequence of ssDNAs (called *annealing*). Primers are very

short DNA sequences that recognize and bind to the target DNA sequence. The solution is then heated to 70–76 °C to maximize the activity of an enzyme, *Taq polymerase*. *Taq polymerase* recruits the dNTPs (deoxyribonucleotide triphosphate), the building blocks of DNA, and assembles the complementary strand of ssDNA. There are four types of dNTPs: A (adenine), T (thymine), G (guanine), and C (cytosine). *Taq polymerase* synthesizes the complementary strand sequentially, starting from the primer to the end of the target sequence: this procedure is called *extension*. This completes one cycle of PCR (*thermocycling*). Two identical copies of the target DNA sequence are obtained from the initial single copy. This cycle can be repeated as many times as possible, since sufficient amount of PCR reagents (primers, *Taq polymerase*, dNTPs, etc.) are added to the target solution. Repeating the cycle for 10 times gives $2^{10} = 1024$ copies and 20 times gives $2^{20} = \text{one million copies}$ (Fig. 14.37).

The DNA/RNA sequence is only amplified if the primers can bind to the target sequence. In other words, the amplification clearly indicates the existence of target sequence. In addition, PCR amplification can provide better sensitivity when the amount of target bacteria/viruses is too low to be detected. Theoretically, only a single copy of genetic sequence is needed for PCR amplification, although this can be quite challenging in practical situations.

The length of the amplified genetic sequence is typically a few hundreds base pairs (bp). To increase the specificity, a longer genetic sequence can be amplified, e.g., a few thousands base pairs (bp), which obviously takes a much longer time to be amplified. (Note: the extension is done sequentially.).

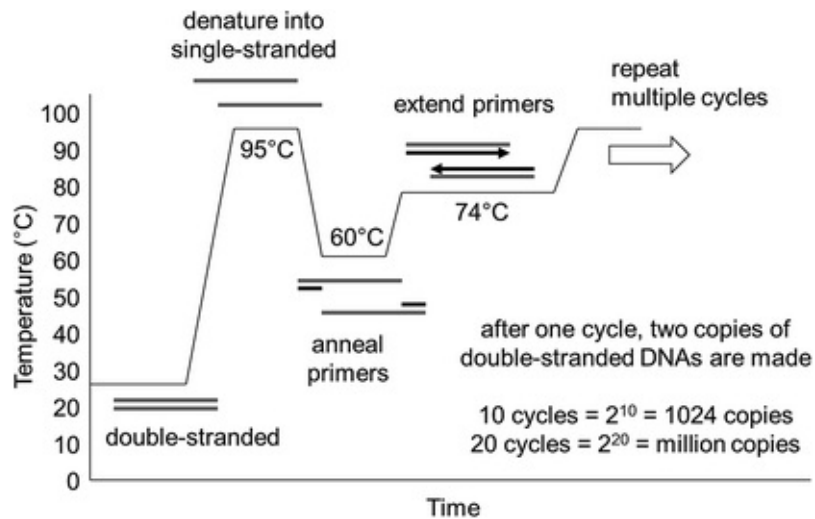


Fig. 14.37 Polymerase chain reaction (PCR)

PCR amplification, or PCR assay, is typically performed in a laboratory setting. The initial lysing and gene extraction requires multiple steps of manual pipetting and/or centrifuging, or a very expensive robotic system. The amplification part is performed using an instrument called *thermocycler*. Once thermocycling is finished, the product is loaded into a gel electrophoresis system, and the length of the amplified product can be identified. If the primers are designed to amplify 380-bp sequence, the gel electrophoresis result should also indicate the band at 380-bp. The actual sequence of the amplified product can be further evaluated using an instrument called *DNA sequencer*, although this is not always required.

Recently, the thermocycler has also become capable of conducting *real-time quantification*. This specific type of PCR is referred to as *real-time PCR*, quantitative PCR or *qPCR*. Real-time PCR should not be confused with *RT-PCR*, which is *reverse transcription PCR*, i.e., amplifying DNAs from RNA. If real-time feature is added to RT-PCR, it is referred to as *real-time RT-PCR* or *qRT-PCR*. Real-time PCR utilizes fluorescent dyes that emit a signal only when they bind to the double-stranded DNAs or the target DNA sequence. Therefore, the increase in fluorescent signals indicates the successful PCR amplification. Since real-time PCR does not tell the length of amplified product, it is less accurate than the gel electrophoresis. However, real-time PCR performs the thermocycling and product identification at the same time, and even allows the user to stop the programmed thermocycling prematurely if the increase in fluorescent signal is apparent.

As discussed previously, PCR is not a stand-alone biosensor, but rather an analytical procedure that involves multiple laboratory equipment and often human labor. In a narrower sense, PCR is not a topic of biosensors. In the past decade, however, scientists and engineers have attempted to incorporate PCR procedures, mostly the thermocycling part, into an LOC platform. Through automation and miniaturization, an easy-to-use and potentially faster PCR assay may become possible towards more specific and sensitive POCT LOC device.

In the conventional PCR, a single tube is repeatedly heated up and cooled down to achieve desired temperatures, typically using a Peltier plate. As this process is primarily based on conductive heat transfer (which is the slowest among the three heat transfer mechanisms: conduction, convention and radiation), it often takes a couple of minutes to complete a single cycle. Thus, it takes over an hour to finish typical 25–30 cycles of PCR. If this liquid is made to move over three different temperature areas within lab-on-a-chip, the time required for heating and cooling may be significantly reduced, thus leading to a faster PCR assay. Additionally, the liquid volume that is needed to be heated and

cooled is so small that the required heat transfer can be completed in much shorter amount of time. The first such demonstration was made by Kopp et al. (1998), where a single serpentine microfluidic channel travels through three different temperature zones to achieve 20-cycle PCR (Fig. 14.38). In this manner, <20-min or even <10-min 25-to-30-cycle PCR has become a possibility. Liquid flows through a microchannel continuously, or as discrete liquid plugs within a microchannel.

Later, other pre- and post-processes required for PCR assay have been demonstrated in microfluidic channels, including cell lysis, capillary electrophoresis to confirm PCR products, or fluorescence microscopy for real-time monitoring of PCR products.

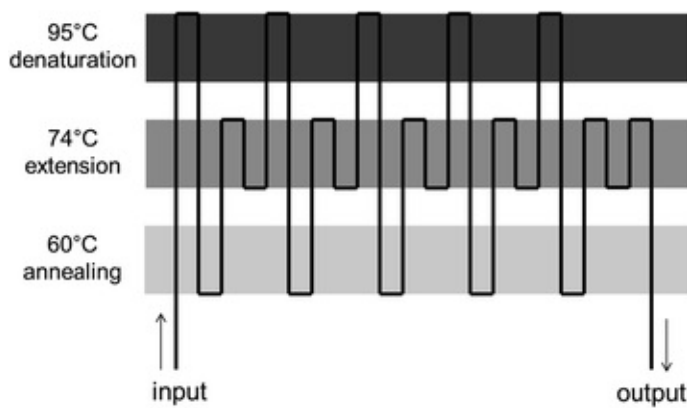


Fig. 14.38 Microchannel PCR on a chip

The problem of these attempts is that the user cannot change the assay protocol easily once the sample is introduced. In addition, the heat transfer throughout the microchannel device makes the heat isolation (required for thermocycling) very difficult, resulting in poor assay results.

The use of droplet microfluidics, including *electrowetting* or *magnetofluidics*, potentially enables this protocol change during experiments and better isolation of heat, which is called reprogrammable digital microfluidics. The use of small droplets allows for significantly lower reaction volumes and decreased assay times for many common laboratory procedures.

In electrowetting, or more precisely electrowetting-on-dielectrics (EWOD), droplets are allowed to move, split, and merge over a checkerboard patterned electrode. The droplet is attracted and moved to the electrode where a voltage is applied (electrowetting). Each electrode is maintained at three different temperatures and a droplet repeatedly moves over three electrodes to achieve thermocycling (Fig. 14.39). However, this method is comparatively more

difficult to fabricate and operate. An example of the issues is dielectric breakdown; other limitations include issues with diffusional mixing and contamination from increased wetting on the surface.

In magnetofluidics, a droplet containing paramagnetic particles moves over a superhydrophobic surface under the influence of an external magnetic field. For PCR, the surface is heated at three different temperatures and causes the droplet to move over three areas repeatedly (Fig. 14.40). However, paramagnetic particles need to be designed so as not to interfere with biological reactions, a capability that has not yet been confirmed. In addition, the paramagnetic particles are not optically transparent, which may also interfere with real-time quantification.

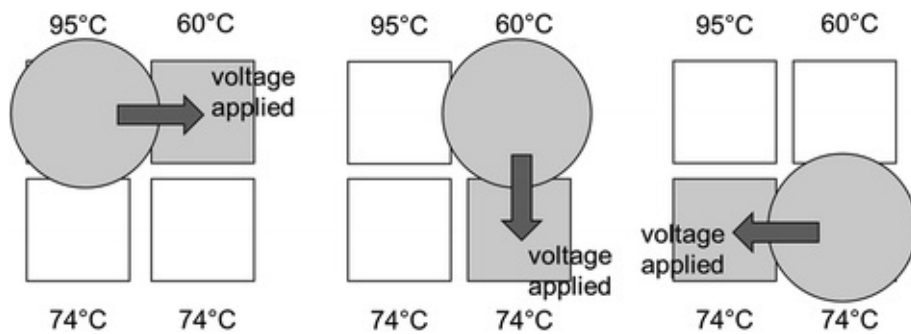


Fig. 14.39 EWOD droplet PCR

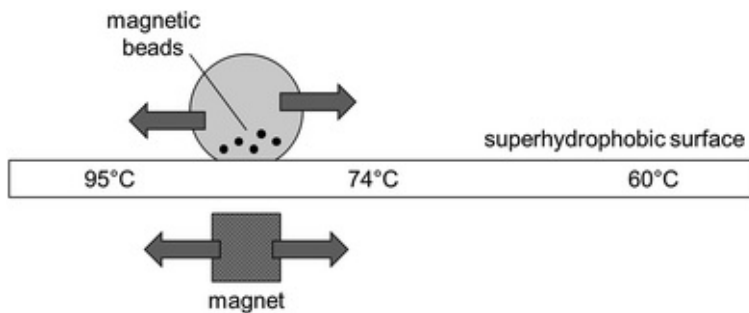


Fig. 14.40 Magnetofluidics droplet PCR

A better, yet simpler droplet-based PCR method has been recently proposed, called *wire-guided droplet PCR* (Harshman et al. 2014, 2015). Rather than using patterned electrode or a magnet superhydrophobic surface combination, it uses a wire or a syringe needle to guide the movement of a droplet. The droplet moves over three silicone oil baths, where it is also vibrated and rotated to achieve better mixing and faster convective heat transfer. All other LOC PCR demonstrations use either conductive heat transfer or very limited convective

heat transfer mechanisms. This method provides much faster thermocycling than the other droplet microfluidic PCR assays, typically less than 5–10 min, and allows easy incorporation of other procedures necessary for PCR assays, such as gene extraction, reverse transcription, and real-time quantification, etc. (Fig. 14.41).

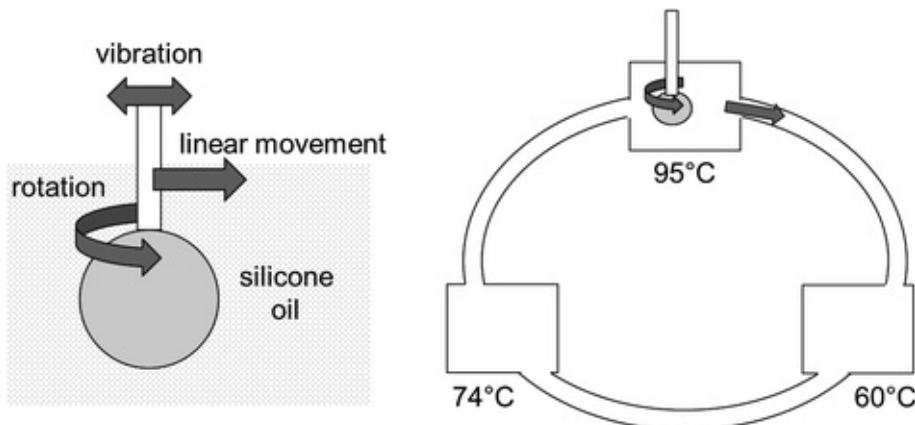


Fig. 14.41 Wire-guided droplet PCR

References and Further Readings

Microfluidics (Sect. 14.1)

Haeberle S, Zengerle R (2007) Microfluidic platforms for lab-on-a-chip applications. *Lab Chip* 7:1081–1220
[CrossRef]

Hogan J (2006) A little goes a long way. *Nature* 442:351–352
[CrossRef]

Lee SJ, Lee SY (2004) Micro total analysis system (μ -TAS) in biotechnology. *Appl Microbiol Biotechnol* 64:289–299
[CrossRef]

Sin MLY, Gao J, Liao JC, Wong PK (2011) System integration—a major step toward lab on a chip. *J Biol Eng* 5:6
[CrossRef]

Whitesides GM (2006) The origins and the future of microfluidics. *Nature* 442:368–373
[CrossRef]

Photolithography and Soft Lithography (Sect. 14.2)

Madou MJ (2002) Fundamentals of microfabrication, 2nd edn. CRC Press, Boca Raton

Saliterman SS (2006) Fundamentals of BioMEMS and medical microdevices. SPIE Press, Bellingham

CE in LOC (Sect. 14.3)

Chabinyc ML, Chiu DT, McDonald JC, Stroock AD, Christian JF, Karger AM, Whitesides GM (2001) An integrated fluorescence detectiodetection system in poly(dimethylsiloxane) for microfluidic applications. *Anal Chem* 73:4491–4498

[[CrossRef](#)]

Gerlach A, Knebel G, Guber AE, Hecke M, Herrmann D, Muslija A, Sshaller Th (2002) Microfabrication of single-use plastic microfluidic devices for high-throughput screening and DNA analysis. *Microsyst Technol* 7:265–268

[[CrossRef](#)]

Locascio LE, Perso CE, Lee CS (1999) Measurement of electroosmotic flow in plastic imprinted microfluidic devices and the effect of protein adsorption on flow rate. *J Chromatogr A* 857:275–284

[[CrossRef](#)]

POCT in LOC (Sect. 14.4)

Ducrée J (2009) Next-generation microfluidic lab-on-a-chip platforms for point-of-care diagnostics and systems biology. *Procedia Chem* 1:517–520

[[CrossRef](#)]

Fu E, Chinowsky T, Nelson, K, Johnston K, Edwards T, Helton K, Grow M, Miller JW, Yager P (2007) SPR imaging-based salivary diagnostics system for the detection of small molecule analytes. *Ann NY Acad Sci* 1098:335–344 (Figure 13.14)

Waggoner P, Craighead H (2007) Micro- and nanomechanical sensors for environmental, chemical, and biological detection. *Lab Chip* 7:1238–1255

[[CrossRef](#)]

Weibel DB, Kruithof M, Potenta S, Sia SK, Lee Am, Whitesides GM (2005) Torque-actuated valves for microfluidics. *Anal Chem* 77:4726–4733 (Figure 13.13)

Yager P, Edwards T, Fu E, Helton K, Nelson K, Tam MR, Weigl BH (2006) Microfluidic diagnostic technologies for global public health. *Nature* 442:412–418

[[CrossRef](#)]

IME Immunosensor in LOC (Sect. 14.4)

Ko S, Kim B, Jo S-S, Oh SY, Park J-K (2007) Electrochemical detection of cardiac troponin I using a microchip with the surface-functionalized poly(dimethylsiloxane) channel. *Biosens Bioelectron* 23:51–59

[[CrossRef](#)]

Varshney M, Li Y (2009) Review: interdigitated array microelectrodes based impedance biosensor for detection of bacterial cells. *Biosens Bioelectron* 24:2951–2960

[[CrossRef](#)]

Yang L, Li Y, Griffis CL, Johnson MG (2004) Interdigitated microelectrode (IME) impedance sensor for the detection of viable *Salmonella Typhimurium*. *Biosens Bioelectron* 19:1139–1147
[CrossRef]

Optical Fibers in LOC (Sect. 14.5)

Han J-H, Heinze BC, Yoon J-Y (2008) Single cell level detection of *Escherichia coli* in microfluidic device. *Biosens Bioelectron* 23:1303–1306
[CrossRef]

Kuswandi B, Huskens J, Verboom W (2007) Optical sensing systems for microfluidic devices: a review. *Anal Chim Acta* 601:141–155
[CrossRef]

Lucas LJ, Han J-H, Chesler J, Yoon J-Y (2007) Latex immunoagglutination for a vasculitis marker in a microfluidic device using static light scattering detection. *Biosens Bioelectron* 22:2216–2222
[CrossRef]

Psaltis D, Quake SR, Yang C (2006) Developing optofluidic technology through the fusion of microfluidics and optics. *Nature* 442:381–386
[CrossRef]

Yoon JY (2008) Latex immunoagglutination assay in lab-on-a-chip. *Biol Eng* 1: 79–84 (Figure 13.15)

Lab-on-a-CD (Sect. 14.6)

Madou M, Zoval J, Jia G, Kido H, Kim J, Kim N (2006) Lab on a CD. *Ann Rev Biomed Eng* 8:601–628
[CrossRef]

Mixing in LOC (Sect. 14.7)

Tabeling P (2009) A brief introduction to slippage, droplets and mixing in microfluidic systems. *Lab Chip* 9:2428–2436
[CrossRef]

Paper-based LOC (Sect. 14.8)

Cheung SF, Cheng SKL, Kamei DT (2015) Paper-based systems for point-of-care biosensing. *J Lab Automat* 20:316–333
[CrossRef]

Cho S, Park TS, Nahapetian TG, Yoon J-Y (2015) Smartphone-based, sensitive μPAD detection of urinary tract infection and gonorrhea. *Biosens Bioelectron* 74:601–611
[CrossRef]

Martinez AW, Philips ST, Wiley BJ, Gupta M, Whitesides GM (2008) FLASH: a rapid method for prototyping paper-based microfluidic devices. *Lab Chip* 8:2146–2150
[CrossRef]

Smartphone in LOC (Sect. 14.9)

Nicolini AM, Fronczek CF, Yoon J-Y (2015) Droplet-based immunoassay on a ‘sticky’ nanofibrous surface for multiplexed and double detection of bacteria using smartphones. *Biosens Bioelectron* 67:560–569
[CrossRef]

You DJ, Park TS, Yoon JY (2013) Cell-phone-based measurement of TSH using Mie scatter optimized lateral flow assays. *Biosens Bioelectron* 40:180–185 (Figure 14.21)

Zhu H, Mavandadi S, Coskun AF, Yaglidere O, Ozcan A (2011) Optofluidic fluorescent imaging cytometry on a cell phone. *Anal Chem* 83:6641–6647
[CrossRef]

Single Molecule Analysis in LOC (Sect. 14.10)

Craighead H (2006) Future lab-on-a-chip technologies for interrogating individual molecules. *Nature* 442:387–393
[CrossRef]

Chemical Analysis in LOC (Sect. 14.10)

deMello AJ (2006) Control and detection of chemical reactions in microfluidic systems. *Nature* 442:394–402
[CrossRef]

Feng X, Du W, Luo Q, Liu B-F (2009) Microfluidic chip: next-generation platform for systems biology. *Anal Chim Acta* 650:83–97
[CrossRef]

Janasek D, Franzke J, Manz A (2006) Scaling and the design of miniaturized chemical-analysis systems. *Nature* 442:374–380
[CrossRef]

MALDI TOF MS in LOC (Sect. 14.10)

Wheeler AR, Moon H, Kim C-J, Loo JA, Garrell RL (2004) Electrowetting-based microfluidics for analysis of peptides and proteins by matrix-assisted laser desorption/ionization mass spectrometry. *Anal Chem* 76:4833–4838
[CrossRef]

Wheeler AR, Moon H, Bird CA, Loo RRO, Kim C-J, Loo JA, Garrell RL (2005) Digital microfluidics with in-line sample purification for proteomics analyses with MALDI-MS. *Anal Chem* 77:534–540
[CrossRef]

Cell-on-a-chip (Sect. 14.10)

El-Ali J, Sorger PK, Jensen KF (2006) Cells on chips. *Nature* 442:403–411

[CrossRef]

Organ-on-a-chip (Sect. 14.10)

Esch MB, King TL, Shuler ML (2011) The role of body-on-a-chip devices in drug and toxicity studies. Annu Rev Biomed Eng 13:55–72
[CrossRef]

Huh D, Matthews BD, Mammoto A, Montoya-Zavala M, Hsin HY, Ingber DE (2010) Reconstituting organ-level lung functions on a chip. Science 328:1662–1668
[CrossRef]

Huh D, Hamilton GA, Ingber DE (2011) From 3D cell culture to organs-on-chips. Trends Cell Biol 21:745–754
[CrossRef]

LIA in LOC (Sect. 14.15)

Fronczek CF, You DJ, Yoon J-Y (2013) Single-pipetting microfluidic assay device for rapid detection of Salmonella from poultry package. Biosens Bioelectron 40:342–349
[CrossRef]

Heinze BC, Gamboa JR, Kim K, Song J-Y, Yoon J-Y (2010) Microfluidic immunosensor with integrated liquid core waveguides for sensitive Mie scattering detection of avian influenza antigens in a real biological matrix. Anal Bioanal Chem 398:2693–2700
[CrossRef]

Heinze BC, Yoon J-Y (2011) Nanoparticle immunoagglutination Rayleigh scatter assay to complement microparticle immuno-agglutination Mie scatter assay in a microfluidic device. Colloids Surf B 85:168–173
[CrossRef]

Song JY, Lee CH, Choi EJ, Kim K, Yoon JY (2011) Sensitive Mie scattering immunoagglutination assay of porcine reproductive and respiratory syndrome virus (PRRSV) from lung tissue samples in a microfluidic chip. J Virol Meth 178:31–38 (Figure 13.28)

You DJ, Geshell KJ, Yoon J-Y (2011a) Direct and sensitive detection of foodborne pathogens within fresh produce samples using a field-deployable handheld device. Biosens Bioelectron 28:399–406
[CrossRef]

Droplet LOC (Sect. 14.16)

Belder D (2005) Microfluidics with droplets. Angew Chem Int Ed 44:3521–3522
[CrossRef]

Berthier J, Silberzan P (2006) Microfluidics for biotechnology. Norwood, Artech House

Cho SK, Moon H, Kim C-J (2003) Creating, transporting, cutting, and merging liquid droplets by electrowetting-based actuation for digital microfluidic circuits. J Microelectromech Syst 12:70–80
[CrossRef]

Egatz-Gomez A, Melle S, Garcia AA, Lindsay SA, Marquez M, Dominguez-Garcia P, Rubio MA, Picraux ST, Taraci JL, Clement T, Yang D, Hayes MA, Gust D (2006) Discrete magnetic microfluidics. *Appl Phys Lett* 89:034106

[CrossRef]

Joanicot M, Ajdari A (2005) Droplet control for microfluidics. *Science* 309:887–888

[CrossRef]

Yoon J-Y, Garrell RL (2003) Preventing biomolecular adsorption in electrowetting-based biofluidic chips. *Anal Chem* 75:5097–5102

[CrossRef]

Yoon J-Y, You DJ (2008) Backscattering particle immunoassays in wire-guide droplet manipulations. *J Biol Eng* 2:15

[CrossRef]

Microchannel PCR (Sect. 14.16)

Huang FC, Liao CS, Lee GB (2006) An integrated microfluidic chip for DNA/RNA amplification, electrophoresis separation and on-line optical detection. *Electrophoresis* 27:3297–3305

[CrossRef]

Kopp MU, de Mello AJ, Manz A (1998) Chemical amplification: continuous-flow PCR on a chip. *Science* 280:1046–1048

[CrossRef]

Lien KY, Lee WC, Lei HY, Lee GB (2007) Integrated reverse transcription polymerase chain reaction systems for virus detection. *Biosens Bioelectron* 22:1739–1748

[CrossRef]

Mohr S, Zhang YH, Macaskill A, Day PJR, Barber RW, Goddard NJ, Emerson DR, Fielden PR (2007) Numerical and experimental study of a droplet-based PCR chip. *Microfluid Nanofluid* 3:611–621

Pal R, Yang M, Lin R, Johnson BN, Srivastava N, Razzacki SZ, Chomistek KJ, Heldsinger DC, Haque RM, Ugaz VM, Thwar PK, Chen Z, Alfano K, Yim MB, Krishnan M, Fuller AO, Larson RG, Burke DT, Burns MA (2005) An integrated microfluidic device for influenza and other genetic analyses. *Lab Chip* 5:1024–1032

[CrossRef]

Droplet PCR (Sect. 14.16)

Angus SV, Cho S, Harshman DK, Song J-Y, Yoon J-Y (2015) A portable, shock-proof, surface-heated droplet PCR system for Escherichia coli detection. *Biosens Bioelectron* 74:360–368

[CrossRef]

Chang Y-H, Lee G-B, Huang F-C, Chen Y-Y, Lin J-L (2006) Integrated polymerase chain reaction chips utilizing digital microfluidics. *Biomed Microdevices* 8:215–225

[CrossRef]

Harshman DK, Reyes R, Park TS, You DJ, Song J-Y, Yoon J-Y (2014) Enhanced nucleic acid amplification with blood in situ by wire-guided droplet manipulation (WDM). *Biosens Bioelectron* 53:167–174

[\[CrossRef\]](#)

Harshman DK, Rao BM, McClain JE, Watts GS, Yoon J-Y (2015) Innovative qPCR using interfacial effects to enable low threshold cycle detection and inhibition relief. *Sci Adv* 1:e1400061

[\[CrossRef\]](#)

Ohashi T, Kuyama H, Hanafusa N, Togawa Y (2007) A simple device using magnetic transportation for droplet-based PCR. *Biomed Microdevices* 9:695–702

[\[CrossRef\]](#)

You DJ, Tran PL, Kwon H-J, Patel D, Yoon J-Y (2011b) Very quick reverse transcription polymerase chain reaction for detecting 2009 H1N1 influenza A using wire-guide droplet manipulations. *Faraday Discuss* 149:159–170

[\[CrossRef\]](#)

15. Nanobiosensors

Jeong-Yeol Yoon¹✉

(1) University of Arizona, Tucson, AZ, USA

✉ Jeong-Yeol Yoon
Email: jyyoon@email.arizona.edu

So far, we have covered several different types of bioreceptors (enzymes, antibodies, nucleic acids, etc.) and transducers (optical, electrochemical, piezoelectric, thermal, etc.) that have commonly been used for biosensors. The performance of these biosensors can be greatly enhanced with the help of nanotechnology. *Nanotechnology*, by definition, deals with fabrication and application of materials that have a controllable feature size from 1 to 100 nm. Controllability is the key. We should be able to fabricate the desired nanometer features, or at least utilize them for our benefit.

Unique physical and chemical characteristics can be obtained with nanometer-sized structures, due to their size similarity to individual proteins or sometimes individual supramolecules, as well as their smaller size compared to the wavelengths of visible light (400–750 nm). Another important feature of nanostructures for biosensor applications is their extremely large surface area, specifically, a higher surface area to volume ratio. This enlarged surface area can accommodate increased numbers of bioreceptors (enzymes, antibodies, nucleic acids, etc.) that would lead to enhanced biosensor performance. In addition, the enlarged surface area also allows larger amounts of electric current or light (photons) to be delivered to optical or electrochemical detectors.

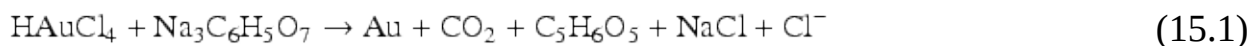
Many different nanostructured materials have been tested to enhance biosensor performance. Since it is impossible to cover in this chapter all the nanomaterials that have been used toward biosensing, we will focus on a couple of popular examples: gold nanoparticles (AuNPs), quantum dots (QDs), zinc

oxide (ZnO) nanostructures, carbon nanotubes (CNTs), and graphene.

15.1 Gold Nanoparticles (AuNPs)

Gold nanoparticles (AuNPs), also known as gold colloids or colloidal gold, are nanometer-sized spheres made primarily of gold. We have briefly touched on this topic in Chap. 13, as many commercial lateral-flow assays (LFAs) use AuNPs as labels. Typically, AuNPs range from 1 to 50 nm in size. Despite the availability of other types of metallic nanoparticles, AuNPs are preferred in biosensing due to their superior stability. In addition, gold itself does not show any adverse effect to the bioreceptors, which can easily be conjugated to AuNPs using *thiol* ($-SH$) chemistry. In addition, AuNPs do not destroy or denature target biomolecules, while many other metal nanoparticles do (e.g., silver nanoparticles destroy most of bacteria). The overall larger surface area accommodates higher number of bioreceptors to be used for a given volume, enhancing the optical or electrochemical signals and signal-to-noise ratio (S/N ratio). AuNPs have also been a popular subject for catalysis and enzyme studies, again due to the larger surface area.

AuNPs can be synthesized in several different ways. One of the most common methods is to reduce gold salt, typically hydrogen tetrachloroaurate ($HAuCl_4$) or potassium tetrachloroaurate ($KAuCl_4$), with citrate, for example, trisodium citrate ($Na_3C_6H_5O_7$). Upon dissolution into water, gold salt becomes gold ion, Au^{3+} , while citrate becomes citric acid ($C_6H_8O_7$). Citric acid reduces gold ion to gold metal in a sphere form, creating AuNPs:



Note that this reaction is just one possibility. Depending on the reaction condition, gold salt cannot fully be reduced and thus carry either hydroxyl (OH) or chlorine (Cl) groups, e.g., $[Au(OH)_2]^-$, $[AuCl_2]^-$, or $[AuClOH]^-$. The negative charges on the surface of the gold will be oriented toward the water phase, making this the major mechanism for stabilizing AuNPs in water (Fig. 15.1): All AuNPs carry negative charges at their surfaces, constantly repelling each other upon their movements, enabling the particles to be suspended in water without precipitating out from solution.

Another method of synthesizing AuNPs is to reduce gold salt with sodium borohydride:



Again, this is not the only possible route, and the end result may vary

depending on the reaction condition. This reaction is typically accompanied by alkane thiol, a long hydrocarbon chain terminated with a thiol ($-SH$) group, e.g., 1-dodecanethiol, $CH_3(CH_2)_{11}SH$ (Fig. 15.1). Among well-known chemicals, thiol is the only one capable of reacting with gold, creating a strong Au–S bond. The linear hydrocarbon chain acts like a spring for AuNPs, allowing them to bounce off one another, again enabling the particles to suspend in water without precipitating out from solution.

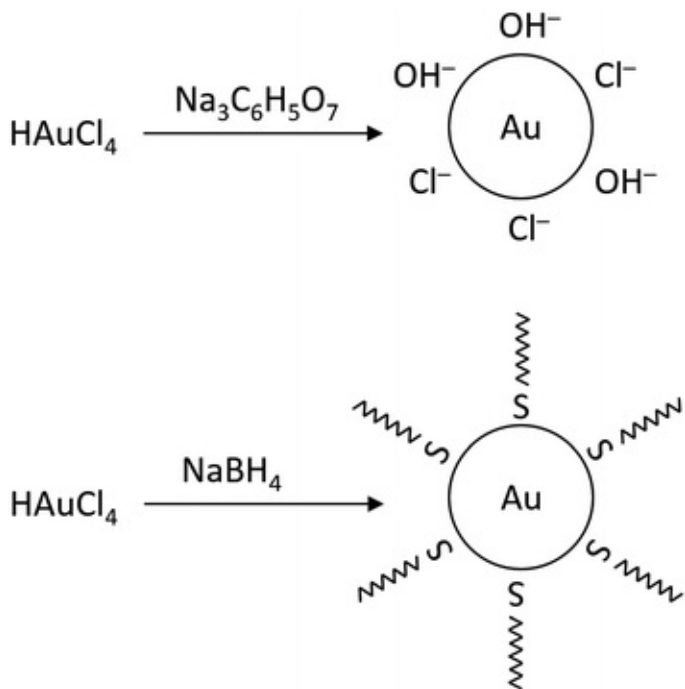


Fig. 15.1 Top: citrate reduction and stabilization by the surface charge. Bottom: borohydride reduction and stabilization by alkane thiol

The size of typical AuNPs, 1–50 nm, is comparable to the wavelength of electron movements in typical metal, about 1 nm. Therefore, the abundant electrons in gold (bear in mind that gold is very conductive both thermally and electrically) are mostly confined, generating a unique feature referred to as the quantum size effect . The theory behind the quantum size effect is quite complicated, and probably out of the scope of this textbook. For AuNPs, it would be sufficient to memorize that there will be a significant absorption band around 530 nm, referred to as the plasmon resonance band (PRB) .

As shown in Fig. 15.2, a strong absorbance in green color (peaked at 530 nm) and moderate absorbance in blue color will result in a pink coloration (strong red + weak blue). Note that this pink coloration is different from the inherent color of gold (shiny yellow). As the diameter of AuNPs increases, the

530 nm peak shifts slightly to a longer wavelength, approaching to the red-colored region. Consequently, more red color is absorbed, resulting in a pale, purple coloration (weak red + weak blue).

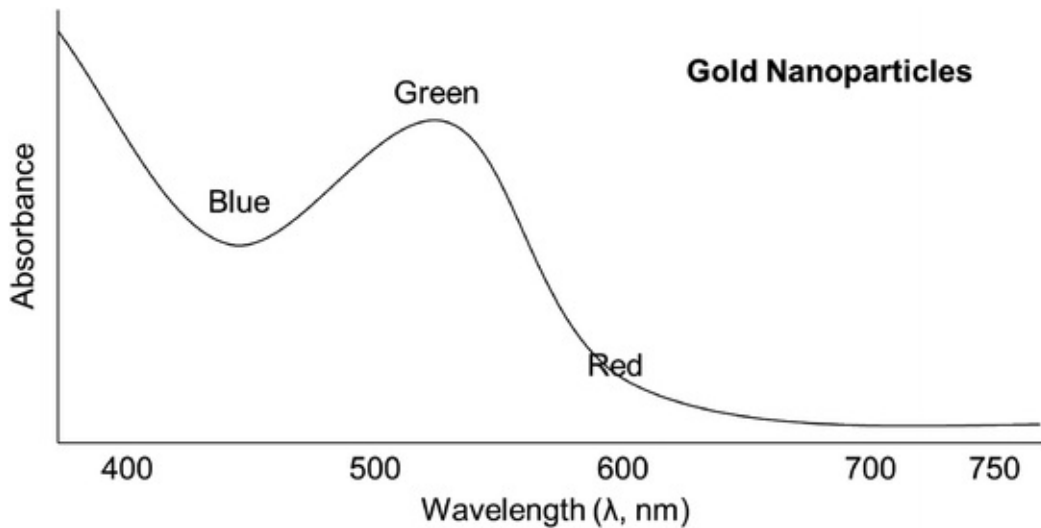


Fig. 15.2 Absorption spectrum of gold nanoparticles (AuNPs), indicating strong absorption in *green*, moderate absorption in *blue*, and almost no absorption in *red*. With *white light*, it will reflect most of *red* and some of *blue*, resulting a *pink* coloration (Identical to Fig. 13.9)

One common biosensor application of AuNPs is the LFA , which we have discussed in Chap. 13. AuNPs are currently being used for almost all types of LFAs, with a few exceptions utilizing fluorescent particles and quantum dots (QDs; which will be discussed in the following section). LFAs performed on paper are beneficial due to the capillary flow of samples through the fibers. The paper strips have no adverse effects on the high number of antibodies conjugated to the AuNPs. In addition, the PRB shows a very distinctive and significant coloration, which does not decay over time, or due to light exposure (while fluorescent dyes typically do decay over time, known as photobleaching; refer to Chap. 9).

Another popular category biosensor application of AuNPs is electrochemical enzymatic sensors, most notably electrochemical glucose sensors . The major advantages of AuNPs for electrochemical enzymatic sensors are (1) large surface area, which accommodates high number of enzymes, and (2) excellent electrical conductance, which leads to high signal-to-noise ratio (S/N ratio) and subsequently to high sensitivity. For this specific application, AuNPs are typically added to an electrode by electro-deposition or physical adsorption. AuNPs can also be mixed directly during the production of electrode. Typical electrodes that have been tested with AuNPs include glassy carbon electrodes

(GCE), crystalline gold, graphite, carbon paste, etc.

AuNP-enhanced electrochemical enzymatic sensors have extensively been tested for glucose sensing (Fig. 15.3). As described in the previous chapters, oxidation of glucose generates H_2O_2 as a byproduct, a target that can be optically or electrochemically detected. Since gold is a good catalyst for oxidizing H_2O_2 , AuNPs have become popular in improving the performance of glucose sensors. Enzymes, including glucose oxidase (GOx), do not lose their biological activity in the presence of AuNPs. Due to this, AuNP-covered electrodes are known to provide suitable microenvironments for enzymes (e.g., GOx). These microenvironments allow a great degree of freedom in molecular orientation, and therefore an increased number of enzymatic reactions. AuNPs also provide excellent electrical conductivity since gold acts as a conducting tunnel. The detection limit for H_2O_2 and glucose using AuNP-enhanced electrochemical sensing is low, typically 1–10 μm (roughly equivalent to a few tens of ng/ml).

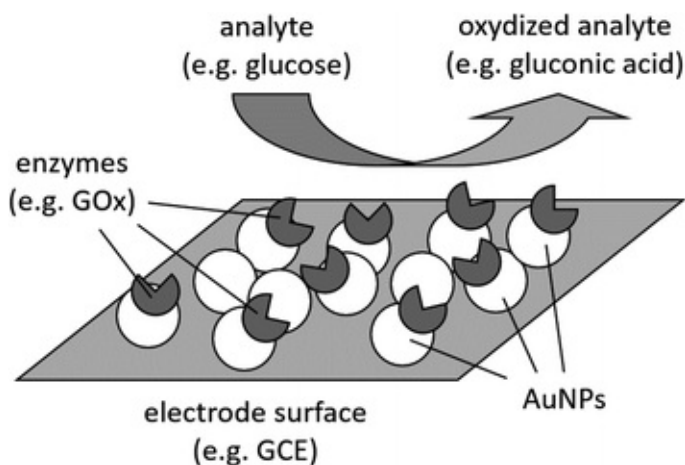


Fig. 15.3 Gold nanoparticles (AuNP) on an electrode surface (e.g., glassy carbon electrode GCE) are used for electrochemical biosensing (e.g., glucose detection using glucose oxidase GOx)

Recently, AuNPs are also being used for electrochemical immunosensing, in which the bioreceptors are antibodies (Fig. 15.4). In this case, ELISA-like assay are typically performed: electrode—AuNP—primary antibody—target—secondary antibody—antibody to antibody—enzyme—substrate (refer to Figs. 13.1 and 13.14). Likewise, aptamers can also be implemented in an ELONA-like assay (refer to Fig. 13.6). It is also possible to detect specific DNA sequences using short, single-stranded DNA probes (refer to Fig. 13.27). Both optical and electrochemical detection methods are possible with AuNP-enhanced ELISA, ELONA, and DNA sensors. Several papers have recently been published involving AuNP-enhanced immunosensing, specifically for the detection of

inflammatory markers, tumor markers, and pathogens from human blood and tissue. The reported detection limits are in the range of 1–100 pg/ml proteins, while the detection limits of conventional immunosensors are in the range of a few ng/ml proteins.

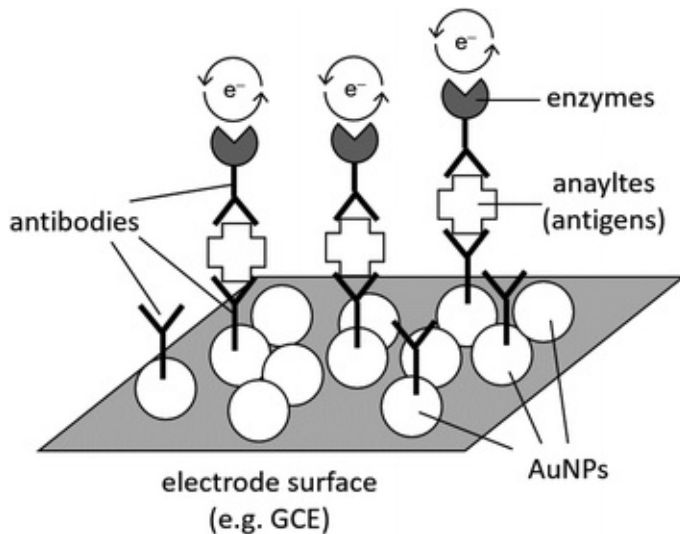


Fig. 15.4 Gold nanoparticle-enhanced ELISA (sandwich immunoassay). Similar schematic can be used for ELONA and DNA sensors

15.2 Quantum Dots (QDs)

QDs are essentially semiconductor nanocrystals. They typically comprise of two different semiconductor materials; examples include lead sulphide (PbS), lead selenide (PbSe), cadmium sulphide (CdS), cadmium selenide (CdSe), cadmium telluride (CdTe), etc. QD sizes are comparable to those of AuNPs, perhaps slightly bigger, thus providing similar characteristics: large surface area to volume ratio, quantum-size effect, etc. The major difference between them and AuNPs is that QDs exhibit fluorescence, or more precisely, *artificial fluorescence*. When the QDs are excited with light, typically UV (ultraviolet) light, the confined electrons (bear in mind that the small size forces the electrons to be confined with the QDs—quantum size effect) relax to the ground state. The extent of such relaxation is a function of the diameter of QDs. The bigger the QDs are the more relaxation of excited electrons is possible. More relaxation leads to a much lower energy light emission, equivalent to a longer wavelength ($E = hc/\lambda$). Emission wavelengths of QDs can easily be controlled by their diameters (referred to as *tunability*) (Fig. 15.5).

It is quite possible to make a mixture of variable-sized QDs, each conjugated

with different bioreceptors (enzymes, antibodies, or nucleic acids). Note that all differently sized QDs can be excited by a single-wavelength light source, typically UV. By looking at the emission wavelength, it is possible to determine which bioreceptor is bound to its target, therefore enabling a multiplexed assay.

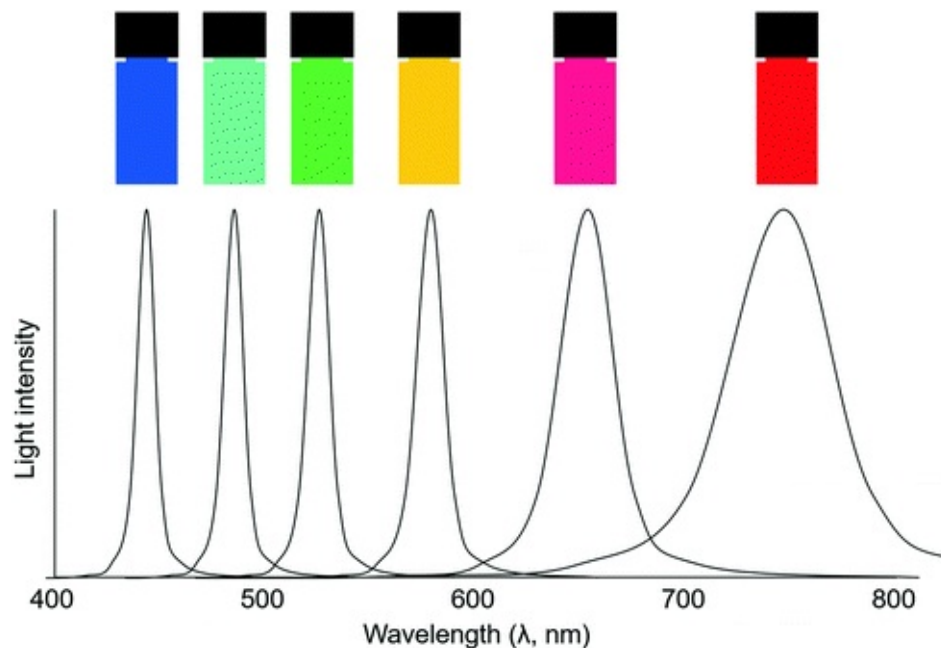


Fig. 15.5 Coloration (top) and emission spectra (bottom) of various CdTe QDs (varying their sizes) upon UV excitation

Due to their unique optical properties, QDs have been exclusively used for optical biosensing. QDs are much brighter and exhibit much less photobleaching than fluorescent dyes, which have been popularly evaluated for various biosensing applications. Unlike AuNPs, however, QDs do exhibit some toxicity to cells, and potentially denature some proteins. After all, they are made of heavy metals such as lead, cadmium, etc. In addition, the stability of QDs in aqueous mediums is not favorable, meaning they often precipitate out from solution if not treated appropriately. Consequently, many commercially available QDs, such as Qdot® Nanocrystal Probes from Molecular Probes® (a division of Life Technologies), are modified with polymer coatings, followed by some linker biomolecules such as streptavidin or neutravidin (popular in conjugating DNA probes), or protein A (has a strong affinity to the Fc portion of antibodies).

15.3 Zinc Oxide (ZnO) Nanostructures

Various nanostructures can be fabricated using metal oxide materials based on

copper, iron, nickel, tin, titanium, zinc, or zirconium. Due to their oxidized status, they are not charged but still hydrophilic (water-loving), thus quite biocompatible, which is a good trait for biosensor applications. Various types of nanostructures have been fabricated using metal oxides such as nanobelts, nanocombs, nanofibers, nanoflakes, nanoforks, nanonails, nanoneedles, nanopores, nanorods, nanosheets, nanoparticles, nanotubes, nanowalls, etc. These nanostructures provide high surface-to-volume ratios, allowing for higher loading of bioreceptors, as well as catalytic capability (similar to AuNPs). ZnO nanostructures are particularly popular in biosensor applications, due to their low material cost, nontoxicity, and high surface charge (advantageous for electrochemical biosensing). In addition, ZnO can easily be incorporated into complementary metal–oxide–semiconductors (CMOS), as both ZnO and CMOS are metal oxides. This similarity allows them to be jointly incorporated into small, integrated biosensor devices. Due to the compatibility with semiconductor devices, ZnO nanostructures have primarily been evaluated for use in electrochemical biosensors. In addition, electrochemical signals (voltage or current) from ZnO nanostructure-based biosensors can also be amplified and transmitted via field-effect transistor (FET) devices, allowing for the possibility of wireless remote biosensing. Implantable monitoring of glucose (and potentially other biomolecules as well) can become a reality with ZnO nanostructure-based biosensors.

ZnO nanostructures can either be grown or deposited on typical electrode surfaces, including carbon, gold, platinum, silicon, and indium tin oxide (*ITO*—another metal oxide similar to ZnO). Both ZnO nanorods and ZnO nanowires have been shown to grow on carbon and gold electrodes. After fabrication, enzymes and electron mediators can be immobilized on the nanostructured surfaces (refer to Sect. 14.1) (Figs. 15.6 and 15.7). ZnO nanoparticles , ZnO nanosheets , ZnO nanotubes have also been deposited onto electrode surfaces, and included the addition of enzymes and electron mediators.

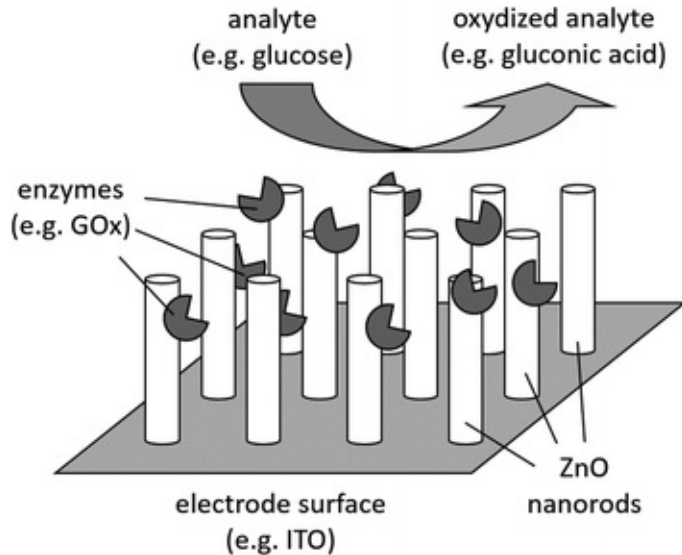


Fig. 15.6 ZnO nanorods on an electrode surface (e.g., indium tin oxide *ITO*) are used for electrochemical biosensing (e.g., glucose detection using glucose oxidase *GOx*)

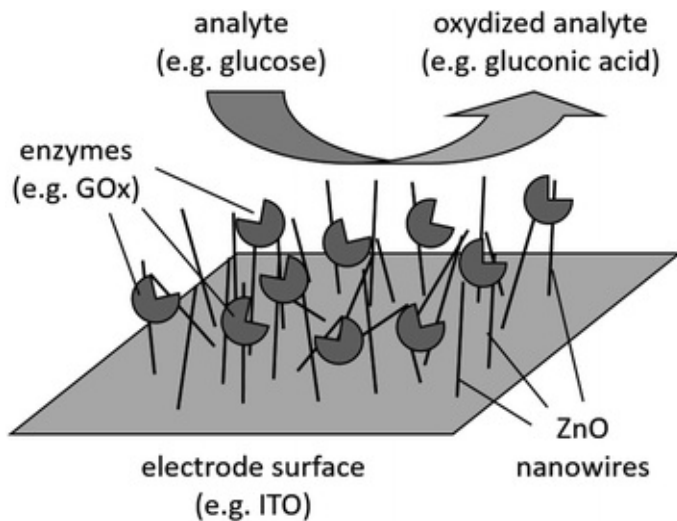


Fig. 15.7 ZnO nanowires on an electrode surface (e.g., indium tin oxide *ITO*) are used for electrochemical biosensing (e.g., glucose detection using glucose oxidase *GOx*)

Porous films of ZnO can also be added to the electrode surfaces, to serve as a membrane filter for sample purification. For example, the ZnO nanowire schematic shown in Fig. 15.8 can only capture target bacteria, but not the human cells.

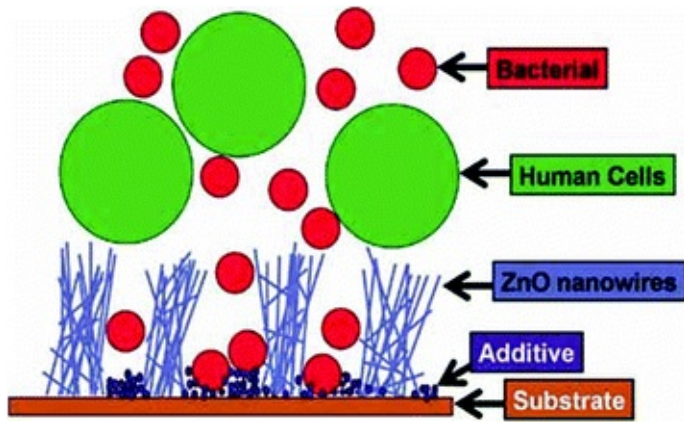


Fig. 15.8 ZnO nanowires act as a filter to capture bacteria in the presence of human cells. Wang et al. (2009), reprinted with permission

Glucose oxidase (GOx; to detect glucose), cholesterol oxidase (ChOx; to detect cholesterol), alcohol dehydrogenase (ADH; to detect alcohol), lactic oxidase (to detect lactic acid), etc., have been used along with ZnO nanostructures. The electron transfer within ZnO nanostructure-based electrochemical biosensors is quite fast, with typical response times of less than 10 s. The rapid response time allows for sensitive and reproducible signals. Typical detection limits are 1–10 μm for most chemicals (glucose, cholesterol, alcohol, lactic acid, etc.), which is roughly equivalent to a few tens of ng/ml. These numbers are essentially within the same range as AuNP-enhanced biosensors. Similar to AuNP-enhanced biosensors, ZnO nanostructure-enhanced biosensors can also be used for immunoassays (ELISA), aptasensors (ELONA), as well as DNA sensors, again with improved sensitivity and lower detection limits.

15.4 Carbon Nanotubes (CNTs) and Graphene

Pure carbon molecules can be interconnected together to form hexagonal- or honeycomb-shaped structures. If these structures form a single-layered, two-dimensional sheet, it becomes graphene . If they make a cylindrical tube, it becomes CNTs (Fig. 15.9). The existence of hexagon-shaped structures made purely out of carbon has long been speculated since the 1950s, but the actual isolation and synthesis came relatively later. The first synthesis of CNTs has generally been attributed to Sumio Iijima at NEC Corporation (Iijima 1991), although there exists some important findings prior to this work. Single-layered graphene synthesis came in even later (Novoselov et al. 2004).

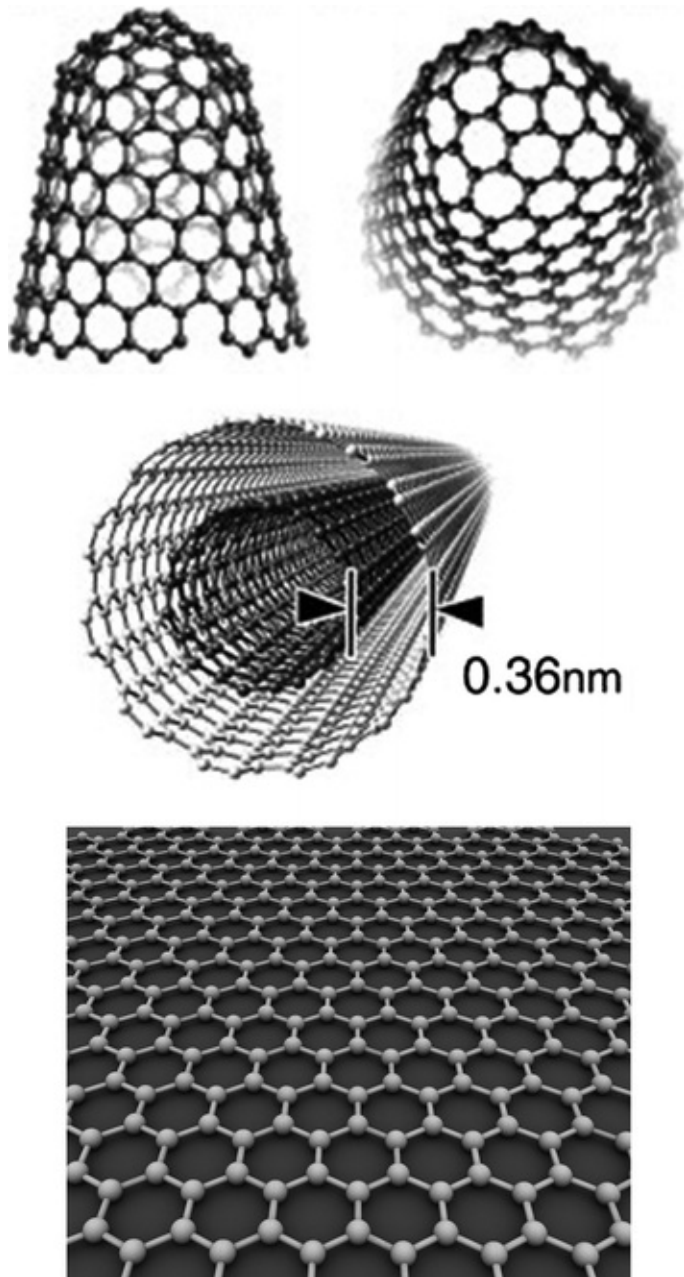


Fig. 15.9 Single-wall carbon nanotube (SWCNT; top), multi-wall carbon nanotube (MWCNT; middle), and graphene (bottom). Top and middle images: Iijima (2002), reprinted with permission. Bottom image Picture taken by AlexanderAIUS in August 2010 and placed in public domain. Accessed October 2015 from <https://commons.wikimedia.org/wiki/File:Graphen.jpg>

CNTs can be made as single-walled tubes, referred to as single-wall carbon nanotubes (SWCNTs), or with multiple layers of tubes, referred to as multiwall carbon nanotubes (MWCNTs). The highly ordered structure of CNTs creates remarkable tensile strength and high resistivity, while the atomic-scale cylindrical structure provides excellent flexibility (i.e., it can easily be bent

without being broken). These unique features have prompted many scientists and engineers to develop much more durable yet resilient materials—for example, addition of CNTs into carbon-fiber composites can significantly enhance the performance of baseball bats or golf clubs. Obviously, we are more interested in utilizing these CNTs toward biosensor applications. Just like other nanomaterials, the surface-to-volume ratio of CNTs is high. This feature leads to more bioreceptor immobilization and improved signal transduction.

Conjugation of bioreceptors to CNTs is difficult, since CNTs are made purely out of carbon. Typically, carboxyl groups are added to CNTs, to accommodate their binding to the amine groups on bioreceptors. It is possible to utilize electrostatic attraction or hydrogen bonding between these carboxyl and amine groups. However, the better-practiced method is to utilize carbodiimide (in the form of $\text{RN} = \text{C}=\text{NR}'$), to covalently conjugate the carboxyl group on CNTs with the amine group on bioreceptors. This forms a very stable peptide bond ($-\text{CO}-\text{NH}-$) between the CNTs and bioreceptors. Alternatively, polymer coatings can be added to CNTs, similar to the QDs, followed by a linker molecule such as streptavidin/biotin or protein A.

Similar to CNTs, graphene can also provide remarkable strength, stiffness, and stability, which can be utilized for various materials applications. Again, graphene can be made into single or multi-layered sheets, analogous to CNTs. Specifically for graphene, excellent heat and electricity conductance have been noted, which is an important characteristic useful in electrochemical biosensing (Fig. 15.10). Graphene is essentially a single-atom-thick (for single layer) sheet of carbon atoms in a honeycomb pattern. This unique structure allows for extremely rapid electron transfer kinetics. Similar to ZnO nanostructure-based biosensors, these electrochemical signals can be amplified via FET devices. Due to these characteristics, graphene has been popularly evaluated for electrochemical kinetic measurements, such as cyclic voltammetry or electrochemical impedance spectroscopy (EIS).

Conjugation of bioreceptors to graphene is typically achieved by oxidizing graphene into graphene oxide (GO), thus making it similar to ZnO. Oxidation is typically made with chemicals or by applying electrical potential. This added oxygen can accommodate the binding of bioreceptors to graphene. Carboxyl or amine groups can additionally be added to this oxygen, and bioreceptors can be conjugated via either hydrogen bonding or covalent conjugation (with carbodiimide). Despite this advantage, GO is less robust, has higher detection limit, and shows slower electron transfer than grapheme. For both graphene and GO, DNA probes can be formed into hairpin shapes, and can be subsequently stacked on top of a hexagonal carbon structure, utilizing π -stacking interactions

(the hexagonal ring structure is stabilized by sp^3 orbital hybrids coming from π bonds among carbon atoms), thus requiring no chemical modification to graphene. Upon binding to a target DNA sequence, the hairpin structure opens up, leading to significant decrease in the charge transfer resistance.

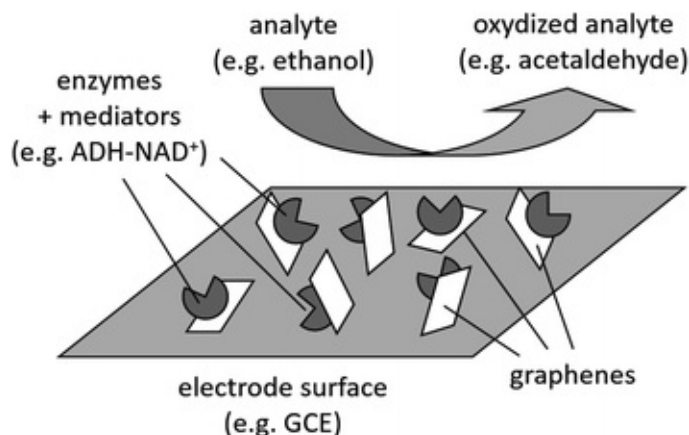


Fig. 15.10 Graphene fragments on an electrode surface (e.g., glassy carbon electrode GCE) are used for electrochemical biosensing (e.g., ethanol detection using alcohol dehydrogenase or ADH and NAD⁺ as electron mediator; refer to Fig. 12.8 for detail reaction scheme)

Similar to other nanomaterials, both CNTs and graphene sheets can be deposited onto an electrode surface, and secondly bioreceptors can be conjugated onto them. The reported detection limits are again in the range of 1–10 μm for most chemicals, roughly equivalent to a few tens of ng/ml. The detection limits for CNTs or graphene in DNA and biomolecule sensing are quite low, typically in the range of pM or sub-pM scale. The mismatch of a single base pair (known as *single* nucleotide polymorphism or SNP) can be detected with this approach, meaning excellent selectivity and sensitivity.

15.5 Nanoporous Gold

All the methods described in the previous sections involved the deposition or growing of nanostructures on top of electrodes, such as GCE or ITO electrodes. In these instances, there is an inherent danger that such nanostructures may be unintentionally removed from the electrode surfaces, or aggregate/agglomerate upon exposure to harsh experimental conditions. Creation of nanoporous materials is generally considered as a good alternative, however, the resulting porous structure can become quite random and difficult to control its dimensions and surface properties. Nanoporous materials can be fabricated in a variety of

methods that are outside the scope of this textbook. One of the most popular nanoporous materials is nanoporous gold (NPG), which can be made by the procedure referred to as *dealloying corrosion*. This process is formed through a 50:50 alloy of gold and silver (known as 12-carat white gold) that can be exposed to a corrosive solution (e.g., nitric acid). Since gold is much more stable than silver, silver is corroded away while gold is not, thus creating nanoporous structures. The resulting NPG can be used for electrochemical enzymatic biosensing, immunosensing, aptasensing, and DNA sensing, as discussed previously for other types of nanostructure biosensing (Fig. 15.11).

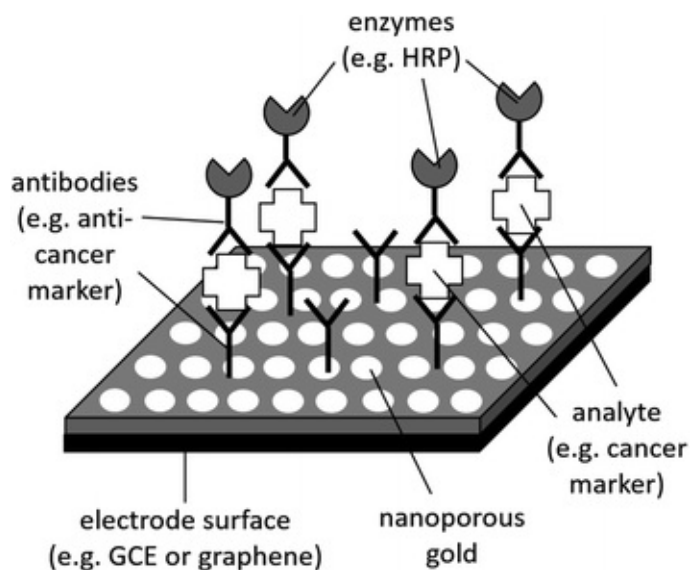


Fig. 15.11 Nanoporous gold on an electrode surface (GCE or graphene) is used for sandwich immunoassay (e.g., cancer marker detection using antibody to cancer marker) in conjunction with an enzyme (e.g., horseradish peroxidase HRP)

15.6 Concluding Remarks

All nano-biosensors described in this chapter have been evaluated and tested for a wide variety of target analytes. While the electrochemical detection of small chemicals using appropriate enzymes have extensively been investigated in the past, such as glucose (using GOx), cholesterol (using ChOx), ethanol (using ADH), lactic acid (using lactic oxidase), etc., recent research efforts are more geared toward immunosensing, aptasensing, and DNA sensing. ELISA-like immunosensing is by far the most studied application of nano-biosensors.

Nano-immunosensors coupled with electrochemical detection have been evaluated for the identification and quantification of protein markers from human bodily fluids (blood, urine, saliva, etc.). A brief list of previously detected

targets includes: inflammatory response markers (such as interleukin 6 = IL-6), and cancer markers (α -fetoprotein = AFP; prostate-specific antigen = PSA; carcinoembryonic antigen = CEA; cancer antigen 125 = CA-125; cancer antigen 15-3 = CA 15-3; carbohydrate antigen 19-9 = CA 19-9; human chorionic gonadotropin = hCG, etc.). Nano-immunosensors with electrochemical detection have also been tested for detecting bacterial and viral pathogens from human bodily fluids, as well as food and water samples. The most commonly studied pathogens are: *Escherichia coli*, *Salmonella Typhimurium*, *Mycobacterium tuberculosis*, human immunodeficiency virus (HIV), influenza A, hepatitis B virus, etc. For both cases, nano-immunosensors with electrochemical detection have shown improved sensitivity, selectivity, and very low detection limits, typically down to 1–100 pg antigens per mL sample. These detection limits are comparable to many other optical-based detection methods, but offer enhanced portability and simplicity since the electrochemical transducers are typically smaller and simpler than the optical transducers.

Although much attention has been paid to the electrochemical detection of nano-immunosensors in the past decade, the optical detection of nano-immunosensors deserves more attention in the future (so far, AuNPs and QDs have been popularly used for optical nano-immunosensing).

References and Further Readings

- Brown LO, Hutchison JE (2001) Formation and electron diffraction studies of ordered 2-D and 3-D superlattices of amine-stabilized gold nanocrystals. *J Phys Chem B* 105:8911–8916
[CrossRef]
- Córcoles EP, Boutelle MG (2013) Biosensors and invasive monitoring in clinical applications. Springer, Heidelberg
- Daniel M-C, Astruc D (2004) Gold nanoparticles: assembly, supramolecular chemistry, quantum-size-related properties, and applications toward biology, catalysis, and nanotechnology. *Chem Rev* 104:293–346
[CrossRef]
- Gu MB, Kim H-S (eds) (2014) Biosensors based on aptamers and enzymes. Springer, Heidelberg
- Iijima S (1991) Helical microtubules of graphitic carbon. *Nature* 354:56–58
[CrossRef]
- Iijima S (2002) Carbon nanotubes: past, present, and future. *Phys B* 323:1–5
[CrossRef]
- Molecular Probes® (2015) Qdot® nanocrystal technology overview. <http://www.lifetechnologies.com/us/en/home/brands/molecular-probes/key-molecular-probes-products/qdot/technology-overview.html>

Novoselov KS, Geim AK, Morozov SC, Jiang D, Zhang Y, Dubonos SV, Grigorieva IV, Firsov AA (2004) Electric field effect in atomically thin carbon films. *Science* 306:666–669
[CrossRef]

Ojea-Jiménez I, Campanera JM (2012) Molecular modeling of the reduction mechanism in the citrate-mediated synthesis of gold nanoparticles. *J Phys Chem C* 116:23682–23691
[CrossRef]

Paulus PM, Goossens A, Thiel RC, van der Kraan AM, Schmid G, de Jongh LJ (2001) Surface and quantum-size effects in Pt and Au nanoparticles proved by ^{197}Au Mössbauer spectroscopy. *Phys Rev B* 64:205418
[CrossRef]

Rahman MM, Ahammad AJS, Jin J-H, Ahn SJ, Lee J-J (2010) A comprehensive review of glucose biosensors based on nanostructured metal-oxides. *Sensors* 10:4855–4886
[CrossRef]

Tiwari A, Turner APF (eds) (2014) Biosensors nanotechnology. Scrivener Publishing, Beverly

Wang X, Zhu H, Yang F, Yang X (2009) Biofilm-engineered nanostructures. *Adv Mater* 21:2815–2818
[CrossRef]

Appendix: Microcontroller

Although this book is designed primarily for studying physical sensors and biosensors, you may want to further “control” the sensor readout, such as:

- Filter, condition, and amplify voltage signals (analog and digital)
- Convert conditioned/amplified analog voltages into digital signals (A/D converting)
- Display digital signals in numeric on an LCD (liquid crystal display) panel
- Store data (data logging)
- Use the sensor output to control the process (e.g., feedback control of temperature)

In Chap. 6 , we learned a great deal of analog signal filtration/conditioning/amplification using op-amp. All other controls, including digital signal filtration/conditioning/amplification, A/D conversion, displaying results, data logging, and process control, have typically been made by using a computer with an appropriate interface board (typically a *data acquisition board* and/or an *A/D converter board*).

Nowadays, all of these controls can be made with a simple *microprocessor-based controller* , or a *microcontroller* (a microprocessor is a special type of integrated circuit, IC). There is an open-source microcontroller that is extremely popular, called *Arduino* . Here is a description on Arduino from its website www.arduino.cc :

Arduino is a tool for making computers that can sense and control more of the physical world than your desktop computer. It's an *open-source* physical computing platform based on a simple microcontroller board, and a development environment for writing software for the board. Arduino can be used to develop interactive objects, taking inputs from a variety of switches or sensors, and controlling a variety of lights, motors, and other physical outputs.

The Arduino board is an open-source physical computing platform. As it is open-source, you can assemble your own Arduino by purchasing the appropriate components. However, we recommend that you purchase the assembled version of it as it is fairly inexpensive (<\$30). Software is free to download from www.arduino.cc . This low cost is made possible as there is no royalty or patent involved (open-source).

Figure A.1 shows one type of assembled Arduino board, called Arduino Uno. The biggest IC in an Arduino board is a microcontroller, which is essentially a cheaper and simpler version of a computer's CPU (central processing unit). On the top left corner, there is a USB jack, where the Arduino board can be connected to and communicate with a computer. The user writes a software code in simplified C programming language, compiles it, and sends its machine code to the microcontroller through this USB connection. This USB connection is essentially a serial port (RS-232C).

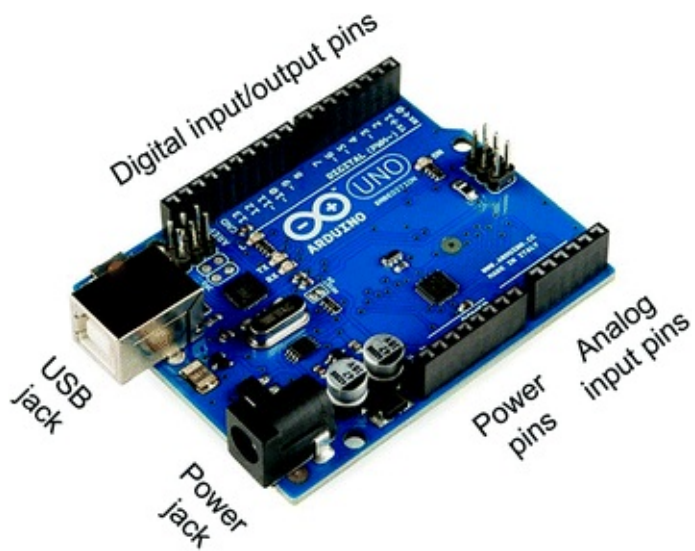


Fig. A.1 Arduino board. Picture taken by SparkFun Electronics in January 2013 and placed in public domain. Accessed October 2015 from https://commons.wikimedia.org/wiki/File:Arduino_Uno_-_R3.jpg

The Arduino board accepts both analog and digital signals. The analog voltage signals are accepted at the analog input pins located at the lower right corner, and converted to digital signals using its own A/D converter. On top of the board there are digital pins, which are used for both input and output.

The Arduino can draw its power from three different sources. It can use external power supply, through a power jack located at the lower left corner, which is connected to an AC-to-DC adaptor. It can also draw power through power pins, located right next to the analog input pins, typically from a breadboard with a separate DC power. Finally, the USB port can also be used to power the Arduino board, which the USB connection is capable of. In this case, the Arduino board draws its power from a computer.

There are many components and devices available in the open-source market that are made to work with the Arduino board. Relays, switches, small keyboards, mice, joysticks, small LCD panels, DC stepper motors, and speakers

are available in the market at relatively cheap prices. The Arduino board can certainly be used for sensor readout, but it can be much more powerful if used for process control. Several different process control algorithms can easily be implemented in C programming language to generate the controller output signals.

There are other types of microcontrollers available, with more memory, faster processor speed, and the ability to communicate with other input/output devices such as keyboard, mouse, monitor, Bluetooth, or even WiFi. *Raspberry Pi* and Intel ® *Galileo* are probably the most well-known and popular alternatives to Arduino. The price tag of Raspberry Pi is slightly higher than Arduino, and that of Galileo is even higher, although all of them are priced at less than \$100.

Raspberry Pi (Fig. A.2) is a good alternative to Arduino, again with open-source and open architecture. The notable difference from Arduino is the inclusion of GPU (graphics processing unit), allowing the board to be connected to monitors, as well as the Ethernet port for networking. Additionally, Linux operating system is loaded on the board, allowing the board to function as a standalone computer.

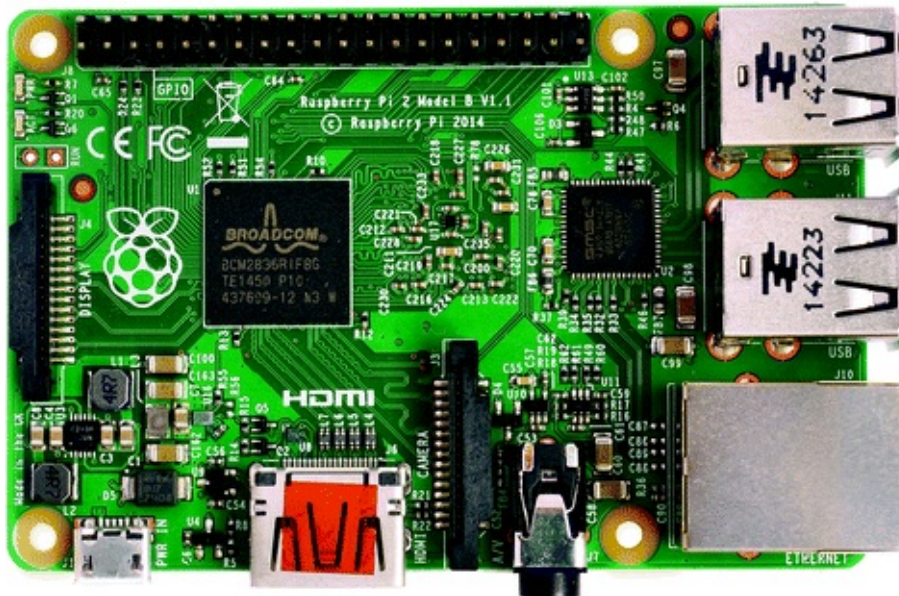


Fig. A.2 Raspberry Pi 2 model B. Picture taken by Lucasbosch in July 2014 and placed in public domain. Accessed October 2015 from https://commons.wikimedia.org/wiki/File:Raspberry_Pi_B%2B_top.jpg

The only downside of Raspberry Pi is that it is not really compatible with Arduino. Therefore, Intel came up with the idea of improving the Arduino board with an Intel-based processor (Pentium-equivalent), called Intel ® Galileo (Fig.

A.3). While equipped with a faster processor, more memory, and the ability to work with various input/output devices, its pin connections are still compatible with Arduino.

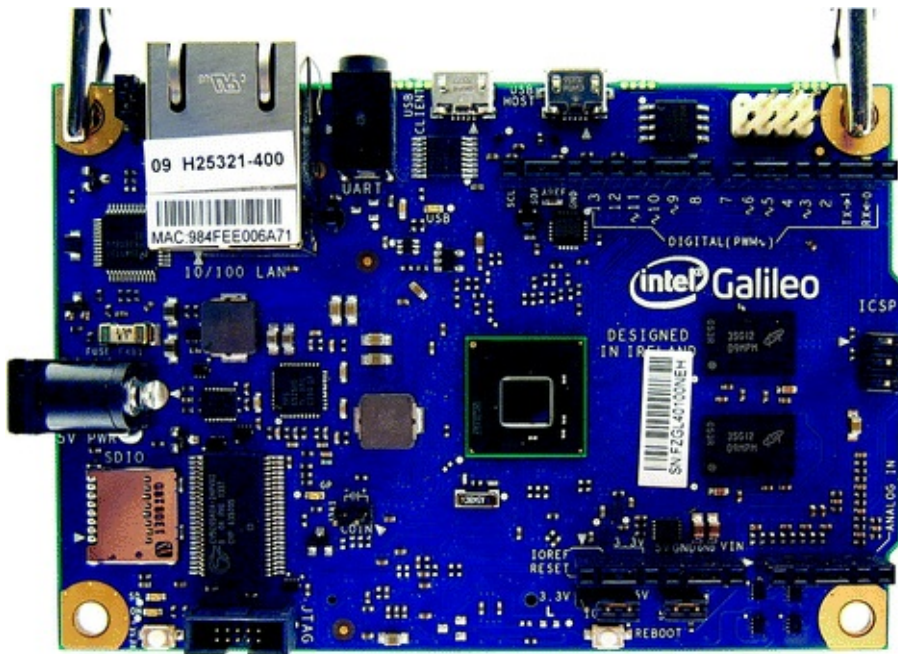


Fig. A.3 Intel® Galileo Gen 2. Picture taken Ordercrazy and Regi51 in February 2014 and placed in public domain. Accessed October 2015 from https://commons.wikimedia.org/wiki/File:Embedded_World_2014_Intel_Galileo_01.jpg

In this chapter, we learned how to use a microcontroller board, specifically the Arduino, toward A/D converting, digital signal processing, displaying sensor readout on an LCD panel, and basic process control (light and temperature control).

Laboratory Task 1: Light Control

In this task we will learn how the Arduino board can accept analog signals and display its reading on an LCD panel. We will repeat Task 2 of Chap. 7 , the photovoltaic operation of a PIN photodiode. In this task, you will need the following:

- A breadboard, wires, wire cutter/stripper, a power supply, and a DMM
- Arduino software (freely available from www.arduino.cc) (Fig. A.4)
- Arduino board (Arduino Duemilanove or equivalent)

- A computer with a USB port (Windows, Mac OS X or Linux)
- Any LCD panel that is compatible with Hitachi HD44780 driver
- One $220\ \Omega$, two $1\ k\Omega$, and two $10\ k\Omega$ resistors
- PIN-040A photodiode
- Op-amp LM741 (or LM324)
- Incandescent light bulbs (with sockets): 15, 40, or 60 W
- Red LED
- Ruler
 - The first thing you need to do is to download and install the Arduino software to your computer. There are three versions of it for Windows, Mac OS X, and Linux (32-bit). The software comes with a compressed (zipped) folder, and all you need to do is to extract them to an appropriate folder.
 - The Arduino board can be powered from an external power supply (7–12 V) through the AC-to-DC power adaptor. Alternatively, it can be powered from a computer through a USB port.
 - Once Arduino board is powered, the V_{out} pin in the power pins can be used to power up the other device. Use $+5\ V_{out}$ and GND pins to power the LCD panel.
 - Connect the Arduino board to a computer using a standard USB cable. Your computer should recognize the Arduino board as a new hardware, and try to install its driver. The driver can be found in the extracted folder of the software.
 - The Arduino board's USB port is essentially a serial port. Therefore, the second driver, “USB serial converter,” needs to be installed. This installation will occur automatically. Again, this driver can also be found in the same extracted folder of the software.
 - Launch the software (arduino.exe) that can be found in the extracted folder. Choose Tools > Serial Port to set up your port. Serial ports that are connected via USB should have port numbers of COM3, COM4, or COM5. If you are not sure, check the Device Manager of your computer to find out the correct port number for the USB serial converter.

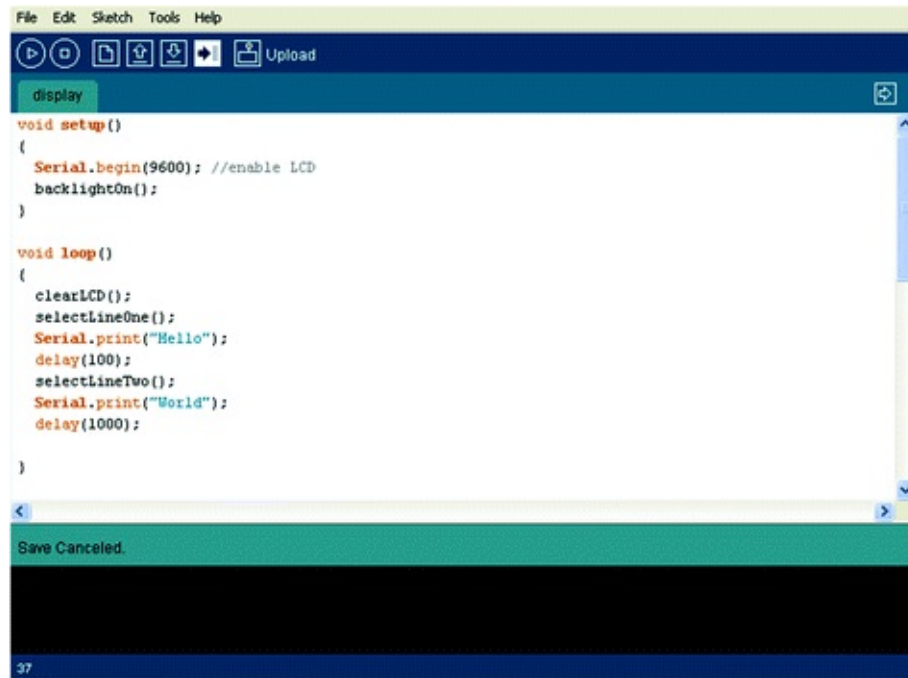


Fig. A.4 Arduino software

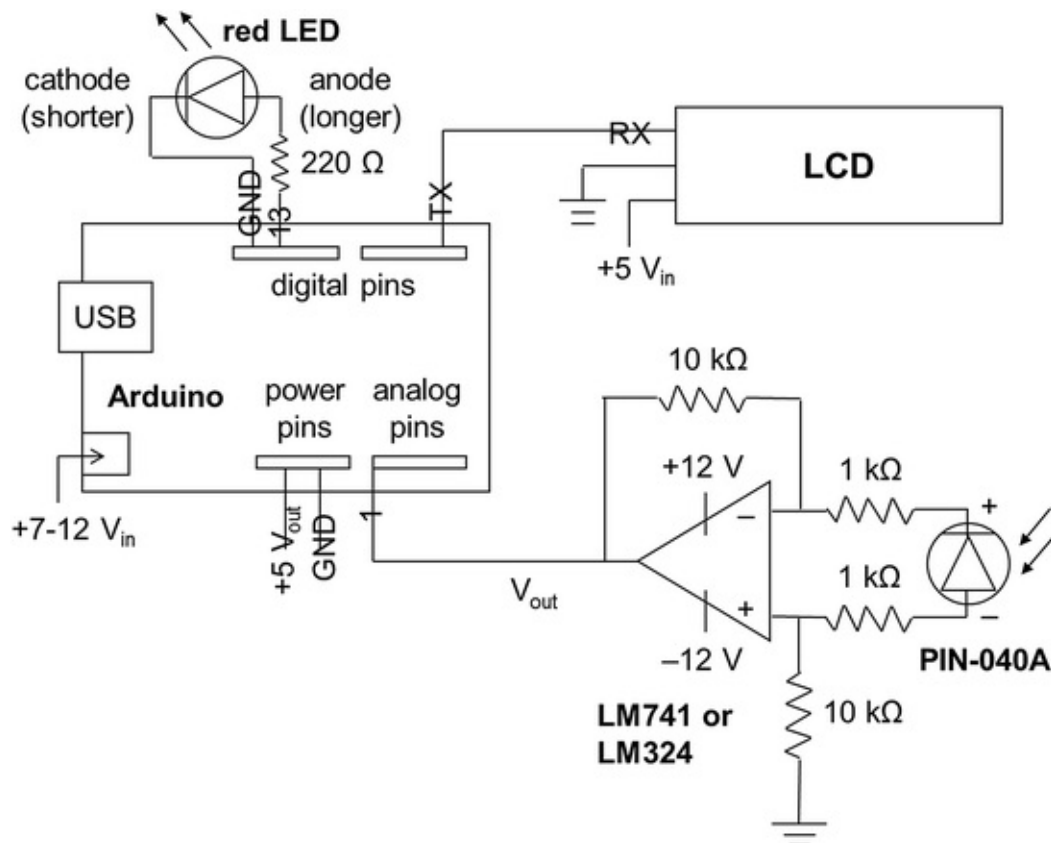


Fig. A.5 Circuit diagram for Task 1. The Arduino board draws power from a computer via USB or from a power adapter. The LCD panel draws power ($+5 V_{out}$ and GND) from Arduino board

via power pins. The op-amp draws power (+12 V, -12 V, and GND) from a separate power supply

Figures A.5 and A.6 show the circuit layout.

- The op-amp LM741 (or LM324) requires ± 12 V, which the Arduino board cannot provide (it generates +3.3 and +5 V), so a separate power supply (the one we have used in the previous chapters) is needed: +12, -12 V, and GND. The LCD panel is powered by +5 V and GND from the power pins of Arduino board. The ground (GND) should not be shared for these two different power sources.
- The analog voltage output from the op-amp is sent to the analog pin #1, which is digitally converted with the analog-to-digital converter (ADC) inside the Arduino board. It accepts between 0 and +5 V with 10-bit resolution. Since $2^{10} = 1024$, +5 V corresponds to the digital signal of 1023 and 0 V to 0. Each unit of this digital signal corresponds to $5/1024 = 0.0049$ V or 4.9 mV.
- Type in the following code. Click “→” button to compile and upload your program to the Arduino board. This program turns the LED on if the photodiode voltage is higher than 300 mV (Fig. A.7).

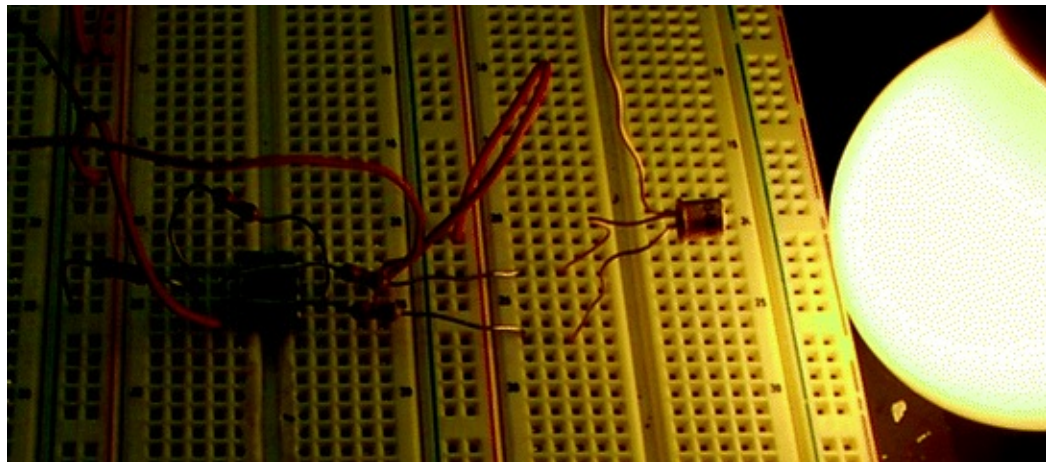


Fig. A.6 Circuit photo of Task 2. Identical to Fig. 7.20

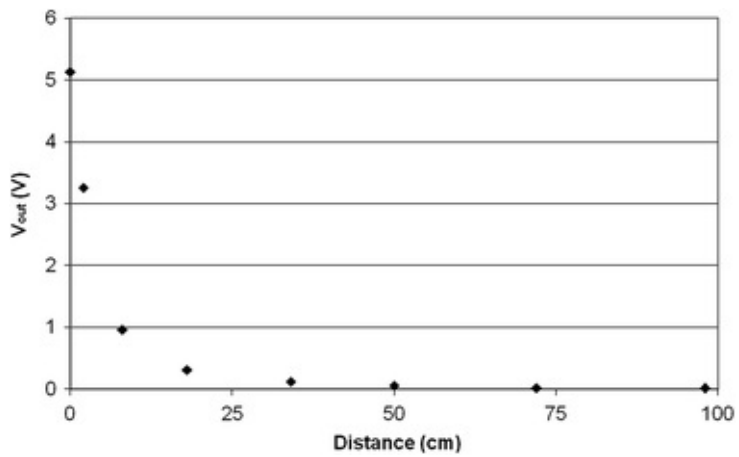


Fig. A.7 V_{out} —distance curve for a 60 W incandescent light bulb. Identical to Fig. 7.22

```

int val1 = 0; //define integer value for analog input
int vout1 = 0; //define integer value for photodiode voltage to LCD

void setup()
{
    Serial.begin(9600); //enable LCD
    backlightOn();
    pinMode(13, OUTPUT); //set digital pin 13 as output
}

void loop()
{
    val1 = analogRead(1); //read photodiode voltage
    vout1 = val1*4.9; //convert to mV unit
    clearLCD();
    selectLineOne();
    Serial.print("Vout = ");
    Serial.print(vout1); //display photodiode voltage on LCD
    Serial.print(" mV");
    delay(100); //pause 100 milliseconds
    selectLineTwo();

    if(vout1 < 300) //300 mV is the threshold
    {
        Serial.print("Nearby Light Bulb = NO");
        digitalWrite(13, LOW); //turn LED off
    }
    else
    {
        Serial.print("Nearby Light Bulb = YES");
        digitalWrite(13, HIGH); //turn LED on
    }

    delay(100); //pause 100 millisecond
}

/* Code for serial-enabled LCD provided by Sparkfun.com */
void selectLineOne(){ //puts the cursor at line 0 char 0.
    Serial.print(0xFE); //command flag
    Serial.print(128); //position
}
void selectLineTwo(){ //puts the cursor at line 0 char 0.
    Serial.print(0xFE); //command flag
    Serial.print(192); //position
}
void clearLCD(){
    Serial.print(0xFE); //command flag
    Serial.print(0x01); //clear command.
}
void backlightOn(){ //turns on the backlight
    Serial.print(0x7C); //command flag for backlight stuff
    Serial.print(157); //light level.
}
void backlightOff(){ //turns off the backlight
    Serial.print(0x7C); //command flag for backlight stuff
    Serial.print(128); //light level for off.
}

```

- The red LED turns on when the incandescent light bulb is close enough to the PIN photodiode.
 - Try to lower the 300 mV threshold to 100 mV, for example, and repeat the experiments with and without ambient light.
-

Laboratory Task 2: Temperature Control

In addition to the equipment needed in Task 1, you will need the following:

- Breadboard, wires, wire cutter/stripper, and a DMM
- 1–5 A power supply
- Thermocouple (type K)
- Thermocouple amplifier AD595
- Relay G5SB (5 A)
- Heating peltier
- Water
- Small beaker (50–100 mL)

Figures A.8 and A.9 show the circuit layout.

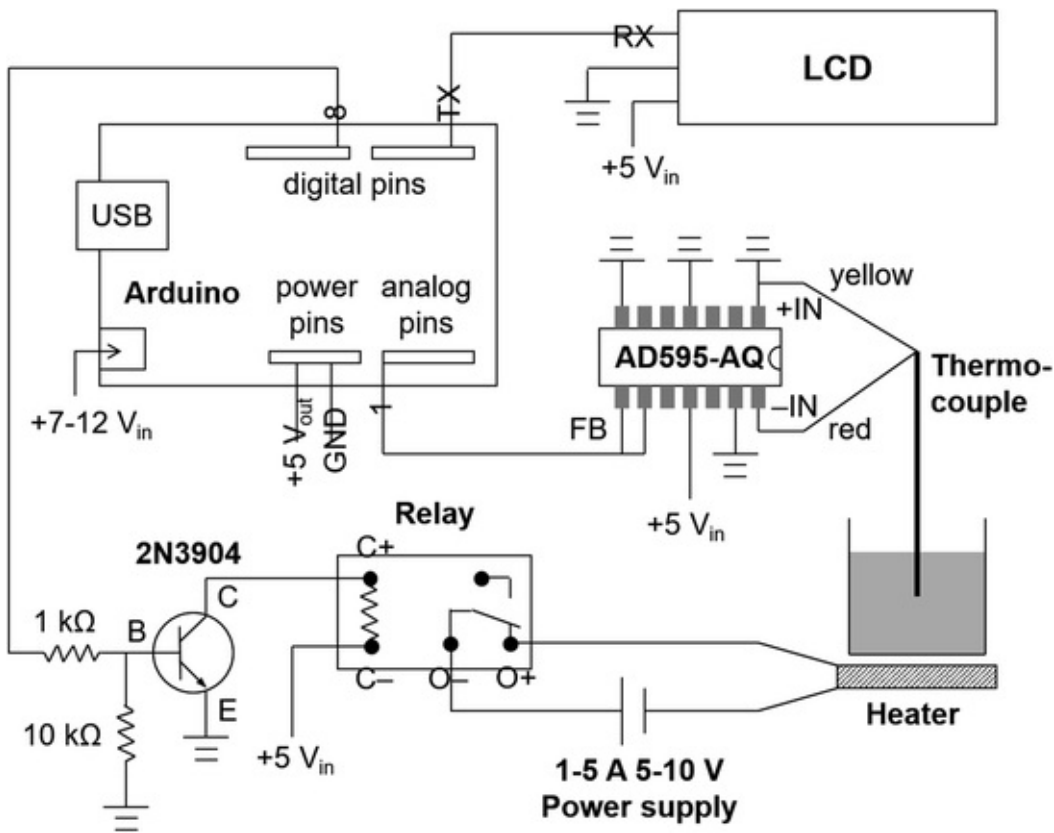


Fig. A.8 Circuit diagram for Task 2. The Arduino board draws power from a computer via USB port or from a power adapter. The LCD panel and AD595 draw power ($+5\text{ V}_{\text{out}}$ and GND) from the Arduino board via power pins. The relay and Peltier heater use a separate power supply ($>1\text{ A}$, 5–10 V), as the Arduino board does not provide enough power

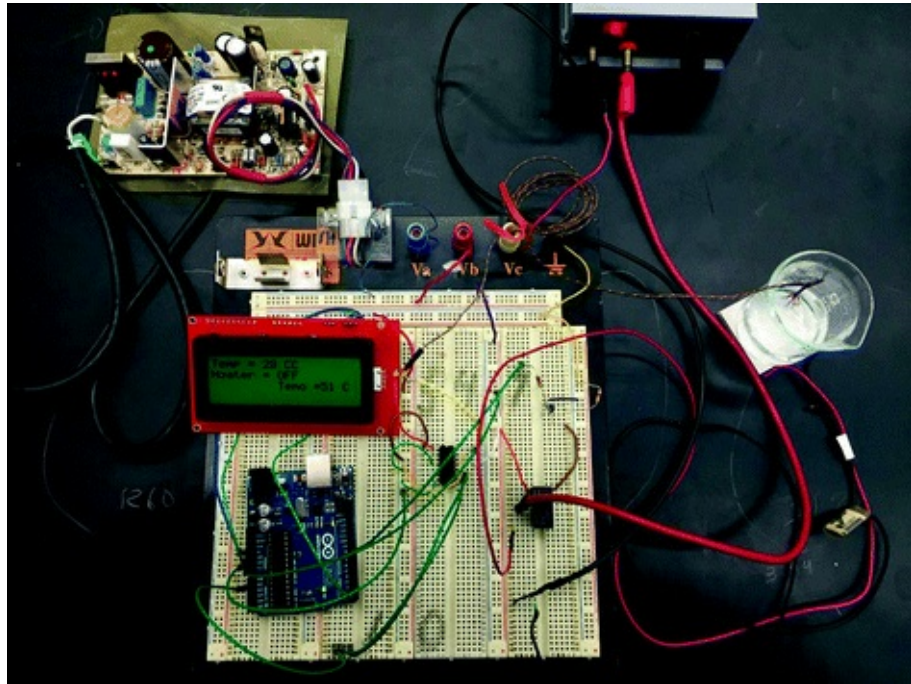


Fig. A.9 Circuit photo of Task 2

– Type in the following code:

```
int vall = 0; //define integer value for analog input
int temp1 = 0; //define integer value for temperature output to LCD

void setup()
{
    Serial.begin(9600); //enable LCD
    backlightOn();
    pinMode(8,OUTPUT); //set digital pin 8 as output
}

void loop()
{
    vall = analogRead(1); //read voltage from thermocouple
    temp1 = vall/2.046; //convert voltage to degrees Celsius

    clearLCD();
    selectLineOne();
    Serial.print("Temp = ");
    Serial.print(temp1); //display temperature on LCD
    Serial.print(" C");
    delay(100); //pause 100 milliseconds
    selectLineTwo();
```

```

Serial.print("Heater = OFF"); //heater displayed on LCD as off
delay(1000); //pause 1 second

if(temp1 < 40) //enter heating mode if temp is below 40 C
{
    while(temp1 < 40) //stay in heating mode until temp is 40 C
    {
        digitalWrite(8, HIGH); //switch relay to turn on heater
        delay(100);
        val1 = analogRead(1); //read voltage from thermocouple
        temp1 = val1*0.49; //convert voltage to degrees Celsius
        clearLCD();
        selectLineOne();
        Serial.print("Temp = ");
        Serial.print(temp1);
        Serial.print(" C");
        delay(100);
        selectLineTwo();
        Serial.print("Heater = ON"); //heater displayed on LCD as on
        delay(1000);
    }
}
digitalWrite(8, LOW); //switch relay to turn off heater
delay(100);
}

/* Code for serial-enabled LCD provided by Sparkfun.com */
void selectLineOne(){ //puts the cursor at line 0 char 0.
    Serial.print(0xFE); //command flag
    Serial.print(128); //position
}

void selectLineTwo(){ //puts the cursor at line 0 char 0.
    Serial.print(0xFE); //command flag
    Serial.print(192); //position
}
void clearLCD(){
    Serial.print(0xFE); //command flag
    Serial.print(0x01); //clear command.
}
void backlightOn(){ //turns on the backlight
    Serial.print(0x7C); //command flag for backlight stuff
    Serial.print(157); //light level.
}
void backlightOff(){ //turns off the backlight
    Serial.print(0x7C); //command flag for backlight stuff
    Serial.print(128); //light level for off.
}

```

- The signal generated from a thermocouple is properly conditioned and amplified with an *AD595* amplifier. This analog voltage signal is then transmitted to analog pin number 1 [analogRead(1)], which is then stored as “val1.”
- The *AD595* amplifier generates 10 mV/°C, i.e., 0 V for 0 °C, 0.25 V for 25 °C, 0.40 V for 40 °C, etc. Since the ADC of an Arduino board accepts analog voltage signals up to +5 V, the circuit can measure the temperature

up to 500 °C.

- Same as Task 2, the number of digital units (val1) can be converted to the temperature in °C as follows:

$$\# \text{ digital units} \times \left(\frac{4.9 \text{ mV}}{1 \text{ unit}} \right) \times \left(\frac{1 \text{ }^{\circ}\text{C}}{10 \text{ mV}} \right)$$

- When the temperature is lower than 40 °C, it switches the relay to turn on the heater by sending signal through digital pin number 8 [digitalWrite(8, HIGH)].
 - The next couple of commands simply show the current temperature in Celsius every 100 ms as well as the heater status.
-

References and Further Readings

Oxer J, Bleatings H (2009) Practical Arduino: cool projects for open source hardware, 1st edn. Apress, New York

Petruzzellis T (2006) Electronic sensors for the evil genius: 54 electrifying projects, 1st edn. McGraw-Hill, New York

Index

A

- Absorption spectrophotometers
- Absorption spectrum
- Acceptance cone (of an optical fiber)
- Acquired immune deficiency syndrome
- AD595
- A/D converter
- A/D converter board
- Adenine (A)
- Agglutination
- Alcohol dehydrogenase (ADH)
- Ames reflectance meter
- Ampere
- Amperometric

Amperometric biosensor
Amperometric electrochemical biosensor
Amplification (of a transistor)
Analog
Analog IC
Analog-to-digital converter
Annealing (in PCR)
Anode
2° antibody
Antibody
Antibody-antigen binding
Antigen
Application (for smartphone)
Aptamer
Aptasensor
Artificial fluorescence
AT-cut
AuNP
Autofluorescence
Avidin

B

B cell
B cell cancer
Back scatter
Band-pass filter (in op-amp)
Band-pass filter (in optical filter)
Barrier voltage
Base (of a transistor)
Bayonet-Neill-Concelman connector
Beer-Lambert law
Binding posts (of a breadboard)
BioMEMS
Biopolar junction transistor (BJT)
Bioreceptor
Biosensor
Biotin
Blood alcohol content (BAC)

BNC connector
Bovine serum albumin (BSA)
Breadboard
Breakdown voltage
Buffer (in chemistry)
Buffer op-amp
Buffer stage

C

Calomel electrode
Cantilever biosensor
Capacitor
Capillary action
Capillary electrophoresis (CE)
Capture probe
Carbon nanotube (CNT)
Cathode
CCD array
cDNA
Cell (as bioreceptor)
Cell constant (of a conductivity cell)
Cell counter
Cell-on-a-chip
Cellulose fibers (of autofluorescence)
Charge-coupled device array
Chlorophyll (of autofluorescence)
Cholesterol oxidase (ChOx)
Cladding (of an optical fiber)
CMOS array
Cold junction temperature
Collector (of a transistor)
Color weakness
Combined pH electrode
Complementary DNA
Complementary metal oxide semiconductor (CMOS)
Complementary metal oxide semiconductor array (CMOS array)
Complex shear modulus
Complex viscosity

Conductivity
Conductivity bridge
Conductivity cell
Conductometric
Conductometric biosensor
Conductor
Cone cell
Constant region Constant region (of an antibody)
Continuous glucose monitoring (CGM)
Core (of an optical fiber)
Corner frequency
Coulomb
Cross-reactivity
Crystal oscillator
Current
Current biasing circuit
Current divider
Current gain
Cut-off frequency
Cuvette
Cy3
Cy5
Cytosine

D

Daniell cell
DAPI
Data acquisition board
Dealloying corrosion
Denaturation (in PCR)
Deoxyhemoglobin
Deoxyribonucleic acid (DNA)
Depletion region
Detection limit
Detector probe
Development (in photolithography)
Dextrostix
Diabetes

Diaphragm
Dichromatic vision
Dichromatism
Differential op-amp
Differential resistance measurer
Digital
Digital IC
Digital multimeter (DMM)
Diode
Diode temperature sensor
Dipole
Dissipation factor (of QCM)
Distribution strips (of a breadboard)
DNA Sensor
DNA sequencer
Dopant
Doping
Double-stranded DNA (dsDNA)
Droop
Dry etching

E

Elastic modulus
Electric circuit
Electric current
Electric double layer (EDL)
Electric voltage
Electrochemical biosensor
Electrochemical cell
Electrochemical glucose sensor
Electrochemical immunosensor
Electrochemical sensor
Electrochemical transducer
Electrolyte
Electrolytic cell
Electromagnetic radiation
Electromotive force (EMF)
Electroosmotic flow (EOF)

Electrowetting
Electrowetting-on-dielectric (EWOD)
ELISA plate
Embedded fiber
Embolus
Emitter (of a transistor)
Enzyme
Enzyme-linked immunosorbent assay (ELISA)
Enzyme-linked oligonucleotide assay (ELONA)
Epitope
Etching
Ethidium bromide
Evanescence wave
EWOD droplet PCR
Extension (in PCR)

F

$F(ab)_2$ fragment
FAD
FADH
 $FADH_2$
Farad (F)
Ferricyanide
Ferrocyanide
Field-effect transistor (FET)
Filter cube
Flame (miniature spectrophotometer)
Flavin adenine
Flavin adenine dinucleotide
Flow cell
Flow cytometer
Fluorescein
Fluorescein isothiocyanate (FITC)
Fluorescence
Fluorescence microscopy
Fluorescent
Fluorescent dye
Fluorescent lamp

Fluorite
Forward bias
Frequency (of light)
FT-IR spectrophotometer

G

Gain medium (of laser)
Gain (of op-amp)
Gain stage
Galileo
Galvanic cell
Gel electrophoresis
GFP
Glass electrode
Glass membrane ISE
Gluconic acid
Gluconolactone
Glucose dehydrogenase (GDH)
Glucose meter
Glucose oxidase (GOx)
Glucose sensor
Gold nanoparticle
Graphene
Graphene oxide (GO)
Green fluorescent protein (GFP)
Ground
Guanine

H

Half-cell
Harmonic oscillation
Heart rate
Hemoglobin
Henderson-Hasselbalch equation
High-pass filter (in op-amp)
High-throughput LOC
High voltage
Hole

Horseradish peroxidase (HRP)
Hot embossing
Hot junction temperature
Human chorionic gonadotropin (hCG)
Human immunodeficiency virus (HIV)
Hybridoma cell
Hydrogen electrode
Hydrophilic
Hydrophobic
Hypervariable region (of an antibody)

I

IME immunosensor
Immunoassay
Immunoglobulin G (IgG)
Immunosensor
Impedance (electrical)
Impedance immunosensor
Indium tin oxide
Infrared (IR)
Insulator
Insulin
Insulin pump
Integrated circuit
Interdigitated array
Interdigitated microelectrode (IME)
Interstitial fluid
Intrinsic layer (of a photodiode)
Inverting comparator
Inverting op-amp
Ion-selective electrode (ISE)
Isoelectric point

J

Junction gate field-effect transistor (JFET)

K

Kirchhoff's current law
Kirchhoff's first law

L

Lab-on-a-CD
Lab-on-a-chip (LOC)
Lactic oxidase
Laser
Laser diode
Lateral-flow assay (LFA)
Lateral-flow immuno-chromatographic assay
Latex immunoagglutination assay (LIA)
Light
Light-emitting diode (LED)
Light sensor
Light transducer
Linear IC
Liquid chromatography (LC)
Liquid membrane ISE
LM324
LM334
LM335
LM741
Logic IC
Low-pass filter (in op-amp)

M

Magnetofluidics
Mask
Mediator (in electrochemical immunosensor)
Megapixel (for smartphone camera)
Methemoglobin
Micro-electromechanical systems (MEMS)
Micro wave
Microchannel
Microcontroller
Microfabrication
Microfluidic chip

Microfluidic device
Microfluidic paper analytic device (μ PAD)
Microfluidics
Microinjection molding (μ IM)
Microplate
Microplate reader
Microprocessor-based controller
Microtransfer molding (μ TM)
Microwell plate
Mie scattering simulation
Miniature spectrophotometer
Modal dispersion
Molar absorptivity
Mold
Monochromatic
Monochromator
Monoclonal antibody (mAb)
Monocrystal
Multimode fiber
Multi-wall carbon nanotube (MWCNT)
Myeloma cell
Myoglobin

N

2N4401
 NAD^+
NADH
Nano-immunosensors
Nanoporous gold (NPG)
Nanotechnology
NA (of an optical fiber)
N-doped
Negative resist
Nernst equation
Neutravidin
Nicotinamide adenine dinucleotide
Nicotinamide adenine dinucleotide (NAD^+)
Non-inverting comparator

Non-Inverting op-amp
Non-specific reaction
NPN transistor
N-type
Nucleic acid
Numerical aperture

O

OceanView™
Ohm's law
Ohm
Op-amp
Op-amp filter
Open-loop voltage gain
Operational amplifier
Optical fiber
Optical filter
Optical glucose sensor
Optical immunosensor
Optical transducer
Organ-on-a-chip (OOC)
Oxygen saturation in blood
Oxyhemoglobin

P

P-doped
P-type
Papain enzyme
Paper-based LOC
Paper (of autofluorescence)
Paper microfluidics
Passivating protein
Passive mixer
Peristaltic pump
pH
pH electrode
pH meter

Phosphate-buffered saline (PBS)
Photobleaching
Photoconductive cell
Photoconductive mode
Photodiode (PD)
Photolithography
Photometry
Photon
Photoresist
Photoresistor
Phototransistor
Photovoltaic cell
Photovoltaic mode
Physical sensor
pI
Piezoelectric effect
Piezoelectric immunosensor
Piezoelectric sensor
Piezoelectric transducer
Piezoelectricity
PIN-040A
PIN photodiode
Plasmon resonance band (PRB)
PNP transistor
Point-of-care testing (POCT)
Polarization (of polycrystal)
Polychromatic
Polyclonal antibody (pAb)
Polycrystal
Polydimethylsiloxane (PDMS)
Polymerase chain reaction (PCR)
Positive resist
Pot
Potentiometer
Potentiometric
PR
Pressure transducer
Primer
Printed circuit board (PCB)

Probe
Proximity fiber
Pulse mixer
Pulse (of heart)
Pulse oximeter
Pyrroquinoline quinone (PQQ)

Q

QCM-D
QCM immunosensor
QRT-PCR
Quality factor (of QCM)
Quantitative PCR (qPCR)
Quantum dots (QDs)
Quantum size effect
Quartz
Quartz crystal microbalance (QCM)

R

Radioisotope dye
Radio wave
Raspberry Pi
Real-time quantification (in PCR)
Real-time PCR
Real-time RT-PCR
Recombinant technology
Rectification
Red blood cell (RBC)
Redox
Reflection probe
Reflection spectrophotometry
Reflectometer
Refractive index
Replica molding
Resistance
Resistivity
Resistor
Resistor-inductor-capacitor circuit

Resistors in parallel
Resistors in series
Resonant frequency
Reverse bias
Reverse transcription PCR
Reynolds number
RGB
Rhodamine B
Ribonucleic acid (RNA)
RLC circuit
RT-PCR
Rules of op-amp

S

Sandwich immunoassay
Saturated calomel electrode
Saturation voltage (of an op-amp)
Sauerbrey equation
ScAb fragment
ScFv fragment
Secondary antibody
Seebeck effect
Semiconductor
Sensor
Serpentine mixer
Side scatter
Siemens
Signal
Signal-to-noise ratio (S/N ratio)
Silicon wafer
Single-chain antibody fragment
Single-chain variable antibody fragment
Singlemode fiber
Single nucleotide polymorphism (SNP)
Single stranded DNA (ssDNA)
Single-wall carbon nanotubes (SWCNT)
Smartphone
Snell's law

Soft lithography
Solar cell
Solid-state ISE
Spectra
Spectrometry
Spectrophotometer
Spectrophotometry
Spectrum
Spleen
 $\text{SpO}_2\%$
SPR immunosensor
Standard curve
Standard electrode potential
Steinhart-Hart equation
Stokes shift
Strain
Strain gauge
Strain transducer
Streptavidin
Subcutaneous
Summing junction (of an op-amp)
Summing op-amp
Surface plasmon resonance immunosensor
SYBR
SYBR Green I
Syringe pump
Systematic evolution of ligands by exponential enrichment (SELEX)

T

Taq polymerase
T cell
Temperature coefficient (of a resistor)
Temperature sensor
Temperature transducer
Tetramethylbenzidine (TMB)
Tetramethyl rhodamine isothiocyanate (TRITC)
Thermistor
Thermocouple

Thermocycler
Thermocycling
Thévenin resistance
Thévenin's theorem
Thévenin voltage
Thickness shear mode
Thickness shear mode resonator
Thiol
Thromboembolism
Thrombus
Thymine
Tissue (as bioreceptor)
TL082
Tolerance (of a resistor)
Total internal reflection (TIR)
Transducer
Transistor
Transistor temperature sensor
Trichromatic vision
TSM resonator
Tuneability (of quantum dot)

U

Ultraviolet (UV)
Uracil
Urobilin
USB4000
UV/Vis spectrophotometer

V

Visible (Vis) light
Voltage (Volt)
Voltage divider
Voltage droop
Voltage drop
Voltage dropper
Voltage follower
Voltage regulator

Voltage rise
Voltmeter

W

Wavelength (of light)
Wave-particle duality
Wet etching
Wheatstone bridge
White LED
Wicking
Wire-guided droplet PCR

X

X-ray

Z

Zener diode
Zener voltage
Zero adjust stage
Zinc oxide (ZnO)
ZnO nanoparticle
ZnO nanorod
ZnO nanosheet
ZnO nanotube
ZnO nanowire